VORTICES OF THE MOZAMBIQUE RIDGE CURRENT

by

Marten Luther Gründlingh

Submitted in partial fulfilment of the
requirements for the degree of
Doctor of Philosophy
in the
Faculty of Science
University of Cape Town

CONTENTS

			Page
PREFACE			(vi)
ACKNOWLEDGEMENTS			(viii)
LIST OF CRUISES EXECUTED ON THIS STUDY			(ix)
CURRICULUM VITAE			(x)
ABSTRACT			(xi)
PART 1		INTRODUCTION AND BACKGROUND	1
CHAPTER 1		MOTIVATION AND SCOPE OF THE INVESTIGATION	2
	1.1	Introduction	2
	1.2	Motivation of the thesis	2
	1.3	Scope of the study	3
	1.4	Definitions and comments	5
CHAPTER 2		THE PHYSICAL ENVIRONMENT OF THE SOUTHWESTERN INDIAN OCEAN	7
	2.1	Introduction	7
	2.2	Historic reports	7
	2.3	Water masses of the southwestern Indian Ocean	9
	2.4	Dynamic characteristics of the Agulhas Current System	10
	2.5	Conclusion	17
CHAPTER 3		CIRCULATION IN THE MOZAMBIQUE RIDGE AREA	18
	3.1	Introduction	18
	3.2	Cruise of the *Robert Giraud*, July 1960	19
	3.3	Cruise of the *Meiring Naudé*, March 1981	22
	3.4	Cruise of the *Meiring Naudé*, October 1981	24
	3.5	Historic observations of deep-sea eddies in the southwestern Indian Ocean	31
	3.6	Discussion	31

PART II DATA COLLECTION AND ANALYSIS 35

CHAPTER 4 OBSERVATIONS OF DEEP-SEA VORTICES : 1975 36

4.1 Introduction 36

4.2 Observations in August 1975 36

4.3 Discussion 45

4.4 Conclusion 48

CHAPTER 5 OBSERVATIONS OF DEEP-SEA VORTICES : 1976 49

5.1 Introduction 49

5.2 Narrative of the June 1976 cruise 50

5.3 Hydrographic results of eddy Charlie 50

5.4 Discussion 59

CHAPTER 6 OBSERVATIONS OF DEEP-SEA VORTICES : 1977 60

6.1 Introduction 60

6.2 Observations in March 1977 60

6.3 Observations in June 1977 67

5.4 Discussion 78

CHAPTER 7 OBSERVATIONS OF DEEP-SEA VORTICES : 1978 79

7.1 Introduction 79

7.2 Observations in April 1978 79

7.3 Observations in May 1978 85

7.4 Observations in June 1978 90

7.5 Satellite imagery 96

7.6 Discussion 98

CHAPTER 8 OBSERVATIONS OF DEEP-SEA VORTICES : 1979 and 1980 101

8.1 Introduction 101

8.2 Narrative of the November/December 1979 cruise 101

8.3 Thermohaline characteristics of Fred 104

8.4 Currents during the November/December cruise 111

8.5 Propagation of the eddy 115

8.6 Volume transport 115

	8.7	Narrative of the January 1980 cruise	118
	8.8	Hydrographic conditions at the Mozambique Ridge	119
	8.9	Section across the Agulhas Current at 30°S	122
	8.10	Observations in March 1980	124
	8.11	Satellite buoy tracks	128
	8.12	Summary	136
CHAPTER 9		OBSERVATIONS OF DEEP-SEA VORTICES : 1981	138
	9.1	Introduction	138
	9.2	Observations in February, 1981	138
	9.3	Observations in April, 1981	140
	9.4	Discussion	150
CHAPTER 10		OBSERVATIONS OF DEEP-SEA VORTICES : 1982	154
	10.1	Introduction	154
	10.2	Observations in April, 1982	154
	10.3	Observations in June, 1982	165
	10.4	Discussion	179
PART III		DISCUSSION AND REVIEW	182
CHAPTER 11		PHYSICAL CHARACTERISTICS OF THE VORTICES OF THE MOZAMBIQUE RIDGE CURRENT	183
	11.1	Introduction	183
	11.2	Thermal structure of the eddies	183
	11.3	Salinity and T/S structure	190
	11.4	Chemistry and biology	195
	11.5	Shape and size of the eddies	196
	11.6	Distribution of eddies	199
	11.7	Summary of main physical characteristics	201

CHAPTER 12	DYNAMIC CHARACTERISTICS OF THE VORTICES OF THE MOZAMBIQUE RIDGE CURRENT	203
12.1	Introduction	203
12.2	Velocity field	203
12.3	Sound velocity in eddies	215
12.4	Volume transport	215
12.5	Kinetic energy	217
12.6	Vorticity field	219
12.7	Advection	223
12.8	Decay and lifetime	225
CHAPTER 13	THE MOZAMBIQUE RIDGE CURRENT	227
13.1	Introduction	227
13.2	Historical reports on the Mozambique Ridge Current	227
13.3	Present observations of the Mozambique Ridge Current	229
13.4	Generation of eddies	233
13.5	Summary of characteristics	240
CHAPTER 14	DISCUSSION AND SUMMARY	242
14.1	Introduction	242
14.2	Origin of the eddies	242
14.3	Physical and dynamic characteristics	243
14.4	Eddy movement	244
14.5	Lifetime and decay	245
14.6	Future research	245
14.7	Conclusions	246
APPENDIX 1	HYDROGRAPHIC EQUIPMENT	248
APPENDIX 2	NAVIGATION ON THE R.V. *MEIRING NAUDé*	257
APPENDIX 3	CALIBRATION OF THE NBIS CTD	260
APPENDIX 4	DATA PROCESSING METHODS	268
APPENDIX 5	THERMOHALINE SECTIONS IN THE MOZAMBIQUE BASIN	275
APPENDIX 6	VERTICAL SECTIONS ON THE NORTHERN MOZAMBIQUE RIDGE	288
APPENDIX 7	FREE-DRIFTING CURRENT METER ARRAY	294
REFERENCES		313

PREFACE

The seed that eventually gave birth to this thesis was planted in August, 1975 when, during a cruise of the Research Vessel *Meiring Naudé* , the existence of deep-sea cyclonic vortices in the South Western Indian Ocean was discovered. Little was it realised during that small, fortuitous beginning in 1975 that the study would develop into the first detailed physical oceanographic investigation of the Mozambique Ridge and adjacent Mozambique Basin areas. It could also not be foreseen that the study would discover what has been called the Mozambique Ridge Current, and thus throw new light on the Agulhas Current System as a whole.

From 1976 onwards, the study of these vortices was incorporated into a project of the National Research Institute for Oceanology of the Council for Scientific and Industrial Research.

Now, after eight years of data collection and analysis, this thesis presents the details of the investigation, its objectives, progress and results. Many of the findings have already been exposed to widespread scrutiny through national and international publications and seminars, and this was considered confirmation of the soundness of the investigation.

The presentation of the thesis is separated into three parts. The function of the first part is to provide a background against which the study itself can be projected. It contains the aim and scope of the thesis, a brief literature survey of historic observations, and also a section on the present state of knowledge of the general circulation in the target area. The latter section was considered a very important part of the thesis, since it provides the oceanographic "climate" of the area against which the phenomena of vortices (oceanographic "weather") can be truly evaluated. The second part is a detailed presentation of the collection and analysis of the data (which have been lodged with SADCO, the South African Data Centre for Oceanography). At the risk of making the thesis too bulky, this part contains the information on which the third part is based. Some of the details presented here may therefore seem superfluous to anybody except the inquisitive reader. A third and conclusive part is a summary and review of the main results of the thesis, a comparison with local and remote observations of vortices and a general outlook for the future. It uses the

information of Part II as basis and by intercomparing results serves as the envelope to bind the various elements of the thesis together.

For the sake of readers who are unfamiliar with operational sea-going procedures of the National Institute for Oceanology, appendices have been added to elucidate equipment and methods of data collection and processing. Other appendices contain vertical sections and information referred to in the body of the thesis.

The thesis moves in the sphere of mainly descriptive physical oceanography. We believe that the opportunity for detailed, theoretical treatment of the features described here lies in the future, and that the thesis should only act as an introduction to the road eventually leading to a complete understanding of these phenomena.

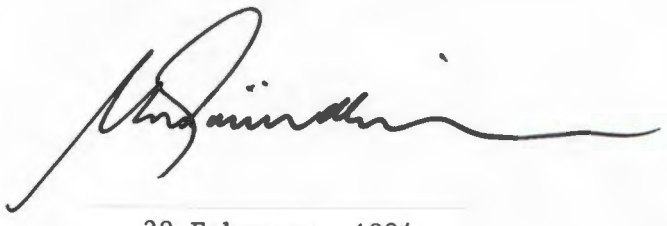

29 February, 1984

ACKNOWLEDGEMENTS

I am grateful to the National Research Institute for Oceanology (NRIO) of the Council for Scientific and Industrial Research for making this study possible.

I would also like to acknowledge the interest of Professor Geoff Brundrit, and the discussions with colleagues at NRIO and the University of Cape Town.

Captain George Foulis and his officers and crew of the R.V. *Meiring Naudé* need a special word of thanks. George was always prepared to help wherever possible, make suggestions and listen patiently and sympathetically to my problems.

My wife Marianne formed an equally important component by providing me with the stability of a happy environment from which to conduct this investigation.

Mrs. Ayliffe Cumming deserves a big hug for her patience and professionality in converting my tatty manuscript into elegant typing.

Mr. Arjoon Singh used his expert draughtsmanship to draw all the figures of this thesis.

In the production of this thesis I had the fond support of many people at the Natal Regional Laboratory of the CSIR in Durban, and I am grateful to them all.

I am indebted to my parents, relatives and friends for their continued interest.

Finally, and above all, my deepest gratitude goes to my Creator, who gifted me with enough insight and interest to execute the study.

LIST OF *MEIRING NAUDé* CRUISES EXECUTED ON THIS STUDY

Cruise Number	Date	Vortex	Number of Stations	Target Depth
MN 75/23	27-31 August, 1975	Alfa, Bravo	31	900 m
MN 76/14	23-29 June, 1976	Charlie	41	1000 m
MN 77/09	17-19 March, 1977	-	21	1000 m
MN 77/17	2-8 June, 1977	Delta	36	1000 m
MN 78/08	7-9 April, 1978	-	11	1750 m
MN 78/11	11-16 May, 1978	Echo	22	1800 m
MN 78/15	15-20 June, 1978	Echo	20	1800 m
MN 79/28	28 November-6 Dec. 1979	Fred	54	1000 db
MN 80/01	16-22 January, 1980	Fred, Golf	25	1050 db
MN 80/07	19-22 March, 1980	Golf	20	1050 db
MN 80/15*	26-27 June, 1980	-	7	1400 db
MN 81/02	6-10 February, 1981	-	23	1050 db
MN 81/05	10-18 March, 1981	-	41	1900 db
MN 81/06	22-27 April, 1981	Harry	29	2500 db
MN 81/13*	23-26 July, 1981	-	10	2500 db
MN 81/17	15-20 October, 1981	-	35	2000 db
MN 82/07	15-21 April, 1982	Ian	35	1050/2000 db
MN 82/13	9-16 June, 1982	John	46	1050 db

Data from the following cruises, not executed as part of this study, is also presented (cruise dates describe only the time spent in our area of interest).

Robert Giraud	9-13 June, 1960	14	4000 m
SAS Natal	4-8 October, 1962	8	3000/4000 m
Meiring Naudé	13-21 August, 1968	49	1000 m

* These cruises were terminated prematurely because of equipment problems, and their data is not included in this study.

CURRICULUM VITAE

Marten Luther Gründlingh was born on the 26th July, 1947 in Krugersdorp, South Africa. His schooling commenced in 1953 in his home town and ended when he gained distinctions in the six subjects required for the University entrance examination.

He was awarded a study-bursary by the South African Council for Scientific and Industrial Research (CSIR), and in 1965 enrolled for the degree of Bachelor of Science at the Potchefstroom University. He completed the degree course in 1967 gaining distinctions in his major subjects of Physics and Mathematics. Two years later he obtained the Master of Science degree in Physics at the same University.

During March 1970 Marten Gründlingh took up an appointment in Durban as Assistant Research Officer in the Oceanography Division of the CSIR's National Physical Research Laboratory.

In January, 1972 he married Marianne Burggraaf, before being seconded to the Institut für Meereskunde at the Christian Albrechts Universität, Kiel, Federal Republic of Germany in October 1972. On his return to South Africa in April 1975, he resumed his post within the Physical Oceanography Division of the newly formed National Research Institute for Oceanology, where he is presently a Senior Chief Research Officer. In December 1980 he was awarded the degree Dr. rer. nat. by the Christian Albrechts Universität. He is the author of a number of international papers.

Marten and Marianne have four children; Christine (1974), Johann (1976) and twins, Nico and Werner (1978).

ABSTRACT

During a cruise of the R.V. *Meiring Naudé* in August 1975, anomalous values for temperature, salinity and nutrients were recorded over a deep-sea region of the Southwestern Indian Ocean. It was thought that this oceanographic anomaly may represent part of a cyclonic mesoscale vortex of unknown origin. The scant information available at the time on the circulation in this area precluded any of the known, steady currents from being possible generators. Only once before, in 1962, had a similar observation been made, and its significance had not been recognised.

In the period 1976 to 1982, several hydrographic cruises were executed on the R.V. *Meiring Naudé* in the region 27 - 33°S, 32 - 43°E, to locate similar features and to find answers to the following questions: Was the 1975 anomaly really a vortex (i.e. a rotating body of water)? What are the physical and dynamic characteristics (i.e. temperature, salinity, density, velocity, volume transport, energy) and distribution of such vortices? How and where are the vortices generated, and what are their lifetime and eventual fate?

In all, more than 500 routine hydrographic stations were occupied to collect data on water properties. Most of these stations extended to a depth of 1 000 m, while about 20% went to at least 1 800 m. Initially, hydrosondes designed and built by the Council for Scientific and Industrial Research were employed, but a Neil Brown Instrument Systems' CTD (conductivity-temperature-depth) microprofiler was used from 1979 onwards. Satellite-tracked buoys and infrared imagery were used to derive information on the circulation patterns, thus extending the coverage of the small research vessel. The drift rate of the ship and current measurements from a drifting array of current meters augmented the calculations of geostrophic velocity, volume transport and energy, and provided insight into the flow dynamics of the water.

During the course of the investigation, eleven additional anomalies were located and surveyed. It was established that these anomalies represented eight individual, cyclonic vortices, thereby

confirming the existence of such entities in the Southwestern Indian Ocean. The vortices were characterised by cold, low-salinity water at the centre at depths below 200 m, where the isopycnals were raised about 250 - 300 m above their ambient or "background" level. If eddy size is defined in terms of the diameter of the 10°C/650m intersection, most of the eddies were elliptical with a diameter typically of about 150 km. Maximum geostrophic velocity was approximately 40 cm/s (relative to 1 000 m) or 60 cm/s (relative to 1 500 - 1 800 m). Volume transport varied considerably within eddies and from one eddy to the next, and a typical volume transport would be 30×10^6 m^3/s (relative to 1 000 m), or 50×10^6 m^3/s (relative to 1 800 m). The maximum kinetic energy amounted to 20×10^{14} J (relative to 1 000 m).

Three eddies were relocated on subsequent surveys (thus enabling a crude estimate of their propagation), but despite this and other measurements to determine the "background" flow in the Mozambique Basin, no consistent evaluation of the vortex drift rate could be obtained. The eventual fate of the vortices therefore remains unknown.

The vortices were generated by a highly-variable current (the Mozambique Ridge Current), the existence of which has now been established for the first time. Flowing either meridionally southward along the Mozambique Ridge, or zonally westward across the Ridge, the Mozambique Ridge Current is induced by the bottom topography to shed cyclonic vortices in the region of 30°S, 37°E. Cyclogenesis has been observed several times, during which the eddies revealed significant increases in volume transport. Evidence was also found of convergence in the upper layers, accompanied by an increase in mixed layer depth at the eddy centre. It was observed that, after occlusion of the loop through which the host current generated the eddies, the vortices became free-drifting in the Mozambique Basin, and it is estimated that they contain sufficient energy to maintain significant existence for a year or more.

PART I INTRODUCTION AND BACKGROUND

It has been said that in science, a good question is very often better than a good answer, since the former tends to excite while the latter tends to stifle. This first of three parts of the thesis attempts to formulate the questions around which the thesis is centred, and to reflect the excitement with which the study was initiated.

To make a true evaluation of the significance of the results of Parts II and III, it is important to present in this first part some insight into the background circulation in the southwestern Indian Ocean. Also included here is the first observation of a cyclonic vortex in this area, made in 1962. This vortex was not identified as such, and it was only in 1975 that new information managed to crystallise the concept of midocean eddies in this region.

CHAPTER 1

MOTIVATION AND SCOPE OF THE INVESTIGATION

1.1 Introduction

As in most other scientific fields, progress in Oceanography has not been one of a continuous, steady nature. Although our knowledge of the ocean in general and its physical characteristics in particular is obviously increasing all the time, it seems that our insight into different aspects of the sea's circulation advances in the form of definite intellectual quanta, providing a step-like feature to the otherwise smooth "curve of knowledge". One of the main factors acting as catalysts in scientific investigation is the discovery and development of new methods and instruments. Among these could be counted the introduction of the bathythermograph, the geostrophic method of current calculation, continuously recording current meters, etc., but the most outstanding innovation of the past few decades must obviously be in the field of satellite oceanography. The capability of satellites to remotely sense oceanic parameters with a frequency and resolution never before possible has stimulated oceanography more than could ever have been foreseen. It was satellite oceanography's stepchild, namely satellite-tracked buoys, developed from a concept for tracking balloons, that can be considered to have initiated the present investigation. It was during a cruise to deploy a satellite-tracked buoy in August, 1975 that the first information was acquired about the intense vortices that form the nucleus of this study. The data from this buoy and other buoys deployed subsequently therefore continuously interleave the treatise below, and provide an important contribution to the more conventionally obtained hydrographic information.

1.2 Motivation of the thesis

It is only during the past decade or so that worldwide interest

in mesoscale motions in the open ocean has flared up. The reasons for this are possibly two-fold : Firstly, the importance of these scales of motion on the larger oceanic circulation has relatively recently been recognised (e.g. BRETHERTON, 1975 and others). Secondly, it is only during the past twenty years that the density of oceanographic stations has increased sufficiently to resolve these scales of motion in many parts of the world.

The acquisition of data for this thesis started in 1975 and is still continuing, although the thesis only covers the period 1975-1982. This data set consisted of 18 cruises with more than 500 hydrographic stations. These were all directly aimed at increasing our knowledge of the deep-sea vortices in the southwestern Indian Ocean. The investigation was undertaken for the following reasons:

a) A study of these vortices could provide the first detailed evidence of their existence in the mid SW Indian Ocean.

b) A knowledge of the characteristics of these eddies could contribute to our understanding of the general circulation in the area, especially in the region between the Mozambique and Madagascar Ridges.

c) The results of the investigation could supply important information to fill the data gap on the worldwide distribution of mesoscale eddies.

d) A last and possibly lower-priority reason tended toward the technical side of our involvement : The study of deep-sea vortices supplied us with the opportunity to outgrow the shoes of a coastally-orientated organisation and attempt to solve the problems involved with deeper (vertical) penetration further from the coast.

1.3 Objectives of the thesis

Very little, if anything, was known about the intense vortices which occur in the SW Indian Ocean at the start of the project in 1975.

The general objective of the thesis is therefore to improve our knowledge of these eddies. The specific objectives are, first, to study the physical (and possibly chemical) composition of the vortices, their dimensions dynamics and volume transport. Second, to determine their origin, evolution mechanism and generating frequency. Third, to investigate the advection of the vortices and their interaction with the environment. The final objective is to estimate their decay, lifetime and eventual destination.

To provide the data base for the treatise, experiments were designed to locate, track and survey the vortices. This location and tracking involved mainly classical ship cruises but use was also made of satellite infrared images. Once located, the vortices were surveyed by obtaining vertical and horizontal distributions of temperature salinity, chemical parameters and velocity.

During the execution of the project it very soon became obvious that we might be dealing with entities that have "lifespans" of several months or longer. It is in this field most of all that the investigation felt the technical and logistic restrictions imposed by a small vessel with limited duration and space, and limitations in the manpower available to participate in data collection and analysis. It was virtually impossible within this framework to observe the slow decay of a vortex and establish an average "life time". The thesis therefore concentrates on the physical characteristics of the vortices.

The title of the thesis is a bit enigmatic, since it suggests that an aspect of an already known current is being studied. This is not the case. The Mozambique Ridge Current - the existence of which has been inferred from other observations - was only surveyed in any detail during the present investigation. It is therefore appropriate that some attention be devoted to the characteristics of this Current *per se* and this is manifested in a separate chapter in Part III.

The study is the first of its kind on a national level and deviates strongly from most other past and present oceanographic projects executed in this country. If the vortices were fixed in space, the investigation

would have deteriorated into the more common of oceanographic surveys where a given area is covered as often and as densely as possible, and where the data is intended to provide insight into the average situation rather than the anomalous. In the present study, there was no foundation to proceed from and no cut-and-dried routines. One of the overruling challenges was to locate the eddy, before any thought could be given to surveying it. Written between the lines of the following chapters is the frustration caused by the many ups and downs which are so common in oceanography.

1.4 Definitions and comments

a) Geostrophy

This is the situation where the pressure gradient in the water is balanced by Coriolis force. In the discussion of vorticular motion, the centrifugal force has to be considered as well due to its compatability to the other two forces, and the current in which these three forces balance is called a gradient current. In the thesis, this terminology is not always distinguished, in that the term "geostrophic current" is sometimes used where the gradient approximation has been applied.

b) Current velocity

Distinction is made between "observed" or "measured" current, which is a current velocity measured mechanically in different ways (see Appendix 1), and "calculated" or "computed" current which is the derivation of current velocity from the density structure (i.e. geostrophic or gradient approximations).

c) Dynamic heights/Geopotential anomalies

These were computerised calculations according to accepted methods (see e.g. NEUMANN and PEARSON, 1966, p 173) and compared with calculations done by other institutes. Where necessary, parabolic interpolation is used between neighbouring data points. An example of the routine processing is given in Appendix 4.
The unit of geopotential anomaly is m^2/s^2 ($10\ m^2/s^2 = 1$ dyn m).

d) Vortex

The terminology "vortex", "eddy" and "gyre" are completely interchangeable.

e) Bottom topography

The bottom topography used in the figures originates from SIMPSON (1974). During the past two years, three revised topographies were produced which agree closely in the area of interest (Chart 526A RabShack, 1980; Sheet 5.09 of the GEBCO Series, 1982; and a combination of these two, Chart 126A by L. Shackleton, 1982). Use of these charts in the final chapters resulted in small differences compared to other Chapters.

f) Salinity is expressed as °/₀₀ (or parts per thousand), while the terminology " 10^{-3} " suggested by the SUN report, is not used.

g) The station spacing during hydrographic surveys was normally defined in terms of nautical miles to simplify navigation (1 n.m. = 1.852 km).

h) Normally, station numbers in the figures are blocked to distinguish them from other values.

i) Smooth isopleths in vertical sections are obtained by visual interpolation between stations.

CHAPTER 2

PHYSICAL ENVIRONMENT OF THE SOUTHWESTERN INDIAN OCEAN

2.1 Introduction

The purpose of this chapter is to briefly describe the general circulation of the southwestern Indian Ocean, since this will allow a proper evaluation of the phenomenon of vortices in this part of the world. Whereas eddies have only been studied over the past decade, the knowledge of the circulation in the southwestern Indian Ocean extends more than 500 years back. For interest sake the reader will be initiated very superficially into these historic quanta of information, to eventually arrive at the present-day status of knowledge relevant to the aims of the thesis.

2.2 Historic reports

A survey of the historic encounters with the Agulhas Current has been compiled by LUTJEHARMS (1972), PEARCE (1980), and the reader is referred to these two works for a more detailed review.

It is considered today that the Phoenicians were the first to circumnavigate the African continent in 600 BC (see PEARCE, 1980), sailing from Arabia around the southern tip of the continent and into the Mediterranean through Gibraltar. The knowledge of this voyage was lost to the Portuguese mariners who attempted to reach India during the fifteenth century. The rather doubtful privilege of being the first to experience the head-on effect of the Agulhas Current (and live to report it) befell Vasco da Gama in 1497, who ranks as the "discoverer" of the passage to the East around Africa.

The exact time at which the occasional, and very often exclusive, entries of ships' captains progressed to a more formal, or even "scientific" evaluation, is not clear. Today, James Rennel's (1778) chart (see PEARCE, 1980) is regarded as the first cartographic evidence of the course and direction of the Southern Agulhas Current and smaller peripheral currents. Not only does Rennel hold the position of pioneer of South African "oceanography", but his career is also one of the longest, since another chart of his

(including more detail about the currents) was published in 1832 - 54 years after laying the foundation of scientific reportage of this area. An image of almost eternal belligerency of the Cape coast is evoked by Rennel's remark that "the borders of the two currents, from the Atlantic and Indian Oceans, appear to often *encroach* on each other ....." (our italics).

It seemed that reported knowledge of the Agulhas Current System promptly entered a dormant phase that lasted up to the 20th century. During this intervening period of about two centuries, observations on winds and ship sets must have been continuously entered into ships' logs, and this enabled the production of the first current atlasses of this area between 1910 and 1920.

It was in more or less the same period (early 20th century) that several research vessels (e.g. the *Gazelle*, *Planet*, *Möwe*) traversed the area. These initial scientific expeditions were followed by the investigations of those well-known oceanographers such as BRENNECKE, MICHAELIS, BARLOW, SCHOTT and MöLLER, and the local oceanography of the western and southwestern Indian Ocean grew at a pace on par with other areas.

The impression is, however, gained that the knowledge of the Agulhas Current System soon seemed to reach a plateau when the basic characteristics of the Agulhas Current were established. Even large, multi-ship surveys only marginally increased the knowledge of the circulation. Investigations were obviously limited by the coverage that can be attained by a research vessel, compared to the significant degree of variability that the system exhibits. To be able to investigate the variability of the system, oceanographers needed the capability of two scientific instruments that were to revolutionise oceanography and oceanographic data collection : satellite technology and continuously-recording current meters.

The introduction of these advanced data-capturing systems led to a strong increase in research projects of the southwestern Indian Ocean and the adjacent areas of the Southern Ocean (see LUTJEHARMS, 1981a). During the 1970s, satellite infrared imagery threw a completely new light on mesoscale (MALAN and SCHUMANN, 1979) and synoptic-scale circulation features. E.g. (HARRIS and VAN FOREEST, 1977). The first satellite-tracked buoy in this area was launched in July, 1973 (STAVROPOULOS and DUNCAN, 1974), and

the first deployment of a continuously-recording, digital current meter was executed in 1976 (SCHUMANN, 1979).

These new types of equipment enabled oceanographers to monitor currents and water profiles remotely. Features were now investigated that had previously been considered too distant for conventional ship's coverage, or of such a nature to make a continuous survey by ship impractical in terms of cost and manpower.

2.3 Water masses of Southwestern Indian Ocean

Since the characteristics of the various water masses in the southwestern Indian Ocean will be referred to repeatedly in the sections to follow, it is important to provide brief descriptions here (see DUNCAN, 1970 and PEARCE, 1977a for a more detailed treatment and other references).

At the surface in this area there are two distinct water masses. Tropical Surface Water (TSW) is characterised by a high temperature (18-29°C) and relatively low salinity (34.8 - 35.0 °/₀₀), and originates in the rainy tropical areas of the Indian Ocean north of about 20°S. From the subtropical areas between roughly 25°S and 40°S comes Subtropical Surface Water (STSW) with a salinity greater than 35.5 °/₀₀ and temperatures between 16°C and 23°C.

The surface of the southwestern Indian Ocean falls within the sphere of influence of both of these water masses, with the Agulhas Current representing roughly the dividing line between them. Given the variability of the Agulhas Current the mixing of these two water masses within the upper 200 m of the ocean is incomplete and can at times be characterised by an interleaving rather than a true mixing (HARRIS, 1972).

Below the 200 m level the surface layers of TSW/STSW overlay the Central Water (CW) which is formed by mixing between the surface waters (STSW) and the Antarctic Intermediate Water (AAIW) in the Subtropical Convergence zone at ~ 42°S. Central water extends from 200 to 800 m and is represented by a linear section on the T/S curve. Further down, South Indian Deep Water (SIDW) extends from 1600 to 4000 m, and inside this depth domain South Atlantic Deep Water is entered eastward around the southern tip of the African continent.

2.4 Dynamic Characteristics of the Agulhas Current System

Apart from the Agulhas Current itself there are various other currents present in the southwestern Indian Ocean. Virtually all of these currents interact with one another and with the Agulhas Current in an almost symbiotic coexistence, and the whole combined circulation is referred to as the Agulhas Current System (see GRüNDLINGH and LUTJEHARMS, 1979).

2.4.1 Tributaries to the Agulhas Current

As the South Equatorial Current impinges firstly on the Madagascar coast and further west on the African continent (Fig. 2.1), portions of the Current are deflected southwards down the eastern coast of Madagascar and down the Mozambique Ridge, respectively. Compared to available information and research done on the Agulhas Current, very little seems to be known about these two currents.

Being exposed to the interior of the Indian Ocean, the East Madagascar Current (EMC) is compatible to the Agulhas Current as a true western boundary current. DUNCAN (1970) used data from the International Indian Ocean Expedition (IIOE) and derived a volume transport (relative to 1000 m) of 23 - 28 x $10^6 m^3 s^{-1}$ for the EMC. In a later survey using XBTs, LUTJEHARMS, BANG and DUNCAN (1981) derived a transport of about 40 x $10^6 m^3 s^{-1}$.

South of Madagascar the circulation seems to be very enigmatic. DUNCAN (1970) maintained that an appreciable portion of the EMC rounded Cape St. Marie (the southern tip of Madagascar) in a westward flow toward the African continent. This situation is also reflected in most current atlasses (see e.g. USN, 1958). On the other hand, WYRTKI's (1971) atlas of the IIOE shows what might be a seasonal pattern in the flow: westward during summer and eastward during winter. This might explain the lack of any westward flow observed by LUTJEHARMS, BANG and DUNCAN (1981). They maintained that water flowing in a westerly direction south of Cape St. Marie is the exception rather than the rule, and postulated that the EMC retroflects southeast of Madagascar in very much the same way as the Agulhas Current does south of the African continent. Spurious (clockwise) eddies are created during the fragmentation process of the current, and these advect in more or less arbitrary directions.

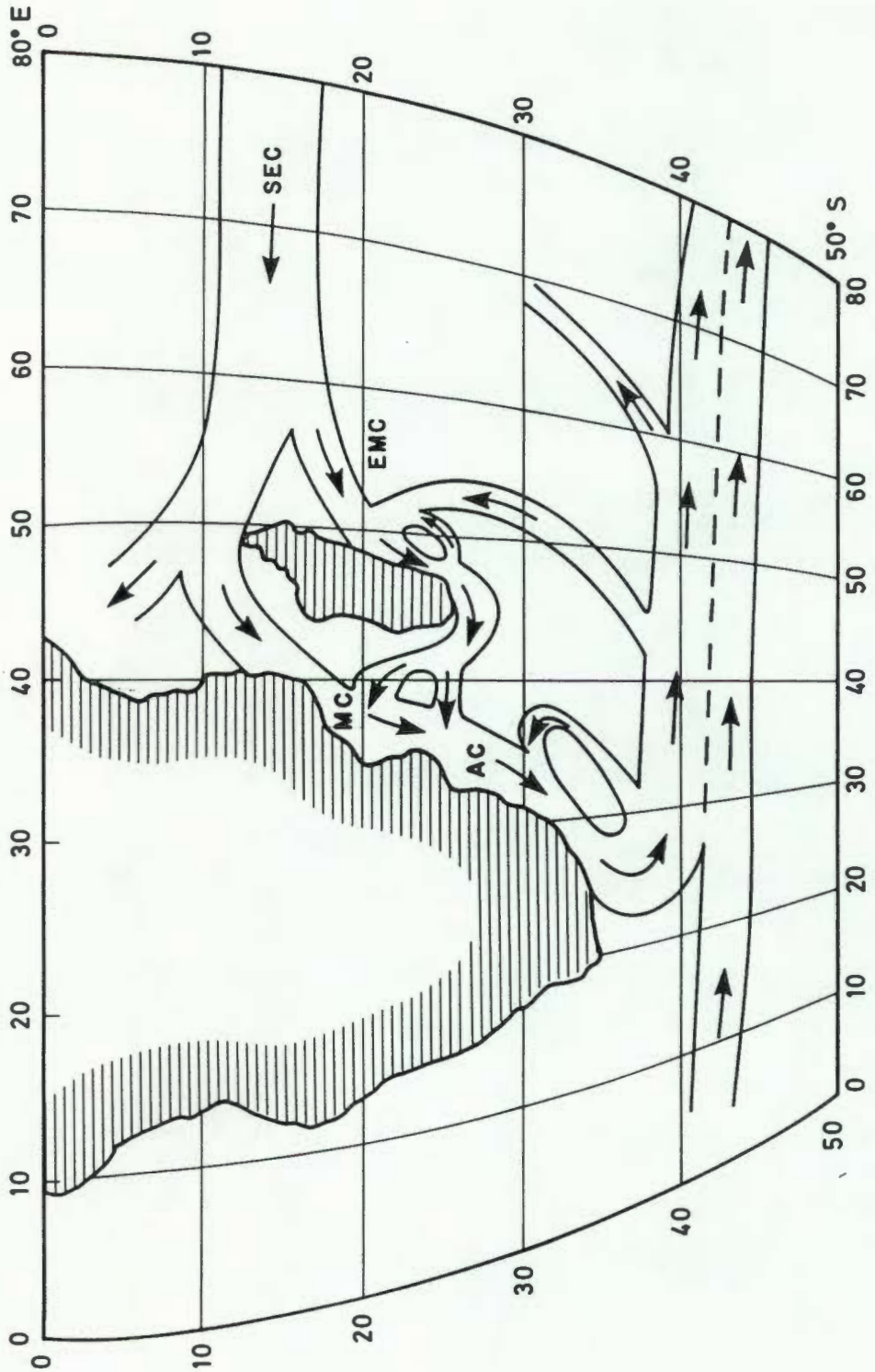

FIG. 2.1 : Representation of the major circulation features in the southwest Indian Ocean. The transport diagram was adapted form DUNCAN (1970). SEC = South Equatorial Current; EMC = East Madagascar Current ; MC = Mozambique Current; AC = Agulhas Current.

The unsteady westward flow southwest of Madagascar was also visible on an infrared image presented by HARRIS, LEGECKIS and VAN FOREEST (1978).

The situation in and at the southwestern entrance to the Mozambique Channel is equally obscure. Circulation patterns presented by MENACHE (1963) seem to have been biased toward the absence of any water mass exchange through the southern entrance, a viewpoint for which there is little, if any, evidence. An excellent insight into the circulation of this area has been provided by DUNCAN (1970), WYRTKI (1971), HARRIS (1972) and LUTJEHARMS (1976). These show that there exists unambiguous evidence of a contribution southward into the Agulhas Current from within the Mozambique Channel. This does not depreciate the existence of an internal circulation in the Channel, but shows that water is moving northward into the Channel mainly on the eastern side along the Madagascar coast, and southward out of the Channel on the western side along the African continent. The variability (possibly seasonal) of the flow pattern must, however, be reiterated.

DUNCAN (1970) postulated a third "tributary" to the Agulhas Current in the shape of a vorticular recirculation within the area bounded by 25°S and 35°S and the African coast and 40°E (see Fig. 2.1). This recirculation (DUNCAN refers to it as the "Agulhas Eddy") withdraws water from the southern parts of the Agulhas,transports it northward again in an anticlockwise and sluggish fashion and supplies it to the Agulhas in its northerly part. The Agulhas Eddy can therefore be regarded as a miniature, localised version of the large-scale oceanic gyre in the southern Indian Ocean.

2.4.2 The Agulhas Current

Somewhere in the vicinity of 25°S, 35°E, the Mozambique Current joins a part of the East Madagascar Current to form the Agulhas Current (see Fig. 2.1). As indicated in the previous section, these two influxes are probably very variable, and details about the dynamics of this mixing region are still virtually non-existent. For the purpose of this thesis, the Agulhas Current will be defined as the intense, more or less continuous coastal current flowing southwestwards within a few hundred kilometers of the African continent, starting at 25°S and "ending" at about 40°S.

a) Course

If it is assumed that the potential vorticity of the Current is conserved, then

$$\frac{f + \xi}{D} = \text{const}$$

where $f = 2\Omega \sin \phi$ is the planetary vorticity at a latitude ϕ due to the rotation rate Ω of the earth, ξ the vorticity $= \partial v/\partial x - \partial u/\partial y$ of a parcel of water due to its speed (u, v) relative to the coordinate frame rotating with the earth, and D the depth of the Current. Since f changes only very slowly compared to topographical changes, it is the relative vorticity ξ inside the water column that compensates for changes in the bottom topography. This will tend to guide the Current along lines of constant f/D, or, over limited meridional distances, constant D. The influence of the bottom topography on the Current has been shown by HARRIS and VAN FOREEST (1977), and GILL and SCHUMANN (1979). In a recent study, GRüNDLINGH (1983a) examined the course of the Agulhas Current from about 28°S to 34°S, and showed that it flowed smoothly along the continental slope.

South of 34°S, the coastline turns away to the west and the continental shelf widens to form the Agulhas Bank. In this area and as the Agulhas Current separates from the coastline, the progressive mesoscale turbulence of the Current is reflected by the almost continuous formation of shear eddies along the edge of the Bank (BANG, 1970). From 35° southward, the Agulhas Current as a whole depicts convulsion-like meandering, while it turns sharply eastward ("retroflects" : BANG, 1970) at 40°S (LUTJEHARMS, 1981b).

b) Velocity

The reports on the velocity of the Agulhas Current originate from calculated (geostrophic) speeds and from directly measured speeds. As far as the geostrophic measurements are concerned, the Agulhas Current lends itself very poorly to this kind of calculation because of the proximity of the continental slope. Because of the problems associated with the choice of a suitable reference level, these computations have been employed on a limited scale only (see e.g. DIETRICH, 1935; DUNCAN, 1970) and almost invariably underestimate the true velocity.

In contrast, current speeds have been measured directly from the R.V. *Meiring Naudé* along the whole length of the Southern African east coast, and we regard these as a closer approximation of the true current velocity. Examples of these speeds have been published by DUNCAN (1976), PEARCE (1977a), HARRIS (1978) and SCHUMANN (1979), where it is shown that the Agulhas Current attains a maximum velocity between East London and Port Elizabeth, where the speed in the core of the Current exceeds 2 m/s on the average. To the North and South of this region, speeds between 1-2 m/s are quite common. The maximum speed of the Agulhas Current lies between 2 and 3 m/s. (See PEARCE, 1977b; SCHUMANN, 1979).

Between the Agulhas Current and the coast there can be eddies of various sizes, depending on the width of the continental shelf. The longest of these shelf eddies is located in the Tugela Bight (see e.g. PEARCE, 1977a and PEARCE, SCHUMANN and LUNDIE, 1978) while southward, where the continental shelf becomes narrower and the continental slope steeper, eddies are normally very small (PEARCE, 1977a) or non-existent.

c) Meanders

The subject of meanders of the Agulhas Current has captured attention since detailed investigations of the Agulhas Current started during the 1960s, and still remains largely unsolved as far as its cause is concerned.

The most common type is characterised by an onshore/offshore displacement with an amplitude of the order of tens of kilometers and a period of a few days (see GRüNDLINGH, 1974). These have been observed almost everywhere along the east coast of Southern Africa where regular hydrographic stations have been occupied, e.g. at Richards Bay (PEARCE, 1976), Durban (PEARCE, 1977b) and Port Edward (HARRIS, 1978).

More isolated occurrences are presented by the large meanders that have been reported by HARRIS, LEGECKIS and VAN FOREEST (1978) and GRüNDLINGH (1979). These are more spectacular in appearance than, but possibly related to the smaller meanders, and have amplitudes (magnitude of the deflection away from the coast) of more than 200 km and "wavelengths" of about 400 km.

South of the continent, large meanders and vortices are a common feature of the Agulhas. In this area the Agulhas has become separated from

the continent before impinging on the subtropical convergence situated approximately at 40°S. LUTJEHARMS (1979) presented some infrared images of the convulsion-like loops exhibited by the Current, and these images provided the first synoptic overview of the circulation features described by DUNCAN (1968). Thus, during the past decade, the oceanic "triple point" of the Atlantic, Southern and Indian Oceans has been shown to contain those variable and intense current patterns that RENNEL (1832) described so vividly about 150 years ago (see section 2.2).

d) Volume Transport

Initial calculations put the volume transport of the Agulhas Current (see e.g. DIETRICH, 1935) at 10-25 x $10^6 m^3 s^{-1}$. More recent measurements have shown these values to underestimate the true volume transport. DUNCAN (1970) estimated that the transport could be 80-100 x $10^6 m^3 s^{-1}$, values that were confirmed by the measurements of GRüNDLINGH (1980). GRüNDLINGH also showed that there is a general increase southward of the transport by a value of about 6 x $10^6 m^3 s^{-1}$ per 100 km. The highest transport reported for the Agulhas was obtained by JACOBS and GEORGI (1977), namely 136 x $10^6 m^3 s^{-1}$, south of the continent. In another study, GRüNDLINGH (1983a) was able to show that the increase in transport coincided quantitatively with an increase in the "intensity" (flow velocity) of the Current.

2.4.3 The Agulhas Return Current

South of the African continent the Agulhas Current turns anti-clockwise through about 135° to form the eastward-flowing Agulhas Return Current. This Current should not be confused with the Antarctic Circumpolar Current, since the latter is characterised by a broad, slow movement of water centred at about 50°S (HARRIS and STAVROPOULOS, 1978). It should rather be regarded as a true extension of the Agulhas Current, and its relatively warm water (see e.g. LUTJEHARMS, 1979) and high speeds (GRüNDLINGH, 1978 reported drifting buoy speeds of more than 2 m/s) give credence to this.

Whereas the Agulhas Current increases intensity and volume transport (GRüNDLINGH, 1980, 1983a) the Agulhas Return Current decreases its speed as it progresses eastward. It is therefore obvious that while the Agulhas Return Current loses volume on a more or less continuous basis and thus forms a source of water, the Agulhas Current forms a sink. Between these two

currents, water is exchanged through a broad, unidentified flow (DUNCAN, 1970). It must be noted that characteristics of this return circulation are based on a few isolated cruises. Station spacings of the order of 200 km (e.g. that of the *Anton Bruun* and *Africana II*) in this region have not been conducive to determining circulation features approaching the mesoscale in size.

2.4.4 Mozambique Ridge Current

The circulation in the Mozambique Basin is discussed in detail in Chapter 3, but it may be appropriate in terms of the scope of the present chapter to provide a brief background to (one of) the currents in this region.

A satellite-tracked buoy entering the "Agulhas area" in the vicinity of 25° (GRüNDLINGH, 1977) was expected - by those who were watching its progress - to approach the edge of the continental shelf and flow down the east coast of southern Africa. Instead, it moved southward along 35°E in a large clockwise route and approached the continent only at 31°S. This aspect coupled with a model of an inertial jet, led HARRIS and VAN FOREEST (1977) to re-inspect some older hydrographic data in this area and to conclude that there is evidence of a southward-flowing current along the Mozambique Ridge. Induced by the bottom topography, this current - the *Mozambique Ridge Current* - seems to separate from the Mozambique Current in the vicinity of 25°S, 36°E, flows southwards along the Mozambique Ridge up to about 32°S before turning westward to join the Agulhas Current off the east coast of southern Africa.

The reason why this Current had not been discovered previously is not clear, but could be contained in its variability and intensity. At the time of its "discovery" it was conjectured that the Mozambique Ridge Current was highly inconsistent in space and time, even to the extent that it would be completely absent at times. In addition, because the Mozambique Ridge is still about 1500 m deep at its shallowest parts, the absence of a rigid boundary along which to flow would diminish the surface signature of the Current.

The study of this Current forms an integral part of the investigation into vortices in the vicinity of the Mozambique Ridge - the nucleus of this thesis. As will be shown below, this study was the first to make a qualitative and quantitative assessment of the nature and

variability of the Mozambique Ridge Current and the vortices spawned by the Current.

2.5 Conclusion

The major part of the oceanographic research executed in the southwestern Indian Ocean was confined to the continental shelf and the deep-sea area within about 200 km from the coast. It is inside this region that attention of oceanographers has been focussed on the Agulhas Current and its variability. Little, if anything, has been done to reveal the mesoscale variability in the open ocean, basically because no-one seriously considered the possibility that such variability could exist away from the energy source of the Agulhas Current. This gap in our knowledge of the circulation has been shown to exist, and the study described in Parts II and III of this thesis represents a purposeful effort to determine the characteristics of this circulation.

CHAPTER 3

CIRCULATION OF THE MOZAMBIQUE RIDGE AREA

3.1 Introduction

Whereas Chapter 2 provided a summarised description of the physical environment of the southwestern Indian Ocean as a whole, and identified the major currents and some of their characteristics, the present chapter will focus on the more localised circulation in the vicinity of the Mozambique Ridge. To set the scene for the study in the following chapters, and to illustrate, by means of contrast, just how remarkable the vortices appear compared to the "background"circulation, it is appropriate that some insight be provided into the steady-state dynamic and thermohaline properties of the area.

As far as oceanographic atlasses are concerned, the most useful is probably the Atlas of the International Indian Ocean Expedition (WYRTKI, 1971). It is believed, however, and will become clear to the readers during this chapter and those following, that various aspects of the IIOE and the production of the IIOE Atlas (e.g. compilation of non-synoptic data) seriously influenced the representation of the regional characteristics. It is by no means our intention to underrate the Atlas of the IIOE, since in our opinion, it forms a cornerstone of research in the Indian Ocean. It will, however, be appreciated that the logistics of any atlas of this kind preclude the detailed consideration of mesoscale features - the very nature of an atlas is to provide the *climate* of the ocean rather than the *weather* of the ocean.

However, it would be misleading to imagine that the "general" circulation in the area is completely featureless. The IIOE Atlas (WYRTKI, 1971) indicates that our area of interest is situated on the eastern and northeastern side of a large, anticyclonic gyre that recirculates some of the water from the Agulhas Current (DUNCAN, 1970). The impression is given that the area is characterised by a weak, steady flow that does not portray any of the energetic characteristics of the Agulhas Current. To prove that this is not the case, it was considered

important that some effort be invested in obtaining some information on the mesoscale characteristics of the Mozambique Ridge and Basin.

First, we will discuss data from a cruise of the *Commandant Robert Giraud* in July 1960. This cruise formed part of the IIOE and is referred to in WYRTKI's (1971) atlas as "unpublished". Second, two cruises were executed by the R.V. *Meiring Naudé* in March and October, 1981. Both of these cruises were designed to provide as much information on the meso- and large-scale thermohaline structure as was possible in a survey of less than two weeks. From the results of these cruises (especially those of the *Meiring Naudé*) it will become clear that this part of the SW Indian Ocean contains intense currents and a large degree of variability.

It was considered appropriate that, within the same chapter, the first (pre-1975) observations of eddies in the vicinity of the Mozambique Ridge be presented. The first eddy appeared in the data collected by the S.A.S. *Natal* in October 1962. Another, smaller eddy, displayed by the track of a satellite-tracked buoy in 1973 (STAVROPOULOS and DUNCAN, 1974) is also discussed briefly. It is believed that this eddy may provide insight into aspects of the circulation that could not be covered by the experimental section of this thesis.

3.2 Cruise of the *Commandant Robert Giraud*, July 1960

This cruise of the *Robert Giraud* lasted from 4 July to 16 September 1960, but only stations 71-84 (9-13 July, 1960) were executed in the area of interest to us. These stations were occupied about 100 km apart along 32°S and between 30°31'E and 43°14'E (see Fig. 3.1). The depth-temperature-salinity data were collected with reversing bottles which were closely spaced at the surface and further apart deeper down.

The temperature data were interpolated to construct the temperature section of the upper 2000 m (Fig. 3.2). The depth extent of the figure was truncated at this level since the interpolation of widely-spaced samples below 2000 m (some samples were obtained deeper than 4000 m) introduced fictitious undulations of the deep isotherms.

The temperature section provides a more-or-less featureless picture of the termal structure. A barely significant rise in the isotherms can be seen between station 83 and 84 at about 43°E. From Fig. 3.1 it can be seen that these stations were located close to the Madagascar Ridge in the eastern perimeter of the Mozambique Basin.

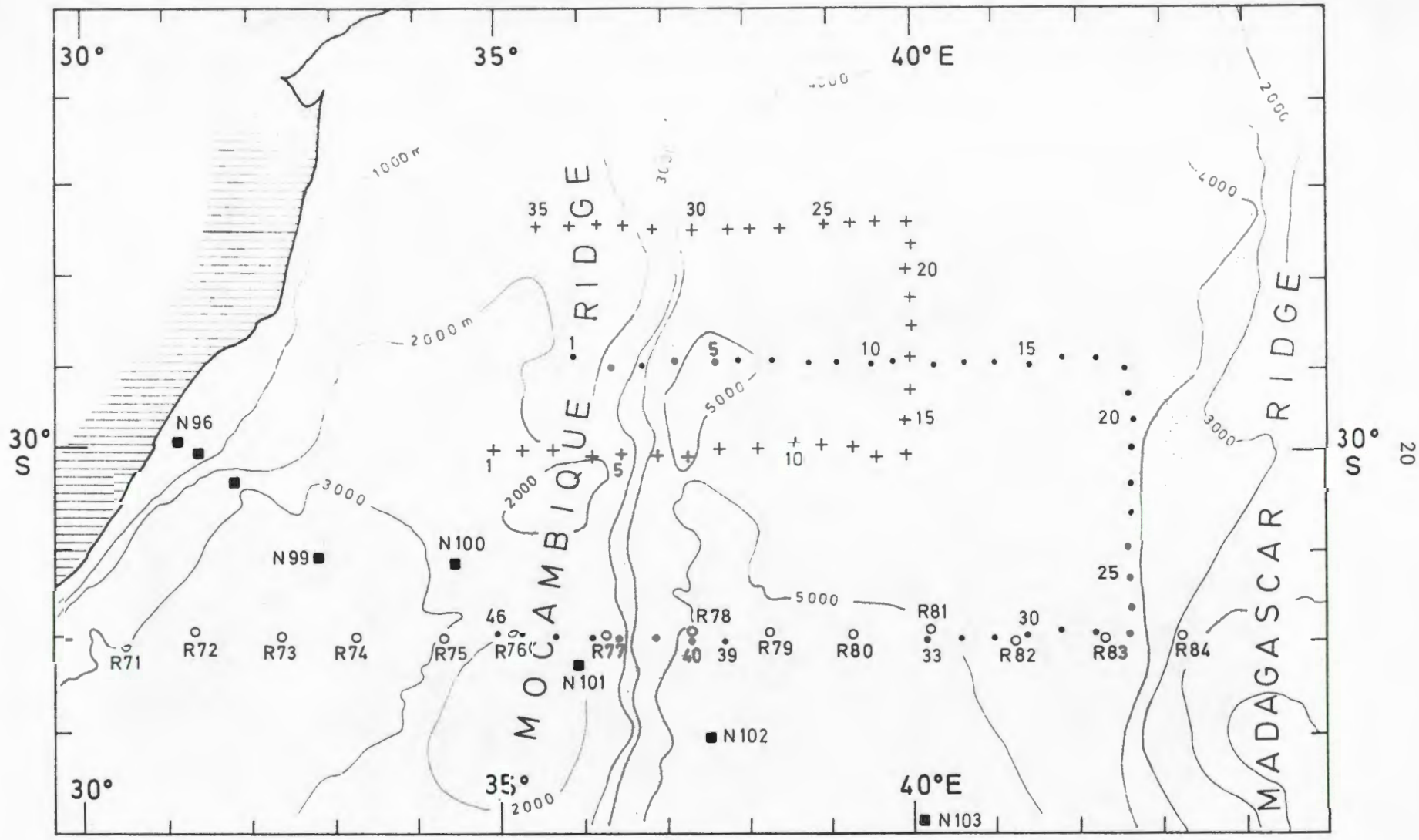

FIG. 3.1 : Stations occupied in the vicinity of the Mozambique Ridge and Basin to illustrate the circulation of the area. Stations R71-R84 (circles) originate from the cruise of the *Commandant Robert Giraud*, July 1960, stations 1-46 (dots, numbers 34-38 omitted) are from the *Meiring Naudé* cruise in March, 1981. Station 1-35 (+) are from the *Meiring Naudé* cruise in October, 1981, and the squares (N96-N103) indicate the stations from the S.A.S. *Natal* cruise in July, 1962.

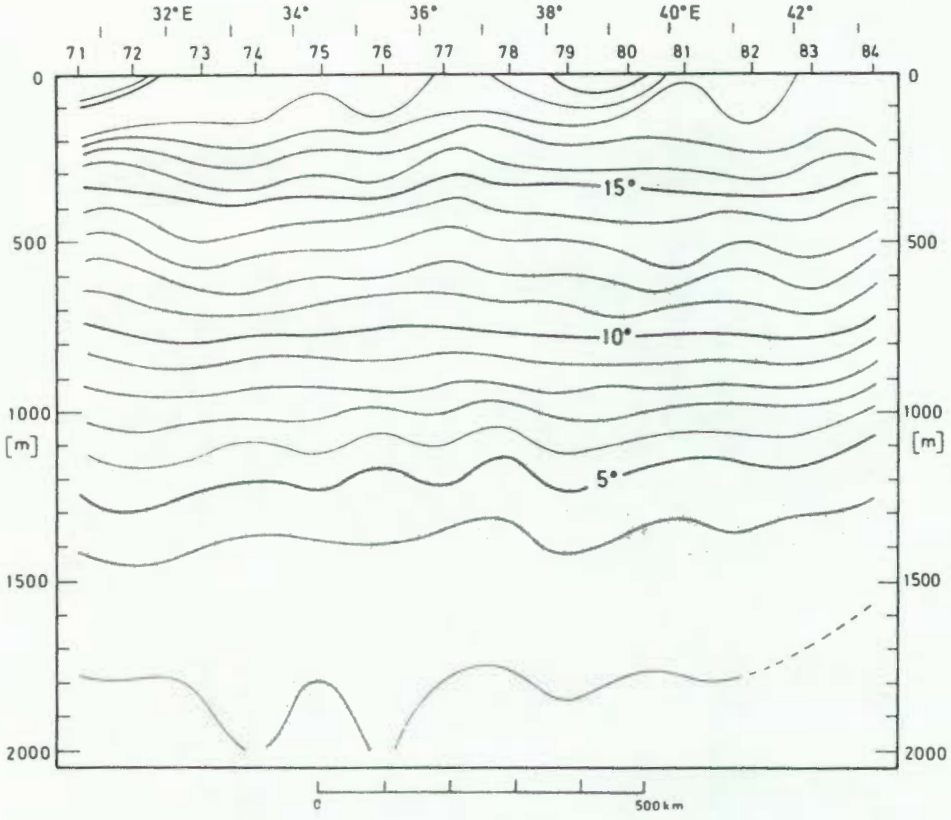

FIG 3.2 : Temperature section from stations 71-84 of the cruise of the *Commandant Robert Giraud*, 9 - 13 July, 1960.

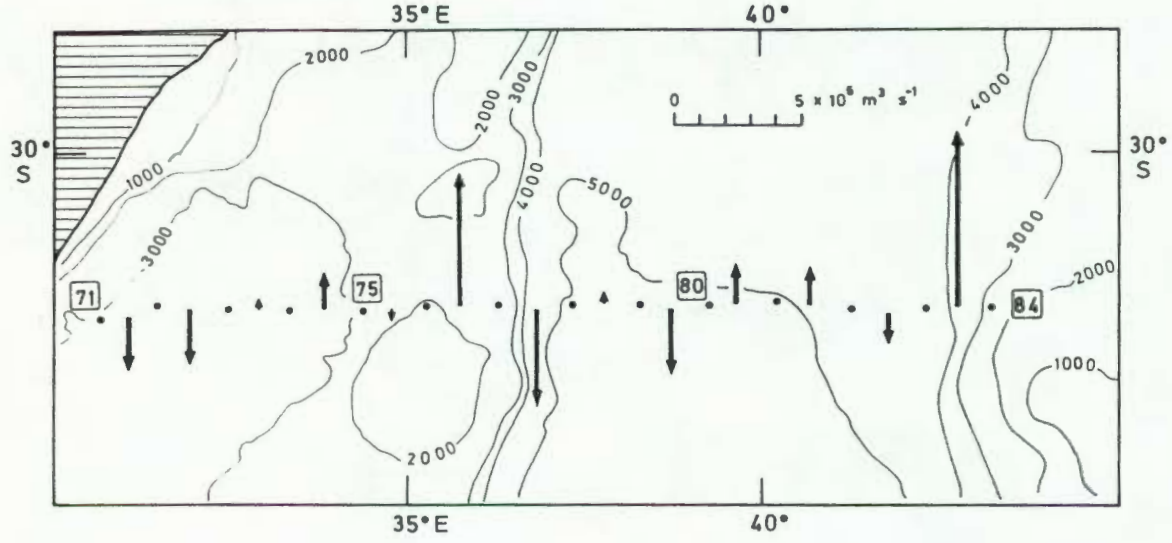

FIG. 3.3 : Volume transports for the *Commandant Robert Giraud* cruise in July, 1960.

It was found that the irregular spacing of samples between 1000 m and 2000 m introduced interpolating problems during the geostrophic calculations and for this reason the volume transport was derived relative to 1000 m only. The transports between adjacent stations were generally less than 2 x $10^6 m^3 s^{-1}$ (see Fig. 3.3), but in the vicinity of the two ridges the transports were higher. Because of their low values, it is not clear whether the transports are spurious and whether they have any physical significance.

3.3 Cruise of the *Meiring Naudé*, March 1981

The cruise of the R.V. *Meiring Naudé*, 10-18 March consisted of three lines : One along 19°S, another along 32°S and a connecting line along 42°30'E (see Fig. 3.1) An NBIS CTD was used on all stations, and represents the first measurements of its kind in the Mozambique Basin. (A description of the data collection and processing methods is given in Appendix 1, 2 and 4, while the calibration of the CTD is discussed in Appendix 3).

Vertical profiling was executed down to a routine maximum of 1900 db, although some stations were occupied to 2000 db. Because of adverse weather, no stations were occupied between stations 33 and 39 although routine underway observations were made. Vertical sections of temperature and salinity and other related data have been reproduced in Appendix 5.

3.3.1 Thermohaline structure

Surface thermal fronts were most noticeable across the Agulhas Current (see Appendix 5), but similar fronts were observed at other places along the ship's track. Some (but not all) of these fronts were accompanied by significant salinity fronts. A strong salinity front occurred between station 7 and 9 with an increase in temperature of about 1°, another front occurred between station 22 and 24. In the southerly leg too, there was a marked increase in salinity between station 33 and 39. It is evident from Fig. 3.4 that these fronts represented transitions from tropical to subtropical water. It is also clear that the water at the northerly leg was more tropical of nature, while water from the southerly leg was more subtropical. Conspicuous is also the solitary intrusion of low-salinity water into the southern leg in the vicinity of station 33.

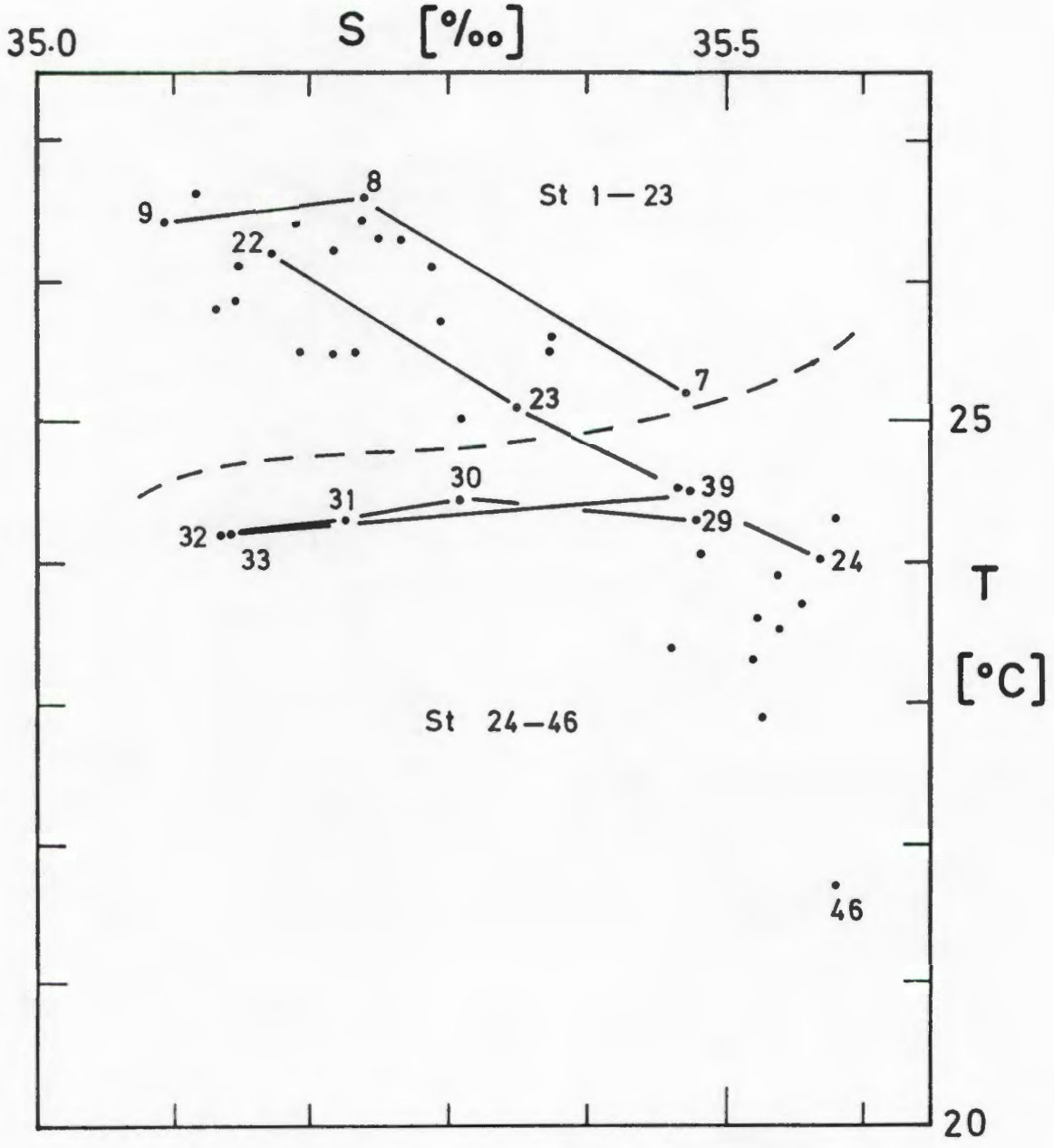

FIG 3.4 : T/S distribution of the surface water on the *Meiring Naudé* cruise, March, 1981. The frontal structures discussed in the text are represented by straight lines, while the apparent geographic division between station 1-23 and station 24-46 is indicated by the dashed line.

In contrast to the data collected via reversing bottles and widely-spaced stations, the CTD sections (see Appendix 5) reveal a considerable amount of finer structure. One of the remarkable features of the thermohaline structure is the "patchiness" of the cores of two of the main water masses, namely the subtropical surface water (STSW) and the Antarctic Intermediate Water (AAIW). This was especially the case on the northern line where the layer with salinity less that 34.5 $^{o}/oo$ was interrupted at stations 4 and between 9 and 12. A tropical water mass seems to have been located between stations 7 and 24 and there is evidence of anticyclonic circulation in this area (Fig. 3.5).

The volume transport (Fig. 3.5 (a) and (b)) reveals a strong southward flux between stations 9 and 15, and this flux is associated in the surface layers with tropical surface water (cf Appendix 5). A similar filament of tropical surface water was located between stations 31 and 33, but the flow rate of this water mass was very low and the direction of flow rather inconsistent.

3.4 Cruise of the *Meiring Naudé*, October 1981

The station spacing of this cruise was the same as that of the March 1981 cruise, namely 20 nautical miles, or about 36 km. The survey consisted of three lines, one along 27°S, another along 30°S and the connecting meridional line along 40°E. The survey as a whole was shifted relative to the March survey in order to investigate more closely the circulation in the northern part of the Mozambique Ridge (see Fig. 3.1). The cruise lasted from 14-22 October, 1981 (departing and returning times from Durban) and a total of 35 stations were occupied. The planned depth was 2000 db but this was not always attained. Equipment problems occurring at station 25 necessitated a repeat of the station, so that the position of station 25 and 26 coincided. Surface profiles and vertical sections of temperature and salinity are represented in Appendix 5.

3.4.1 Thermohaline variation

Variation of surface temperature and salinity (see Appendix 5) show different frontal structures to those observed during the March cruise.

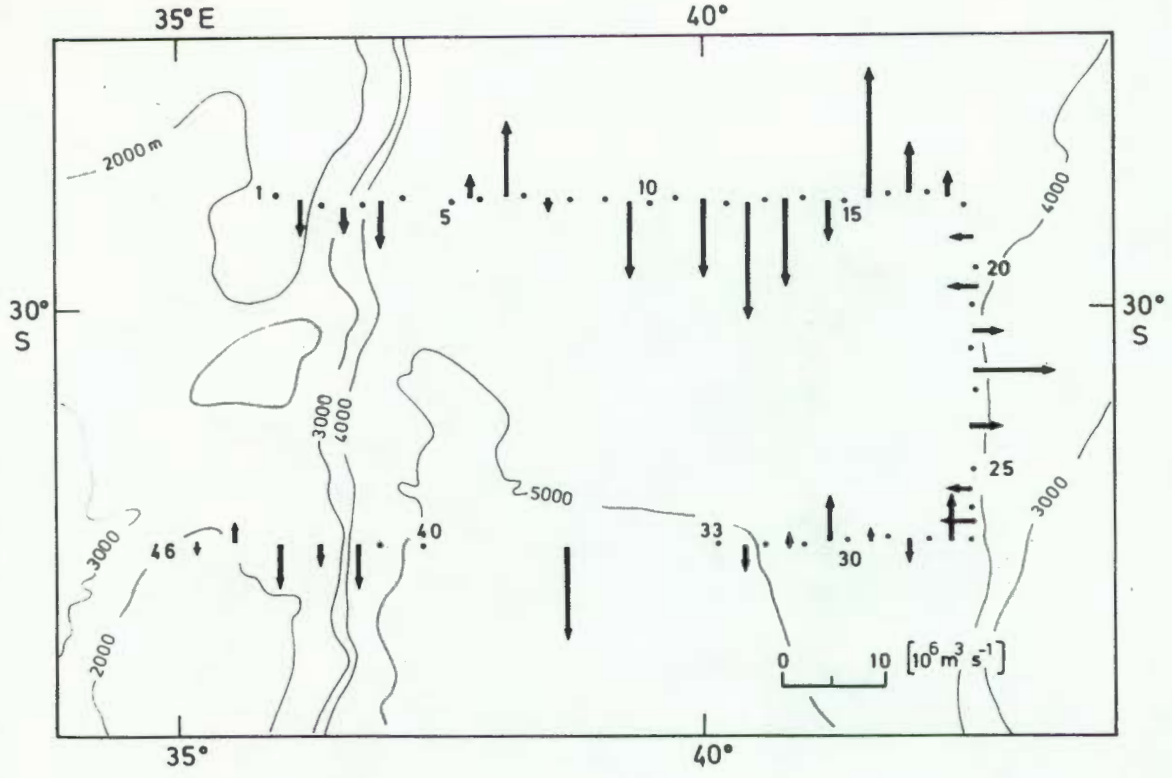

FIG. 3.5(a) : Volume transports for the *Meiring Naude* cruise in March, 1981. Values were calculated relative to the deepest common depth between station pairs (usually about 1800-1900 m). Direction of flow is nominally indicated N/S or E/W. Transports less than 1 million cubic metres per second have been omitted.

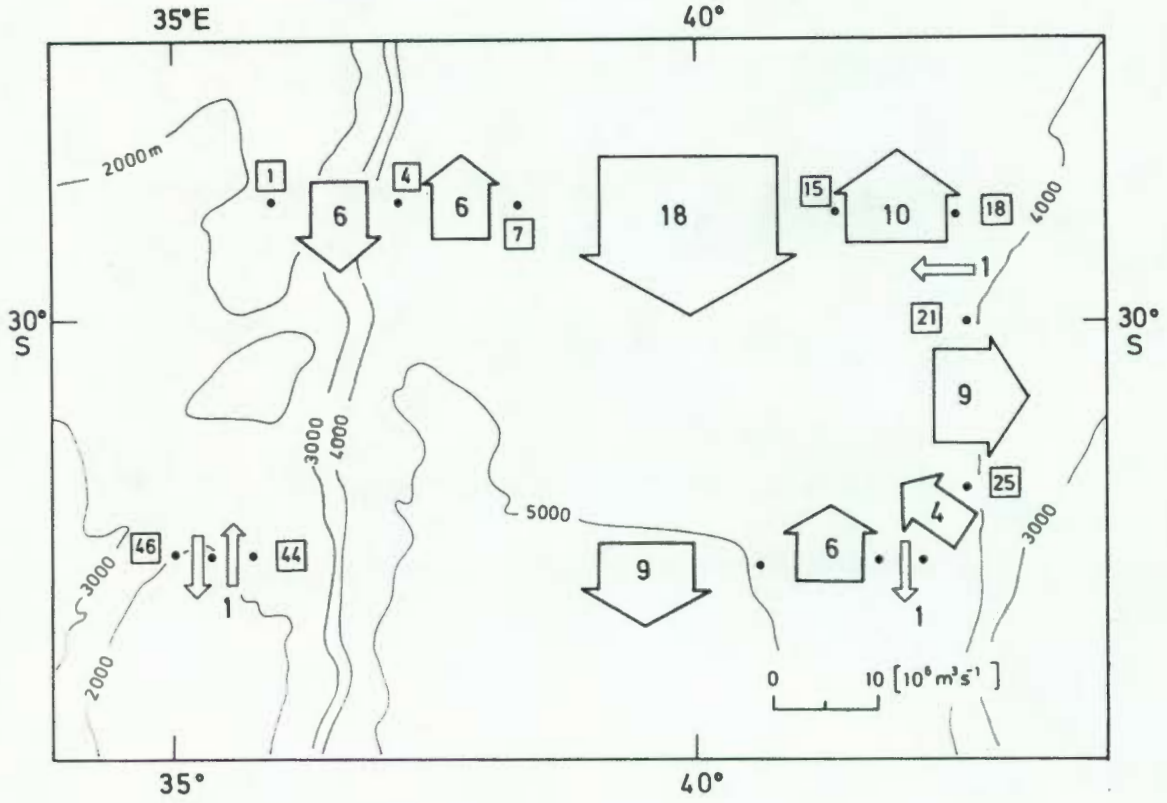

FIG. 3.5(b) : Volume transports relative to 1500 m for the *Meiring Naude* cruise in March, 1981.

The only thermal fronts that occurred in more-or-less the same position were those associated with the Agulhas Current. In the survey area, salinities varied between 35.4 and 35.6 °/oo, except for a few isolated observations on the southern leg. Here, marked discrepancies occurred between the salinity from the surface samples and the surface salinity of the CTD. These values have been bracketed since they are considered to have been caused by malfunction of the salinometer used to analyse the surface samples. In one case only (station 10), both the surface sample and the CTD recorded high salinities (~ 35.7 °/oo).

The subsurface thermohaline variation (Appendix 5) show similar variations in the depth of the isotherms and isohalines. Most conspicuous is the upheaval of isopleths between station 29 and 34 in the vicinity of the Mozambique Ridge. There is also, especially on the northerly line (stations 22-35), a considerable amount of variation at the depth of the Antarctic Intermediate Water (~ 1000-1500 m). This variation seems to have been the result of fine structure (see Fig. 3.6) involving the intrusion of "Red Sea Water". To illustrate this phenomenon, the T/S profiles of the stations were grouped according to the presence or not of Red Sea Water (Fig. 3.7). This seems to indicate that Red Sea Water was mainly present on the northerly line between stations 25 and 30, although the area cannot be sharply delineated.

To make an evaluation of the intensity of vortices that will be discussed in this and subsequent chapters, in terms of the elevation of isotherms from their "unperturbed" levels, we have obtained the average depth of some isotherms. For this, we used all the stations of the *Meiring Naudé* cruise in March 1981, and all except station 30-35 of the cruises in October 1981.

TABLE 3.1 : Average depth of isotherms in the Mozambique Basin (n=73)

Temperature	15°	10°	5°
Depth (m)	325	741	1159
Standard deviation (m)	42	42	61

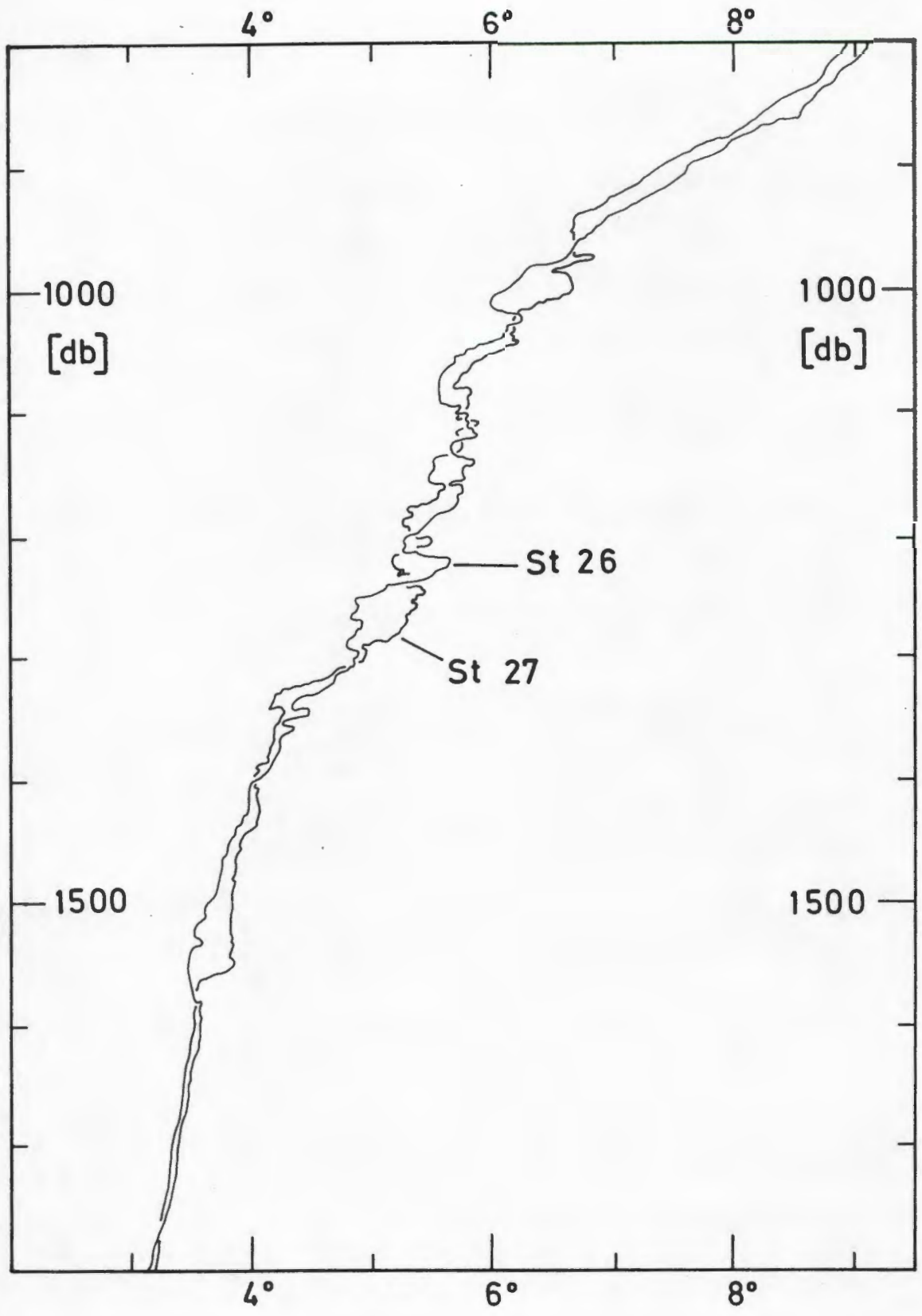

FIG. 3.6 : Vertical profiles of temperature from two stations of the *Meiring Naudé* cruise in October, 1981, to illustrate the fine structure at the depth of the Antarctic Intermediate Water.

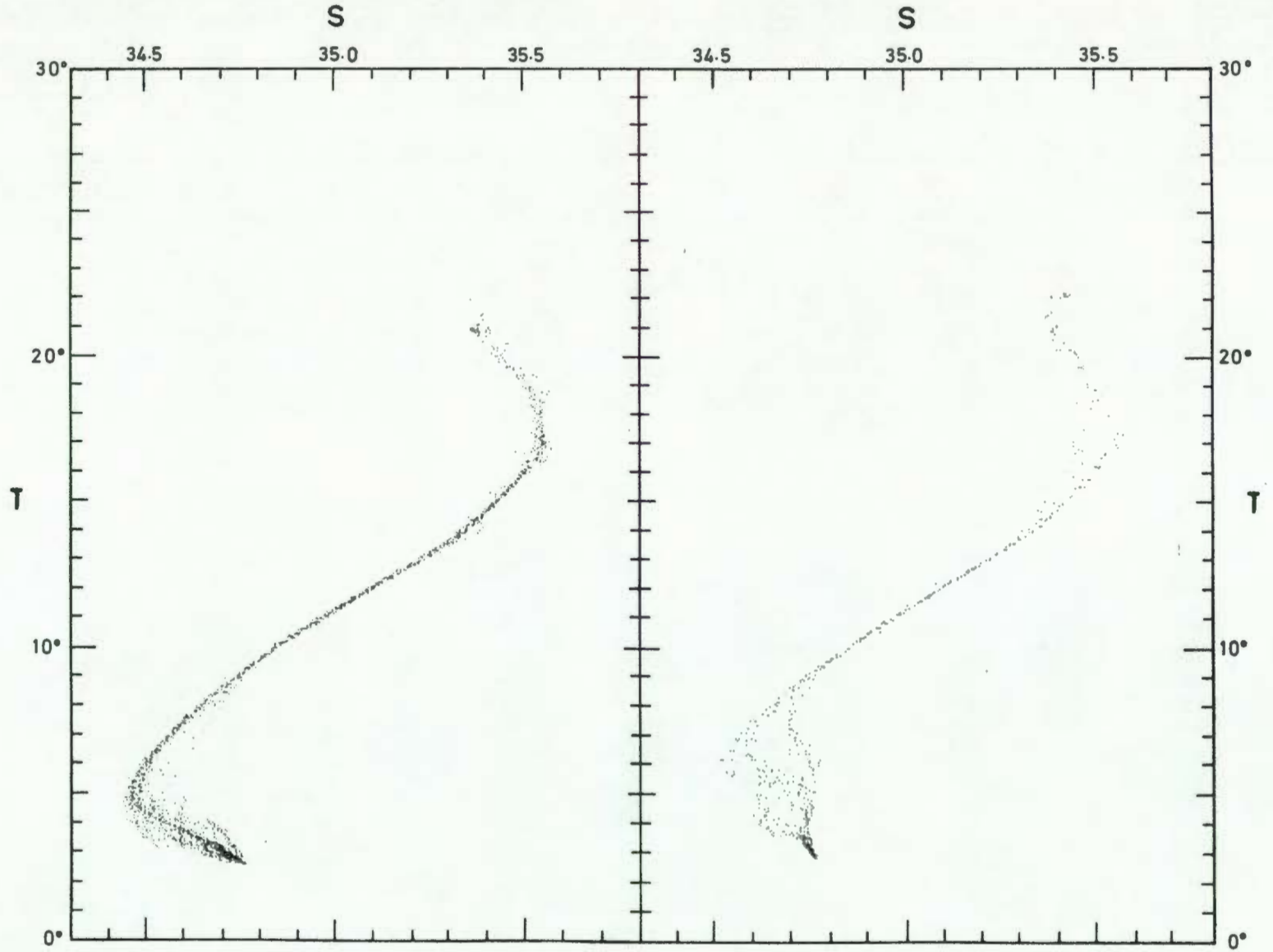

FIG. 3.7 : T/S profiles (interpolated at 20 db intervals) from the *Meiring Naudé* cruise in October, 1981. Left: Profiles from stations 4-23. Right: Profiles from stations 25-30. Note the difference between the two graphs in the range 3-8°, indicating the presence of Red Sea Water.

3.4.2 Dynamics and volume transport

In Fig. 3.8(a) the volume transport for this cruise is presented. All transports were calculated relative to the deepest common depth between stations, and this was about 1800-2000 m for most stations, except those in the vicinity of the Mozambique Ridge (Stations 32-35). The volume transports are indicated as flowing either N-S or E-W (because of the stations orientation) which need not necessarily have been the case. In addition, all transports less than 1 x $10^6 m^3 s^{-1}$ have been omitted.

The features that are particularly noteworthy are, first the strong southward flow of 34 x $10^6 m^3 s^{-1}$ over the Mozambique Ridge between stations 35 and 30. Second, the net southward flow on the Ridge at 30°s and between stations 1 and 7 amounted to 21 x $10^6 m^3 s^{-1}$. Third, there is a consistent flow on the southern line between stations 7 and 14, totalling 28 x $10^6 m^3 s^{-1}$.

Compared to these three "major" flows, the transport through the whole of the meridional section amounted to 0.7 units to the east, and the flow between stations 22 and 29 amounted to 3.3 units to the north.

To enable the construction of a flow budget, the geostrophic computations were limited to 1500 m, which, except for stations 22, 32 and 35, was the deepest common depth. The results (Fig. 3.8(b))show that a cyclonic circulation existed around station 34, while an anticyclonic circulation existed around station 7. The magnitude of these transport figures contrast strongly with the transport figures derived by DUNCAN (1970) for the IIOE cruises and it is not sure whether the *Meiring Naudé* cruises are representative of the "background" circulation in this area.

It seems to be evident that the vicinity of the Mozambique Ridge is characterised by a high volume flux. At the same time that these two cruises were executed (1981), this was not an unknown feature, but it was the first time that the Mozambique Ridge area could be contrasted hydrographically to the rest of the Mozambique Basin.

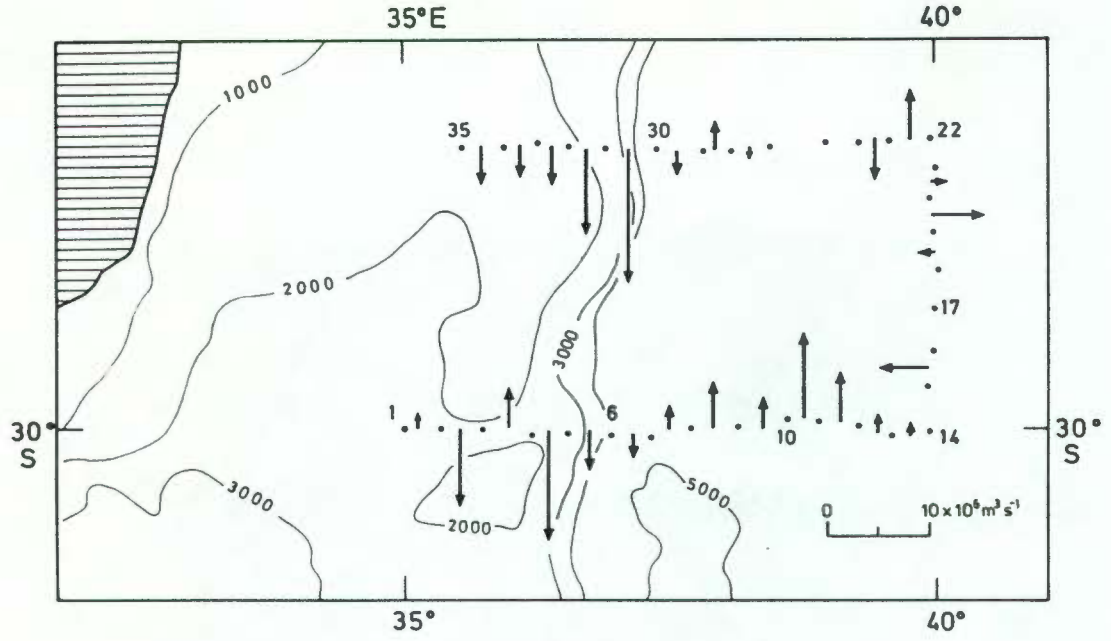

FIG 3.8(a) : Volume transports for the *Meiring Naude* cruise in October, 1981. Values were calculated relative to the deepest common depth between station pairs (1400-2000 m). For further details see Fig. 3.5(a).

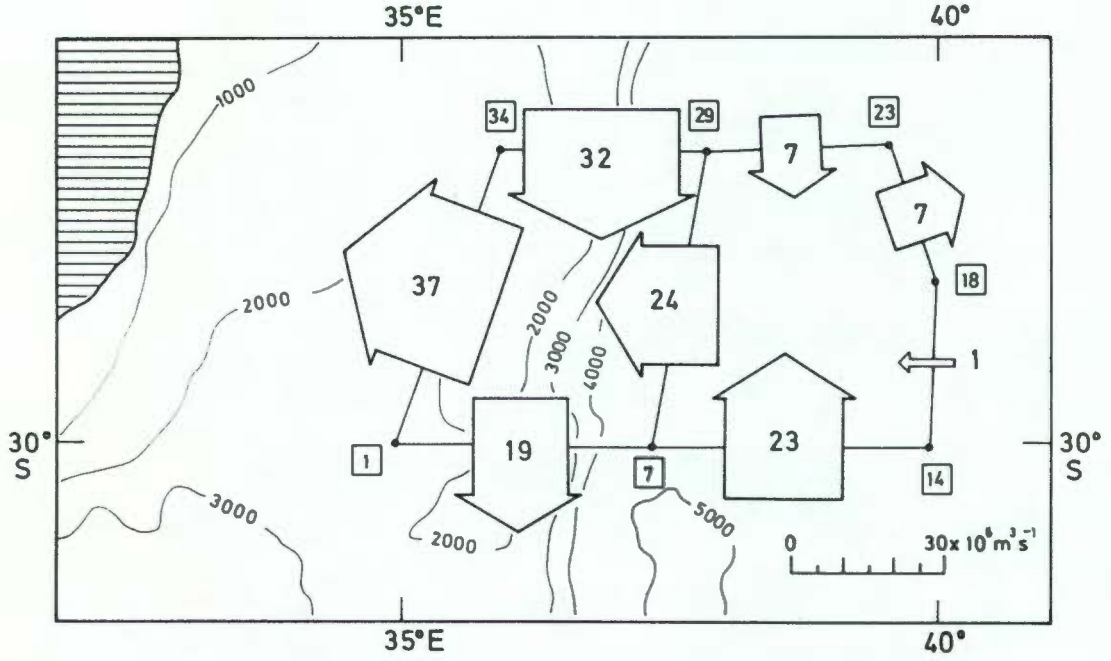

FIG. 3.8(b) : Volume transports relative to 1500 m for the *Meiring Naude* cruise in October, 1981.

3.5 Historic observations of deep-sea eddies in the Southwest Indian Ocean.

The first vortex of considerable size and intensity in the southwestern Indian Ocean was observed in 1962 during a cruise of the S.A.S. *Natal*. The data of this cruise were published by SHIPLEY and ZOUTENDYK (1964), and discussed by HARRIS (1970), HARRIS and VAN FOREEST (1977) and GRüNDLINGH (1983b).

The temperature section for stations 96-103 of this cruise is presented in Fig. 3.9. Close to the coast the upheaval of isotherms in the Agulhas Current can be seen, and centred at station 102, another upheaval of much greater magnitude (viz. the elevation of the 5° and 10°C isotherms). The large station spacing (~ 200 km) tends to enhance the horizontal extent of the upheaval.

The geostrophic profiles of stations 102 and 103 were used to estimate the depth of the "level of no motion" namely 2180 m, (see Fig. 3.9), and the volume flux between station 102 and 103 was then determined at $50 \times 10^6 m^3 s^{-1}$ relative to this depth (no gradient effects were considered). Since station 101 went to only 1432 m, volume transport was not calculated between station 101 and 102. Judging by the magnitude of the volume transport (compared to transports observed during this study) it was estimated that station 102 must have been located very close to the centre of the vortex.

Another, smaller eddy was observed in 1973 during the deployment of a satellite-tracked buoy (STAVROPOULOS and DUNCAN, 1974). As with the previously-described observation of HARRIS (1970), the eddy was cyclonic, but it appeared to be much smaller (~ 50 km diameter). During the first few days after deployment, the buoy was followed by the R.V. *Meiring Naudé* and current velocities of 0.5-1.0 m/s were recorded. The buoy remained in the eddy for two weeks before drifting into the offshore perimeter of the Agulhas Current at 32°S.

3.6 Discussion

A considerable amount of data were collected during the IIOE, and it would be presumptuous to claim that the two cruises forming part of this

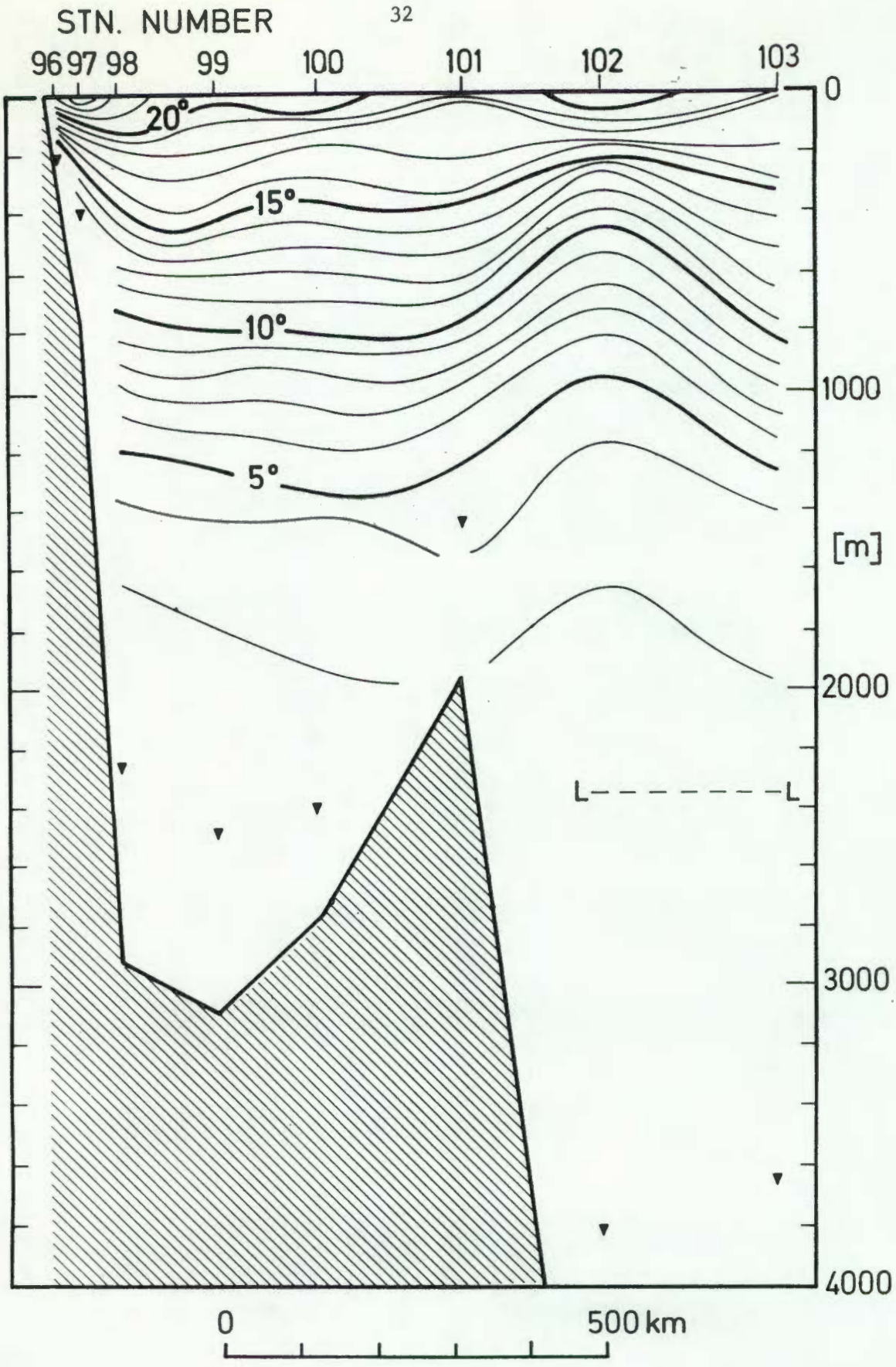

FIG. 3.9 : Vertical section of temperature of stations 96-103 of the S.A.S. *Natal* cruise in July, 1962. L-L indicates the level-of-no-motion derived from the geostrophic profiles.

study and aimed at obtaining information on the "background" circulation present a better impression. However, there is a subtle point that emerges upon close inspection of the IIOE Atlas : The cruise of the SAS *Natal*, the data of which was reported by HARRIS (1970) and discussed above, was an official cruise of the IIOE (WYRTKI, 1971), but the explanatory notes of the Atlas state that only 108 of the 129 stations were used in the preparation of the Atlas. The Atlas itself does not reflect the anomaly portrayed in Fig. 3.9, and it can be concluded that these stations were excluded from the Atlas and from the calculations of DUNCAN (1970). We believe that this could be the first reason for possible discrepancies between our data and that of the IIOE.

A second reason could be situated in the difference in equipment. The IIOE surveys made use of reversing bottles and other discrete sampling devices, while the 1981 surveys used a CTD. This could influence the amount of interpolation to be done during the geostrophic calculations.

Finally, the production of a coherent picture for the Atlas, using data of different cruises in different years in slightly different locations, may have knowingly or unknowingly smoothed any irregularities in the data. We have therefore concluded that the IIOE Atlas represents a several-year, smoothed condition, while the two *Meiring Naudé* cruises represent a much shorter time scale.

An interesting fact emerging from the results of the two *Meiring Naudé* cruises is that the northerly line of each cruise revealed stronger flow than the two southerly lines. That is, on both cruises a large amount of water passed southwards through the northerly lines, and was deflected westwards across the Mozambique Ridge. During the March cruise, this southerly flux through the northern line occurred in the Mozambique Basin, whereas it occurred over the Mozambique Ridge during the October cruise. (cf Figs. 3.5 and 3.8).

On both cruises, little or no zonal flux occurred through the meridional line of stations east of 40°E. On the other hand, strong (zonal) fluxes were recorded over the Mozambique Ridge, and it was unfortunate that a line of stations was not executed here to determine the exact location and structure of this flow.

The variability of flow that emerges when the results of one cruise is compared with the others (including the cruise of the *Robert Giraud*), seems to indicate that the concept of a steady, consistent, background flow in the Mozambique Basin is not established.

PART II : DATA COLLECTION AND ANALYSIS

This section contains details of all the *Meiring Naudé* cruises that form part of this thesis. Each cruise is presented in a fair amount of detail, including items such as the objective of the particular cruise, a short narrative of the progress and duration of the cruise and finally the results. As explained previously, the presentation of the data in this way was essential since the bulk has not been published elsewhere before. As far as the cruise results are concerned, the hydrographic data are not portrayed in the same format for each cruise.

There is no intercomparison between cruises (this is left for Part III) except where a cruise is based directly on the results of previous cruises. Where cruises were designed and executed as a group, they are included in the same chapter, while solitary cruises (e.g. one cruise per year) are discussed in individual chapters.

For purposes of comparison, the vortices located during this study have been identified alphabetically (Alfa, Bravo, etc.).

CHAPTER 4

OBSERVATIONS OF DEEP-SEA VORTICES IN 1975

4.1 Introduction

As described in Chapters 2 and 3, there was no reason up to 1975 to believe that the deep-sea area of the southwestern Indian Ocean contained anything but a slow, steady flow forming the eastern flank of a large recirculatory gyre (DUNCAN, 1970).

It therefore came rather as a surprise when strong anomalies were observed in the depth of the isotherms during a cruise in August 1975 (see section 4.2 below). The features were so anomalous that considerable effort was initially put into checking the data acquisition system for faulty equipment! At the same time, a thorough literature search provided evidence of a previous, similar sighting(recalled in section 3.5), and only after all this effort was it realised that a significant aspect of the circulation in the southwestern Indian Ocean had been lying undiscovered : the existence of large, intense cyclonic vortices. In the following sections of this chapter, the details of this "discovery" are presented. Further results have been given by GRüNDLINGH (1977), and this chapter will partially follow the discussion of that paper.

4.2 Observations in August 1975

The object of this cruise was very remote from the study of vortices. In this year, the CSIR (Council for Scientific and Industrial Research) was engaged in a feasibility study concerning free-drifting buoys tracked by the NIMBUS VI satellite. The cruise from 25 to 31 August 1971 formed part of this study and was intended to deploy a satellite-tracked buoy at 28°S, 40'E. It was hoped that this would put the buoy in the vicinity of the (suspected) westward-flowing East Madagascar Current (EMC). On the way back to Durban, the *Meiring Naudé* executed a series of hydrographic stations between the deployment position and Durban.

4.2.1 Buoy's drift track

After deployment the buoy set off in a NW direction with a speed of 51 cm/s , increasing to 65 cm/s the following day (28 August)

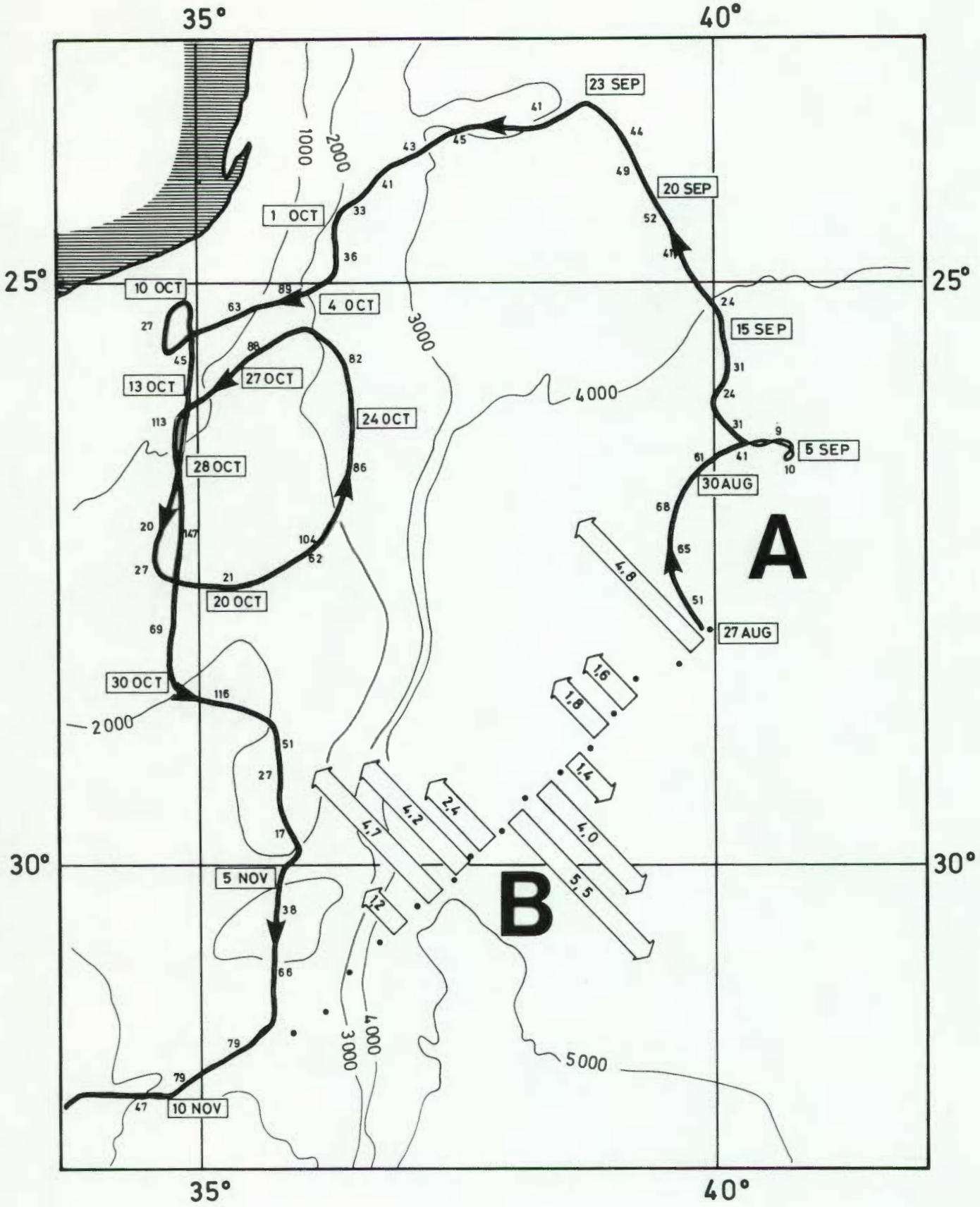

FIG. 4.1 : Course of a satellite-tracked buoy (bold curce) between 27 August and 15 November, 1975, in the southwestern Indian Ocean. Dots indicate stations of the *Meiring Naudé* in August, 1975. A and B designate eddies Alfa and Bravo, respectively. Figures accompanying drift track are drift velocities over 24 hours (cm/s). Geostrophic volume transport relative to 900 m are indicated by arrows (in units of 10^6 $m^3 s^{-1}$)

(Fig. 4.1). During the first week after deployment, the buoy's track described part of a mesoscale cyclonic circulation. Soon thereafter, between 1 and 9 September, the buoy decelerated, reversed its track and accelerated again in a general NW direction, then followed a general NNW course for 15 days.

The buoy proceeded northward until it reached its maximum northward penetration into the Mozambique Channel at 23° 26'S on 23 September, then moved closer to the African coast and eventually southwards, roughly along the Mozambique Ridge. Here, the buoy returned along its track between 25° and 27°30'S around a seemingly oval-shaped track of about 200 km diameter centred at 26°30'S, 35°30'E. The northward movement on the eastern flank of the eddy and the subsequent southward movement were at considerably higher speeds than the initial southward traverse between 13 and 20 October (Fig. 4.1).

Next, the buoy moved eastward at 28°S, drifted meridionally along the peak of the Mozambique Ridge and then swung westward again at 32°S. After this, the buoy left the area which is of concern to us now, drifted southward in the Agulhas Current and was eventually washed ashore at Waenhuiskrans, a little village in the vicinity of Cape Agulhas (see GRÜNDLINGH, 1977).

4.2.2. Hydrographic observations

On the return leg after the deployment, the *Meiring Naudé* executed a series of stations, first to 32°S, 35°E and from there into Durban. The data obtained from this section were intended to assist in the interpretation of the buoy's drift pattern, and 32°S 35°E would have been the deployment position of a second buoy which started malfunctioning during the cruise and was returned to the laboratory. A continuous vertical profile of temperature was measured at each station, while salinity and nutrients were measured at 0, 10, 50, 100, 150, 200, 300, 400, 500, 700 and 900 m. (See Appendix 1 for further details). The vertical section of temperature for the whole traverse is indicated in Fig. 4.2, while Fig. 4.3 contains the sections of salinity and nutrients for stations 1-15 only.

4.2.3 Thermohaline results

The vertical section of temperature (Fig. 4.2)shows the following noteworthy features: First, the deeper isotherms (< 15°) slope downwards between station 1 and 5, then rise abruptly to a peak at station 8 before dropping again to seemingly "undisturbed" levels (cf. Table 3.1). Within 150–200 km from the coast (stations 25-31), the Agulhas Current is visible from the rise of the deeper isotherms.

The most conspicuous anomaly in the temperature section is obviously the thermostat centred at station 8. Above the colder water below 300 m was situated a bowl of warm water depressing the isotherms in the centre of the anomaly. To quantify the anomalous elevation of isotherms, the 10°C isotherm is chosen, and Fig. 4.2 shows that this isotherm rose to about 480 m, which was about 300 m above the ambient depth of 800 m at stations 13-25.

It is interesting to note that the Agulhas Current reflects the same thermal structure as the offshore half of the thermostad in the vicinity of station 8: Between station 6 and 8 the deeper isotherms rise, similar to what occurred between stations 26 and 28. Between station 6 and 8 the shallower isotherms go deeper, again similar to what happened between stations 26 and 28.

Compared to the "ambient" level of the isotherms between stations 18 and 25, the isotherm levels between stations 1 and 5 are also anomalous. There are definite indications that a similar thermal structure existed in this area than at station 8.

The existence of a thermal anomaly centred at station 8 is also reflected in the salinity and nutrient sections between stations 1 and 15 (Fig. 4.3). The rise in the deeper isolines of nitrates and silicates between station 1 and 3 was even stronger than at station 8, indicating that the phenomenon at station 1 was possibly just as intense as the one at station 8.

It is obvious from the thermal structure at station 8 that we are dealing with two opposing flows : a southeastward flow between stations 5 and 8 and a northwestward flow between stations 8 and 12. This feature, and the northwesterly flow in the vicinity of station 1, contrast

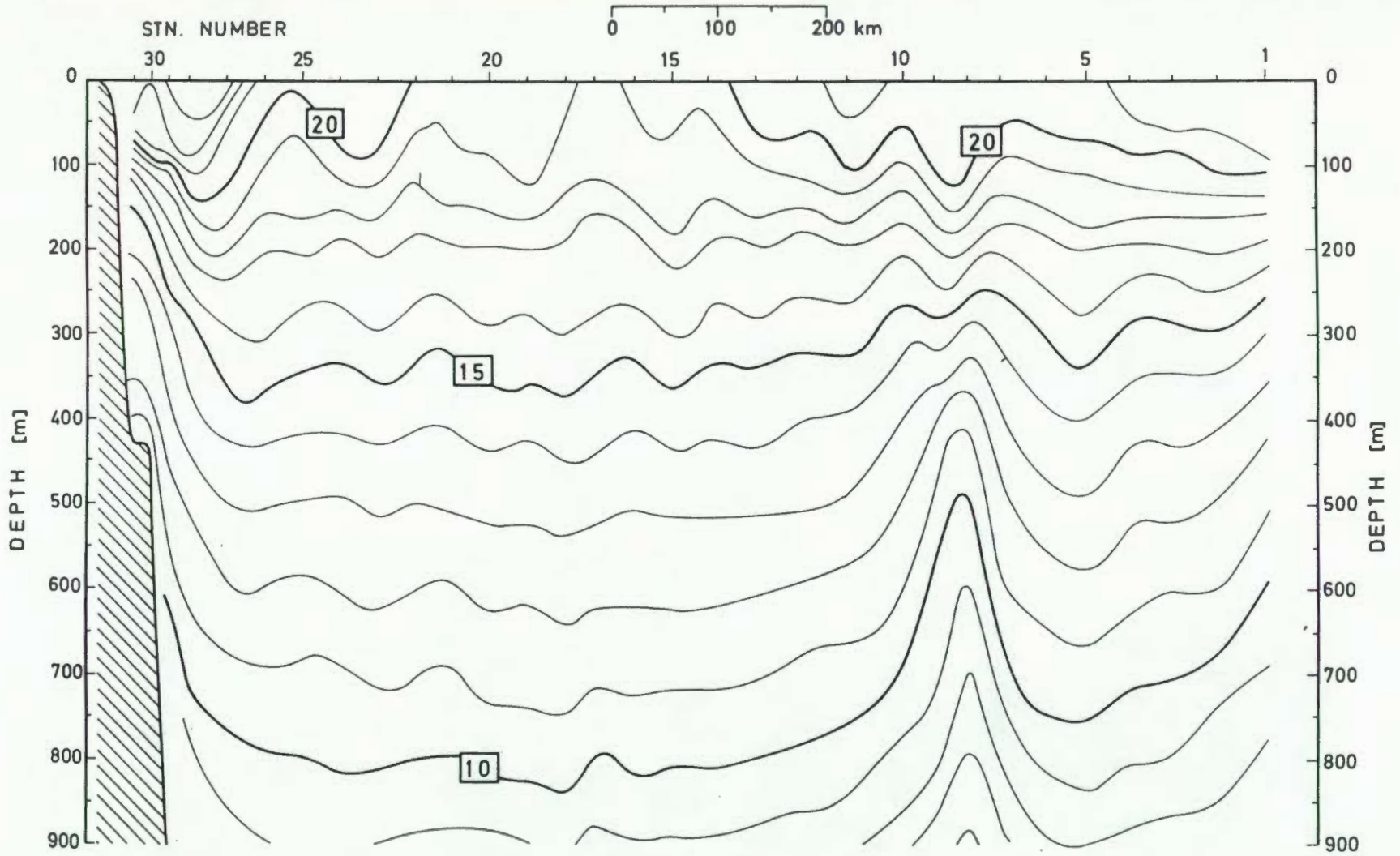

FIG. 4.2 : Temperature section of the *Meiring Naude* cruise in August/September 1975. A satellite-tracked buoy was deployed at station 1, and the isotherms show the presence of eddy Bravo at station 8 and the Agulhas Current close to the coast.

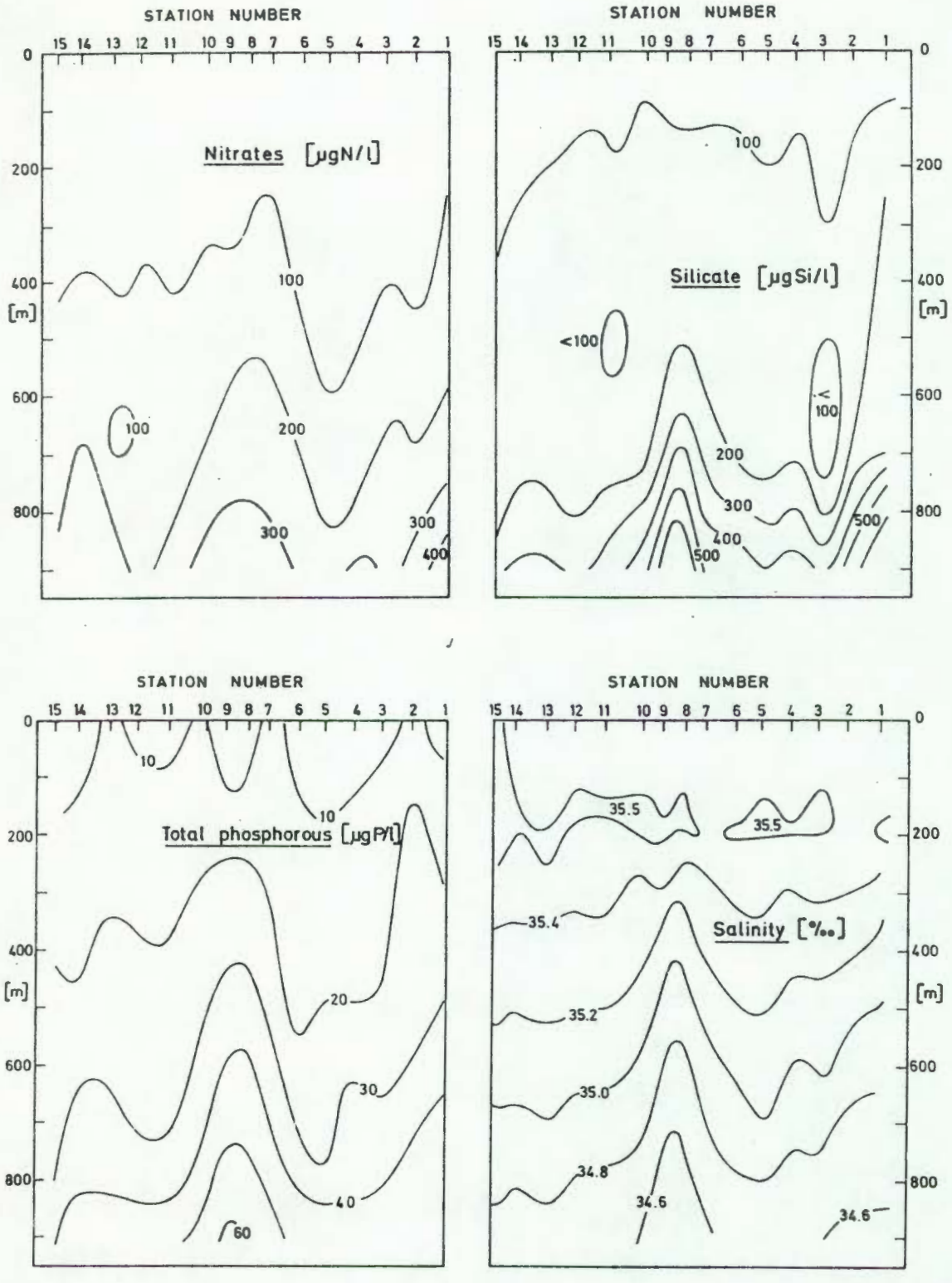

FIG. 4.3 : Vertical section of nitrates, silicate, total phosphorous and salinity obtained during August/September, 1975, showing the upheaval of isopleths in the eddy Bravo centred at station 8.

starkly with the broad, unconfirmed flow portrayed by the IIOE Atlas (WYRTKI, 1971) and the analysis of DUNCAN (1970).

Considering the two features simultaneously, one can come to virtually only one conclusion, and that is that they were eddies. Both circulation patterns have namely the same sense of rotation and approximately the same size (cf. the buoy track NE of station 1). In addition, there is no evidence of a strong, ribbon-like flow in the Mozambique Basin that, by meandering, could simulate the concurrent flow patterns of these features. Moreover, eddies with characteristics similar to the ones reported here have been observed previously. There are namely great similarities with the eddy discussed by HARRIS (1970, see section 3.5), and there are also indications of similar situations in the results presented by VISSER and VAN NIEKERK (1965). The northernmost eddy has been called Alfa, the other Bravo (see Fig. 4.1).

4.2.4 Dynamic results

Geostrophic velocities calculated relative to 900 m were below 10 cm/s everywhere except in the Agulhas Current, eddy Alfa and eddy Bravo. The velocity distribution in Alfa and Bravo (Fig. 4.4) showed that the peak velocity was not attained at the surface, but at about 300 m depth. This is reflected in the temperature section by the downward dip of the isotherms over the centre of the eddy, which reversed the geostrophic shear in the upper few hundred meters. Since it is not sure whether the hydrographic transect crossed the centre of the eddy, the calculated velocities are possibly underestimates of the true velocity. The limitation of the reference level would tend to reduce the calculated velocities even further.

The volume transport (relative to 900 m) totalled 12.5 x $10^6 m^3/s$ through the southwesterly sector of Bravo and 10.9 x $10^6 m^3/s$ through the northeastern sector (Fig. 4.1). The southwestern sector of Alfa reflected the same pattern of volume transport as Bravo, confirming the similarity between the two eddies. The stronger flux toward the northwest in Bravo resulted in a much higher kinetic energy here (see Fig. 4.5) than on the other side (the calculation procedures of these parameters are described in Appendix 4).

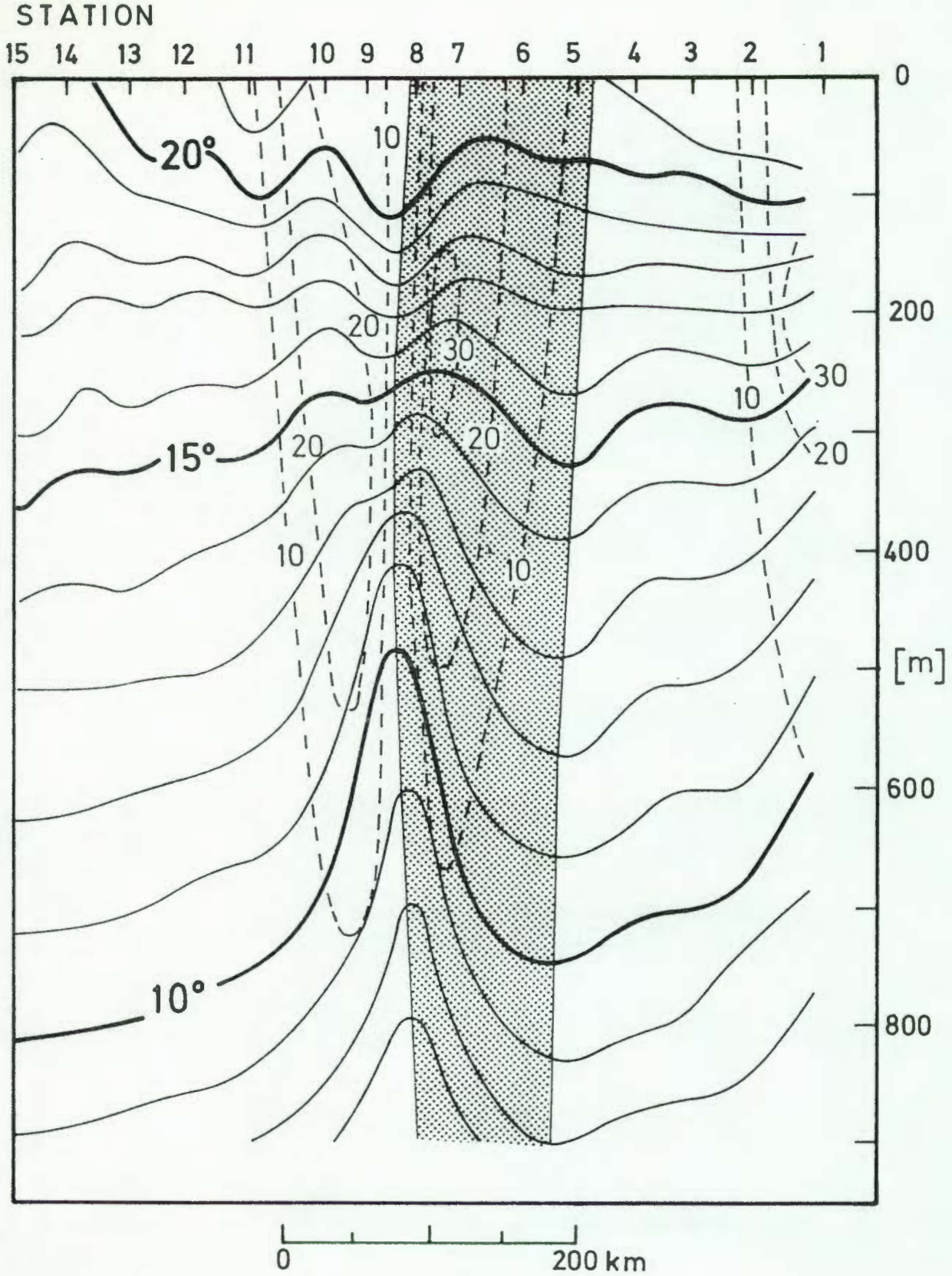

FIG. 4.4 : Gradient velocity in cm/s superimposed on the temperature structure of station 1-15 in August/September, 1975. Shaded area indicates flow out of the page. Velocity calculations were relative to 900 m.

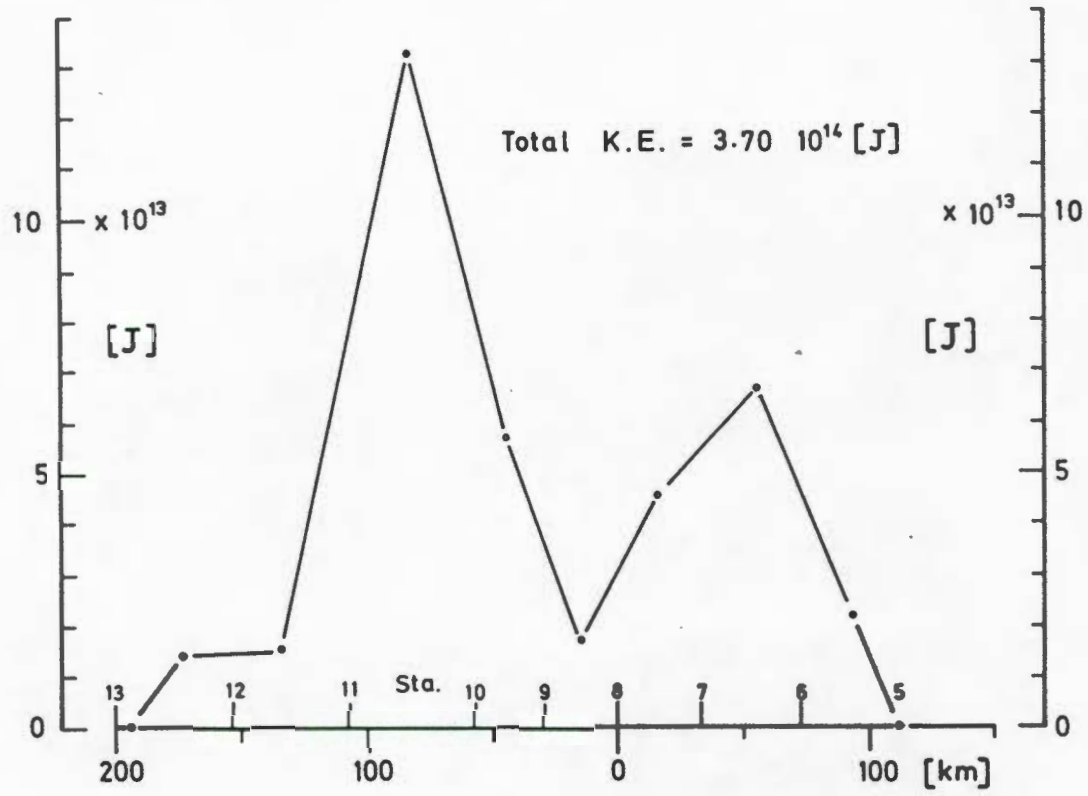

FIG. 4.5 : Kinetic energy across the eddy in August, 1975.

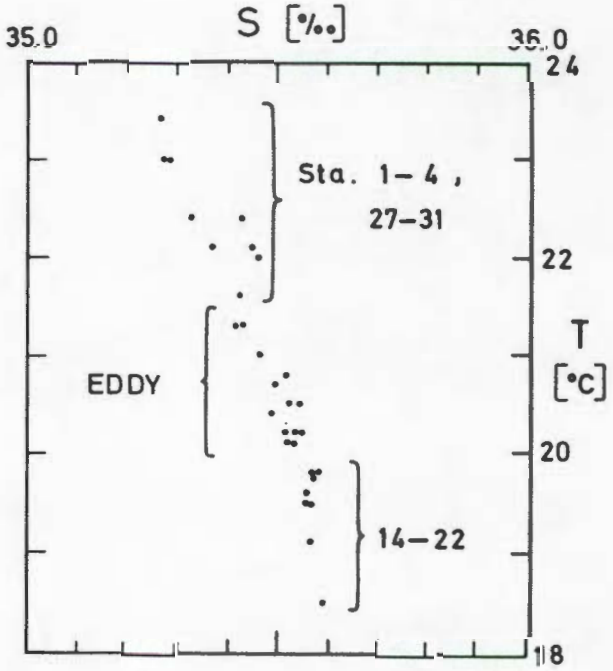

FIG. 4.6 : Surface T/S diagram of the cruise in August, 1975.

4.3 Discussion

Having identified the circulation patterns and thermohaline anomalies as eddies, it is important to devote some attention first to the relevance of the eddies to the circulation in the southwest Indian Ocean and second to their possible origin.

4.3.1 Relevance

In his seasonal charts of the dynamic topography of the SW Indian Ocean, DUNCAN (1970) invariably indicated an anticyclonic gyre (which he called the "Agulhas Eddy") off the southeast coast of South Africa. He showed, however, that considerable variations can occur, superimposed on the large scale circulation. HARRIS (1972) also admitted that time variations of a period of less than 4 weeks took place during his survey. Historic measurements therefore seem to be inadequate to resolve the time fluctuations in the large-scale circulation, mainly due to the non-synoptic nature of the data.

Now, for virtually the first time, evidence has been found of the existence of mesoscale eddies in an area that has been considered void of any mesoscale activity. In addition, the cyclonic sense of rotation presents a contradiction to the opinions of DUNCAN (1970), HARRIS (1972) and others who regarded the circulation off the South African east coast as consisting of various sizes of *anticyclonic* eddies.

The difference of opinion concerning the possible circulation can be resolved by concluding that the current system bordering the Agulhas Current on the seaward side is probably very variable. STAVROPOULOS and DUNCAN (1974) could explain some of their results in terms of a moving anticyclonic eddy, with a diameter of 80 km. According to HAMON (1970) the East Australian Current *consists* of a succession of anticyclonic eddies moving southwards, rather than a continuous boundary current.

The eddies observed in August 1975 represent isolated quanta of energy that were generated by some mechanism and will eventually either decay by themselves or interact with other elements of the circulation in the region. An eddy such as Bravo advecting eastwards and coalescing with the Agulhas Current could impart a considerable amount of water and cyclonic

vorticity into the Agulhas Current, and this could have an important effect on the behaviour and course of the Current.

The significance of the eddies lay, however, to a large extent in their tantalising novelty. For many years of oceanographic surveying they had remained undetected. Now, during a single cruise, two eddies were fortuitously discovered. If two could be discovered during a solitary survey, the southwestern Indian Ocean may be teeming with eddies - or so we thought. By and large, the academic questions raised by this rather fortunate observation were so interesting that a cruise was immediately planned to survey the area again a year later.

4.3.2 Origin

In the discussion of the possible origin of the eddies described above we are drawn toward either of two approaches. Either we can follow the arguments that were thrown around at the time of the eddies' discovery, or we can replace those ideas with the ones that have developed through the surveys of later years. In retrospect, many of the considerations based on the first survey in August 1975 seem clumsy and immature, and it would be easy, even inviting, to replace these deliberations with the knowledge of the eddies and their creation that we have today.

If we chose the latter course, many of the subsequent surveying approaches would however be difficult to explain. It was therefore decided to follow more-or-less the thoughts as given in GRüNDLINGH (1977), and, where necessary, indicate the clues to the riddle of the eddies' origin that were not identified at the time.

At the time (1975/76), a satellite-tracked buoy had been drifting in the Agulhas Return Current along 40° (GRüNDLINGH, 1978). The course of this Current revealed some very intense *cyclonic* eddies in the vicinity of the Agulhas Plateau and at the southern tip of the Mozambique Ridge. These eddies were more-or-less the same size as Alfa and Bravo, and one of them seemed to be occluded. The possibility therefore existed that Alfa and Bravo was one of these eddies that had become entrained by the large, anticyclonic gyre (Agulhas Eddy : DUNCAN, 1970) recirculating water in the southwestern Indian Ocean (see section 2.4.3), and, in the

process, had advected northwards to 30°S. A similar process has been observed in the case of the cyclonic Gulf Stream rings (see e.g. RICHARDSON, 1980; WATTS and OLSON, 1978) that advect toward the upstream regions of the Gulf Stream.

In contrast to this possibility of an eddy spawning in 40°S and drifting to 30°S, a closer inspection of the thermohaline characteristics of the eddy yielded a different picture. An analysis of the surface T/S relation (Fig. 4.6) along the whole section (station 1-31) shows that those stations which seem to have been in or close to the eddy belonged to a water mass in between the more tropical and the more subtropical water (see section 2.3 for details of water mass definition). It is noteworthy that stations 1-4 revealed the same characteristics as stations 27-31 which were inside the Agulhas Current, while Bravo contained water normally characteristic of the offshore flank of the Agulhas Current (DARBYSHIRE, 1966). This seemed to suggest that Bravo was different from Alfa, and that Bravo did not have a direct relation with the Agulhas Current itself.

What about Alfa? A comparison of the hydrographic results (see Fig. 4.2) of the *Meiring Naudé* at the start of the transect (stations 1 to 4) with those of LUTJEHARMS (1971) from a cruise of the *Atlantis II*, it initially seemed that the northern-most part of the *Meiring Naudé* section penetrated the East Madagascar Current (EMC). If this were the case, the satellite buoy would have continued drifting in a northwesterly direction. Instead, it moved in the semi-circular fashion described in section 4.2.1.

After the buoy was expelled from Alfa on the 2nd September it started moving toward the NNE with an average speed of 15-25 cm s^{-1}. Its subsequent behaviour to the north and west (see section 4.2.1) led to the conclusion that it was drifting inside the EMC. The drift speed between 9 and 23 September agreed well with the current velocity observed by other authors (MARTIN *et al*, 1965; LUTJEHARMS, 1976, accepting what they observed *was* the EMC).

It was therefore concluded that Alfa was either embedded inside the EMC, or adjacent to it to allow the buoy to enter the EMC directly.

It was not realised at the time (1975) that the course of the satellite buoy as it drifted southward along the Mozambique Ridge could provide the key to the whole riddle concerning the existence of Alfa and Bravo. In 1975 our knowledge about the circulation was insufficient to be able to connect the eddies with the buoy track. It was only in December 1979, more than four years later, that other buoys, launched during the First Global Garp Experiment (FGGE) revealed more-or-less the same drift pattern and thereby provided an important clue to the origin of the eddies.

4.4 Conclusion

With a reasonable amount of certainty, two eddies were positively identified in the buoy drift track and hydrographic stations' data in 1975. Although the encounter was completely fortuitous, it was possible to estimate the surface velocities, volume transport and some T/S characteristics of the eddies. The origin of the eddies remained a matter of conjecture, so do aspects such as lifetime and eventual fate.

CHAPTER 5

OBSERVATIONS OF DEEP-SEA VORTICES : 1976

5.1 Introduction

The cruise in June 1976 was the first cruise in the southwestern Indian Ocean specifically aimed at locating and surveying a vortex of the kind that had been described in Chapter 4.

The problem of locating an eddy might sound quite trivial initially, but in fact represented the biggest challenge of the data collection aspect of the study. This becomes evident when considering, first, that the R.V. *Meiring Naudé* has a duration of about 12 days in terms of water, fuel and food (not to mention the limited endurance of the scientists!). After subtracting about three days for transit time between Durban and the target area, approximately 9 days are left for hydrographic stations. If the weather remains favourable and the equipment operable throughout a cruise, a maximum of 40-50 stations are possible. Second, to positively identify an eddy, a hydrographic station must be located within that area of the eddy where the depth of the 10°C isotherm surface is less than 650 m. This was expected to occur within a radius of 50 km from the eddy centre, and thus represented a "target" of about 8×10^3 km^2. Third, it was assumed that the eddy could be free-drifting, which meant that it could be anywhere in the Mozambique Basin region. The latter is crudely estimated to have an area of about 8×10^3 km^2. Statistically, the chance of locating such an eddy using one station only is therefore almost negligible. To *locate* it during a cruise and still have sufficient time available to *survey* it seemed even more remote, although 40-50 stations improved the chances. Hydrographic stations were executed along a more-or-less constant heading and the isotherm progress monitored continuously.

The cruise in June 1976 (this Chapter) and March 1977 (Chapter 6) were the only cruises to start with stations in the south and proceed northwards. The reason for this was that it was considered a strong possibility that the vortices were generated in the region of the Subtropical Front at 40°S and drift northwards inside the recirculatory gyre (DUNCAN, 1970). By starting in the south it was hoped that eddies

may be encountered in an area where their characteristics would be more pronounced, thus making location easier.

The station interval on most of the cruises would be 20 nautical miles (about 37 km). This interval fitted in with operational requirements of the equipment (see section A1.3(f)), while providing sufficient resolution of the hydrographic data.

5.2 Narrative of the June 1976 cruise

The *Meiring Naudé* left port on 21 June and proceeded to a position about 34°S, 36°E (see Fig. 5.1). At the start of the survey (station 1), a slight anomaly in the depth of the isotherms (not shown here) caused the course to be revised. The existence of an eddy could not be confirmed, even though station 1 was almost completely circumnavigated. At the end of station 18 it became obvious that it had been a false alarm.

The vessel's course was altered in a general northeasterly direction, and hydrographic stations were initially spaced further apart before returning to the 20 n.m. interval. During the execution of station 25 the hydraulic system of the hydrographic crane on board the *Meiring Naudé* became inoperable. Subsequent handling of the equipment became so difficult under adverse weather conditions that the rosette sampler was removed and the collection of subsurface water samples on the remaining stations forfeited.

The course (chosen more or less arbitrarily after station 18) eventually carried the vessel across an eddy (Charlie) in the vicinity of 30°30'S, 39°E (see Fig. 5.1). After the initial traverse across Charlie, it was estimated from the results that station 25 had been located close to the centre of the vortex, and a second traverse, almost at right angles to the first, was executed in a northwesterly direction. Stations were spaced close together in the centre of the eddy. The hydrosonde failed during the completion of station 41 and the survey was abandoned. The *Meiring Naudé* returned to Durban on 30 June.

5.3 Hydrographic results of eddy Charlie

Eddy Charlie had very similar characteristics and was positioned

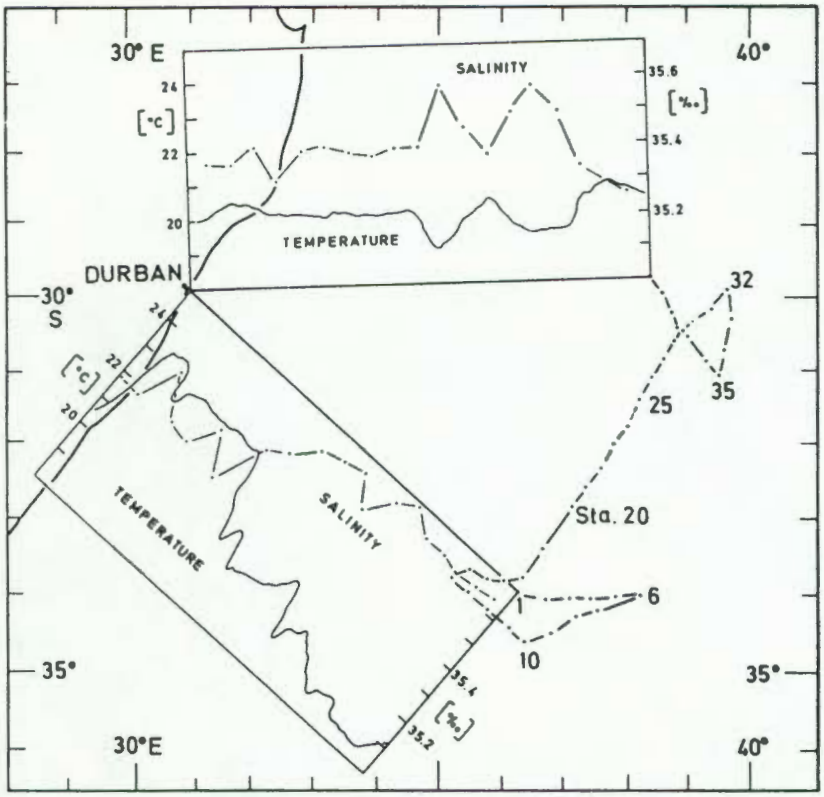

FIG. 5.1 : Track chart of the cruise in June, 1976, with the variation of sea surface temperature and salinity on the outward (southeasterly) and homeward (westerly) traverses.

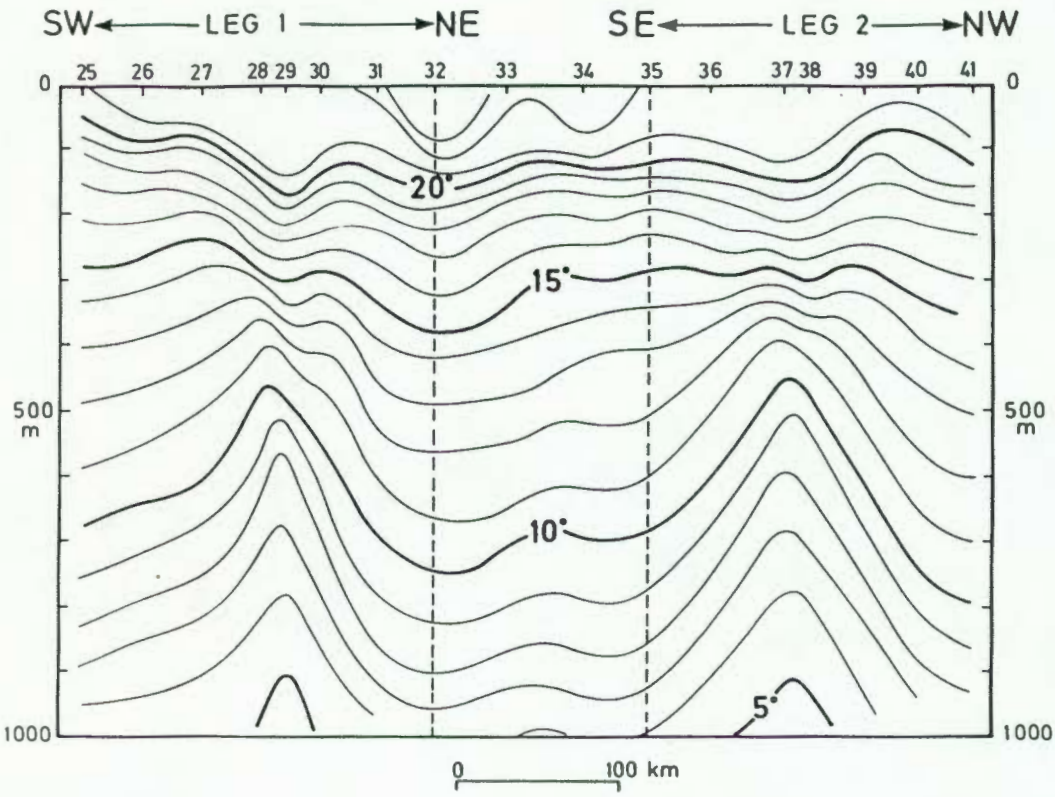

FIG. 5.2 : Vertical section of temperature along the SW-NE traverse (Leg 1) and the SE-NW traverse (Leg 2) of the cruise in June, 1976.

very closely to eddy Bravo (August 1975).

a) Temperature structure (Fig. 5.2).

The thermal structure is characterised by the strong upheaval of isotherms below about 300 m, i.e. the water colder than about 15°C. The maximum vertical displacement was 320 m of the 8°C isotherm and occurred between stations 29 and 32. Similar to Bravo, the temperature field was again characterised by the reversal of the domed structure in the upper 300 m, caused by the presence of warm water at the surface.

The peaked structure of the colder isotherm presented unambiguous and conclusive evidence that the thermostads seen here (Fig. 5.2) and before (e.g. Bravo, Fig. 4.2) were more-or-less circular. This was also the first time that a cruise had been organised in the southwestern Indian Ocean to locate an eddy, and executed successfully.

The shape and size of the eddy can be derived from the topography of the 10°C isotherm (Fig. 5.3). Using the 10°C/650 m interaction as a guide, Charlie was slightly oval-shaped with axes lengths 130 and 150 km.

b) Mixed layer

The variation of the depth of the mixed layer along the SW-NE traverse across Charlie is shown in Fig. 5.4. Outside the eddy (stations up to number 22), the mixed layer was typically 100-125 m thick. At the edge of the eddy, the layer shoaled to a minimum of 45 m at station 26, then deepened over the centre of the eddy to about 100 m at stations 28 and 29, and finally shoaled again on the northeastern side of the eddy to 20 m at station 31. A similar variation was evident for the SE-NW section from stations 35 to 41 (not shown here): the mixed layer deepened from 70 m at station 35 to 90 m at 37 and virtually disappeared again at station 40 (20 m deep).

c) Surface temperature and salinity

The profile of sea temperature and salinity in a NE-SW direction across the eddy yielded the following results:

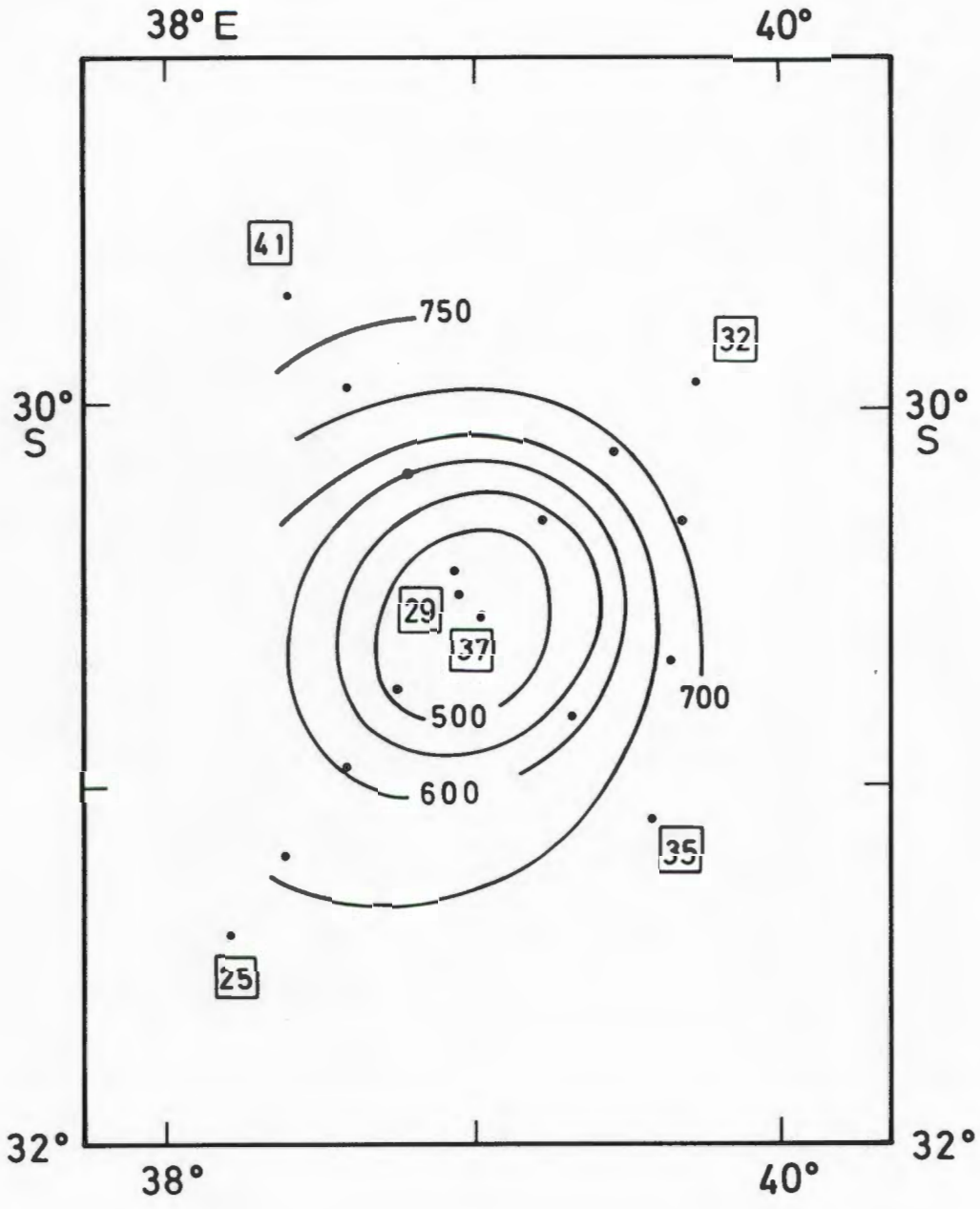

FIG. 5.3 : Topography of the 10°C isotherm (in m below sea level) for the cruise in June, 1976.

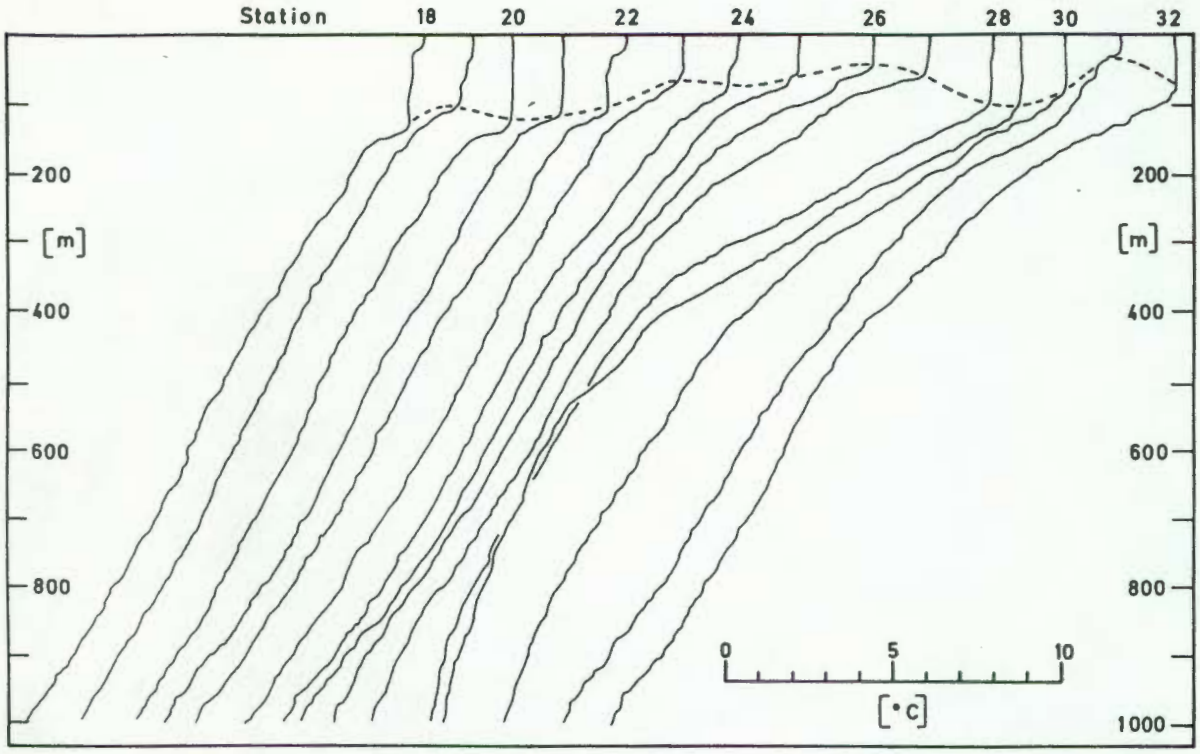

FIG. 5.4 : Profiles of temperature in the vicinity of eddy Charlie, illustrating the variation in depth of the mixed layer.

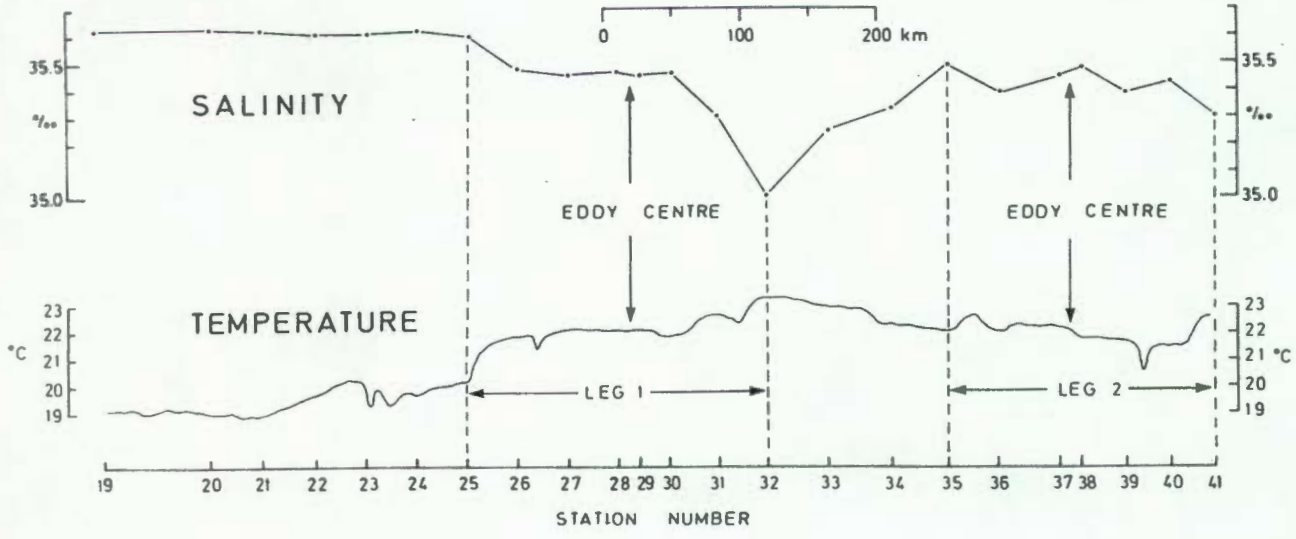

FIG. 5.5 : Surface profiles of temperature and salinity through eddy Charlie.

i) To the south of the eddy (i.e. south of station 25), the salinity varied only very slightly between 35.50 and 35.63 °/oo (Fig. 5.5), indicating the sub-tropical origin (salinity 35.5 °/oo : DUNCAN, 1970) of this water mass.

ii) On its southern edge the eddy was delineated quite clearly by a 2°C temperature front and 0.13 °/oo salinity front (Fig. 5.5). To the north the eddy appeared to be fringing on a water mass of tropical origin (salinity ~ 35 °/oo).

iii) An investigation of the T/S characteristics at the surface (Fig. 5.6) shows that the eddy seemed to have entrained very little of the subtropical water adjacent to the south, but more of the tropical surface water (temperature ~ 23°C, salinity ~ 35 °/oo), and was by-and-large composed of what DARBYSHIRE (1966) referred to as "boundary water". Referring to DARBYSHIRE's distribution chart, the tentative conclusion was reached that the vortex was alien in its environment and had originated to the west and northwest of where it was encountered.

d) Dynamics

Since no subsurface water samples were obtained inside and in the vicinity of the eddy, subsurface salinities were inferred from a T/S graph of stations occupied during the August 1975 cruise, in conjunction with the temperature profiles observed during the present cruise. This method has been used successfully elsewhere (EMERY, 1975) due to the weak dependence of density on salinity (provided that the T/S graph has a "tight" fit).

The gradient velocities calculated in this way indicated an intense flow through the northerly part of the eddy (between stations 40 and 41) and a weaker flow through the southern sections (Fig. 5.7). This asymmetry in the velocity distribution was also reflected in the kinetic energy (Fig. 5.8) and the volume transport relative to 1000 m (Fig. 5.9). A general easterly flow was maintained through the vortex, and a maximum transport of 22 x $10^6 m^3 s^{-1}$ was derived. Of this maximum, only about 50%

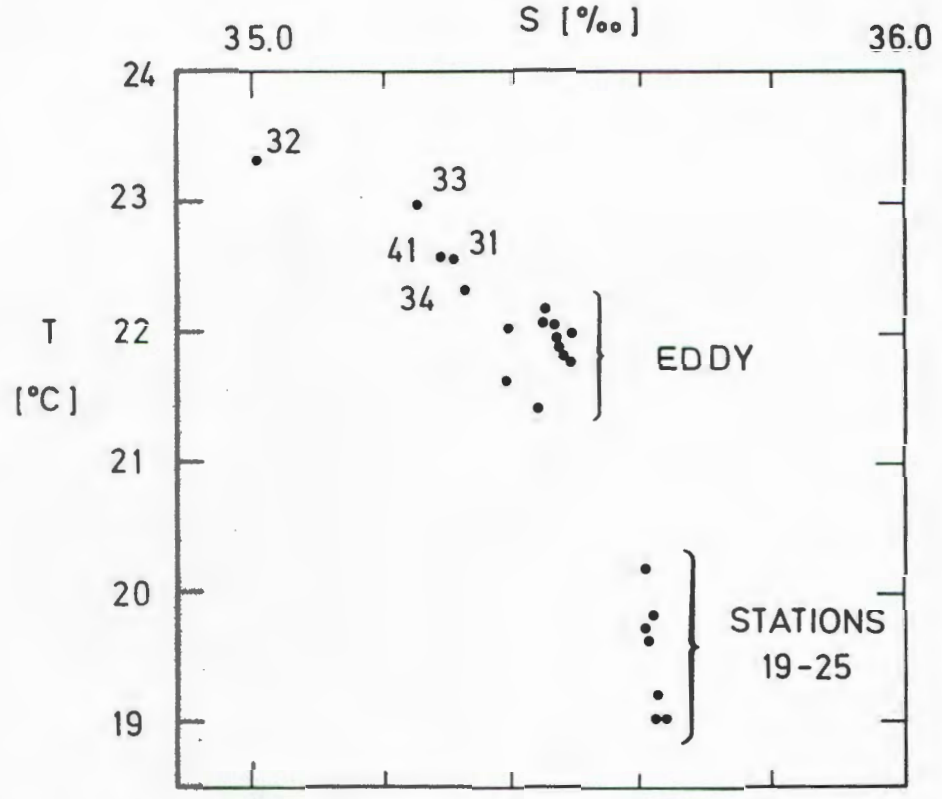

FIG. 5.6 : T/S distribution of surface values from some of the stations of the cruise to survey eddy Charlie.

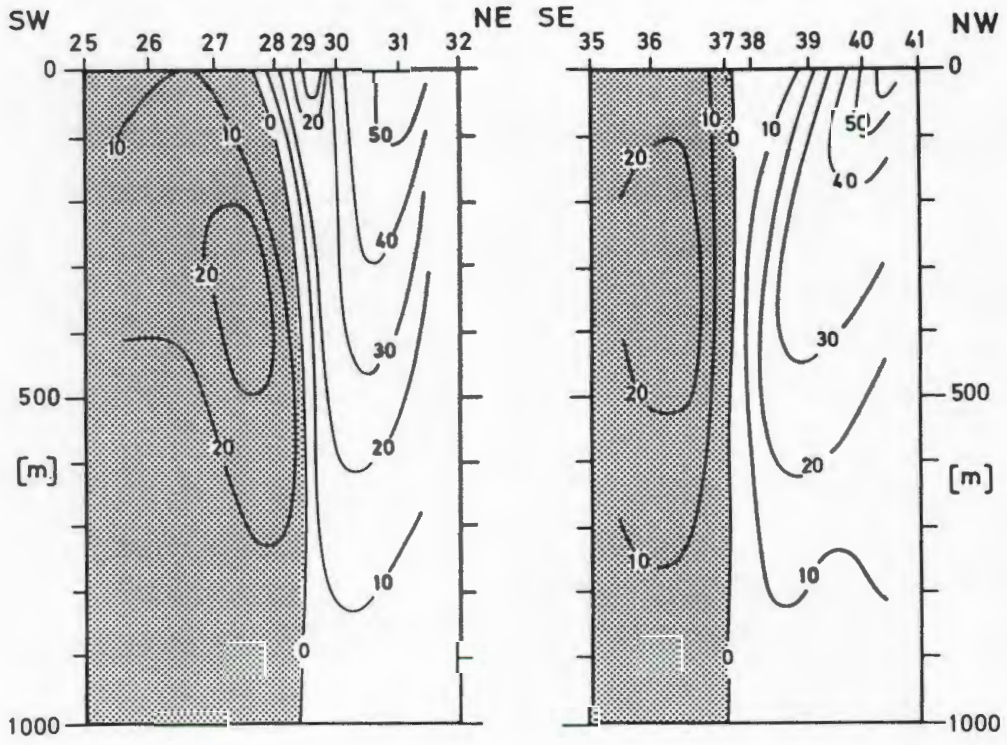

FIG. 5.7 : Gradient velocities in the vicinity of eddy Charlie.

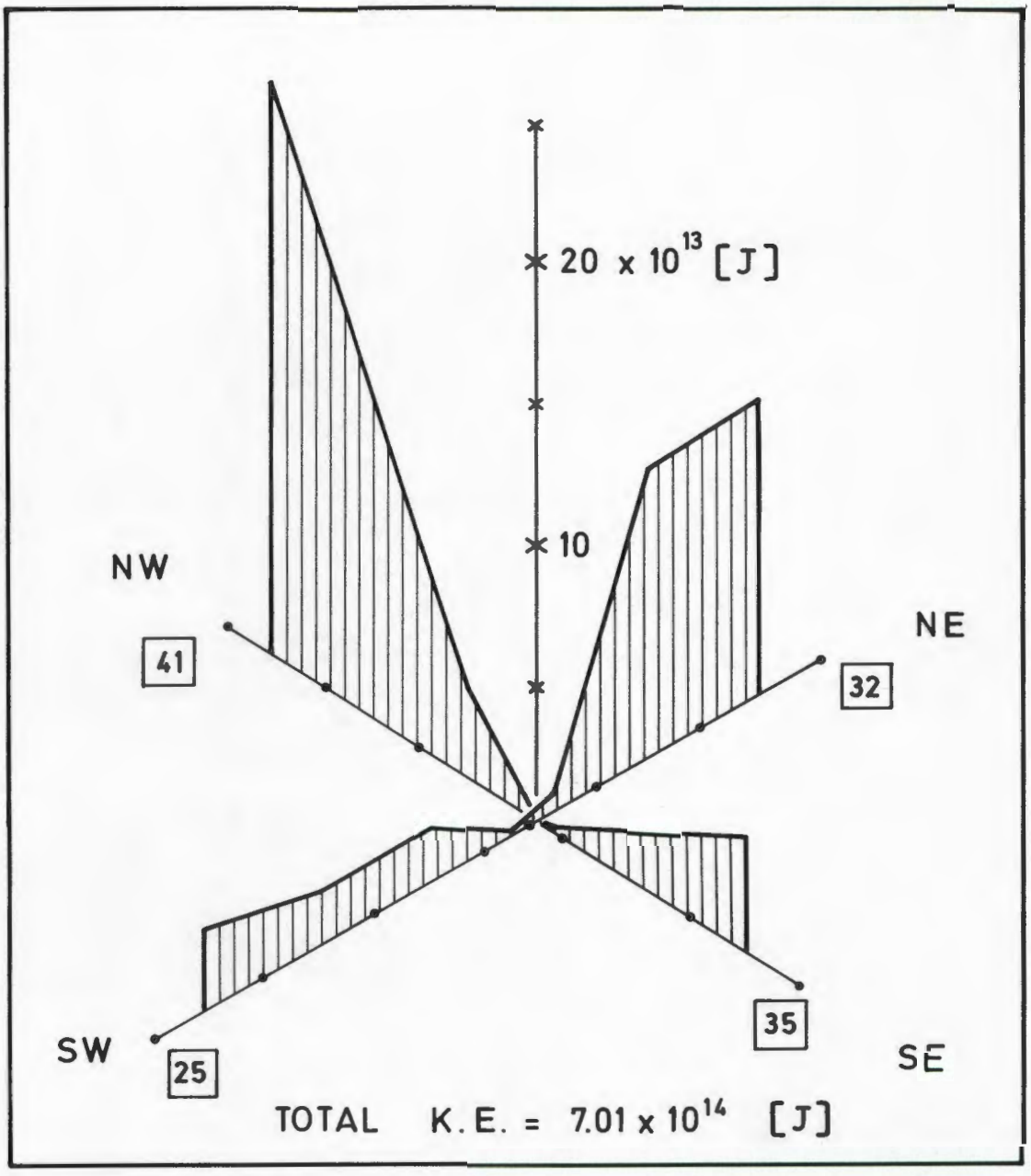

FIG. 5.8 : Kinetic energy of eddy Charlie.

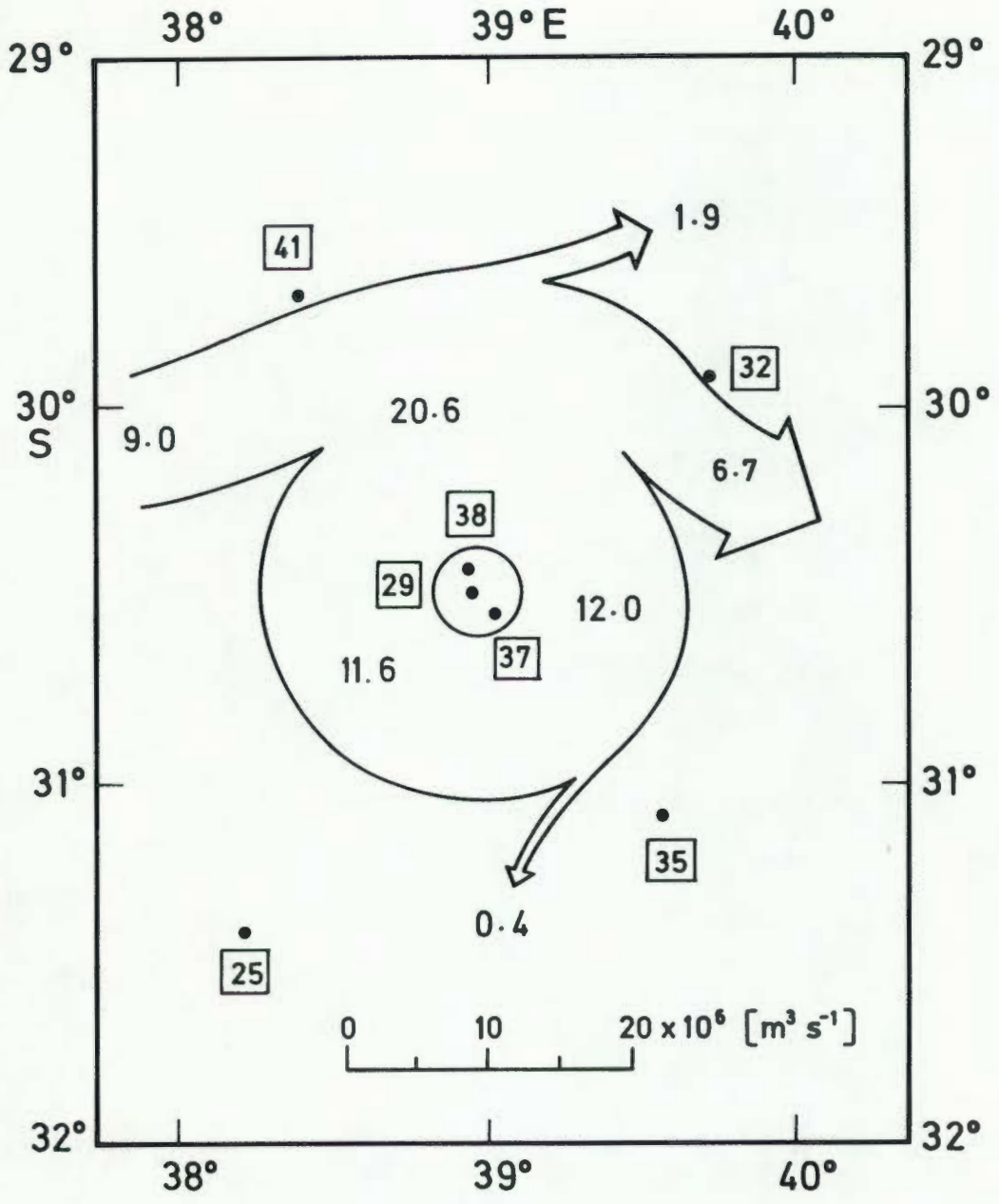

FIG. 5.9 : Volume transport (in units of 10^6 m^3 s^{-1}) of eddy Charlie.

originated from water moving around the eddy, while the rest was made up of water joining and leaving the eddy before completing a full revolution. These sections convey the impression that the flow extended beyond station 41 on the northwesterly traverse and beyond station 32 on the northeasterly traverse.

5.4 Discussion

Apart from the discovery itself, the characteristics of Charlie represented some of the main results of this expedition. The volume transport and associated variables indicated that Charlie was not free-drifting but that it was interacting with the environment.

In addition, although Charlie was separated from its environment by significant fronts in the surface thermohaline structure, the T/S analysis indicated that Charlie was associated with the water to the north rather than with the water to the south of where it was located.

Both the dynamics and the physical structure of the eddy therefore suggested that Charlie did not originate from the area of the subtropical convergence ($\sim$40°S). This aspect would need confirmation during future cruises.

It was not clear why Charlie was located in almost the same spot where Bravo had been the year before (Chapter 4). Even though there was a similarity between Bravo and Charlie, it was never seriously considered that the two eddies were the same, since there were no indications of the decay that would have been visible. CHENEY and RICHARDSON (1976) found that the decay of a Gulf Stream ring was manifested in the collapse of the cold "dome" at the eddy centre at an average rate of 0.4 m per day. Over a period of one year this would amount to about 140 m, and this subsidence is not reflected by Bravo (Fig. 4.2) and Charlie (Fig. 5.2). It was therefore considered that the collocation was purely fortuitous.

CHAPTER 6

OBSERVATIONS OF DEEP-SEA VORTICES : 1977

6.1 Introduction

In this year, two cruises (March and June) were planned and an eddy was located on one of them (June). Results of the March cruise are also presented and although the expedition was unsuccessful in the sense that no eddy was surveyed, evidence to promote the idea of cyclogenesis in 25°-30°S was found. This evidence was collected fortuituously and was speculative at best, but was confirmed by the results obtained during the June cruise - thus paving the way for an improvement in the efforts to locate the eddies.

6.2 Observations in March 1977

6.2.1 Narrative of the cruise

The *Meiring Naudé* left Durban on 15 June and started on 17 June executing a single transect along 37°30'E between 37°30' and 27°S (Fig. 6.1). This line of stations passed through the area where Bravo had been located (see Fig. 4.1).

The weather was exceptionally adverse during the cruise, with the wind velocity remaining between 8 and 20 m/s from the southeast (gusting up to 28 m/s), and swell heights up to 6 m. On two occasions, namely in the vicinity of stations 7 and 20, the data suggested that the edge of an eddy had possibly been traversed. This was, however, not confirmed by additional data collected in the area. The mental depression caused by the weather conditions, as well as the failure to observe any encouraging signs in the data, eventually caused us to abandon the cruise. Because of these dejecting circumstances, a "golden" opportunity that eventually presented itself was not grasped, even though its importance was recognised at the time. This occurred namely at station 22 (a test station) at 27°46'S, 35°32'E, where the only positive results of the

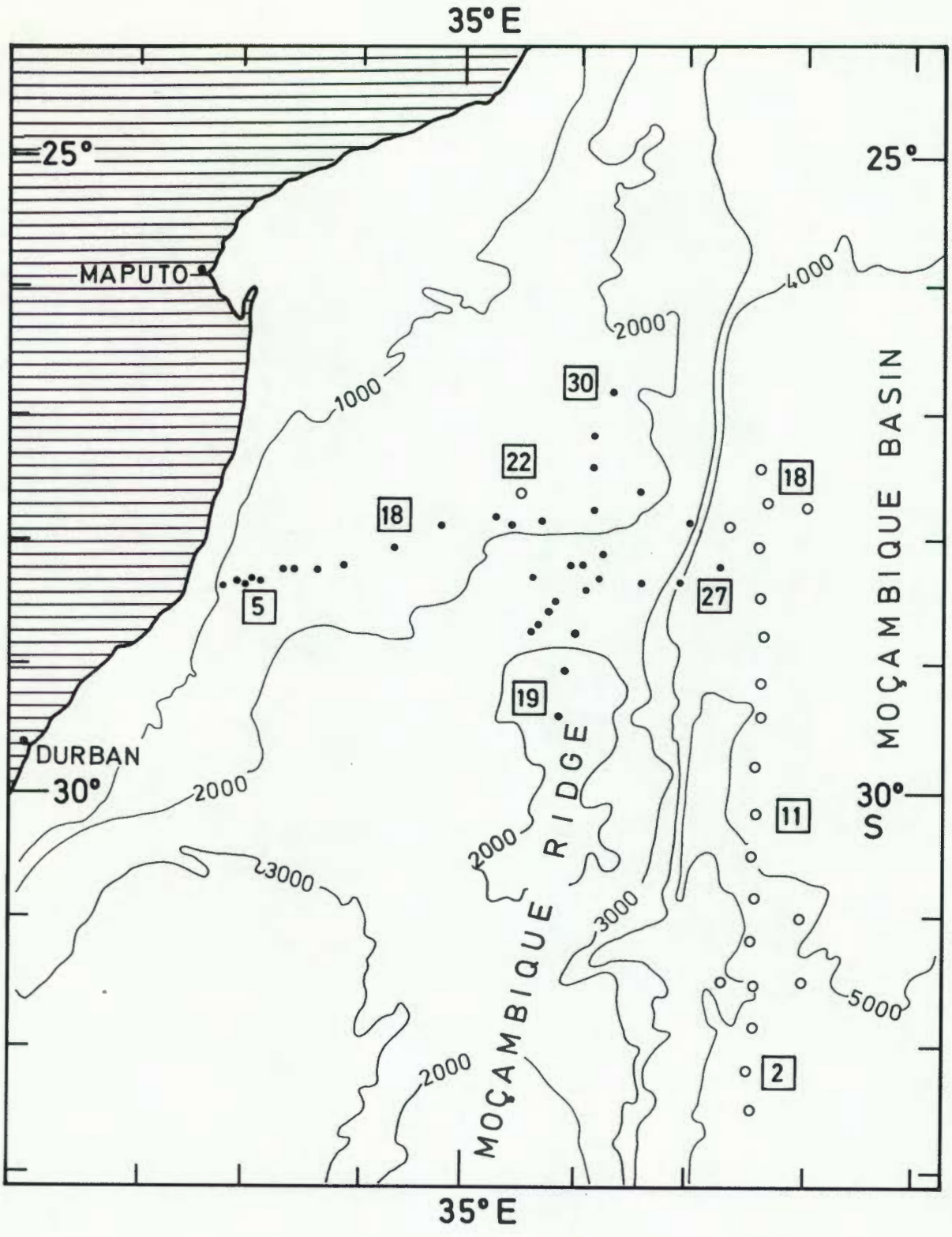

FIG. 6.1 : Bathymetry of the northern Mozambique Ridge with the station positions of the R.V. *Meiring Naude* cruises in March 1977 (stations 1-22, o) and June 1977 (stations 1-35, •).

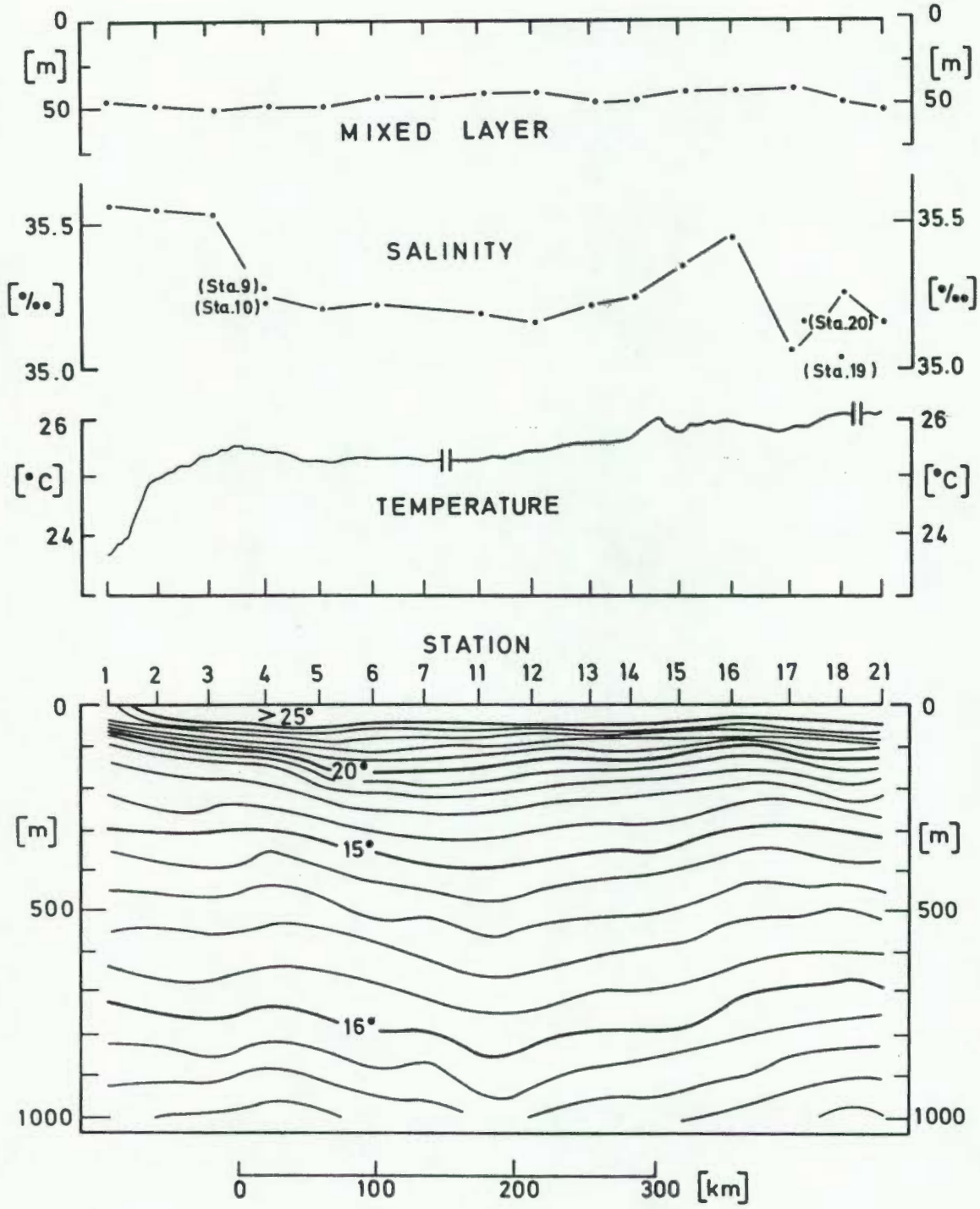

FIG. 6.2 : Top : Variation of mixed layer depth, surface salinity and surface temperature.

Bottom : Vertical section of temperature for the cruise in March, 1977.

cruise were collected. At that stage our demoralised spirits were beyond repair, and the home journey was continued without interruption.

6.2.2 Section along 37°30'E

The vertical section of temperature (Fig. 6.2) presents a more-or-less featureless situation with no evidence of eddies. The cruise was executed in late summer, and the temperatures in the upper 150 m are therefore higher than on the previous cruises, which were all done in winter.

There were some strong fronts in the surface temperature and salinity, especially at the beginning and end of the line of stations. A T/S analysis of the surface water (not shown here) indicated that the first three stations were located in water of subtropical origin, while the rest (particularly stations 17 and 19) were in water of more subtropical nature.

6.2.3 Test station (station 22)

A test station for equipment was occupied on the northern Mozambique Ridge at 27°46'S, 35°32'E. It would, in retrospect, be very nice to claim scientific foundation for the location of this test, but the position was chosen more-or-less arbitrarily.

A vertical profile of temperature down to 720 m was obtained, and to illustrate the anomalous conditions at this station, the temperature profile is compared with a selection of other profiles from the same cruise (Fig. 6.3). Below the seasonal thermocline, the water at station 22 is 4°-5°C colder than the water at any of the other stations. In Bravo and Charlie, the minimum depth of the 10°C isotherm was 510 m and 450 m respectively, while at station 22 it was 345 m. A deeper isotherm, such as 6°C, was at 890 m and 790 m in Bravo and Charlie, respectively, while it was 685 m at station 22.

A surface profile of temperature along the ship's track was only obtained for a limited distance after station 21, and this showed an irregular increase in temperature from 26° at station 21 (38°E) to 27°C at 36°30'E on the Mozambique Ridge. The ship's set (using the SATNAV

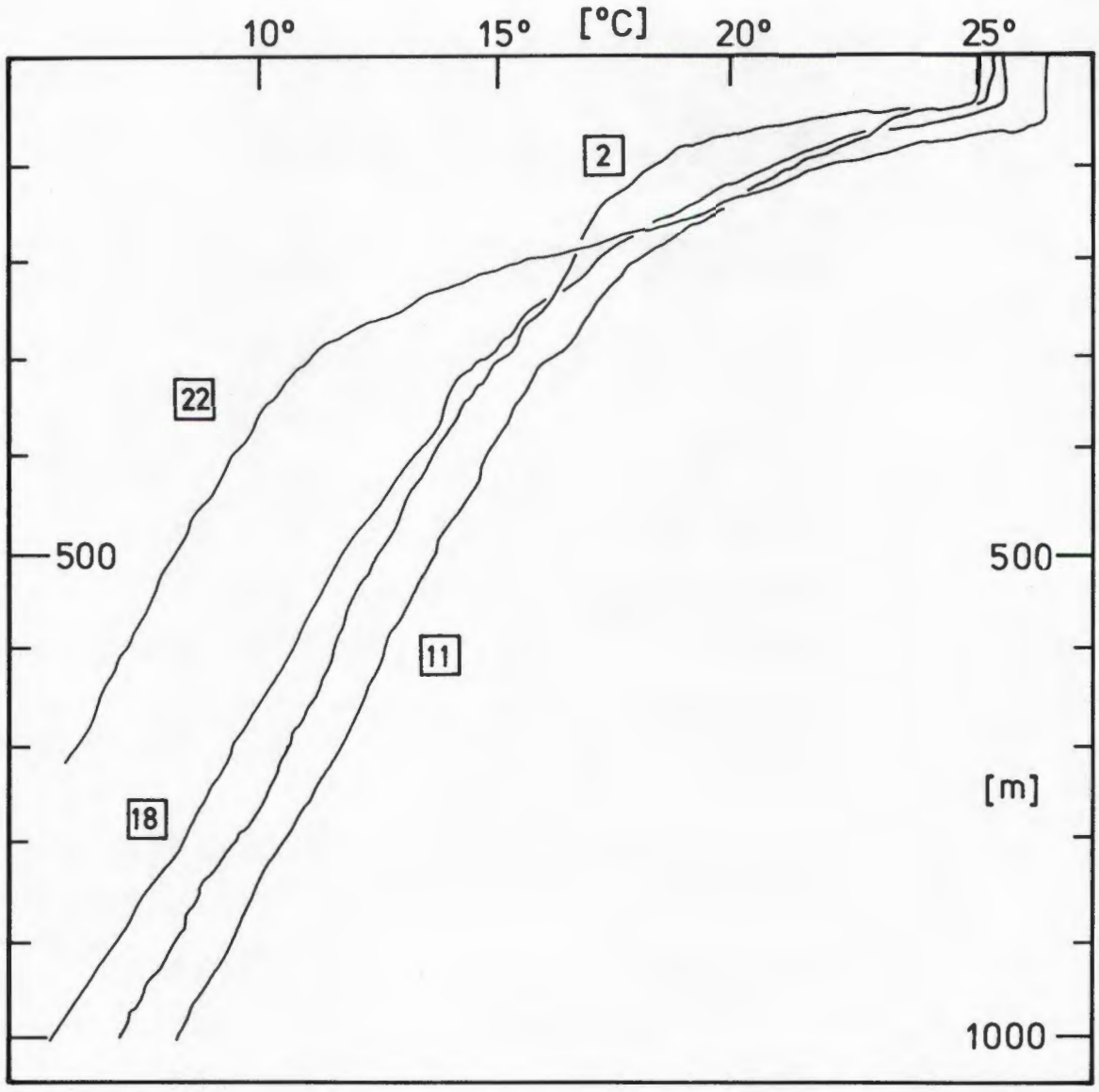

FIG. 6.3 : Vertical profiles of temperature obtained on stations 2, 11, 18 and 22 of the cruise in March, 1977.

positions) showed a 35 cm/s set toward the south between 36° and 37°E (i.e. east of station 22) and a northwesterly set of 0.7 cm/s between 34° and 35°E, west of station 22.

Although station 22 was separated geographically from and lacked the more detailed results of the other stations of this cruise, its relevance to the present discussion cannot be ignored. Considering the surface temperature front to the east of station 22, the direction of the ship sets on either side of this station, and the strong southward geostrophic flow implied by the subsurface temperature decrease from station 21 to 22, it was concluded that station 22 was situated close to the centre of an intense cyclonic vortex.

This represented the first time that a vortex was observed in this position, and although the dimensions of the vortex were unknown, it was intuitively felt that the diameter of the eddy was 200 km or more. A circulation feature of this magnitude in this region was obviously large enough to have been directly or indirectly involved with the Agulhas Current, and our attention involuntarily shifted towards the behaviour of the Agulhas Current in this area.

Considerable evidence exists that the Agulhas Current adheres to the coast south of 30°S (e.g. DIETRICH, 1935; DUNCAN, 1970 and 1976; PEARCE, 1977b). GRüNDLINGH and SNYMAN (1972) also presented radiometer evidence of the Agulhas within 100 km of the coast from 28°S southwards. On the other hand, HARRIS (1972) indicated a high transport of water ($40 \times 10^6 m^3/s$) as far east as the Mozambique Ridge at 29°S, directed roughly in a SW direction. His data did not reveal any coastal current at that latitude, and he concluded that at the time of the survey, the $40 \times 10^6 m^3/s$ *was* the Agulhas Current - approximately 400 km east of its expected position. GRüNDLINGH's (1977) satellite buoy track (Fig. 4.1) confirmed the possibility of a circuitous cyclonic route between 25° and 30°S, but it was not suggested that the bulk of the Agulhas Current supply from the north followed this route. For example, the volume transport of Bravo ($11 \times 10^6 m^3/s$) and Charlie ($13\text{-}20 \times 10^6 m^3/s$) were much less than the transport of the Agulhas Current, since the latter has a geostrophic transport (relative to 1000 m) exeeding $30 \times 10^6 m^3/s$ (DUNCAN, 1970).

In 1968, the R.V. *Meiring Naudé* executed a series of stations

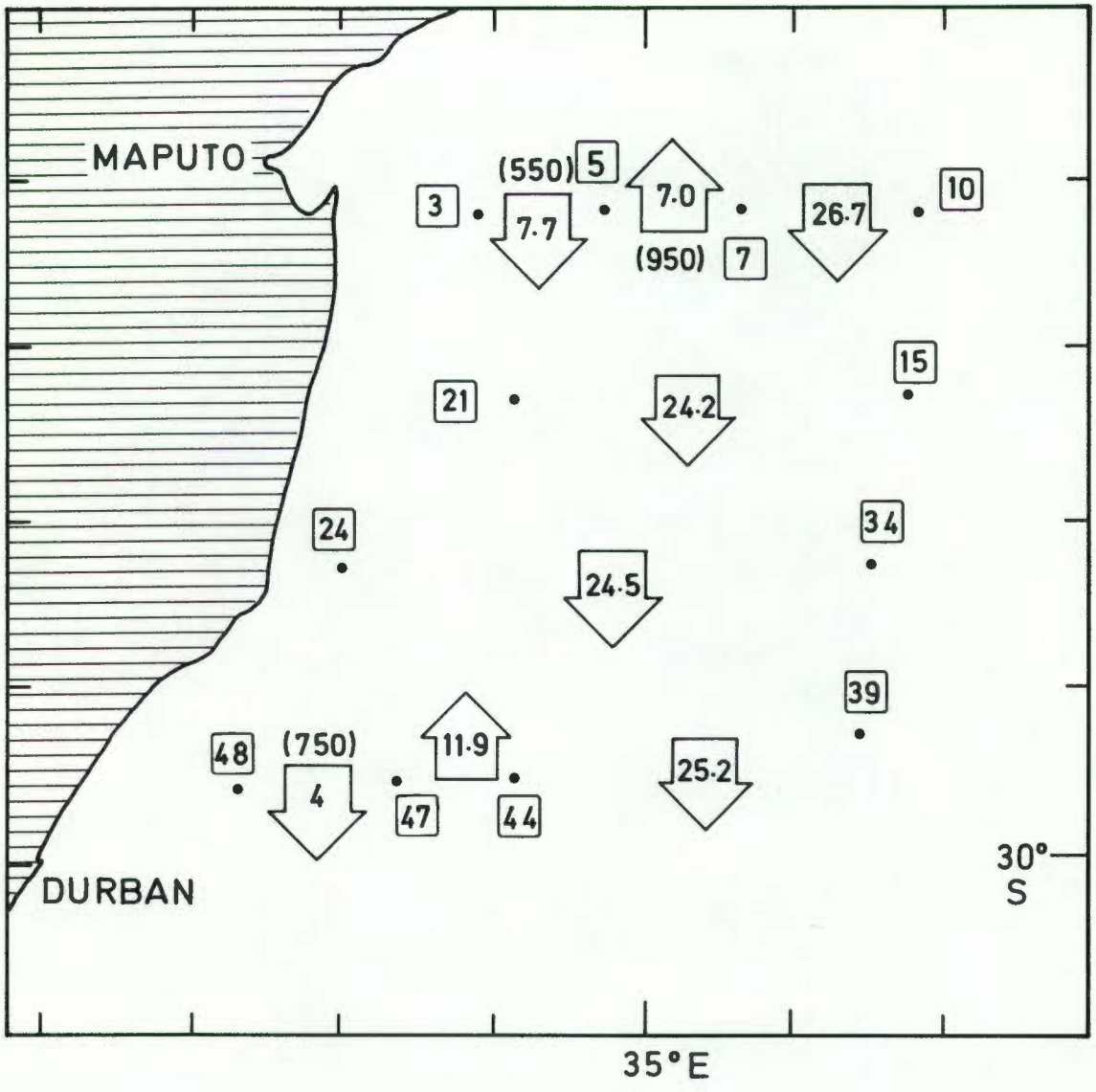

FIG. 6.4 : Volume transports (in units of 10^6 m^3 s^{-1}) between selected stations of the *Meiring Naude* cruise in August, 1968. All transports were calculated relative to 1000 m, except where the reference level is indicated in brackets.

in the area between Maputo and Durban, mainly to test the ability of the vessel to operate far offshore for a longer time (having just been commissioned a few months before). The data from this cruise remained dormant for many years because the equipment with which the data was collected underwent considerable modification in the meantime, and the data is now published for the first time (see Appendix 6).

The vertical sections of temperature show the Agulhas Current on all traverses, although there is evidence of some subsurface eddy activity, especially on the northernmost and southernmost lines. There is a fair amount of consistency in the volume of water transported through the four transects (Fig. 6.4). The offshore limit of significant southward flow formed a more-or-less straight line, running through stations 10, 15, 24 and 39 on the Mozambique Ridge.

These results seemed to indicate that, on occasion, there can exist significant flow in the vicinity of the Mozambique Ridge. This current can be accompanied by a filament closer to the coast, giving the circulation a biaxial appearance. The coastal branch seemed to be more intense, but transported less water because it was shallower and narrower than the offshore branch. The possibility existed that the offshore branch could act as a source of the flow observed in this area in March 1977. The cruise in June 1977 was therefore planned to confirm the existence of a "coastal" Agulhas Current and simultaneously identify possible offshore filaments or eddies in the vicinity of the Mozambique Ridge.

6.4 Observations in June 1977

6.4.1 Narrative of the cruise

The *Meiring Naudé* left port on 1 June and a line of stations was started off Cape St. Lucia the next morning. A total of 36 stations were completed up to 8 June, and the vessel returned on the 9th. About 24 hours were lost due to equipment problems during the survey. With the aid of DECCA, some current measurements were obtained close inshore (stations 1-7) and offshore (stations 12, 13, 15 and 23) using SATNAV drifts (Fig. 6.5). Vertical profiling was done to 1000 m depth.

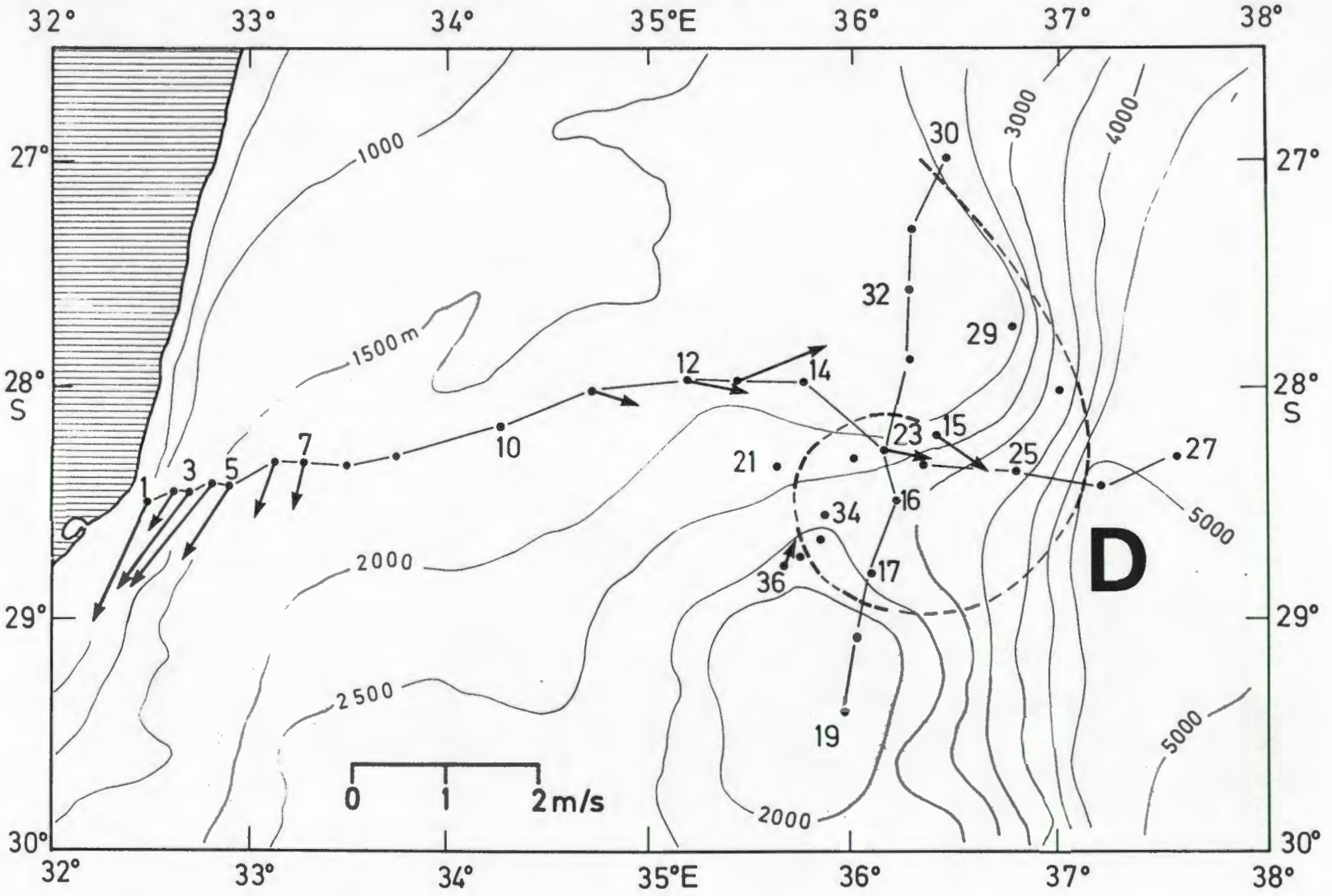

FIG. 6.5 : Station chart of the cruise 2-8 June 1977. The arrows represent current velocities while the ship was drifting on station. Bold dashed lines represent thermal fronts (see Fig. 6.6 and 6.7) which were interpolated (light dashes).

An eddy (Delta) was located over the Mozambique Ridge with its centre at approximately 28°17'S, 36°05'E. Two traverses were executed across the eddy and care was taken to proceed as far beyond the position where the depth anomaly of the isotherms becomes relatively small, to see whether thermal fronts existed similar to those observed at Charlie.

6.4.2 Thermohaline structure

The zonal and meridional sections of temperature are shown in Figs. 6.6 and 6.7 respectively, and the following points are noteworthy:

a) The rise of isotherms toward the coast in Fig. 6.6 indicated the position of the Agulhas Current. The Current was also reflected by the vectors of current speed at 50 m depth in Fig. 6.5. The width of the Agulhas Current was about 150 km.

b) Beyond 150 km offshore the isotherms tended to become level although there was still a small downward slope. Between station 12 and 13 they started rising again, reaching a maximum amplitude between stations 23 and 24. The maximum displacement was experienced by the 9°C isotherm, namely about 300 m. An anomaly of similar magnitude occurred in the meridional transect (Fig. 6.7). The topography of the 10°C isotherm surface provides some insight into the shape and size of Delta (Fig. 6.8). Delta had dimensions (based on the 10°C/650 m intersection) of about 50 X 80 km, making it much smaller than Bravo or Charlie.

c) In depths shallower than 300 m the eddy centre coincided with an amount of warm water at the surface, causing a concave shape of the isotherms. This feature had also been observed in the thermal structure of Bravo and Charlie.

d) Surface thermal fronts were observed at irregular distances from the eddy centre. With a certain amount of freedom, these fronts were interpolated between their observed positions (Fig. 6.5) to yield a helix spiralling clockwise toward the centre of the eddy. These temperature fronts were only rarely accompanied by salinity fronts.

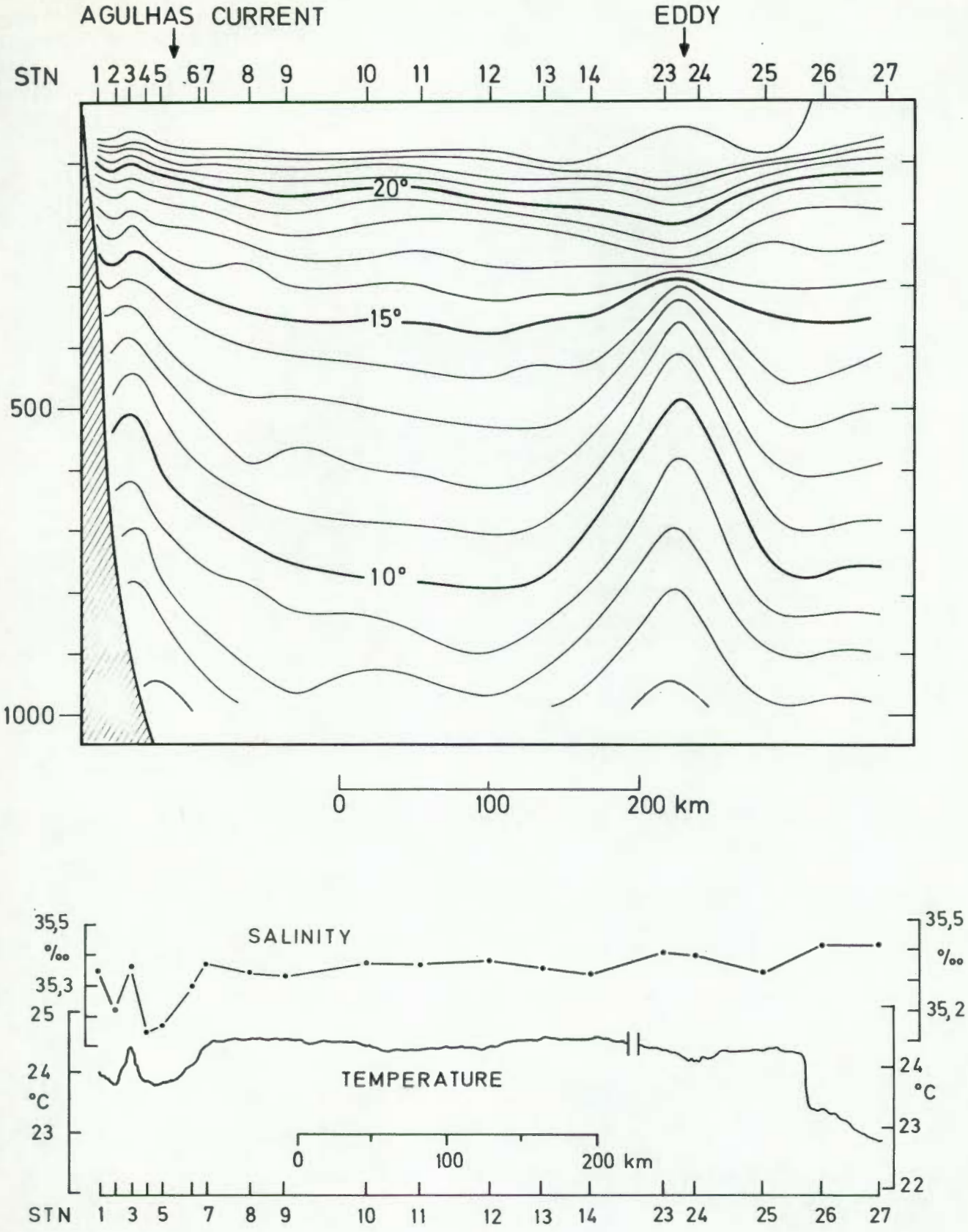

FIG. 6.6 : Zonal temperature section (top) in June 1977 across the Agulhas Current and eddy Delta. Surface fronts are visible from the variation of surface temperature and salinity (bottom).

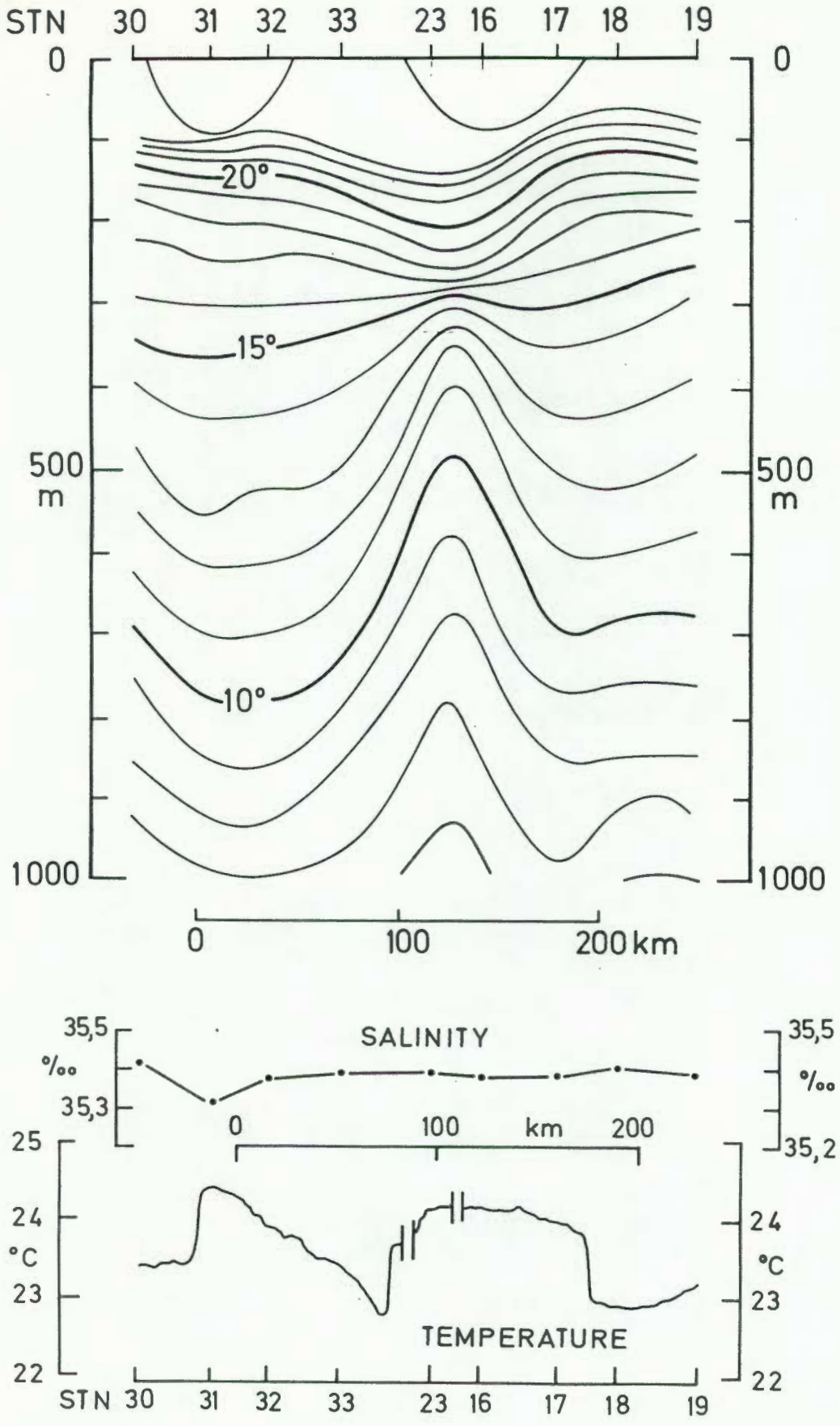

FIG. 6.7 : Meridional temperature section (top) and surface temperature and salinity variation across eddy Delta in June, 1977.

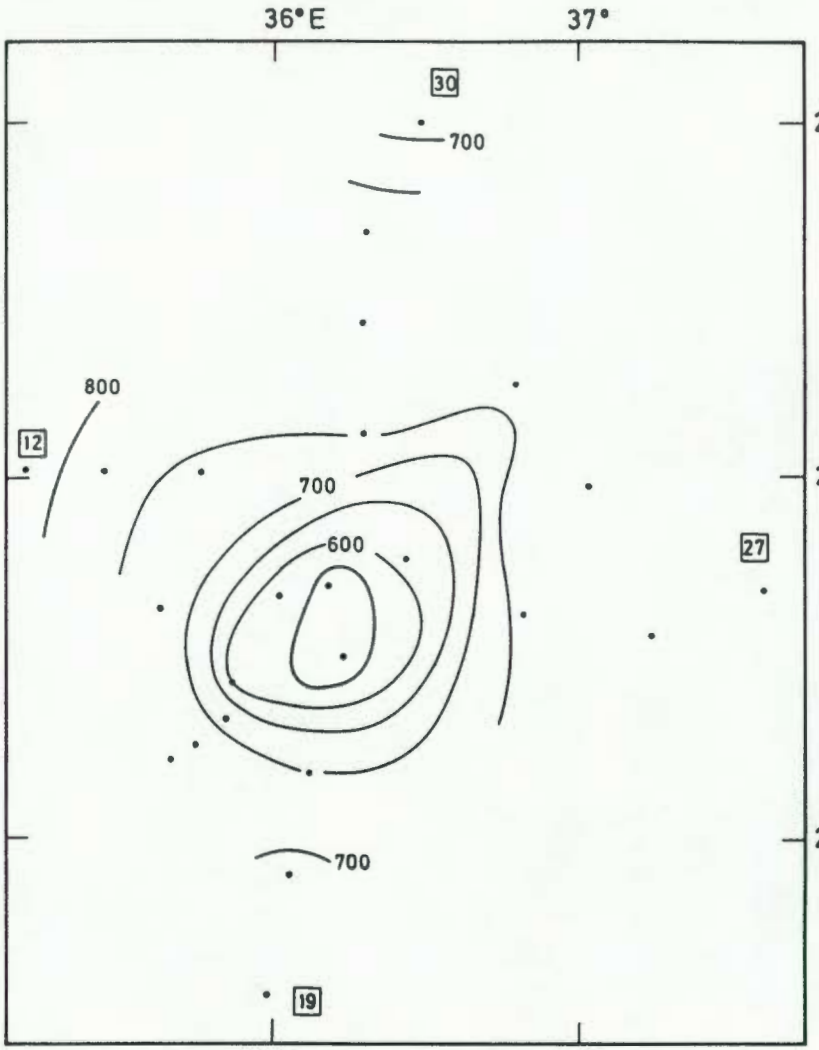

FIG. 6.8 : Topography of the 10°C isotherm (in m depth) in eddy Delta, June 1977.

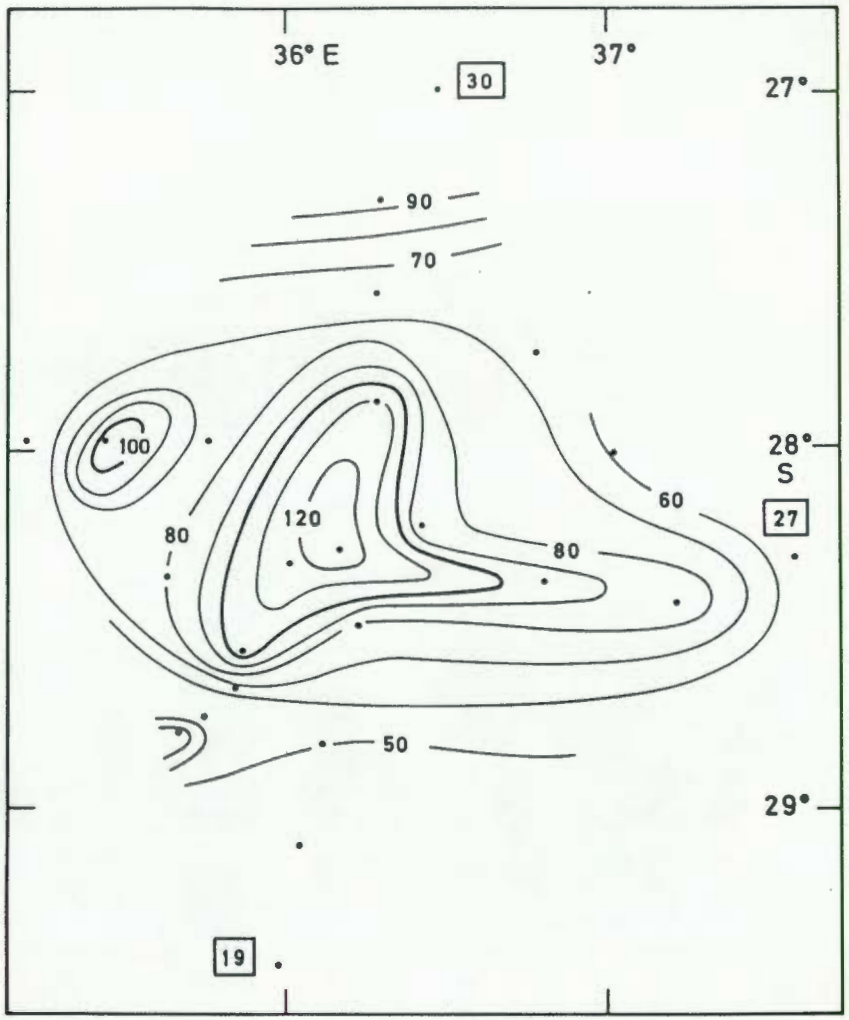

FIG. 6.9 : Depth of the mixed layer (m) in eddy Delta.

e) An investigation into the depth of the mixed layer (Fig. 6.9) confirmed the results obtained on previous cruises: The mixed layer deepened over the centre of the eddy to a depth of 125 m, and shoaled outward to approximately 50-60 m.

f) A remarkable intermediate minimum of 34.8-35.3 $^{o}/oo$ was observed in the salinity of stations 2, 4, 13, 21, 29, 30 and 33 (see examples in Fig. 6.10), This seems to indicate the penetration of tropical water along the upper part of the seasonal thermocline, and progressing unmixed between layers of higher salinity tropical water. (Due to its high stratification, the seasonal thermocline customarily coincides with the spreading depth of the subtropical water, but here it seemed to perform the same function for tropical water).

6.4.3 Dynamical structure

The few isolated current velocities that could be measured directly in the vicinity of Delta (Fig. 6.5) confirmed its clockwise motion, the speeds directly inside the eddy attained a maximum of 0.62 cm/s (station 15). Maximum gradient current velocities were recorded between stations 14 and 23 (46 cm/s), 33 and 23 (47 cm/s), 29 and 23 (42 cm/s), 25 and 24(48 cm/s), 17 and 16 (42 cm/s), 20 and 16 (38 cm/s), 21 and 23 (39 cm/s), and these maxima were all located at 300 $\pm$ 50 m depth.

A representation of the volume transport is given in Fig. 6.11 and two aspects are noteworthy:

a) The transport around Delta reached a minimum of 6.4 x $10^{6} m^{3}/s$ along its southern flank, and this value gained 11.6 units along the eddy's western flank and lost a corresponding amount along its eastern and southeastern flank. Less than 50% of the volume flux was being rotated by the eddy, and this gives an indication of the interaction between Delta and its environment.

b) Whereas the major exchange of volume flux occurred in the south, the surface fronts in Delta seemed to indicate a

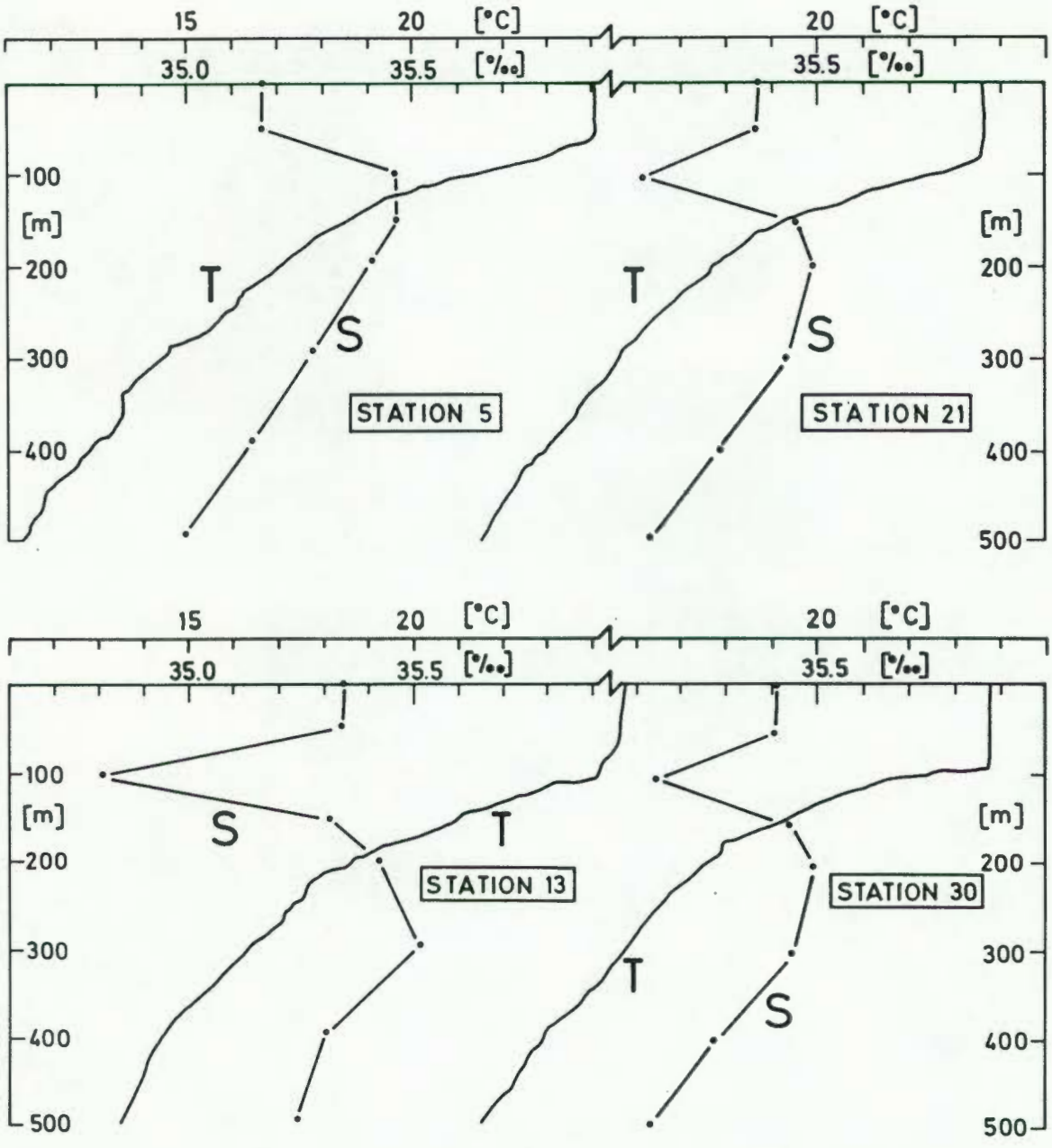

FIG. 6.10 : Vertical profiles of temperature and salinity for selected stations of the cruise in June, 1977, to illustrate the intrusion of low-salinity, tropical water within the seasonal thermocline ($\sim$ 100 m).

circulation being supplied from the north (with no losses). Warm surface water from the north was flowing clockwise into the helix while colder surface water was being fed from the southwest between stations 13 and 21. If the surface water was converging into the centre of the eddy as the frontal helix suggests, the warm water must have downwelled at the centre for reasons of continuity. The shape of the isotherm anomaly suggests that the downwelling was confined within the upper 300 m.

Combining the flow pattern that has emerged from the dynamics of Delta with the pattern of sea-surface (SST) temperature, it seems that Delta had a complicated layered structure.

On the one hand, the SST suggested a convergence of surface water into the centre (Fig. 6.11) and this was confirmed by the presence of a bowl of warm water at the centre, as well as by the increase in depth of the mixed layer. Consider the behaviour of the Agulhas Current, the warmest water and maximum mixed layer depth are normally located above the velocity maximum. For Delta, this maximum was situated approximately 30 km away from the centre, and it was concluded that the thermal features (SST and mixed layer maxima) had advected from here to their observed position at the centre. To assess the magnitude of these radial velocities, it was assumed that the downstream flow rate of the surface was 30 cm/s (based on the geostrophic velocity). Converging in the way shown in Fig. 6.5, the frontal system would require an inwardly-directed velocity component of about 10 cm/s.

On the other hand, the flux budget (Fig. 6.11) showed no inflow from the north corresponding to the surface flow pattern. This is even more remarkable when a possible exchange mechanism is sought for the southerly inflow. It was concluded that the dynamics of Delta could not be explained in terms of existing knowledge of the circulation.

The kinetic energy of the eddy (Fig. 6.12) is approximately half the value of Charlie observed in June 1976. Since the distribution of energy indicates that the survey encompassed the whole of the vortex, it is concluded that Delta was much weaker than Charlie.

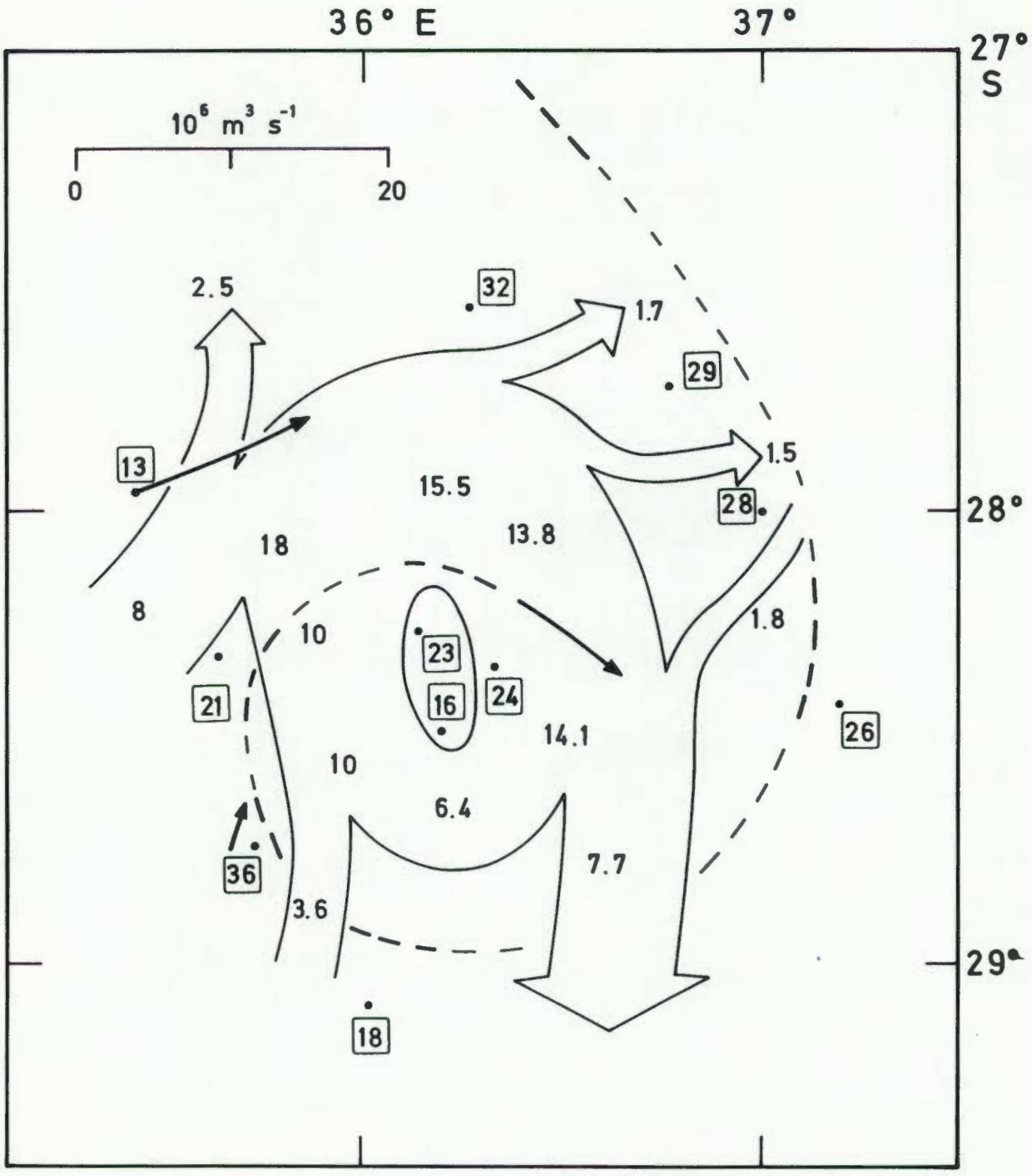

FIG. 6.11 : Volume transport (in units of 10^6 m^3 s^{-1}) of eddy Delta. The vectors represent directly-measured current speeds, while the dashed lines represent thermal fronts observed during the cruise (see Fig. 6.5).

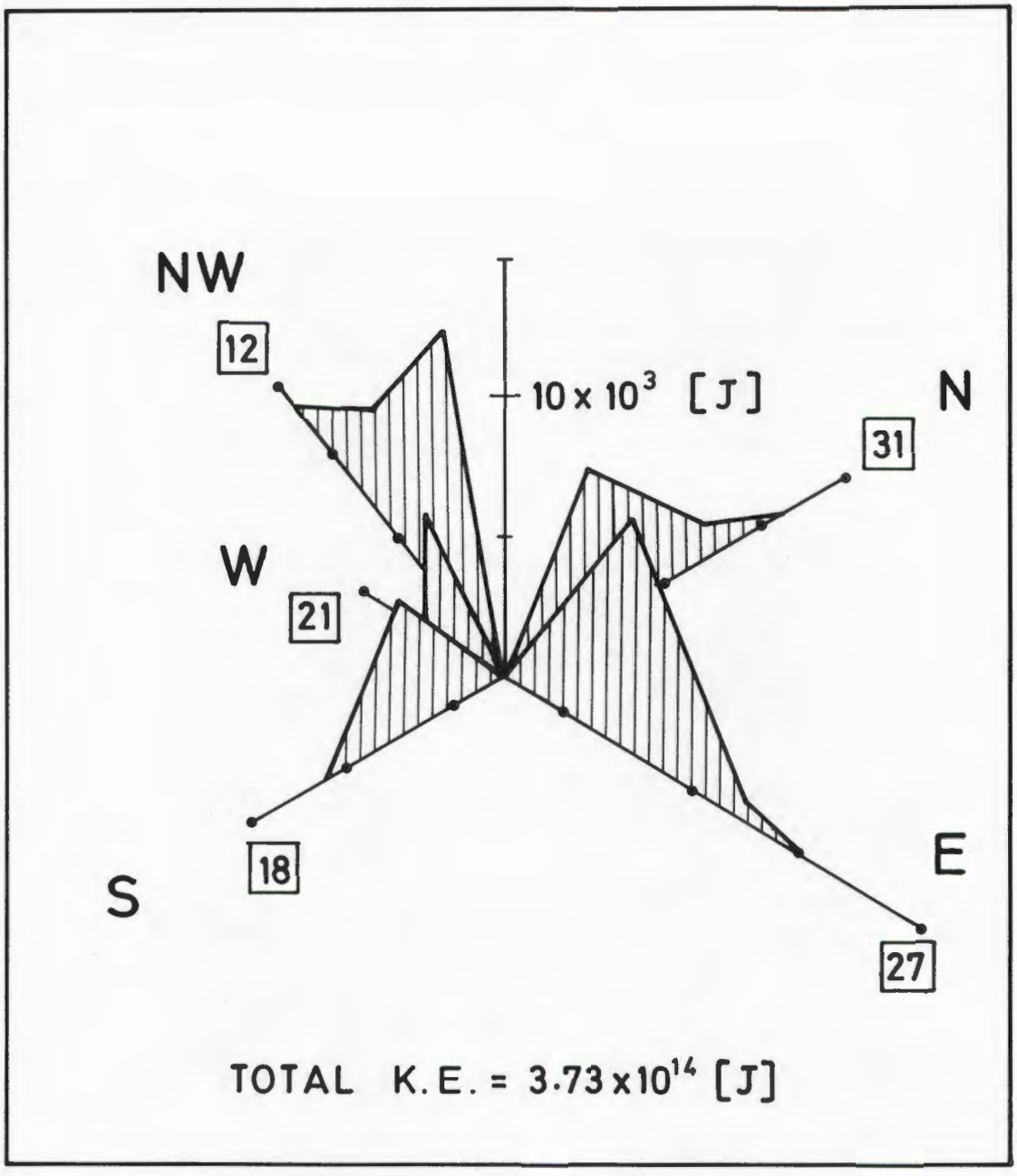

FIG. 6.12 : Kinetic energy distribution of eddy Delta, June, 1977.

6.5 Discussion

The centre of Delta was located at 28°20'S, 36°15'E (Fig. 6.8), about 90 km southeast of where station 22 of the cruise in March (three months before) detected a significant thermal anomaly. At that station, the 10°C isotherm was observed at a depth of 345 m, while the shallowest depth of this isotherm in Delta was about 500 m, (the interpolated section in Figs. 6.6 and 6.7 showed a depth of less than 500 m). Assuming that these two cases represent the same eddy, and assuming further that station 22 of the cruise in March was located in the centre of the eddy, the observations suggest that the centre was becoming warmer, resulting in a subsiding of the isotherms. This could have been caused by a decreasing spin rate of the eddy. The vertical rate of collapse of the eddy centre amounted to about 1.6 m/day, which is larger but still of the same magnitude as reported by PARKER (1971, 0.6 m/day) and CHENEY and RICHARDSON (1976, 0.4 m/day) for Gulf Stream rings. The vortex would have drifted at a speed of about 1 cm/s to have advected to the position where Delta was located. This, too, is of the same order as the translation rate of Gulf Stream rings (cf. WARREN, 1967, 4-10 cm/s; PARKER, 1971, 3-8 cm/s; RICHARDSON, CHENEY and MANTINI, 1977, 9 cm/s). In other words, it is quite possible that the two observations originated from the same vortex, even though the phenomenon of a large, intense, semi-stationary vortex, such as this one, has not been reported off the South African coast before.

An important conclusion that was reached after the surveys in 1977 was that the northern Mozambique Ridge could serve as a theatre for the generation of cyclonic eddies. This conclusion is contrasted by the complicated dynamics of Delta, and the relationship between Delta and the eddies in the Mozambique Basin (Alfa, Bravo and Charlie) that could not be explained in terms of the available knowledge of the general circulation in the region. Further information was only collected during a cruise in June 1982 (see Chapter 10) when it was confirmed that the Agulhas Current as a whole can be involved in major disruptions of the flow in the region of the northern Mozambique Ridge.

CHAPTER 7

OBSERVATIONS OF DEEP-SEA VORTICES : 1978

7.1 Introduction

After the cruise in June 1977 during which eddy Delta was observed, attention was focussed on the vicinity of the Mozambique Ridge north of 30°S as the possible spawning area of eddies. The first cruise of 1978 was therefore planned to start in this area after crossing the Agulhas Current at Cape St. Lucia. It was hoped that once an eddy had been located, subsequent cruises could try and follow its propagation to get some idea of its destiny. This turned out to be quite difficult, and after the first cruise (April) was aborted due to equipment problems, an eddy was only located during the second and eventually surveyed on the last cruise of the year (which made the location virtually useless for tracking purposes). A rough estimate of its progression could, however, be obtained).

The cruises of this year were the first to go down to 1900 m on a routine basis, and this new step in the process of data collection was the main cause behind the malfunction of the equipment. Water leaked into the hydrosonde at the high pressure and caused malfunction of the electronic circuitry. Only after the May cruise were these problems solved to such an extent that data could be collected relatively fault-free.

7.2 Observations in April 1978

7.2.1 Narrative of the cruise

The *Meiring Naudé* left port on the 6th April 1978 and steamed to Cape St. Lucia where stations were commenced at approximately noon on 7 April (see Fig. 7.1). The vessel experienced strong southward drifts inside the Agulhas Current, and severe problems were experienced in getting the hydrosonde to go down instead of "floating" away from

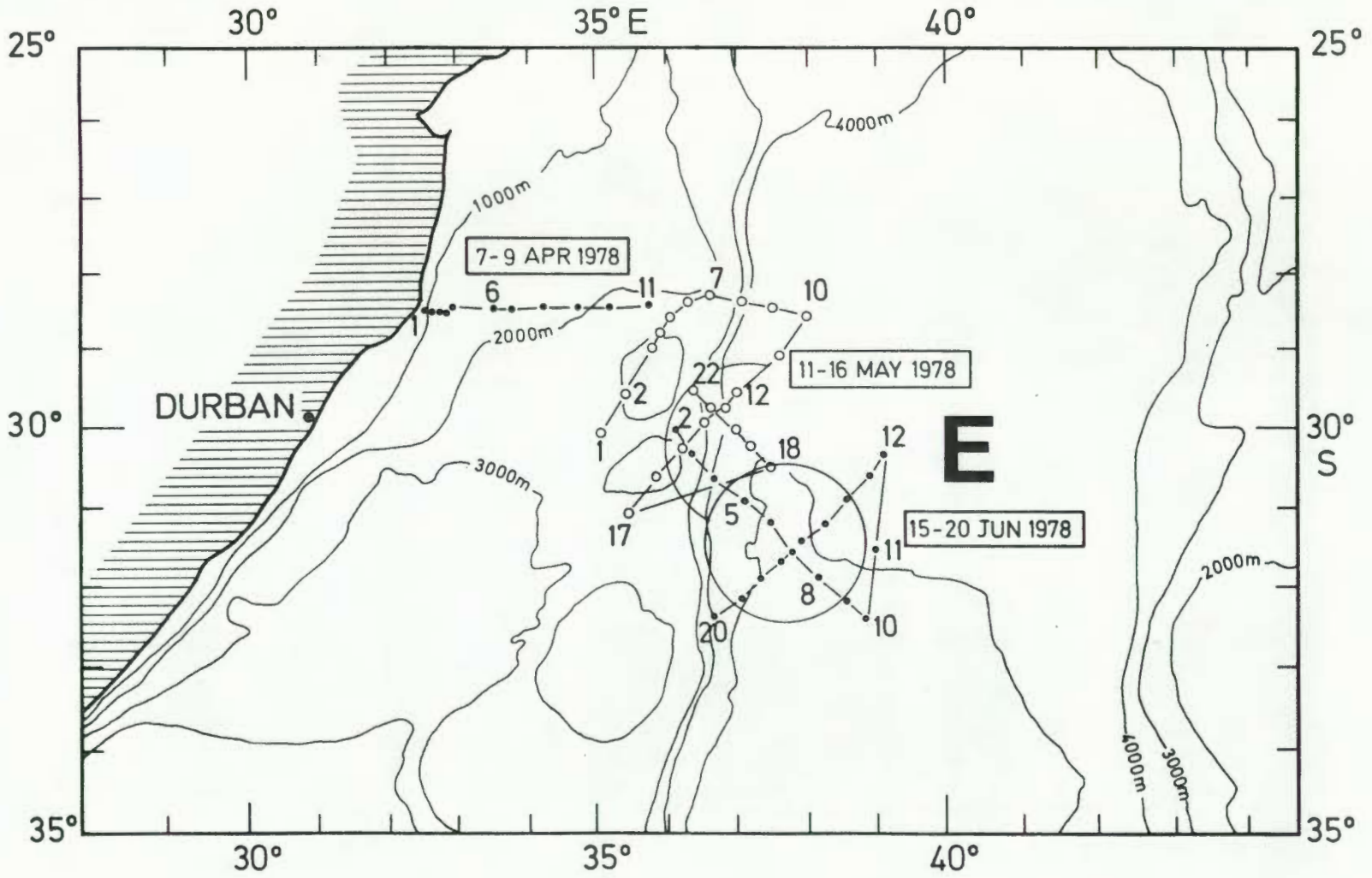

FIG. 7.1 : Station disposition of the *Meiring Naudé* cruises in April, May and June 1978. The semi- and full circles indicate more or less the position of eddies observed during the May and June cruises.

the ship (due to the strong current, the angle on the cable became so great that the hydrosonde was moving horizontally away from the ship faster than it was going vertically downwards).

For purposes of current measurement, the first seven stations were completed in daylight hours on 7 and 8 April. On station 11, the pressure transducer in the hydrosonde failed, and with no standby systems on board, the cruise was abandoned. The vessel arrived back on 10 April.

Temperature, salinity, current velocity and nutrients were measured. The cruise was unsuccessful in the sense that no eddies were located. Similar to the cruise in March 1977, where the bulk of the data showed no evidence of vortices (section 6.2), the results of the present cruise are briefly included here since they show certain features relevant to the circulation.

7.2.2 Results

The surface temperature profile (Fig. 7.2) showed a very sharp front of the Agulhas Current in the vicinity of station 1, and again on the return journey to port. The high surface temperature ($\sim 28°C$) inside the Current and further offshore indicated the summer-autumn character of the water. The surface salinities (and, for that matter, salinities down to about 200 m) were much lower than one would have expected, indicating that a large amount of low-salinity, tropical water was present in the surface layers.

The presence of the Agulhas Current was confirmed by the strong, although not undirectional ship drift vectors off Cape St. Lucia (see Fig. 7.2). The influence of the Agulhas seems to have extended beyond station 7, with a northerly set between station 9 and 11.

The temperature section in Fig. 7.3 shows the Agulhas Current within about 100 km from the coast, probably extending right to the bottom (about 1700 m). Beyond station 7-8 the isotherms started curving upward again throughout the water column. The upheaval of isotherms in the area of station 9-11 could possibly have been an indication of an eddy

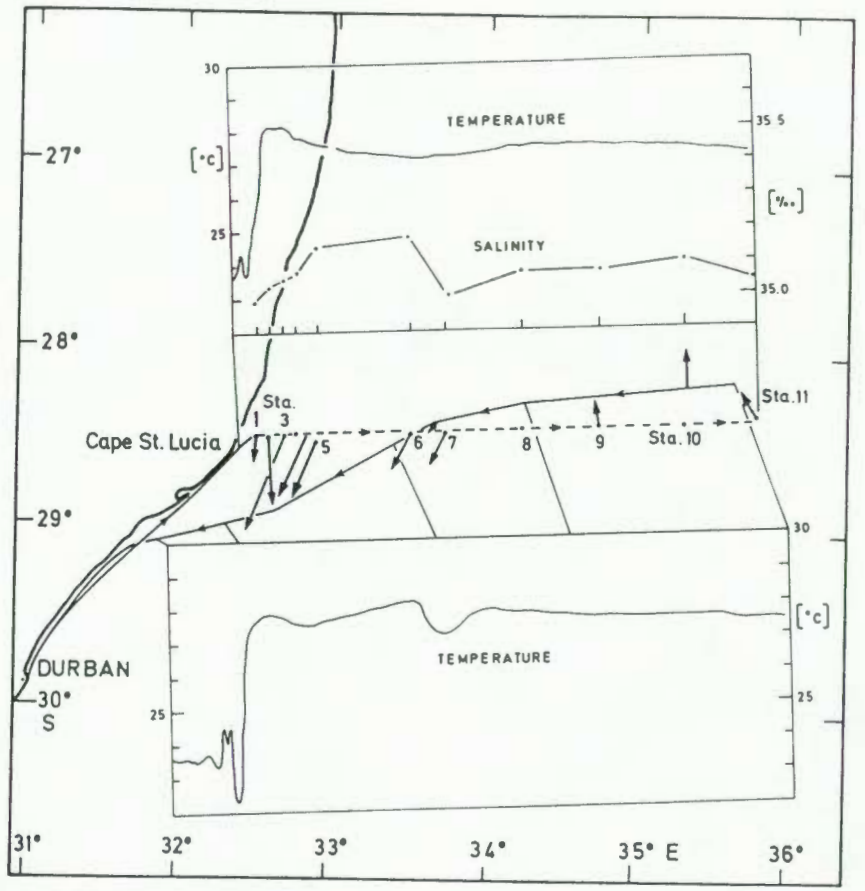

FIG. 7.2 : Surface temperature and salinity during the April 1978 cruise, as well as directly-measured current velocities and ship sets.

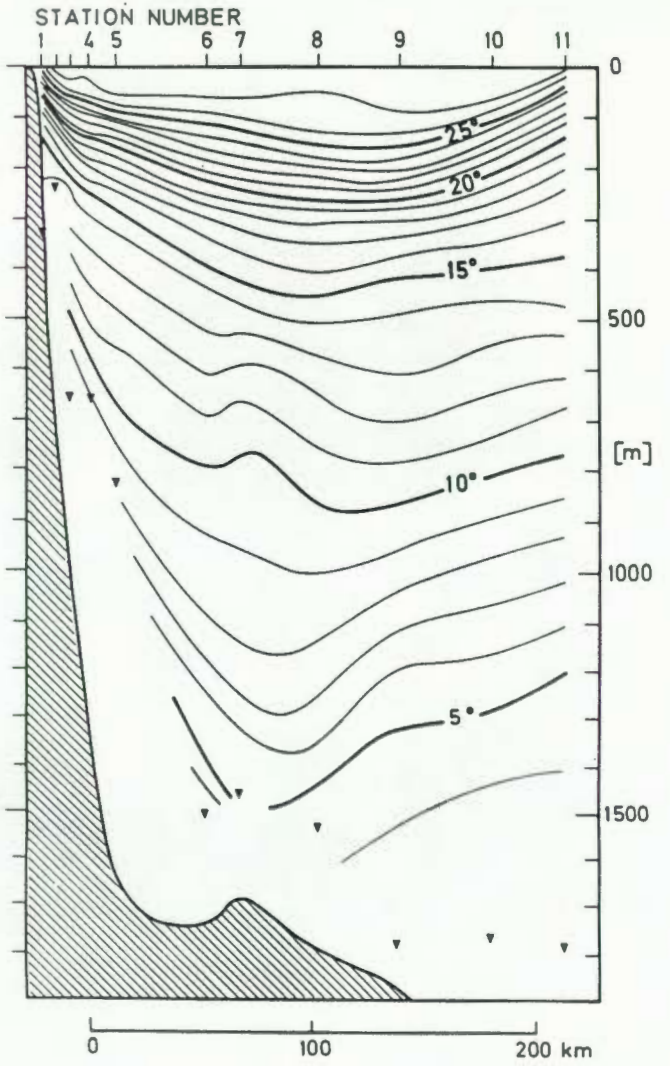

FIG. 7.3 : Vertical section of temperature during the cruise in April, 1978.

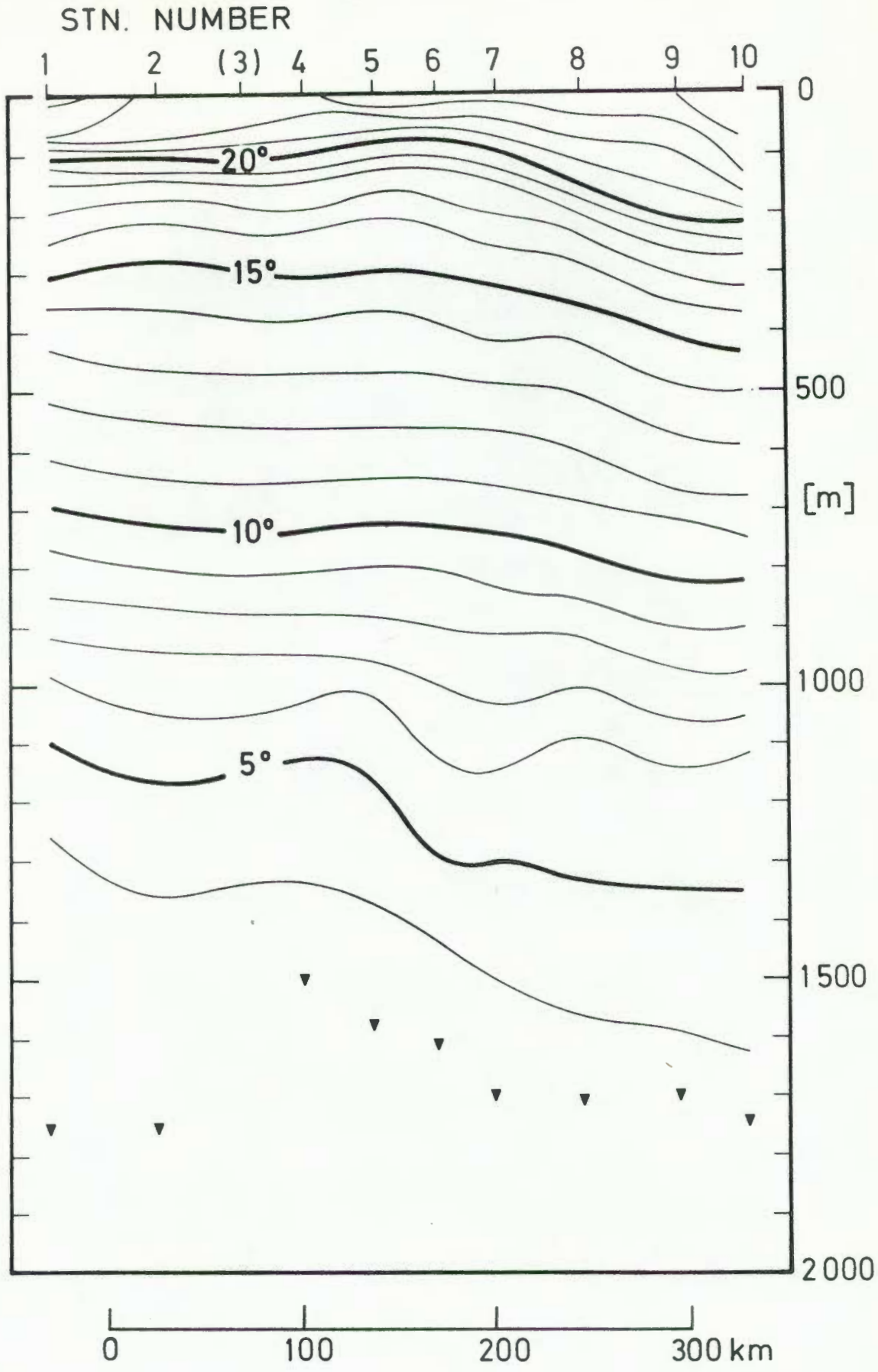

FIG. 7.4 : Vertical section of temperature for stations 1-10, April 1978. Subsurface data from station 3 was considered suspect because of equipment problems, and was therefore omitted from the analysis.

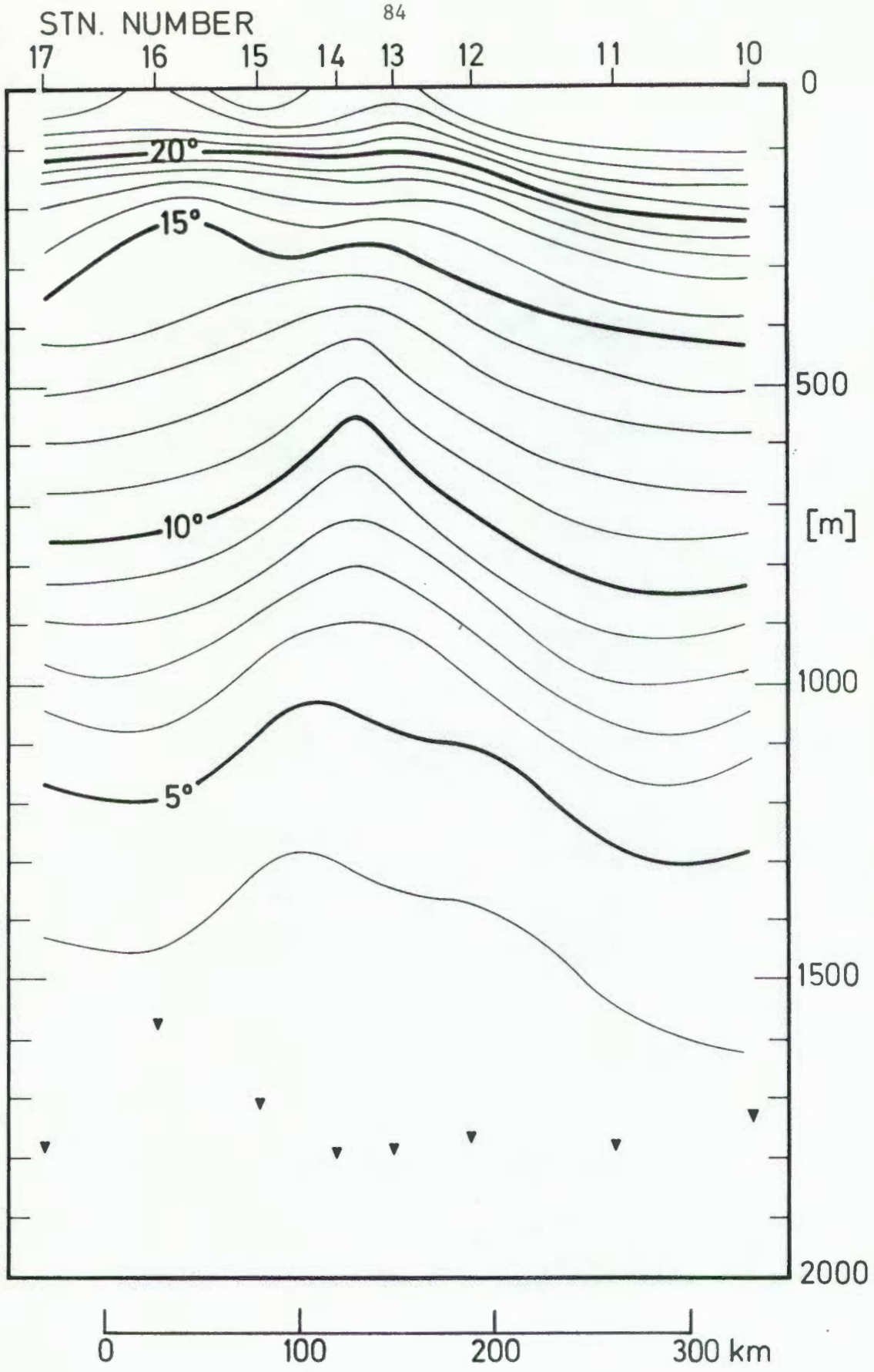

FIG. 7.5 : Vertical section of temperature for stations 10-17, April 1978. Note the upheaval of isotherms around station 13 and 14.

situated in more or less the same location as the one observed in June 1977, but the 10°C isotherm had not reached a conspicuous elevation by station 11 ($\sim$ 770 m), nor had isotherms in the upper 300 m started to deepen, as would have been expected if an eddy was situated east of station 11. In addition, no conspicuous thermal fronts were observed in the vicinity of station 11, and it is therefore dubious whether the upheaval of the isotherms can be regarded as indicative of a vortex.

7.3 Observations in May 1978

The primary objective of this cruise was to continue the search for an eddy with stations also covering the region to the east of where the April cruise was abandoned (see Fig. 7.1).

7.3.1 Narrative of the cruise

The ship left port just after noon on 10 May and proceeded on a general easterly course toward a position about 30°S, 35°E (Fig. 7.6) A major setback was experienced during the first two stations, when both the temperature channel on the hydrosonde and the depth channel of the XY recorder failed. The standby hydrosonde was employed from station 3 onwards, and only the analogue representation of the temperature-depth profile was lost.

The cruise proceeded in a general northeasterly direction up to station 7, when it became clear, from the absence of any conspicuous upheaval of the isotherms, that there was no eddy situated where the April cruise had been terminated the previous month. The course of the survey was then turned toward the ESE (see Fig. 7.1). Rough sets calculated on board indicated a general displacement toward the southwest between stations 7 and 10, and this was confirmed by the downward trend of isotherms east of station 6 (Fig. 7.4). The course was therefore altered to survey the area into which there seemed to be flowing a rather strong current.

On some stations, the hydrosonde had to be opened to remove the water that was penetrating under great pressure. (It was later concluded that a section of the hydrosonde's stainless steel casing had deformed under high pressure). The leaking eventually damaged some of the electronic

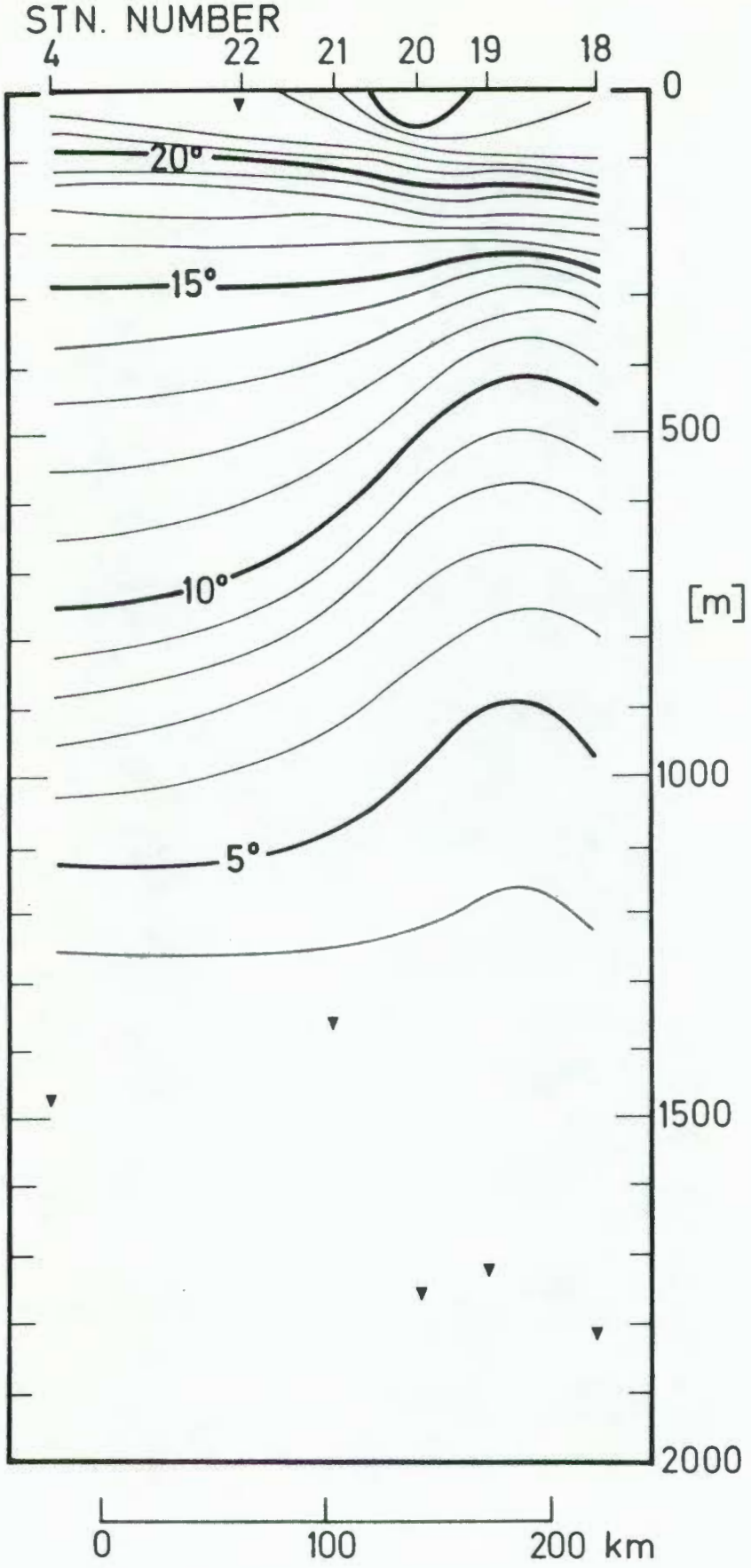

FIG. 7.6 : Vertical section of temperature, April 1978.

components, and the circuitry controlling the water sampler became inoperative. No more water samples (for salinity determination) were therefore obtained after station 10. Salinities for geostrophic computations were subsequently obtained from a T/S curve.

The southwesterly traverse from stations 10 to 17 showed an upheaval of the isotherms, roughly centre between stations 13 and 14 (Fig. 7.5). The course was changed after station 17 to enable another right-angled transect through the feature.

The eddy (code-named Echo) turned out to be situated further to the southeast than initially estimated, but a failure of the second hydrosonde on station 22 made it impossible to return and complete the data set in the southeastern sector of the eddy (see Fig. 7.6). The vessel returned to Durban on 17 May.

7.3.2 Results

The most conspicuous feature in the vertical sections of temperature (Figs. 7.5 and 7.6) was the elevation of the isotherm at stations 13-14 and stations 18-19. This upheaval was visible right down to the deepest measurement ($\sim$ 1800 m), and the maximum displacement of the 10°C isotherm from its normal level was about 300 m. The topography of the 10°C isotherm (Fig. 7.7) shows that Echo was elliptical with its major axis orientated NW-SE and dimensions 90 X 240 km.

Using the salinities obtained from the T/S curve, geopotential relative to 1500 m were calculated (Fig. 7.8). Also entered in this figure are ship sets derived from the intended (= autopilot) and true (= SATNAV) course and speed. These two current speed indicators compare favourably as far as direction is concerned. Largest ship sets were 1.24 m/s in 108° between stations 11 and 12, and 1.25 m/s, 062° between stations 19 and 20.

The gradient currents provided the basis for the calculation of volume transports relative to 1500 m between various stations in the vicinity of Echo (Fig. 7.9). If station 19 is considered to have been the centre of the eddy as far as the volume transport is concerned, the transport diagram shows that there was a considerable amount of water that was not rotating with the eddy. It is estimated that the amount

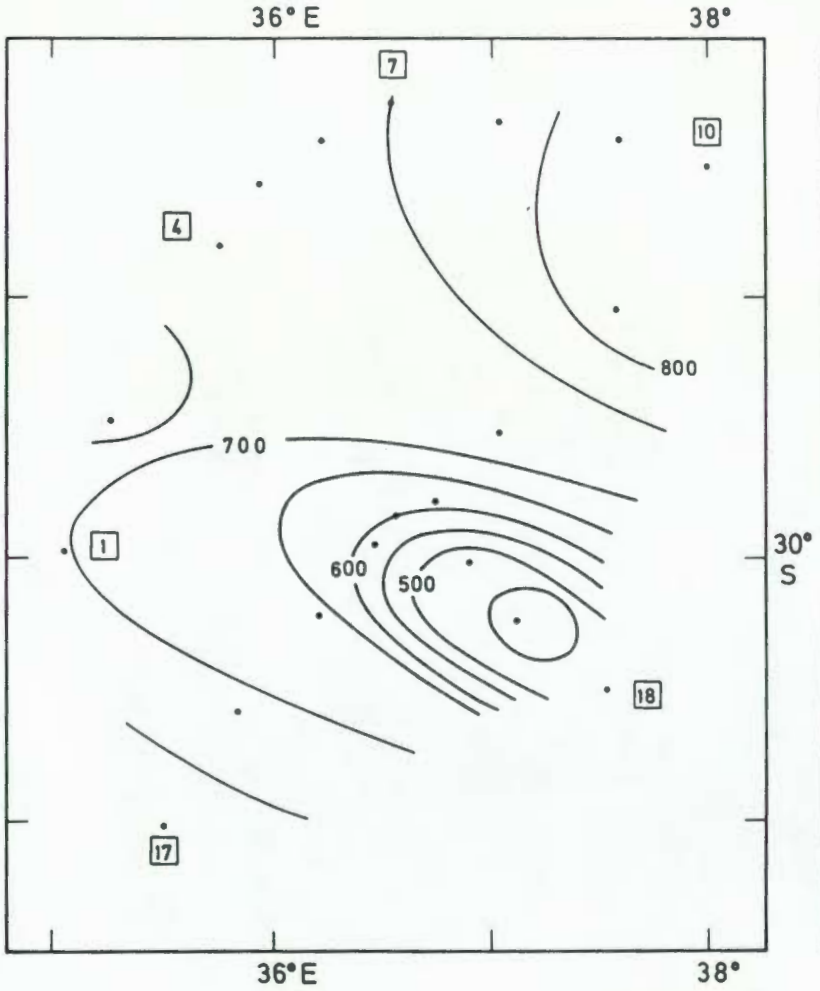

FIG. 7.7 : Topography of the 10°C isotherm surface (in m depth) across eddy Echo, May , 1978.

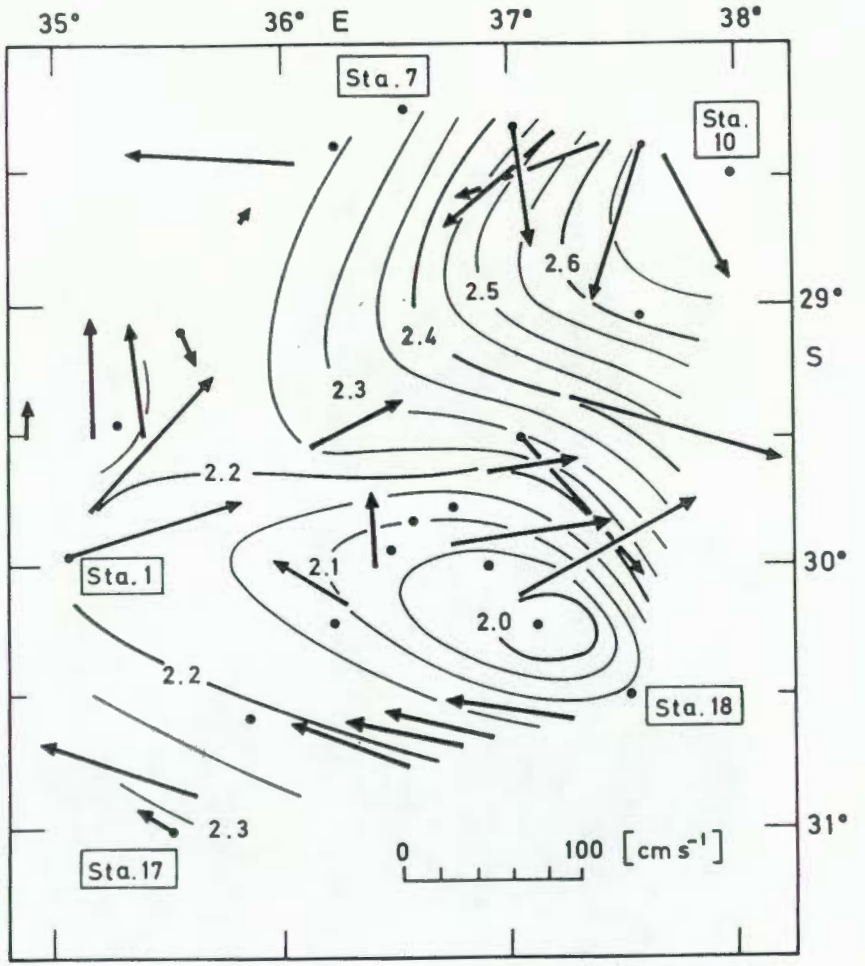

FIG. 7.8 : Geopotential topography of the sea surface relative to 1500 m during the cruise in May, 1978.

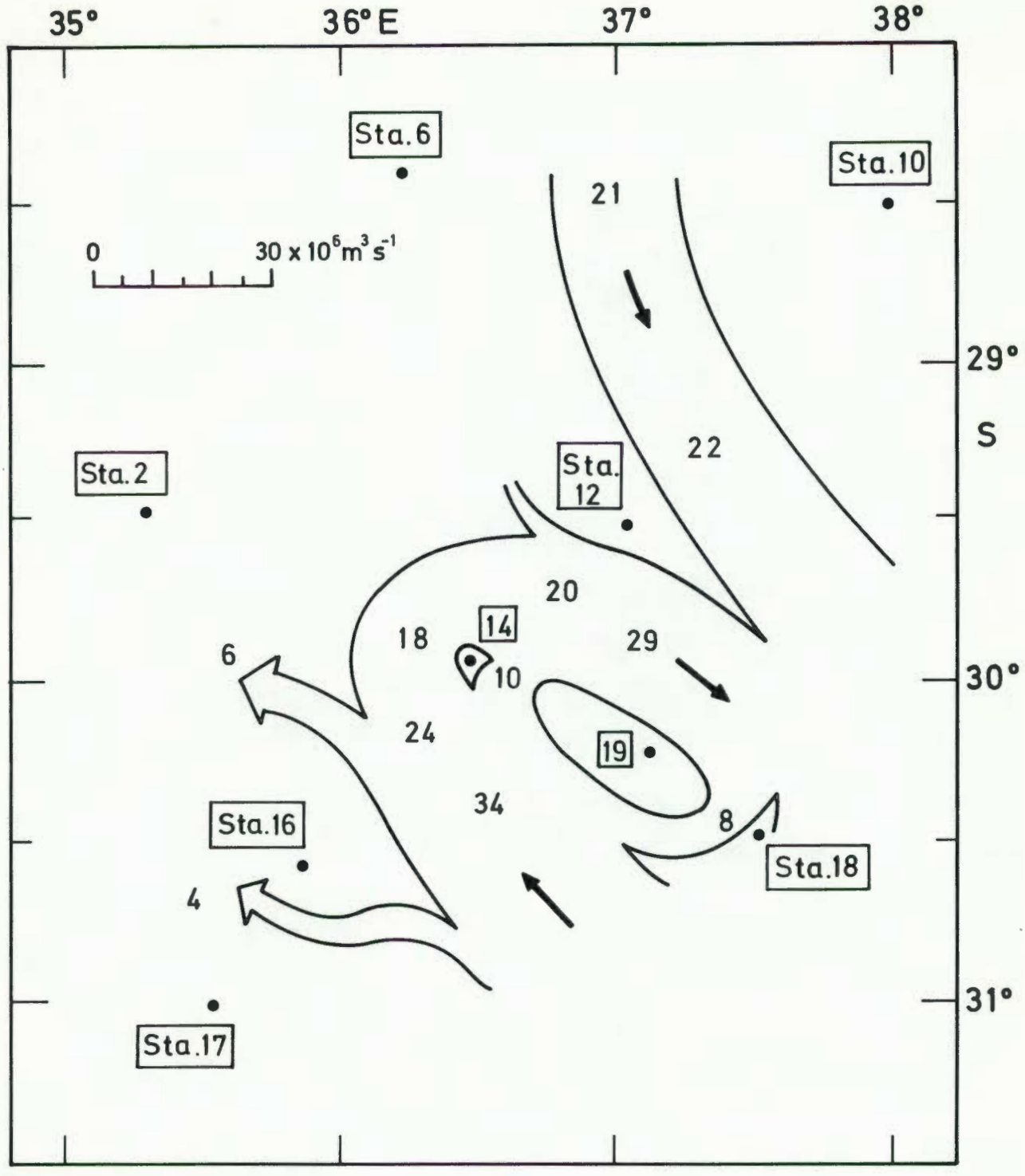

FIG. 7.9 : Volume transport, calculated relative to 1500 m, of the cruise in May 1978.

of water actually circulating the vortex was 25-30 x $10^6 m^3 s^{-1}$ (the transport between stations 19 and 2), while between stations 6 and 10, and between stations 10 and 12, there were 21 x $10^6 m^3 s^{-1}$ moving in a roughly southeasterly direction. The presence of this current led to the conclusion that Echo was not a free-drifting, solitary entity, but was somehow being supported or supplied by this current. Because of the "incomplete" section along the southeasterly line of stations 2-14-19-18, it is difficult to consider what the current did eastward of station 18. It is conjectured that the current turned clockwise in this region and northwestwards again (Fig. 7.9) in a tightening elliptical pattern.

7.4 Observations in June 1978

Since it was managed to locate and partially survey Echo in May, the June cruise was aimed at relocating it to determine its rate of advection and possibly any change in characteristics.

7.4.1 Narrative of the cruise

The ship left port on Tuesday, 14 June. The target area was the region to the southeast of where the estimated Echo's centre had been during the May cruise, but the survey was planned so as to partially cover the region of the previous cruise (see Fig. 7.1).

After completion of a test station (station 1), operational work started without problems. It was planned to obtain casts down to at least 1800 m, and this was achieved on all the 20 stations executed on the cruise, (see Figs. 7.10 and 7.11).

The rosette sampler of the hydrosonde started giving trouble soon after the start of this transect, and failed completely on station 3. It was decided to use reversing bottles to obtain samples of sea water, and from station 4 onwards, seven bottles were attached to the hydrographic cable and tripped by messenger when the hydrosonde attained the maximum depth. To complement the salinity profile, isolated values of salinity were read from a T/S graph during the subsequent processing ashore.

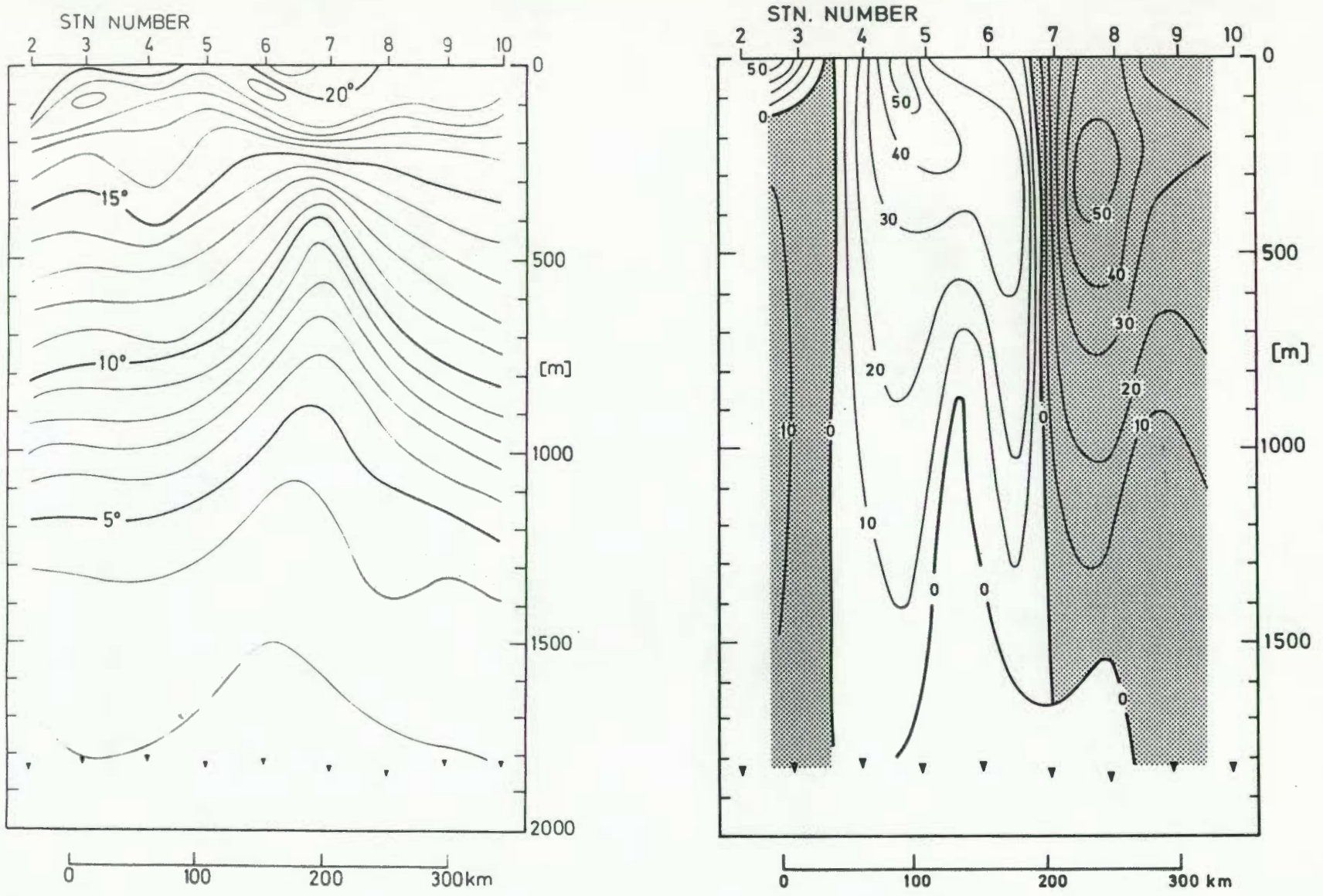

FIG. 7.10 : (a) Vertical section of temperature for stations 2-10 in eddy Echo, June 1978.
(b) Gradient velocities (in cm/s) relative to 1800 m in eddy Echo, June 1978. Shaded areas indicate flow out of the page.

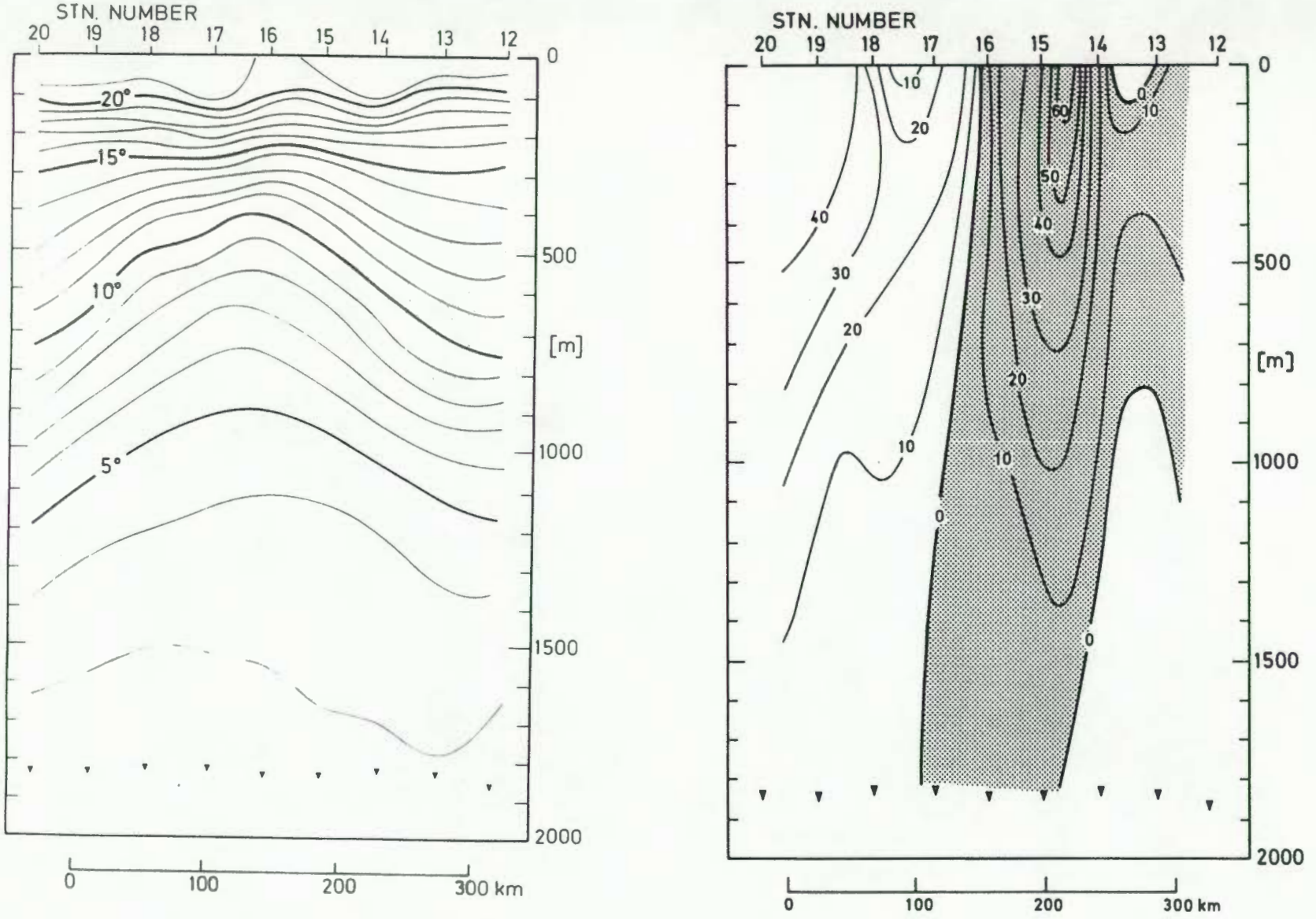

FIG. 7.11 : (a) Vertical section of temperature for stations 12-20 in eddy Echo, June 1978.
(b) Gradient velocities (in cm/s) relative to 1800 m in eddy Echo, June 1978. Shaded areas indicate flow out of the page.

From stations 4 and 5 onwards the isotherms below about 15°C started curving upwards, while those near the surface (16°-20°C) dipped downwards. The upheaval of the 10°C isotherm culminated at station 7 (420 m depth) although the interpolated representation in Fig. 7.10(a) actually shows the peak to be between stations 6 and 7 at a depth of 390 m. Beyond station 7 the isotherm started deepening again and at station 10 attained more-or-less the same height as they had at the start of the survey. The proximity of this eddy to where Echo had been observed, suggested that the same eddy had been located again.

The transect from station 12 toward the southwest revealed a shoaling of the isotherms that reached their shallowest depth at station 16 and deepened again in the southwestern section of Echo. The upheaval of isotherms was not as pointed as during the previous transect (compare Fig. 7.10(a) and 7.11(a)), and it was apparent that Echo had an oval rather than a circular shape, with the major axis in line with the section between stations 12 and 20.

On station 17 the weather worsened and because of the violent movement of the ship, the reversing bottles were not used again. With winds gusting more that 17 m/s and swells of up to 8 m, the survey was abandoned and the vessel steamed back to Durban, arriving on 22 June.

7.4.2 Results

The shape and size of Echo can be seen from the topography of the 10°C isotherm surface (Fig. 7.12). The eddy was again elliptical, but the major axis was now orientated NE-SW, compared to NW-SE in May (Fig. 7.7). The dimensions of Echo were now 120 km by 240 km.

The circulation is portrayed by a combination of the dynamic topography and the true currents (Fig. 7.13). In this case, the ship sets between stations were used to estimate the true drift on station, and these drifts in turn were used to correct the relative currents measured from the drifting ship. The shape of the contours of dynamic topography was adapted to the direction of the current vectors.

The gradient velocities relative to 1800 m (Figs. 7.10(b) and 7.11(b)) reveal a maximum of 60 cm/s. There was also a significantly-strong contra-rotating flow between stations 2 and 3 (see Fig. 7.14),

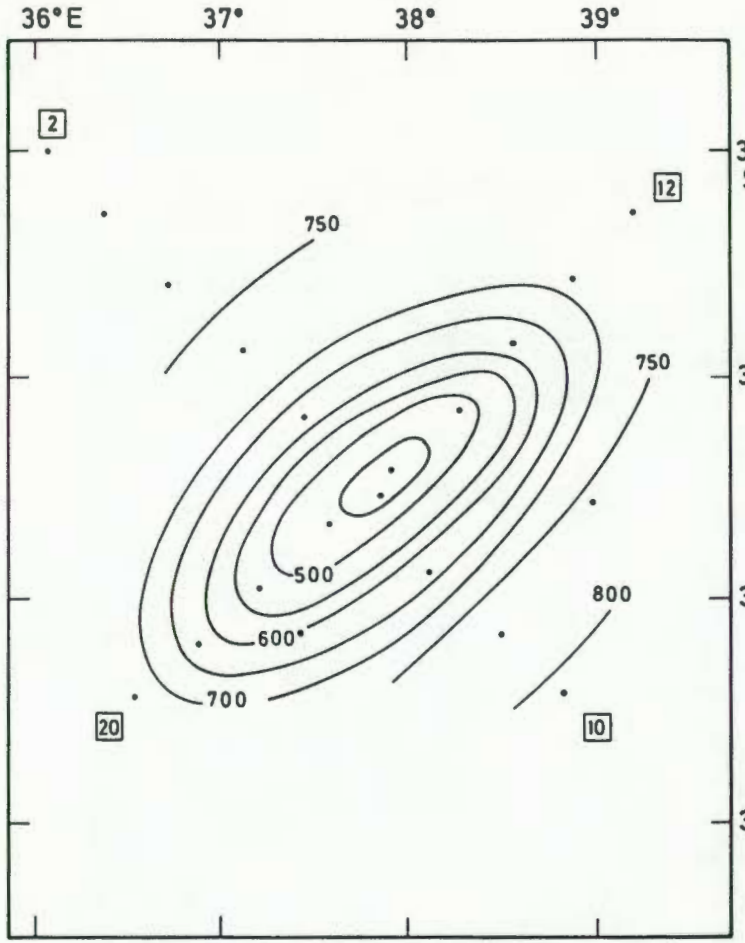

FIG. 7.12 : Topography of the 10°C isotherm surface (in m depth) across eddy Echo in June, 1978.

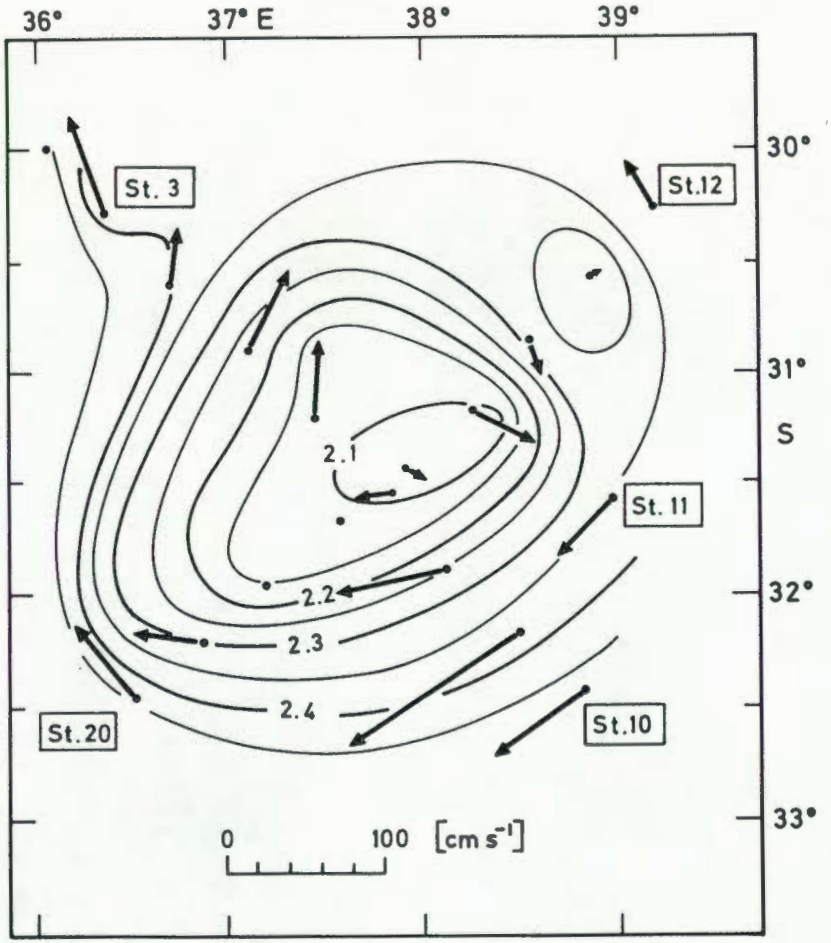

FIG. 7.13 : Geopotential anomaly (in 10^{-1} m^2/s^2) of the sea surface relative to 1800 m in eddy Echo, June 1978. Vectors represent measured current velocities at 10m depth.

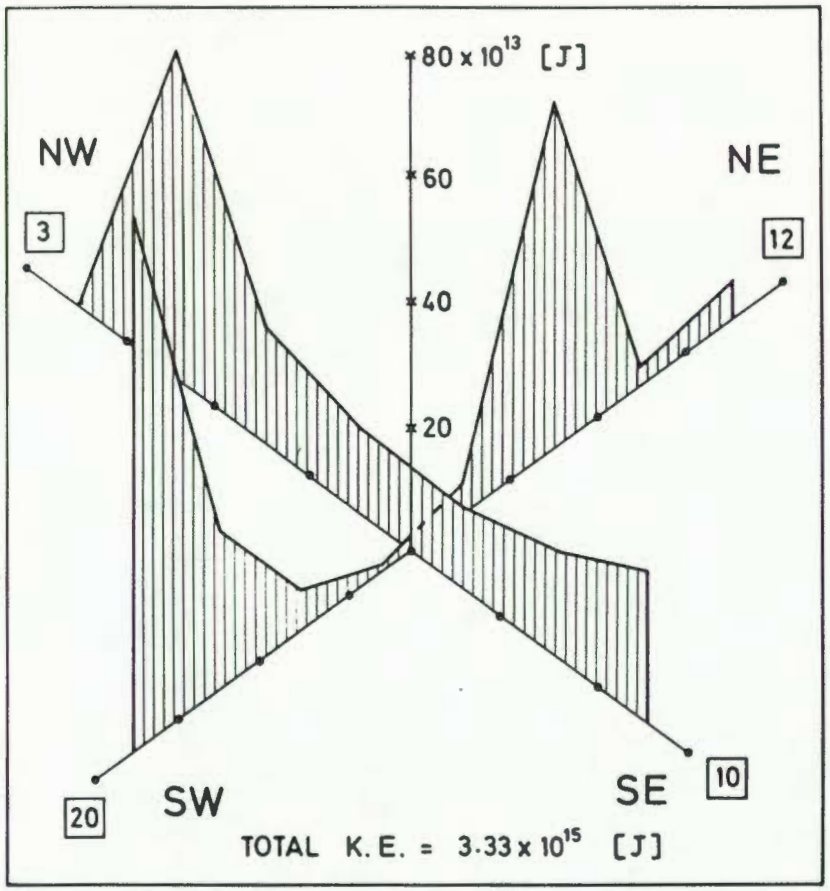

FIG. 7.14 : Kinetic energy (relative to 1800 m) of eddy Echo in June, 1978.

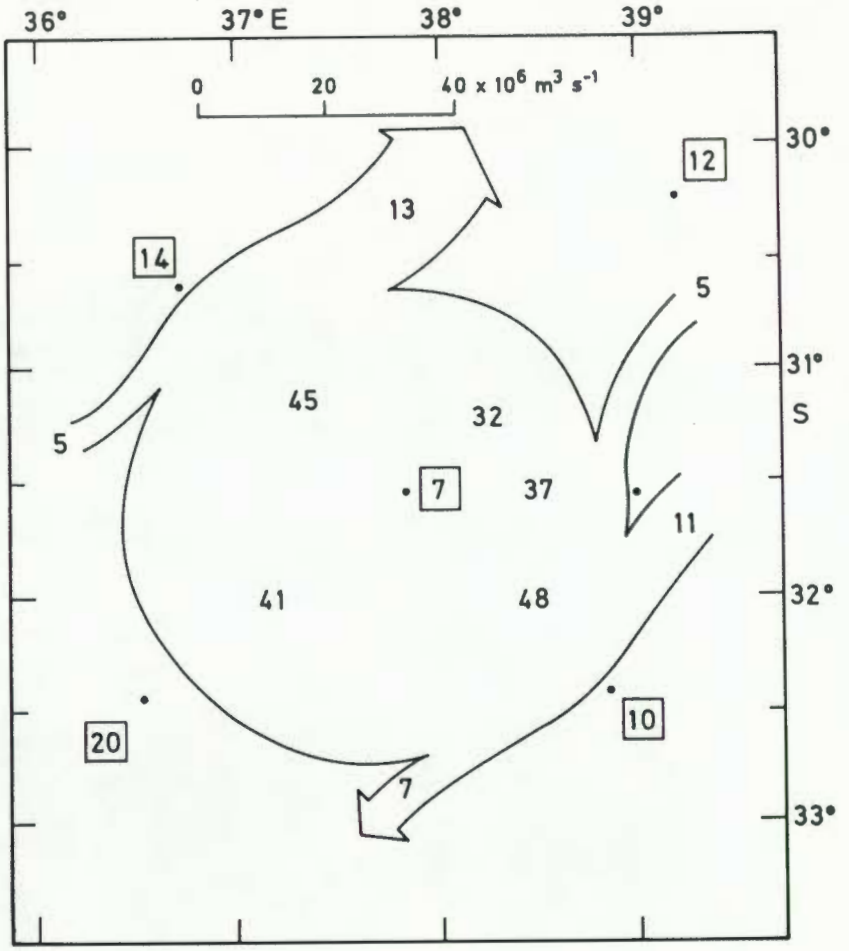

FIG. 7.15 : Volume transport relative to 1800 m of eddy Echo in June, 1978.

although this was confined to the upper 200 m.

The distribution of kinetic energy in Echo (Fig. 7.14) showed peaks in all sectors except the southeasterly part of the eddy. This is the only region where the maximum current velocity was located at 300 m depth, whereas in the other sectors the maximum velocity was situated at the surface.

The volume transport (Fig. 7.15) confirmed the high values derived from the May cruise (Fig. 7.9), with fluxes ranging from 32 to 48 x $10^6 m^3 s^{-1}$.

7.5 Satellite imagery

For the duration of the three-cruise experiment, infrared images from two satellites were obtained. First, NOAA-5 scanned the area off Southern Africa on the average every second or third day. These images had been enhanced by the NOAA (National Oceanic and Atmospheric Administration) Satellite Data Services Division according to a more-or-less standard enhancement curve, and the surface temperature patterns were very indistinct. In addition, the orbiting satellites such as NOAA view a different part of the ocean each time, making it difficult to correct for the distortion. For these reasons, the NOAA images were not very useful.

Second, images were also received from the METEOSAT satellite. METEOSAT was placed in a geostationary orbit above 0°S, 0°E and images were obtained on a daily basis from the Satellite Remote Sensing Centre of the CSIR. Although the satellite images are also distorted because of the earth's curvature, the distortion is the same in all scenes and therefore easier to accommodate.

Because of the almost-perpetual cloud cover over the target area, only a few scenes were useful in the sense that a reasonably clear impression of the sea-surface temperature (SST) patterns are obtained. These covered mainly the period of the May cruise, and in Fig. 7.16 two of these images are portrayed in the form of line-drawn representatives.

On the 9th May (Fig. 7.16) a broad flow entered the target area from the north and revealed a meandering, bifurcating pattern in the

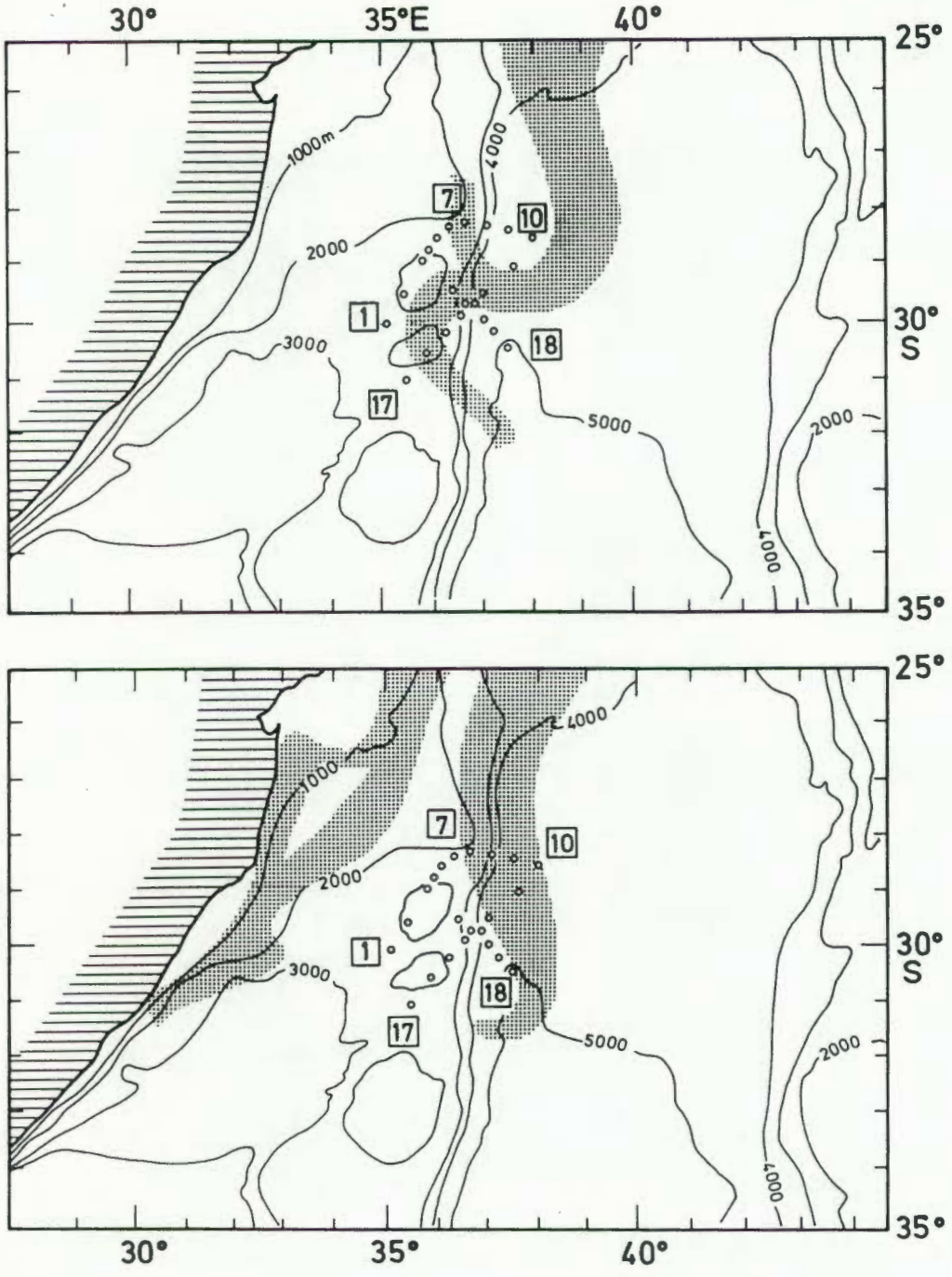

FIG. 7.16 : Representation of two infrared images obtained from the METEOSAT satellite on 9 May (top) and 20 May 1978 (bottom). Shading represents warmer water; the stations of the cruise in May, 1978 are indicated.

vicinity of 30°S 38°E. Another image was obtained after the cruise (20 May, see Fig. 7.16) and this shows that the SST pattern had shifted further south. Close to the coast, the cloud cover had decreased sufficiently to enable the Agulhas Current to be recognised. To the north of 25°S the SST was so high that the enhancement had been unable to distinguish any patterns.

The satellite SST agreed very well with the ship observations and increased the coverage of the flow patterns. The images showed how a current formed an eddy-like circulation at 29°S, 37°E on 9 May, and how this circulation advected at about 20 cm/s southward to reach 31°S, 37°E on 20 May (all values are very approximate).

7.6 Discussion

Based on the proximity of the eddies observed in May and June, and the satellite imagery, it is safely assumed that the eddies were one and the same, namely Echo. There are, however, noticeable changes in Echo's characteristics from the one survey to the next. First, Echo was more symmetric in June than in May. This is not solely an effect of the partial coverage attained during the May cruise, nor can it be the result of the shallower reference level during the May cruise (1500 m) compared to the June cruise (1800 m).

Second, the "intensity" of Echo seems to have increased from the May to the June cruise. In terms of the geopotential topography, Echo's centre was depressed 15 dyn cms (=1.5 $m^2 s^2$ relative to 1500 m) more than in May. This seemed to indicate that the eddy had still been in a formative stage during May.

Third, there was evidence of a strong input current from the north during the May cruise, a feature that was completely absent in June. This "source current" injected 20 x $10^6 m^3 s^{-1}$ into the system, and it seems that the transport distribution of Echo in June gave account of this added amount.

By considering the cruises in May and June, the following tentative conclusions about the characteristics of Echo can be drawn:

a) Propagation course and speed

Since the "centre"of Echo could not be geographically determined closer than the station interval, it has been assumed that the centre was first located at 30°14'S, 37°8.5'E (station 19, 21h38, 15 May) and later at 31°25'S, 37°54'E (station 16, 16h59 19 June) respectively. This displacement represents a speed of 5 cm/s toward 151°. This should not, however, be considered as evidence that the eddy was free-drifting, which obviously was not the case in May 1978. From the satellite images, the advection speed at the time of the May survey was 20 cm/s.

b) Surface temperature

The maximum temperature recorded at the surface in May was close to 25.0°C (in the vicinity of station 8 and 12), while the "input" current from the north had a temperature of about 24°C. The temperatures in June were much lower, with maximum temperatures of just over 22°C recorded in the vicinity of stations 2 and 8, and this suggests that Echo had cooled by about 2-3°C during the month between cruises.

c) Dimensions and orientation

During both surveys, Echo had an elliptical shape of about 100 km by 240 km. The increase in the amount of water transported within this frame, was taken as indicative of the "growth" of Echo, similar to the increase in topographic depth of the centre. Another noteworthy aspect is the apparent horizontal rotation of the eddy axes. During the survey in May, Echo's major axis was orientated NW-SE, while a month later it was orientated NE-SW.

The observation of Echo had clearly confirmed that the Mozambique Ridge was a generation area of eddies. Since the Agulhas Current had been observed in April and May close to the African coast off Cape St. Lucia, the eddies were spawned by another current much further offshore.

This current was much stronger during the cruises in 1978 than it was at the time of Delta (1977). Echo was also much larger than all the previously-observed eddies.

Some comments have been made above about the changes observed in Echo between the May and June surveys. Equally relevant to the existence and characteristics of Echo was the disappearance of the "host current" in the time between surveys. This means that in the month between surveys this current had either stopped flowing or became displaced outside the survey area. Although the origin of the current was unknown, such variability of a current that transported some 20 x $10^6 m^3 s^{-1}$ one month and vanished the next was quite remarkable.

At this stage of the study, it became obvious that the investigation had two distinct but nevertheless related aspects: On the one hand the existence of intense, cyclonic eddies had been established. In fact, it had been possible to show that these eddies were more common than originally imagined. On the other hand, the eddies must have been generated by a current of which there has been only a passing glimpse. This current represented the major component of the interaction between the eddies and their environment. Surveys that included this current as a target (besides the vortices themselves) were important, but would be difficult to execute because of the limited duration of the vessel. It was hoped that, similar to the observation of this current in May, more information could be gathered of the current without impeding the surveys of vortices.

CHAPTER 8

OBSERVATIONS OF DEEP-SEA VORTICES : 1979 AND 1980

8.1 Introduction

The cruises in December 1979, January and March 1980 that are discussed here were chosen about six to eight weeks apart since it was hoped that an eddy could be located during the first cruise and tracked during the other cruises. Included in this chapter are the tracks of satellite-tracked buoys that were launched in 1979 and fortuitously drifted into the area. The presence of these buoys in the vicinity of the Mozambique Ridge during the summer of 1979/80 was an unexpected but very welcome bonus to the hydrographic surveys. The drift of these buoys enabled us to see the hydrographic data collected through the rather limited coverage of the ship against the background of the larger-scale circulation in the southwestern Indian Ocean. The results obtained during this time proved to be the most enlightening of the whole study.

Apart from being an attempt to locate and survey any vortices in the Mozambique Ridge region, the cruise in December 1979 had two additional aims: First, an NBIS CTD, which had been acquired during 1979, was to be tried operationally for the first time. Second, if an eddy was located, a free-drifting array of five current meters would be deployed from and tracked by the *Meiring Naudé*. The objective of the deployment of current meters would be to ascertain whether there was any significant radial motion away from the eddy centre, as the results of the cruise in June 1977 (Chapter 6) had suggested.

8.2 Narrative of the November/December 1979 cruise

Shortly before the cruise commenced, a visit was paid to the CSIR's Satellite Remote Sensing Centre at Hartebeeshoek. There, the most recent infrared images from METEOSAT were inspected for evidence of any conspicuous thermal patterns in the vicinity of the Mozambique Ridge.

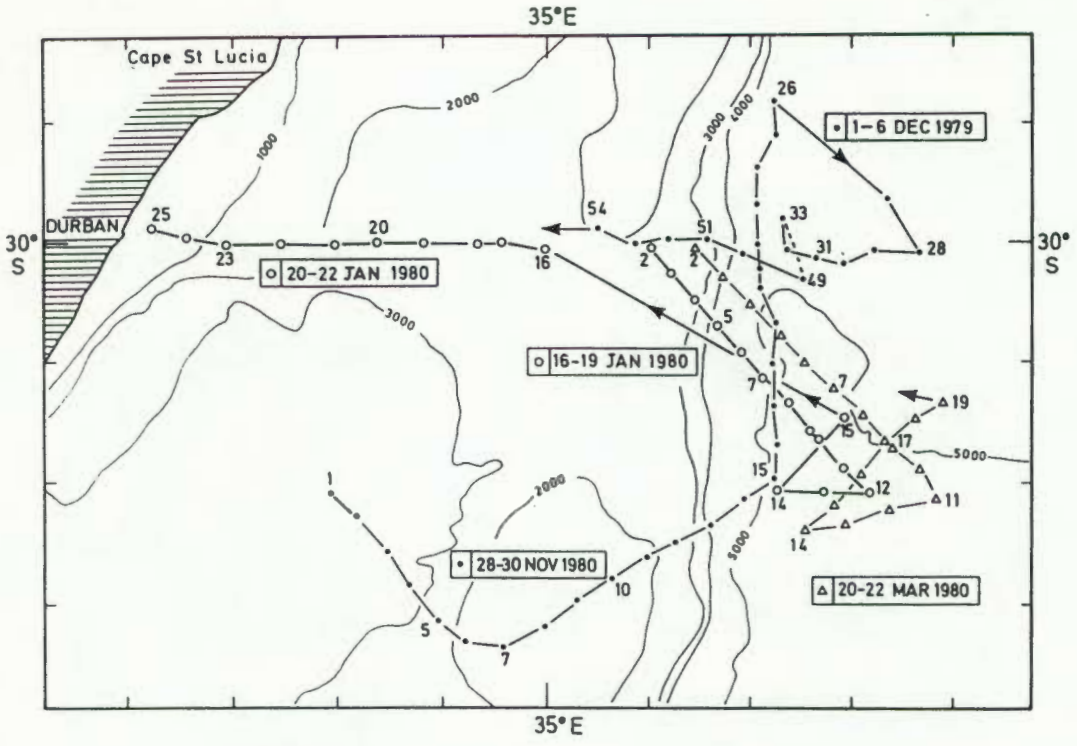

FIG. 8.1 : Station chart og the *Meiring Naudé* cruises in November/December, 1979 (dots), January, 1980 (circles) and March, 1980 (triangles).

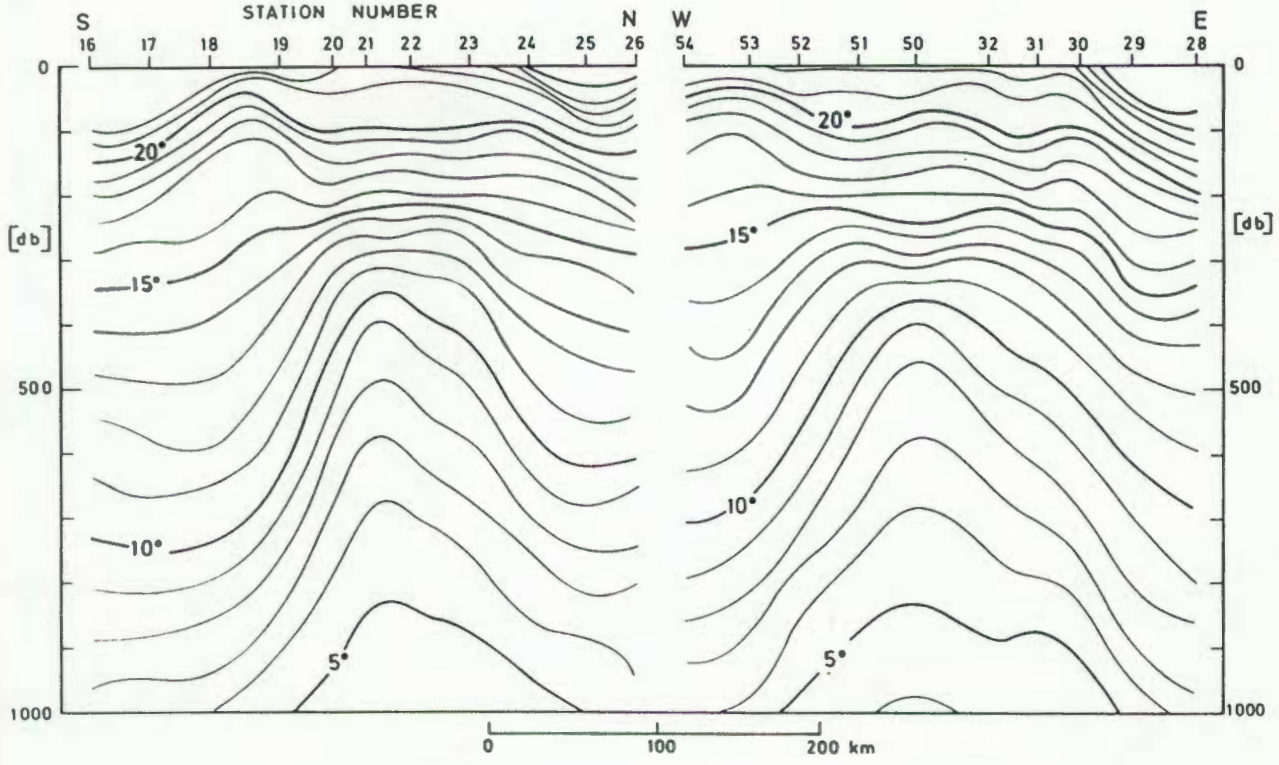

FIG. 8.2 : Vertical sections of temperature across eddy Fred during the cruise in November/December, 1979.

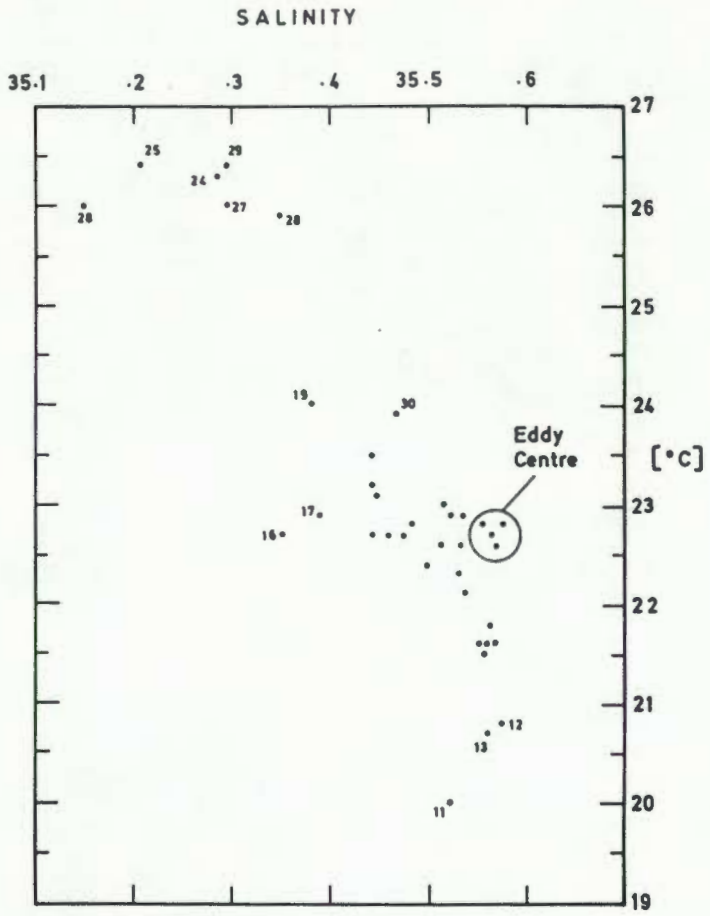

FIG. 8.4 : T/S diagram of surface values during the cruise in Nov. /Dec., 1979.

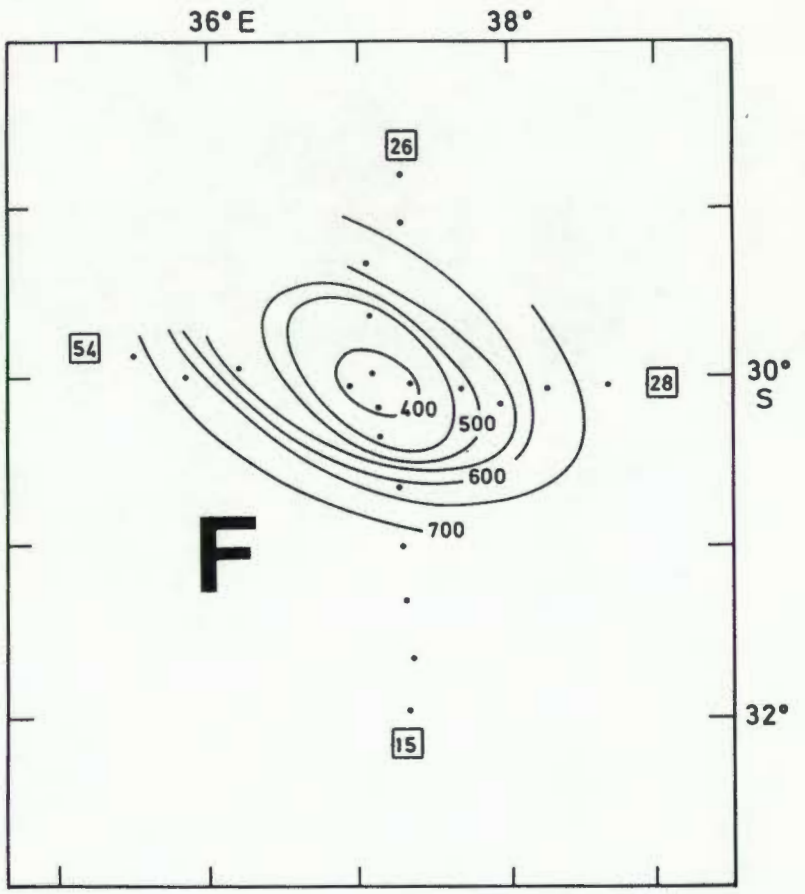

FIG. 8.5 : Topography of the 10°C isotherm (in m depth) of eddy Fred, Nov./Dec., 1979.

Unfortunately, the Ridge area itself was covered with cloud, but the clear area to the southwest of the Ridge showed some faint "ribbons" of warmer water. It was considered that these filaments of warm water may be associated with currents or vortices, and the cruise plan was amended to include the area of the thermal patterns.

The *Meiring Naudé* left Durban on 27 November, and hydrographic stations were started the next day at approximately 32°S. 33°E (see Fig. 8.1). From this position, stations were continued along a direction of 135°T.

After six stations that failed to produce any signs of strong currents or a vortex, the course was altered at station 7 to 060°T and after station 15 to 000°T. These course changes carried the vessel progressively northwards into an area where vortices had previously been observed (see Chapters 4-7).

The northward leg after station 15 eventually revealed a significant upheaval of the isotherms signifying an eddy (codenamed Fred) at about 30°S (Fig. 8.2). Upon completing this northerly traverse, an east-to-west section along 30°S was started at about 38°S 43'E (station 28).

At station 32, this section was interrupted to deploy an array of current meters about 40 km to the northeast of the eddy centre. The array was designed to drift freely and was tracked by the vessel over a distance of approximately 60 km. Hydrographic stations were continued at two-hourly intervals during the deployment period, but adverse weather conditions caused a cessation of the profiling at 15h00 on 4 December (i.e. after the array had been drifting for about 30 hours). The weather was worsening continuously, and the eventual recovery of the array turned out to be quite an experience (see Appendix 7).

The east-west section across the eddy centre and further westwards was then completed with stations 50 to 54. At station 54, about 150 km west of the eddy centre, the isotherms had levelled again (Fig. 8.2) and the survey was terminated. The *Meiring Naudé* returned to Durban on 7 December.

8.3 Thermohaline characteristics of Fred during November/December 1979

8.3.1 Isotherm depth changes

As mentioned above, the isotherms tended to be very much horizontal

up to station 6. Between stations 7 and 15 there was a general rise in the deeper-level isotherms while the shallower layer (0-300 db) exhibited some significant variations between stations 10 and 14. Corresponding fluctuations are visible in the thermograph record and sea-surface salinity variations (Fig. 8.3). It is possible that the thermal fronts encountered during this traverse were responsible for the infrared patterns observed in the satellite images. Water with surface T/S characteristics similar to those at station 11-13 is normally found only at deeper levels (100-200 db), indicating that water of subtropical-central origin has risen to the surface in this area. Some of the variations may have been a result of the proximity of an eddy east of station 15 - a feature that was only discovered during the cruise in January 1980 (see section 8.7).

At station 19 there was a conspicuous filament of almost-tropical water (Fig. 8.3), and this is considered to have been a branch of the tropical water located north and east of Fred (e.g. stations 25 and 28). The vertical section of temperature (Fig. 8.2) indicates that this branch was associated with the westerly flow along the southern flank of Fred.

From station 18 to 21 (Fig. 8.2) the isotherms exhibited a strong upward displacement. Elevations of 250-400 db were displayed by most of the isotherms below 10°C. In the surface layers above 300 db there was a marked reverse inclination of the isotherms, so that the upward trend of the deep isotherms coincided with a downward trend of the shallower ones between stations 19 and 20.

The north-south traverse located Fred's centre between stations 21 and 22, but the isotherms were not as "cusped" here as with previous eddies. So, e.g., the 11°-14°C isotherms displayed a "tabular" formation rather than a pinnacle. The colder water below 300 m coincided with a broad bowl of warm water at the surface. The T/S values of the surface water at the centre of the eddy did not appear any different from those originating from areas to the south of the eddy (Fig. 8.4).

The initially hesitant descent of the isotherms between stations 21 and 23 was followed by a sharper slope between stations 23 and 25 (Fig. 8.2). This coincided with a sharp thermohaline front at the surface immediately south of station 24 (Fig. 8.3). The surface T/S values of station 24-26 (Fig. 8.4) show that the water in this area was of tropical origin.

Surface data showed (Fig. 8.4) that the other stations along the northeastern flank of the eddy (stations 27-29) were all situated in the same tropical water mass. Along the east-west section this water mass extended up to station 29, and was again separated from the water of more subtropical origin by a strong thermohaline front (Fig. 8.3).

The slightly elongated shape of the isotherm elevation was also evident in the east-west section. Sharp changes in depth of the isotherms between stations 28 and 30, and between station 50 and 53 were separated by a much weaker variation. The 10°C isotherm rose from about 700 db at station 28 to 370 db at station 50, then dropped again to 700 db at station 54. Fred was elliptical (see Fig. 8.5) with its major axis orientated NW-SE, and its size was aboug 170 x 210 km.

No further thermohaline surface fronts were observed in the western sector of the eddy, indicating that the westward intrusion of semi-tropical water across the N-S line at station 19 did not extend much further westward.

8.3.2 Variations in the mixed layer depth

In contrast to the results obtained in previous eddies, no consistent trends were found in the variation of the mixed layer depth this time. At most stations inside Fred there was no mixed layer at all, which was very surprising if only in the light of the high wind and swell conditions that were experienced.

8.3.3 T/S structure in the upper 300 db

Some of the stations with tropical-water characteristics also displayed anomalous T/S structure at subsurface levels. A T/S analysis of the data above 15°C at station 27 showed evidence of incomplete horizontal mixing, or interleaving, between the tropical and subtropical surface water masses.

8.3.4 Subthermocline anomalies

For most of the stations inside the eddy, the deep temperature profiles were relatively smooth (see Fig. 8.6). However, some stations revealed conspicuous layering characteristics below 700 db with water at some depths up to 0.5°C *warmer* than the layers immediately above. The

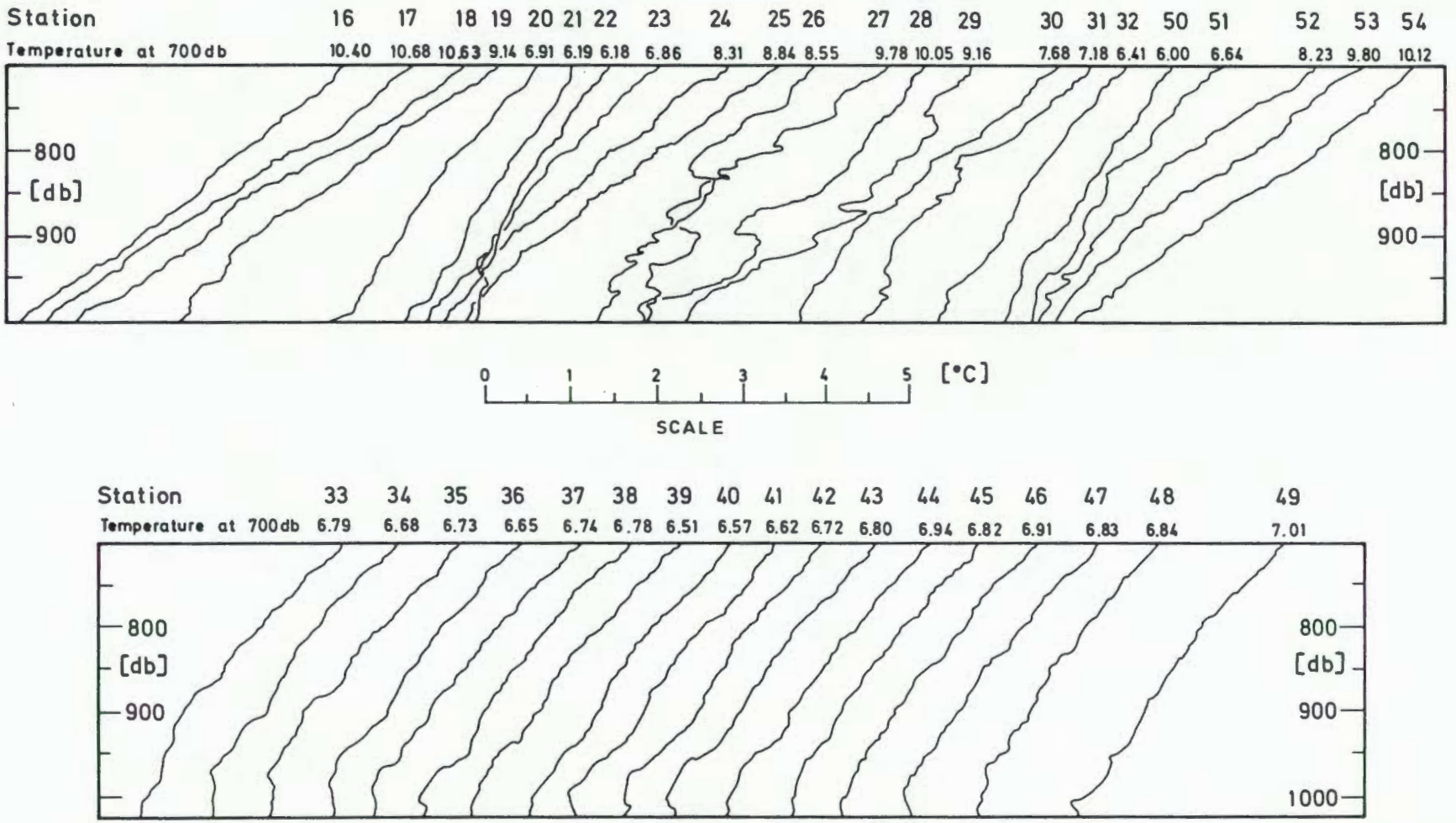

FIG. 8.6 : Vertical profiles of temperature between 700 and 1000 db for selected stations of the *Meiring Naude* cruise in November/December, 1979. Note the anomalously-high temperatures in 800-1000 db of stations 26-29, as well as some inversions on other stations.

upper edge of the anomalies was manifested by a sharp discontinuity in temperature and salinity, while the characteristics of the lower edge are unknown since profiling was only done to 1000-1025 db. The anomalies were most conspicuous at stations 26-29 and 31, and to a lesser extent at stations 23, 30, 50-52. Some irregularities also appeared in the vertical profiles of the drift stations. Most of these stations were situated to the north and east of the eddy centre, while station 26-29 formed part of the group of stations where tropical surface water was observed. At station 26 the discontinuity in the temperature/salinity profile was located at 825-835 db, while at station 27 and 28 it was about 75 db deeper, namely at 895-915 db. At station 29 it was shallower again at 765 db. This difference in depth can be explained in terms of the dynamics of Fred, stations 26 and 29 having been closer to the centre of the eddy than the other two stations.

In Fig. 8.7 a comparison is drawn between the T/S distribution of "normal" stations and those of stations 26-29. The T/S points belonging to the anomalous strata between 700 and 1000 db of station 26-29 form a cluster in the vicinity of T = 7.34°C, S = 34.78 °/oo and have σ_T = 27.23 According to the data collected throughout the Indian Ocean during the International Indian Ocean Expedition (WYRTKI, 1971), these anomalous points originate from the Red Sea. WYRTKI'S (1971) distribution charts show that water from the Red Sea has preference of advecting down the Mozambique Channel instead of along the eastern coast of Madagascar.

The appearance of Red Sea water on the northeastern perimeter of the eddy is slightly problematic. If the pocket of Red Sea water under discussion did in fact reach the area of the eddy via the Mozambique Channel, there is very little reason why it should be confined to one side of the eddy only. The issue will be raised again during the discussion in section 8.11.

8.3.5 Temperature time-series

The five current meters recorded temperature every 10 minutes while the array was drifting from 10h00 on 3 December to 05h00 on 5 December. The time series of temperature (Fig. 8.8) for the five meters show fluctuations with amplitudes up to 0.5°C and periods of the order of hours.

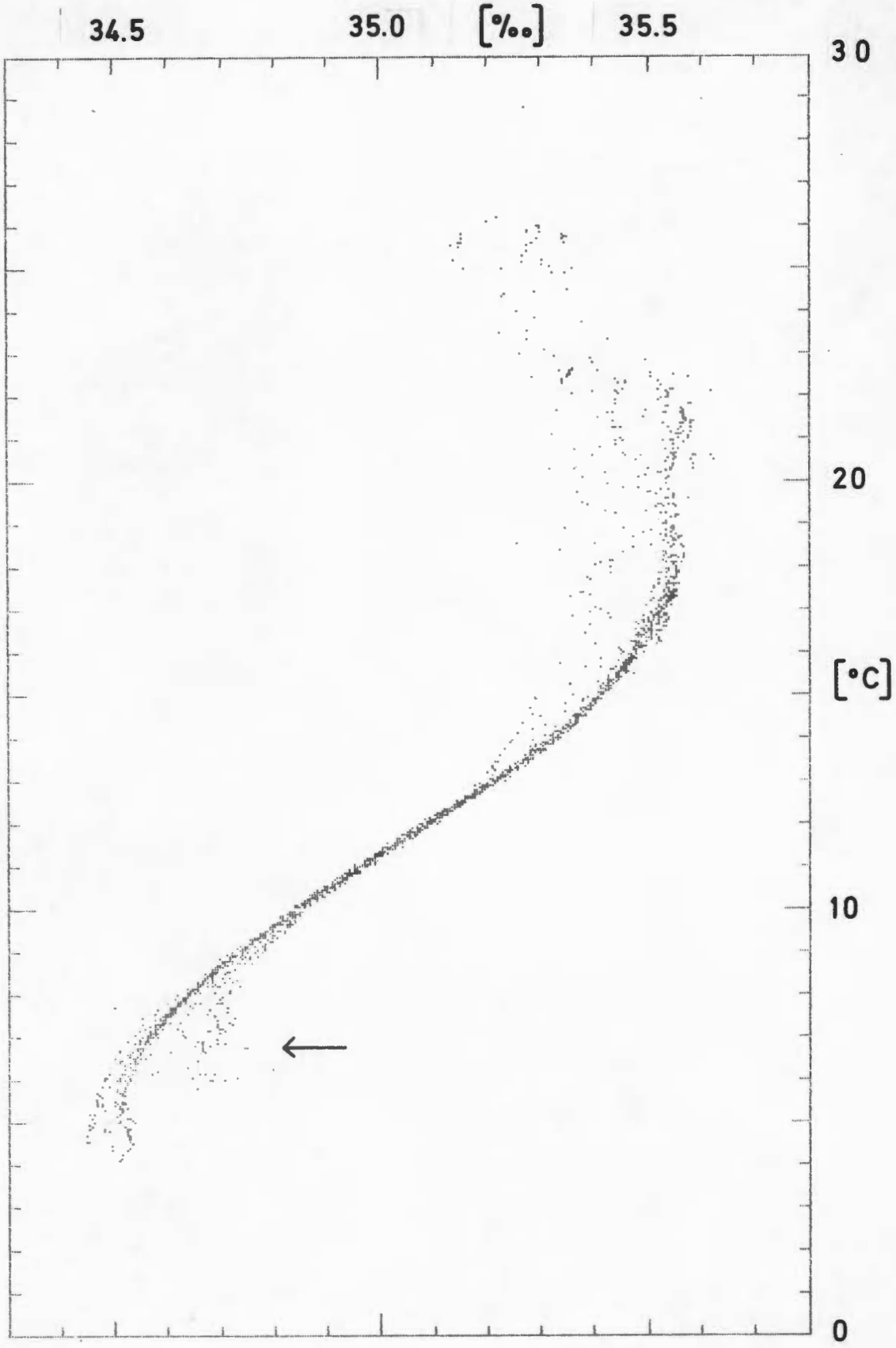

FIG. 8.7 : T/S plot (interpolated at 10 db intervals) of 20 selected stations of the *Meiring Naudé* cruise in December 1979. Between 5° and 9° the higher-salinity points, originating from stations 26-29, can be seen.

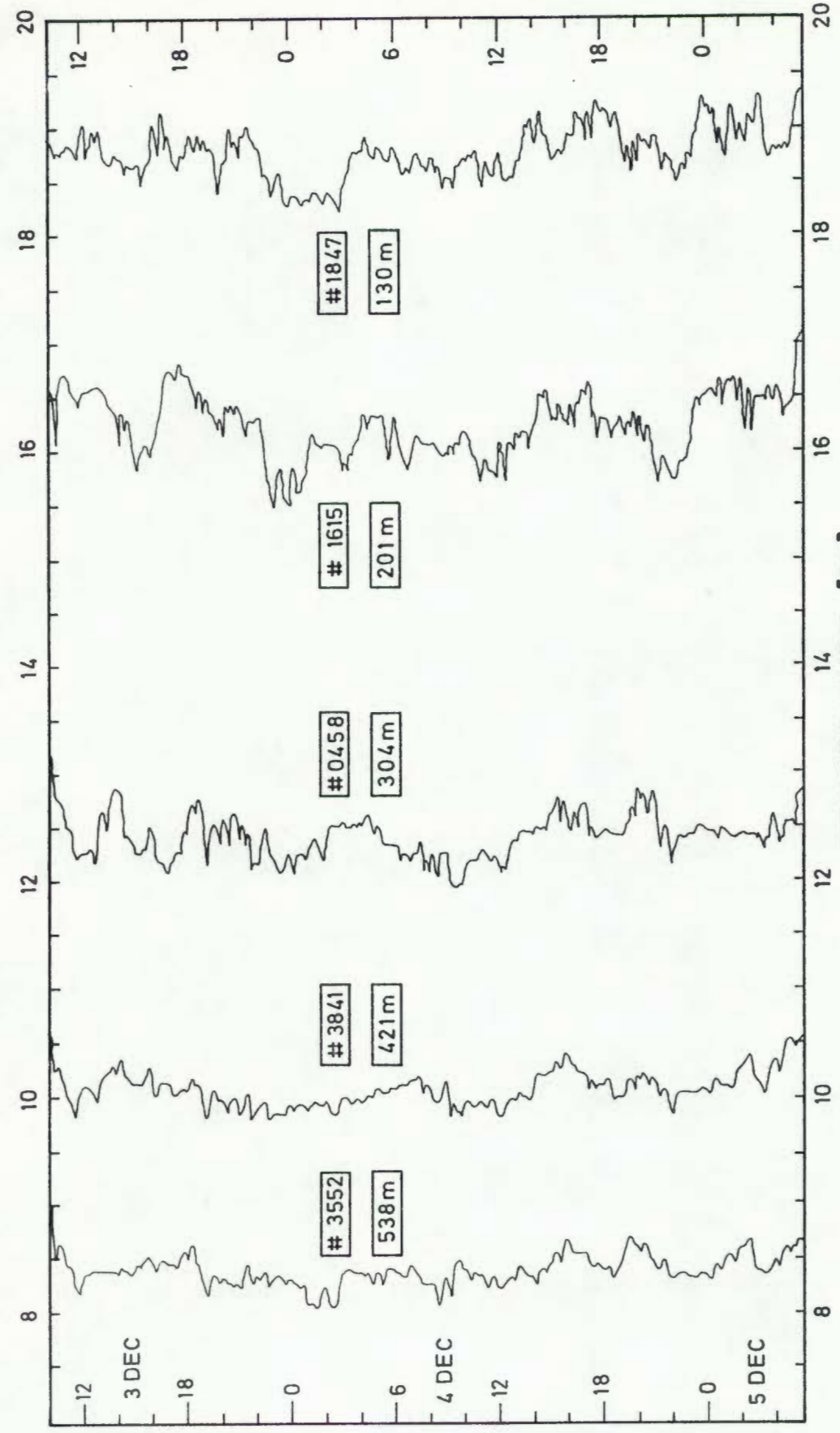

FIG. 8.8 : Time series of temperature from an array of five current meters that drifted between station 33 and 49 of the cruise in November, 1979.

Variations of this magnitude could not be explained in terms of a vertical motion of the array. The swell-induced motion of the array was shown (see Appendix 7) to have been very small, while a 0.5°C variation at the deepest meter (No. 3532) corresponded to a vertical displacement of approximately 50 m, using the temperature gradient recorded by the CTD. There was no evidence that the array became inclined because of vertical shear in the current velocity. Successive CTD records obtained at 2-hourly intervals during the drift station revealed that fluctuations in the temperature profile with amplitudes of 0.1–0.5°C were not uncommon. The time-series therefore confirmed that variations of this magnitude can occur, even at depths of 500 db.

8.4 Currents during the November/December cruise

Information on currents in the vicinity of the eddy originates from the following four sources: gradient currents, ship's drift, current meter array and satellite-tracked free-drifting buoys. The results of the buoy tracks will be discussed in section 8.10 below since their drift period and course encompassed both the December 1979 as well as the January 1980 cruises.

8.4.1 Geostrophic (gradient) currents

The geopotential topography (Fig. 8.9) of the stations in the eddy indicated that the centre of Fred was located at 30°2'S, 37°E. Fred's shape was clearly delineated by the equipotential lines, the drawing of which was guided by the ship sets. The geopotential confirmed the elliptic shape derived from the 10°C topography (Fig. 8.5)

After determining the position of the eddy centre, gradient currents were calculated for the transects across the eddy. The motion of the water relative to 1000 db (Fig. 8.10) showed a filament of high speed current flowing between stations 23 and 25 through the northern part of Fred, and continuing to intensify while passing between stations 29 and 30 in the eastern part. Comparison with the variation of surface temperature and salinity across Fred (Fig. 8.3) showed that the high-speed filaments coincided more-or-less with the positions of strong thermohaline surface fronts. A remarkable aspect of the velocity structure is that the maximum current was located at the surface in the northern and eastern parts, but became submerged in the other sectors.

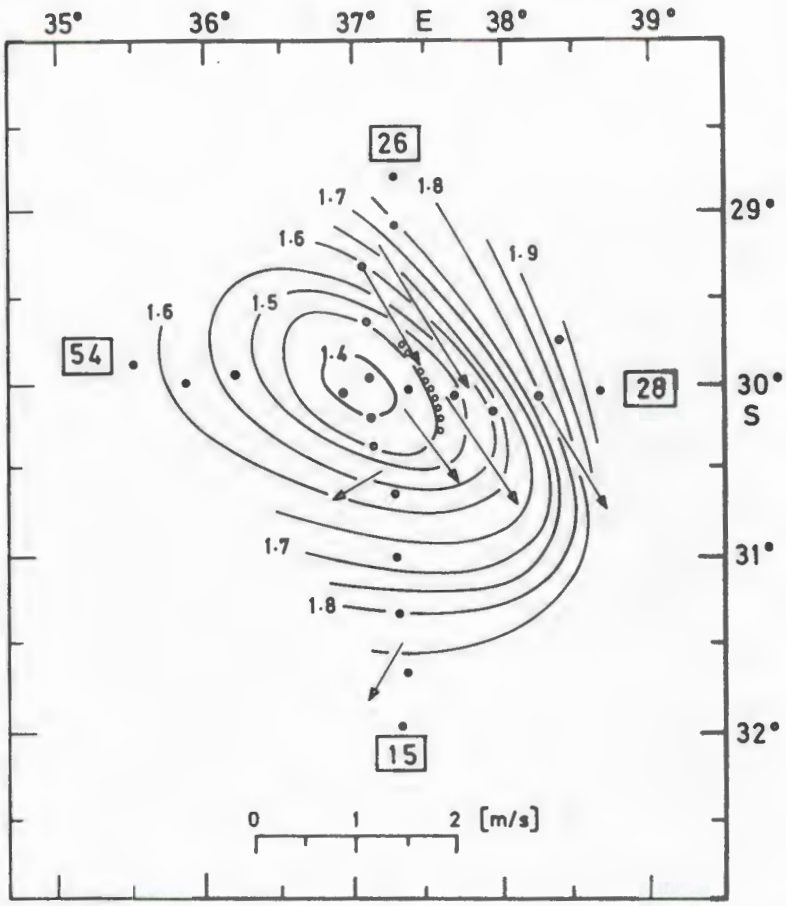

FIG. 8.9 : Geopotential topography of the sea surface relative to 1000 m (in units of 10 m^2/s^2) of eddy Fred in November/December 1979. Also included are ship set vectors (arrows) and the drift track of the current meter array (circles).

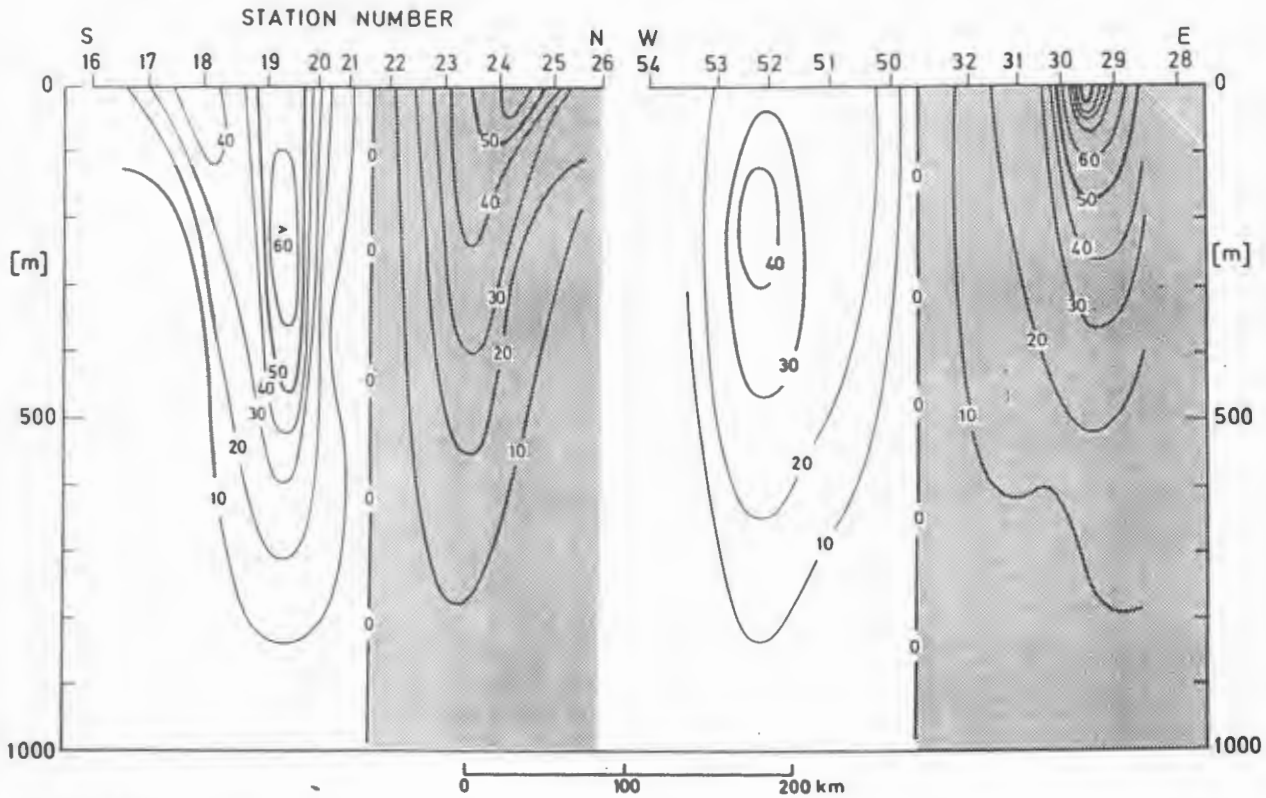

FIG. 8.10 : Gradient current velocity (cm/s) for two transects across eddy Fred, November/December, 1979.

Fred's kinetic energy (Fig. 8.11) was much higher than that of other eddies when measurements were also done to 1000 m. The total kinetic energy of the eddy amounted to 1.74×10^{15}(J).

8.4.2 Ship's drift

Disagreement between some of the ship sets and the geopotential topography (Fig. 8.9) could be due to any combination of the reasons listed in Appendix 3. As stated in section 8.4.1, the equipotential lines were drawn using the set vectors as a guide, so that any disagreement was minimised. Included in Fig. 8.9 is a representation of the drift of the current meter array, which closely followed the equipotential lines.

8.4.3 Current meter array

The objective of the deployment of current meters was to ascertain whether there was any significant radial motion away from the eddy centre, as the results of the cruise in June 1977 (Chapter 6) had suggested. The plan was therefore firstly to position the current meter array relatively close to (but not inside) the centre of the eddy, and secondly to measure the current in about 200-300 m (the depth in which the geostrophic maximum was expected). A total of five current meters were attached to the array in various depths from 130 m to 540 m.

Current velocities recorded by the five current meters that drifted between station 33 and 49 have been evaluated in Appendix 7. It was shown that, except during the first 12 hours or so of the deployment, when swell-induced vertical motion of the array probably falsified the records, the speeds should be a fairly accurate representation of the true current velocities at the time. Since the drift of the array could only be verified at about 6-hourly intervals every time the ship approached the array, average relative velocities were calculated for each period for which a drift speed was available, and the drift vector used to provide an absolute velocity (see Table A7.2).

(i) It can be seen from Fig A7.9 that during the four periods into which the deployment was separated, the current turned progressively clockwise through approximately 78°. This rotation of the vectors was

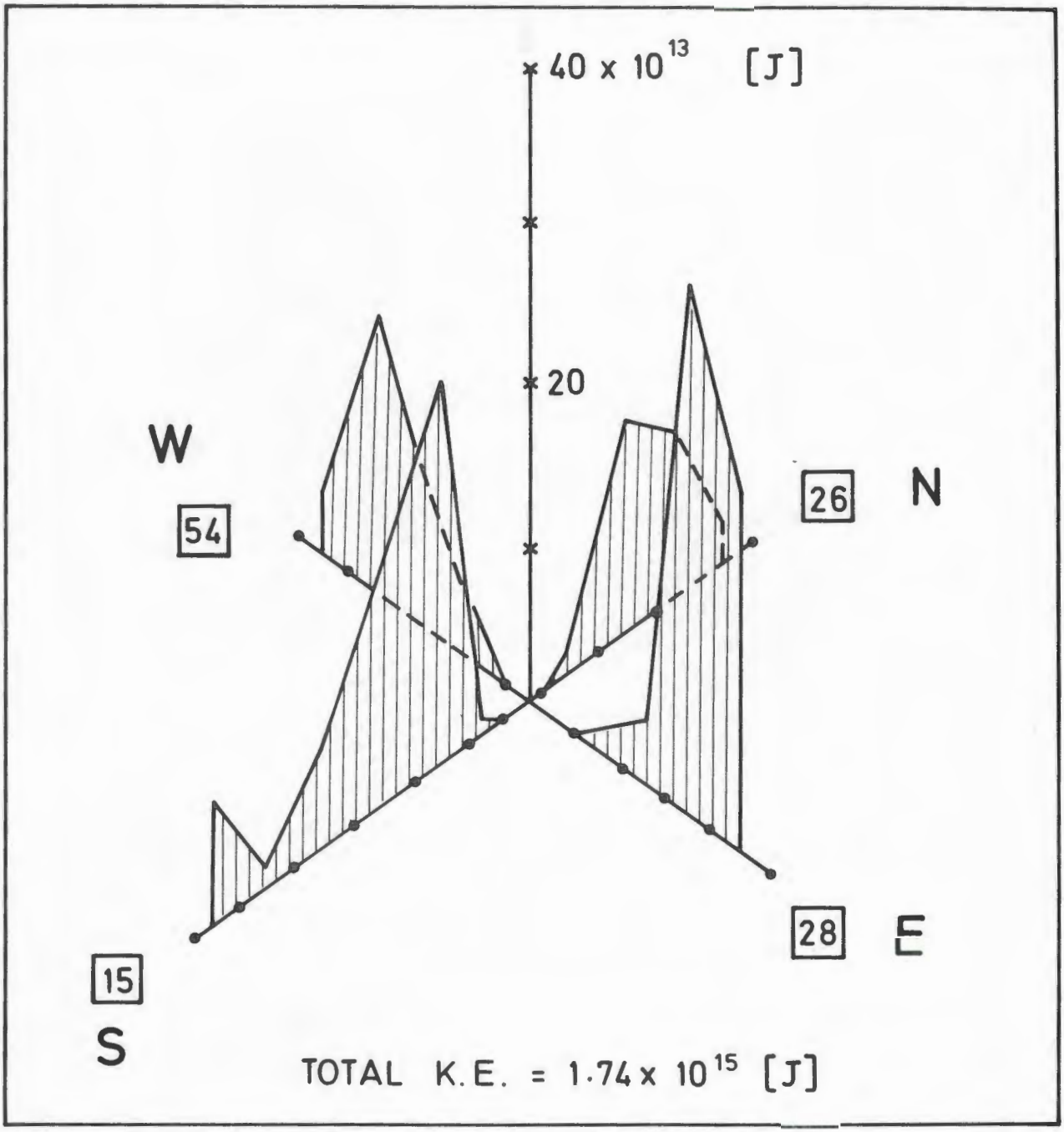

FIG. 8.11 : Distribution of kinetic energy along two transects across eddy Fred in November/December 1979.

explained in terms of the drift of the array from a direction of about 60° relative to Fred's centre at deployment to about 138° at recovery (see Fig. 8.9).

(ii) There does not seem to be any consistency in the relative orientation of the current vectors at different depths (Fig. A7.9). E.g. during period I the current vectors turned clockwise with depth, but they were not orientated in any consistent pattern during the other periods. This seems to answer the main objective of the current meter deployment, namely that the current vectors do not show any evidence of a significantly strong radial motion outward from the centre. This result is not altogether unexpected, since the surface thermal fronts (see Fig. 8.3) did not reveal the same helix shape as was the case with Delta (June 1977, Fig. 6.5). Failure to observe this phenomenon therefore does not exclude its existence at other vortices in this study.

(iii) The true current velocities recorded by the current meters during period III and IV respectively, are compared in Fig. 8.12 with the geostrophic velocity profiles from various stations in the vicinity of the array drift track. This comparison shows that the geostrophic velocities underestimated the true current on the average by approximately 20 cm/s, suggesting that the reference level for geostrophic computations should be much deeper than 1000 m.

8.5 Propagation of the eddy

Fred was estimated to have been drifting at 5-10 cm/s toward 160° during the time of the survey, based on the current meter data (see Appendix 4). It must be pointed out that, apart from being a very crude approximation of Fred's propagation, the value was probably only applicable during the few days of the array drift.

8.6 Volume Transport

The volume transport was calculated from the gradient currents. The results (Fig. 8.13) show that transport was greatest in the southern part of Fred and smallest in the northern part. Although the geopotential (Fig. 8.9) and gradient current velocity (Fig. 8.10) gave the impression that the current and concomitantly, the volume transport, was much higher in the northern and eastern section, this turned out to be not the case, and values ranged from 17 to 28 x $10^6 m^3/s$.

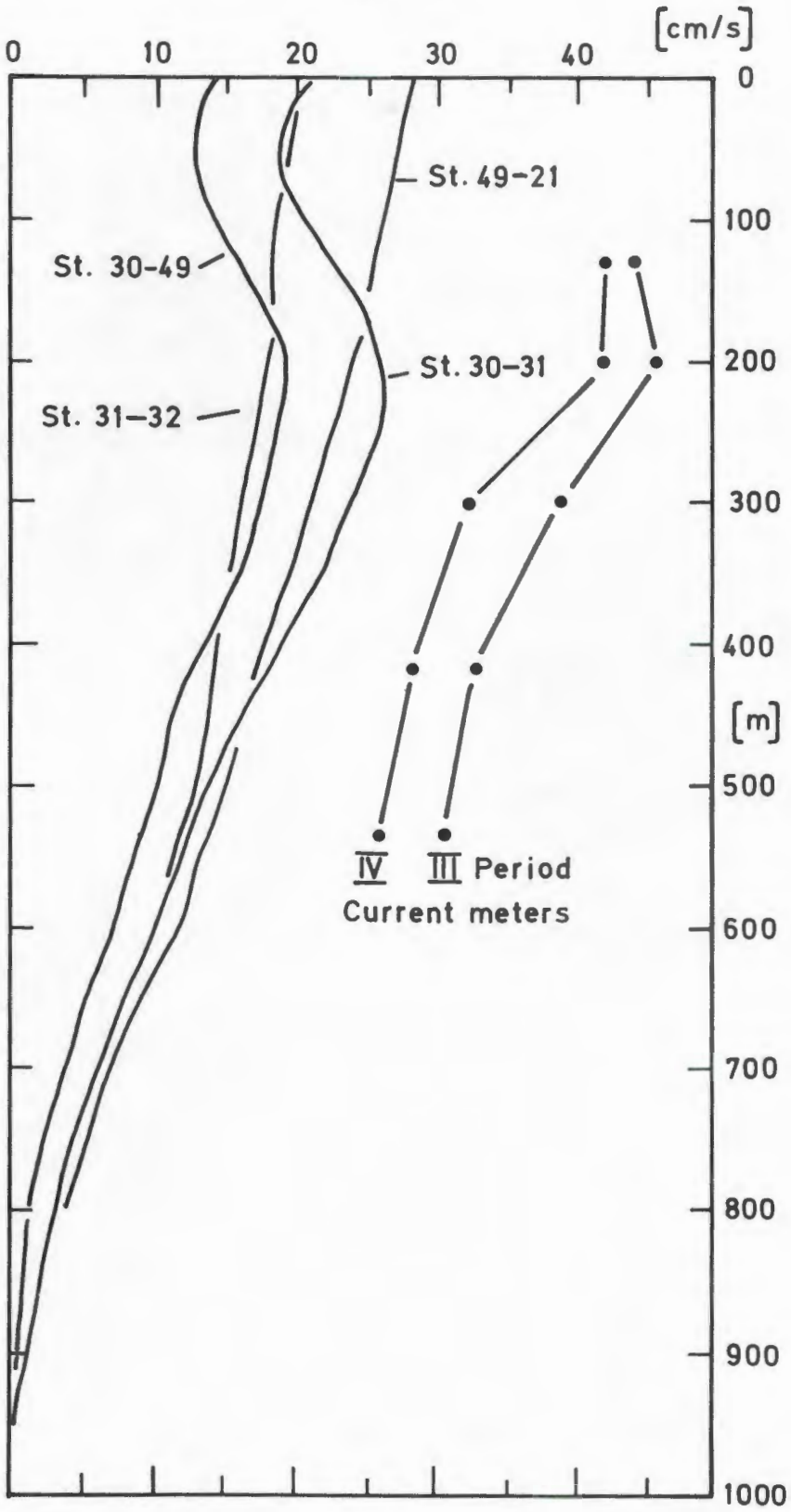

FIG. 8.12 : Vertical profiles of gradient velocity between four pairs of stations in the vicinity of the drifting current meter array, and the true velocity of the current meters during two periods of their drift (see Table A7.2).

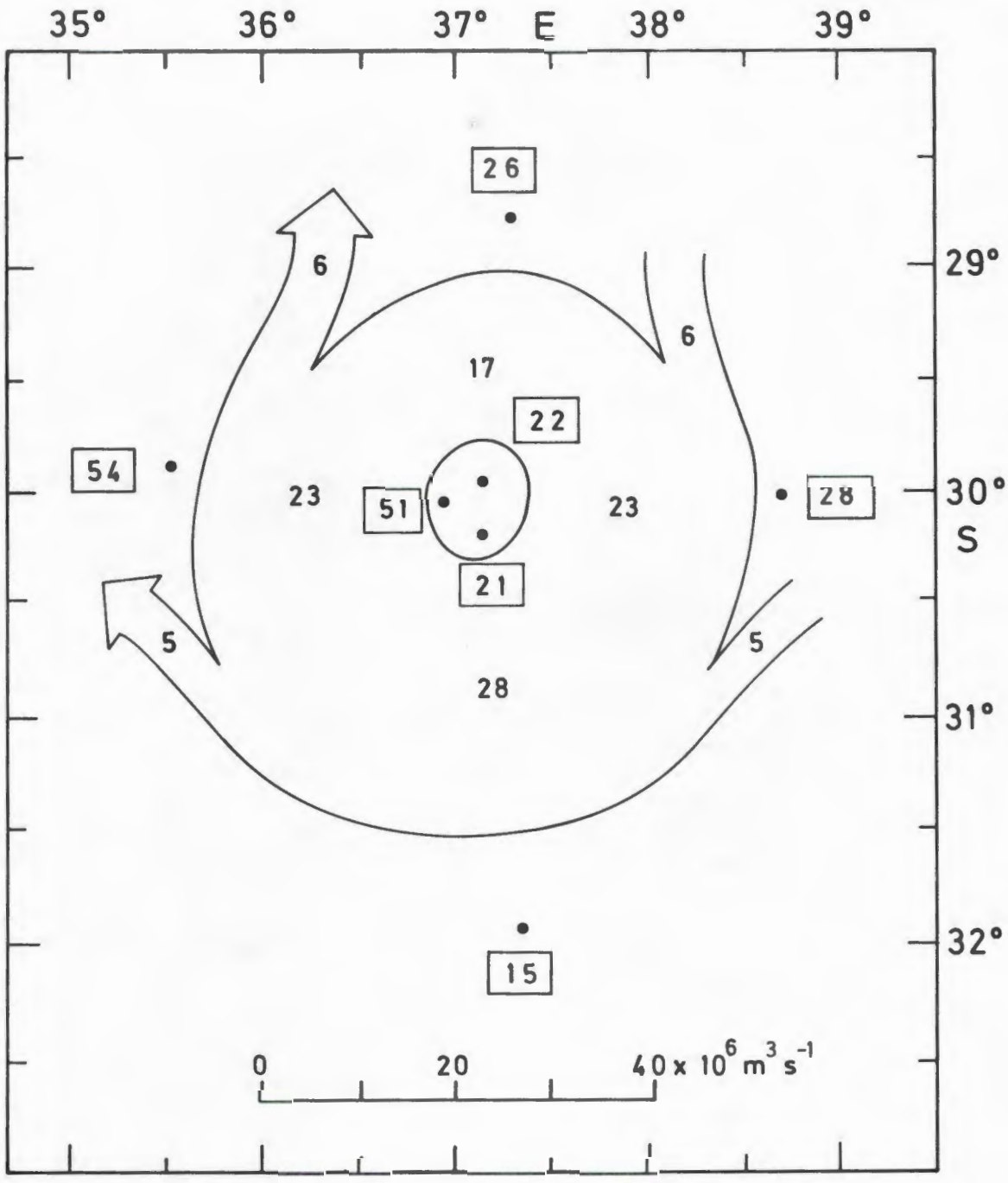

FIG. 8.13 : Volume transport of eddy Fred in November/December 1979.

8.7 Narrative of the January 1980 cruise

The cruise plan of the expedition in January 1980 was designed to relocate Fred. The results from the current meter array suggested that Fred might have been drifting toward 160°T, and the station grid in January 1980 was planned accordingly. The information that two free-drifting, satellite-tracked buoys were at that very moment passing through the study area was received much later, and it was therefore unknown that the buoys' tracks were delineating the flow pattern of the currents as well as the position of eddies in the area. This *a priori* knowledge would certainly have had a profound influence on the design of the cruise.

The *Meiring Naudé* left port on 15 January 1980 and set an easterly course toward the target area. A test station (station 1) was occupied at noon on 16 January to check the equipment, after which the vessel continued on the same heading. The survey was commenced at 16h45 (17 January) at approximately 30°S, 36°E, and from this position, stations were occupied at 20 n.m. intervals in a southeasterly direction (see Fig. 8.1).

The trend of the isotherms from the first few stations (see Fig. 8.14) seemed to indicate the existence of an eddy somewhere in the vicinity, with the centre situated on a line running in a NE-SW direction between stations 3 and 4. This evidence was considered to confirm the position of Fred in more-or-less the same location as in December 1979. Since this was still at the start of the cruise, it was decided to continue on a southeasterly heading to ascertain whether more than one eddy could exist at the same time. Fred could then be resurveyed on the way back to Durban.

At station 12 the isotherms showed a significant variation in depth (Fig. 8.14), and it was estimated that a cyclonic eddy was possibly situated to the northeast of the station line. To make full transect of the eddy, the course was initially changed to southwest (stations 13 and 14) to put the vessel on a SW-NE line passing through the centre of the eddy.

During this time, a problem developed in the navigation of the *Meiring Naudé* and the position of the ship was becoming increasingly unsure. By the time the vessel reached station 15, accurate navigation had become impossible and, the survey was reluctantly discontinued on 19 January.

In the time still left on the cruise it was decided to execute a transect across the Agulhas Current and thereby confirm its existence simultaneous to that of the vortices further offshore. The *Meiring Naudé* therefore proceeded to a position 30°S, 35°E where the vessel was within range of the DECCA transmitters ashore. From here, a line of stations at 25 n.m.intervals was executed up to Durban, where the ship arrived on 22 January.

8.8 Hydrographic conditions at the Mocambique Ridge

8.8.1 Isotherm and T/S structure

The temperature section in Fig. 8.14 displays two separate features, each of which was interpreted as signifying the existence of a cyclonic eddy.

The first feature visible in the data of station 2-6 is the upheaval of isotherms below 16°C (i.e. in depths exceeding 200 m) with a deepening of those isotherms in depths less than 200 m. The 10°C isotherm was elevated from about 700 m on station 6 to about 470 m on stations 3-4. During the December 1979 cruise the shallowest depth attained by the 10°C isotherm inside Fred was 360 m, while about 50 km away from the centre the level of the 10°C isotherm dropped to about 470 m. If the eddy suggested by the isotherm pattern at stations 2-6 in Janaury 1980 was indeed Fred, the thermal structure seems to indicate that the eddy had remained stationary or moved slightly toward the southwest during the intervening six weeks. This movement was in contrast to the speed and direction derived from the current meter results (section 8.5), suggesting that Fred's advection was unsteady.

The southerly eddy (codenamed Golf) was situated approximately 200 km southeast of Fred (see Fig. 8.15), and this was only the second time that two eddies have been located simultaneously in this study (the first occasion having been in 1975, see Chapter 4).

The thermograph trace (Fig. 8.16) indicated that Fred and Golf were separated by a mass of cold water situated between stations 6 and 8. From the surface T/S diagram (Fig. 8.16) it can be seen that station 7 was situated in water of a more subtropical nature than the other stations.

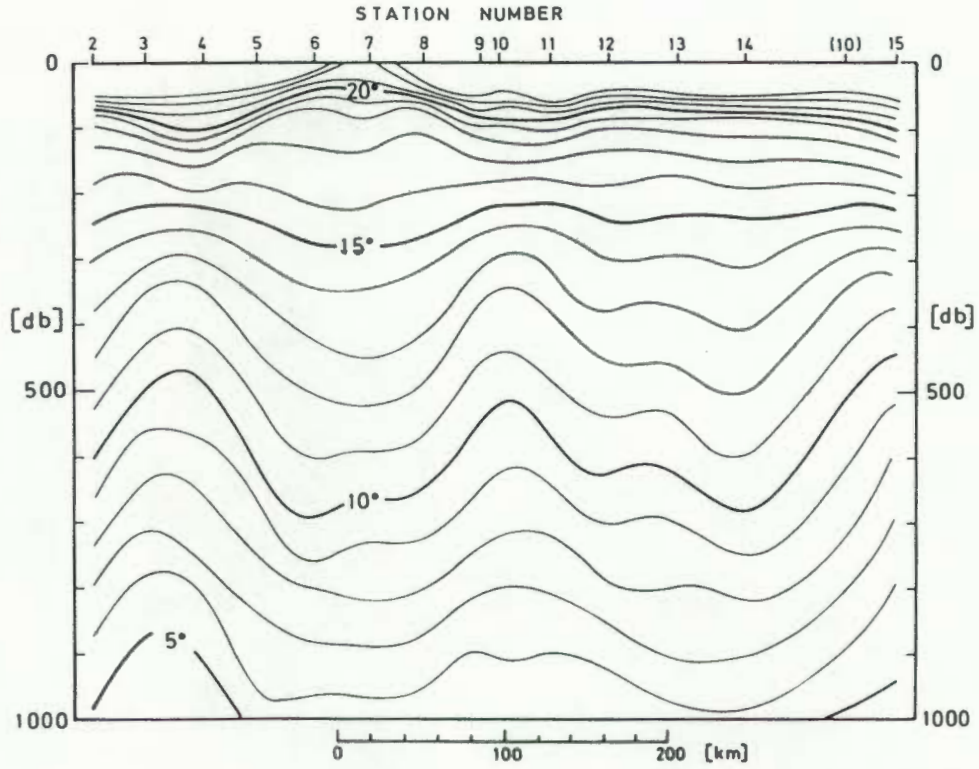

FIG. 8.14 : Vertical section of temperature for stations 2-15 of the *Meiring Naudé* cruise in January, 1980.

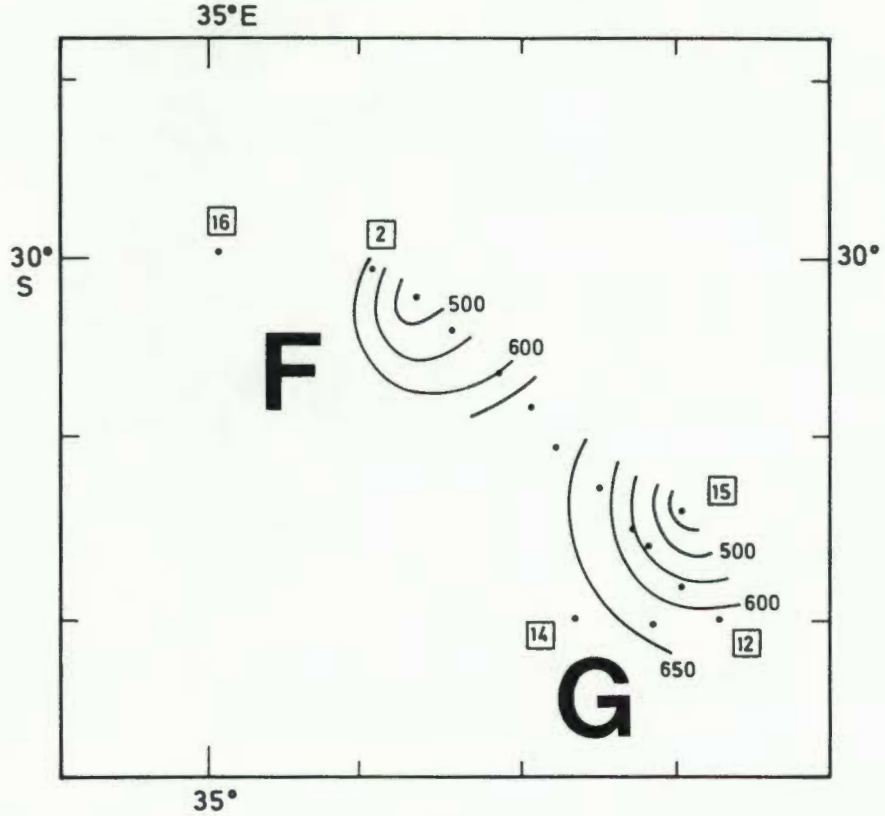

FIG. 8.15 : Topography of the 10°C isotherm surface (in m below sea level) showing eddy Fred (top) and eddy Golf during two grazing encounters in January, 1980.

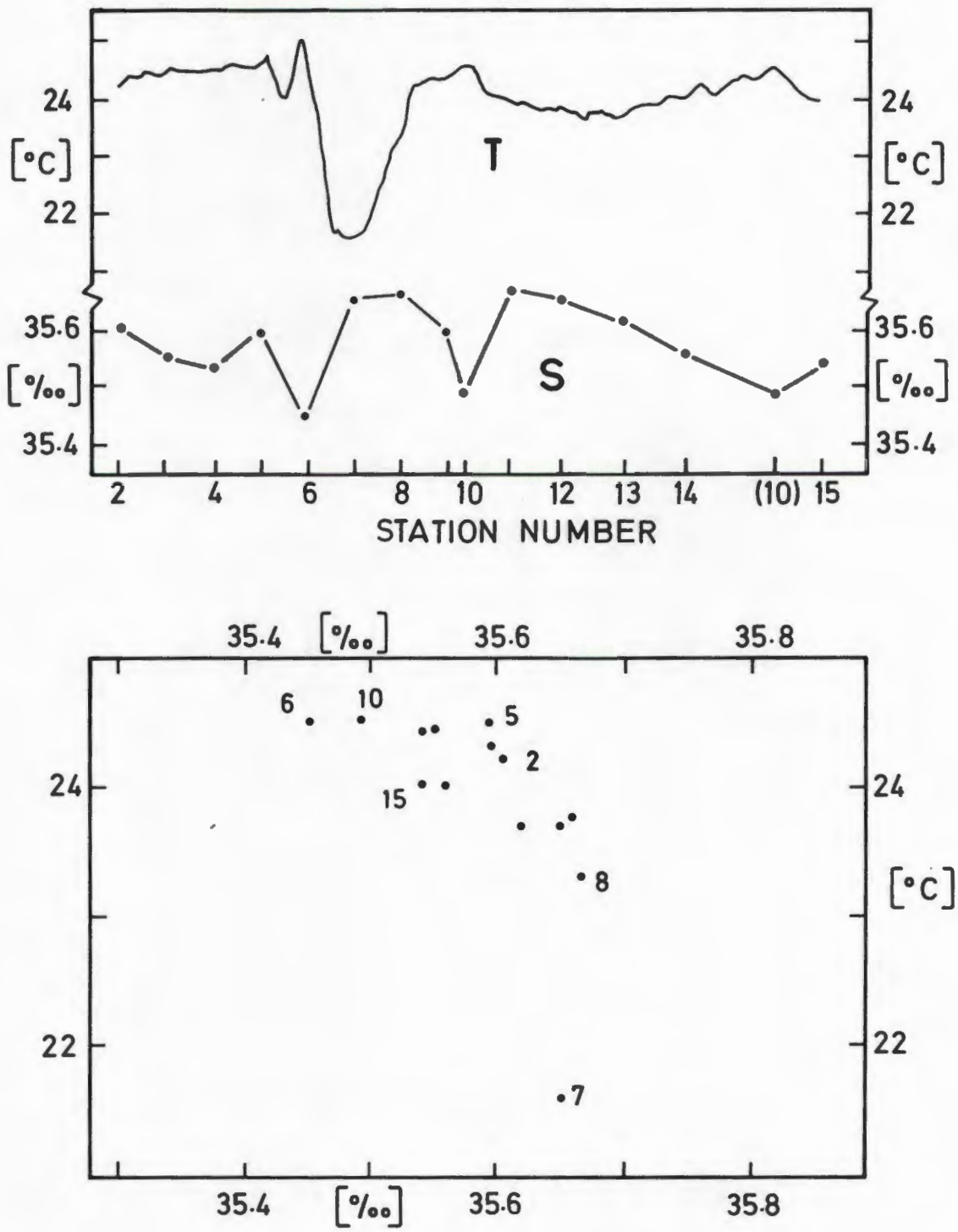

FIG. 8.16 : Variation of surface temperature and salinity (top) and T/S distribution at the surface (bottom) from the stations of the *Meiring Naudé* in January, 1980.

As far as the subsurface T/S relationship of station 2-15 is concerned, only station 5 showed the presence of any Red Sea Water. This station was located on the southeastern flank of Fred (see Fig. 8.15).

8.8.2 Current velocity and kinetic energy

Geostrophic velocities for the hydrographic section portrayed in Fig. 8.14 were calculated using 1000 db as a uniform reference level (Fig. 8.17). These velocities reached a maximum of 40 cm/s between stations 8 and 9. It is noteworthy that almost all the velocity maxima were located not at the surface but at about 200 db depth.

Because the vertical section did not pass through the centre of Fred, its kinetic energy could not be calculated. The kinetic energy of Golf can only be estimated roughly since the transect was incomplete. Using the hydrographic data of stations 15, 10 and 14, the total kinetic energy of Golf is estimated at 33×10^{13} J, which was much lower than the $1{,}74 \times 10^{15}$ J derived for Fred (section 8.4.1).

8.8.3 Volume Transport

The volume transports were calculated relative to 1000 m and are presented in Fig. 8.18. According to these results, Fred and Golf transported more-or-less the same amount of water. However, if the partial traverse of Fred is taken into consideration, it is estimated that Fred's transport was two or three times as high as that of Golf.

8.9 Section across the Agulhas Current at 30°S

En route to Durban, a section was executed across the Agulhas Current. Where possible, profiling was done to 2300 db (stations 17-20), while the other stations on this section were shallower (mostly about 800 db) depending on the bottom depth or the vertical current shear.

Although of only peripheral interest to the present study, a T/S analysis for the data collected on this section revealed quantities of Red Sea Water at 1200 db at station 19.

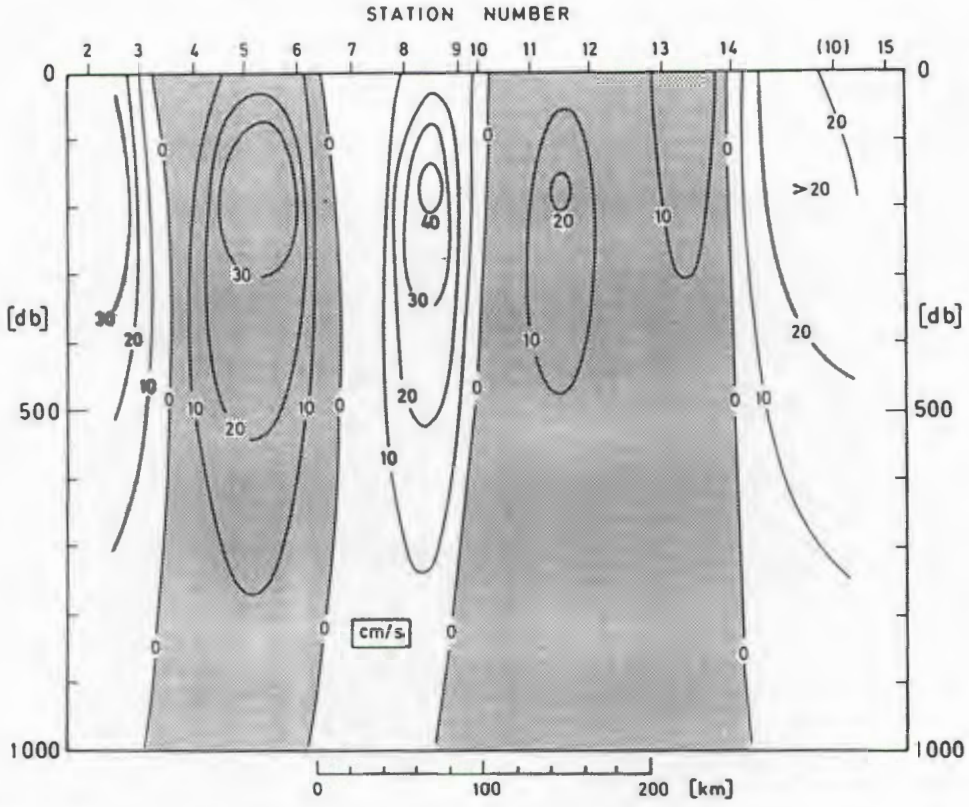

FIG. 8.17 : Geostrophic current velocity for the stations of the *Meiring Naudé* cruise in January, 1980. Shaded areas indicate flow out of the page.

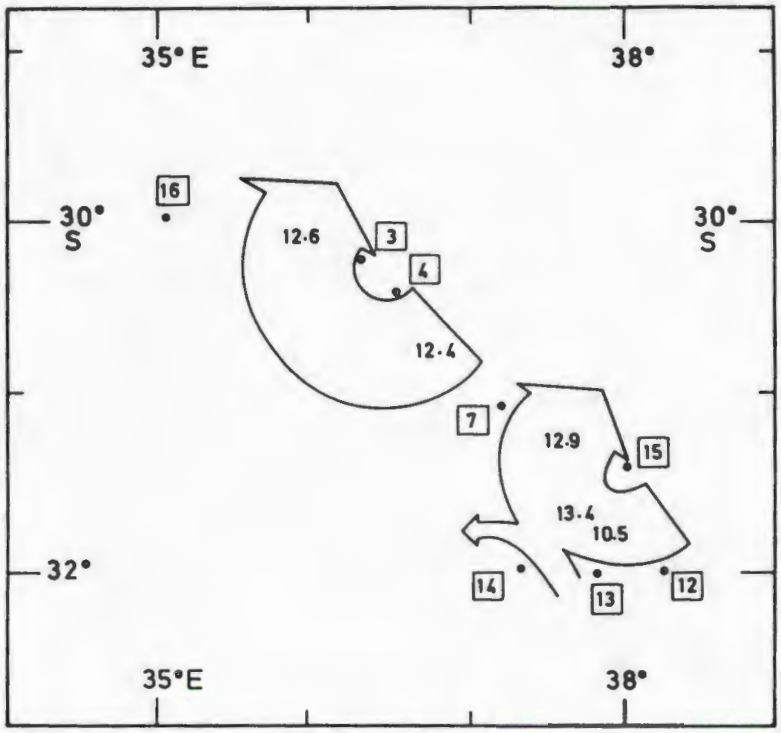

FIG. 8.18 : Volume transport (in units of 10^6 m^3 s^{-1}) for the stations in January, 1980, showing the grazing encounters of Fred (top) and Golf (bottom). A certain amount of subjectiveness was used in the derivation of the flow continuity, considering that only a single transect through Fred was availlable.

The intermediate maximum of 7,8 x $10^6 m^3 s^{-1}$ between stations 22 and 23 of the cross-current profile of volume transport (Fig. 8.19), is considered to signify the centre of the Current. It can be mentioned as corroborating evidence of the high current velocities in this area that the current shear at stations 22 and 23 prevented sufficient penetration of the CTD and caused wire angles as high as 50°. Although the transport values seem low initially, this was mainly because of the shallow reference level. A rough estimate of what the transport would have been had the profiling been deeper, raised the flux to the same magnitude of volume transport values commonly measured in the Agulhas Current (DUNCAN, 1970; GRüNDLINGH, 1980).

8.10 Observations in March 1980

8.10.1 Narrative of the cruise

The *Meiring Naudé* left port on the evening of Tuesday, 18 March and set course due eastwards. After a test station (station 1), the vessel proceeded toward the target area to initiate the survey at 30°S, 36°30'E. From this point onwards, stations were occupied at 20 n.m. intervals in a southeasterly direction (Fig. 8.1). The reason for this orientation of the station grid was to occupy a line of stations that would pass just east of station 15 of the cruise two months previous. It was hoped that these stations would thus traverse the centre of Golf observed during the January cruise. It may be mentioned that the cruise was executed still unaware of the drift tracks of the satellite buoys in the area.

The present cruise followed very much the same procedure as the January cruise, and this can also be seen from the similarity of their cruise tracks. In both cases the southeasterly course was maintained until a significant upheaval of the deeper isotherms was detected. In both cruises the course was altered but equipment problems eventually prevented a completion of the survey. On the present cruise, data collection was terminated at station 20 (station 19 having been the last one to contain profiling data), on 22 March, and the ship returned to port on 25 March.

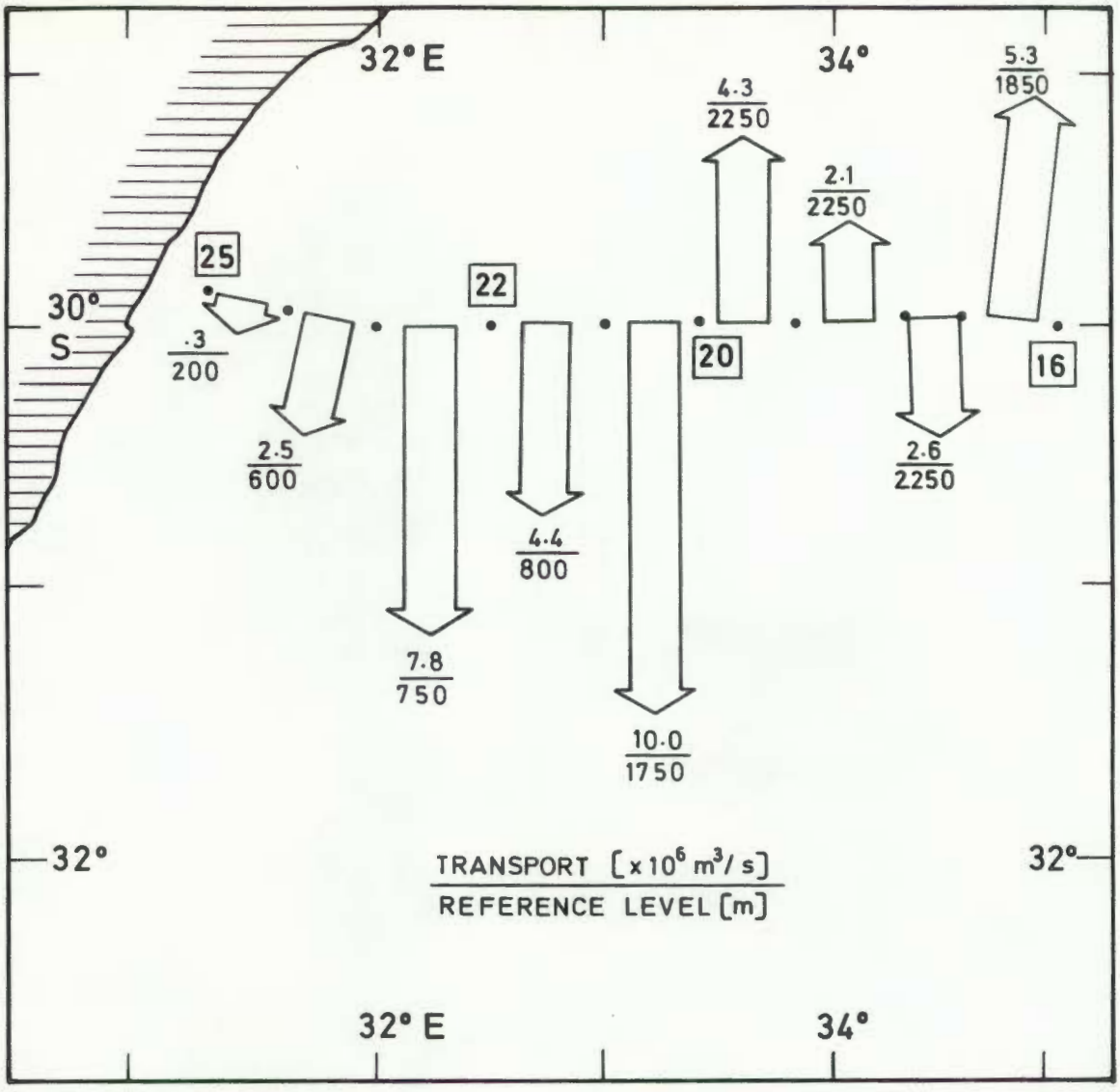

FIG. 8.19 : Volume transport for stations 16-25 of the *Meiring Naudé* cruise in January, 1980.

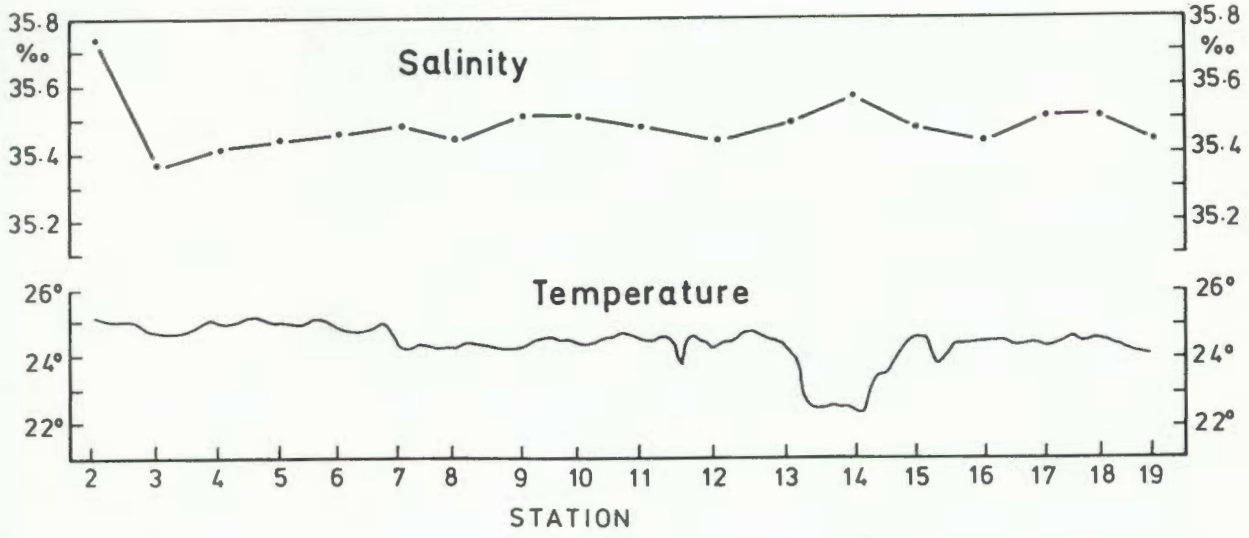

FIG. 8.20 : Variation of surface temperature and salinity during the cruise in March, 1980.

8.10.2 Thermohaline data

As far as the surface temperature and salinity are concerned, the only conspicuous variation occurred in the vicinity of station 14 (Fig. 8.20). This station was located on the southwestern perimeter of the survey area (see Fig. 8.1), and the thermohaline values indicated the presence of water of subtropical character.

During the execution of the survey, a conspicuous upheaval of the isotherms and isohalines occurred in the vicinity of station 9, (see Fig. 8.21), and this warranted a change in the course as indicated in Fig. 8.1. A northeasterly heading through the position of station 9 produced a strong upheaval with a maximum that seemed to have been centred between stations 18 and 19. The location of this maximum could not be determined unequivocally since the equipment failure prevented a completion of the transect. The presence of colder water in the layers deeper than 200-300 m (Fig. 8.21(a)) coincided with a bowl of warm water in the upper 200 m. The warmer surface water revealed a lower salinity (Fig. 8.21(b)), and this reduced salinity was evident throughout the water column.

The shape of the isotherm upheaval, in which the 10°C isotherms rose to a depth of approximately 460 m, indicated that the centre of the eddy was located between station 18 and 19 (31°20'S, 38°45'E). The topography of the 10°C isotherm surface and the variation of the mixed layer depth (Fig. 8.22) confirmed that the NE-SW line of stations succeeded in traversing the eddy through its centre. The proximity of the eddy to the position where Golf had been observed (31°22'S, 38°10'E) suggested that the present eddy and Golf were one and the same.

8.10.3 Circulation

The dynamic topography of the sea surface relative to 1000 m (Fig. 8.22) indicated that the centre of the eddy was located between station 17 and 18, rather than between station 18 and 19. This discrepancy between the topography of the 10°C surface and the dynamic topography of the sea surface can be attributed to the bowl of warm water in the upper layers, producing an anticyclonic tendency close to the surface. All the geostrophic/gradient velocity maxima (20-30 cm/s) were located at a depth of about 200 m (not shown here).

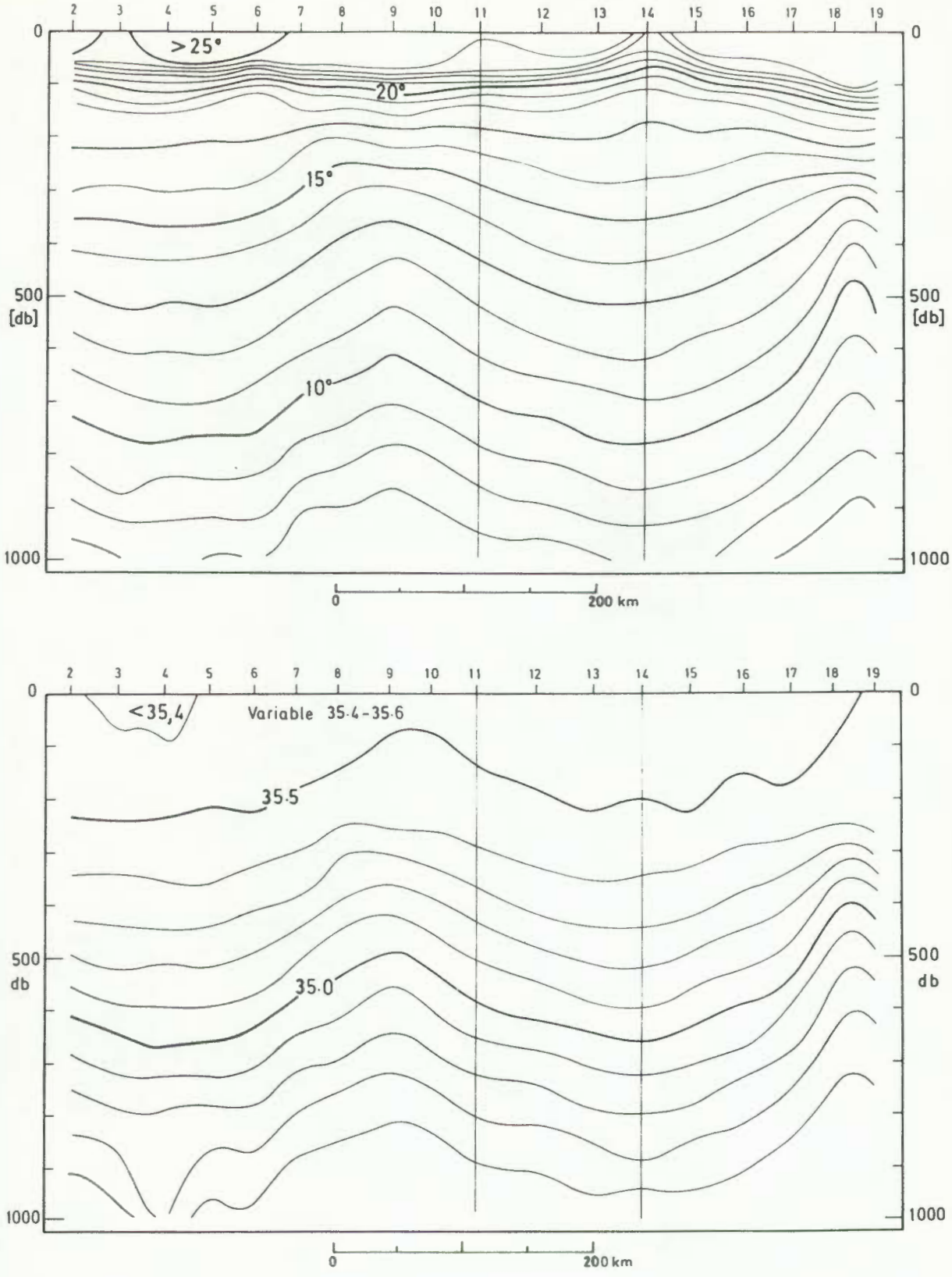

FIG. 8.21 (a) Vertical section of temperature for the cruise in March, 1980. Major course changes (see Fig. 8.1) are indicated by the two vertical lines.

(b) Vertical section of salinity for the cruise in March, 1980.

The volume transports in the vicinity of Golf (Fig. 8.22) amounted to 14-18 x $10^6 m^3 s^{-1}$ circulating the eddy. These amounts are compatible to the volume transport derived when Golf was observed in more-or-less the same position in January 1980.

The kinetic energy calculated for the line of stations passing through the centre of Golf shows a maximum in the vicinity of station 17, some 50 km from the estimated position of the centre (Fig. 8.23). The total kinetic energy of Golf was estimated at 4 x 10^{14} J.

8.11 Satellite buoy tracks

During the First GARP (Global Atmospheric Research Project) Globe Experiment, a large number of free-drifting, satellite-tracked buoys were deployed. In the area around the African Continent, these buoys were mainly of Canadian, French and South African origin.

The buoys of relevance to the present study were all deployed in the area east of Madagascar in the beginning of 1979. These buoys were drogued and were designed to measure sea temperature and atmospheric pressure (EERM, 1979). Unfortunately, the temperature sensors on the buoys failed before the end of 1979, and for this reason, no conclusions can be made concerning the water masses the buoys were following. Some statistics about their drifts are given in Table 8.1.

TABLE 8.1 STATISTICS OF BUOY DRIFTS IN 1979/80

Buoy ID	Deployed		Lost	
	Date	Position	Date	Position
14621	12 Jan '79	23°30'S, 54°E	30 Jan '80	30°20'S, 75°E
14622	7 Jan '79	23°50'S, 58°E	20 Sept '79	33°S, 30°30'E
14627	13 Jan '79	29°S, 53°20'E	10 Feb '80	30°30'S, 33°E

Some of the buoys deployed east of Madagascar cross the Madagascar Ridge and entered the area defined in section 1.4 as the "Southwest Indian Ocean". The drift tracks of those buoys that remained in the area immediately south of Madagascar, and those that drifted northwards up the west coast of Madagascar remained outside the "target area" and are considered irrelevant to the present discussion and have been omitted.

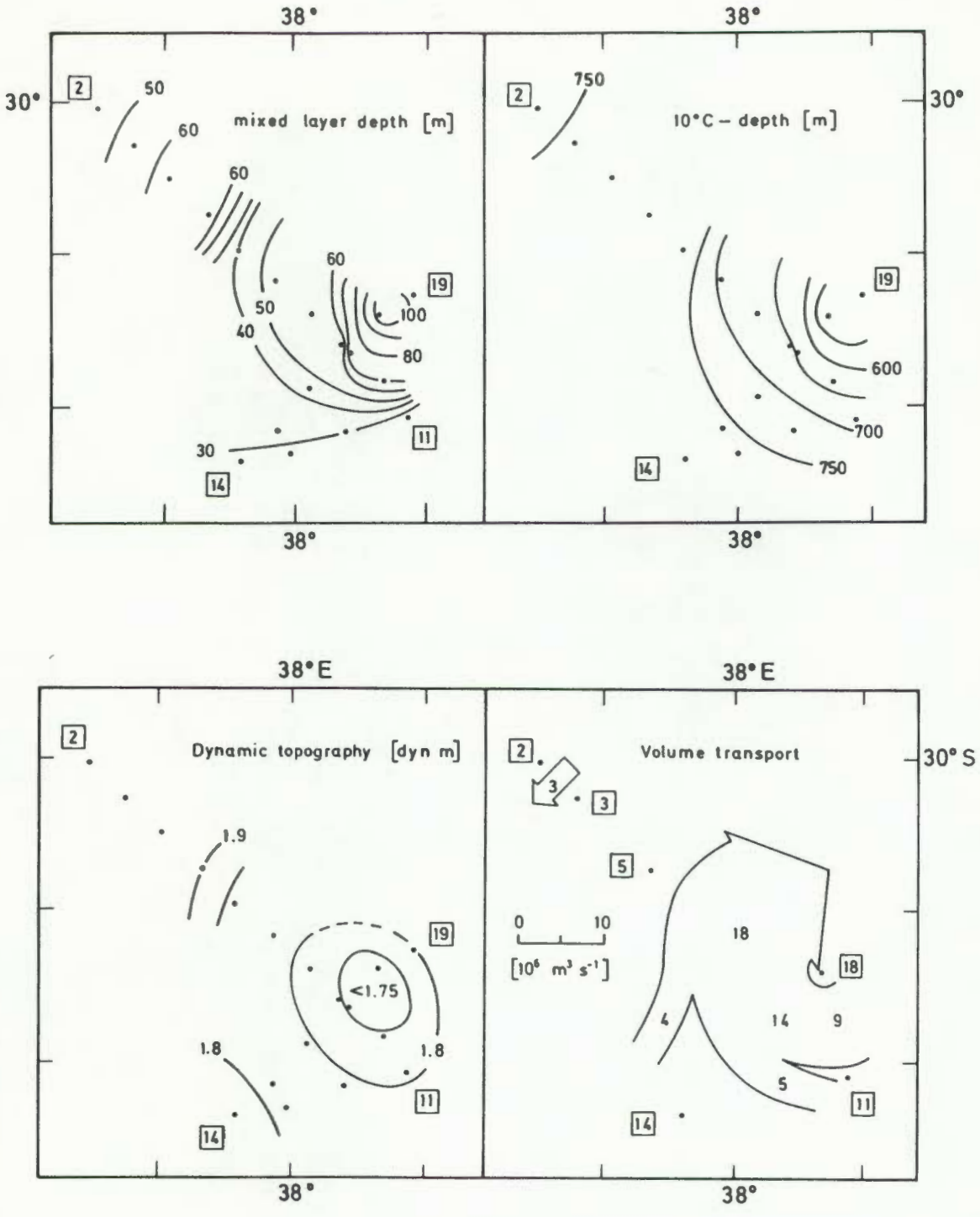

FIG. 8.22 : Mixed layer depth, 10°C-isotherm topography (in m below surface), topography of the geopotential anomaly and volume transport in the vicinity of eddy Golf in March, 1980. Geopotential anomaly and volume transport were calculated relative to 1000 m.

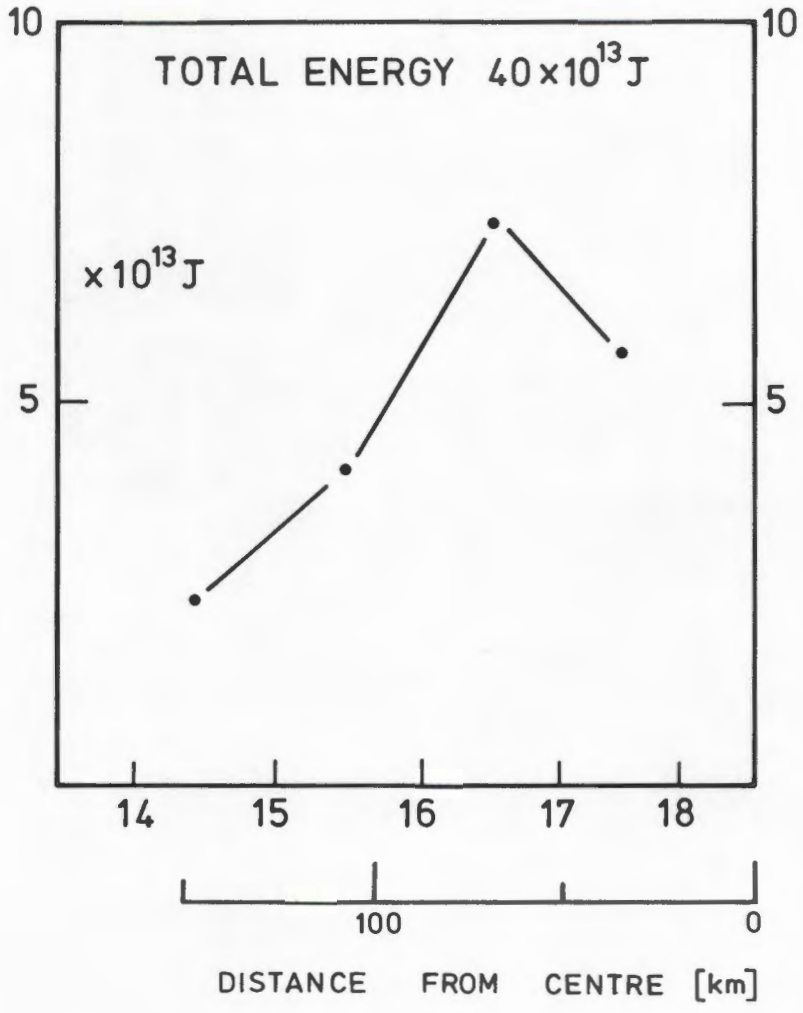

FIG. 8.23 : Kinetic energy of the flow in the vicinity of eddy Golf, March, 1980.

Three buoys (code numbers 14621, 14622 and 14627) entered the Mozambique Basin and Mozambique Ridge area and their drifts will be discussed here. The tracks have been divided into two periods since it will be seen that the tracks underwent notable changes from one period to another. These two periods are, first, the time from the moment the buoys entered the area west of about 45°E up to 30 November 1979 and second, from 1 December 1979 to 31 January 1980 - the period encompassing the two *Meiring Naudé* cruises. As can be seen in Table 8.1 only two buoys remained active up to this period and both failed shortly afterwards.

8.11.1 Period I : Up to 30 November 1979

The tracks during the first period are shown in Fig. 8.24, and the drift of the two buoys depicted there show the following noteworthy features:

a) Buoy 14627 was trapped in an advecting, cyclonic eddy south of Madagascar during May and June 1979 before leaving the eddy at the beginning of July. The eddy seems to have originated from the area southeast of Madagascar (possibly the East Madagascar Current) and the buoy displayed a regular rotation rate of once every 4-6 days (LUTJEHARMS, BANG and DUNCAN,1981).

This buoy was subsequently carried much further northwards into the Mozambique Channel than buoy 1116 in 1975 (see Chapter 4), before drifting southwards in a flow that can probably be attributed to the Mozambique Current. Similar to the behaviour of buoy 1116, buoy 14627 did not follow the "coastal" route of the Agulhas Current south of 25°S, but moved away from the coast and eventually drifted onto the Mozambique Ridge at 28°S.

During October the buoy became entrained in a cyclonic eddy east of the Mozambique Ridge at 31°S, 38°E. The buoy completed three revolutions at an average velocity of 55 cm/s before leaving the eddy in a northeasterly direction.

b) Buoy 14622 completed a large oval-shaped circuit at 29°S, 43°E before drifting steadily westwards onto the Mozambique Ridge. There it remained for two months moving in a seemingly irregular pattern. From the

beginning of July 1979 it started drifting in a general westerly direction along 32°S toward the African coast. The buoy's drift on the Mozambique Ridge between 30°S and 32°S neither confirms nor denies the existence of the eddy at 34°S, 38°E described by buoy 14627.

The station patterns executed during the December 1979 and January 1980 cruises of the *Meiring Naudé* have been included in Fig. 8.24. In this regard, two points are noteworthy at this stage.

First, toward the end of April, buoy 14622 was drifting southwards along 37°E between 29°S and 31°S. This part of its track was situated in the same area as the hydrographic stations occupied by the *Meiring Naudé* during December - 7 months later. Similarly, buoy 14627 drifted through the same area (in a southeasterly direction) during September. Neither of these buoys' tracks showed any evidence of the eddy (Fred) observed during the ship's survey in December, even though they moved against the rotation of Fred (had it been there). It was therefore concluded that Fred had not been in existence in that area during the period April-September.

Second, buoy 14627 became entrained in an eddy at 31°S, 38°E in October 1979. This was the same position where Golf was observed during January 1980 (i.e. 2½ months later). It was tentatively concluded that the eddy described by the buoy track and the one located during the ship survey were one and the same (Golf). It is remarkable that the cruise in December 1979 narrowly missed traversing Golf (see Fig. 8.24).

8.11.2 Period II : 1 December 1979 - 31 January 1980

During December 1979 and January 1980 the drift position and velocity of buoys 14621 and 14627 seemed to undergo a notable change. After buoy 14627 was ejected from Golf at 31°S, 38°E, it moved northeastwards towards Madagascar in November, then accelerated rapidly westwards during December (Fig. 8.25). By coincidence, buoy 14621 was in the same area at that time (having drifted into the region from the east), and experienced the same westward acceleration as buoy 14627. During the following two months, these two buoys followed more-or-less the same route. As the buoys drifted onto the Mozambique Ridge at 27°S, the current in which they were obviously embedded first turned anticlockwise on the Ridge, then clockwise again as it left the Ridge and flowed into the Mozambique Ridge,

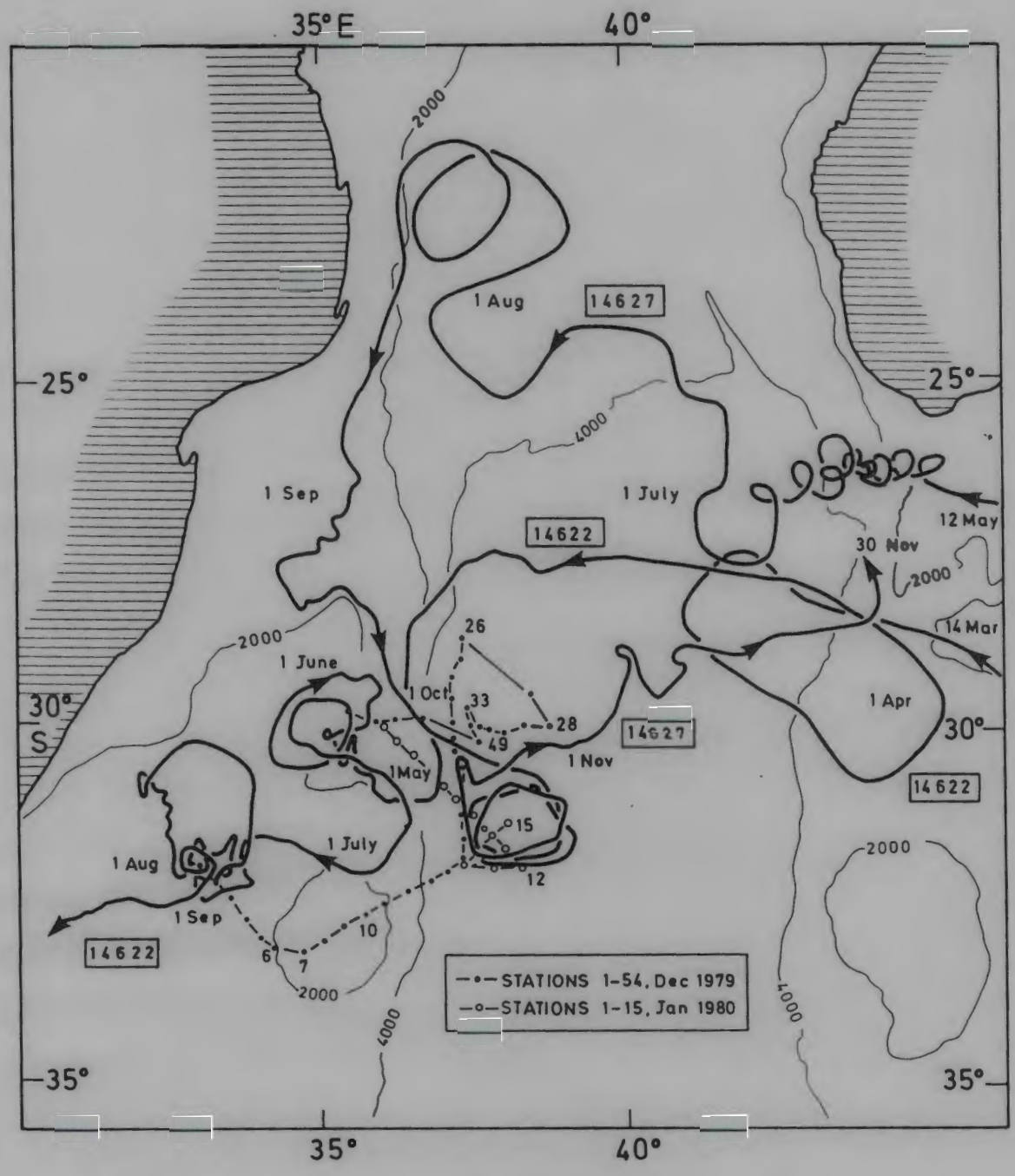

FIG. 8.24 : Composite of satellite-buoy drift tracks (identification numbers 14622 and 14627) in the Mozambique Basin area during 1979, and the hydrographic stations of the *Meiring Naude* in December 1979 (dots) and January 1980 (circles).

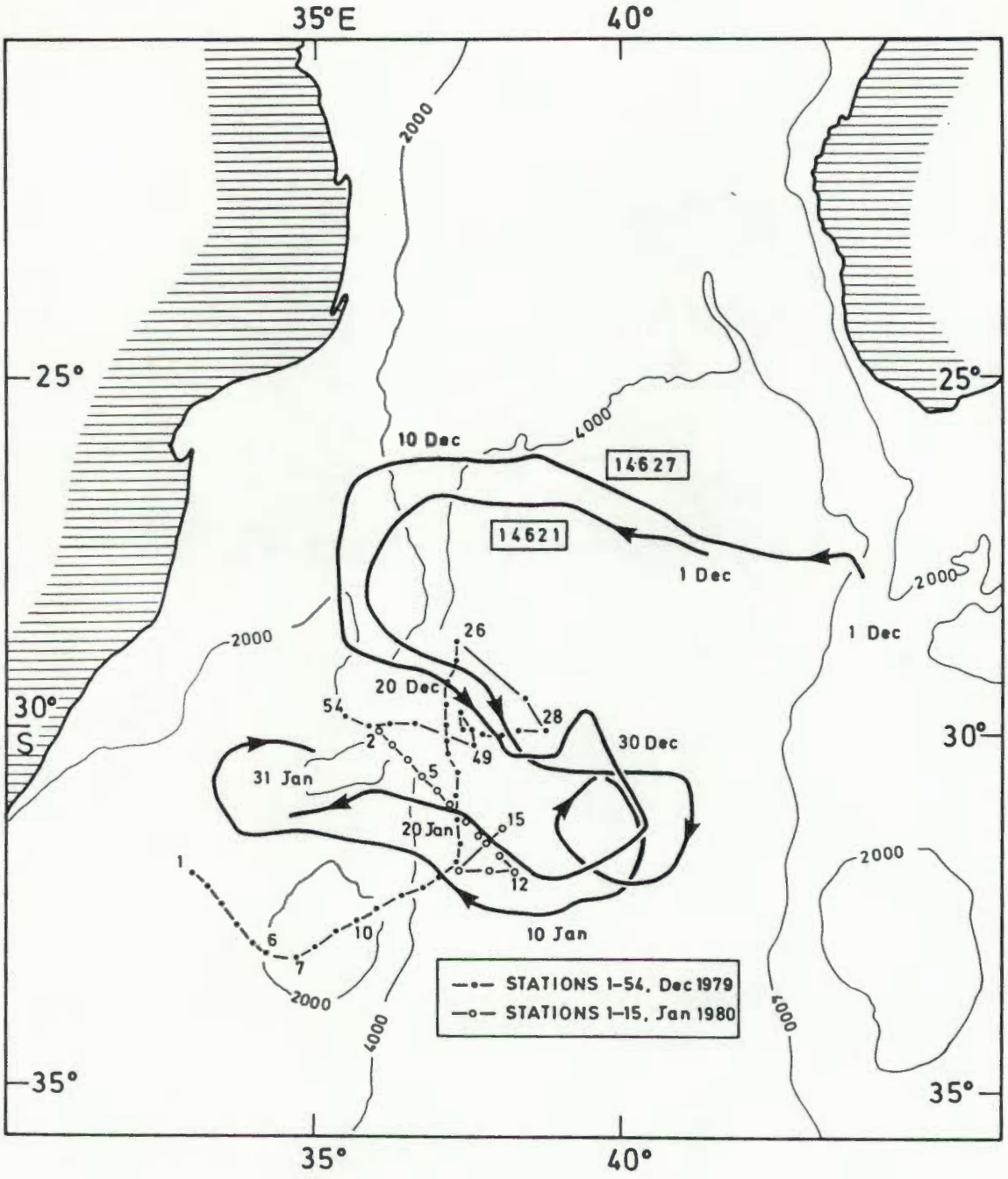

FIG. 8.25 : Satellite-buoy tracks during December, 1979 and January, 1980 and the station positions of the *Meiring Naude* in the same months.

and then flowed onto the Ridge again at 32°S. It is interesting to notice that a current approximately 100 km wide could account for the drift patterns of the buoys.

The drift tracks of these two buoys formed an envelope around Fred and Golf located during the cruises in December 1979, January and March, 1980 . By combining the drift tracks of Figs. 8.24 and 8.25 with the hydrographic results, the following tentative statements can be made about the circulation in the area:

(a) The host current

The tracks of buoys 14621 and 14627 during December 1979/January 1980 differed significantly from the drift tracks of the previous months. During December and January the tracks portrayed the existence of a strong, consistent current flowing westwards at 27°S and subsequently describing an "S" shape in the Mozambique Basin/Ridge area (Fig. 8.25). In April 1979, buoy 14622 followed more-or-less the same route westward, but deviated from the December tracks by remaining on the Mozambique Ridge. This seems to suggest that the current in which buoys 14627 and 14621 became embedded in December had not been in this region a few months before. The speed of the current (as evidenced by the drift rate of the buoys) was about 80 cm/s. This current will hereinafter be referred to as the Mozambique Ridge Current.

(b) Eddy Fred

The buoy tracks during the months preceding the December 1979 cruise (Fig. 8.24) seem to indicate that Fred had either not existed at the time of their drift through the area, or it was situated in a different position. If it had been situated in a different area it must have moved into position at some stage, to be enveloped by the current reflected in Fig. 8.25. Intuitively this movement seems rather unlikely, and the large amount of energy contained in the eddy rather suggests a relatively recent creation. It is therefore postulated that the Mozambique Ridge Current, into which buoys 14621 and 14627 had become entrained, was the generator of Fred. The reason why the buoys failed to execute a tight loop around Fred, but moved off southeastwards,

can be explained in terms of the proximity of Golf. In other words, the presence of Golf caused filaments of the host current to enclose Fred and Golf simultaneously.

(c) Eddy Golf

The first conclusive observation of this eddy occurred when buoy 14627 became trapped in it for about one month in October 1979. By the time it was located in January 1980 it was therefore at least 3 months old, and 5 months when it was observed in March 1980. In Chapter 13 it will be argued that Golf might have been generated as early as April/May 1979, making it eleven months in March 1980.

8.12 Summary

Evidence in the form of buoy tracks and hydrographic data indicated the simultaneous existence of two cyclonic eddies along the eastern edge of the Mozambique Ridge. It is further suggested that these eddies were, possibly at different times, created by an eastward flow of the Mozambique Ridge Current through a narrow window of the Mozambique Ridge between 29° and 31°S.

The two eddies, Fred and Golf, were not of compatible intensity since the hydrographic measurements indicated that Fred had a larger volume transport and kinetic energy than Golf. This difference in characteristics, coupled with the buoy data, suggested that Golf was older than Fred.

This is the first time that evidence of the age of an eddy has been found. It is also the first time that the Mozambique Ridge Current is coupled unambiguously to the cyclonic eddies east of the Mozambique Ridge. This aspect provides an important insight into the circulation of the region, and could be considered a significant breakthrough in this project.

Apart from the fact that the existence of significantly-strong, concentrated radial velocities inside Fred could not be established, the presence of Red Sea Water (RSW) remains a mystery. It is namely unknown, first, why RSW penetrates this far southward (30°S) when it is customarily found only much further northward. Second, why RSW always seems to be

confined to the anticyclonic (outer) side of the current in the eddies (and on the offshore side of the Agulhas Current). Third, why the distribution of RSW seems to take the shape of unmixed, localised "patches". Neither of these aspects can be explained in terms of existing knowledge and become even more problematic if it is considered that the eddies are generated by the Mozambique Ridge Current which in turn originates south of Madagascar. This would namely indicate the unlikely event that RSW penetrated southward along the *eastern* side of Madagascar.

CHAPTER 9

OBSERVATIONS OF VORTICES : 1981

9.1 Introduction

After the successful cruises of the previous year the cruises that were executed in 1981 had the following aims: First a cruise was planned to locate and and survey vortices in the vicinity of the Mozambique Ridge and Mozambique Basin, in order to increase the information about the characteristics of eddies. Second, an additional three cruises (those in March and October) were aimed at the "background" circulation in the Mozambique Basin, and thus provide an insight into where the eddies, once they became free-drifting, should advect to.

As it turned out, an eddy was located on one of the "background" cruises, and the cruise plan was altered accordingly. Only these two "vortices" cruises, executed in February and April, are reported here, the other two having already been discussed in Chapter 3. Because of the contemporary nature of all the cruises in 1981, however, a certain amount of cross-referencing is essential.

9.2 Observations in February 1981

9.2.1 Narrative of the cruise

The *Meiring Naudé* left port on 5 February and steamed northeastwards inshore of the Agulhas Current (see Fig. 9.1 for the track chart). Since many of the vortices observed previously were generated in the northern part of the Mozambique Ridge (between 17° and 29°S, and between 35° and 37°E), the present cruise was planned to start at 28°30'E and then proceed in a southeasterly direction into the Mozambique Basin. To expedite the survey, CTD casts were restricted to the upper 1000 m (Fig. 9.2).

Between Durban and station 1 the sea-surface temperature did not reveal any conspicuous fronts (not shown here), and this trend was continued during the first few stations. The isotherms (Fig. 9.2) were also at their expected depths (cf Chapter 3) at station 1 and it was concluded that the ship had not inadvertently crossed (part of) an eddy before arriving at station 1.

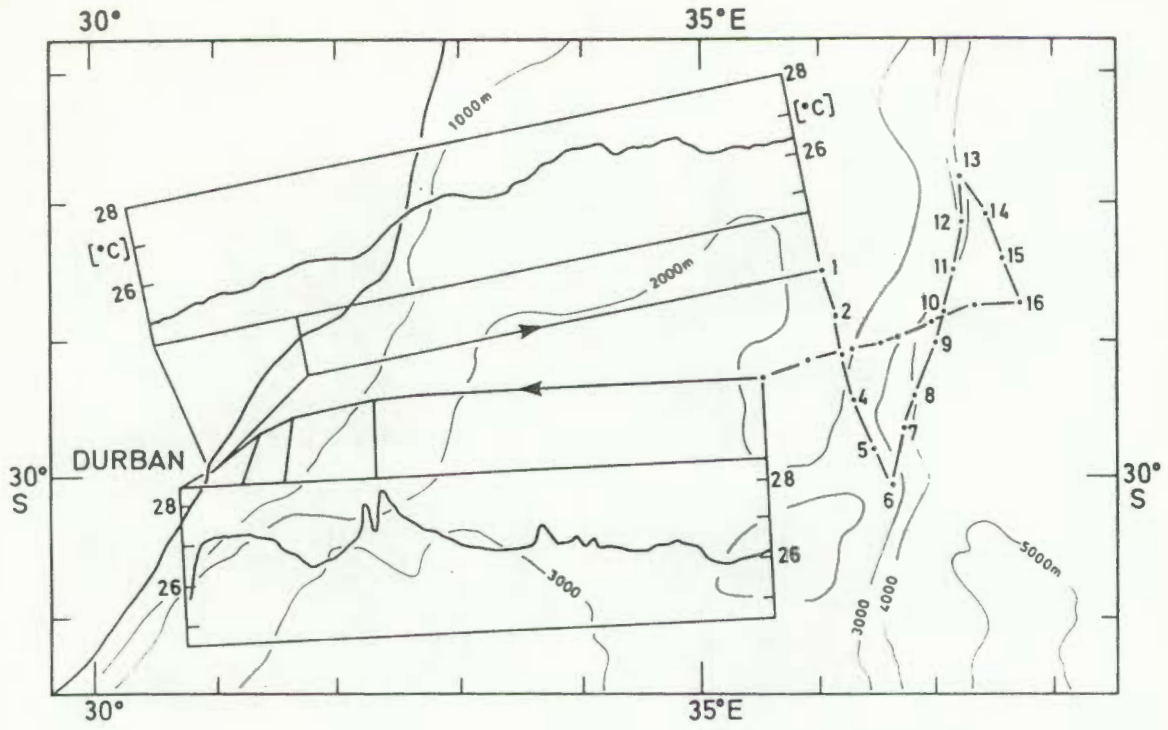

FIG. 9.1 : Track chart of the *Meiring Naudé* cruise in February, 1981, with the variation of surface temperature between Durban and the target area.

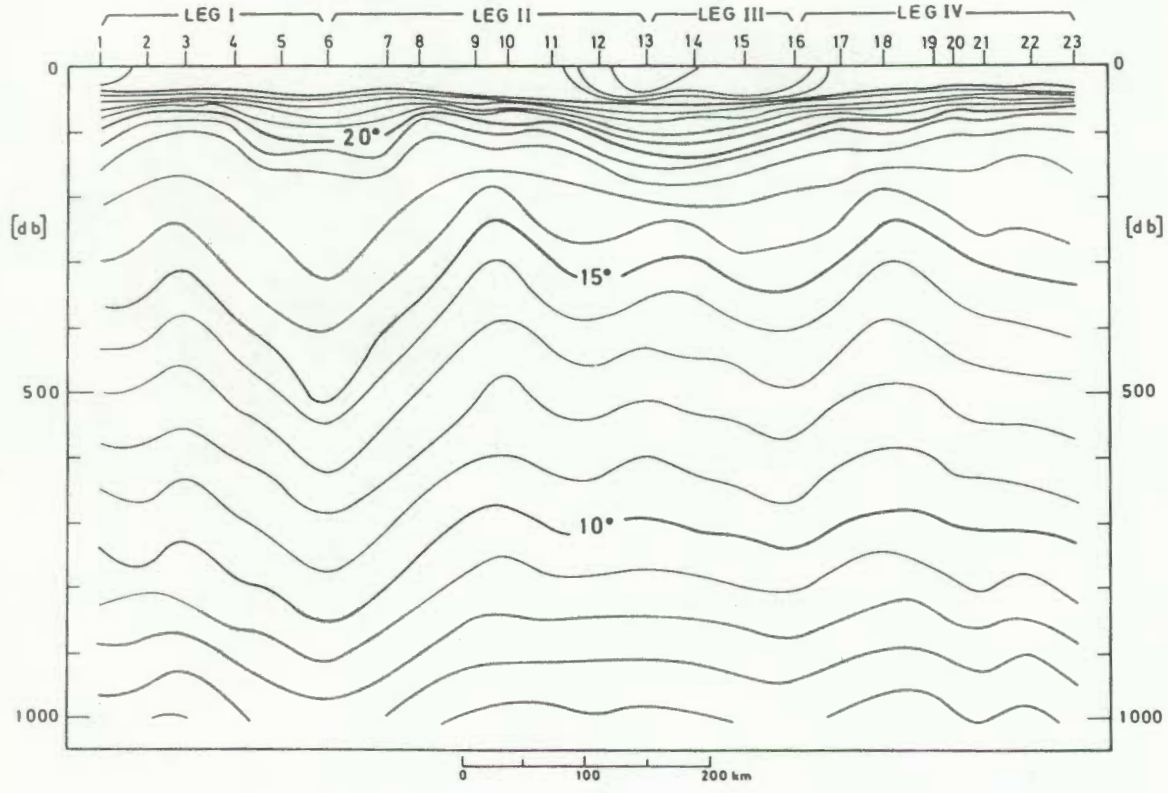

FIG. 9.2 : Vertical section of temperature in February, 1981.

Between station 3 and 6 the isotherms showed a steady downward trend. Since this was indicative of a current with a weak westward component, it was considered that an eddy was possibly situated east of station 3, and the survey was directed into the area closer to the eastern edge of the Mozambique Ridge.

Although the isotherms rose steadily up to station 9 (Fig. 9.2), they did not deepen again after reaching a peak. The search area was therefore extended even further eastwards, but the southeasterly line of stations up to station 16 revealed no evidence of strong vorticular motion. The survey was concluded with a line of stations running through stations 10 and 3 (see Fig. 9.1), still without any significant sign of an eddy. The *Meiring Naudé* arrived back in Durban on 12 February.

9.2.2 Results

The group of stations 12 to 16 were the only ones to indicate the presence of tropical surface water (high temperature, low salinity). The presence of this water mass can also be seen in the vertical section of temperature (Fig. 9.2) as a layer of warm water in the upper 50 m between station 11 and 17.

The geopotential of the sea surface (Fig. 9.3) showed a weakly-defined eddy with an oval shape centred in the vicinity of stations 18-20. There was a relatively strong flow in westerly direction through the southern part of the eddy. According to the distribution of the volume transport calculated relative to 1000 m only about $4 \times 10^6 m^3 s^{-1}$ were circulating the eddy, although the westerly flow through the southern flank was 3-4 times as high. This westerly flow was orientated almost diagonally across the eastern escarpment of the Mozambique Ridge (cf Fig. 9.1).

9.3 Observations in April 1981

The *Meiring Naudé* cruise of April 1981 would have been the second of three cruises which were initially aimed at studying the "background" circulation in the Mozambique Ridge. For this reason, the cruise was planned to fit in geographically between the areas covered by the March and October cruises of that year (see Fig. 3.1). As it happened, the results collected during the initial stages of the April cruise warranted a deviation from the planned track.

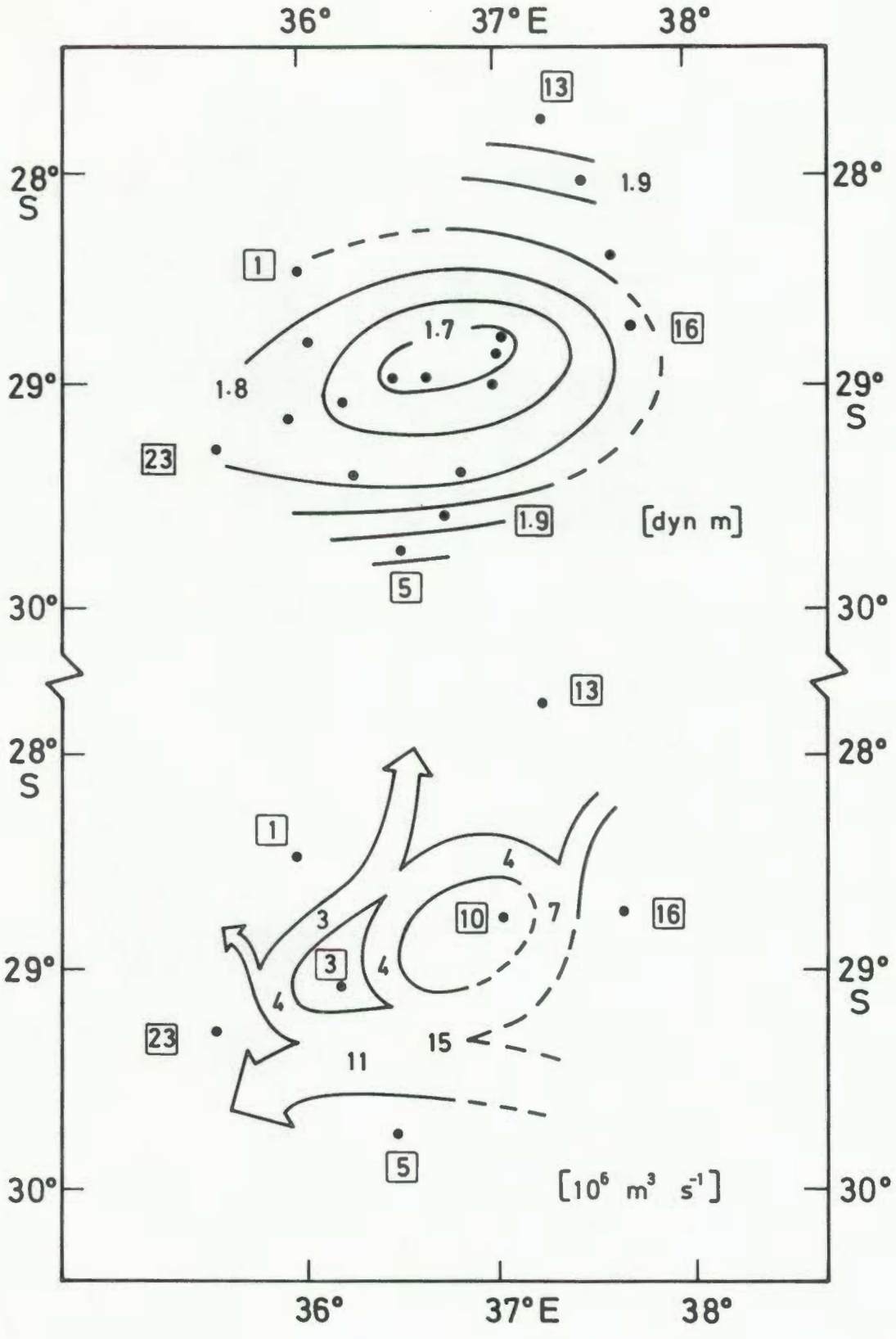

FIG. 9.3 : Top: Topography of the geopotential anomaly (in units of $10m^2/s^2$) of the sea surface relative to 1000 m. Stations 6, 11 and 12 were not used because of gaps in the digitised profiles. Bottom: Volume transport relative to 1000 m.

9.3.1 Narrative of the cruise

The *Meiring Naudé* left Durban on 21 April 1981 and proceeded up the coast close inshore. Just south of 28°S, the course was altered to the east in order to cross the Agulhas Current and proceed toward the target area. A test station was occupied in the evening of the 22 April and some equipment problems eliminated.

Operations were started with station 1 inshore of the Mozambique Ridge early on 23 April (see Fig. 9.4). The initial plan was to continue on an easterly course along 28°S with hydrographic stations spaced approximately 20 nautical miles ($\sim$ 37 km) apart.

The surface temperature and salinity (see Fig. 9.5) underwent some significant variations between stations 5 and 8. This variation was accompanied by a cooling of the whole water column (see Fig. 9.6). It was concluded that a strong, southward-setting current was flowing between station 4 and 8, and it was decided to deviate from the planned survey grid and survey the area to the south of these stations.

The current filament was again evident on this southwesterly line of stations by the heating of the water column between stations 8 and 12 (Fig. 9.7). After the isotherms had levelled off again, the course was altered at station 15 and the survey proceeded in an ESE direction. The isotherms now showed a slight, almost insignificant shoaling between station 15 and 20 (Fig. 9.8).

At this point (station 20) it was decided to proceed northeastwards to investigate some features observed during the March cruise. The abrupt cooling in the water column between station 20 and 21 was so significant that the course was reversed toward the south (station 22) and then toward the southwest, in order to join the imagined line passing at right angles between station 19 and 20. This line traversed an eddy (codenamed Harry) centred in the vicinity of station 24-25 (Fig. 9.9).

The CTD failed on station 26 and use was made of the hydrosonde and sampler for stations 27-29. On station 29 the hydrosonde also failed, and the survey had to be abandoned. The vessel returned to Durban on 29 April.

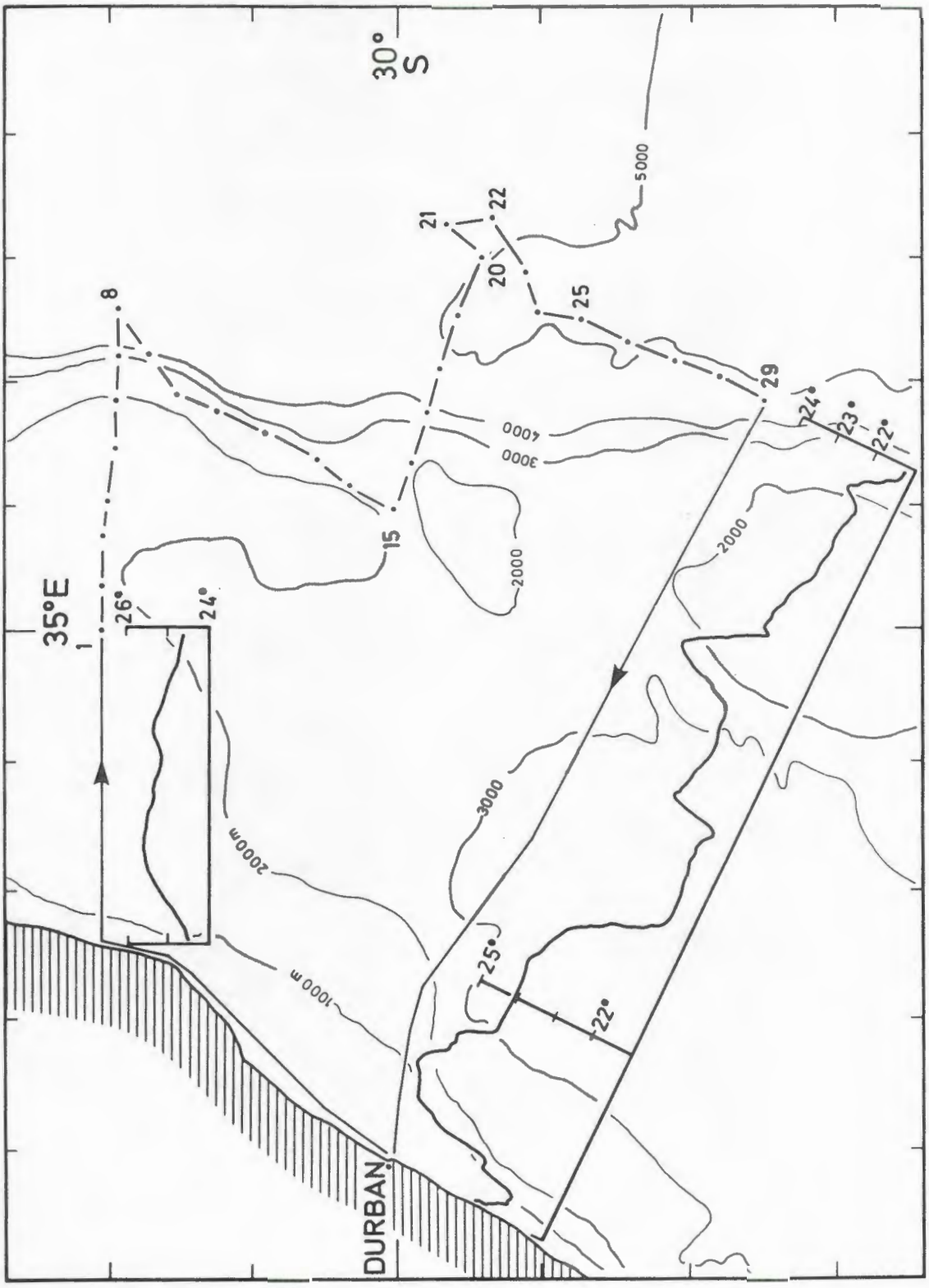

FIG. 9.4 : Track chart and thermograph trace of the *Meiring Naudé* cruise in April, 1981.

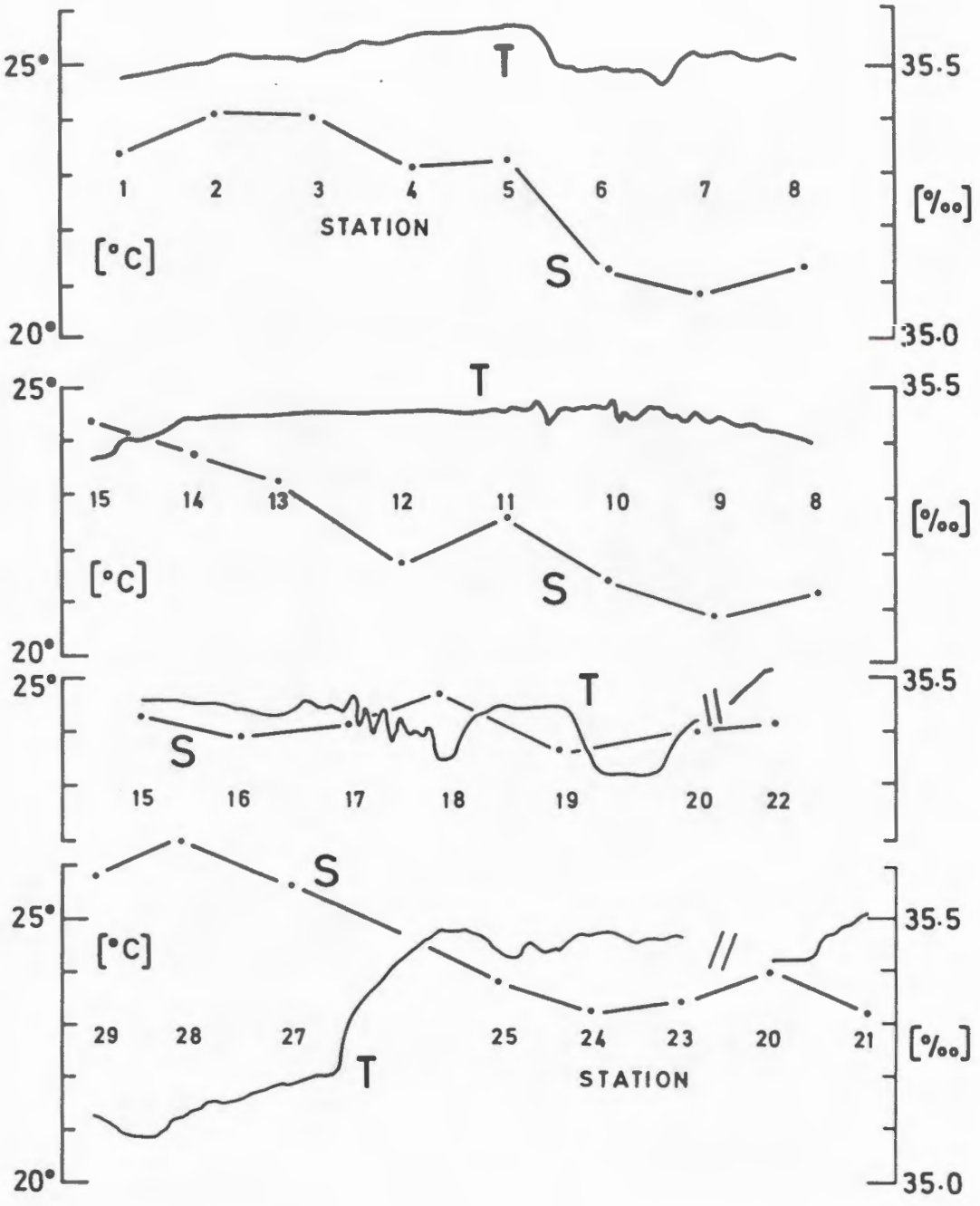

FIG. 9.5 : Variation of sea surface temperature and salinity for the cruise in April, 1981.

9.3.2 Thermohaline results

The variation of surface temperature during the outward and inward journeys (Fig. 9.4) seemed to indicate the existence of the Agulhas Current adhering to the coast off Durban and northward. Although not clearly evident on the journey up the coast and eastward towards the target area, the sea-surface temperature rose significantly as the *Meiring Naudé* penetrated the Agulhas Current off Cape St. Lucia. In this area, the Current normally comes to within a few kilometers off the coast (GRüNDLINGH, 1974; PEARCE, 1977b), and it is virtually impossible for the vessel to remain inshore of the Current. By the time the vessel headed eastwards, it was therefore already inside the Current, and the temperature did not rise any further.

The values of surface temperature and salinity east of 35°E (Fig. 9.5) indicated the presence of a water mass of tropical character (stations 6-12), and a water mass of subtropical character (stations 27-29), while the other stations represented a mixture of these two water masses.

Evidence was found in the subsurface thermohaline structure of the presence of Red Sea Water, as was the case during previous cruises. A lens of RSW (see Fig. 9.10) was observed at station 7 and again at station 9, while the neighbouring stations were affected to a much lesser degree or not at all. The lens of water extended vertically from about 1300 to 1500 db and is estimated to have been about 35 km wide (judged from the separation of stations 6, 7 and 8). Its extent in the N/S direction could not be ascertained, except that it exceeded about 15 km (the distance between station 7 and 9).

Harry was characterised by a rise of the deeper isotherms (Fig. 9.10) while the isotherms in the upper 200 m displayed the presence of a bowl of warm water. The vertical section across the eddy (Fig. 9.9) did not provide any answer about the exact position of Harry's centre, but the topography of the 10°C isotherm (Fig. 9.11) indicated that the centre was located more-or-less at the position of station 24, namely 30°57'S, 37°34'E. According to the usual definition of eddy shape and size, Harry was approximately circular with a diameter of 130 km.

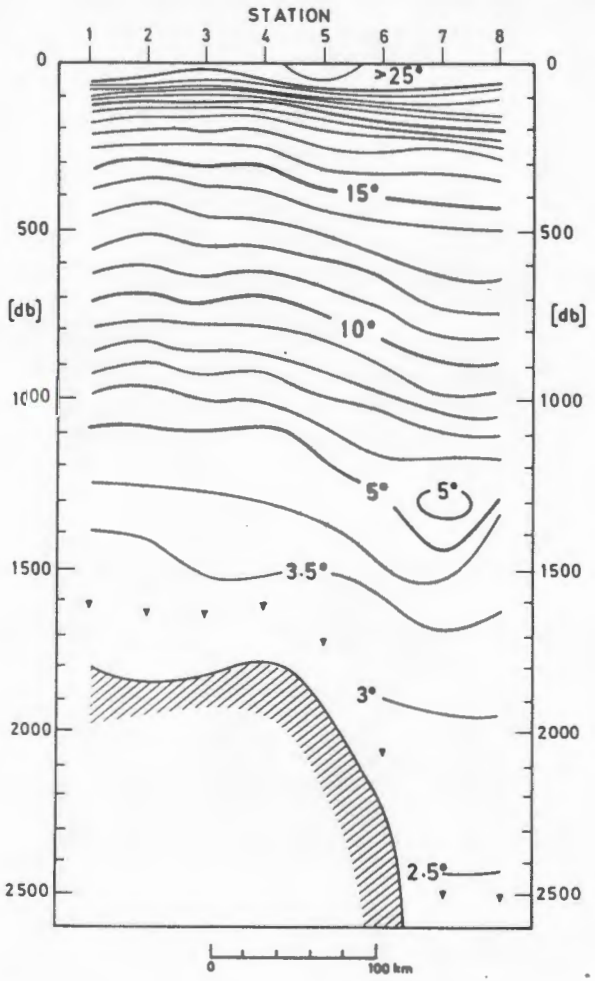

FIG. 9.6 : Vertical section of temperature of stations 1-8 of the cruise in April, 1981.

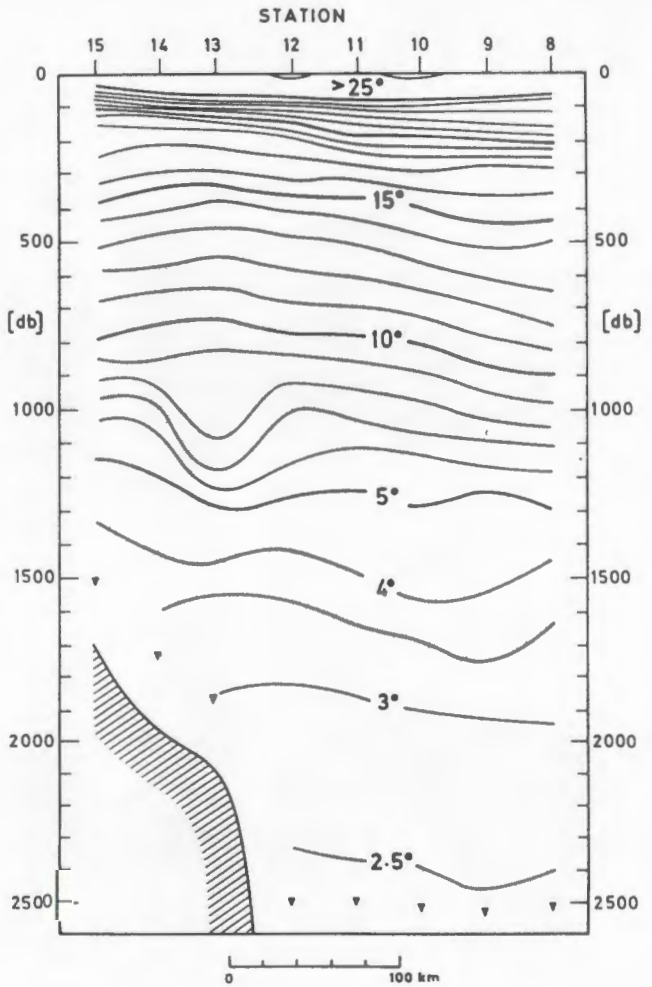

FIG. 9.7 : Vertical section of temperature of stations 8-15 of the cruise in April, 1981.

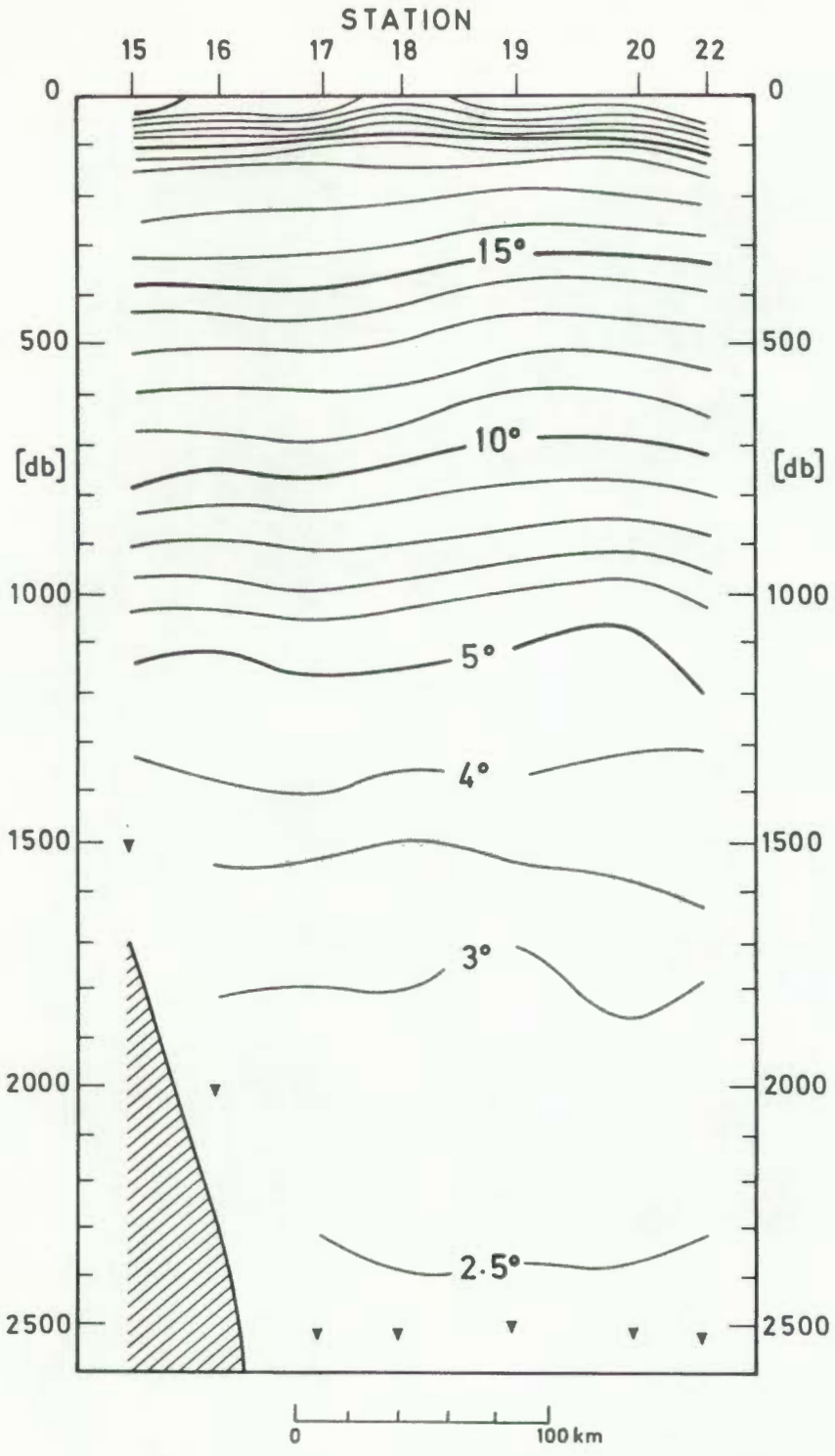

FIG. 9.8 : Vertical section of temperature on stations 15-22 of the cruise in April, 1981.

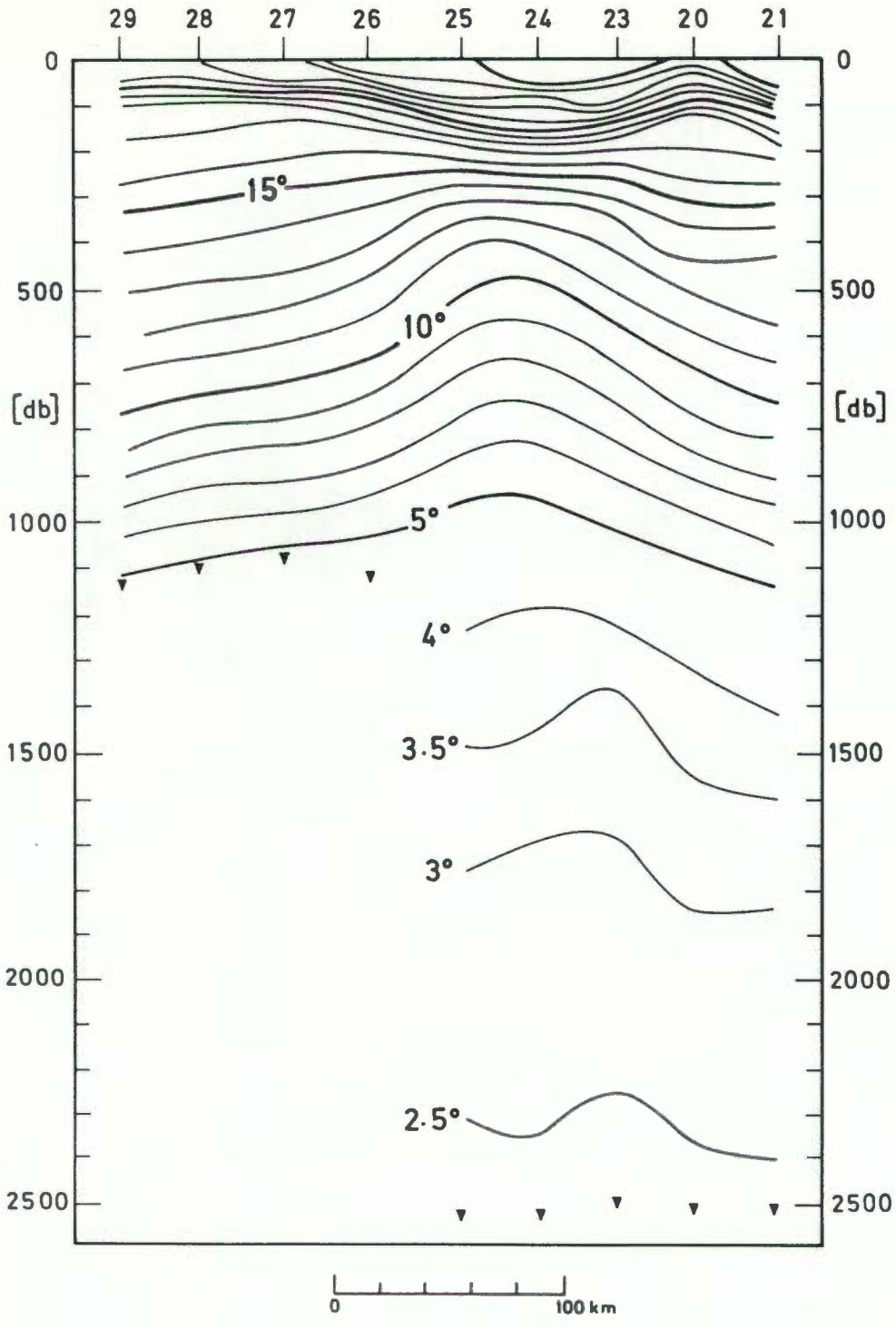

FIG. 9.9 : Vertical section of temperature for stations 20-29 of the cruise in April, 1981. Failure of the CTD at station 26 and subsequent equipment problems resulted in only limited coverage of temperature profiles on stations 27-29.

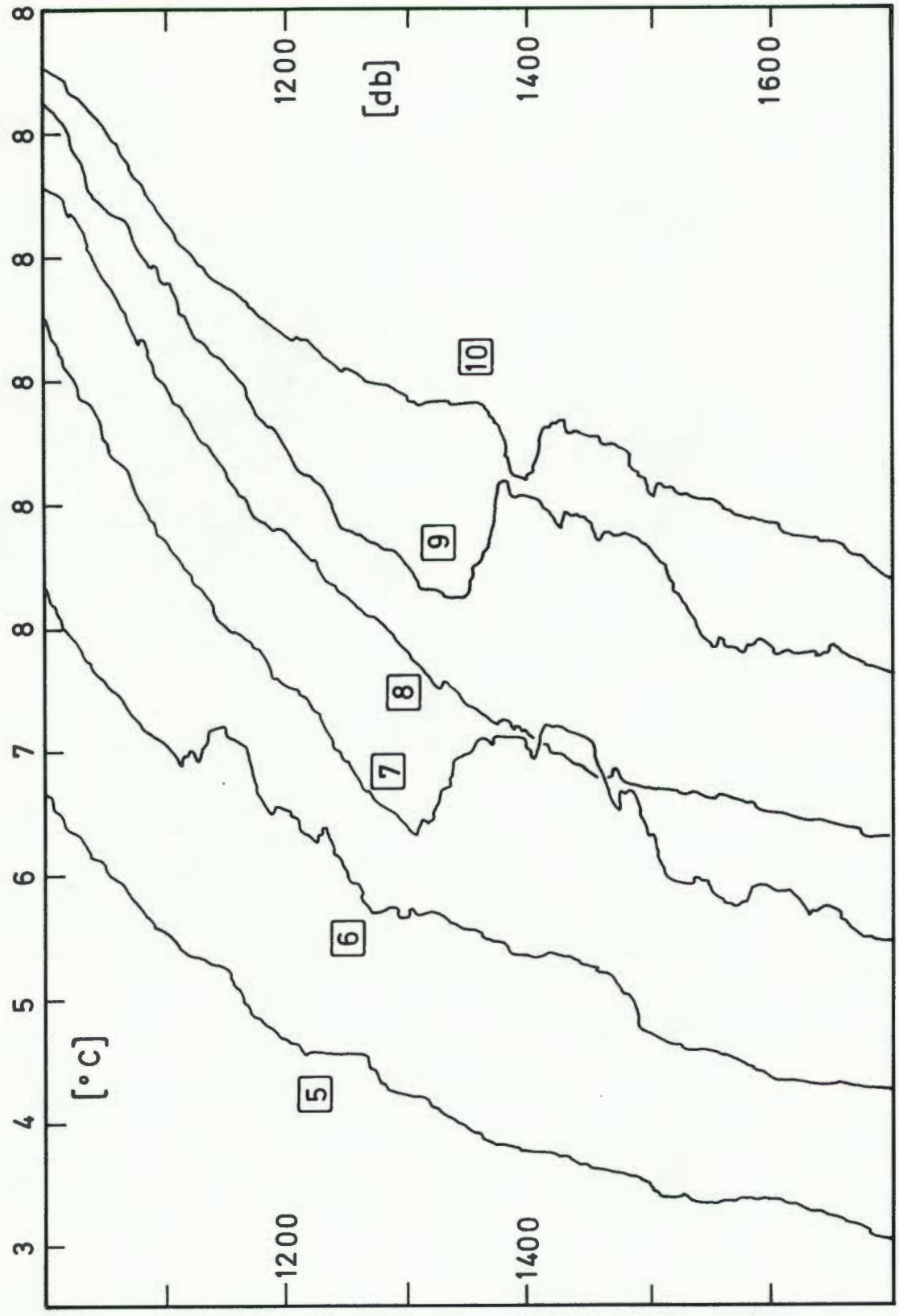

FIG. 9.10 : Vertical profiles of temperature from stations 5-10 and in the depth range 1000-1700 db. Successive profiles have been offset by one degree for separation. Note the high temperatures at stations 7 and 9 in 1400 db depth.

9.3.3 Dynamics

Because of the malfunction of equipment from station 26 onwards, geopotentials were not calculated for these stations and the circulation reflected by the geopotential is therefore incomplete. For the stations where full hydrographic data were available, the geopotential distribution was compared with the topography of the 10°C isotherm, and it was concluded that the 10°C topography (Fig. 9.11) could be used equally well to portray the circulation features of the cruise.

North of 30°S there was an anticyclonic circulation, while south of 30°S there was an intense cyclonic eddy. The circulation pattern as a whole closely resembled the flow observed during the surveys in December 1979 and January 1980 (Chapter 8), and this correspondence will be discussed in section 9.4.

The volume transports (Fig. 9.12) calculated relative to 1500 m, indicated that the "input" flow from the north amounted to 36 units of $10^6 m^3 s^{-1}$, a portion of which seemed to remain on the Mozambique Ridge. The 21 units diverging from the Ridge were augmented by some 31 units that seemed to represent the eddy itself, to total more than 50 x $10^6 m^3 s^{-1}$ passing between stations 8 and 24. Volume transports that were derived relative to the deepest depth common to each pair of stations (the maximum having been 2400 m), showed that the flux between station 8 and 24 amounted to 67 x $10^6 m^3 s^{-1}$.

9.4 Discussion

The cruise in February located an eddy that was defined so weakly so as to make it virtually insignificant compared to the other eddies discovered in this study. On the other hand, the eddy (Harry) located during the April cruise was intense and transported a large amount of water.

Harry seems to have represented the same flow pattern observed in eddy Fred, and the following points of comparison can be elucidated (using Figs. 8.25 and 9.11).

(a) At 28°S there was essentially a southward flow in both cases. In the case of the buoy tracks (Fig. 8.25), this flow was located between

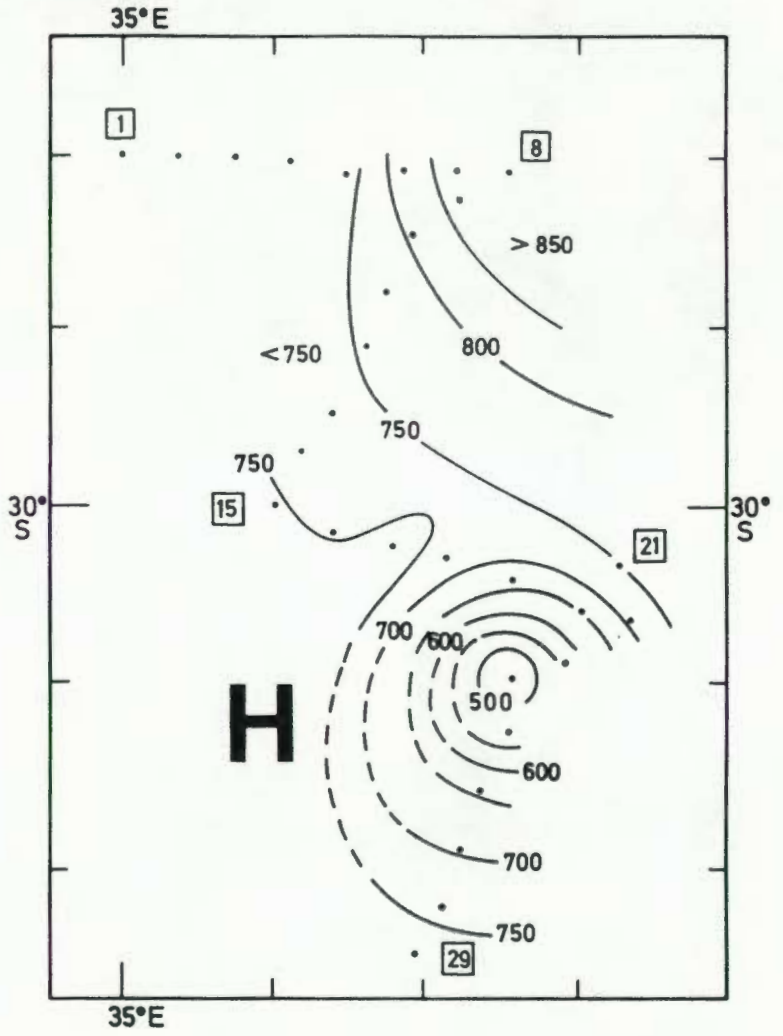

FIG. 9.11: Topography of the 10°C isotherm (in m depth) in April, 1981. Eddy Harry can be seen in the lower part of the figure.

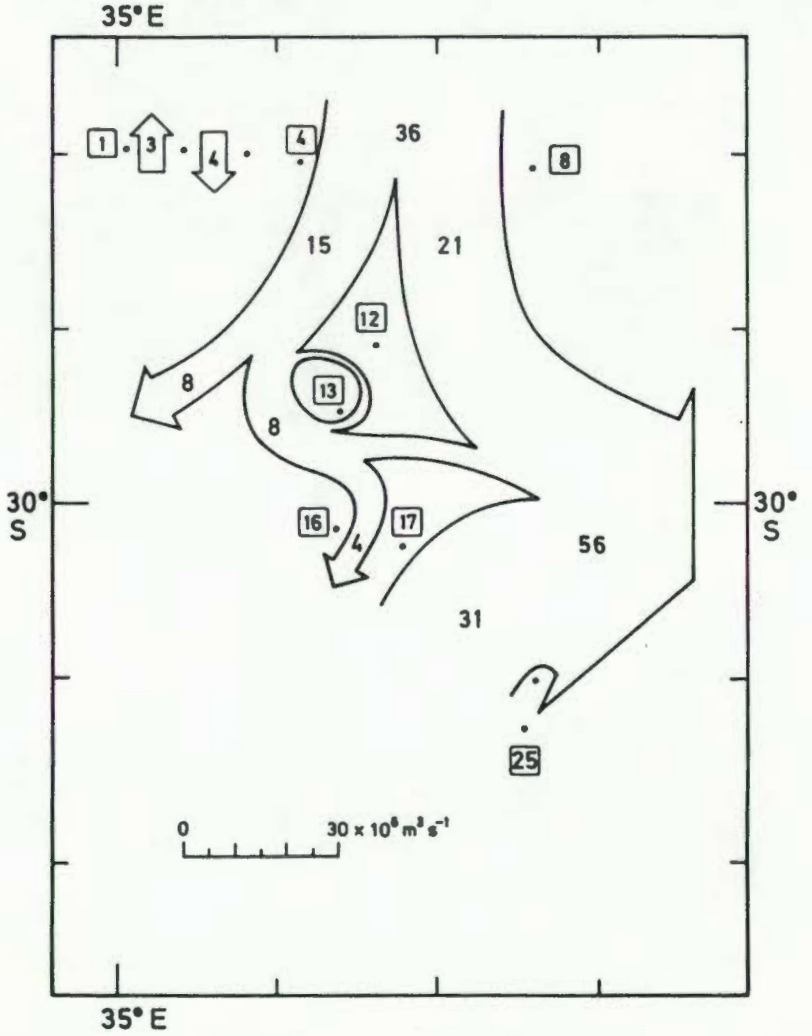

FIG. 9.12 : Volume transport (in $10^6 m^3/s$) calculated relative to 1500 m for the cruise in April, 1981.

35° and 36°E, i.e. above the Mozambique Ridge. During the present survey, this flow was located between 36° and 37°E, i.e. over the eastern escarpment of the Ridge.

(b) At 29°S, the flow in Fig. 8.25 turned sharply eastward and southeastward off the Ridge and into the Mozambique Basin. A similar bend is apparent in the flow regime of Fig. 9.11.

(c) In the area immediately south of this eastward jet there were two eddies (Fred and Golf, Fig. 8.25) situated above the eastern edge of the Mozambique Ridge. During the present survey, there was an eddy (Harry) situated in more-or-less the same place.

(d) The westward return flow of the looping current in Fig. 8.25 occurred at 31-32°S (37°E), and this agrees with the flow indicated in Fig. 9.11.

(e) The agreement also extended itself to the surface thermohaline structure. In November/December 1979 survey, the surface T/S distribution (Fig. 8.4) indicated the presence of water of a tropical nature at those stations in the northern part of the survey where the flow was by-and-large orientated toward the southeast, and subtropical water in the other areas. During the present survey, this distribution of water masses was also present.

On the basis of this evidence it seems reasonable to assume that the flow pattern that existed during the November/December 1979 survey was almost identical to the one during the present survey.

The question that immediately arises is whether the present circulation *is* not perhaps the same one that existed more than a year before? In the light of the results obtained in February 1981 (see section 9.2) the answer must definitely be no. The stations of that cruise covered the area between 28° and 29°S, (where the present cruise observed first indications of a strong southward flux at stations 5-8), without evidence of a significant southward-flowing current.

How do the results obtained in February, March, April and October 1981 fit together then? Since there seems to be no (visual) relation between the flow regimes that existed in February, March and April, it must be concluded that Harry was generated between the March and April

cruises. This would indicate that the cyclogenesis, as well as the Mozambique Ridge Current, have onset periods of the order of 1 month, which agrees with the conclusion in section 8.11.2. Unfortunately, the cruise in October (Fig. 3.8(a)) did not cover the area south of 30°S where Harry was initially situated, so that the possibility of fortuitously relocating Harry was excluded. It is significant, though, that a strong current (the Mocambique Ridge Current?) was situated on the eastern escarpment of the Mozambique Ridge (see Fig. 3.8(a)), similar to where Fig. 9.12 showed the MRC at 28°S. The possibility that Harry still existed in the area south of 30°S in October can therefore not be excluded.

One of the interesting features of the Mozambique Ridge Current is the recurring presence of Red Sea Water (RSW). For the cruise in April it has been possible to allocate some physical dimensions to this water mass. The position at which it was located ($\sim$ 28°S, 37°E) agreed with the position where it was observed in October (27°30'S, 38°E), and in both cases RSW was situated on the anticyclonic side of the Mocambique Ridge Current. The local origin of RSW, its course and relevance to the regional circulation and the eddies remain enigmatic.

CHAPTER 10

OBSERVATION OF DEEP-SEA VORTICES : 1982

10.1 Introduction

Two cruises were executed in 1982, and these were to be the last major data-collection exercises of this thesis. The cruises were executed in April and June, respectively, and both were aimed at locating and surveying vortices in the vicinity of the northern Mocambique Ridge. Both cruises started at 28°30'S, 35°E and proceeded in an easterly direction. As it turned out, an eddy was located on each cruise, albeit in markedly different circumstances.

10.2 Observations in April, 1982

10.2.1 Narrative of the cruise

The *Meiring Naudé* left port on 13 April 1982, and steamed toward the target area (see Fig. 10.1). Whereas the sea-surface temperature had remained constant while the ship was close inshore, there was a significant increase in the temperature (not shown here) soon after the vessel moved away from the coast at Cape St. Lucia.

Hydrographic stations were started at 10h00 on 15 April at a position that was regarded to be beyond the Agulhas Current. However, the data collected at the first few stations (Fig. 10.2) showed that the water column below about 200 m was much cooler than anticipated, and becoming colder. The line of stations was continued about 500 km offshore where the isotherms reached their expected levels again.

The course was altered toward the southwest (station 10, Fig. 10.1) to enable a line of stations to be occupied that would pass through the point where the deeper isotherms were at their maximum elevation. Two sections were planned to cover the northern part of the survey area, namely stations 20-24 and 27-30, and the zonal line (stations 1-10) was eventually augmented toward the coast by stations 31-35.

The CTD failed on station 28, and the standby hydrosonde suffered from electromechanical problems that first prevented salinity samples to be collected and eventually caused a complete failure after station 35. The cruise was therefore terminated and the vessel returned to Durban on 22 April.

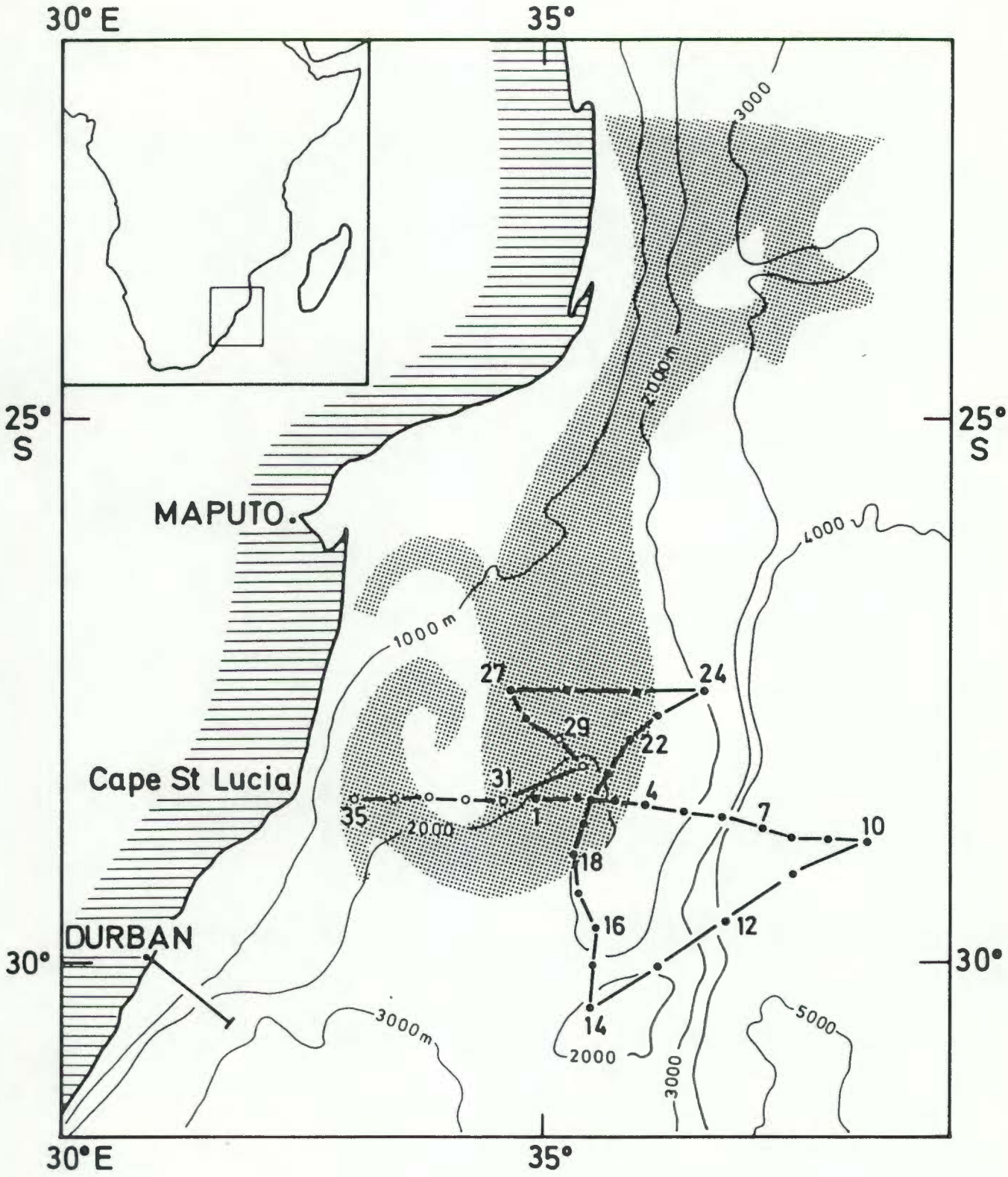

FIG. 10.1 : Cruise track of the *Meiring Naudé* in April, 1982. Dots represent CTD stations, while circles indicate stations with temperature profiles only. Shading represents an enhanced infra-red pattern observed from METEOSAT on 15 August, 1978.

10.2.2 Thermohaline results

The sections of temperature (Figs. 10.2 and 10.3) show an upheaval of isotherms that reached a maximum in the vicinity of station 2 and 20. This maximum elevation that raised e.g. the 10°C isotherm from its "normal" depth of approximately 700-800 m to as little as 320 m (see Fig. 10.4) represented one of the largest displacements observed on this project. The data obviously reflected the characteristics of a cyclonic eddy, codenamed Ian.

Horizontally, Ian extended much further in an easterly direction than towards any other direction. Toward the east, the isotherms (Fig. 10.2) levelled off only at station 8, some 210 km from the point of maximum displacement, whereas in the other directions it seemed to level off (albeit not at the same depth as at station 8) at station 16 (140 km from the centre), station 24 (160 km). At station 27 (the northwesterly limit of the survey) the isotherms had not levelled off yet.

There seemed to be a mismatch between the data collected on 20 and 21 April (station 27 to 35) and the data collected during the rest of the survey, resulting in an inability to align the isotherm pattern of stations 31-35 with the pattern of station 1-10 (Fig. 10.2). This was interpreted as indicating that Ian had shifted toward the coast during the survey, and that the point of maximum elevation of the isotherms had moved westwards by approximately 70 km in the period between the time of stations 2 and 3 and the time of station 31, namely 130 hours. This amounted to an advection rate of approximately 15 cm/s. According to Fig. 10.4 Ian seemed to have been elliptical with dimensions of 180 km x 260 km.

There were consistent changes in the depth of the mixed layer throughout the survey area, and this depth varied from about 95 m in Ian's centre to 60-70 m away from the centre (Fig. 10.5). Toward the eastern perimeter of the area, i.e. east of station 7, there occurred a significant deepening of the mixed layer. This coincided with a small surface thermohaline frontal system that existed between station 6 and 7.

Although the nominal station depth was 1000 m, selected stations were occupied to 2000 m, depth permitting. Some of these deeper stations revealed the existence of temperature fine structure in the depth range

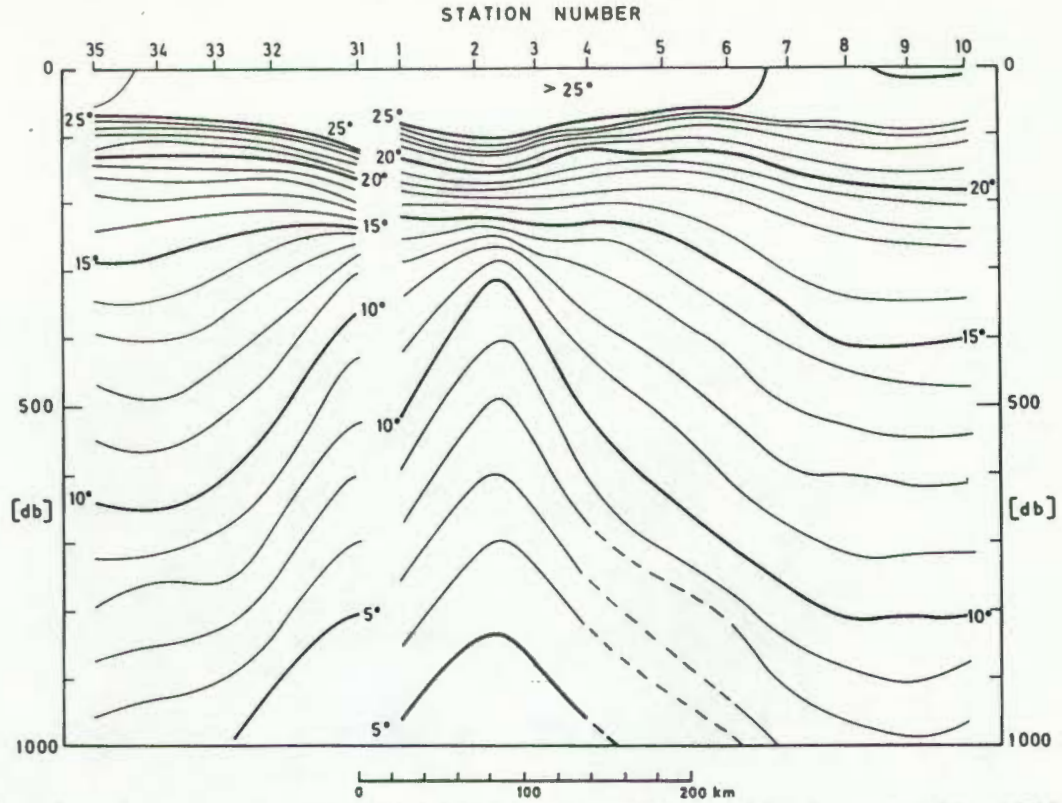

FIG. 10.2 : Quasi-zonal section of temperature across eddy Ian, April, 1982. Isotherms have been interrupted between stations 1 and 31 because of data mismatch.

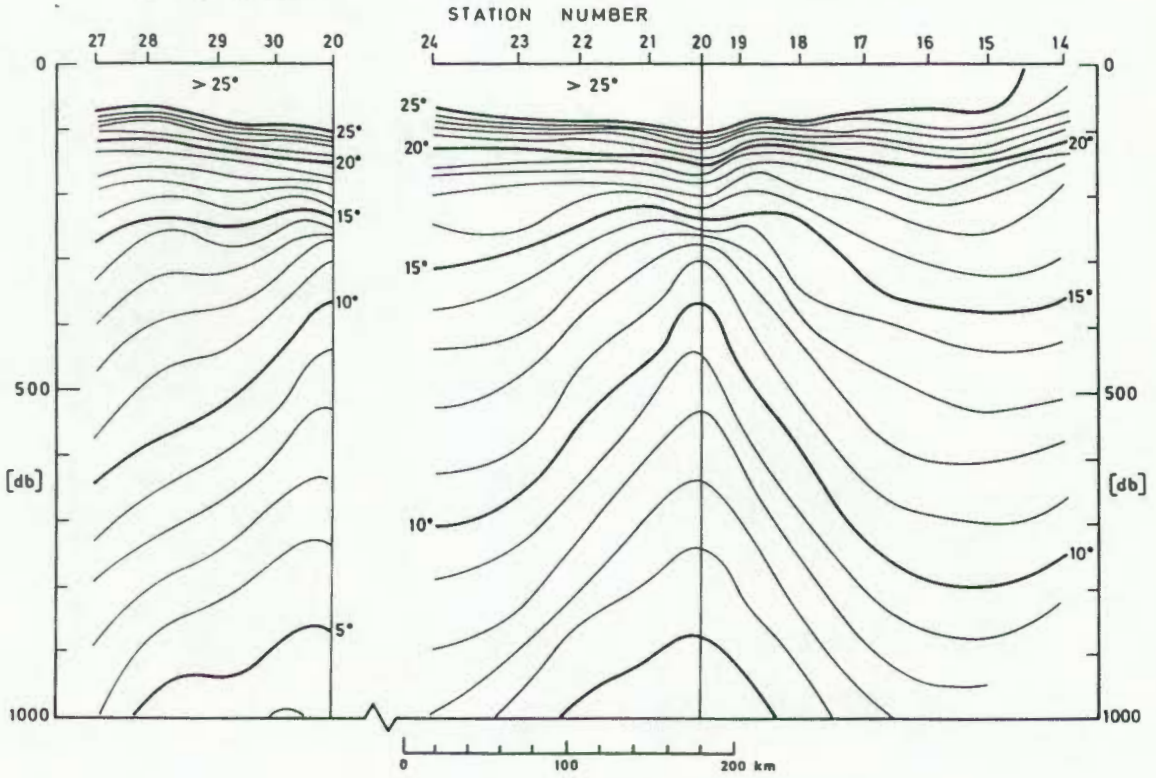

FIG. 10.3 : Quasi-meridional sections of temperature across eddy Ian in April, 1982.

1000-2000 m, but it would be impossible to present a reasonable geographical distribution of these anomalies since many of the stations were possibly just too shallow to have observed it.

10.2.3 Dynamical structure

Ian's oval shape as suggested by the topography of the 10°C isotherm surface (Fig. 10.4) is confirmed by the geopotential of the sea surface relative to 1000 m (Fig. 10.6), derived from the CTD stations only. This topography shows that the vortex maintained a depth of approximately 35 cm below its surroundings. Unfortunately, the geopotential could not be completed in the western half of the vortex because of the absence of any salinity readings. Many of the topographical contours of the 10°C surface were closed in the western sector (Fig. 10.4) and it would be reasonable to assume that this was the case too for the geopotential topography.

The gradient current velocities along a quasi-meridional section (Fig. 10.7) revealed maximum speeds of 40-50 cm/s about 80-100 km from Ian's centre. This distribution was also reflected by the profiles of kinetic energy across the eddy (Fig. 10.8). The maximum kinetic energy seemed to be the same in all sectors of the eddy, and Ian's total kinetic energy (relative to 1000 m) was estimated (see Fig. 10.8) at 1.8×10^{15} J.

The amount of water transported through the various transects across Ian is portrayed in Fig. 10.9. This shows that the transports varied between 17 and 34 x $10^6 m^3 s^{-1}$, the larger flux having occurred in the eastern and southern sectors of the vortex. Relative to the deeper reference levels, a maximum of 71 x $10^6 m^3 s^{-1}$ was derived through the easterly part between station 20 and 10. The impression is gained that the flow consisted on the one hand of an amount of water coming into (12 units) Ian down the Mozambique Ridge at 36-37°E and leaving in a westerly direction (13 units), and on the other hand of an amount of water circulating the eddy(13-17 units). Attention must be drawn to the incompleteness of the transport diagram in that no transports could be calculated for the western sector.

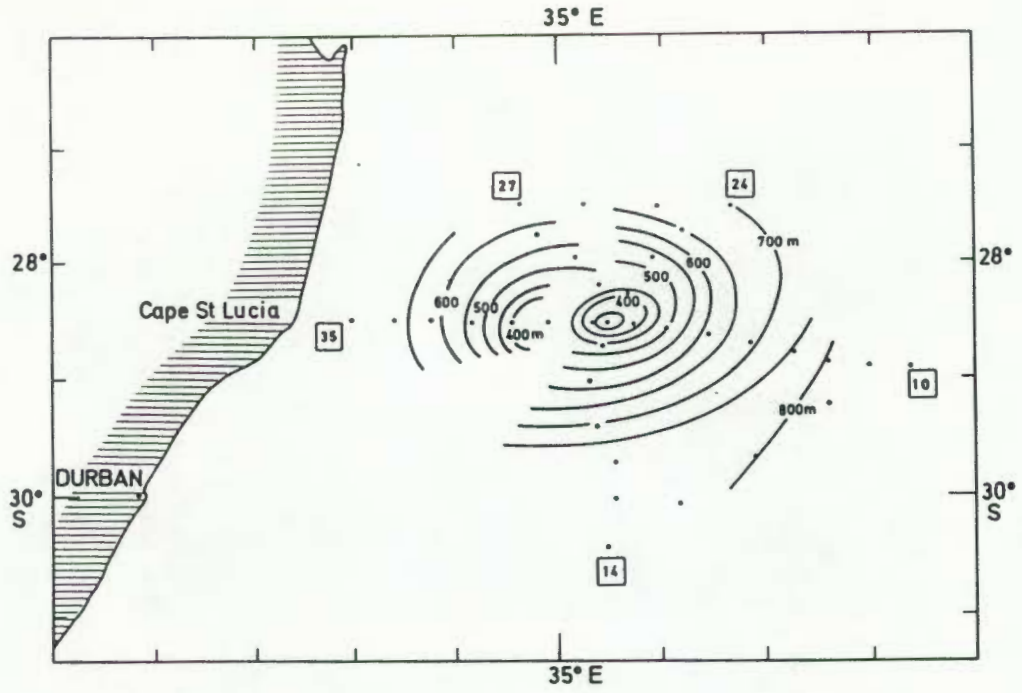

FIG. 10.4 : Topography of the 10°C isotherm (in m depth) in April, 1982, showing the size and shape of eddy Ian.

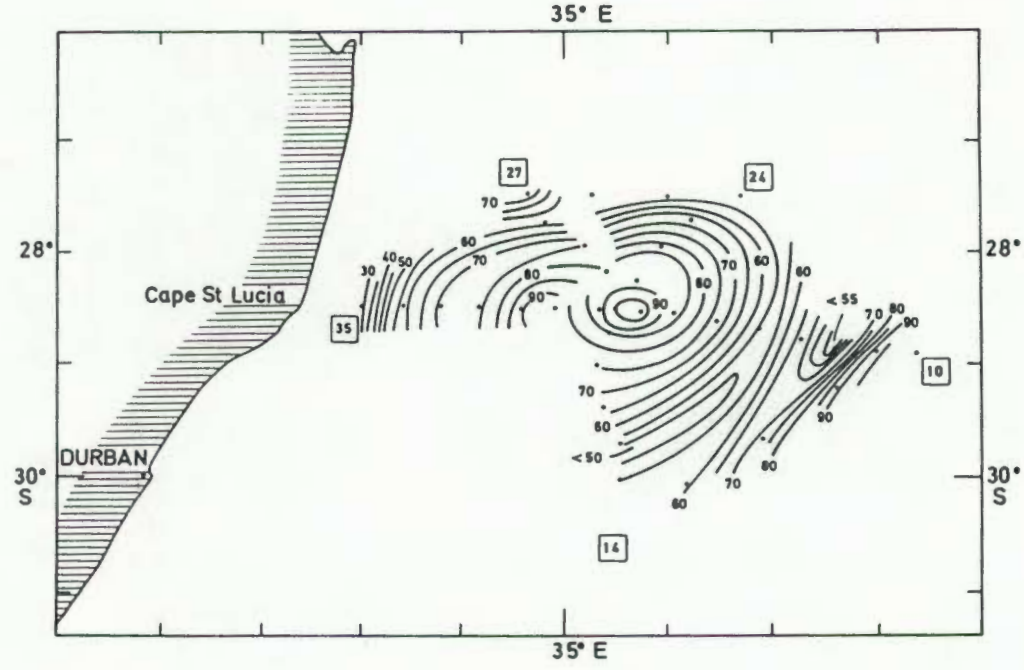

FIG. 10.5 : Depth of the mixed layer (m) in the vicinity of eddy Ian in April, 1982. Because of the mismatch in the data (see text), the contours were interrupted at station 27.

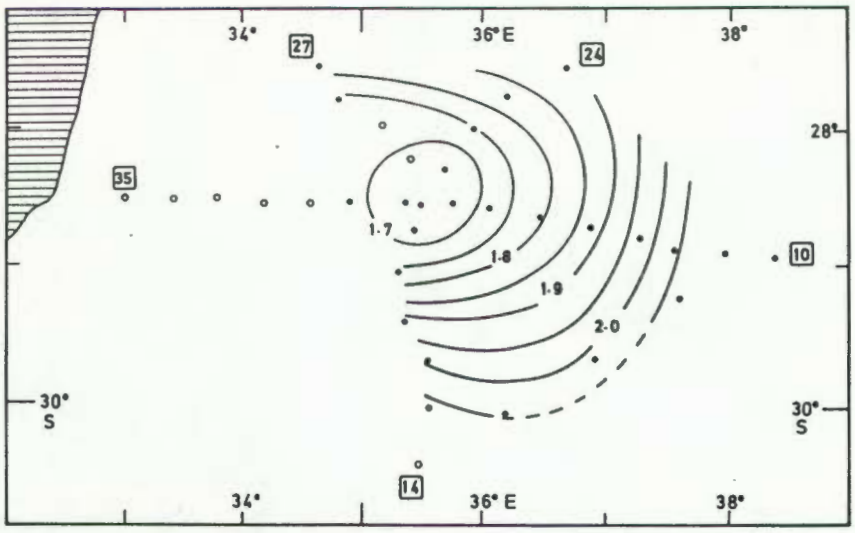

FIG 10.6 : Geopotential anomaly (in units of 10 m^2/s^2) of the sea surface relative to 1000 m, derived from the CTD stations' (dots) data. Circles indicate stations on which temperature profiles only were obtained.

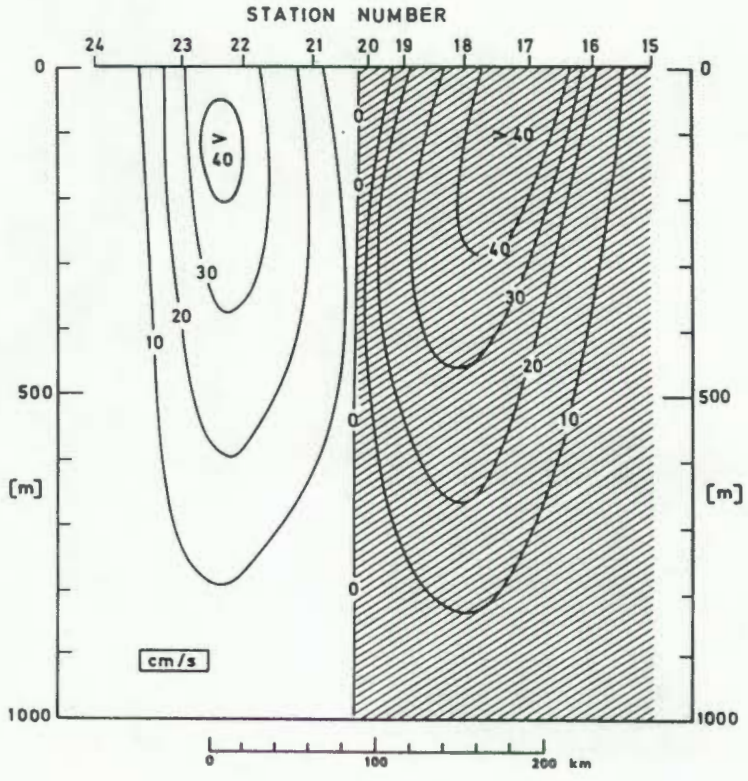

FIG. 10.7 : Gradient current velocity from the quasi-meridional section across eddy Ian in April, 1982.

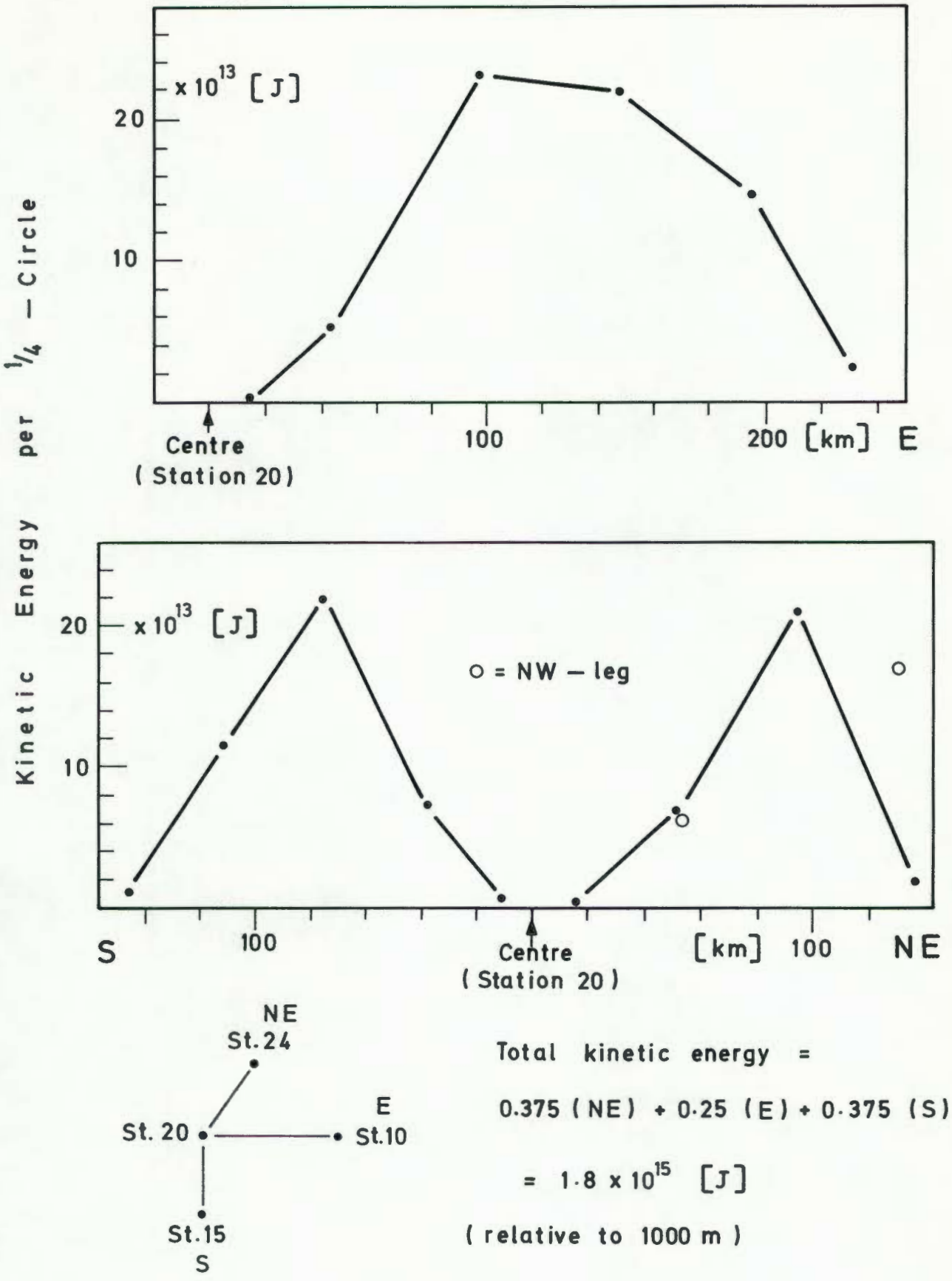

FIG. 10.8 : Kinetic energy across eddy Ian observed in April, 1982.

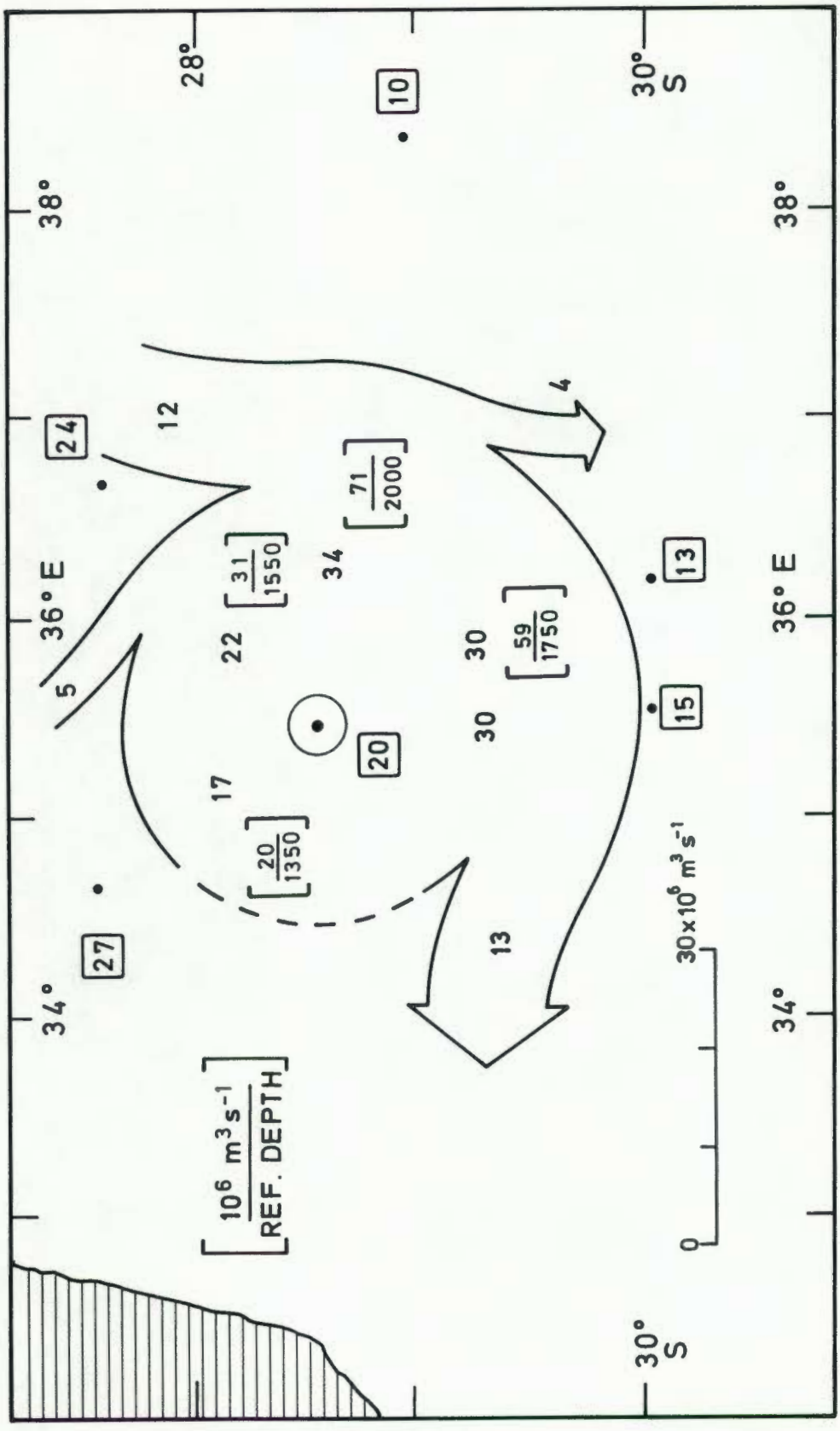

FIG. 10.9 : Volume transport relative to 1000 m of eddy Ian observed in April, 1982. Isolated transports, derived relative to deeper reference levels are indicated.

10.2.4 Discussion

From the apparent mismatch in the data collected during the cruise, it was concluded that Ian had advected at about 15 cm/s during the time of the survey. This speed is of the same order as the 20 cm/s derived by HARRIS and VAN FOREEST (1977) and GRüNDLINGH (1979) for the movement of large, wavelike distributions further down the coast (34°S). The elliptical shape of the eddy as it appeared in Fig. 10.4 could have been the result of this advection.

A significant conclusion drawn from the zonal temperature section (Fig. 10.2) is that the Agulhas Current seems to have been absent in the area close to the coast. In the region immediately south of Cape St. Lucia, the Agulhas Current is normally located 10-20 km from the coast (see PEARCE, 1977; GRüNDLINGH, 1983). According to Pearce, the "width" of the Current (taken as the region where the velocities exceed 1 m/s) varies between 5 and 50 km. However, the region of significant southward flow extends beyond 100 km offshore. Although the hydrographic stations during the present survey did not extend right up to the coast but stopped some 60 km short, the temperature section (Fig. 10.2) did not contain evidence of any significant southward flow at the coast. The existence of a narrow coastal current can, however, not be excluded (this, in fact is confirmed by the thermal front off Cape St. Lucia).

Evidence of a similar synoptic-scale anomaly in the flow of the Agulhas Current was observed in the infrared image taken on 15 August 1978 (superimposed in Fig. 10.1) by the METEOSAT 1 weather satellite. The image was received and processed at the Satellite Remote Sensing Centre at Hartebeeshoek, Pretoria, and has been enhanced to reveal features of the sea surface temperature pattern. While it is true that surface temperature patterns as observed by a radiation thermometer are not *per se* equal to the circulation patterns, there is evidence that in the strong flow of the Agulhas Current, surface temperature is generally a good indicator of circulation elements (see GRüNDLINGH and SNYMAN 1972; GRüNDLINGH, 1974). Satellite images have also been used with great success south of the continent (LUTJEHARMS, 1978; 1981b), and we assume here that the surface temperature patterns reflect the movement of the water.

In Fig. 10.1 the main influx from the northeast (as portrayed

by the infrared pattern) seems to have converged at 26°S, while immediately southward there is evidence of an offshore divergence. Why the flow should first converge and then diverge is not clear, but it could be related to variations in the bottom topography. The topography namely shows that the steepness of the continental slope reduces from north to south in the bight off Maputo, and at 25°30'S the 1000 m contour separates from the coast to form a "bank" almost 200 km wide in this area.

Further south, at 27-28°S, the whole of the 150 km-wide flow turned clockwise to form an eddy with its centre at 27°S, 33°30'E. It is depicted by an inward-spiralling helix of warm water that seems to have completed at least a full revolution at the time the image was scanned.

The visible waveband of the satellite revealed various patterns of cloud southward from Cape St. Lucia, and through a clearing in the cloud formation south of Durban (not included in Fig. 10.1), a surface temperature pattern resembling the Agulhas Current could be seen. However, careful inspection of the satellite image indicated that there was no connection between the eddy at 27°S and the flow south of Durban, i.e. the flow of the Agulhas Current was completely interrupted at 29°S.

A feature of this magnitude has not previously been observed in this area. The inshore current reversals described by GRüNDLINGH (1974) involve much smaller phenomena between the Agulhas Current and the coast. Although of the same nagnitude, larger meanders observed further southward (e.g. GRüNDLINGH, 1979) seem to display the characteristics of a wave rather than that of an eddy, although a progressive transformation of the one into the other cannot be excluded.

The impression is gained that the ship's survey in April 1982 stumbled upon a feature very similar to the one recorded by the satellite four years previously. In both cases the eddies were large, and, more important, generated by the Agulhas Current. The main difference between the two observations lies in the flow south of the eddy: In the satellite image, the Agulhas Current was interrupted by the presence of the eddy, while the ship survey showed that the Agulhas Current continued southwards after having been deflected offshore around the eddy.

10.3 Observations in June 1982

The cruise in June 1982 was not aimed primarily at recording the vortex (Ian) observed two months previously, since the vortex was not expected to have remained in the area for very long. This conclusion was based on the movement of the vortex during the survey (at a rate of about 15 cm/s), which would advect the eddy through a distance of about 700 km over the intervening two months. However, to make sure of Ian's absence, the survey started in the area where Ian's centre had been located (27°30'S, 35°E).

10.3.1 Narrative of the cruise

The *Meiring Naudé* left harbour at 20h00 on Tuesday, 8 June. A course was set northward along the coast inshore of the Agulhas Current, and at St. Lucia the Current was traversed as the vessel proceeded eastward (see Fig. 10.10). A test station (station 1) was occupied on Wednesday 9 June, and some problems with the equipment were rectified.

The first leg of the planned grid (28°30'S, 35°E - 28°30'S, 38°E) was completed with stations 2 to 10 (at 20 nautical mile intervals) and no conclusive evidence was found of vortices in the area. The results also confirmed that Ian had moved from its original location. The cruise then proceeded toward the second leg (which would have run from 30°S 38°30'E to 30°S 35°30'E), executing hydrographic stations *en route* at 30 nautical mile intervals. The isotherms, plotted as the cruise progressed (Fig. 10.11) revealed a slight disturbance in the vicinity of stations 13 and 14 and the line of stations was promptly terminated. The set of the ship indicated that an eddy was possibly situated to the east of the line of stations 10 to 14, but it was nevertheless decided to check the area between station 14 and the edge of the Mozambique Ridge first. The results of station 15 clearly indicated that the eddy centre *was* located east of station 14, and the survey was focussed on this region (see Fig. 10.10).

A very intense vortex (codenamed John) was discovered, centred at station 31. The east-west traverse through John's centre was eventually augmented with stations 41 and 42 located west of station 15. Deep (2 000 m) stations were executed in the centre and on the perimeter of John except on the western edge.

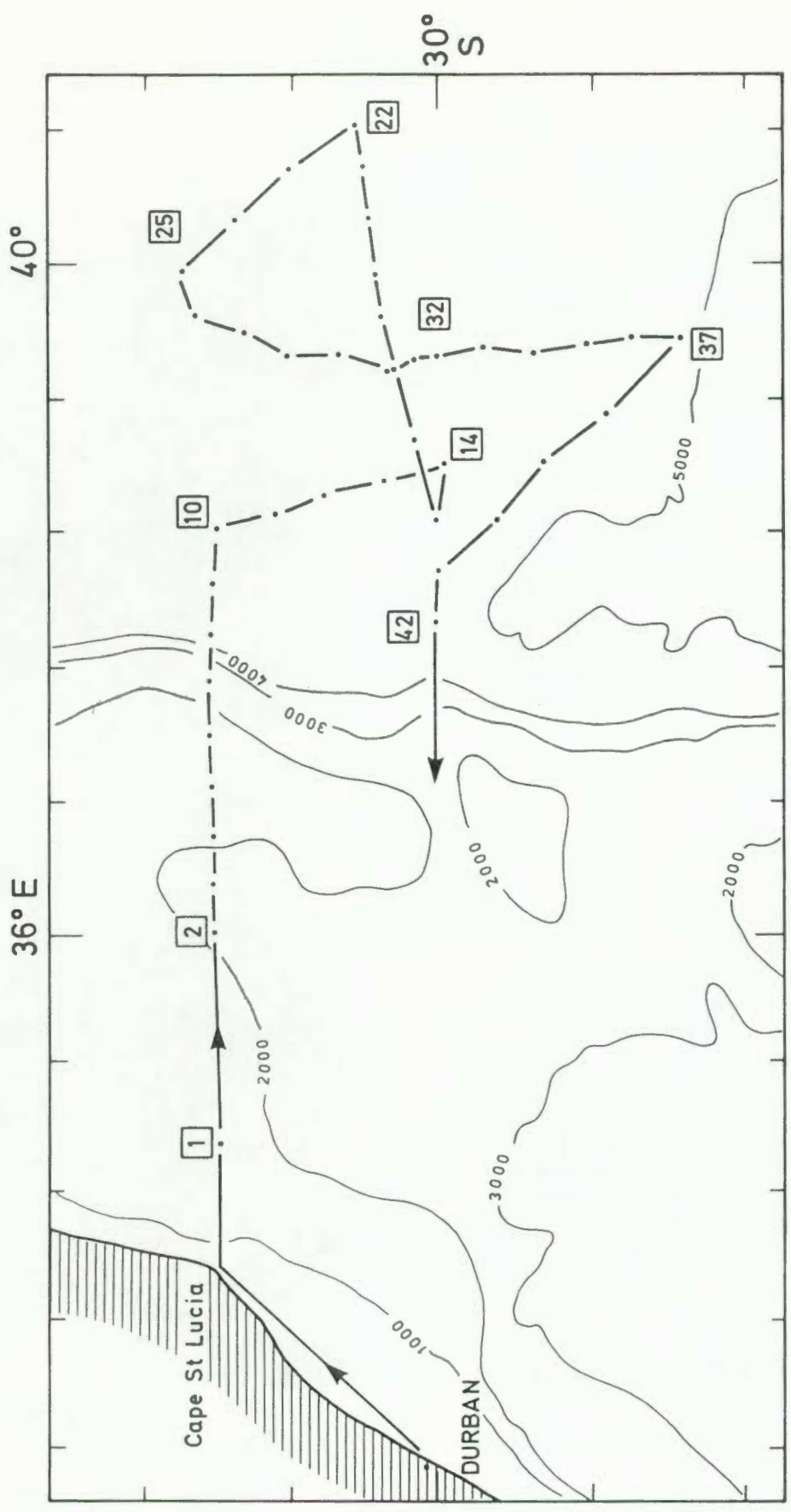

FIG. 10.10 : Track chart of the *Meiring Naudé* cruise during the survey of eddy John in June, 1982.

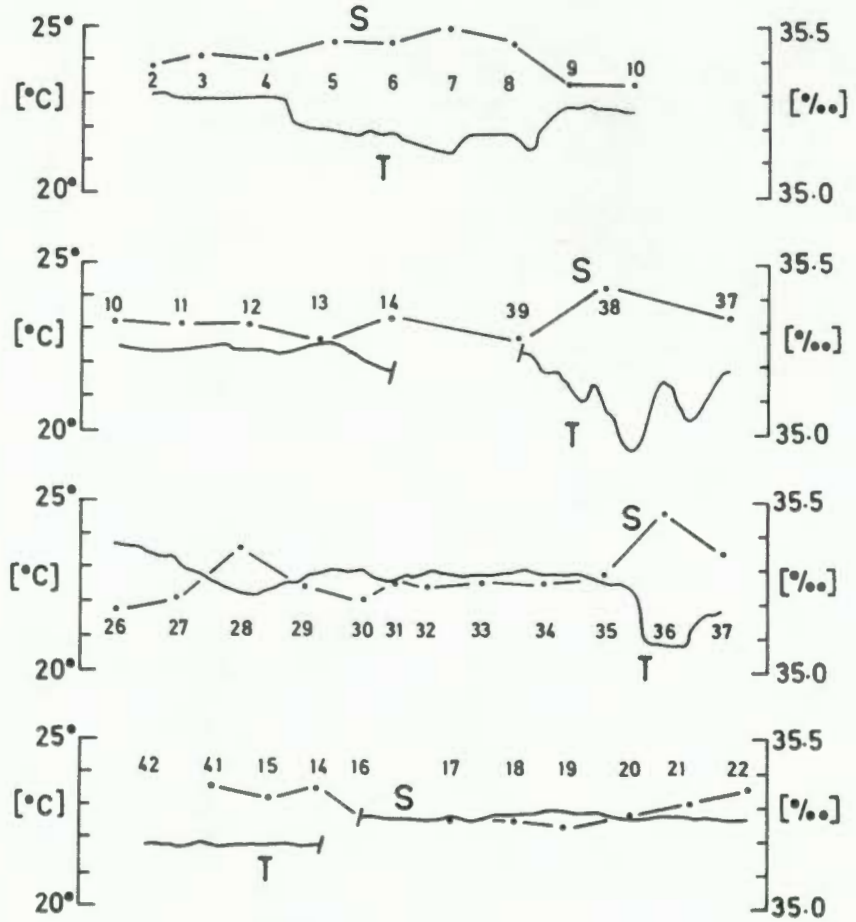

FIG. 10.11 : Variation of surface temperature and salinity during the cruise in June, 1982.

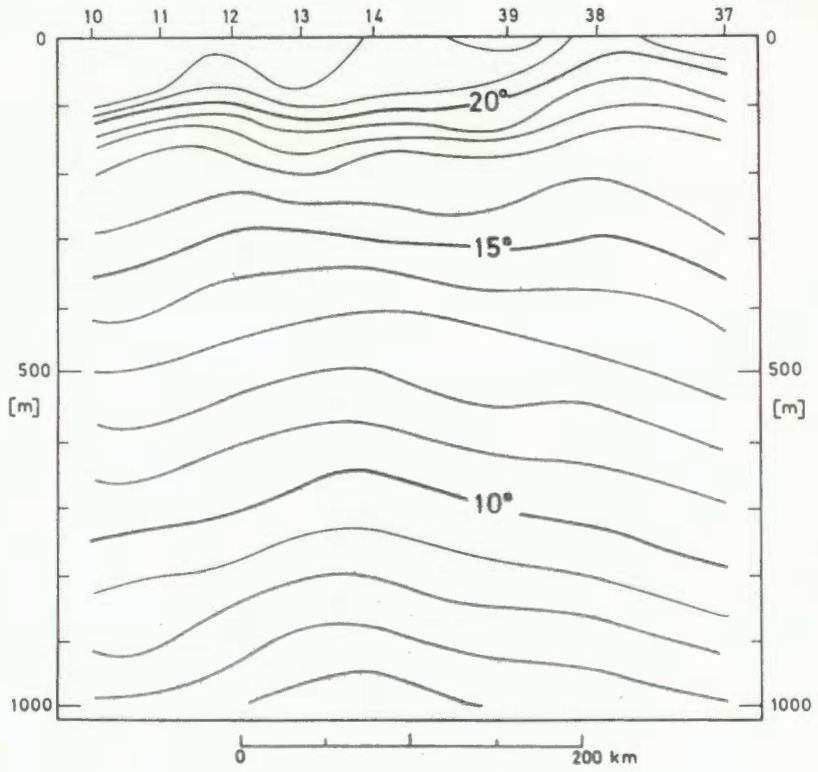

FIG. 10.12 : Vertical section of temperature on a line between stations 10 and 37 in June, 1982.

The *Meiring Naudé* returned to Durban on Thursday, 17 June 1982.

10.3.2 Thermohaline results

For most of the stations, the surface temperature and salinity showed very little variation (Fig. 10.11). The thermal fronts were very small, except in the vicinity of stations 36-39. Here, on the southern perimeter of the survey area, the temperature at times dropped to 2-3°C below the surface temperature over the rest of the eddy. At the same time the surface salinity rose by 0.1-0.2 °/oo. The higher salinity and lower temperature indicated that these stations were situated in a water mass with a stronger subtropical character, while all the other stations tended to contain water of a more tropical nature.

The southerly traverse from station 10 onwards revealed a small but significant upheaval of the isotherms (Fig. 10.12), with the vertical displacement of the 10°C isotherm between station 10 and 14 amounting to about 100 m. From station 15 to 20 the deeper isotherms showed a conspicuous upheaval, coinciding with a slight deepening of the isotherms in the upper 200 m (Fig. 10.14). The centre of this cold water mass below 300 m was in the vicinity of station 17, where the 10°C isotherms rose to 436 m. The traverse was extended well beyond the point where the isotherms seemed to level off again.

Between station 22 and 25 there was a slight heating of the water column below 300 m. On the southerly transect (stations 26 to 37), the line of stations was orientated in such a way as to pass through the centre of the upheaval encountered on station 17. As the line of stations progressed, the deeper layers cooled even further, the coldest temperatures occurring only at station 32 (Fig. 10.16), approximately 40 km south of station 17.

A bowl of warm water was located at station 32, causing a deepening of the isotherms. At this station, which is considered to have been situated in John's centre, the 10°C isotherm rose to 395 m. At a depth of about 200-300 m, there was virtually no horizontal temperature gradient (see Figs. 10.14 and 10.17).

The lateral extent of the upheaval can be seen from the topography of the 10°C isotherm (Fig. 10.17), which shows that John was almost perfectly circular with a diameter of about 180 km.

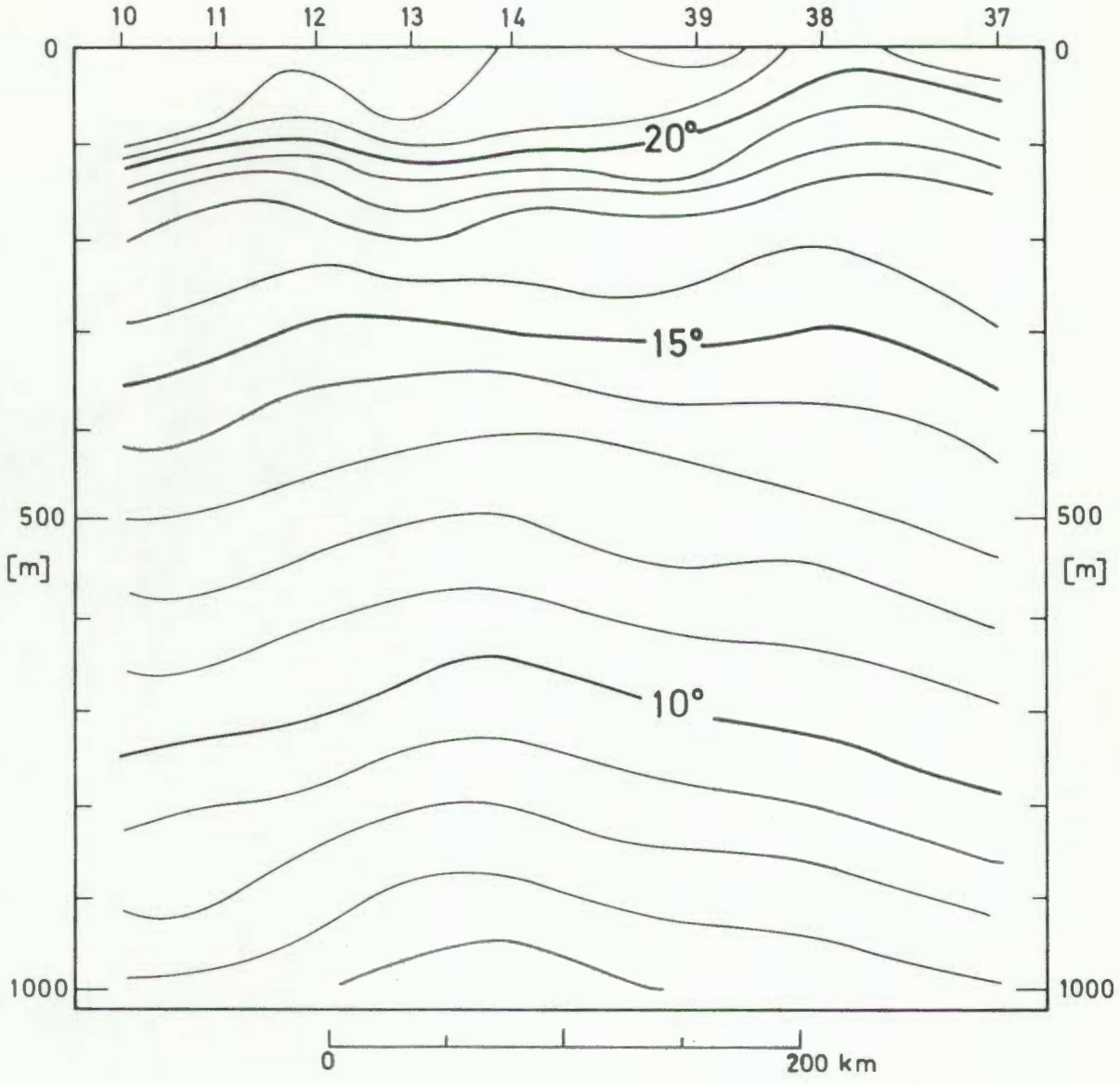

FIG. 10.12 : Vertical section of temperature on a line between stations 10 and 37 of the cruise in June, 1982.

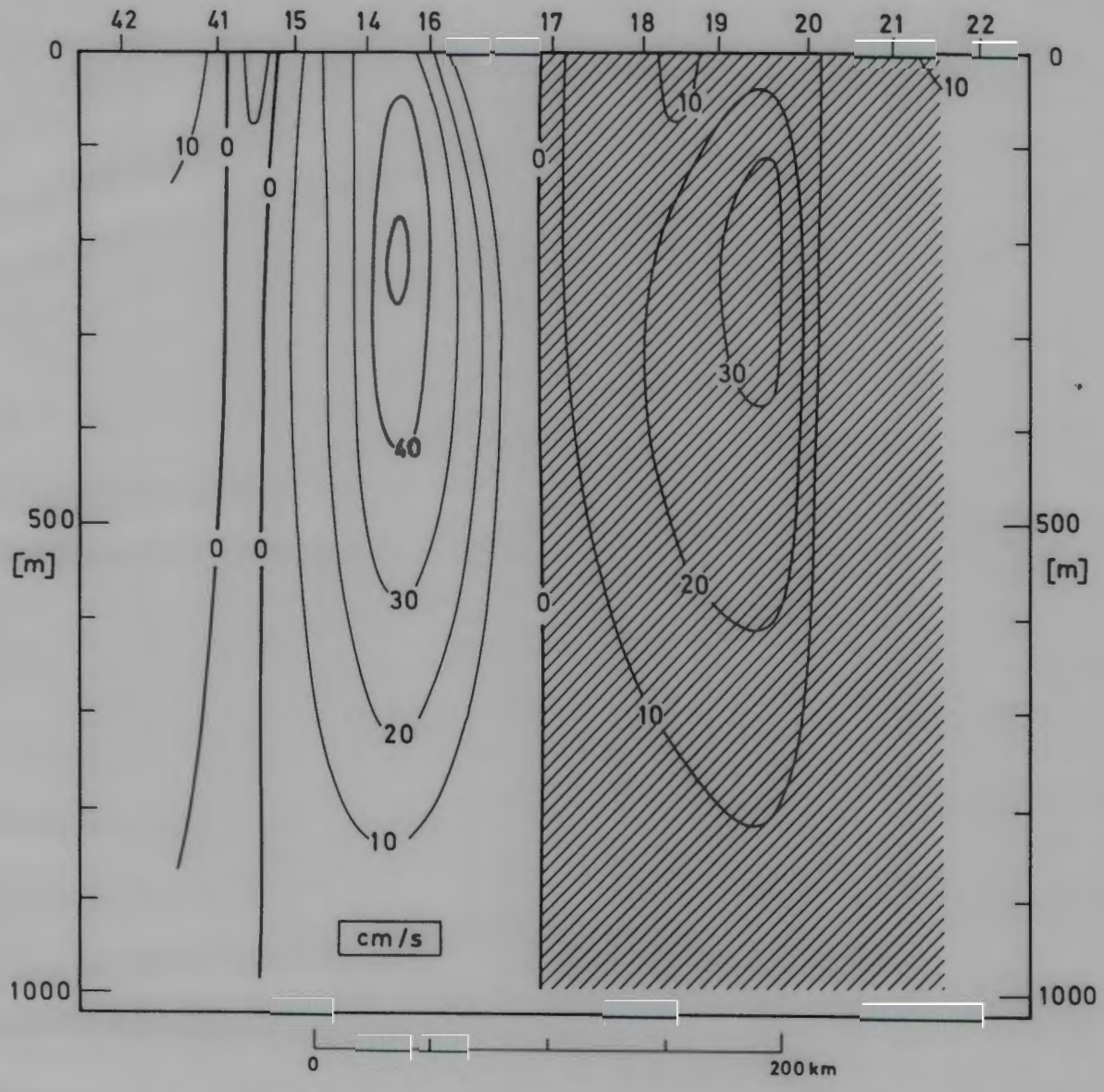

FIG. 10.13 : Gradient currents relative to 1000 m in the quasi-zonal section across eddy John in June, 1982. Shaded areas represent flow out of the page.

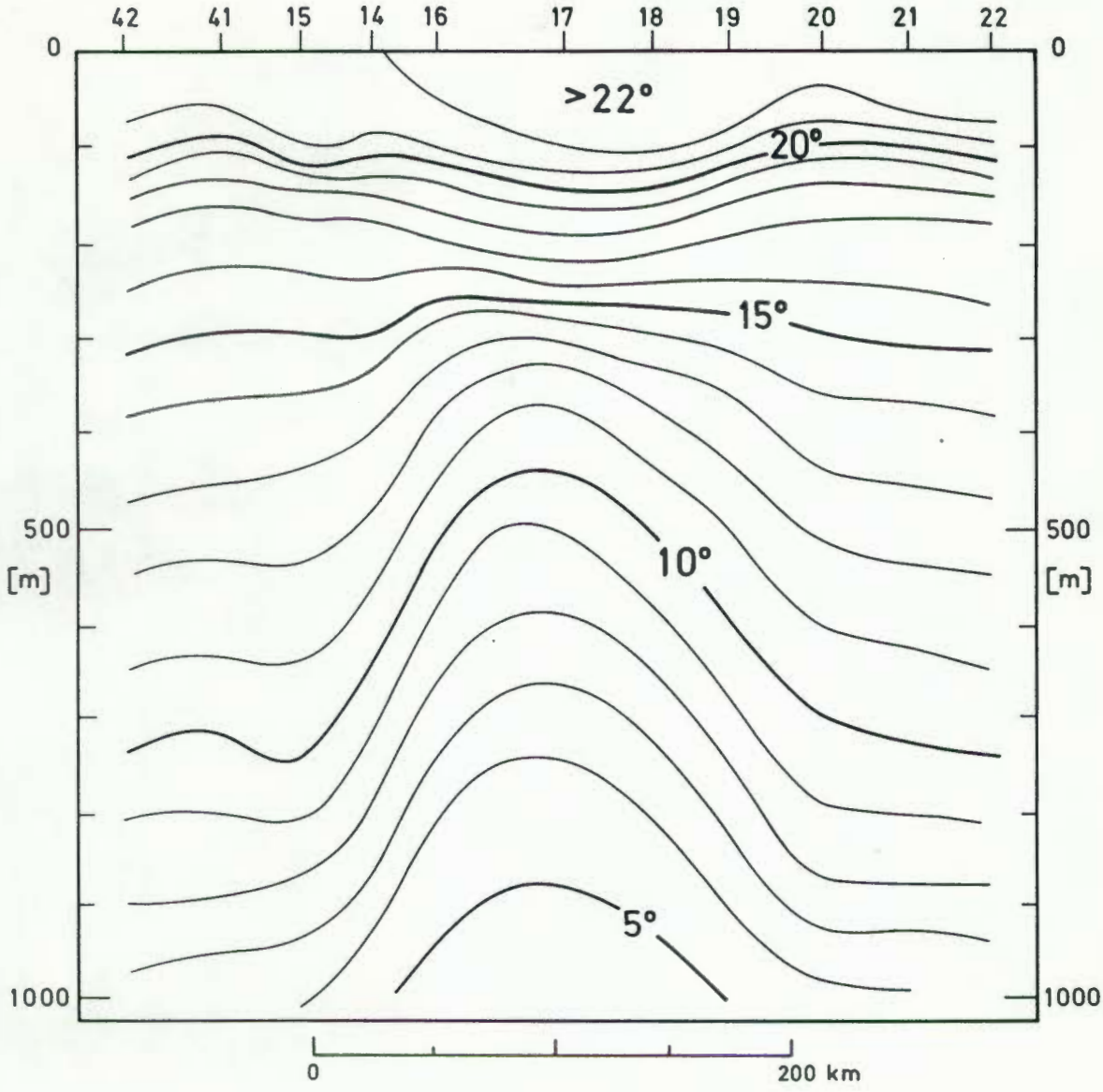

FIG. 10.14 : Vertical section of temperature in a quasi-zonal direction across eddy John in June, 1982.

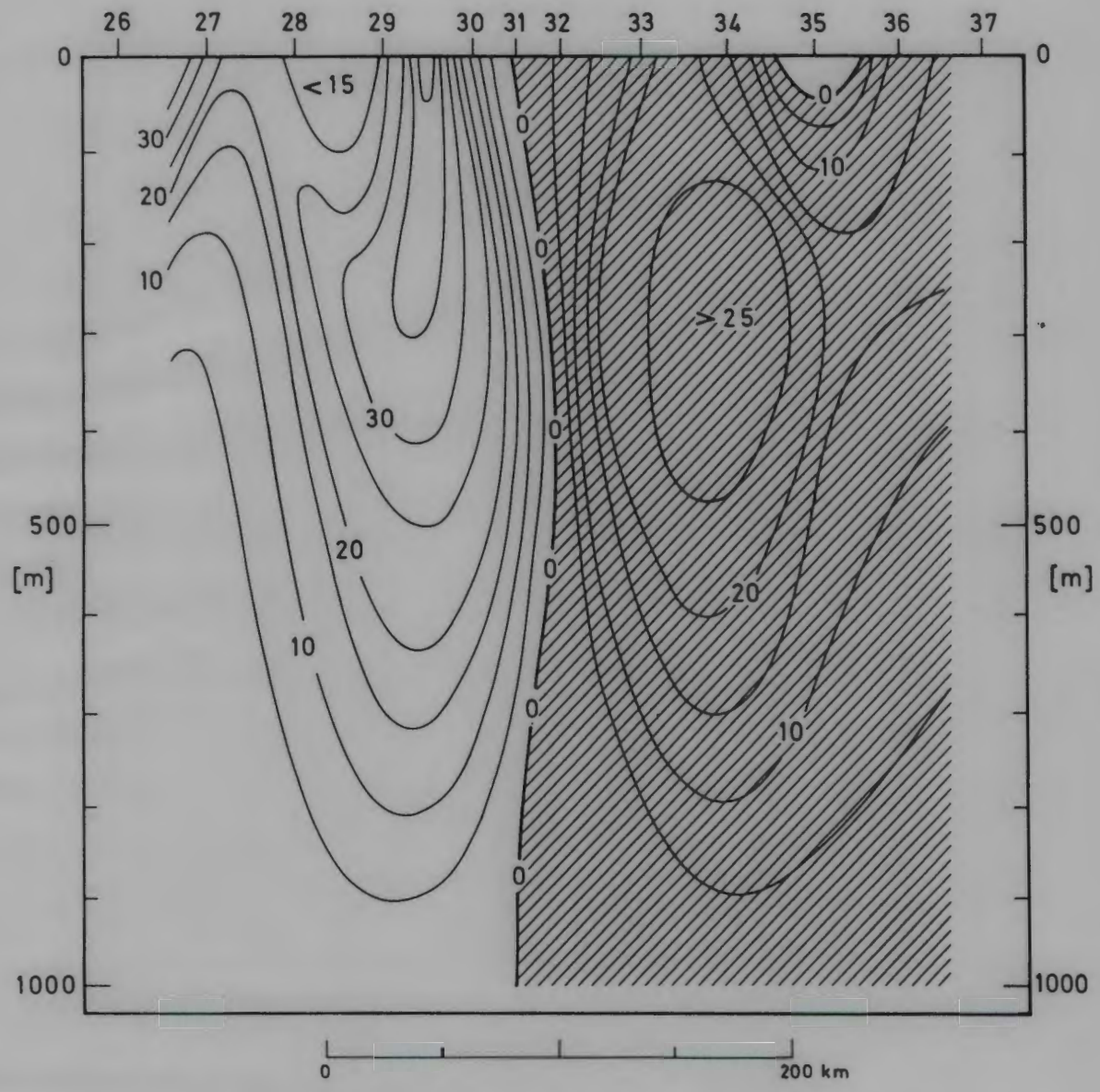

FIG. 10.15 : Gradient currents (in cm/s) relative to 1000 m in a quasi-meridional section across eddy John observed in June, 1982. Shaded areas indicate flow out of the page.

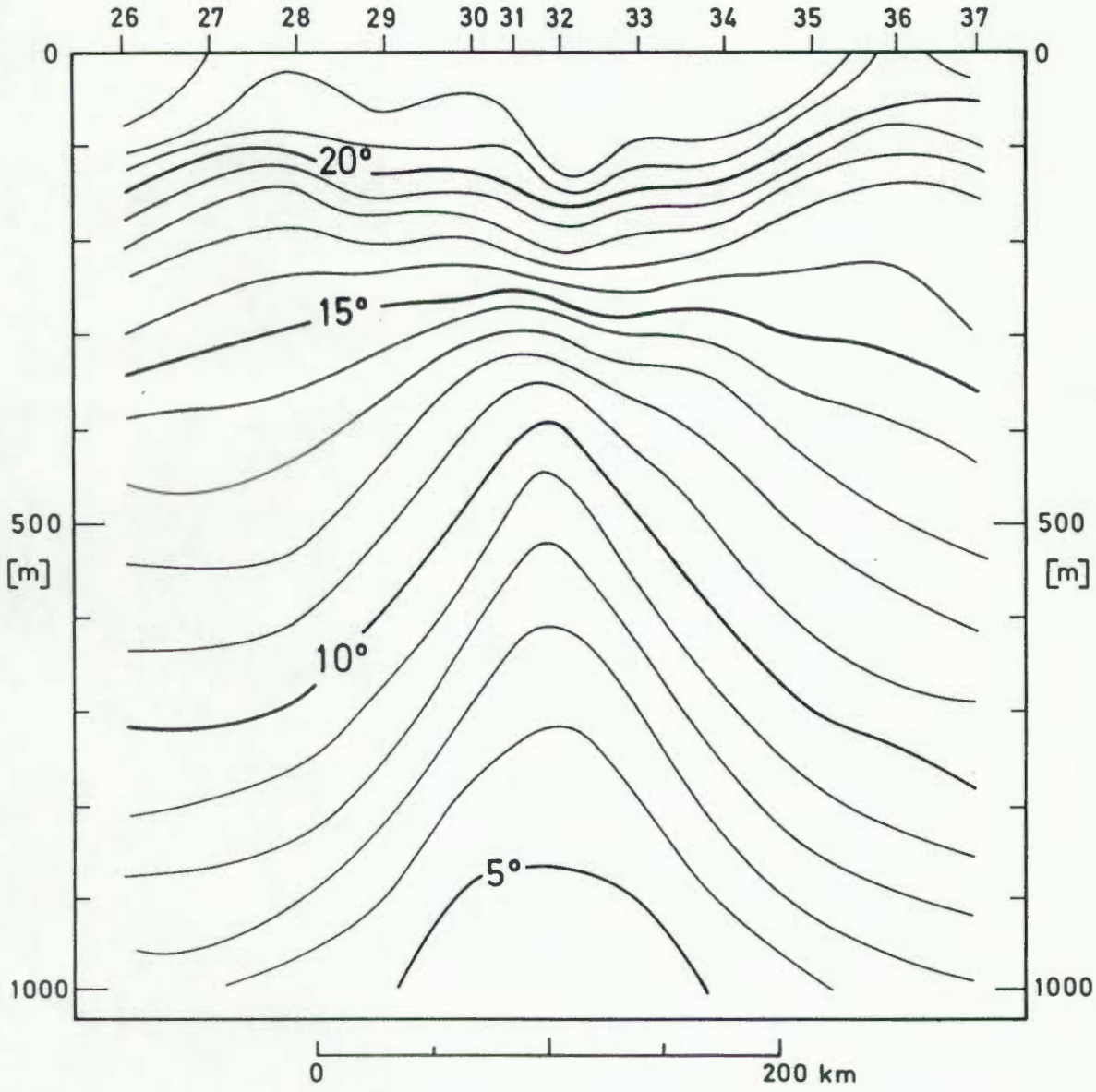

FIG. 10.16 : Vertical section of temperature in a quasi-meridional direction across eddy John in June, 1982.

Very little evidence was found of any anomalies (e.g. the presence of Red Sea Water) in the vertical profiles of temperature, but this may have been because of the limited penetration (1000 m) of most of the stations.

10.3.3 Dynamic results

The topography of the 10°C-surface (Fig. 10.17) indicated that John was symmetric with its centre situated at station 32. The geopotential of the sea-surface relative to 1000 m (Fig. 10.18) did not reflect this quasi-circular shape, nor did it indicate that the centre of the eddy was located at station 32. This difference must be ascribed to the trough-like configuration of the isotherms in the upper 300 m, producing an anticyclonic tendency in the upper layers and deforming the almost circular shape of the circulation in the deeper layers. This is confirmed by the symmetry of the geopotential topography of 300 m relative to 1000 m (Fig. 10.19).

Taking the position of station 32 as John's centre, gradient currents were calculated for the two transects across the eddy (Figs. 10.13 and 10.15). In the southerly sector (station 32-37) the maximum gradient velocity (29 cm/s) was located at a depth of approximately 300 m at station 34 (Fig. 10.15) while in the northerly sector (stations 26-32), the maximum of 41 cm/s was located at the surface between stations 29 and 30. High gradient velocities (exceeding 50 cm/s) occurred in the western sector between station 16 and 14 (Fig. 10.13), and in this sector and the easterly sector, the maximum velocity was attained at a depth of 200 m.

John's distribution of kinetic energy (Fig. 10.20) shows that the energy maximum was located approximately 70 km from the centre, with a total energy of 2.14×10^{15} J.

The volume transport (Fig. 10.21) also reflected the circular nature of the flow. John transported 21-25 x $10^6 m^3/s$ (calculated relative to 1000 m), and these values increased to 41-50 x $10^6 m^3/s$ when calculations were referred to 2000 m. Significant transports were also derived in the vicinity of the Mozambique Ridge. Between station 3 and 6, a northerly transport of 11 x $10^6 m^3/s$ was calculated, and in conjunction with the 5 x $10^6 m^3/s$ flowing southward between station 8 and 10 represented an anticyclonic eddy over the eastern edge of the Ridge.

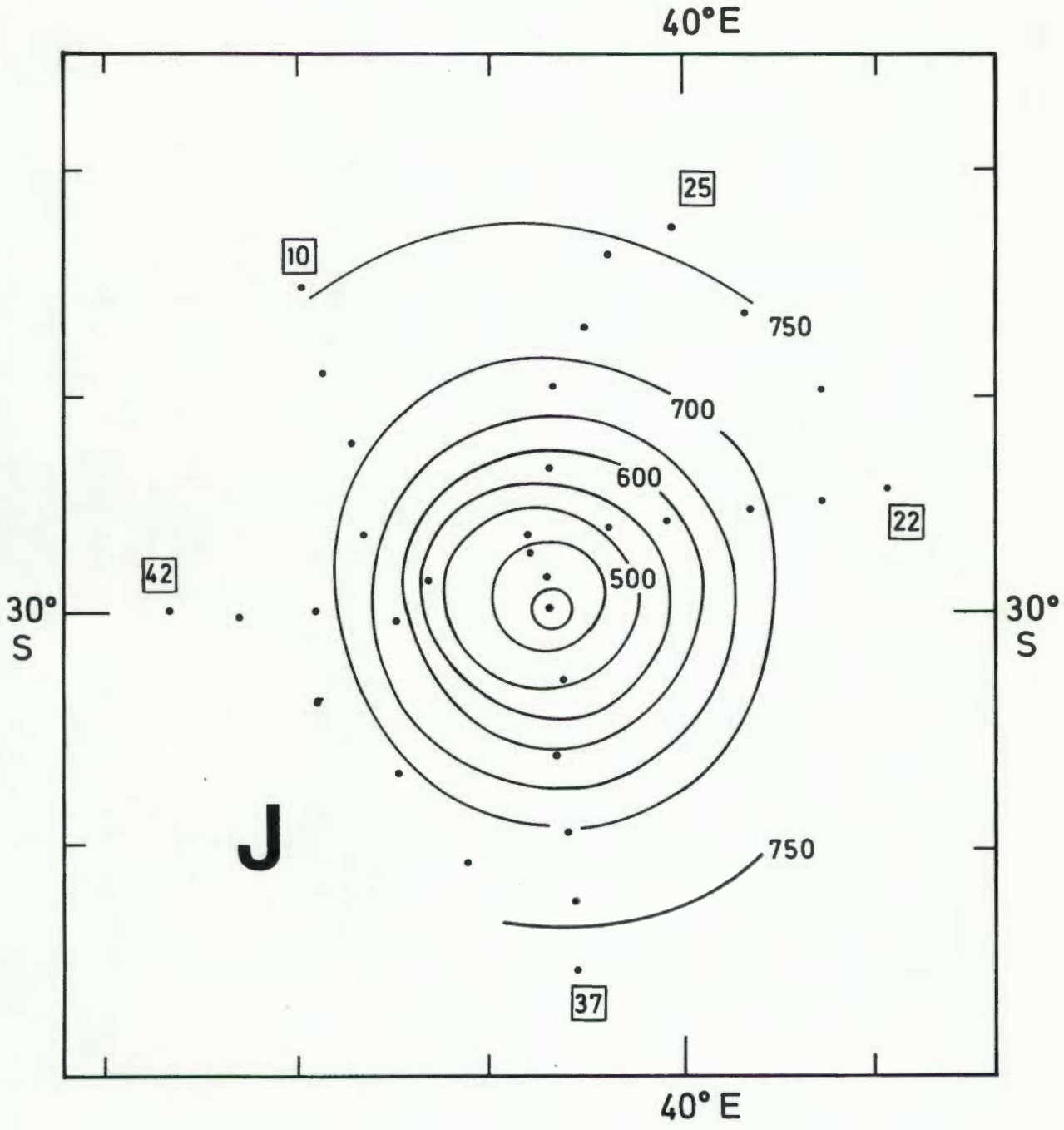

FIG. 10.17 : Topography of the 10°C isotherm surface of eddy John observed on the cruise in June, 1982.

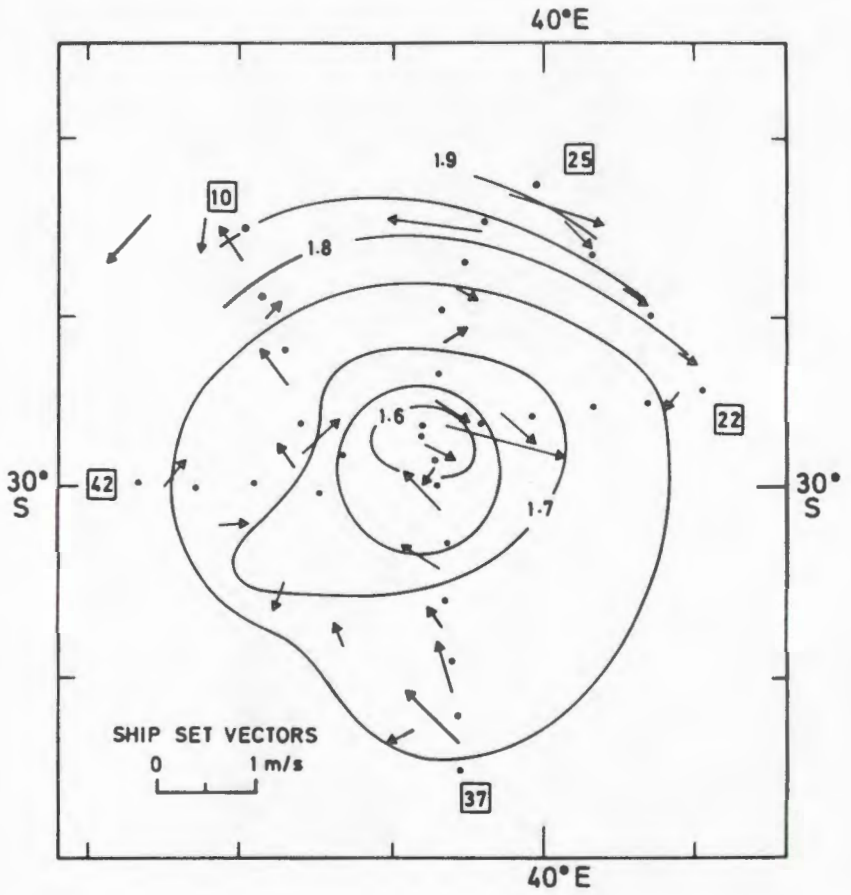

FIG. 10.18: Geopotential anomaly (in 10^{-1} m^2/s^2) of the surface relative to 1000 m in eddy John. Also included are the ship's set vectors.

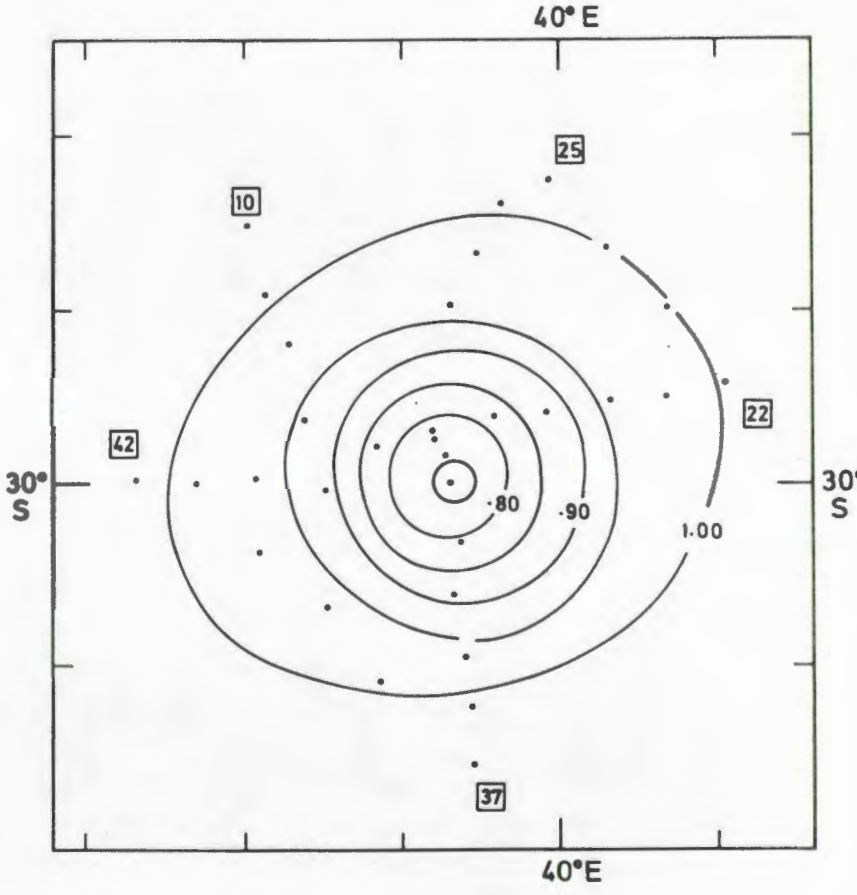

FIG. 10.19: Geopotential anomaly (in $10^{-1}m^2/s^2$) of the 300 m surface relative to 1000 m in eddy John, June 1982.

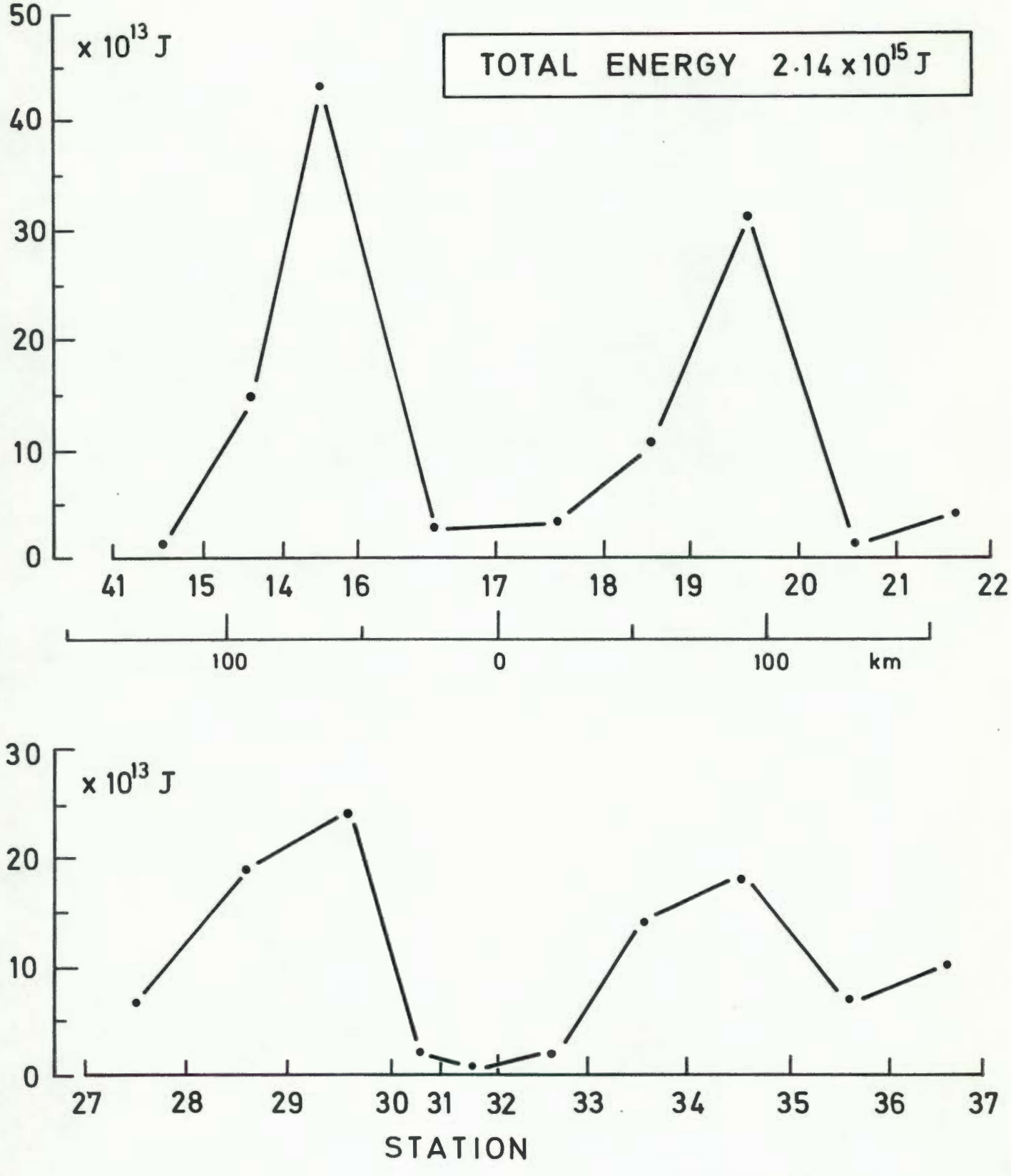

FIG. 10.20 : Distribution of kinetic energy along the zonal (top) and meridional (bottom) transects across eddy John obeserved in June, 1982.

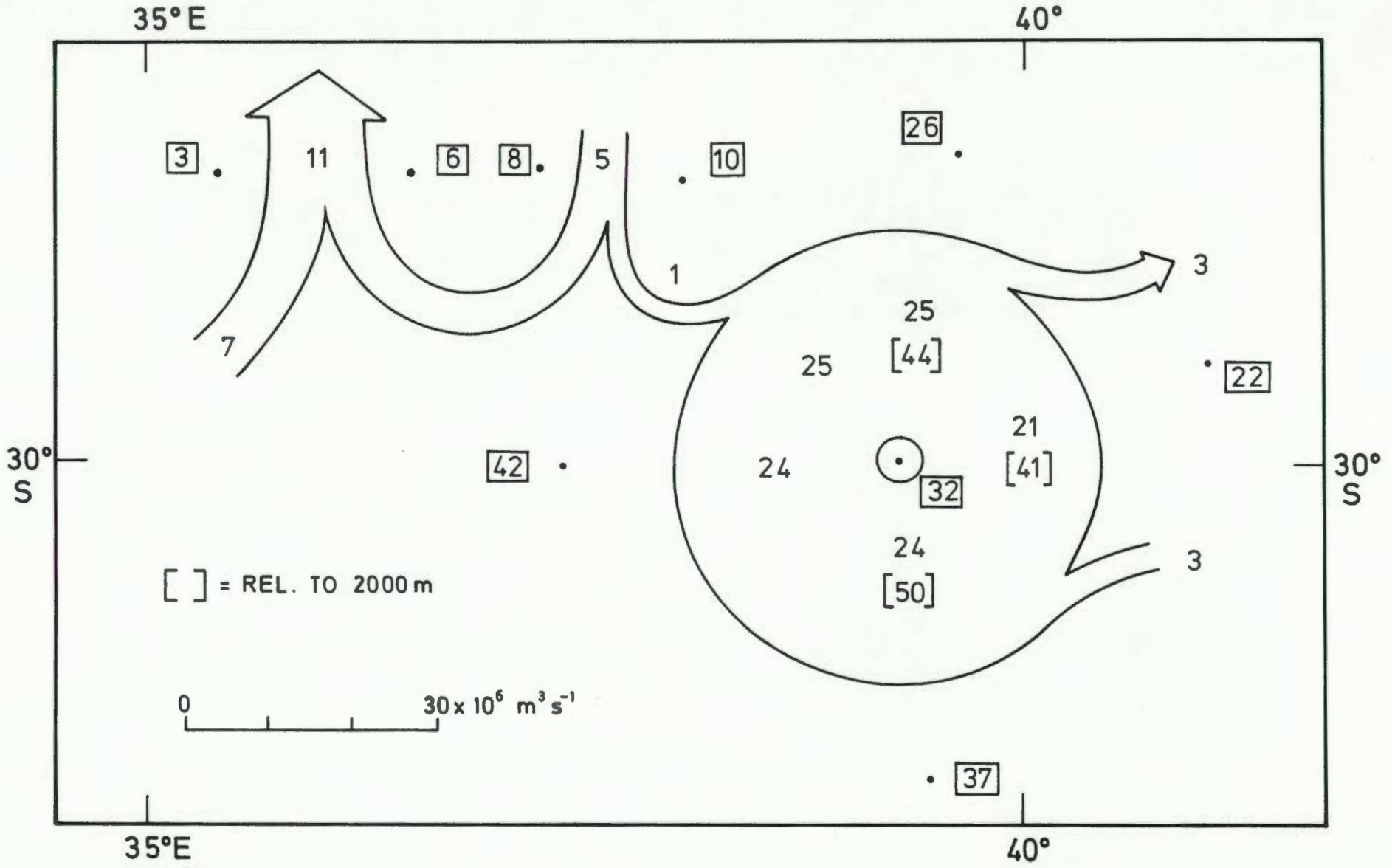

FIG. 10.21 : Volume transport (in units of 10^6 m^3 s^{-1}) relative to 1000m in the vicinity of eddy John observed in June, 1982. Isolated transports relative to 2000 m are also indicated.

10.3.4 Discussion

The first and overriding impression gained from the results presented of the cruise in June 1982 is John's near-circular shape. This was taken as an indication that John was rotating virtually independently of the surrounding water. Only as far as the volume transport relative to 2000 m is concerned was there a significant variation across the eddy, and this could have been the result of a variation in the level-of-no-motion.

A certain amount of ambiguity is situated in two of John's characteristics. On the one hand, its shape (see e.g. Fig. 10.17) and the isolation of the circulation (see e.g. Figs. 10.19 and 10.21) seem to indicate that John was independent of and free-drifting in the surrounding water mass. On the other hand, its intensity portrayed by the volume transport (Fig. 10.21), the kinetic energy (Fig. 10.20) and the elevation of the 10°C isotherm (Fig. 10.17) seems to indicate that John had not entered any stage of significant decay (although the latter concept cannot yet be defined for the present study). John was therefore considered to have been still fairly "young". Following some of the arguments of Chapters 4 and 8, the "source current" - the Mocambique Ridge Current - should then still be visible in the vicinity of the Mocambique Ridge. However, the flux of 5 x $10^6 m^3/s$ that was observed between stations 8 and 10 (see Fig. 10.21) does not seem sufficiently large to fulfil this role.

10.4 Discussion

On the one hand, the two eddies (Ian and John) discovered during 1982 were markedly different in many important aspects. First, Ian was observed between the coast and the Mozambique Ridge, while John was situated in the Mocambique Basin. Second, Ian was generated by and still firmly attached to the Agulhas Current, while John was free-drifting.

On the other hand, there were features that corresponded well in the two eddies. First, the volume transports were compatible (Ian : 17-30 x $10^6 m^3/s$; John : 21-25 x $10^6 m^3/s$, relative to 1000 m). Second, the kinetic energy of Ian (estimated at 1.8 x 10^{15}J) agreed closely with that of John (2.14 x 10^{15} J). Third, Ian's size was 180 x 260 km whereas John was circular with a diameter of 180 km.

In the light of the agreement between the two observations, the question arises whether Ian and John could have been the same eddy? If it is assumed that Ian became displaced eastwards shortly after the April cruise, it would have required an average speed of 7 cm/s to arrive at the position where John was observed. Taking into consideration that Ian was not free-drifting at the time of its observation but being displayed toward the west, it is crudely estimated that an advection speed of less than 10 cm/s would be required to displace Ian to the position where John was observed. A speed of this magnitude would not necessarily be visible in the configuration of John's thermal structure.

Another point that can be considered lies in the generating mechanism of Ian and John. If John was about two months old, and if it was created by the Mozambique Ridge Current as indicated by the results of Chapters 8 and 9, it would require the simultaneous presence of the Agulhas Current (creating Ian) and the MRC (creating John) in the vicinity of the Mozambique Ridge. The close proximity of these two intense currents does not seem justifiable. On the other hand, if John were 3-4 months old, the necessity of the simultaneous side-by-side existence of two very intense currents would be obviated.

It is therefore concluded that the following possibilities exist:

(a) Ian and John are "snapshots" of the same eddy two months apart. The eddy (Ian) was created by the Agulhas Current, became detached from the Current and advected eastward about 400 km where it was observed as John about two months later.

(b) John was created by the Mozambique Ridge Current before April 1982 and advected toward the position where it was observed in June (making it more than 3 months old at that time). In April, Ian was generated by the Agulhas Current and swiftly advected southwards with the Current.

To ascertain whether any connection between Ian and John existed, infrared images obtained from the METEOSAT and NOAA-7 satellites were

inspected. It was found that these images were unable to provide sufficient evidence to substantiate or disprove the possibility whether Ian and John were identical. The reason for this failure was partially situated in the large amount of cloud-cover, but mainly in the uncertain relationship between the surface temperature characteristics and the dynamics of the eddies (cf Fig. 10.11 and Fig. 10.17). The question whether an eddy such as Ian can advect eastwards at the rate indicated must remain open.

PART III

DISCUSSION AND REVIEW

After the presentation in Part II of the data collected during this project, the purpose of Part III is to provide an overview of the project.

A total of fourteen cruises (separated into nine different experiments) surveying the vortices of the Mozambique Ridge Current were executed. Through these cruises, ten different eddies were located and a large amount of information about various aspects of the circulation was collected. The first objective of Part III will be to identify and synthesize the main characteristics of these eddies through intercomparison and assessment, and to produce a profile of the typical eddy (if there is one) of the Mozambique Ridge Current.

Because of the limited geographical coverage that could be achieved by the *Meiring Naudé*, each cruise presented a very restricted "snapshot" of the circulation in the target area. Even where experiments consisted of two or three cruises, the extent to which the vessel could survey a particular eddy as well as the area around it proved completely unsatisfactory. The second objective of this part will be to see how and where these eddies fit into the larger-scale circulation. As stated in Chapter 2 and 3, the Mozambique Ridge Current had not been defined previous to this study, and the results of Chapters 4-10 will now be used to assess the characteristics of this Current.

The final objective of this part will be to redefine the general circulation of the southwestern Indian Ocean in terms of the knowledge gained from the present study. Guidelines will also be presented for further investigations of a similar kind.

CHAPTER 11

PHYSICAL CHARACTERISTICS OF THE VORTICES OF THE MOZAMBIQUE RIDGE CURRENT

11.1 Introduction

The aim of this chapter is to extract the most important physical characteristics of the ten vortices located during the field exercises (i.e. thermohaline) (Chapters 4-10). Although this number of eddies appears insignificant compared to the large number of rings observed in the North Atlantic (see e.g. LAI and RICHARDSON, 1977 , 163 observations; PARKER, 1971, 62 observations), an attempt will also be made to compare the local eddy characteristics with observations made elsewhere (mainly Gulf Stream rings). The reader will repeatedly be referred back to the relevant sections and figures of previous chapters to obviate unnecessary repetition of data.

11.2 Thermal structure of the eddies

11.2.1 Deep Isotherm deflection

When the physical characteristics of the eddies are discussed, it is appropriate that we start with the temperature structure. It is namely the temperature of the water that was used during the field experiments as primary indicator of the presence of a vortex.

In Chapter 3, where the oceanographic "climate" of the Mocambique Basin was presented, a "background" temperature profile was derived (Table 3.1). The hydrographic stations from which this profile was determined were located in the area that could be considered representative of all the stations executed on this project. It is relative to this climate that we will consider the thermal structure of the vortices.

Whereas the isotherms are more or less horizontal in the open ocean away from the vicinity of eddies or strong currents (see Appendix 5, and also the sections in the southwest Indian Ocean presented by WYRTKI, 1971 and HARRIS and VAN FOREEST, 1977), the edge of a vortex was signified by a consistent decrease in temperature at all levels below about 200 m. The

concomitant rise in isotherms was on most occasions accompanied by a temperature *increase* in the layer above 200 m, although this increase was not as steady as the temperature decrease deeper down.

To derive the exact depth to which the isotherms became elevated, or, alternatively, to determine the coldest temperature at the eddy centre, depended very much on whether a hydrographic station was located at this position. With a station spacing of approximately 30-40 km it is quite likely that this "peak" would be missed, and it therefore became custom to decrease the station interval when the centre of the eddy was approached. In those cases where subsequent data analysis showed that the peak was situated between two stations, a parabolic interpolation was made between adjacent stations' data to ascertain the point where the isotherms reversed. To enable an intercomparison of the various eddies, the minimum depth of the 10°C isotherm, and the depth of the 5°C and 15°C isotherms in the same vertical plane are listed in Table 11.1.

On the average the 5°C isotherm surface was elevated 269 m above its normal level, the 10°C surface 351 m and the 15°C surface 62 m. The standard deviation of, e.g. the 10°C depth indicates that elevations of 400 m above ambient level were possible.

How do these figures compare with observations from other regions? To provide some values for comparison, a number of those reports dealing with cyclonic eddies were selected more-or-less arbitrarily, and the results about isotherm elevation above the unperturbed level were extracted (see Table 11.2). Also included in this table are the results reported by BANG (1970) of a section through an unoccluded meander of the Agulhas Return Current over the Agulhas Plateau.

The results of Table 11.2 indicate that the eddies studied in this thesis were compatible in isotherm elevation to eddies located elsewhere in the world. It can be expected that the magnitude of isotherm elevation is primarily related to the slope of the thermocline in the host current. Added to this is the age of the vortices, since the decay is eventually related to the collapse of the cold dome of the eddies (This aspect will be discussed again in Chapter 12).

TABLE 11.1

DEPTH OF SELECTED ISOTHERMS AT EDDY CENTRE

Cruise	Eddy	5°	10°	15°
Aug 75	Bravo	-	480	260
June 76	Carlie	910	450	295
Mar 77		-	530 *	250 *
June 77	Delta	-	480	290
May 78	Echo	890	420	240
June 78	Echo	890	495	250
Dec 79	Fred	820	350	210
Jan 80	Fred	900 @	470 @	215 @
	Golf	940	440	210
Mar 80	Golf	-	475	280
Apr 81	Harry	950	480	250
Apr 82	Ian	850	320	240
June 82	John	870	390	370
Average $\pm$ std. dev. (excluding *,@)		890 $\pm$ 44	390 $\pm$ 59	263 $\pm$ 45
Background (from Chapter 3)		1159 $\pm$ 61	741 $\pm$ 42	325 $\pm$ 42
Elevation		269	351	62

* Single station

@ Grazing encounter

TABLE 11.2

ISOTHERM ELEVATIONS OF CYCLONIC EDDIES FROM OTHER REGIONS

Source	Isotherm (°C)	Elevation (m)	No. of Observations
Gulf Stream:			
JAMES and CHENEY (1977)	12.8	450	1
KHEDOURI and GEMMIL (1974)	15	410	1
LAI and RICHARDSON (1977)	"Thermocline"	500	1
McCARTNEY, WORTHINGTON and SCHMITZ (1978) @	15	130-430	10 *
Southern Ocean:			
SAVCHENKO, EMERY and VLADIMIROV (1978)	5	330	2
Kurushio:			
CHENEY, RICHARDSON, NAGASAKA (1980)	"Thermocline"	300	1
Agulhas Return Current:			
BANG (1970)	10	650	1
Present Study :	10	351	12

* grazing encounters not included

@ These refer to the socalled "big babies" of the northeast Sargasso sea.

In some eddies (see e.g. eddy Echo, Fig. 7.10), the rotating axis of the eddy seemed to be displaced from the vertical, although the station spacing was too large to resolve this inclination unequivocally. This orientation has also been observed in Gulf Stream rings (VUKOVICH, 1976).

11.2.2 Surface layer (0-150 m)

A noteworthy feature of the eddies' configuration was the bowl of warm water constituting the upper part of the eddies. The presence of warm water here was reflected by the inversion in the shape of the isotherms (from convex below 300 m to concave above 200 m). Examples of this feature are visible in Figs. 4.2 and 6.7. On the other hand, some eddies did not portray the bowl of warm water, and an example of this can be seen in Fig. 8.2.

Of the two questions, first why there should be a bowl of warm water at all, and second, why there should be a bowl of warm water in some eddies but not in others, only the first can be answered with any amount of confidence.

An inspection of vertical sections across the Agulhas Current (see e.g. WYRTKI, 1971; PEARCE, 1977a and others) invariably shows that the core of the Current (i.e. the area of highest velocity) is characterised by the presence of a mass of higher, warmer water at the surface. In other words, the Agulhas Current, similar to any other western boundary current, is not merely a front where geostrophy separates a denser from a less dense water mass. If this were the case, the water at all depths on one side of the Agulhas could be warmer than the water on the other side. Whereas this holds true for depths exceeding 100 m or so, the surface layers reveal a ribbon of warm water situated directly above the Current and coinciding more-or-less with the "core" of the Current. This feature is e.g. used to track the Current through infrared satellite imagery (see e.g. LUTJEHARMS, 1981b), and is also characteristic of the Gulf Stream (see e.g. GOTTHARDT, 1973; PARKER, 1971). This filament of warm water must be considered to have its origin in lower latitudes since it is this part of the Current that consists mainly of the TSW (tropical surface water) (see DARBYSHIRE, 1966). Since the Agulhas does not entrain any TSW in mid-latitudes (because there isn't

any available to entrain), the warm-water filament does not signify a zone of convergence. In other words, if the Mocambique Ridge Current resembles the Agulhas Current, it should contain a similar ribbon of warmer water, situated over the high-velocity part of the Current.

As the host Current performs a cyclonic loop, the high-temperature surface core remains positional over the highspeed axis of the current (see e.g. the case of Gulf Stream ring formation : FUGLISTER, 1977; RICHARDSON, CHENEY and WORTHINGTON, 1978). However, in the eddies studied in this thesis, the warmer water was not found over the region of maximum velocity (since the latter is normally located some 50-100 km from the eddy centre, see Chapter 12), but over the *centre*. This seems to indicate that the warm surface core had advected inwards, suggesting that the centre of the eddy represented a zone of convergence for the surface layers. This aspect of eddy circulation is evidenced by the results of the cruise in June 1977 (section 6.4), where the surface temperature was characterised by fronts spiralling into the centre of the eddy.

Depressions of the near-surface isotherms (indicating the presence of a bowl of warm surface water) are also visible in the results of CHENEY (1976), FUGLISTER (1977), VASTANO, SCHMITZ and HAGAN (1980) but do not appear in e.g. the diagrams of MIED, LINDEMANN and BERGIN (1983) or WIEBE (1982). (By and large, the impression was gained that Gulf Stream rings retain their warm water above the high-speed filaments of the ring, and not above the centre).

On the other hand, convergence did not seem to have been present in all the eddies studied in this thesis since the bowl of warm water was absent in some cruises (see e.g. the well-developed eddy, Golf, located in November 1979, section 8.3).

Coinciding with the presence of a bowl of less dense water at the centre of the eddy was an occasional increase in the mixed layer depth (MLD). Typically, the MLD would increase from about 50 m on the perimeter of the eddy to 100 m or more in the centre of the eddy (see Figs. 6.9 and 10.5). This seems to indicate that the central region of some of the eddies was either characterised by increased mixing and turbulence, or by the advection of

already-mixed water from the high-speed filaments of the eddy further away from the centre, or both. E.g. on the cruise in June 1977, special reference was made in the scientific log of station 22 to "rip currents" in the vicinity of the vessel. This station was located about 20 km away from the centre of the eddy but well within the region of deep MLD (see section 6.4).

It is considered that the depression of isotherms over the eddy centre and the increase in MLD here were signatures of convergence in the upper layers. This is supported by the conclusions of VASTANO and HAGAN (1977) (see also LAMBERT, 1974, who studied variations of dissolved oxygen in cyclonic eddies). OLSON (1980) concluded that the depressions in near-surface isotherms represented zones of convergence for Gulf Stream rings, and used the fact that satellite-tracked buoys, drogued at 200 m, moved into the region of convergence and stayed there.

This is confirmed by the results of SCHMITZ and VASTANO (1975) who found that convergence resulting from entrainment (with radial velocities of about 0.03 cm/s) in the upper 600 m and divergence in the depths below 600 m could explain the temperature variations in Gulf Stream rings.

This would tend to answer the first question presented above, namely why these features occur in the eddies, but the second question, namely why warm-water bowls were observed in some eddies and not in others, cannot be answered satisfactorily at present, but will be discussed again when the dynamic characteristics of the eddies are addressed (Chapter 12).

It is appropriate at this stage to say something about the paucity of information on the surface temperature characteristics of water immediately outside the perimeter of an eddy. To collect information on the surface frontal systems while a cruise was in progress invariably brought about a clash of interests. On the one hand, a knowledge of the fronts could assist in decipering the structure, dynamics and origin of the eddies. On the other hand, surveying the area "outside" the eddy (i.e. the area where the 10°C elevation became insignificant) required considerable time, often involving precious hours that could possibly have been better spend *inside* the eddy. For this reason, the information on surface fronts associated with eddies was often incomplete.

The results of one cruise (Fig. 4.2) revealed the existence of wave-like features in the isotherms. These waves were smaller than those predicted by FLIERL (1977) as a mechanism whereby Gulf Stream rings could radiate energy into the surrounding sea.

11.3 Salinity and T/S structure of the eddies

It can be seen from the various salinity sections that have been included in this thesis that the salinity and temperature fields in the vicinity of an eddy are generally homotropic. What has been said about the thermal patterns associated with an eddy therefore holds just as well for the salinity patterns, and we will refrain from repeating the discussion. This section will therefore concentrate on T/S (rather than just salinity) structures encountered in the Mocambique Basin in general and the eddies in particular.

11.3.1 Deep (~ 1000 m) T/S anomalies

A brief description of the water masses present in this depth has been given in section 2.3. At a depth of about 800–1000 m in the southwestern Indian Ocean, the salinity profile reaches a minimum which indicates the core of the Antarctic Intermediate Water (AAIW). AAIW is initially found at the Antarctic convergence at 45–55°S where the water has a temperature of 2.2°C and salinity 33.8 °/oo. This water mass sinks to about 900 m while spreading northward, and is characterised in the southwestern Indian Ocean by T = 5°C and S = 34.4–34.6 °/oo.

Anomalies at the depth of the AAIW are caused mainly by the intrusion of Red Sea Water (RSW). According to the IIOE Atlas (WYRTKI, 1971), RSW enters the Indian Ocean from the Red Sea at depths of 500–600 m. Initially, the salinity inside the core of the RSW is about 37–38 °/oo, but rapidly dilutes to about 35.5 °/oo off the horn of Africa. The RSW has been traced to many parts of the Indian Ocean (see e.g. ROCHFORD, 1964), and is characterised by a high-salinity layer of warm water. In the region south of 10°S, the core of the RSW has subsided to 1000–1100 m with a salinity of 34.8 °/oo and temperature of about 5.5°C (WYRTKI, 1971). According to WYRTKI, RSW penetrates southward in the Mozambique Channel to 25°S before it disappears, while on the eastern side of Madagascar it does not extend much

further southward than about 12°S. It is possible that isolated observations of RSW south of these latitudes would have been disregarded in the establishment of distribution charts for RSW in the Atlas production. The results of CLOWES (1950) and, more recently, of JACOBS and GEORGI (1977) confirm that RSW penetrates further than 30°S. The STD measurements of JACOBS and GEORGI were the first to reveal the layered structure of the AAIW-RSW interaction at σ_T = 32.00

In the present study, RSW has been identified on several occasions in the vicinity of 30°S. E.g. on the cruise in October, 1981, RSW was observed at 27°30'S and only between 37° and 39°E (see Fig. 3.7). This seems to indicate that in the area south of the Mozambique Channel, RSW spreads in ribbons of limited lateral extent, rather than in a broad layer. The observed RSW extended from about 950 db to 1400 db (see Fig. A5.12).

On the cruise in March 1981, the AAIW revealed a patchiness in 29°S reminiscent of the intrusion of RSW, but the data contained no real evidence of RSW (section 3.3).

The whole issue of RSW presence in higher latitudes in the southwestern Indian Ocean may have remained of merely academic importance, and the isolated observations reported above just a few added statistics for a distribution map, were it not for the simultaneous presence of the RSW on the one hand and the Mozambique Ridge Current (MRC) and its vortices on the other hand. In all the cases reported here, the observation of RSW was namely coupled to the presence of the MRC, and specifically, its *anticyclonic* side. Examples of this can be found in Figs. 8.5 and 8.6, in Figs. 9.10 and 9.11 and in Figs. 3.7 and 3.8(a).

Two possible explanations came to mind: First, the RSW could have been entrained by the MRC and travelled along with this Current. In the case of eddy Fred (December 1979), where it was concluded that the MRC had flowed westwards from the area south of Madagascar, it would imply that the RSW had been entrained and carried southward along the *eastern* side of Madagascar. Although not impossible, this conclusion seems doubtful, considering that the "normal" penetration of RSW along this route is not further than 10°S.

Second, the RSW could have flowed down the Mozambique Channel in the form of a ribbon of salty, warm water at depths of 900-1600 m. At these depths it would automatically tend to be situated offshore of the main currents (Mozambique and Agulhas Currents) and possibly tend to flow on the eastern side of the Mocambique Ridge. In the case of the December 1979-flow pattern, a fast westward flowing MRC could have penetrated this slow southerly drift of RSW along the eastern escarpment of the Mozambique Ridge. The disruption of the (initially) continuous flow of RSW could have caused its irregular distribution over the target area.

Although the second explanation is preferred, neither of the explanations can be fully justified in the light of the inadequate geographical coverage of the data.

As far as the meridional flow of RSW is concerned, we would like to briefly draw attention to some recent results. QUADFASEL and SCHOTT(1983) investigated the existence of a southward subsurface flow below the Somali Current (as a transporting mechanism of RSW toward the south) and found that such a current exists but does not extend further southward than 30°N before turning offshore. In addition, QUADFASEL (1983) reported virtually no net southward flow into the northern Mozambique Channel. The question in this instance is therefore: How does the RSW observed at 30°S reach such a high latitude? The answer is probably situated in the seasonality of the flow, since the presence of RSW south of the equator has been established beyond doubt (see e.g. KRAUSE, 1968, WYRTKI, 1971, and others).

11.3.2 T/S anomalies in the upper thermocline

The T/S structures referred to here are those low-salinity intrusions that were observed in the upper thermocline in depths of 100-150 m. Examples of this can be seen in Fig. 6.10 and similar (but not so marked) cases were observed during other cruises. It would be difficult to define the origin of this low-salinity layer although a possibility is that water with a strong tropical component at the surface was at some stage exposed to strong (winter) cooling. This could have resulted in a downwelled mixing of the low-salinity water, which was subsequently overlaid by warm, higher-salinity water. Another possibility is that the interleaving could be indicative of the exchange mechanism between the tropical water inside the eddy and the subtropical water outside, as reported by FEDEROV, GINZBURG and ZATSEPIN (1981) for the exchange of Slope and Sargasso water in Gulf Stream rings.

11.3.3 Surface T/S anomalies

The first and important observation that can be made as far as the surface T/S characteristics of the eddies are concerned, is that there existed conspicuous thermal fronts in the vicinity of the eddies. Examples of this feature abound in the data presented in Part II. Salinity fronts, on the other hand, were sometimes weak or absent. Where the surface thermohaline fronts were pronounced, they represent rapid transitions from water of a tropical character to water of a more subtropical character. Evidence of this can be seen in Fig. 3.4 where temperature changes of 1-2°C were accompanied by salinity changes of about 0.4 °/oo. These values of 2°C/0.4 °/oo probably represent extreme cases, and more typical values would be 10°C/0.2 °/oo.

In Table 11.3 the thermohalines observations in the vicinity of the eddies located during this survey have been summarised. On the average, the area to the north of the eddies contained mainly tropical surface water (TSW), while the area to the south of the eddies contained subtropical surface water (STSW). The surface T/S character of the eddies normally reflected a mixture of these two water masses.

DARBYSHIRE (1966) maintained that this mixture of TSW and STSW forms a water mass - socalled "boundary water" - in itself, which is normally located between the Mozambique Ridge and the southern African continent. The location of this boundary water (in the vicinity of the eddies) was some hundreds of kilometres removed from its common area, indicating that either the boundary water extended eastward from its region reported by DARBYSHIRE, or the water mass of the eddies had basically the same generating mechanism as boundary water.

As explained in section 11.2.2, the survey of the sea-surface frontal systems was invariably insufficient. We believe that this factor is responsible for many of the difficulties arising from attempts to construct a comprehensive and consistent hypothesis of the surface T/S distribution. Encouraging results were obtained during the survey of June 1977 (Chapter 6.4) where the transects were extended well outside the perimeter of the eddy. These results managed to indicate the dynamics of the eddy (and its complexity!) better than a mere calculation of the geostrophic currents and volume transport.

TABLE 11.3

MAIN SURFACE T/S OBSERVATIONS ASSOCIATED WITH EDDIES

Cruise	Eddy	Observations
August 1975	Bravo	Eddy situated between TSW to NE and STSW to SW
June 1976	Charlie	Eddy situated between TSW to NE and NW and STSW to SW
June 1977	Delta	Thermal front spiralling inward
May 1978	Echo	Eddy situated between TSW to NE and STSW to SW
June 1978	Echo	Thermal fronts present, eddy consisted of warmer water
December 1979	Fred	Strong T/S fronts, TSW to N & NE of eddy, eddy itself containing STSW
January 1980	Fred	Variable
March 1980	Golf	STSW to SW of eddy
February 1981	-	TSW to NE of eddy
April 1981	Harry	Eddy situated between TSW to NE and STSW to S
April 1982	Ian	Variable
June 1982	John	STSW to S of eddy

TSW = Tropical Surface Water

STSW = Subtropical Surface Water

The problem as far as the surface T/S patterns are concerned is quite obvious: If TSW exists mainly to the north of the eddies, and STSW to the south, there must exist a more-or-less zonal boundary between these two water masses extending eastwards from the eddy. This would suggest that for some reason, the eddies were often situated on the boundary between these water masses.

Confirmation of this hypothesis is found in the data of the March 1981 cruise (see Fig. 3.4). There, the hydrographic stations 36° and 43°E but north of 31°S contained mostly TSW, and stations south of 31°S contained STSW, with a strong frontal system at 31°S. This separation was not verified by the data from a similar cruise in October of the same year, when salinities in the range 35.5 - 35.6 °/oo were found throughout the area 27° - 30°S. Seasonality could have played a role in these discrepancies.

The lack of sufficient ground-truth measurement of the sea surface temperature (SST) patterns, and the discrepancy between these patterns and the deeper (integrated) circulation (cf Fig. 6.11), detracted from the usefulness that satellite imagery could play in the survey of eddies in this region. Only in isolated occasions (cf Fig. 7.16) could SST be fruitfully employed to reveal the circulation over larger areas. Satellite images have been used with great success to portray the flow of the Agulhas Current (cf. LUTJEHARMS, 1978) in higher latitudes. Gulf Stream rings have also been studied from satellite (cf. RICHARDSON, STRONG and KNAUSS, 1973; DOBLAR and CHENEY, 1977; VUKOVICH and CRISSMAN, 1978; WIEBE, 1982). It is possible that the stronger thermal fronts that exist at higher latitudes are more closely related to the subsurface structure and the circulation dynamics than at lower latitudes where thermal patterns are more diffuse.

11.4 Chemistry and biology of the eddies

The eddies were studied mainly from a physical oceanographic point of view, with very few chemical samples taken during the surveys (partly because of the extra time and cost involved). The increased use of the CTD from 1979 onwards made sampling very difficult because of the absence of a proper rosette sampler.

Figure 4.3 gives an idea of the distribution of nitrates, silicates and phosphorous in the vicinity of eddy Bravo observed in August, 1975. The graphs show the general increase of nutrients toward the centre of the eddy. In the layers between 600 and 900 m this increase amounted to

two- or three-fold the ambient nutrient levels. In spite of these increases, it might be unwarranted to refer to an event of this description as "upwelling" since the higher nutrient levels did not penetrate the euphotic zone and should therefore not enhance the existing plankton communities. Bravo was one of the weaker eddies observed during the present survey. According to Table 11.1 the 10°C isotherm was elevated less than the average compared with other eddies. In the case of eddies such as Fred (December, 1979) and John (June 1982) one would expect the nutrient levels to have been elevated much more than the August 1975 case.

Only one eddy (Charlie, June 1976) of the present study was sampled biologically, and then only with plankton nets that were hauled vertically through the water column. It falls beyond the scope of this thesis to present the results. It is, however, the unequivocal opinion of the author that a multidisciplinary (physical-chemical-biological) investigation of the eddies should be a worthwhile exercise. In comparison, Gulf Stream rings which are created in such a way that biological quanta originating from Slope Water are introduced in to the Sargasso Sea, have proved fertile breeding grounds (sic!) for biological research (see e.g. BACKUS and CRADDOCK, 1982; BOYD, WIEBE and COX, 1978; WIEBE et al, 1976).

11.5 Shape and size of the eddies

There are many parameters that can be employed to define the shape and size of an eddy, e.g. geopotential anomaly of the surface relative to some deeper level, surface thermohaline structure, volume transport, etc. It was decided for this study to use the topography of the 10°C isotherm as indicator. The 10°C surface provides a straightforward means of displaying the form of an eddy and it is simple to interpret. In addition, the thermal structure in general and the depth of the 10°C isotherm in particular were used during field surveys as primary indices of the existence of eddies. In addition, the thermal structure has been used to represent eddies in one way or another by many authors. Some authors display the depth D_T of a fixed temperature T (e.g. CHENEY et al (1976), CHENEY (1976), RICHARDSON, CHENEY and WORTHINGTON (1978) and VASTANO, SCHMITZ and HAGAN (1980) used D_{15}, while FUGLISTER (1972) used D_{10}), whereas others prefer the temperature T_D at a fixed depth D (e.g. GOTTHARDT (1973) used T_{200} and T_{300}, HOWE and TAIT (1967) used T_{390} and SCHMITZ and VASTANO (1975) used T_{500}).

TABLE 11.4

SIZE AND SHAPE OF EDDIES

Date	Eddy	Shape	Figure	Dimensions (km) (10°C/650 m)
June 1976	Charlie	Elliptic	5.3	130 x 150
June 1977	Delta	Eggshaped	6.8	50 x 80
May 1978	Echo	Elliptic	7.7	90 x 240
June 1978	Echo	Elliptic	7.12	120 x 240
December 1979	Fred	Elliptic	8.5	170 x 210
April 1981	Harry	Circular	9.11	130
April 1982	Ian	Elliptic	10.4	180 x 260
June 1982	John	Circular	10.17	180

The two-dimensional topography of the 10°C isotherm surface has been shown in Chapters 4-10 for all those eddies where more than just a single transect was executed. Admittedly, two transects only does not provide a detailed representation of the two-dimensional structure of the eddies, but basic features of the eddy shapes can be discerned.

The eddies assumed many forms, and only in isolated cases were they quasi-circularly shaped. The size of the eddies was defined as the area enclosed by the intersection of the 10°C and 650 m depth. The choice of the 650 m depth meant that the size of the eddy was not influenced by the variations ($\pm$ 42 m see Table 11.1) in the 10°C depth encountered in the absence of eddies. Defining the size of an eddy in terms of its thermal structure in this way is quite acceptable. E.g. RICHARDSON, MAILLARD and STANFORD (1979) used the 15°/650 m intersection and RICHARDSON, STRONG and KNAUSS (1973) used 15°/500 m intersection to define the size of Gulf Stream rings. The smallest eddy (see Table 11.4) was Delta (50 x 80 km) while the largest was Ian (180 x 260 km), and it is obvious that with variation of this magnitude there can be no meaningful "average" eddy size.

In comparison Gulf Stream rings have diameters of 130 km (RICHARDSON, CHENEY and MANTINI, 1977), and 150 km RICHARDSON, STRONG and KNAUSS, 1973) while RICHARDSON, CHENEY and WORTHINGTON (1978) reported dimensions ranging from 45 km (circular) to 80 x 220 km (elliptical). All these dimensions were based on the 15°C/500 m intersection. The "overall size" (indicating the largest dimensions of the anomalous elevation of the 15°C isotherm) ranged from 100 to 250 km. The impression is gained that Gulf Stream rings are larger than the eddies of the Mocambique Ridge Current, but that both eddy types are of compatible magnitude.

There is no conclusive evidence of any geographical variation of eddy shape. According to FUGLISTER (1977), Gulf Stream rings evolve from elliptical to a more circular shape as the ring moves away from its host current. VASTANO, SCHMITZ and HAGAN (1980) also attributed eccentricity in the ring shape to dynamic processes (current-ring and ring-ring interaction). This would suggest that an eddy such as John (see Fig. 11.1) was more independent than most of the other eddies.

As has become evident through Chapters 4-10, the study suffered from the availability of "time series" observations of eddy development, propagation and decay. Separate surveys of the same eddy were obtained in only two cases: Echo (May and June, 1978) and Golf (January and March, 1980). Although the aspect of eddy advection will be dealt with in Chapter 12, we would like to draw attention to one aspect of eddy Echo's drift. During the first observation, Echo's major axis was orientated roughly NW-SE, while it was orientated NE-SW a month later. SPENCE and LEGECKIS (1981) attributed the elliptical shape to the presence of a wave propagating around the perimeter of the eddy, and concluded that a decay of this wave's amplitude may lead to more circular flow. The wave rotated in the same sense as the current in the eddy, and at a rate of about 5% of f (the Coriolis parameter). In our case this would imply clockwise rotation and a full revolution every 20 days. In the $\pm$ 30 days between the two surveys, eddy Echo could have rotated 1½ times, which could agree roughly with its orientation during the June 1978 survey (see Fig. 11.1).

11.6 Distribution of eddies

In Fig. 11.1 the 10°/650 m intersections of all the eddies surveyed in this project have been portrayed. Also included are the estimated positions of eddies Alfa and Bravo of whose dimensions little is known.

Most of the eddies (except Alfa, Delta and Ian) were located between 29°S and 32°S, immediately east of the Mozambique Ridge. The concentration of eddies in this area may, on the one hand, be an artificial result of the survey technique, since eddies were only looked for in this region. On the other hand, their concentration may be related to their mode of generation (see Chapter 13).

Through comparison (above) with results from other parts of the world, it has been attempted to show that the eddies located in this study are now unique, and this aspect of the results must be reiterated. Although eddies in this abundance have not been reported in this area before, eddies in general and cyclonic eddies in particular have been observed all over the globe. GRüNDLINGH (1983b) has given a review of eddies in the southern Indian Ocean and the Agulhas Current, but the reader is also

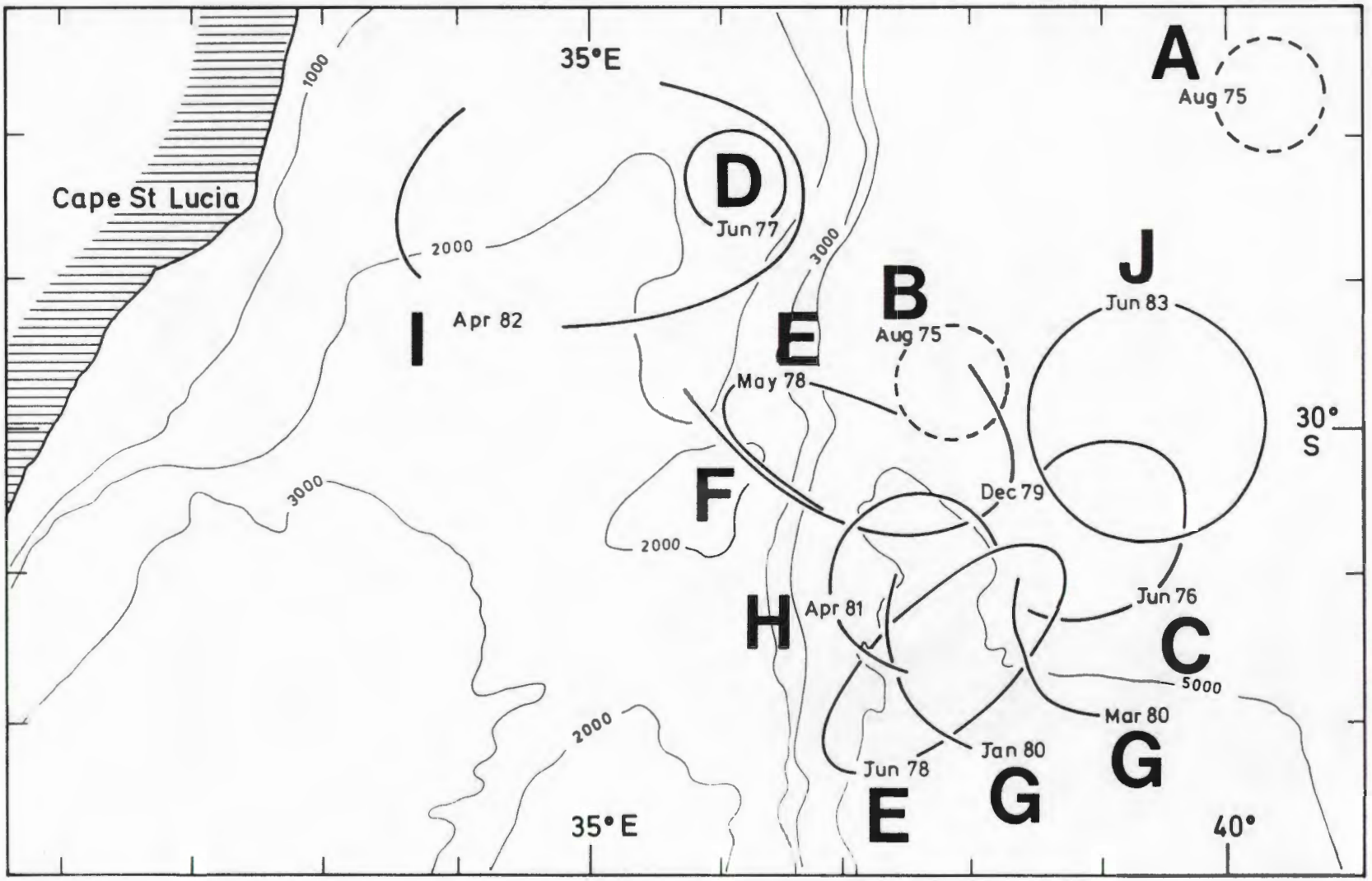

FIG. 11.1 : Distribution of vortices located and surveyed during the present study. The vortices are represented by the 10°C/650 m intersection.

referred to LUTJEHARMS (1981b) and SZEKIELDA (1983) for further examples of eddies in the Agulhas retroflection area. Slightly further afield, but still in the western boundary of the Indian Ocean, BRUCE (1979), BRUCE, QUADFASEL and SWALLOW (1980) and COX (1979) discussed the eddies of the Somali Current. Other examples of eddy research (excluding the Gulf Stream cold and warm eddies) are given by CRESWELL (1982) and NILSSON, ANDREWS and SCULLY-POWER (1977) for the East Australian Current, JOYCE and PATTERSON (1977) and PETERSON, NOWLIN and WHITWORTH (1982) in the Drake Passage, SAVCHENKO, EMERY and VLADIMIROV (1978) in the Antarctic Circumpolar Current south of Australia, STUMPF and LEGECKIS (1977) in the eastern Pacific, BERNSTEIN and WHITE (1974) in the north Pacific. CHENEY, RICHARDSON and NAGASAKA (1980) in the Kuroshio, MADELAIN and KERUT (1978) in the northeast Atlantic and HANSEN and MEINCKE (1979) in the far north Atlantic, to name but a few. Under this list also belong the results of the MODE experiment (see MODE Group, 1978) which had a much wider scope than to simply study eddies. SWALLOW (1976)presented a brief review of the varied geographical distribution of eddy observations. It is therefore clear that the uniqueness of the eddies under discussion does not lie in their existence, but only in their discovery.

11.7 Summary and main physical characteristics

The eddies observed during this survey were by and large characterised in the deeper layers ($\sim$ 500 m) by the presence of water that was 2-3°C cooler than the ambient water. This was portrayed by an upheaval of the isotherms below 10°C to approximately 300 m above their normal levels, an elevation that was also reflected in the behaviour of the isohalines as well as the nutrient levels. A deepening of the mixed layer at the centre was a typical feature of many eddies.

The shapes of the eddies ranged from circular to elliptic and considerable variability was evident. The dimensions of the smallest eddy were 50 x 80 km (taken as the transverse distances over which the water temperature was $<$ 10°C at a depth of 650 m) and of the largest were 180 x 260 km. The "areas" of the eddies thus varied by an order of magnitude from 3.14×10^3 km^2 to 36.7×10^3 km^2 .

In isolated cases, Red Sea Water was observed in the vicinity of some of the eddies, while the upper 200 m showed interleaving of tropical and subtropical water masses. At the surface, evidence was found that the eddies were often located between water of a tropical origin to the north and subtropical to the south.

CHAPTER 12

DYNAMIC CHARACTERISTICS OF THE VORTICES OF THE MOZAMBIQUE RIDGE CURRENT

12.1 Introduction

Having defined the eddies in terms of size, shape and main thermohaline characteristics in Chapter 11, the present chapter will provide an insight into the dynamics of the eddies. This will involve aspects such as velocities, volume transport, energy, etc. It is believed that the generation of these vortices are directly linked to the existence and behaviour of the Mozambique Ridge Current, and a discussion of this aspect of eddy dynamics as well as of the Mozambique Ridge Current *per se* has been retained for Chapter 13.

12.2 Velocity field

The velocity of flow in the eddies was measured in the following four ways. First, gradient velocities were calculated for those stations where a "centre of curvature" was present and where station pairs were orientated in line with the centre of curvature (see Appendix 4). For all the other station pairs, simple geostrophic currents were computed. In almost all the cases, the greatest common depth of measurement of a station pair was selected as the reference level, but since many stations went to only 1000 m, the geostrophic velocities are only approximations of the true velocity (not even considering all the other inaccuracies involved with geostrophic currents). Second, estimates of the surface velocity were obtained by determining the set of the ship(see Appendix 4). Third, satellite-tracked buoys ventured into the surveying area in 1975 and in December 1979, and their drift velocities could be determined between successive fixes. Finally, an array of current meters was deployed during the cruise in December 1979, and currents were measured at five levels for a period of approximately 2 days (see Appendix 7).

As far as the study of the dynamics of eddies is concerned, attention should be drawn to three novel ways of investigation (not employed in this study); namely radar altimetry, synthetic-apperture radar (SAR) and acoustic

tomography. The radar altimeter flown during the SEASAT mission in 1978 enabled the resolution of the sea surface height within about 10 m, and this was used to study currents and eddies in the North Atlantic (e.g. CHENEY and MARSH, 1981; CHENEY, 1982) and the Agulhas Current retroflection region (COLTON and CHASE, 1983). The potential of SAR in the detection of eddies was shown by FU and HOLT (1983). Recently, acoustic tomography has come to the foreground as a tool in the detection of mesoscale features (such as eddies) in the sea. By tracing acoustic ray paths from an array of transmitters and receivers, eddies can be detected over large distances (e.g. MERCER and BOOKER, 1983).

12.2.1 Geostrophic velocities

By far the most information on the velocity distribution of the eddies has been obtained from the geostrophic/gradient currents, especially since this method provides details of both horizontal and vertical distribution of velocity. Examples of the distribution of these velocities in the vicinity of eddies can be found throughout the thesis, and there are a few points that can be elucidated:

(a) Maximum velocity

In Table 12.1 the maximum geostrophic velocity has been listed for all the vortices encountered on this project. This table shows that a typical maximum velocity (relative to 1000 m) would be about 40 cm/s, and that although this maximum was located at the surface in the majority of cases, in some eddies it was located at 200-300 m depth.

These velocities seem to be much lower than the velocities calculated in the Gulf Stream rings (see e.g. KHEDOURI and GEMMIL, 1974; RICHARDSON, MAILLARD and STANFORD, 1979) where values larger than 1.5 m/s have been computed (OLSON, 1980). In several of the cases reported in the literature, the velocity maximum was located below the surface ($\sim$ 100 m depth).

(b) Reference level

In all cases, the reference level or "level of no motion" has been taken equal to the maximum depth of measurement. With an exponential decrease in velocity, as is customarily the case, the possible error incurred

TABLE 12.1

MAXIMUM GEOSTROPHIC VELOCITIES Vmax

Cruise	Eddy	V_{max} m/s	Depth of V_{max} (m)	Ref Depth (m)
August 1975	Bravo	0.30	200	900
June 1976	Charlie	0.5	0	1000
June 1977	Delta	0.48	300	1000
May 1978	Echo	0.49 (0.65)	0	1000 (1700)
June 1978	Echo	0.48 (0.67)	0	1000 (1800)
December 1979	Fred	1.07	0	1000
January 1980 *	Golf	0.4	180	1000
March 1980 *	Golf	0.2	180	1000
February 1981	-	0.54	0	1000
April 1981	Harry	0.51 (0.67)	0	1000 (1500)
April 1982	Ian	0.45	0	1000
June 1982	John	0.55	0	1000

* grazing encounter

TABLE 12.2

CHARACTERISTICS OF THE VELOCITY MAXIMUM Vmax IN EDDY FRED DECEMBER, 1979

Eddy Sector	Magnitude (m/s)	Depth (m)	Distance from Centre : (km)
East	1.07	0	100
South	0.36 and 0.65	0 and 200	100 and 60
West	0.42	200	100
North	0.64	0	100

by a wrong choice of this level decreases with increasing depth of the reference level. During only two cruises where eddies were located (May and June 1978) did the measuring depth extend to 1800 m on a routine basis (in contrast to other cruises where profiling was extended beyond 1100 m only at isolated stations). It would be unrealistic to claim that Echo was an example of a "typical" eddy, but these measurements provide the only cases where some insight can be obtained into the deeper reference depth.

In Fig. 12.1 a selection of geostrophic profiles from Echo are presented, and these show the sharp decline of velocity in the upper 800 m or so, and the almost asymptotical approach to zero in depths greater than 1000 m. At 1000 m the profiles had dropped to about 30% of their surface value, while at 1500 m it was about 7%. By assuming the reference level at 1000 m instead of 1800 m, geostrophic velocities would therefore tend to be about 30-40% too low. (The stations of which the geostrophic profiles are presented in Fig. 12.1 were all situated in more than 4000 m depth). The impression is gained that the eddies only extend to about 1800-2000 m depth, but more measurements of this kind will be required before any confidence can be placed on the results of just a single eddy. It may be mentioned in passing that geostrophic currents have been compared to current meter observations (BROENKOW, 1982), and good agreement has been found.

(c) Geopotential

The geopotential anomaly (or dynamic topography) of the sea surface relative to 1000 m or the deepest common depth during a cruise, has been presented for various surveys (see Chapter 4-10). The subsurface maximum attained by the velocity field on some occasions lead to a noticeable distortion of the flow pattern derived intuitively from the vertical sections of geostrophic velocity or the temperature sections. This can be seen from a comparison of the surface geopotential and topography of the 10°C isotherm surface (e.g. Figs. 10.17-10.19). Relative to 1000 m, the sea surface in the eddy centre was depressed above 30 cm below the ambient sea level.

(d) Three-dimensional motion

During some of the cruises where it was possible to execute two or more transects of an eddy it was noticed that the maximum velocity was

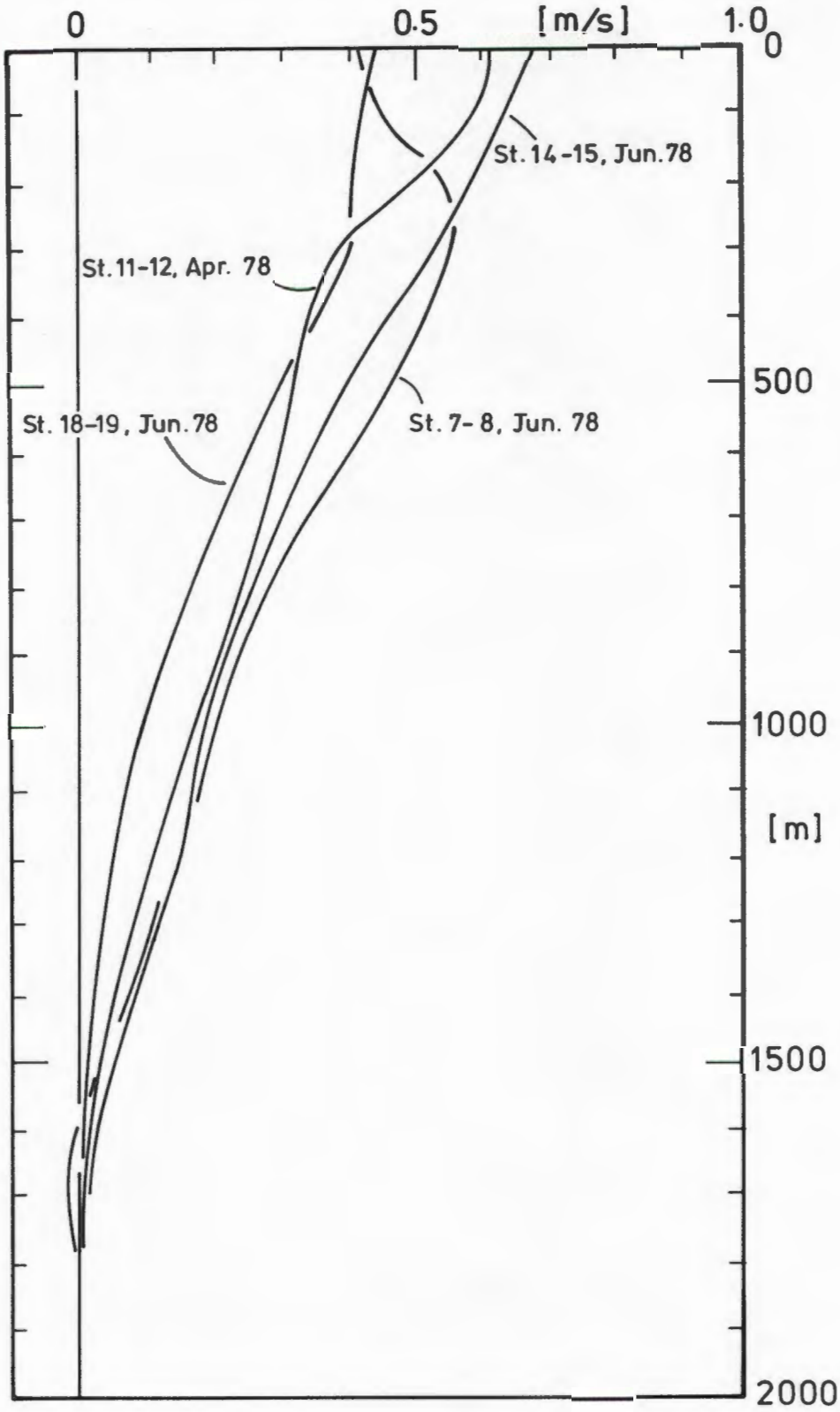

FIG. 12.1 : Profiles of geostrophic velocity from four station pairs during April and June, 1978.

located at the surface in parts of the eddy and at subsurface depths in other parts of an eddy. An example of this can be seen in the results of the cruise in November/December 1979 (e.g. Fig. 8.10), Table 12.2 provides some details of the position of the high-velocity core of the current constituting the eddy.

From this table it is clear that the eddy had a rather complicated velocity structure with, at times, two separate velocity filaments at different depths. The undulating nature of the velocity field (maximum velocity sometimes at the surface and sometimes below the surface) was also observed in other eddies (cf. eddy Echo Fig. 7.10 and Fig. 7.11; eddy John Figs. 10.13 and 10.15) as well as in Gulf Stream rings (e.g. OLSON, 1980).

The results seem to indicate that the eddies were very seldom (if ever) symmetrical or uniform and could be considered anything but smoothly-rotating bodies of water. The information suggests that some eddies had a distinct two-layered flow distribution: A surface flow involving the upper 100 m or so, and a deeper layer from about 200 m downwards. Where the velocity maximum of the surface layer $V_{1\ max}$ and that of the bottom layer $V_{2\ max}$ were at the same distance from the centre, they combined to present an overall maximum at the surface. If $V_{1\ max}$ and $V_{2\ max}$ did not coincide vertically, two separate filaments were formed or if either $V_{1\ max}$ or $V_{2\ max}$ is absent, the remaining jet was the only one visible in the velocity distribution.

This is obviously an oversimplification of the eddy circulation, but is in line with the layered structure suggested by the thermohaline distribution (see Chapter 11).

12.2.2 Ship's set

There are many factors that influence the "ship's set" i.e. the difference between the planned (DR) course and the true course of a vessel. Factors such as wave height and direction, wind speed and direction, etc. all have to be considered in the derivation of an accurate set. One of the main sources of error lies in the inaccurate assessment of the ship's speed through water, and this often reduces the usefulness of the ship's set to the component normal to the ship's heading only (NILSSON, 1977).

The best calculations of the set are therefore obtained when the vessel is allowed to drift passively in fair weather over a prolonged time. This was done during the cruise in December 1979 when the *Meiring Naudé* followed the free-drifting array of current meters (see Fig. 8.9). Although the vessel had to be repositioned every now and then to keep the array in sight, this allowed a fairly accurate determination of the set, or drift, of the array. This drift velocity has been presented in Table A7.1. During the period of drift, the array passed through the region previously occupied by the *Meiring Naudé* on stations 31 and 32, and this enabled a comparison between the drift and the geostrophic velocities. Extrapolating the surface geostrophic speed between stations 31 and 32 by 40% from the 1000 m reference depth to about 1800 m (see section 12.2.1(b)),a value of 28 cm/s (corrected for gradient effects) is derived. If it is assumed that this represented only a component of the true gradient velocity (since the array drift direction differed from the alignment of stations 31-32), the value was "rotated" to produce a true velocity of 37 cm/s . This agrees very well with the 35 cm/s drift speed of the array during this period (see Table A7.1).

Whereas the drift velocity used in this comparison is probably quite accurate, the ship sets calculated over shorter periods show greater variation. Table 12.3 presents a few examples and these show some large differences between the ship set and the extrapolated-rotated geostrophic speeds. Some other extreme cases can be seen in the superposition of ship set and geopotential for the cruise in June 1982 (Fig. 10.18). It seems that although the ship sets can produce some indication of the current flow (especially in real time conditions), great care must be exercised in the selection of appropriate satellite fixes, while also considering other contributing factors such as wind effects.

It is concluded that the ship sets confirm the order of magnitude of the geostrophic velocities, although the geostrophic velocities provide much greater consistency in the velocity field.

12.2.3 Satellite-tracked buoys

In section 8.10 the tracks of several buoys were discussed in terms of the shape and periodicity of their courses. In the present section

TABLE 12.3

COMPARISON OF GEOSTROPHIC VELOCITY AND SHIP'S SET (m/s)

Cruise	Stations	$V_{1000\ m}$ +	$V_{1800\ m}$ (V_{1000} + 40%)	$V^{\S}_{rot}$	Ship Set
May 1978	11-12	0.49	0.65@	0.71	1.24
	20.21	0.11	0.28@	0.39	0.87
	14-15	0.15	0.25@	0.34	0.48
	19-20	0.16	0.25@	0.24	1.25
Dec. 1979	31-32	0.20	0.28	0.37	0.35
	24.25	0.64	0.90	1.10	1.21
	29-30	1.07	1.50	1.53	1.23
	17-18	0.42	0.59	0.60	0.78
Apr. 1981	4.5	0.67 (0.81)*	0.94	0.95	0.67
	6-7	0.37 (0.5)*	0.52	0.55	0.41
	9-10	0.16 (0.22)*	0.22	0.24	0.54

\+ Subscript denotes reference level depth.

§ velocity in direction of ship set

* velocity calculated relative to 1500 m

@ observations extended down to 1700 m (not extrapolated).

attention will be focussed on the drift speeds of these buoys and the buoy of Fig 4.1 while they were trapped inside two eddies but also while drifting in the area surrounding the eddies (e.g. the Mozambique Ridge Current). The relevant sections of the tracks with the drift speeds have been reproduced in Fig. 12.2.

Buoy 14627 performed almost three complete revolutions inside an eddy 31°30'S, 38°E (shown in Chapter 8 to have been eddy Golf), and over a period of 24 days drifted at an average rate of 0.53 m/s. The average radius of curvature inside Golf was approximately 70 km. This velocity can be compared with the hydrographic data obtained at the last few stations in January 1980 (i.e. 3 months after the buoy track). The surface gradient velocity between stations 14 and 10 (60 km from the eddy centre) was 0.23 m/s relative to 1000 m (or 0.32 m/s, extrapolated by 40% to simulate the 1800 m reference level).

Buoy 14621 that drifted in a southeasterly direction in the vicinity of 30°S, moved at a rate of about 0.8 m/s before also decelerating to 0.3-0.5 m/s in the eddy region.

Buoys 14622 and 1116 did not enter the eddy region, but continued on a more-or-less meridional course between 29°S and 31°S, and their speeds during this time were significantly lower than any of the other buoy drifts. The areas of high-speed drift ($>$40 m/s) of the buoys southward along the Mozambique Ridge between 28° and 19°S and the high-speed drift (40 - 70 cm/s) westwards over the Ridge at 31°S were obviously separated by a region of fairly slack water ($<$30 cm/s) between 29°S and 31°S. The significance of this will be discussed in Chapter 13.

These results seem to indicate that the drift velocity of satellite-tracked buoys inside the eddies are in fair agreement with the velocities derived from other methods.

Remote-tracked buoys have been used fairly extensively to study the dynamics of eddies in many parts of the world, especially in rings of the Gulf Stream (see e.g. RICHARDSON, 1980; RICHARDSON, CHENEY and MANTINI, 1977) and the Kuroshio (CHENEY, RICHARDSON and NAGASAKA, 1980). Drogued floats, tracked by surface vessel, have also been used to explore an eddy off California (REID, SCHWARTZLOSE and BROWN, 1963). The most interesting performance of a single buoy inside a Gulf Stream ring was presented by

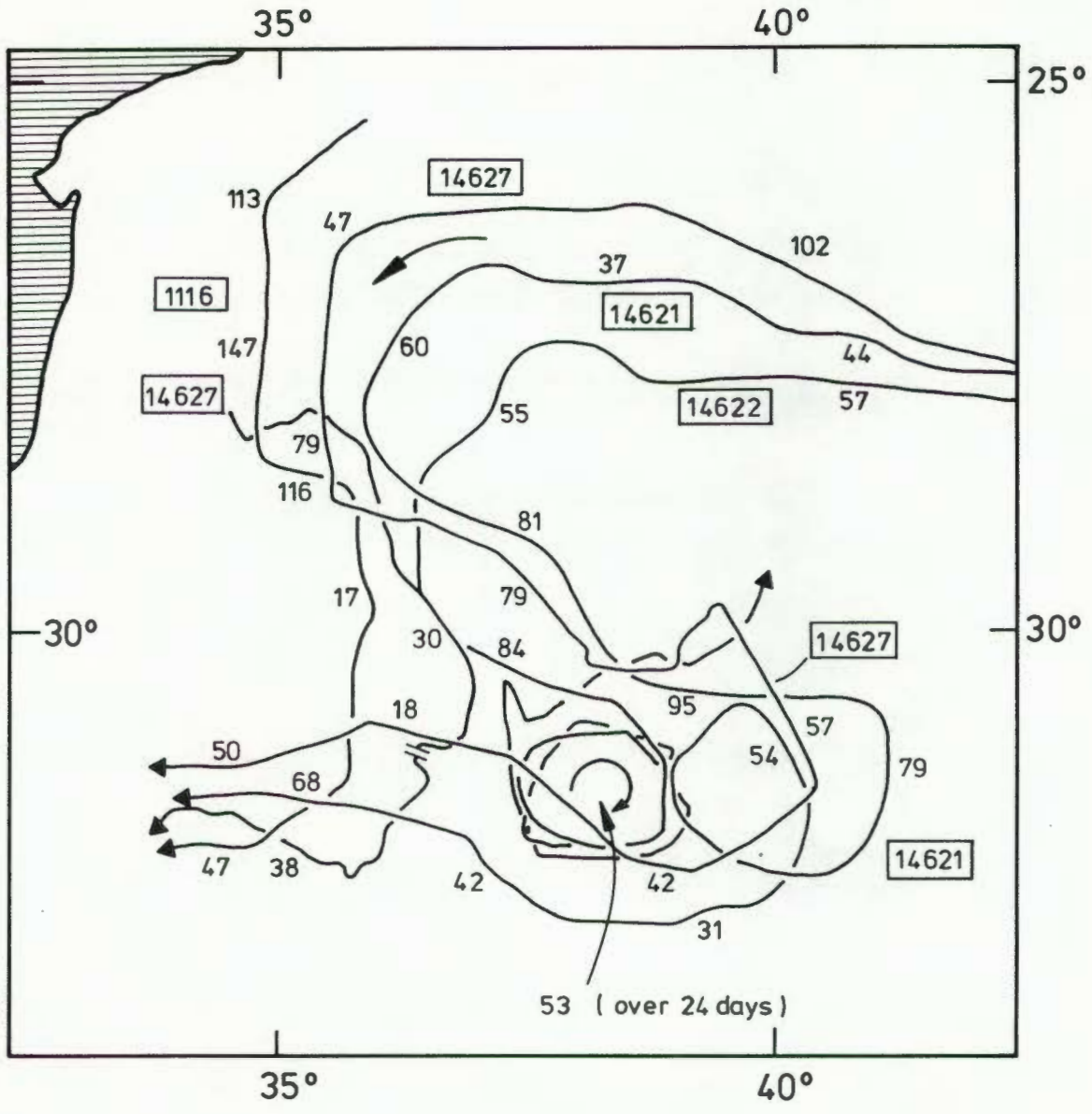

FIG. 12.2 : A selection of satellite-buoy tracks in the vicinity of the Mozambique Ridge and - Basin. Blocked figures are buoy ID numbers, while figures accompanying tracks are drift velocities in cm/s, calculated over approximately 24 hours.

RICHARDSON (1980), when a buoy remained in a ring for 8 months while making 86 loops. The buoy's velocity at this time was 125 cm/s at a mean radius of 40 km.

12.2.4 Current meters

Since the velocities recorded directly by the drifting current meter array (December 1980, Chapter 8) were very low (see Appendix 7), the true current velocity was not significantly different from the drift rate of the array itself. What is of interest in this section are some aspects of the vertical distribution of velocity and direction.

A profile of the current velocity was presented in Fig. 8.12. In Fig. 12.3 the relative currents (i.e. relative to the drift of the array) have been superimposed on the drift track. Assuming that the array was fixed to a body of water moving around the eddy, then, even if the eddy was not perfectly circular, a line normal to the drift track will coincide more-or-less with the direction into and out of the eddy. Although the tolerance of the current velocities measured by the current meters is not very great (see Appendix 7), there is still a remarkable consistency between the currents recorded at the different levels.

Within the framework of these restictions, it seems that a certain amount of (consistent) variation occurred during the drift period of the array. Initially, the relative currents were directed outwards (i.e. away from the eddy centre which was located to the east of the array position), while near the end of the drift period the vectors were directed mainly inward. There is no indication of anomalously-high velocities at certain layers, with speeds generally of the order of 10 cm/s. In Chapter 11 it was derived that the structure of some eddies was consistent with convergence in the surface layers. If this surface convergence was balanced by a subsurface divergence extending over a few hundred meters' depth, the outward radial velocities would be less than 5 cm/s. These low speeds would not be detectable by conventional equipment, and especially not by the free-drifting array. It is concluded that the results of the free-drifting current meter array did not negate the existence of any radial movement of water in and out of the eddy.

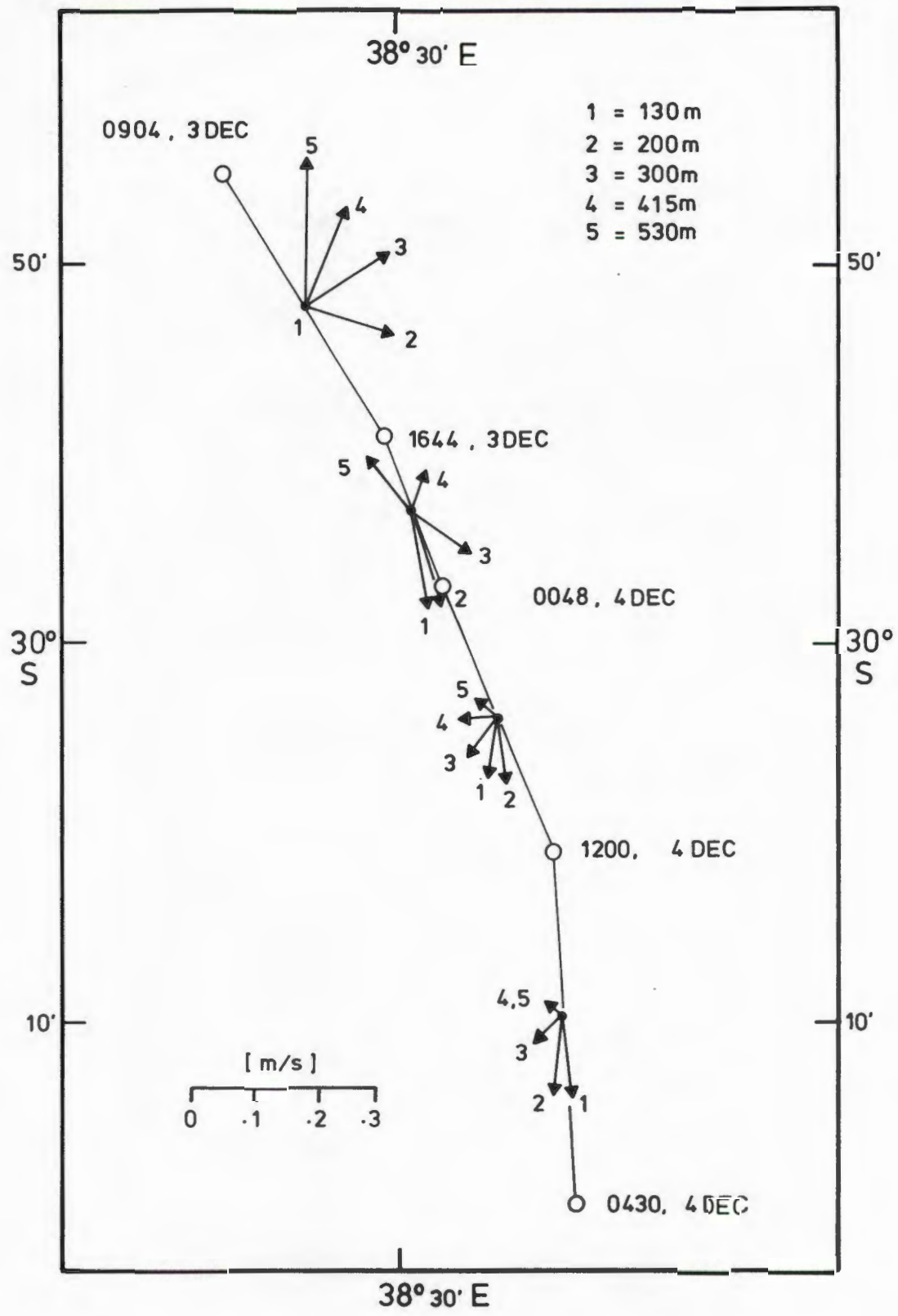

FIG. 12.3 : Drift of the current meter array deployed in December, 1979. Superimposed on the drift track are the current velocities (relative to the drift of the array) measured by the five current meters.

12.3 Sound velocity in eddies

Although the velocity of sound was calculated as one of the routine parameters during data processing, it was not used during this thesis. It is, however, appropriate to mention briefly some results obtained in the study of acoustic characteristics of rings and eddies in other parts of the world.

Transmission of acoustic signals has been used for quite some time to track neutrally buoyant SOFAR floats (e.g. ROSSBY and WEBB, 1970). These floats are deployed in or close to the SOFAR channel and are tracked over great distances. On occasion, it has occurred that a Gulf Stream ring advected in between the SOFAR float and the listening station, and this resulted in significant distortions of acoustic ray paths (e.g. BECKERLE *et al*, 1980).

Because of the lower temperature of the water inside a cyclonic ring, the ring represents an area of relatively low sound velocity, and as such severely distorts the path of acoustic rays that propagate through the ring. Using inverse methods, the distortion can be used to glean information about the structure of eddies - the principle of acoustic tomography (MERCER and BOOKER, 1983). It has also been shown (VASTANO and OWENS, 1973) that the ring can transfer acoustic energy from a near-surface layer to the SOFAR channel. A detailed treatise of the present status of acoustic investigation of eddies has been given by SPINDEL and DESAUBIES (1983).

12.4 Volume transport

Normally, volume transports varied considerably inside a particular eddy, with large fluxes being exchanged with the environment. For the sake of intercomparison between vortices, Table 12.4 contains the range of volume transport variation (where the coverage of an eddy was only partial e.g. with grazing encounters or where only one complete transect is available, only one value has been entered) relative to 1000 m, as well as the transport relative to a deeper level if measurements extended beyond 1000 m.

TABLE 12.4

VOLUME TRANSPORT T AND KINETIC ENERGY$^{\neq}$ OF THE EDDIES

Cruise	Eddy	$T_{1000}^{@}$	$T_{>1000}$ (ref. depth)	$T_{1000}/T_{>1000}$	$K.E._{1000}^{@}$
August 1975	Bravo	11-12*			3.7*
June 1976	Charlie	12-21			7.0
June 1977	Delta	10-18			3.7
May 1978	Echo	36	51 (1500)	0.70	
June 1978	Echo	20-25	32-48 (1800)	0.62-0.52	33.3+
December 1979	Fred	17-28			17.4
January 1980	Fred	12§			
	Golf	13§			
March 1980	Golf	18			4.0
February 1981	-	4-15			
April 1981	Harry	32	56 (1500)	0.57	
April 1982	Ian	17-34	20-71 (1350-2000)	0.85- .48	18
June 1982	John	21-25	41-50 (2000)	0.51-0.50	21.4

≠ transport $10^6 m^3/s$; KE in 10^{14} J

@ subscript denotes reference level depth (m)

* relative to 900 m

§ grazing encounter

+ relative to 1800 m

Excluding the data from eddy Ian (April 1982), a vortex that seemed to be part of the Agulhas Current itself, the maximum volume transports of the vortices seem to be in the region of 50 x $10^6 m^3/s$. The transport of eddy John located in June 1982, which is considered to have been one of the more symmetrical of the eddies, varied between 41 and 50 units. Interaction of this eddy with the environment in terms of flux exchange was minimal (see Fig. 10.21), and this was considered to indicate that the eddy had grown to maturity and had become free-drifting.

Although the evidence is very scant, the data seem to suggest the existence of a relationship between the transport in the upper 1000 m, T_{1000} and the "total" transport, $T_{>1000}$ (referred to levels deeper than 1500 m. In eddy John, which was considered to have been "independent", $T_{1000}/T_{>1000}$ was about 0.5. The possibility exists that this figure (0.5) may be characteristic of fully-developed, mature eddies, whereas younger eddies reflect a higher value. In comparison, DUNCAN's (1970) results show that a figure of 0.35 may be applicable to the Agulhas Current.

According to Table 12.4, the volume transport of eddy Echo decreased from the survey in May to the one in June 1978. This was reflected in the shallower and deeper calculations. The relationship between T_{1000} and $T_{>1000}$ also decreased, suggesting that the flux had become distributed over greater depth range during the developing stage of Echo.

12.5 Kinetic energy

The energy contained by an eddy can be partitioned into two components: potential energy and kinetic energy.

Potential energy in the sea arises from the density stratification of the water, irrespective of whether the isopycnals are sloped or not. The upheaval of isopycnals in cyclonic eddies means that the potential energy can be separated into a portion that arises from the upheaval and which can be converted into kinetic energy (referred to as the available potential energy, or APE), and a large portion that is associated to the potential energy inherent to a horizontally uniform density stratification.

For the Gulf Stream rings, APE has been calculated by BARRET (1971), CHENEY and RICHARDSON (1976), KHEDOURI and GEMMIL (1974), and others. OLSON (1980) reported ratios of KE (kinetic energy) to APE between 0.3 - 0.47 so that the APE exceeds the KE by a factor of 2. Because of the relation between potential energy and the density inside the eddy, the potential energy resembles the shape of the isopycnals in the main thermocline (see e.g. KHEDOURI and GEMMIL, 1974). The peak of the APE coincides with the peak in the isopycnals, and for that reason the maximum APE is located in the centre of the eddy. Although APE was not calculated for the eddies of this thesis (mainly for logistic reasons), it remains a valuable tool in the study of eddy decay.

The residual component of energy, namely KE, is associated with the (circular) motion of fluid particles. For the eddies of this thesis, KE was calculated using equation (4) in Appendix 4. An inspection of the distribution of kinetic energy in all these eddies shows that the eddy centres coincided with an energy minimum. The energy increased with distance from the centre and reached a maximum between 50 and 100 km from the eddy centre.

Table 12.4 contains an estimate of the total kinetic energy of the eddies that were surveyed with sufficient detail in this study, while grazing encounters or temperature-only surveys have been omitted. These values seem to indicate that the maximum total kinetic energy in an eddy (calculated relative to 1000 m) was approximately 20×10^{14} J. Because of the paucity of the data base, it has been impossible to relate the KE to either the "age" of the eddies or its geographic location.

The values of KE in Table 12.4 ($3\text{-}20 \times 10^{14}$ J) are comparable to the KE reported for cyclonic Gulf Stream rings by CHENEY and RICHARDSON (1976 : $9\text{-}24 \times 10^{14}$ J, relative to 1000 m). On only one occasion was it possible in the present study to calculate the KE relative to a deeper level (1800 m), and in this case the KE (33.3×10^{15} J) is also compatible to the estimates of CHENEY and RICHARDSON (1976: 135 and 56×10^{14} J, relative to 1500 m and 3500 respectively) KHEDOURI and GEMMIL (1974: 85×10^{14} J, relative to 2500 m), and RICHARDSON, MAILLARD and STANFORD (1979: 30×10^{14} J, relative to 4700m).

Because the APE reaches a maximum at the centre of an eddy and decreases outward, while the KE increased from 0 at the centre to a maximum 50-100 from the centre, the KE exceeds the APE in the region of the KE maximum. This requires the transfer of APE or KE outward to the region of KE maximum in order to maintain the KE against viscous dissipation (CHENEY and RICHARDSON, 1976; OLSON, 1980).

12.6 Vorticity field

According to PEDLOSKY(as quoted by OLSON, 1980), the conservation of potential vorticity can be expressed as follows

$$\frac{d}{dt}\left[\frac{\partial \rho}{\partial r}\left(\frac{1}{r}\frac{\partial w}{\partial \theta} - \frac{\partial v}{\partial z}\right) + \frac{1}{r}\frac{\partial \rho}{\partial \theta}\left(\frac{\partial u}{\partial z} - \frac{\partial w}{\partial r}\right) + \frac{\partial \rho}{\partial z}\left(\frac{v}{r} + \frac{\partial v}{\partial r} - \frac{1}{r}\frac{\partial u}{\partial \theta} + f\right)\right] = 0 \quad (1)$$

The equation relates the components of velocity u, v and w the density ρ, radius or curvature r and the Coriolis parameter f, in terms of cylindrical coordinates r, θ and z. OLSON estimated the magnitude of each of the terms in equation (1) to determine their relative contribution to the vorticity balance. Using the data obtained during the survey of a cyclonic Gulf Stream ring in 1977, he concluded that the conservation of potential vorticity can be approximated by

$$\frac{d}{dt}\left[\frac{\partial \rho}{\partial z}\left(\frac{v}{r} + \frac{\partial v}{\partial r} + f\right)\right] = 0 \quad (2)$$

with the other terms in eq (1) at least one order of magnitude smaller than the terms in eq (2).

To examine the distribution of potential vorticity for the vortices of the Mozambique Ridge Current, we selected an eddy (John) that was considered to have passed the formative stage and was probably free-drifting. Although John was symmetrical, it should not necessarily be considered a typical example of eddies in this area, since most of the other eddies were assymetrical and close to the Mozambique Ridge - an indication that the eddies were probably still attached to the host current (see Chapter 13).

For this eddy, the density was used to derive $\partial\rho/\partial z$, and the gradient current distribution was used to obtain $v/r + \partial v/\partial r$

Finite differencing for the meridional and zonal sections provided the distribution of potential vorticity π where

$$\pi = \frac{\partial \rho}{\partial z}\left(\frac{v}{r} + \frac{\partial v}{\partial r} + f\right) \qquad (3)$$

displayed in Figures 12.4 and 12.5. A superficial estimate of the magnitude of the terms in (1), using eddy John as an example, confirmed their relative magnitude as derived by OLSON (1980).

There is a certain amount of incompatability between these two sections, a disparity that was also evident from the temperature and velocity sections (see Chapter 10). This was the result of the zonal transect not having passed through the centre of the eddy (see the topography of the 10°C isotherm, Figure 10.15).

Most of the eddy's potential vorticity seems to be located in the upper 300 m. This is due to the large contribution of changes in the vertical stratification $\partial\rho/\partial z$ to the potential vorticity (eq (3)). In the deeper layers ($>$ 500 m) the isopleths of vorticity are characteristic of a poorly-defined field with values less than 1×10^{-7} kg m^{-4} s^{-1}. The vorticity values derived for this eddy are compatible to the values obtained from a Gulf Stream ring (OLSON, 1980).

An interesting feature that emerges from the combined distribution of σ_T and potential vorticity (Figures 12.4 and 12.5) is that the two fields are homotropic (orientated similarly) in certain depths and heterotropic in others. Homotropy seems to exist in the upper part of the thermocline ($\sim$ 200 m) and in the deeper layers ($\gtrsim$ 800 m). This was also found by FLIERL (1979), who used a two-layer model to represent the flow in the eddy.

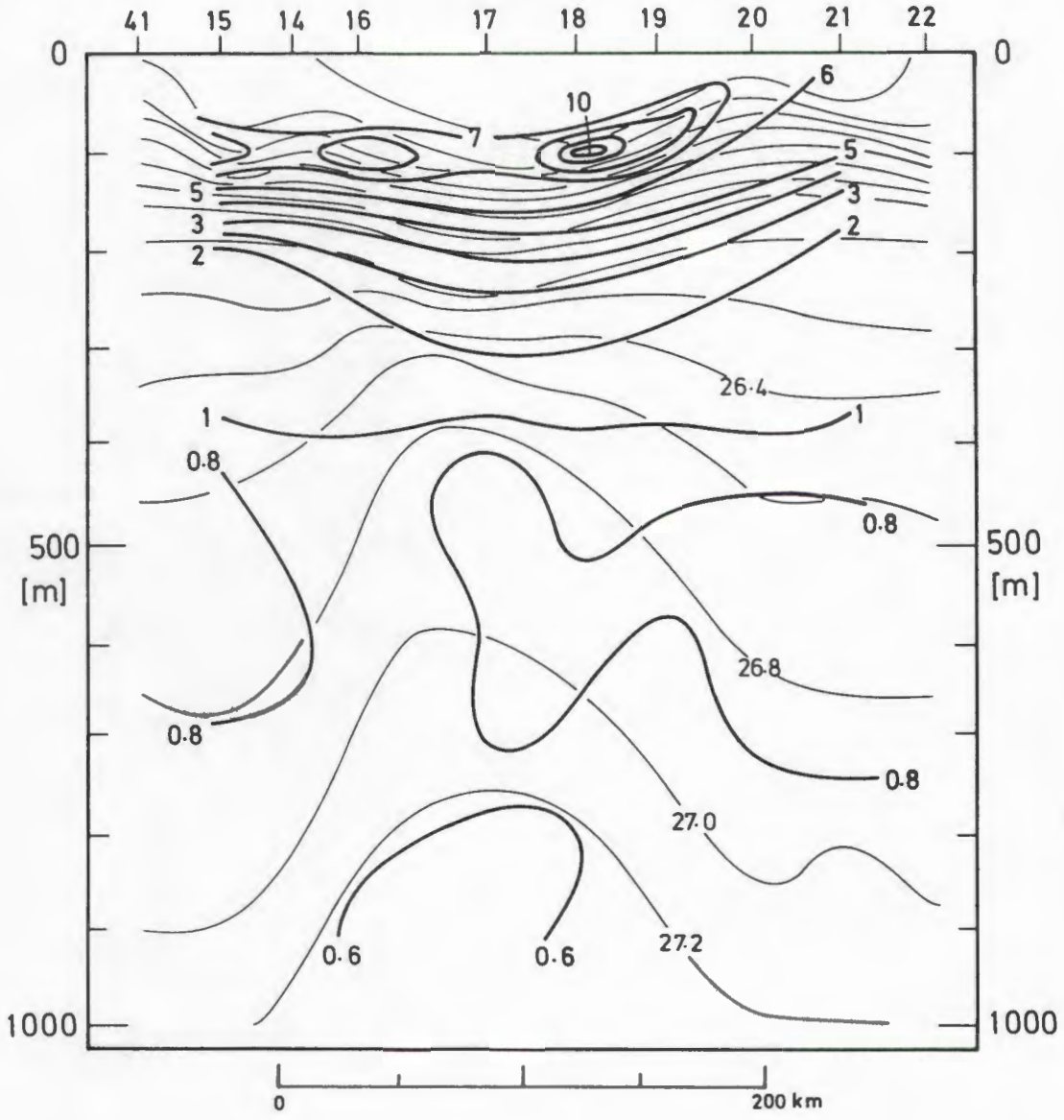

FIG. 12.4 : Potential vorticity (bold lines, x 10^7 kg m^{-4} s^{-1}) and potential density σ_τ (thin lines, kg^{-3}) for the zonal section across eddy John, June 1982.

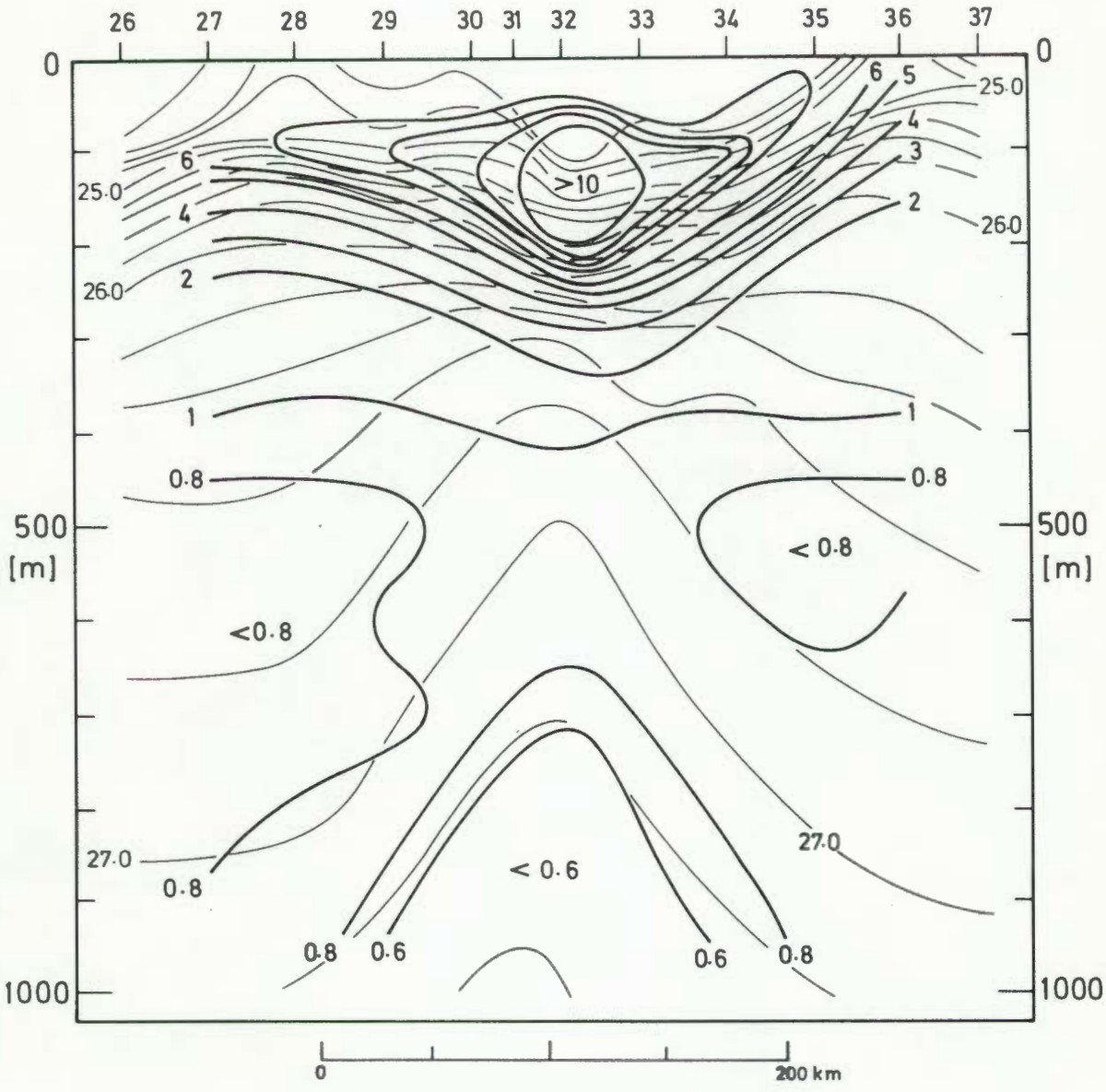

FIG. 12.5 : Same as Fig. 12.4, but for meridional section.

Assuming that vorticity and density are two conservative properties of a fluid parcel as it moves around the eddy, homotropy of the two fields indicates that the fluid parcel can move along a density interface, radially in- and outward from the centre. Where heterotropy exists, this type of movement is obstructed and fluid parcels are trapped. Fluid parcels can therefore enter or leave the eddy in the vicinity of $25 \leq \sigma_T \leq 26$ and $\sigma_T \geq 27.2$, while in the density range $26 \leq \sigma_T \leq 27$ there is a restraint on radial motion. This agrees well with the results obtained in the case of Gulf Stream rings (CHENEY *et al*, 1976; OLSON, 1980). In conjunction with this radial convergence and divergence there must be vertical motion in the eddy centre. In an eddy in the Drake passage, a vertical current meter recorded velocities of 10-20 m/day during the formative stage of the eddy (JOYCE, PATTERSON and MILLARD, 1981).

The restriction to convergent flow in the surface layers of this eddy is at variance with the convergent flow observed in some of the eddies discussed previously. It must be remembered that the eddies, where evidence of convergent flow was found, were mostly still being formed, and the distribution of vorticity could be quite different in the surface layers.

12.7 Advection

It is obvious from Chapters 4-10 that pitifully little is known about the advection of the cyclonic eddies studied in this thesis. Fig. 11.1 shows only two cases in which eddy advection could be positively identified: Eddies Echo (May-June, 1978; 5 cm/s in 151°T) and Golf (January - March 1980; 0.7 cm/s in 086°T). Apart from these two cases, the propagation of eddies could also be tentatively derived from their positions. In Chapter 13 it will be argued that the Mozambique Ridge at 30°S may be favoured for the generation of vortices. It can be seen from Figure 11.1 that the eddies observed in this study were scattered in all directions relative to this point. In addition to these positions, the vortex from HARRIS' (1970) data was located at 33°S, 38°E, and the one reported by Stavropoulos and Duncan (1974) at 31°S, 33°E. If it is considered that, in many cases, the eddies were still in a formation stage, the data base itself is obviously insufficient to produce a "preferred" propagation direction.

In contrast, Gulf Stream rings have been tracked on several occasions as they drift through the North Atlantic. CHENEY (1976) reported a value of the drift speed of 3 cm/s, CHENEY and RICHARDSON (1976) 2 cm/s, FUGLISTER (1977) 4 cm/s, GOTTHARDT (1973) 2-12 cm/s, LAI and RICHARDSON (1977) 1-4 cm/s, RICHARDSON (1980) 5 cm/s. CHENEY *et al* (1976) used SOFAR floats to track the rings and derived a rate of 6 cm/s, while RICHARDSON, STRONG and KNAUSS (1973) followed a ring for more than 14 months during which time the ring advected at about 2 cm/s. In other parts of the world, similar values were found: JOYCE, PATTERSON and MILLARD (1981) recorded 5-10 cm/s in the Drake passage, and CHENEY, RICHARDSON and NAGASAKA (1980) measured 5-8 cm/s for a Kuroshio eddy although there were short-term fluctuations, it therefore seems that a typical drift speed is 0-10 cm/s, and that the rather crude values derived for eddies Echo and Golf are quite realistic.

The propagation direction of free-drifting cyclonic Gulf Stream rings has also been considered from analytical, numerical or experimental bases. FIRING and BEARDSLEY (1976) studied the propagation of two cyclonic,circular barotropic eddies on a beta plane, and the results of their experiments are 1-1.5 cm/s, roughly toward the northwest. This is of the same order as found by BRETHERTON and KARWEIT (1975), who modelled the propagation of a circular cyclonic eddy using a six-layer quasi-geostrophic model, and MIED and LINDEMANN (1979), who studied the advection numerically. FLIERL (1977) obtained similar values, and also found that the orientation of large elliptic eddies influenced the north/south component of the advection rate. The westward translation rate, v_w of an eddy with radius R is given in simplified form by

$$v_w = \lambda R^2 \beta \qquad (\beta = \partial f / \partial y)$$

According to PETROV (1980), λ should have the value of 0.25, while WARREN (1967) reported 0.5. For anticyclonic eddies in the Gulf of Mexico, NOF (1981) obtained a value of 0.32 for λ (for a circular eddy with the velocity varying in a parabolic way from the centre outwards). With $\beta = 2 \times 10^{-13}$ cm^{-1} s^{-1}, the westward advection amounts to 2-4 cm/s for a 60-km eddy and 5-10 cm/s for a 100-km eddy. The propagation rate is always much smaller than that of a Rossby wave (βR^2).

The advection of cyclonic eddies in the northern hemisphere can be explained in the following simplified representation. As the eddy rotates cyclonically, water to the west of the eddy is moved southward, i.e. from

an area of larger planetary vorticity to a region of lower planetary vorticity. This translation means that positive vorticity is increased to the west and decreased to the east of the eddy, which simply implies a westward displacement of the eddy centre. Added to this is the flow induced by the cyclonic tendency to the west and the anticyclonic tendency to the east of the eddy. This flow pushes the eddy northward, and the net effect of these two components is an advection toward the northwest. In the southern hemisphere, the advection is toward the southwest.

At the low, "self-propelled" speeds, it can be expected that an eddy is strongly influenced by the mean (barotropic) flow. The result has been, for the case of the Gulf Stream rings, that the direction of eddy drift has varied considerably (see e.g. PARKER, 1971; RICHARDSON, 1980) although many of them drifted toward the southwest (e.g. LAI and RICHARDSON, 1977), where they eventually merged with the Gulf Stream.

It would be difficult to predict where the eddies discussed in this thesis would have drifted once cyclogenesis was completed. If the example of the Gulf Stream rings is considered, our eddies should have drifted toward the northwest, and not the southwest as theory predicts. This would also be more-or-less in agreement with the large-scale, "average" circulation in the area (DUNCAN, 1970). It has however been shown in Chapter 3 that the "average" circulation is probably overshadowed by shorter-term variations in the circulation. It is nevertheless our opinion that the eddies will advect in a general northerly direction, possibly toward the Mozambique Channel or the northern parts of the Agulhas Current.

12.8 Decay and lifetime of eddies

Eddy spindown, or decay, is defined as the ageing process experienced by eddies between creation and disappearance. In cyclonic eddies, the rotational speed decreases to zero, so does the elevation of the isopycnals above their ambient levels. There are various opinions about the way in which the decay is manifested. According to OLSON (1980), it is impossible to arrive at a quantitative estimate of eddy decay (over short periods) by using the isotherm elevation in the eddy centre. An eddy can namely adjust its thermal structure without necessarily decaying. In a study that remains one of the most enlightening as far as the observed behaviour of cyclonic Gulf Stream rings is concerned, RICHARDSON (1980) noted that a buoy implanted in a ring rotated at a fairly constant radius for

about 5 months while its period increased from 1.9 days to 2.9 days. This is more-or-less consistent with the observation of RICHARDSON, MAILLARD and STANFORD (1979), who found that although the isotherms in a ring gradually subsided (over 7 months), the mean slopes of the isotherms remained nearly constant. PARKER (1971) derived a subsidence of the 17°C isotherm of 0.6 m/day. CHENEY and RICHARDSON (1976) derived an average subsidence rate of 0.4 m/day (over a period of 12 months), although short-term shrinkages were higher. The eddy decay was mainly confined to the horizontal shrinkage of the cold dome, rather than vertical collapse. GOTTHARDT (1973) also found a subsidence of 1 m/day.

Basically, eddies lose their intensity by transformation of kinetic energy into heat. Since kinetic energy (KE) can be supplemented by the available potential energy (APE) a true measure of eddy decay is the *total* energy. Whereas the thermohaline structure of an eddy may provide ambiguous information about the spindown, estimates of energy decreases are quite significant and unambiguous. CHENEY and RICHARDSON (1976) found that the APE and KE both decreased although the relation APE : KE remained more-or-less constant. FLIERL (1977) calculated that a ring decays with time t according to a $t^{-2/3}$ law, but admitted that the predicted decay rate over the first six months may be too high. According to the decay rates quoted above, Gulf Stream rings have "life times" between one and four years.

Further to the comment at the start of the previous section about the lack of information on the drift of eddies in the southwestern Indian Ocean, even less is known about the decay of eddies in this area. Only one of the eddies, John, is considered to have been free-drifting. Using a value of 0.4 m/day for the subsidence of the cold dome, John had a potential lifetime of about 2½ years. A decay rate of 2×10^{12} J/day for the KE (from CHENEY and RICHARDSON, 1976) provided John with a potential lifetime of 2.7 years. Whether it would remain in the open ocean while decaying steadily is a different matter. According to RICHARDSON (1980), the usual fate of Gulf Stream rings is to coalesce with the Stream, thereby truncating their "lifespan". It is, however, clear that most of the eddies reported in this thesis would have had lifespans of 1 year or more, in the event that they became and remained free-drifting. As stated in the previous section, the questions of advection rate, decay rate, lifetimes and eventual fate of the eddies in the southwestern Indian Ocean remain the major outstanding issues of this thesis, and worthwhile topics for future study.

CHAPTER 13

THE MOZAMBIQUE RIDGE CURRENT

13.1 Introduction

In the previous two chapters, detailed reference to the origin of the eddies observed in this thesis has purposefully been avoided, mainly for the following reasons. First, it is believed that the creation of these vortices represent a very important aspect of their characteristics and therefore deserve more than a fleeting reference. Second, throughout much of the study, the vortices were like foundlings, with no parents in sight. In this regard the study must rank among the first of its kind where eddies of the size and intensity reported in this thesis have been discovered without any indication of their origin.

A discussion of the Mozambique Ridge Current (hereinafter referred to as MRC) therefore forms an important component of this thesis, and the reasons are twofold: First, the MRC is believed to be the host current of the eddies standing at the centre of this study. For this reason, the characteristics of the eddies (such as variability, intensity, composition, etc) are closely linked to the characteristics of the MRC. Second, the MRC has been nothing more than an abstract conception up to now, having been unthought of up to about 6 years ago and only vaguely inferred from historic data of the region (see HARRIS and VAN FOREEST, 1977). The present set of information represents the first clear evidence of the existence of the MRC, and represents an important contribution to our knowledge of this Current, even though the MRC deserves an investigation more detailed than what can be offered here from the data at our disposal.

The purpose of this chapter is therefore to elucidate some of the qualities of the MRC *per se* as well as to establish qualitative and quantitative relationships between it and the eddies off the Mocambique Ridge.

13.2 Historical reports on the Mozambique Ridge Current

The first, (indirect) reference to the MRC was made by HARRIS (1972) while discussing the tributaries to the Agulhas Current. He concluded

that an amount of 35 x $10^6 m^3 s^{-1}$ crossed the Madagascar Ridge westwards into the Mozambique Basin. Of this, a certain amount (22 units), joined the Agulhas Current between Durban and Maputo, but he noted that the rest ($\sim$ 13 units) was possibly diverted by the Mozambique Ridge into a southerly direction. He concluded that this flow might recirculate *anticyclonically* afterwards. Although not referred to, this flow is also suggested in the diagrams of DUNCAN (1970) and WYRTKI (1971).

HARRIS and VAN FOREEST (1977) reported further evidence of an easterly tributary to the Agulhas Current just south of Durban (30°S). Using the results of the *Agulhas Current Project* in 1969, they concluded that this inflow from the east had a different origin from the Agulhas Current itself. Whereas stations inside the Agulhas Current were related hydrographically to the water inside the Mozambique Channel, the eastern tributary contained water from an area South of the Mozambique Channel. They found additional evidence of the eastern tributary in the data of the *SAS Natal* in 1962 and 1967, and it was possible to arrive at an estaimte of the magnitude of this tributary, namely 11-29 x $10^6 m^3 s^{-1}$ (relative to 2000-4000 m). In conclusion, they applied the inertial-jet model of WARREN (1963) to the Agulhas Current at 25°S in very much the same way as DARBYSHIRE (1972) did further south. The model indicated that water flowing southwestwards into the "Agulhas Current area" at 25°S will tend to be divided into two branches: Water in shallow areas will tend to flow along the African coast, while water in deeper areas (i.e. further offshore) will diverge from the coast, flow southward along the Mozambique Ridge and rejoin the "coastal" Agulhas Current at about 30°S . The main results from this report were included in the paper by HARRIS and VAN FOREEST (1978), Here, the westward influx was given as 10 x $10^6 m^3 s^{-1}$ relative to 1100 db.

In conclusion, DUNCAN (1970) found a steady seasonal contribution from the East Madagascar Current (EMC) into the Agulhas Current, whereas LUTJEHARMS, BANG and DUNCAN (1981) found little evidence of this, and concluded that the contribution from the EMC into the Agulhas Current system is only sporadic.

We believe (and the thesis supports this view) that there is more variability in the circulation in the SW Indian Ocean than initially anticipated. The mesoscale variability of the Agulhas Current dominates

the variability in the Indian Ocean (CHENEY, MARSH and BECKLEY, 1983). Inside the Agulhas Current, the eddy energy is twice as high as the energy of the mean flow, while at 30°S, 40°E the ratio is 20 : 1 (WYRTKI, MAGAARD and HAGER, 1976). The large amount of *in situ* mesoscale data (this is the scale where variability is probably concentrated) collected as part of this thesis allows a much better insight to be obtained of the aspect of mesoscale dynamics than has been possible so far.

13.3. Present observations of the Mozambique Ridge Current

The existence of cyclonic eddies in the Mozambique Basin has by itself been considered as evidence of a "host" current in the vicinity from which the eddies were spawned. However, the assumption that the vortices are created from a current in the *vicinity of the Mocambique Ridge* (i.e. by the MRC) could not be accepted forthwith, since a very intense vortex (Ian) was observed being formed by the *Agulhas Current* northeast of Cape St. Lucia (see Chapter 10), and it is not impossible that such an eddy could have become detached and drifted eastward into the Mocambique Basin. To prove therefore that there *is* an MRC, and to illustrate the relation between the MRC and the eddies observed during this study, three cases will be presented.

Case 1 : May 1978

A simultaneous observation of the MRC in the process of forming an eddy (Echo) is presented by the data collected in May 1978. The relevant results are portrayed in Figs. 7.7 and 7.9. Especially important to note is the influx of about 21 x $10^6 m^3 s^{-1}$ (relative to 1500 m) through the zonal section at 29°30'S. According to the geopotential and ship's set (Fig. 7.8), the input direction of this flow was from the NE, while the volume transport diagram indicates a flow from N or NNW. This influx was situated on the eastern escarpment of the Mozambique Ridge, and flowed from the Ridge into the Basin at about 29°S. The geostrophic velocity profile in this flow is portrayed in Fig. 13.1 below. The maximum speed of 0.68 m/s was located at the surface of a flow that is estimated to have been about 100 km wide.

It is interesting to note that the volume transport of eddy Echo

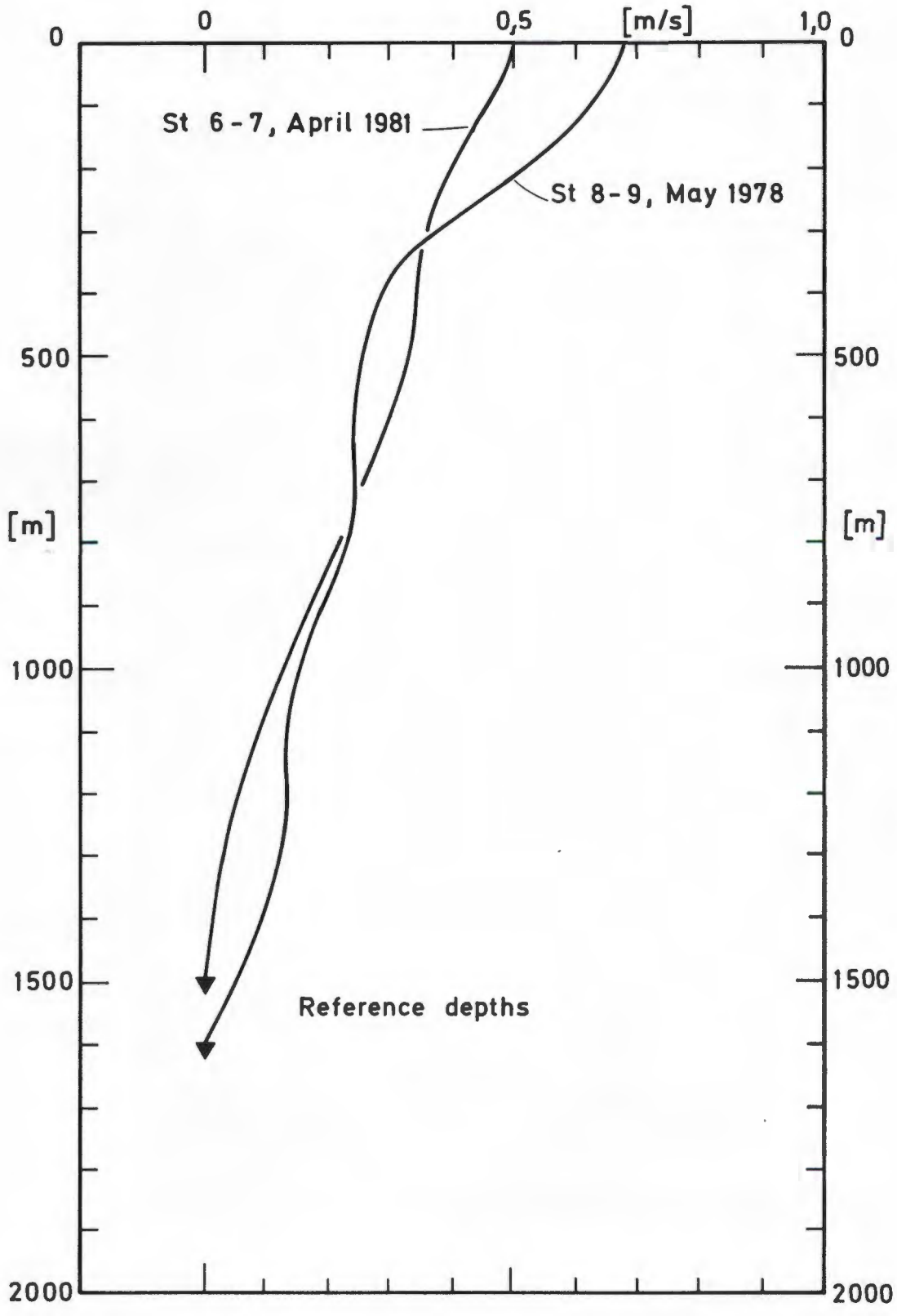

FIG. 13.1 : Geostrophic velocity profiles in the Mozambique Ridge Current

one month later (June 1978, see Chapter 7) was 32-48 x $10^6 m^3 s^{-1}$, i.e. approximately double its transport in May. Since there is every reason to believe that it was the same eddy on both occasions, it seems to indicate that Echo "absorbed" about two full turns (or about 1000 km) of the host current (before separating from it). In other words, the generating process was not a simple occlusion of a loop in the MRC as customarily occurs when a Gulf Stream ring is generated (e.g. FUGLISTER, 1972), but a "termination" of the MRC.

This is obviously a very simplistic view of what must be a complex process, but if this representation is true, it means that an eddy such as Echo containing approximately 1000 km length of the MRC at a nominal average flow speed of .25-.50 m/s requires a generating period of 3-6 weeks, which agrees with the eddy growth rate evident over the 5 weeks between the two observations. FUGLISTER (1972) used a similar argument (i.e. relating the eddy transport to the length of Gulf Stream "contained" in a ring) to estimate the generating frequency of a Gulf Stream ring. What happens to the MRC after this stage is pure conjecture, since the generating process has not been observed beyond this point. However, it will be attempted in section 13.4 to show that an MRC of given intensity will invariably form an eddy off the Mozambique Ridge escarpment. Two alternatives about the typical behaviour of the MRC therefore spring to mind: The first possibility is that the MRC flows for a very limited time of approximately the same duration as required to form an eddy (i.e. of the order of weeks). The eddy completely "absorbs" the MRC, becomes a free-drifting entity, and there is no contribution into the Agulhas Current (unless the vortex coalesces with the Agulhas Current). The second possibility is that the MRC flows for a much longer time than required to form an eddy (i.e. of the order of months). An eddy is nevertheless formed during the first weeks, and during the remaining time the MRC starts interacting with the eddy in such a way that the eddy becomes free-drifting while the MRC contributes to the Agulhas Current. We feel that the solution might be hinted at by either or both of these alternatives, but refrain from further speculation.

Case 2 : December 1979, January 1980 and March 1980

The three cruises and the satellite-buoys tracked in 1979/80 were discussed in Chapter 8. The conclusions reached in that chapter were that there were two vortices (Fred and Golf) in the area of the 4-month period between December 1979 and March 1980. There is, however, some doubt whether

the two eddies were generated at the same time, since Golf was delineated by the tracks of a buoy in October 1979 (Fig. 8.24) and the same buoy drifted freely through the area where Fred was observed two months later.

The buoy tracks (see Fig. 8.25) provided the first glimpse of how the vortices are generated: A westward flow at 27°S became deflected anti-cyclonically at 36°E as it encountered the northern Mozambique Ridge. Turning through 180°, the current flowed southeastwards off the Ridge and into the Basin at 29°S. At 31°S the flow returned cyclonically through 180° and flowed westward from the Basin onto the Ridge again. The drift velocities of the buoys can be seen in Fig. 12.2, from which the variability of the speeds is evident. It seems, however, that a surface velocity of about 0.5-0.6 m/s for the current is not inappropriate.

The S-shaped meandering of the current can be explained in terms of the conservation of potential vorticity: As the MRC flowed westward (at 27°S) from the Basin onto the Ridge, the reduction in depth decreased the vorticity (i.e. made the flow more anticyclonic) and the Current turned anticlockwise back into the Basin. The increase in depth from the Ridge to the Basin increased the vorticity and the Current turned clockwise back toward the Ridge. This behaviour of the flow is tested with a very simple model in section 13.4.

The buoy tracks are therefore considered to be a realistic representation of a current that flowed in December 1979. The tracks also agree with the hydrographic results obtained in December 1979 (see Chapter 8 and Fig. 13.2) and thus show the connection between the input current and the position of the eddy off the Mozambique Ridge. This information is regarded as the best example found so far of the existence of such a current (the MRC)' and the simultaneous existence of an intense cyclonic eddy.

Case 3 : April 1981

The cruise in April 1981 is described in Chapter 9, and the figures relevant to our present discussion are represented in Figs. 9.11 and 9.12. In Fig. 9.12, the "input" volume transport across 28°S totalled

$36 \times 10^6 m^3 s^{-1}$ (relative to 1500 m), which was larger than the input transport of the MRC obtained in Case 1. Of this amount, 21 units became deflected eastwards off the Ridge to contribute directly to the eddy (Harry). Although the survey did not extend far enough southwards, there is no indication of a westward flow at 32-33°S that was detached from the eddy. It seems therefore that an almost similar situation reigned as during May, 1978 (case 1, above) where eddy Echo "absorbed" the MRC. This is supported by the agreement between geostrophic velocity profiles inside the MRC (see Fig. 13.1). During the previous month (March, 1981), a cruise was executed across the Mocambique Basin to throw some light upon the "background" circulation in the area (see Section 3.3). The region of 29°S, 37°E was traversed on 11 March 1981, 44 days before the MRS was observed during the April 1981 cruise. Although the temperature section (Fig. A5.2) showed a weakly-defined geostrophic current in the vicinity of stations 3 and 4, the volume transport diagram (Fig. 3.5) does not contain any conspicuously-high fluxes in this area. This seems to indicate that the flow pattern observed during the April 1981 cruise did not exist 44 days before, which tends to confirm the high initiation rate of the MRC derived from the results of May 1978 (Case 1).

13.4 Generation of the eddies

Since the Gulf Stream rings represent the richest source of eddy research, it is appropriate that we turn our attention to the generating mechanism of those eddies.

After the initial observations of ISELIN (1936), and ISELIN and FUGLISTER (1948), FUGLISTER and WORTHINGTON (1951) were the first to document the creation process of Gulf Stream rings. The occlusion of a meander of the Gulf Stream has since then been observed on several occasions (see e.g. DOBLAR and CHENEY, 1977; FUGLISTER, 1972; GOTTHARDT, 1973).

Without going into details of theory that has been developed to explain the behaviour of the Gulf Stream and the gyres (cyclonic and anticyclonic) that are generated, we would like to briefly indicate the results of some of the methods.

WARREN (1963) predicted the path of the Gulf Stream on the basis of potential vorticity conservation. The model could not, however, delineate

details of the generation of eddies, although it showed the influences of the bottom topography on the path of the Current. This was also found by the refined model of NIILER and ROBINSON (1967), who concluded that steady-state, non-divergent theory cannot account for details in the path of the Gulf Stream.

During the 1970s there has been a dramatic increase in attempts to numerically simulate the oceanic circulation and to reproduce the mesoscale eddies observed in the ocean. HOLLAND and LIN (1975 a, b) showed that a wind-driven, baroclinic ocean model (of the northern hemisphere) will generate vortices spontaneously if the viscosity is small enough. The unpremeditated generation of eddies was also one of the main conclusions of SEMTNER and MINTZ (1977) and HOLLAND (1978). IKEDA and APEL (1981) admitted that the bottom topography could have an important influence on the meanders generated by the Gulf Stream. IKEDA (1981) proceeded to show that a submarine ridge, located at the point where eddies normally (i.e. in the flat-bottom model) become detached from an eastward-flowing jet, strengthens cyclonic eddies south of the jet and upstream of the ridge (and *vice versa* for anticyclonic eddies). An excellent review of many of these models is given by HOLLAND, HARRISON and SEMTNER (1983).

Mention has been made in the previous section that a form of topographical control was exhibited by the MRC under the conservation of potential vorticity. To test this hypothesis, the simple numerical model of an inertial jet proposed by WARREN (1963) was used. This model was also applied by DARBYSHIRE (1972), HARRIS and VAN FOREEST (1977) and GRüNDLINGH(1978) to explain features of the circulation pattern in the Agulhas Current System.

In this model, the change in curvature $C(x,y) - C_o(x_o,y_o)$ of a current with volume transport V, momentum transport M and volume transport T across unit depth near the bottom is approximated by

$$C(x,y) = C_o - \left|\beta V (y-y_o) + f T (D-D_o)\right| / M$$

where $\beta = \partial f / \partial y$, the meridional change of the Coriolis parameter f and $D_o = D(x_o, y_o)$, is the depth at the origin. The

Runge-Kutta method is used to estimate the curvature $C(x, y)$, which is integrated piecewise to yield the current path. As in the treatment of GRüNDLINGH (1978), the coordinate axes are rotated continuously to avoid singular points of dy/dx.

Using arbitrary values for V/M and T/M, the model was used to simulate the satellite buoy drift tracks observed in December 1979 (Fig. 8.25, Case 2 above), and in this way derive parameter values that could be compared with the observations. The computation was started at a position 27°30'S, 41°E, indicated by the buoy tracks to have represented a position of zero curvature of the MRC.

In Fig. 13.2 the model curves representing the best visual simulation are compared with the two satellite-buoy tracks and the 10°C topography of the cruise in December 1979. Two model curves were required as it was found that one set of parameters was needed for the curve north of 29°S, and another set south of 19°S. The "northerly" values for T/M and V/M were 0.55×10^{-4} $(m^2/s)^{-1}$ and 3.5 $(m/s)^{-1}$ respectively, and the corresponding "southerly" values were 1.2×10^{-4} $(m^2/s)^{-1}$ and 3.5 $(m/s)^{-1}$ respectively.

Unfortunately, these values could not be compared to the hydrographic data of Case 2, since the observations of this Case did not extend beyond the eddy perimeters into the "supply current" of the eddies. In Cases 1 and 3 hydrographic sections were executed across this current to the north of Echo and Harry, and these measurements could be used for comparison.

For eddy Echo (Case 1), the total transport V (relative to 1600 m) amounted to 26×10^6 m^3/s between stations 7 and 9, and the momentum transport M amounted to $10^7 m^4/s^2$. From these values, V/M = 2.5 $(m/s)^{-1}$. Because the observations were limited depthwise, a reliable value for T/M could not be derived. For eddy Harry (Case 3), the total transport (relative to 1500 m) between stations 4 and 7 amounted to $36 \times 10^6 m^3/s$, while the momentum transport amounted to $13.8 \times 10^6 m^4/s^2$. This too, resulted in V/M = 2.5 $(m/s)^{-1}$. Using NIILER and ROBINSON's (1967) velocity distribution, the model values predict surface velocities of 1.0-1.2 m/s, which are of the same order as the geostrophic velocities of 0.5 cm/s in Fig. 13.1.

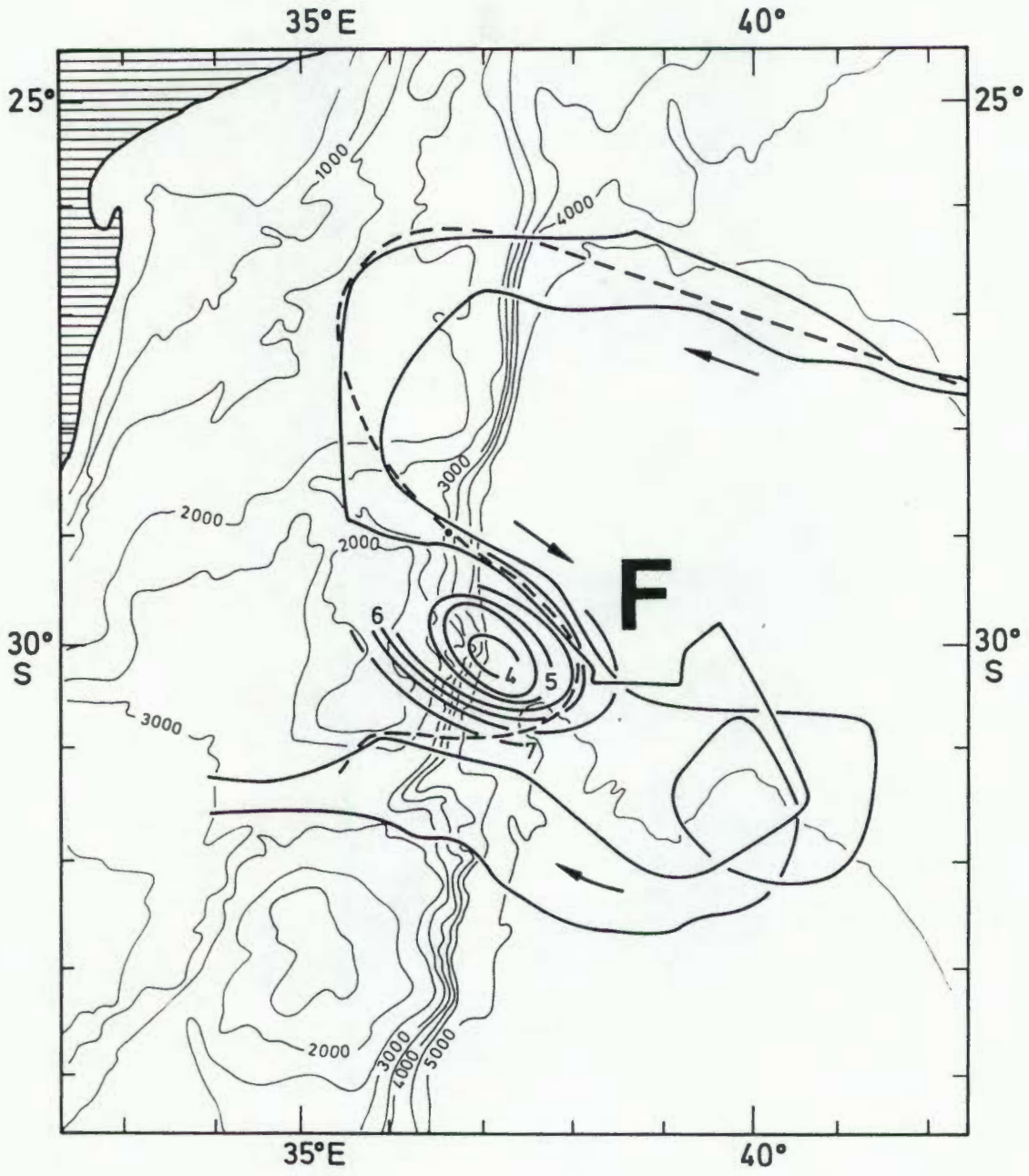

FIG. 13.2 : Tracks of two satellite-buoys in December, 1979 (see Fig. 8.25). Elliptic lines at 30°S, 37°E are contoured depths (in hectometre) of the 10°C isotherm in eddy Fred. The dashed line is the course of the inertial jet model obtained with one set of parameters north of 29°S and another south (see separating dot).

The fair agreement between the model and measured values was considered to be an indication that the flow pattern reflected by the satellite-buoy tracks was induced to a large extent by the bottom topography.

An important result following from the discussion so far is that eddies in the western Mocambique Basin at 30°S can only be generated by an MRC initially flowing *westward* at 27°S. The results of HARRIS and VAN FOREEST (1977) indicate that a current flowing more-or-less meridionally southward on the Mozambique Ridge may spawn cyclonic eddies *on* the Ridge but seemingly never to the *east* of the Ridge (where most of our eddies were observed).

It is clear that if the topographic control of an inertial jet as postulated above is accepted, the consequences for the circulation in this region are profound.

First, the phenomenon referred to in this study as the "Mozambique Ridge Current" seems to assume an ambiguous character. It has previously been tacity accepted that the MRC is that current that flows more-or-less meridionally along the Mozambique Ridge between 25° and 30°S. The model, however, suggests that eddies in the Mozambique Basin were formed by a strong current that spent very little time on the Ridge. It therefore seems that there may be a case for considering the existence of two types of MRC: One that flows along the Ridge (The MRC) and the other that briefly resides on the Ridge because of the deflecting nature of the topography. For the latter case, "MRC" may be a misnomer, but the nomenclature will be retained.

We believe that there is evidence of the existence of both these currents, but suggest that they are possibly different manifestations of the same phenomenon. On the one hand, an intense westward zonal flow at 27-28°S will invariably be deflected by the Ridge to form vortices of the type observed in the Mozambique Basin at 30°S. On the other hand, a weaker zonal flow will probably be unable to exist in the same shape as e.g. reflected by the satellite-buoy tracks, but will tend to flow along the northern perimeter of the Mozambique Basin and then curve anticyclonically to merge with the Mozambique Current. This weaker current will also undergo topographic induction, but will form eddies in the region suggested by HARRIS and VAN FOREEST (1977, Fig. 8.2(c)) which coincides with the area of eddy Delta observed in June 1977 (see Chapter 6 and Fig. 11.1).

These two possible alternatives for the flow of the MRC are represented in Fig. 13.3. If this assumption holds, it implies that eddies on the Ridge will be relatively weak, while eddies in the Basin will be relatively intense. In addition, this implies that the eddies observed at about 30°S on the western side of the Mozambique Basin were all basically of the same intensity. Eddies that were significantly weaker than the others (e.g. the weaker eddies of August, 1975, June 1976) were either older and have dissipated some of their energy, or advected from the Ridge into the Basin.

Second, the model suggests that vortices will always be found within 200 km or so from the eastern escarpment of the Ridge. Eddies observed further eastward (e.g. Charlie, June 1976; John, June 1983 see Fig. 11.1)as well as the eddy Golf, observed in January and March 1980 must have been "older" eddies, i.e. their existence and geographic position are not directly associated with the Mozambique Ridge any more.

In the light of this discussion it is important to deviate slightly from the present line of thought and focus our attention once more on the satellite-buoy tracks in Figs. 8.24, 8.25 and 12.2. Eddy Golf was delineated by the track of buoy 14627 in October 1979. Hydrographic measurements in January and March 1980 showed that the Golf was much weaker than eddy Fred, located in December 1979. It is interesting to note that buoy 14622 drifted in an almost similar position as 14621 and 14627 (Fig. 12.2) but whereas 14621 and 14627 drifted in an anticlockwise curve at 28°S and subsequently moved southeastward off the Ridge at 30°S, 38°E, buoy 14622 continued southwards between 29°S and 31°S. This drift pattern (May 1979) was similar to the behaviour of buoy 1116 in November 1975. Recalling from Fig. 4.1 that eddy Bravo was located in the Mozambique Basin just east of this southward drift of buoy 1116, it is suggested that there must have been an eddy in a similar position east of the southward drift of buoy 14622. The only eddy that could fill this role was Golf. It is therefore suggested that Golf was generated in the first half of 1979, and later interacted with the Current that spawned Fred. Why Golf had not advected from this area during this period of about 10 months is not clear.

If the ideas suggested above seem realistic the classic concept of the East Madagascar Current (EMC) contributing to the Agulhas Current should be reconsidered. The question is namely raised: If the MRC always forms an

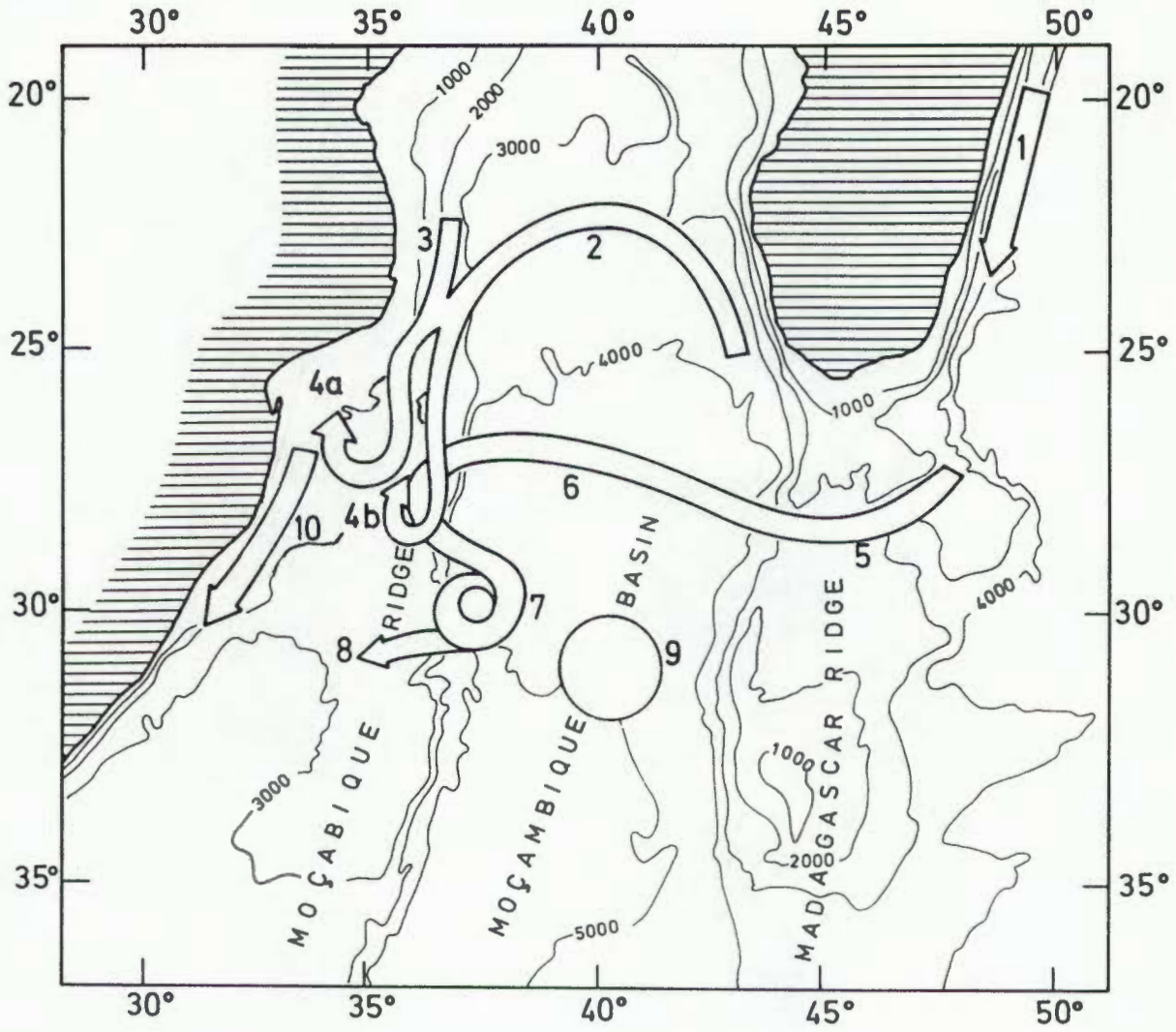

FIG. 13.3 : Conceptual representation of the circulation in the Mozambique Basin and vicinity. 1 = East Madagascar Current; 2 = path of weak quasi-zonal flow; 3 = Mozambique Current; 4a and 4b = vortices formed by Mozambique/Agulhas Currents; 5 = path of stronger EMC across Madagascar Ridge; 6 = quasi-zonal flow across Mozambique Basin; 7 = vortex of the Mozambique Ridge Current; 8 = contribution of MRC to the Agulhas Current; 9 = free-drifting cyclonic vortex; 10 = Agulhas Current.

an eddy of some kind, either a weak eddy on the Ridge at 28°S, or more intense ones in the Mozambique Basin at 30°S, how does the contribution of the EMC reach the Agulhas Current? We suggest that either of the following possibilities exist (we will only consider the case of an intense MRC creating an eddy in the vicinity of 30°S, 38°E) :

On the one hand, the data collected on this study suggest that the MRC can spiral by completing two revolutions and thereby doubling the volume transport of the eddy. This seems to be an important difference between the way the MRC can create an eddy and the way the Gulf Stream creates a ring. If the MRC flows only for about the same time as it takes to generate the eddy (i.e. about 4-6 weeks), the whole of the MRC can become "absorbed" by the eddy. The latter, after becoming deprived of its host current, becomes free-drifting inside the Mozambique Basin. On the other hand, if the MRC flows for any longer period, or if it does not spiral, a certain portion of the MRC possibly continues toward the African coast, after forming an eddy. One way or the other, the cyclonic vortices in the Mozambique Basin represent a separation point of possible recirculatory flow(in the shape of eddies containing quanta of water) and the contribution to the Agulhas Current further west.

It seems logic to conclude that the energetic flow such as exhibited by the MRC on its passage across the Mozambique Basin and by its subsequent cyclogenesis can only originate from the East Madagascar Current (EMC). LUTJEHARMS, BANG and DUNCAN (1981) considered that (in 1975) there was no direct link between the EMC and the Agulhas Current System, and concluded that the EMC probably contributes to the Agulhas Current only sporadically. Our present results are in full agreement with this. We are of the opinion that, at times, an energetic filament of the EMC penetrates the Madagascar Ridge (possibly at 28°S) and proceeds westwards to form the MRC.

13.5 Summary of the characteristics

The following should be considered as *indications* of the characteristics of the MRC rather than hard-and-fast qualities:

(a) Volume transport : It is considered that the typical transport is about 20 x $10^6 m^3/s$ relative to 1500 m.

(b) Current velocity : The maximum surface geostrophic current velocity (relative to 1500 m) is approximately 0.5-0.6 m/s. Since this value is confirmed by observations using other methods, it could be an indication that the "depth" of the MRC does not extend much deeper than about 1500-1800 m.

(c) Width : A typical width would be about 100 km.

(d) Origin : The MRC seems to originate from the area of the Madagascar Ridge at about 27-28°S. In the intense case (i.e. when the MRC transports about 20 x $10^6 m^3/s$), the MRC flows more-or-less zonally across the Mocambique Basin to the Mozambique Ridge at 26-28°S. In the weaker case, the MRC probably follows the northern edge of the Mozambique Basin and then flows down the Mocambique Ridge. There is a strong possibility that, in the intense case, the MRC is a direct extension of the East Madagascar Current.

CHAPTER 14

DISCUSSION AND SUMMARY

14.1. Introduction

The purpose of this chapter is primarily to review the results of the thesis in terms of its aims as set out in section 1.3. It is also appropriate at this point to reflect on the existing (or new) deficiencies in our information and to suggest possible avenues and methods for future investigations into this field.

14.2 Origin of the eddies

It has been established that the source of the eddies located in this study was the Mozambique Ridge Current. Although the variability of the Current itself falls outside the scope of this investigation, it is believed that the fluctuations of the Current could play an important role in the dynamics and generating frequency of the eddies. Evidence was found that, at times, the MRC flowed more-or-less zonally along 27-28°S between the Madagascar (45°E) and Mozambique Ridges (36°E). This location presupposed that the MRC had a certain intensity (volume transport and flow speed) without which it would probably have looped northwards into the Mozambique Channel. Upon arriving at the Mozambique Ridge (36°E), the MRC acquired anticyclonic vorticity and retroflected from the Ridge into the Basin and back onto the Ridge at 30°S. This second, cyclonic loop spawned the eddies studied during this investigation. There seems to be evidence that the cyclonic vorticity acquired by the MRC at 30°S was sometimes sufficient to cause instability of such a nature that the Current spiralled into itself. The latter process enhanced the volume transport of the eddies beyond the transport of the MRC itself.

Apart from the spiralling phenomenon there also seems to have been a certain amount of water exchange between the vortices and their environment. This interchange could have been imaginary because the flow in some parts of a particular eddy could have been deeper than in other parts, an aspect that the geostrophic calculation, through its choice of reference level, would not have been able to recognise. Evidence was found of a convergence in the upper layers of the vortices, giving rise to a bowl of warm water at the eddy centres.

Satellite buoy tracks suggested that the MRC occasionally extended beyond the cyclonic loop, i.e. the MRC did not terminate at the eddy but continued across the Mozambique Ridge and westward possibly to the Agulhas Current.

The generating frequency of the eddies would be difficult to assess from the rather sparse coverage achieved by the ship surveys. The discussion of section 13.6 suggested that an eddy could be formed within 4-6 weeks but it is not known how often this process would repeat itself. There was evidence of a particular eddy (Golf) remaining in more-or-less the same position for at least 6 months (and possibly 11), while another (Fred) was created (and disappeared) in this period. It would therefore seem that a generating frequency of one or two eddies per year would probably be appropriate.

It has been tacity assumed that the cruises of each year were not studying the same eddy every time, but the variability that has been observed (even over periods of a few months) seems to exclude this possibility altogether.

14.3 Physical and dynamic characteristics

The eddies were cyclonic and characterised by a cold, low-salinity, core situated at depths greater than about 100-200 m. This core manifested itself as a three-dimensional peak in the isotherms and isohalines. Typically, the 5°-10°C isotherms were raised about 250-300 m above the "background" or ambient level of these isotherms.

The intersection of the 10°C surface with the 650 m level was used to define the shape and size of the eddies. According to this definition, the eddies varied considerably in shape and size, and a circular eddy was the exception rather than the rule. This may be ascribed to the fact that vortices were mostly searched for (and therefore located) in the vicinity of the Mocambique Ridge, and these eddies (it was concluded later) were mostly in the process of being created. A typical eddy "radius" would be about 75 km.

The available information on the dynamics of the vortices is, of course, closely associated to the thermohaline structure through the geostrophic relation. It was for this reason that the temperature data was used as primary indicator of the shape and size of the eddies, and not the velocity field or volume transport. A typical geostrophic velocity maximum was about 40 cm/s relative to 1000 m and 60 cm/s relative to 1500-1800 m. Indications were found that the eddies do not display significant velocities below 1800 m, although some motion probably exists below this level.

The highest volume transport recorded was 71 x $10^6 m^3 s^{-1}$ which was calculated relative to 2000 m. Relative to 1000 m, volume transports varied considerably within an eddy and from one eddy to the next, and a typical volume transport would be in the region of 30 x $10^6 m^3 s^{-1}$. A maximum volume transport (relative to the deepest possible level) is estimated at 60 x $10^6 m^3 s^{-1}$, based on the relationship that was found between transports relative to 1000 m and deeper. The maximum total kinetic energy in an eddy was approximately 20 x 10^{14}J (relative to 1000 m).

14.4 Eddy movement

No consistent movement of the eddies over large distances, compatible to that observed in the Gulf Stream rings, was observed. Many of the Gulf Stream cyclonic eddies form part of the recirculation system whereby water is transported in a southwesterly fashion to the area where the Stream still adheres to the American coast. Like Rossby waves, eddies should also have a significant westward translation, and one would expect the eddies of the MRC to move northwest in the Mocambique Basin.

There is, however, still some doubt about the "background" circulation in the Mozambique Basin. The measurements of this study failed to confirm the anticyclonic flow found during the IIOE (DUNCAN, 1970), and it is therefore uncertain where the eddies will drift to.

On a few occasions it was possible to derive some advection rate of a vortex, but in almost all the cases these vortices were not free-drifting yet and the observed advection could be ascribed to the meandering or instability of the host current. The aspect of advection and eventual fate of the eddies remains one of the unfulfilled aims of this study, and the one which will require particular attention during future projects of this nature.

14.5 Lifetime and decay

The eddy observed for the longest time was eddy Golf located at approximately 38°20'S, 38°E and was observed during 1979 and the first quarter of 1980. It was concluded that it had been in existence for at least 6 months. Unfortunately, hydrographic coverage was incomplete during January and March 1980 and although volume transports of the eddy were more-or-less the same during these surveys, the evidence is too scant to be able to conclude that the eddy had remained unchanged. Using the decay rate determined from Gulf Stream rings, most of the vortices located in this study had lifetimes of more than one year.

If eddies are generated at the rate of one or two per year and each eddy potentially lasts for a year or more, there must obviously be a sink where eddies are removed from the Mocambique Basin. In conjunction with the advection of the eddies (section 14.4), this sink (as the termination stage for the "life" of the eddies) remains one of the aims of the study about which nothing is known. For Gulf Stream rings it is uncommon to dissipate in the open ocean as they typically coalesce with the Gulf Stream after about one year. On this basis it seems likely the MRC eddies also become absorbed into the currents of this region.

14.6 Future research

Within the terms of reference of this study, a certain amount of information has been collected about the physical and dynamic characteristics of the eddies. In addition, their origin and generating mechanism have been established. On the other hand, comparatively little or nothing is known about the eddies after they are spawned, i.e. their lifetime, advection, decay and eventual fate. It is firstly in this field that a future project can make a significant contribution.

It is felt that a major contribution of this thesis lies in the documentation of some of the characteristics of the MRC. Comparatively little was known about the existence of this Current,(let alone its characteristics) before the present study, even though only the surface has been skimmed. The evidence that has been uncovered about the MRC throws a completely new light on the eastern contribution into the Agulhas Current

and therefore on the circulation in the whole southwestern Indian Ocean. It is therefore secondly considered important to follow up this initial survey by one that is dedicated to study this Current and its variability.

The two studies proposed above are not completely separate, since they deal with more-or-less the same phenomenon but only at different stages. Well-founded knowledge of the MRC can, e.g., aid in the location and tracking of the vortices that are shed by the MRC at the Mozambique Ridge.

As a side issue, consideration should be given to the survey method that should be employed. At present, it falls beyond the scope and means of the National Research Institute for Oceanology to conduct an experiment where regular (one every two months or so) deep-sea surveys of this kind are required. Rather should methods of remote sensing of the sea be investigated, such as colour imagery, infrared imagery (although the latter has not proved of very great use) and free-drifting, satellite-tracked buoys. The advantage of buoys and the valuable information that can be obtained from them has already been evidenced by the results of this thesis.

14.7 Conclusion

In retrospect it is considered that most of the objectives of the study were met. Although the more ambitious aims (e.g. decay and fate of the eddies) could not be reached, some aspects (e.g. the generation of the eddies) provided a far greater amount of information than had been anticipated (e.g. the "discovery" of the MRC). In addition it is felt that a worthwhile foundation has been created on which to base future projects in this field.

Since the study of Gulf Stream rings has been considered an appropriate norm against which to measure our research results, it is also interesting to estimate where achievements of the present study fit in on the chronological ladder of Gulf Stream ring investigation. It is crudely estimated that in many respects, present knowledge on MRC eddies could slot in quite comfortably in that stage reached by Gulf Stream ring research in the

middle 1960s. On the one hand, the lag of about 20 years should correct any gradiloquence about the results of this study. On the other hand, the decade following 1965 proved to be the most rewarding as far as insight into Gulf Stream rings is concerned. Maybe we can achieve the same during the next ten years for the vortices of the Mozambique Ridge Current.

*** SOLI DEO GLORIA ***

APPENDIX 1

HYDROGRAPHIC EQUIPMENT

A1.1 Introduction

As stated in the preface, hydrographic equipment really forms the backbone of oceanographic research at sea. No matter how important the oceanographic feature awaiting discovery is, badly calibrated or failing equipment can have a disastrous influence on the data collection. It is therefore important that we review the performance of the equipment, also because the challenge of deep-sea cruises necessitated some changes in the oceanographic hardware of the *Meiring Naudé*.

The following is a brief, non-technical description of this system with emphasis on some of the physical aspects relevant to and changes required by the present study. A more detailed description of the data acquisition system on board the *Meiring Naudé* has been given by STAVROPOULOS (1971), and an excellent treatise was done by SNYMAN (1980) who has been deeply involved with the software and some hardware on board the vessel.

A1.2 The research vessel *Meiring Naudé*.

The hydrographic data used in this thesis (except those of the *Commandant Robert Giraud*, section 3.2) were collected by the R.V. *Meiring Naudé*. She is a 360-ton, 32 m vessel owned and operated by the National Research Institute for Oceanology (NRIO) of the Council for Scientific and Industrial Research (CSIR). The *Meiring Naudé* was built by the Barens Shipbuilding Company, Durban, and was commissioned in April 1968. Some of her features are a 430 kW engine providing a maximum speed of about 10.5 knots, a variable-pitch propellor, slave-flap rudder, bow-thruster, and anti-roll tank. Details about the navigational facilities are provided in Appendix 2.

Apart from the captain, two officers and two engineers there is a crew of 8 and provision for 8 scientists. The vessel is airconditioned throughout and the laboratories are relatively spacious. Having been designed mainly as a coastal vessel, the *Meiring Naudé* has an endurance of 10-14 days (dictated to a large extent by the freshwater capacity).

A1.3 The NRIO hydrosonde

The first NRIO hydrosonde was constructed in Durban about 15 or more years ago by the electronic personnel of the National Physical Research Laboratory (Oceanography Division) and the instrument-makers of the Technical Services Department. The instrument was based on components that could be obtained commercially, coupled with the innovative designing and improvising that has characterised this group of people to the present. The hydrosonde is continuously undergoing modifications to improve its accuracy and reliability. In 1982/83 (i.e. after the present study), the hydrosonde was redesigned completely and the instrument type described below became redundant. On most (but not all) cruises, a standby hydrosonde and sampler were taken along. The hydrosonde measured temperature, pressure and current velocity, and could take 12 1000 cc samples of seawater in any one cast. These samples could be analysed in the laboratory for salinity and nutrients.

The hydrosonde's internal batteries required about 1½ hours' recharging after every deep station, and this necessitated a station spacing of about 20 nautical miles.

a) Temperature

Temperature was measured through a platinum resistance element removed from the electronic housing (or "body") of the hydrosonde by a rubber hose of approximately 20 cm length, ensuring that any heat contained by the body of the hydrosonde did not influence the recording. To explain the operational procedure of the hydrosonde, consider the following:

The Newtonian law of cooling states that the time rate of change of a body with Temperature T, exposed to an ambient temperature T_A, is proportional to the temperature difference $T-T_A$, i.e.

$$\frac{dT}{dt} = -\frac{1}{k}(T - T_A)$$

Integrations to an initial temperature T_o and solving for k gives

$$k = \frac{t}{\ln\left[\frac{T_0 - T_A}{T - T_0}\right]}$$

Here, k is the time constant of the temperature sensor. If the expression has to be transformed for the case that the "time constant" is expressed as the time t_{90} required to attain, say 90% of the temperature difference,

$$t_{90} = k \ln\left[100/90\right]$$

If the constant temperature T_A changes linearly with time, i.e.

$$dT_A/dt = \lambda$$

the indicated temperature on the sensor will lag with ambient temperature by

$$\delta t = k\lambda = 9.49\, t_{90}\, \lambda$$

The platinum resistor of the hydrosonde had a t_{90} of 1.8 seconds. If the recorded temperature was to be within 0.1°C of the true temperature when the hydrosonde was raised/lowered through a given temperature profile, the raising/lowering speed had to be varied according to the steepness of the temperature profile. In Fig. A1.1 this speed has been calculated using an already recorded profile as an example. The slow speeds (~ 0.1 m/s) required to accurately record the main thermocline would have made the profiling unfeasible, and the profiles were therefore obtained at 1 m/s and used only as indicators of temperature/depth *trends*.

Because these measurements would be much too inaccurate for geostrophic calculations, temperature was also recorded when the hydrosonde was stationary, i.e. lowered to a required depth and the measurements taken by the computer-controlled automatic sampling sequence (see below).

The temperature channel of the hydrosonde was calibrated regularly (at least before every cruise) using a temperature-controlled bath and a Hewlett-Packard quartz thermometer (which was checked against the national standard). The resolution of the quartz thermometer is 0.001°C,

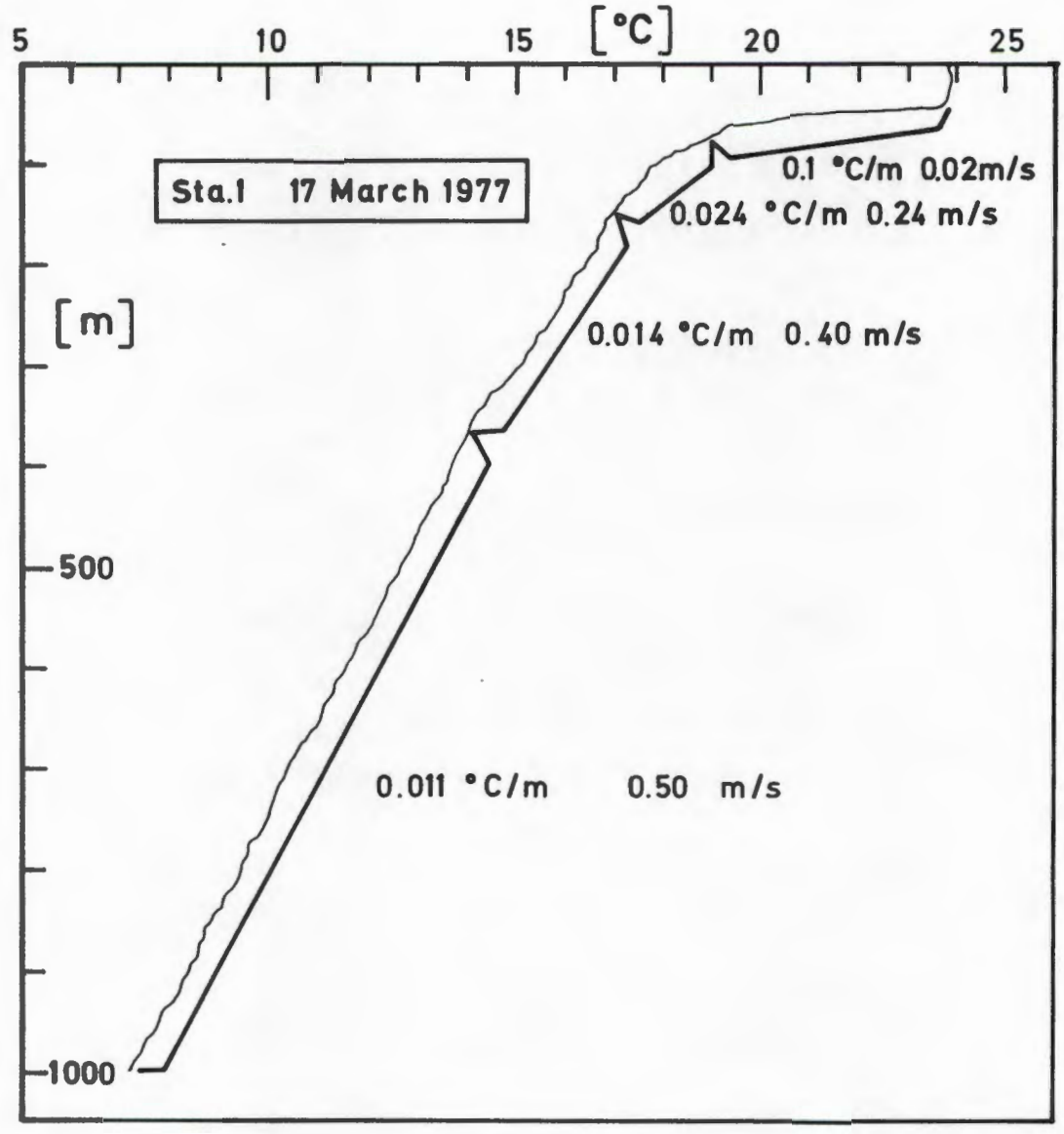

FIG. A1.1 : Vertical profile of temperature of station 1 on 17 March, 1977. The temperature gradients are indicated, as well as the profiling speed of the NRIO hydrosonde to achieve an accuracy of better than 0.1°C.

but that of the hydrosonde thermometer was only 0.03°C, giving it a calibrated accuracy of better than 0.1°C.

b) Pressure

Pressure was measured with a strain-gauge with a range up to 3400 db. The calibration in the laboratory (on a Budenberg pressure balance) provided it with an accuracy of about 5 m. Before March 1977 the hydrosondes were equipped with vibratons, but this system was phased out due to the difficulty in obtaining spares and the improved performance of the strain gauges.

c) Current velocity

In some cases during this thesis, "directly-measured current velocities" are reported. These were derived from the rotating rate of a Savonius rotor as water flowed past the hydrosonde.

There are many factors influencing the response of a rotor of this kind, e.g. the inclination of the rotor axis to the flow direction, the vertical "pumping" of the instrument, higher frequency fluctuations in the flow velocity, etc. These were compensated for by cradling the hydrosonde in a frame which allowed it to hang vertically in the water (irrespective of the cable angle), by having an accumulator on the winch with a take-up capacity of about 4 m, and by sampling the velocity over longer periods (three periods of 10 seconds each).

One of the main problems in the measurement of current velocity is the fact that only the flow rate of water past the hydrosonde is recorded, and this did not necessarily equal the absolute flow speed (i.e. relative to the sea bottom). To determine the absolute velocity, the drift rate of the ship was continuously monitored where sufficient navigational accuracy was available (see Appendix 2). A representative value of this drift (normally derived from a straight line fitted to the position fixes) was then added to the relative speed recorded by the hydrosonde to obtain an absolute velocity. The process assumed that the ship and hydrosonde are drifting at the same rate, which was only true over periods of the order of several minutes. The deeper the hydrosonde and the larger the current shear, the more unreliable this assumption becomes. Current measurements were therefore limited to about 300 m, and the estimated tolerance was 10-20 cm/s.

d) Current direction

The direction of the current was indicated by a vane which had a magnetic coupling into the electronic housing of the hydrosonde. Here it moved the wiper of a potentiometer, the base of which was attached to a magnetic compass. The resolution of the current direction was approximately 6°.

e) Water samples

The detachable rosette sampler had 12 individually-released sampling tubes of 1000 cc capacity each. This sampler was one of many designed and constructed by the Durban branch of the CSIR's Technical Services Department.

After a cast, the samples were tapped to be analysed ashore for salinity and sometimes also for phosphates, nitrates and ammonia. Salinity was measured by a Plessey model 6230N salinometer, calibration of which was done with every batch of samples by using IOS Standard Seawater providing the reported salinities with a tolerance of 0.003 $^{o}/_{oo}$.

Nutrients were measured on a UNICAM auto analyser.

f) Automatic sampling sequence (ASS)

The hydrosonde was powered by internal batteries and parameter signals transmitted through the sea cable were identified by frequency. To enable accurate evaluation and recording of the underwater data, and to monitor the drift of the ship, as well as other relevant information, a Hewlett-Packard 2100A mini-computer was used.

Whenever detailed measurements of the underwater parameters were needed, the hydrosonde was kept at the required depth and the ASS was activated through the control panel scanned by the HP 2100A. After the sampler had been triggered the frequencies transmitted up the hydrographic cable from the hydrosonde were then monitored in the following order: pressure (3 seconds), temperature (3 seconds), current velocity and direction (3 x 10 seconds), pressure (spot check). The first pressure reading, the average temperature, velocity and direction, along with other information were recorded onto paper tape and various analogue displays.

A1.4 Conductivity-temperature-depth (CTD) instrument

The CTD was bought from Neil Brown Instrument Systems Inc., and has been the major data capturing device on this project since December 1979. This system is commercially available and is being used by several oceanographic institutes across the world. The main difference between the CTD and the hydrosonde lay in the CTD's greater accuracy, its capability of providing a continuous salinity profile and its digital mode of operation (compared to the analogue mode of the hydrosonde).

Temperature is recorded by a dual system consisting of a thermistor probe for fast response (time constant = 30 ms), and a precision platinum resistance thermometer for slower response (250 ms) and increased linearity. It has a rated accuracy of 0.003°C. Conductivity of the seawater is measured by a platinum conductivity cell situated close to the temperature sensors and has an accuracy of 0.003 mmho. Pressure is recorded by a strain gauge transducer with an accuracy of 0.1% of full scale, i.e. 3 m.

The NBIS CTD was more than an order of magnitude more accurate than the NRIO hydrosonde as far as temperature was concerned. The CTD also provided a continuous profile of conductivity (from which salinity could be calculated), compared to the limited number of samples taken by the hydrosonde. Appendix 3 discusses the calibration and handling of the CTD, while data processing is dealt with in Appendix 4.

A1.5 Echosounding

A SIMRAD echosounder (model EH 4 R) was used to determine the water depth at or between stations. It operates an 11 kHz signal, has an accuracy of 3% of the recorded depth and has a maximum range of 5200 m. The bottom depths reported in this thesis have not been corrected for the change of sound velocity in water.

Profiles of the sea bed could also be obtained on an EPC graphic recorder, whereby the scale could be expanded significantly and the range increased to 7000 m with an accuracy of 0.01% of reading.

A SIMRAD Sonar (model SK 3) operating on 29 kHz with a range of 1500 m in all directions was used to track a free-drifting array of current meters to which a transponder had been attached (see Chapter 8).

A1.6 Satellite-tracked buoys

The satellite-tracked buoys described in the present study were followed by the NIMBUS VI and NOAA satellites, respectively. A description of the NIMBUS VI buoy configuration is given by GRüNDLINGH (1977a). To illustrate the position-fixing capability of the system, positions reported by the satellite of a buoy moored on the Mocambique Ridge in 1500 m of water(see GRüNDLINGH, 1977b) were inspected. It was considered that the scatter in the calculated position did not arise from a possible swaying movement of the buoy at anchor, but was solely due to the tolerance in the satellite system's ability to pinpoint the buoy's location. The standard deviation of the buoy's positions was of the same order as the resolution of the reported locations, namely 1 km x 1 km. Due to the influence on the calculated drift, all buoy velocities reported in this study have been calculated over approximately 24 hours.

The buoys were all fitted with a "window shade" drogue of plasticised nylon. Without any strain gauge sensors attached to drogues, there was no way of telling directly whether the drogue was still attached to a buoy. The response of the buoy to wind was therefore used as an indicator: If the buoy started to react in a different way to the wind, e.g. if its drift velocity component in the wind direction suddenly increased to, say 3-5% of the wind speed, where it normally should be less than 1½%, it was assumed that the drogue had probably been damaged or disconnected (see e.g. GRüNDLINGH, 1978).

A1.7 Winch and cable

a) Old system : The hydrographic winch (installed when the *Meiring Naudé* was built) had a drum diameter of 25 cm and the pulleys had diameters of 30 cm. The winch was capstan-driven (as opposed to drum-driven) to ensure that the cable was not laid under tension and thus reduce corrosion. The cable on this winch was a single conductor, steel cable with a thickness of 4.6 mm and a breaking strain of 1230 kg. The safety factor (nominally set at 50% of the breaking strain) with the hydrosonde and 1000 m cable was 3.7, and with 2000 m it was 2.2.

b) New system (from January 1980 onwards) : To enable deeper penetration, a thicker cable was required and the one chosen was a 5.72 mm stainless steel, single conductor cable. It has a breaking strain of 2170 kg. The winch is electrical and drum-operated with a drum diameter of 36 cm.

c) Cable maintenance

The relatively thin hydrographic cable forms an irreplaceable link between the researcher and his data, but this wire is very seldom awarded the attention it deserves. Whereas the hydrosondes are regularly checked and calibrated before each cruise, the cable is only inspected when it starts malfunctioning, and then it is usually too late.

To increase the reliability of the system through proper and detailed maintenance, the recommendations of Woods Hole Oceanographic Institution (see BERTEAUX et al, 1979) are followed as closely as possible.

APPENDIX 2

NAVIGATION ON THE R.V. *MEIRING NAUDé*

A2.1 Introduction

As stated in section A1.2, the *Meiring Naudé* was designed as a coastal vessel, and as such lacked the navigational aids common to large, ocean-going vessels. However, most of the work described in this thesis was executed beyond the reach of the more common navigational aids available closer to the coast (e.g. radar, radio direction finding, etc). In this respect, satellite navigation proved the most reliable and was eventually the only system used, but, depending on the circumstances, two other methods were initially used as well.

A.2.2 DECCA Navigator

This is a well-known system used internationally. The east coast of South Africa is served by different DECCA chains, each consisting of three 100 kHz transmitters (one master and two slaves). The hyperbolic lines of constant phase difference between master and each slave intersect each other over the coverage area, and the position of the ship can be derived from this intersection, using charts with DECCA lattices. DECCA can be used to about 250 nautical miles (~ 460 km) from the coast and has a typical accuracy of ½-4 km. It was employed on those cruises that involved stations closer inshore. Because of the effect of the ionosphere, DECCA reception is normally good during daylight but virtually useless during dusk/dawn and at night. Direct current measurements could therefore only be made during daytime.

A.2.3 Astral Navigation

Some of the first cruises outside DECCA range on this project were forced by circumstances to make use of an ordinary sextant for navigation. This caused some inaccuracy in the station positions, since reasonably reliable fixes could only be obtained during sunrise and sunset, and the amount of cloud-cover at that time played a decisive role. Loss of an accurate position fix would cause the "dead reckoning" to extend over

24 instead of 12 hours. Station positions were interpolated and extrapolated between fixes with the aid of the ship's heading and speed, the reigning weather and estimated currents as best as was possible, but the tolerance probably remained at about 5 km in some cases.

A2.4 Satellite Navigation

During the early 1970s, satellite navigation was still a novelty and very much a luxury item for small coastal vessels. The *Meiring Naudé* acquired her own satellite navigator (SATNAV) only after 1976.

The SATNAV system used during this study was a Redifon single channel SATNAV, although this has lately been replaced by a Navidyne. In satellite navigation, the doppler shift of a signal emitted by a satellite passing overhead is used to derive the position of the ship.

To illustrate the accuracy and frequency of the fixes, the SATNAV was run in harbour for a few days and the computed positions compared with the true position of the ship (see Fig. A2.1). The following features are noteworthy:

a) Within a period of 3½ days from 26 February to 2 March 1981, 51 good position fixes were obtained at an average of a position fix every 1 hour 40 minutes.

b) The latitudes of all the fixes combined had a standard deviation of 170 m, while the standard deviation of the longitude was 480 m. A rectangle of 340 m x 960 m centred around the average latitude and longitude enclosed 66% of all the fixes as well as the actual position of the vessel (as derived from a trigonometric chart).

c) From this positional variance the tolerance on the drift velocity of the vessel, (derived from two satellite fixes an hour apart) can be estimated. For zonal drift, the inaccuracy of the velocity is about 0.25 m s^{-1} and of direction it is less than 9°. For meridional drift, the velocity tolerance is 0.10 m s^{-1} and the directional tolerance is less than 17°. This directional tolerance seems to vary inversely with velocity, increasing from the values given above at a drift of 1 m s^{-1} to 23° and 34° (for zonal and meridional drifts respectively) at 0.5 m s^{-1}.

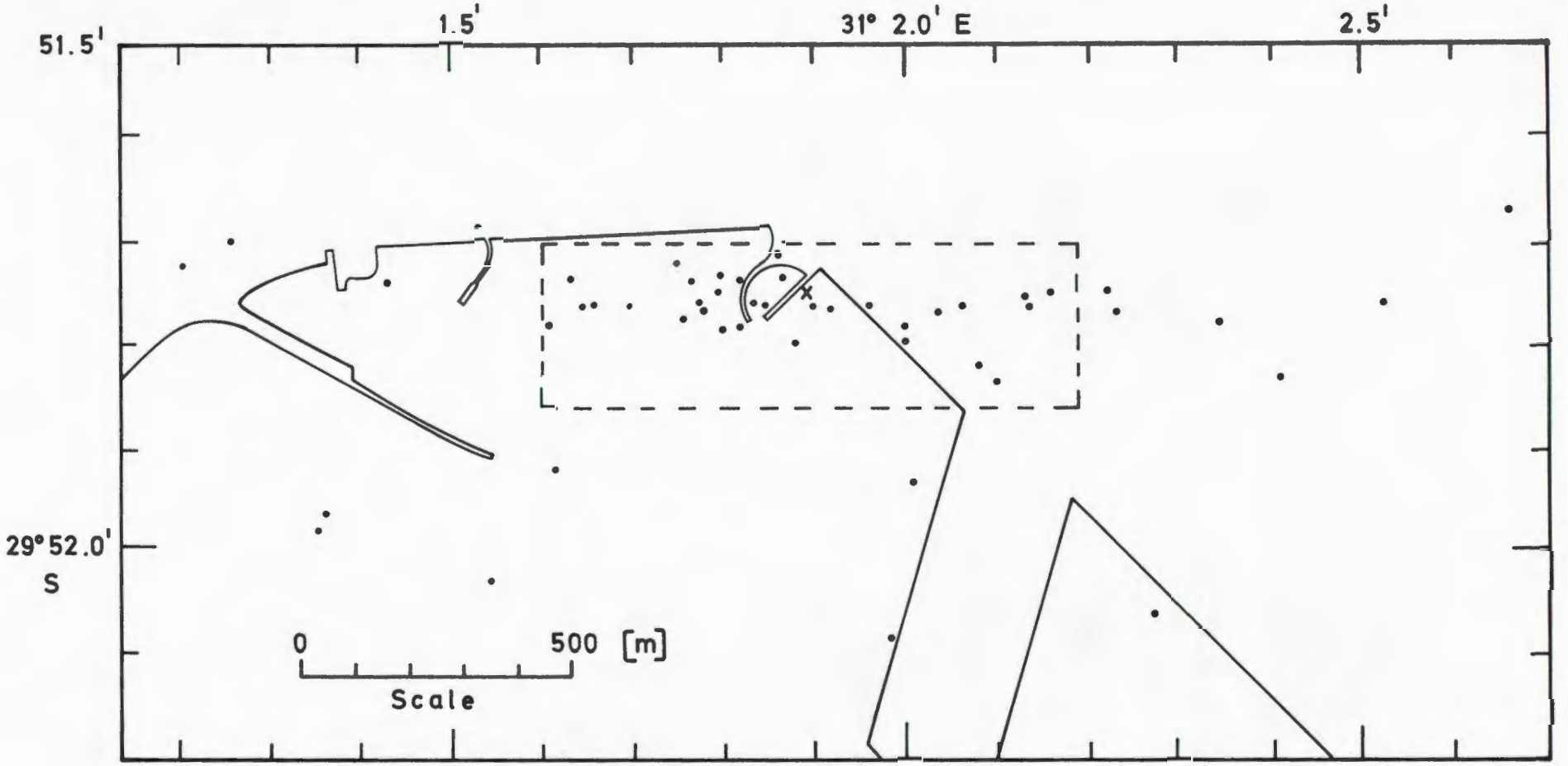

FIG. A2.1 : Series of position fixes (indicated by dots) obtained by the satellite navigator while the *Meiring Naudé* was moored (position indicated by cross as derived from navigational charts) in Durban Harbour, February - March, 1981.

APPENDIX 3

CALIBRATION OF THE NBIS CTD

A.3.1 Introduction

A conductivity-temperature-depth probe (hereafter referred to as a CTD), manufactured by Neil Brown Instrument Systems, was acquired by the National Research Institute for Oceanology in 1979 and has been in use since December, 1979. Since the CTD was acquired specifically to serve the needs of the present investigation, it is appropriate that we briefly present the results obtained in calibrating the CTD. A detailed description of the attempts at calibration (and all the problems that were encountered in the process), and the formulæ to convert readings of pressure, temperature and conductivity into salinity, are given by GRüNDLINGH, BROWN and SMITH (1981).

A.3.2 Standards

The following standards were used to check and eventually calibrate the CTD.

a) Temperature

(i) Kurt Gohla Reversing Thermometers: These are highly accurate (to within 0,01°C) thermometers that were calibrated in Germany before their delivery. They were new and unused at the time of their employment, and it was accepted that their calibration still held.

(ii) Hewlett-Packard Quartz Thermometer Model 2801A: During the calibration of the quartz thermometer against the national standard in Pretoria in 1980, the probe started to malfunction and a new probe ordered. When it was delivered, the thermometer and its new probe was calibrated on 21 April 1982 by the CSIR in Pretoria to within 0,001°C of the national standard.

(iii) Hewlett-Packard Quartz Thermometer, Model 2804A: This instrument was bought in 1981 and is stationed at the CSIR in

Stellenbosch. It was the acquisition of this instrument that eventually enabled the first calibration of the CTD to be carried out. The quartz thermometer was recalibrated at the CSIR in Pretoria on 17 August 1981, and the reading of the thermometer was within 0,004°C of the temperature standard over almost the full range of temperatures. At 0°C, the correction was 0,000°C. The uncertainty in the temperatures of the standard was 0,003°C.

b) Conductivity

Presently there is no conductivity standard available to calibrate the conductivity of the CTD. The only equipment to which the conductivity could be compared was a Plessey Model 6230N salinometer. This is a small portable salinometer and although the manufacturer claims an accuracy of 0,003 °/oo, the instrument drifts and has to be continuously recalibrated using standard seawater obtained from the Institute of Oceanographic Sciences, England. Since the CTD measures conductivity, whereas the salinometer measures salinity, the CTD conductivity is transformed into salinity (using the temperature calibration) in order to make it compatible to the salinometer reading.

c) Pressure

The pressure standard is a Budenberg Dead-weight Pressure Tester Model 280H.

A3.3 Temperature calibrating procedure

The CTD was checked and calibrated in the laboratory and at sea, and the results of these checks and calibration are illustrated in Fig. A3.1. We differentiate between "checks" and "calibration", the former being cruder comparisons between the CTD and the standards at isolated values, while "calibration" indicates a full-range, laboratory comparison, the results of which are used in the processing of the field data.

a) Laboratory check, 13-14 March 1980

The CTD temperature was checked twice against the HP quartz thermometer model 2801A by immersing the sensor head in a container filled with tap water at room temperature, and in melting, deionised, ice.

b) Check at sea, 10 September 1980

A release was manufactured to enable one reversing bottle to be clamped onto the CTD. This release was remotely triggered from the vessel by changing the polarity on the sea cable voltage. The CTD was lowered from the ship but kept within the mixed layer to ensure that it was in a thermally stable environment. Two checks were made, each time using two reversing thermometers (RTs).

c) Laboratory calibration, June 1981

A calibration was executed between 10 and 16 June 1981 by comparing the CTD with the Hewlett-Packard quartz thermometer 2804A. A thermosflask was used for the ice-point test using iced, deionised distilled water. To raise or lower the temperature from a particular level, hot or cold water was added while keeping the water well stirred.

d) Laboratory calibration, May 1982

The second, full-scale temperature calibration of the CTD was executed on 19 May 1982, using the HP Quartz Thermometer Model 2801A (with the new probe). The results (see Fig. A3.1) indicate the shift in calibration that the CTD had experienced in one year.

In Fig. A3.1, the line(s) representing the calibration curve used to process data from the cruises 1979-1982 are indicated. These lines are based on the June 1981 calibration only, since this calibration seemed to be more representative as far as spanning the time of the CTD-data collection was concerned.

The calibration seems to be approximated by three straight lines, one from 0-2°C, the next from 2-15°C and the last from 15-30°C. The intermediate "knee" at 15°C in the calibration curve was to be expected, considering the electronic construction of the temperature recording channel. The origin of another "knee" at 2°C was probably due to the insulating problems at these low temperatures. A least-squares straight line was fitted to the data points within the temperature ranges 3-16°C and 16-31°C. The three curves which are considered to represent the result of the calibration are :

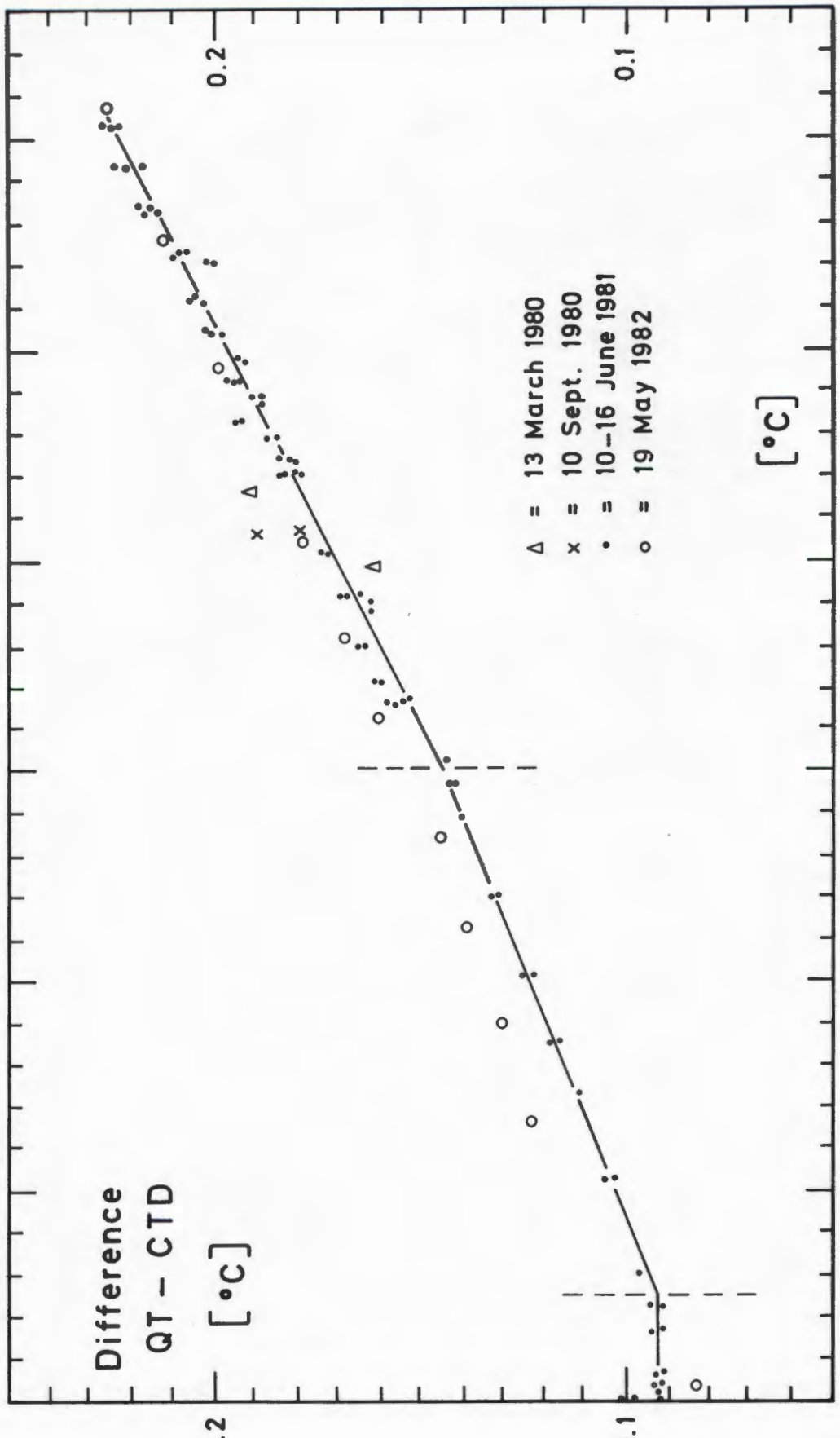

FIG. A3.1 : Temperature difference between the quartz themometers (QT) and the CTD for various checks and calibrations. The three lines seperated by dashes, represent the June 1981 calibration.

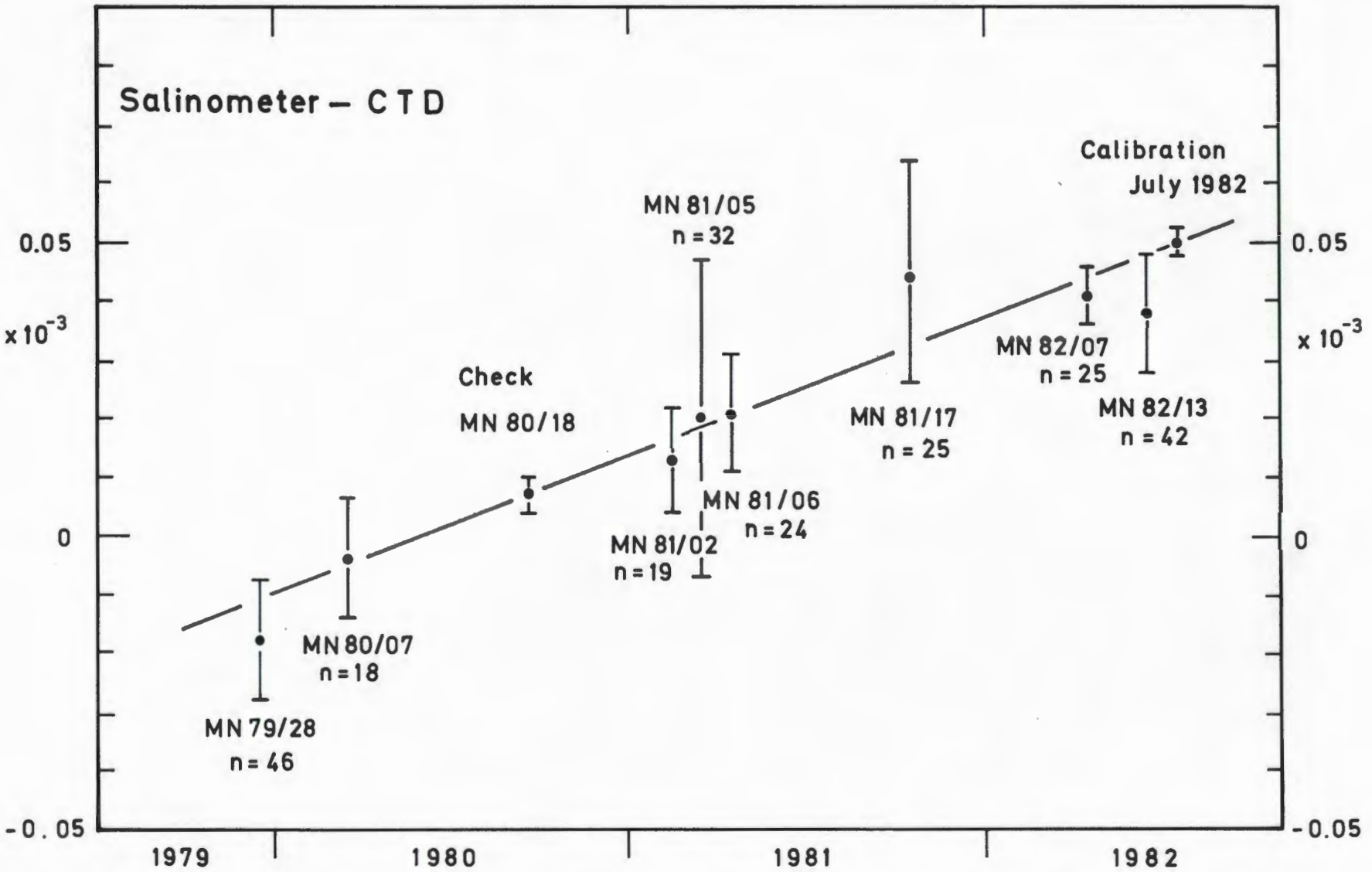

FIG. A3.2 : Salinity difference between the salinometer and the CTD from 1979 to 1982 (see text for full description). The cruise numbers of the *Meiring Naudé* are indicated, as well as the numbers of comparisons on each cruise (n). The straight line was used to process the data.

For temperatures below 2,5°C:

True temp = CTD temp + 0,0925°

For temperatures between 2,5°C and 15°C:

True temp = CTD temp + 4,1666 x 10^{-3} x CTD temp + 0,0824°

For temperatures above 15°C:

True temp = CTD temp x 5,1538 x 10^{-3} x CTD temp + 0,0676°

The calibration confirmed the results obtained through intermediate checks, namely, that the CTD temperature had differed from the true temperature by as much as 0,2°C. *The temperature calibration listed below was used to process all the CTD data reported in this study.* A rough inspection seems to indicate that accuracies of about $\pm$ 0,005°C are possible (this is mainly the scatter in the data).

A3.4 Conductivity calibrating procedure

All salinity comparisons have been entered in Fig. A3.2

a) Check at sea, September 1980

During the test cruise MN 80/18 in September 1980 (see A3.3(b) above), samples of seawater were obtained from the reversing bottles. These were subsequently analysed on the Plessey Salinometer, and compared with the salinity calculated from the *in situ* conductivity, temperature and depth of the CTD.

b) Routine comparisons at sea

It has become routine practice to tap a surface sample of seawater on every station. The water for these samples is drawn from about 3 m below sea-level on the port side of the vessel and pumped to the wet laboratory where the sample is tapped. The samples are taken ashore and analysed for salinity which is then compared with the surface salinity of the CTD. However, the CTD is lowered from the starboard side of the ship, and is thus removed from the seawater at the pump-intake by several meters. In addition, sea-surface samples are not necessarily tapped at the same time as the CTD surface measurement. The salinities from

the surface samples and the salinities calculated from the surface readings of the CTD therefore have intrinsic differences. This is evidenced by the large error bars in these comparisons (Fig. A3.2).

c) Laboratory calibration, July 1982

Although this occasion is termed a "calibration", it was really only a careful comparison at one salinity value only. This was done by immersing the whole CTD in a container with seawater that was stirred continuously. A plastic tube was attached to the Plessey salinometer and allowed to draw samples at regular intervals (about every 30 minutes) from a point a few centimeters away from the CTD sensors. This resulted in about 10 comparisons of which the differences (CTD-salinometer) scattered within less than 0,005 ppt.

Included in Fig. A3.2 is a line drawn through the value obtained in the check of September, 1980, and the calibration of July 1982. This straight line passes through (the error bars of) all the values obtained through the routine surface comparisons. It is therefore assumed that the CTD conductivity sensor had drifted steadily over the three years of use between 1979 and 1982. It was tacitly assumed that the constant that is added/subtracted from the CTD salinity is independent of salinity, and is just a function of the time of the cruise. *This line was used to correct the salinities calculated from all the CTD data reported in this thesis.*

A3.5 Pressure calibrating procedure

The CTD pressure has been checked regularly during its use, and has not drifted during the years covering this thesis. The only problem encountered in the pressure channel was a failure of the internal circuitry. The circuit board with the fault was exchanged and the pressure had to be set again.

A3.6 Handling the CTD

It will become clear to the reader that, although everything

possible has been done to ensure the accuracy and reliability of the data, the operational procedures have been unsophisticated by overseas standards.

During the period of CTD use in this study, the facility did not exist at the Institute to analyse the large quantity of data emitted by the CTD. Instead of recording and processing the CTD data as three separate time series (i.e. each of T, C and D vs time at 30 frames per second), provision existed to handle T and C vs depth only. In addition, the amount of data was reduced even further by recording data at regular depths only. This meant that, instead of about 30 000 frames (each containing a value of depth, temperature and conductivity) per 1000 m profile (at a m/s), the data was reduced by a factor of 1 in 50. Admittedly, this reduced data had undergone some real-time editing by computer, but only as far as spurious "spikes" were concerned. Having lost the time base of the parameters, time series analyses such as those developed and reported by FOFONOFF, HAYES and MILLARD (1974), CHANDLER *et al* (1978) and lately by GILBERT, HUYER and SCHRAMM (1981) and PERKIN and LEWIS (1982) could not be implemented. The result was not only a loss of vertical resolution (for which there was no need at that stage) but, more important, the inability to correct the raw data for the different response times of the temperature and conductivity sensors. The determination of the time response of the temperature sensors (see PAIGE, 1980; GREGG *et al*, 1982) and the effect of sensor response mismatches (RODEN, 1974; HORNE and TOOLE, 1980) remain an inherent problem in CTD operation.

To evaluate the performance of the CTD, the temperature error was estimated through the example given in section A1.3(a). As a true constant for the temperature sensor, a value of 50 ms was used (PAGE, 1980). Since this is an "e-folding" time constant, the temperature lag is given by

$$\Delta t = 2.2\, t_{63}\, {}^{\partial T}/_{\partial t}$$

The maximum error is experienced as the thermistor moves through the steepest part of the thermocline where ${}^{dT}/dt = 0.1°C/s$ (at a lowering/raising rate of 1 m/s), and the error amounted to 0.01°C. By lowering the winch speed, the accuracy of the readings is accordingly enhanced. Customarily, the winch speed was 0.7-1.0 m/s, and this means that the tolerance on the CTD temperature readings reported in this thesis was about 0.01°C in steep parts of the thermocline and better in other depths.

APPENDIX 4

DATA PROCESSING METHODS

A4.1 Introduction

The method by which data collected by the *Meiring Naudé* is checked and processed has been developed over many years at the East Coast Branch of NRIO and is therefore not applicable to the data of this project only. The routine processing of raw data (BIMA, 1974), makes provision for elimination of errors as far as possible, both through visual as well as computerised intercomparison of different data sets.

A.4.2 Pre-processing of CTD data

Because of the different response times of the temperature ($\sim$ 100 m s) and conductivity sensors ($\sim$ 30 m s), a mismatch in values occurs when salinity is to be calculated from these two parameters. Since the conductivity sensor has the faster response, it can be assumed that the true variation of conductivity is almost perfectly reflected by the output of the conductivity sensor, while the temperature output lags behind the true variation of temperature (Fig. A4.1).

When the CTD passes through a step-like change in temperature and conductivity, the calculated salinity shows opposite responses, depending on whether the step change is an increase or a decrease. When, e.g. there is a steep thermocline, the calculated salinity will show a transient *decrease* compared to the expected salinity if the CTD is lowered and an *increase* when the CTD is raised (see Fig. A4.1).

By keeping the raising/lowering speed of the CTD $\lesssim$ 1 m/s, it was found that spikes in the resulting salinity were very few and so small ($\lesssim$ 0.01 ^{o}/oo) that detailed correction of the raw data was unnecessary. It was accepted that the tolerance of the temperature was 0.01°C and that of the salinity 0.01 ^{o}/oo.

From the depth, temperature and conductivity, salinity was calculated using the formulæ given in the NBIS CTD manual. In this calculation, the value of C (35, T, 0), the conductivity as a function of temperature at 35 ^{o}/oo salinity and zero pressure, is required. KNOWLES (1974) quoted values ranging from 42.698 to 42.929 (mmho/cm). It was

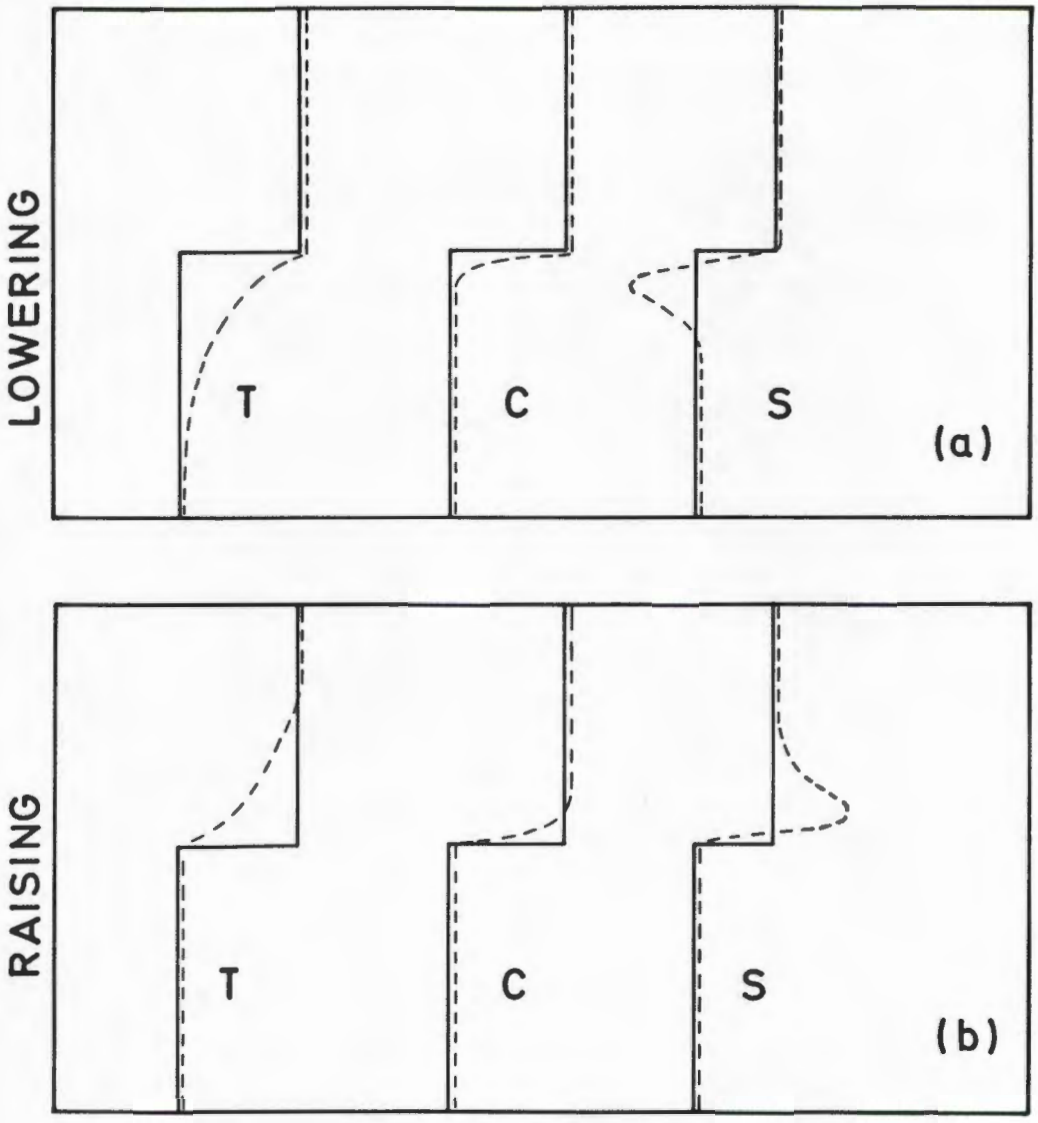

FIG. A4.1 : Representation of the response of the temperature and conductivity sensors (dashed line) to a steplike change in the temperature (T) and conductivity (C) profiles.
(a) : Lowering the CTD through this interface produces a salinity spike toward *lower* salinity values *below* the interface.
(b) : Raising the CTD through the interface produces a salinity spike toward *higher* values *above* the interface.

decided to use the value of LaFOND (1951), namely 42.893 mmho/cm, although a value of 42.900 may have been closer to the average of the listed values.

A4.3 Calculation of oceanographic parameters

The input data of depth, temperature and salinity were used to calculate various parameters, and the subroutines are listed below.

(a) Sigma-t

```
CL = S/1.80655
R1 = -.069+1.4708*CL-(1.57E-3)*CL^2+3.98E-5*CL^3
R2 = (4.53168*T-0.545939*T^2-1.98248E-3*T^3-1.438E-7*T^4)/(T+67.26)
R3 = 1.-4.7867E-3*T+9.8185E-5*T^2-1.0843E-6*T^3
R4 = 1.803E-5*T-8.164E-7*T^2+1.667E-8*T^3
R5 = R2 + R3*R1 + R4*R1^2:REM THIS IS SIGMA-t
R6 = 1000/(R5 + 1000)
```

(b) Sound velocity

Sound velocity was also calculated as part of the basic data processing, but since the velocity of sound is not used anywhere in this thesis, the subroutine will not be reproduced.

(c) Density and specific volume anomaly

Referring to some variables calculated for sigma-t in (a) above, the *in situ* density and specific volume are calculated as follows:

```
D0 = 4886/(1.+ 1.83E-5*Z)
D2 = 227+28.33*T-.551*T^2+.004*T^3
D3 = (105.5+9.5*T - .158*T^2)*1.E-4*Z
D4 = 1.5E-8*T*Z^2
D5 = 147.3-2.72*T+.04*T^2
D6 = (32.4-.87*T+.02*T^2)*1.E-4*Z
D7 = 4.5+.1*T-(1.8-.06*T)*1.E-4*Z
G  = (R1-28)/10
G1 = R6-R6*(D0-D2+D3-D4-G*(D5-D6) +G^2*D7)*1.E-9*Z
REM G1 IS THE SPEC. VOLUME
RHO = 1./G1:REM RHO IS THE in situ DENSITY
```

(d) Geopotential anomaly (dynamic height)

The specific volume anomaly δ between adjacent observations was

used to obtain the anomaly of dynamic depth or geopotential anomaly ΔD

$$\Delta D = \int_{p_0}^{p_1} \delta \alpha p \qquad (1)$$

where P_0 and P_1 designate successive pressure levels. The true dynamic depth was then obtained by summing ΔD from the surface downwards. The reader is referred to oceanographic textbooks (e.g. NEUMANN and PIERSON, 1966) for a more detailed description.

A.4.4 Interpolation and geostrophic currents

To calculate geostrophic currents between stations, data have to be interpolated to "standard" depths (normally every 50 m). Temperature and salinity were interpolated to these depths in the following way: A Lagrangian interpolation was applied, first using two values above and one below. The average was finally taken of the two interpolated values. Density-related parameters were then calculated from these interpolated values, as well as geopotential anomalies. These were used to calculate the geostrophic velocity between stations.

A4.5 Gradient currents

In the case of circular, stationary, frictionless currents, the pressure gradient force is balanced by the Coriolis force and the centrifugal force

$$\frac{1}{\rho} \frac{\partial p}{\partial r} = \frac{v_{gr}^2}{r} + f v_{gr} \qquad (2)$$

Here, v_{gr} is the gradient velocity, i.e. the tangential velocity in the circle, r is the radius and p, ρ and f are the pressure, density and Coriolis parameter, respectively. Here r is taken radially outwards from the centre of the circular motion. When $r \to \infty$ (linear motion), $v_{gr} \to v_g$ (geostrophic velocity), so that the gradient current can be obtained from the geostrophic current:

$$v_{gr} = -\frac{rf}{2} + \left[\frac{r^2 f^2}{4} + f |v_g| r \right]^{1/2} \qquad (3)$$

This equation holds for cyclonic motion, in which case the gradient current is always less than the geostrophic current. The correction from geostrophic to gradient current increases with speed and decreases with distance from the eddy centre (see Table A4.1).

TABLE A41 : GRADIENT CURRENT FOR VALUES OF r AND GEOSTROPHIC SPEED v_g ($f = 10^{-4}$/sec)

v_g	r (km) 5	10	20	30	50
100	50	62	73	79	85
80	43	52	61	66	70
60	35	42	48	51	54
40	26	31	34	36	37
20	15	17	18	19	19

To determine the radius for the eddies studied in this thesis, it was imperative that stations be occupied as close to the centre of the eddy as possible. In this way, the geographic resolution of the centre could be improved.

From the contours of the eddy geopotential, the radius of curvature needed in equation (3) could be obtained. In all cases it was assumed that the eddy was circular, and that the curvature therefore was only a function of the distance from the centre.

A4.6 Volume transport

After the gradient/geostrophic currents had been derived, the volume transport was calculated by integrating the velocity depthwise and multiplying by the station separation. Since the volume transport is independent of station separation, the volume transported in an eddy was often obtained by considering a station in the eddy centre and another outside the eddy (as indicated by, say, the 10°C topography).

A.4.7 Kinetic energy calculations

The kinetic energy (KE) of an eddy with radius R and depth h

is given by (in cylindrical coordinates):

$$K.E.\ [J] = \pi \int_0^R \int_0^h \rho v^2 \, dz \, r \, dr \qquad (4)$$

where v = current velocity (m s^{-1})

r = radial distance to eddy centre (m)

ρ = density of the water (kg m^{-3})

z = depth (m)

Alternatively, by writing the kinetic energy in terms of pressure, p (N m^{-2}), rather than geometric depth, this equation becomes:

$$K.E.\ [J] = \frac{\pi}{g} \int_0^R \int_0^p v^2 \, dp \, r \, dr \qquad (5)$$

The vertical step distance was normally taken as 100 m, while the magnitude of the horizontal steps was governed by the station separation (normally 20-40 km).

A4.8 Ship's set

While steaming at a constant speed and heading, a ship's course can be affected by the wind and currents in such a way that a difference exists between the intended velocity vector and the true velocity. This difference is referred to as the *ship's set*. To determine this set, the planned (or socalled "dead reckoning" or DR) speed and heading must be known (this is normally obtained from the ship's gyro and log), as well as the true speed and heading (derived from, e.g. two SATNAV fixes).

The ship's set is obviously a result of both the wind and the currents. Because the density of air is approximately 1000 times smaller than that of water, the wind stress is also about 1000 times smaller. Given equal exposure of the ship, a 10 m/s-wind has the same drag on the ship as a 30 cm/s current. However, it becomes virtually impossible to calculate the influence of both current and wind because of the uncertainty in area size exposed to the wind/current, the uncertainty in the drag coefficients

at different speeds, the tendency for the vessel to sail (i.e. drift at an angle to the wind direction), etc. Because of this inaccuracy, the ship's set was only considered as an indication of current flow conditions.

APPENDIX 5

THERMOHALINE SECTIONS IN THE MOZAMBIQUE BASIN

The discussion in Chapter 3 of the circulation in the Mozambique Basin was to a large extent based on the results gained during two cruises of the *Meiring Naudè* in this region. The purpose of this Appendix is to present the temperature and salinity sections of these two cruises. The location of the sections has been presented in Fig. 3.1, but for the sake of convenience, Fig. A5.1 and A5.7 contains the station disposition and the sea-surface temperature and salinity variation for each cruise, respectively.

The first cruise was executed 10-18 March 1981, and the second cruise 14-22 October 1981.

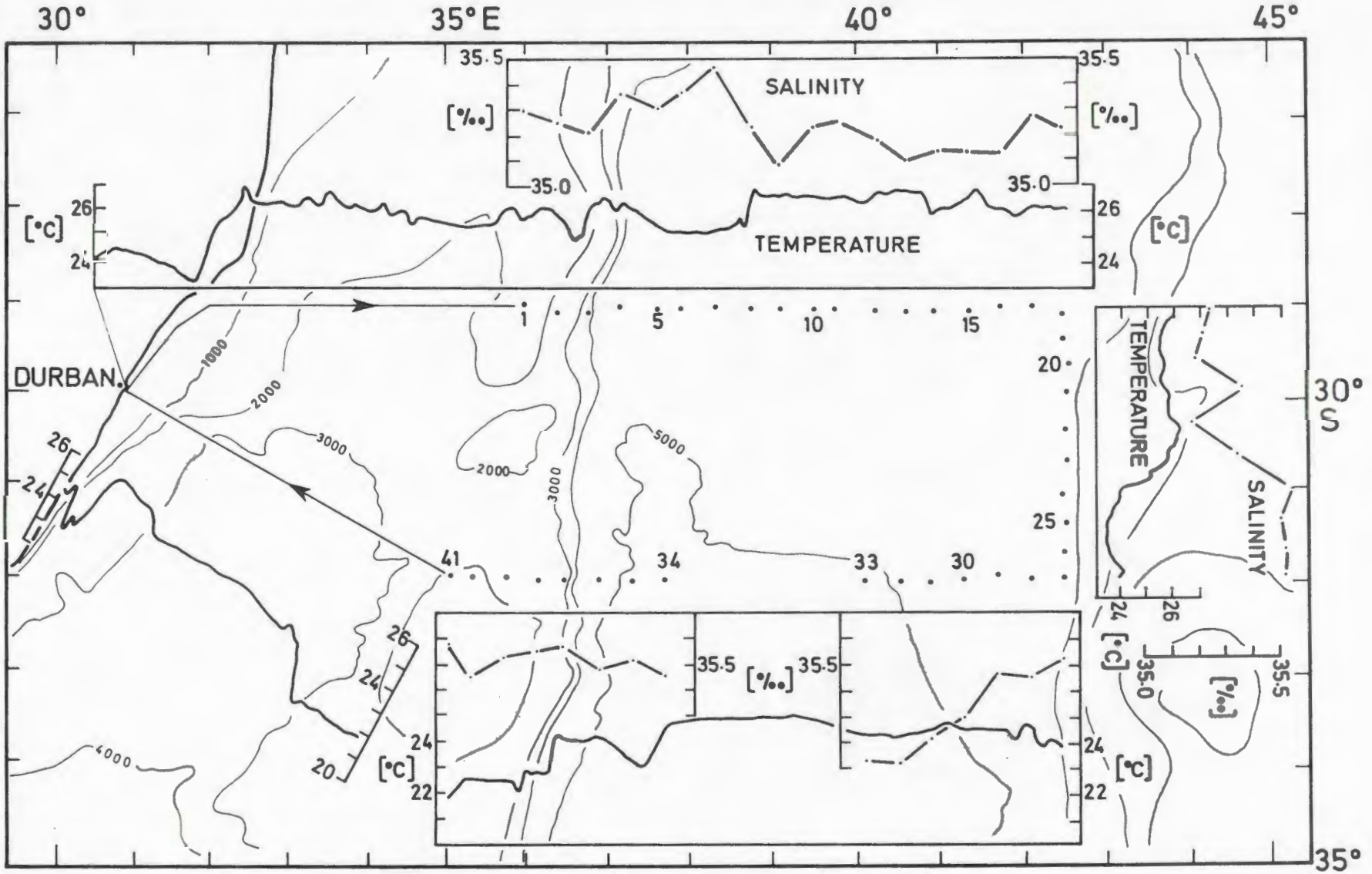

FIG. A5.1 : Track chart of the *Meiring Naudé* cruise in March, 1981, with surface thermograph traces and variation of surface salinity (samples collected only on station).

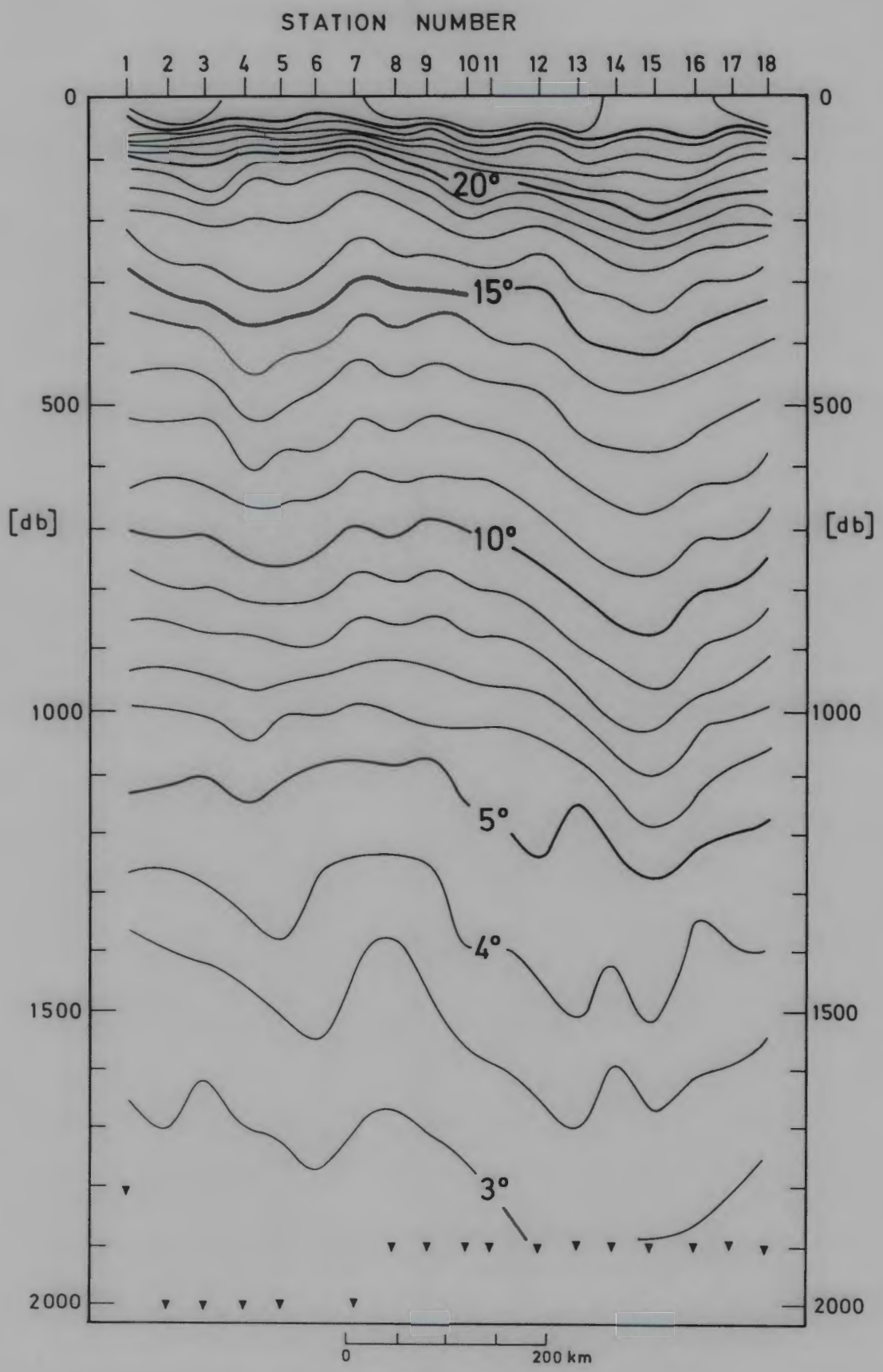

FIG. A5.2 : Vertical section of temperature for stations 1-18 of the *Meiring Naudé* cruise in March, 1981.

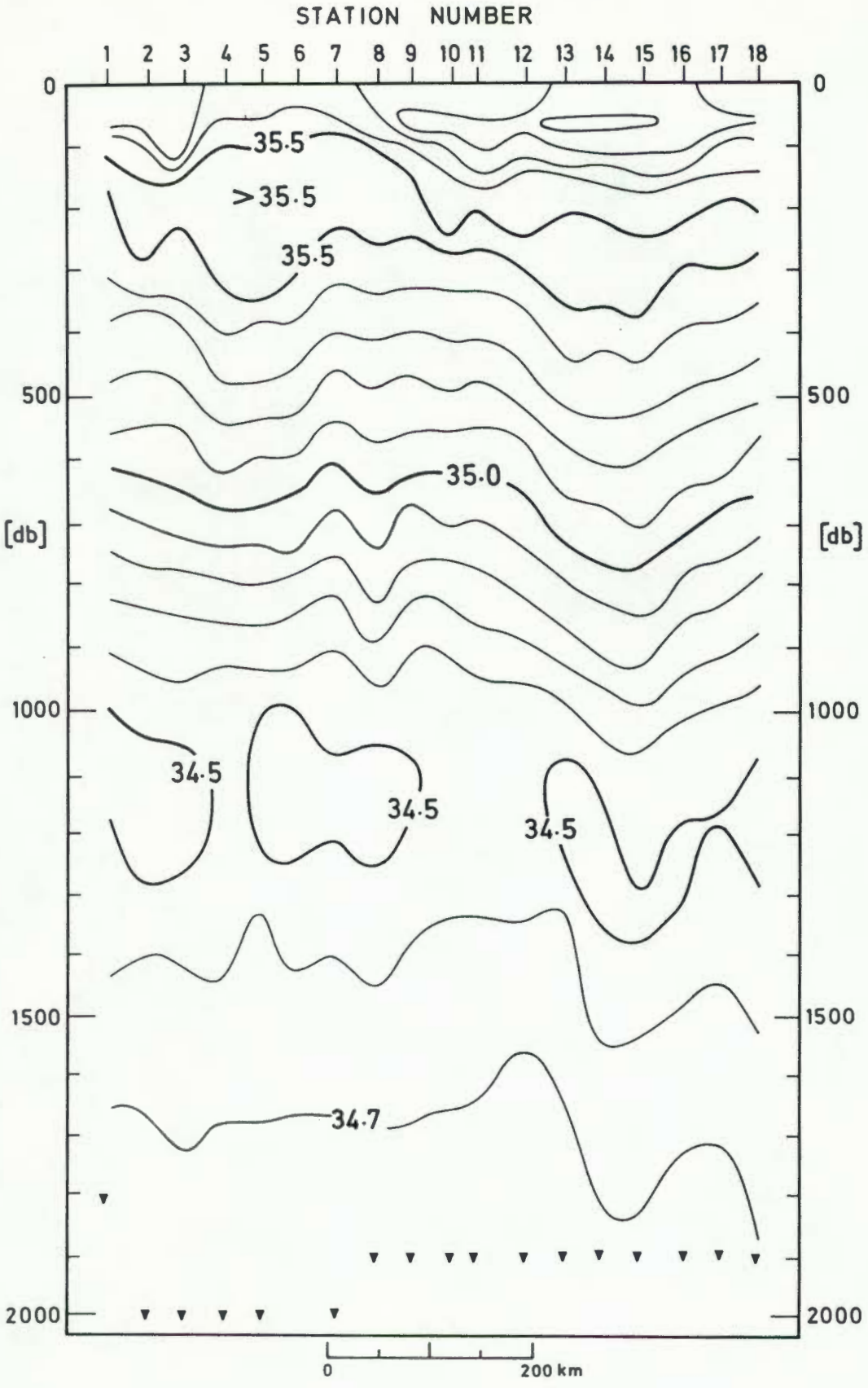

FIG. A5.3 : Vertical section of salinity (in parts per thousand) of stations 1-18 of the *Meiring Naudé* cruise in March, 1981.

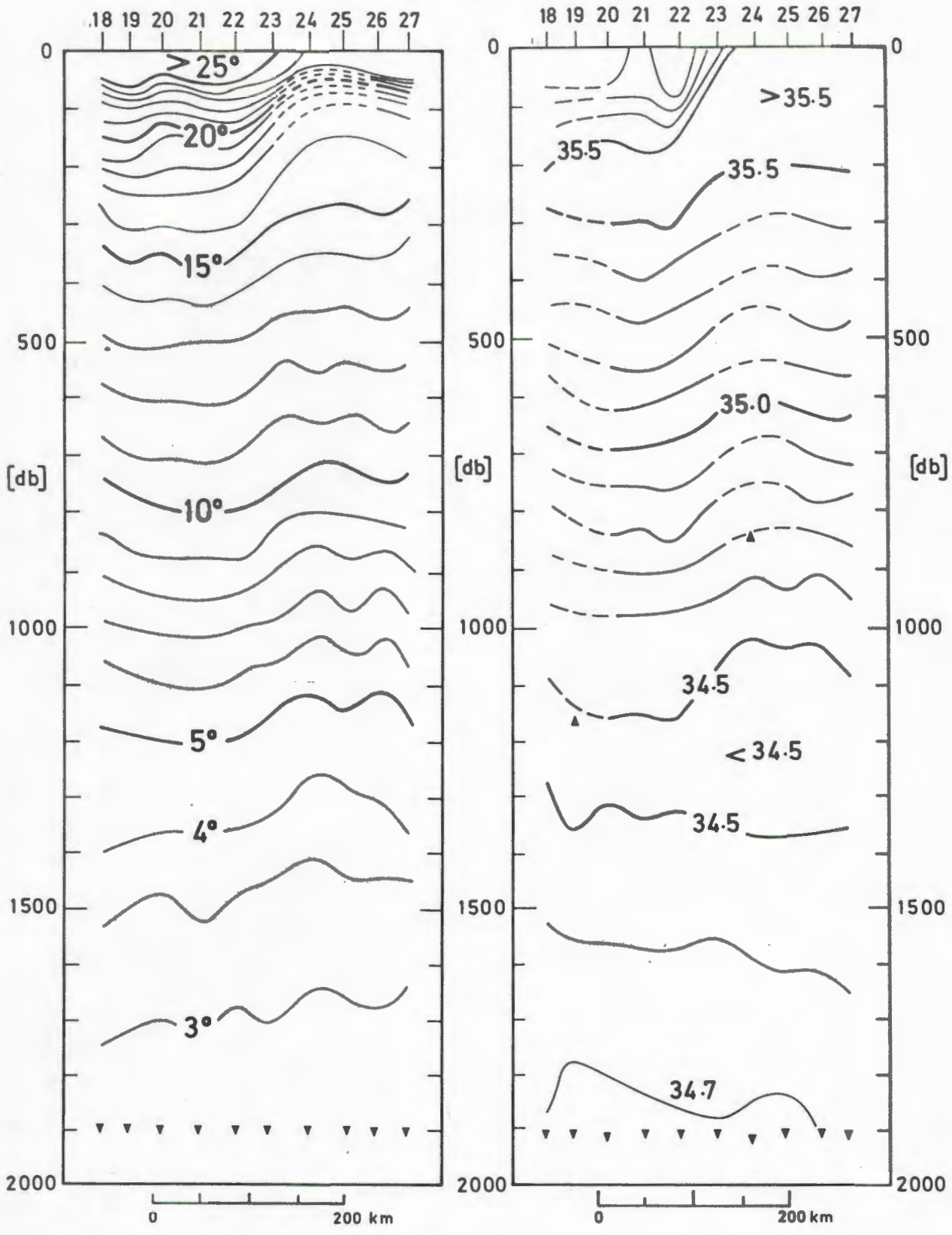

FIG. A5.4 : Vertical section of temperature (left) and salinity (right) of stations 18-27 of the *Meiring Naudé* cruise in March, 1981.

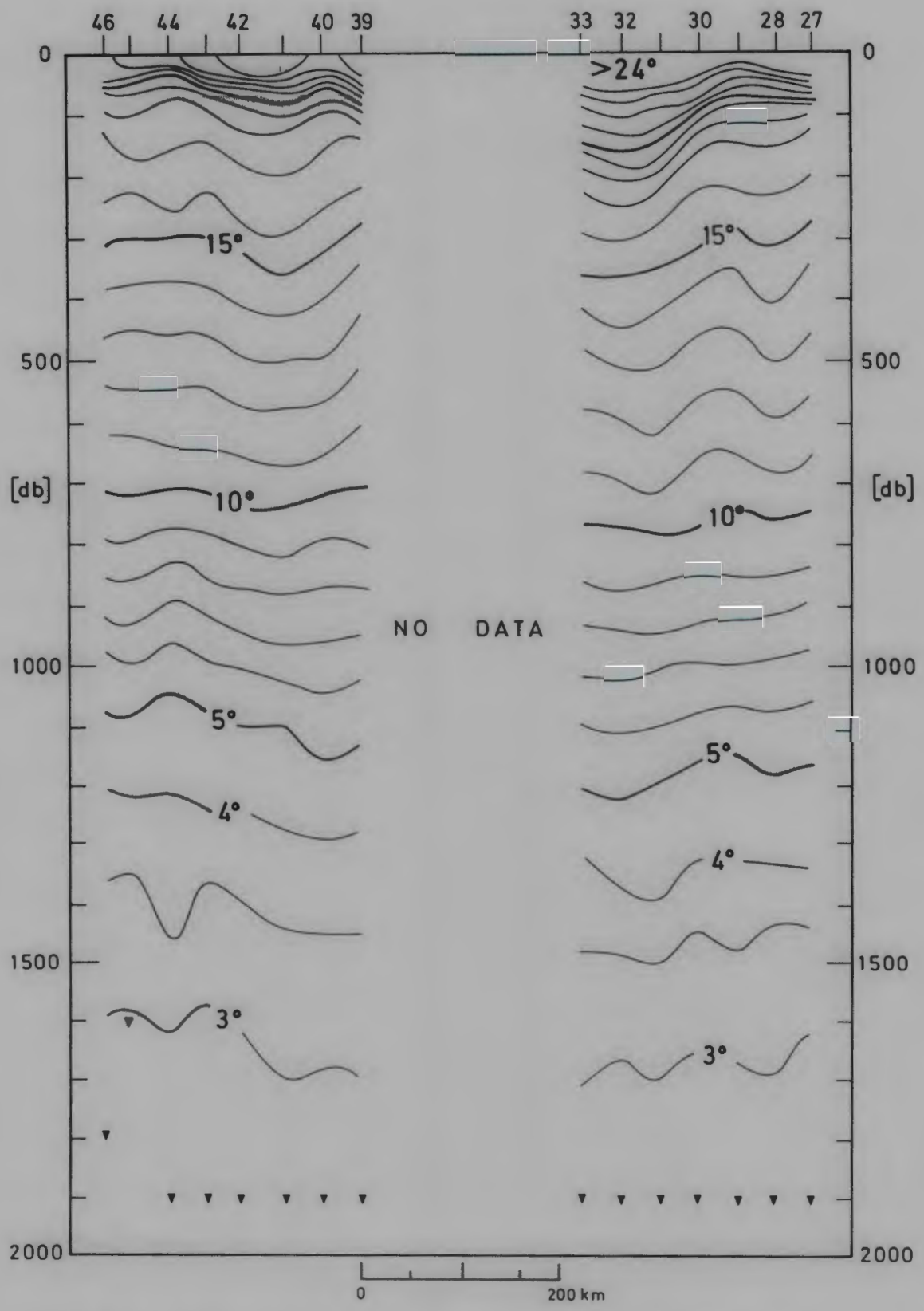

FIG. A5.5 : Vertical section of temperature for stations 27-46 of the *Meiring Naudé* cruise in March, 1981. No subsurface data were collected on stations 34-38.

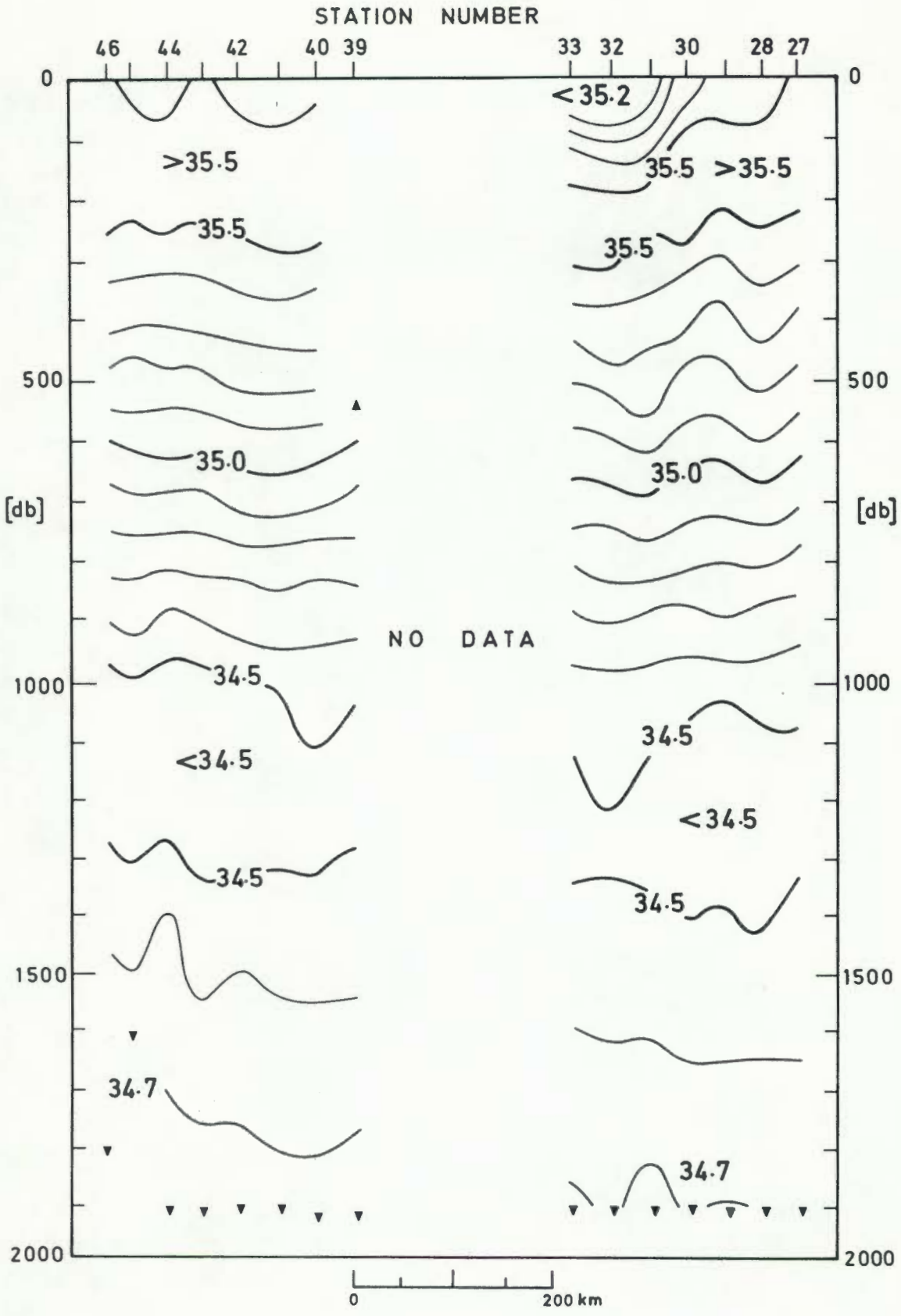

FIG. A5.6 : Vertical section of salinity (in parts per thousand) of stations 27-46 of the *Meiring Naudé* cruise in March, 1981. No subsurface data were collected on stations 34 - 38.

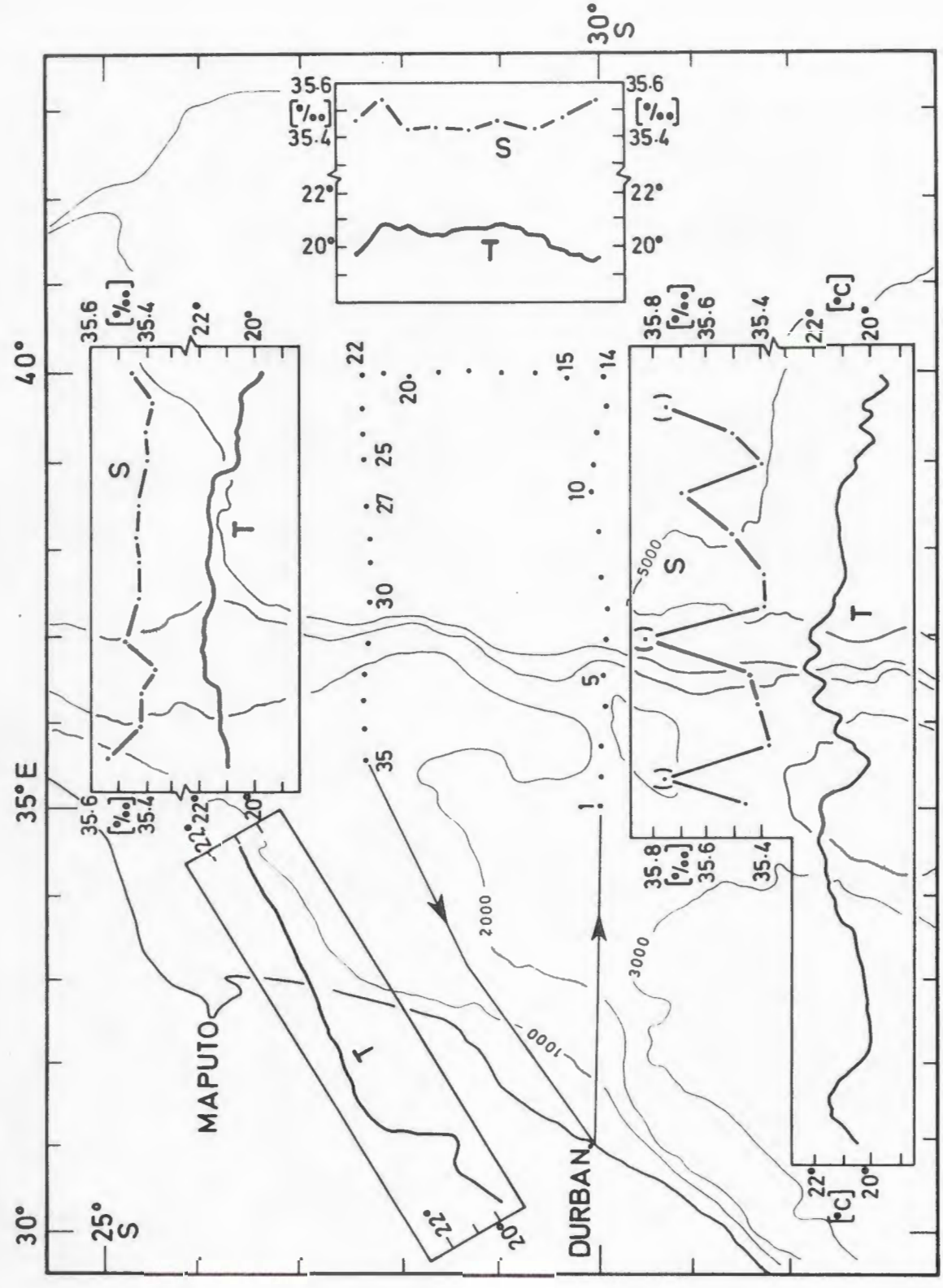

FIG. A5.7 : Track chart of the *Meiring Naudé* cruise in October, 1981, with surface thermograph traces and variation of surface salinity (samples collected on station only).

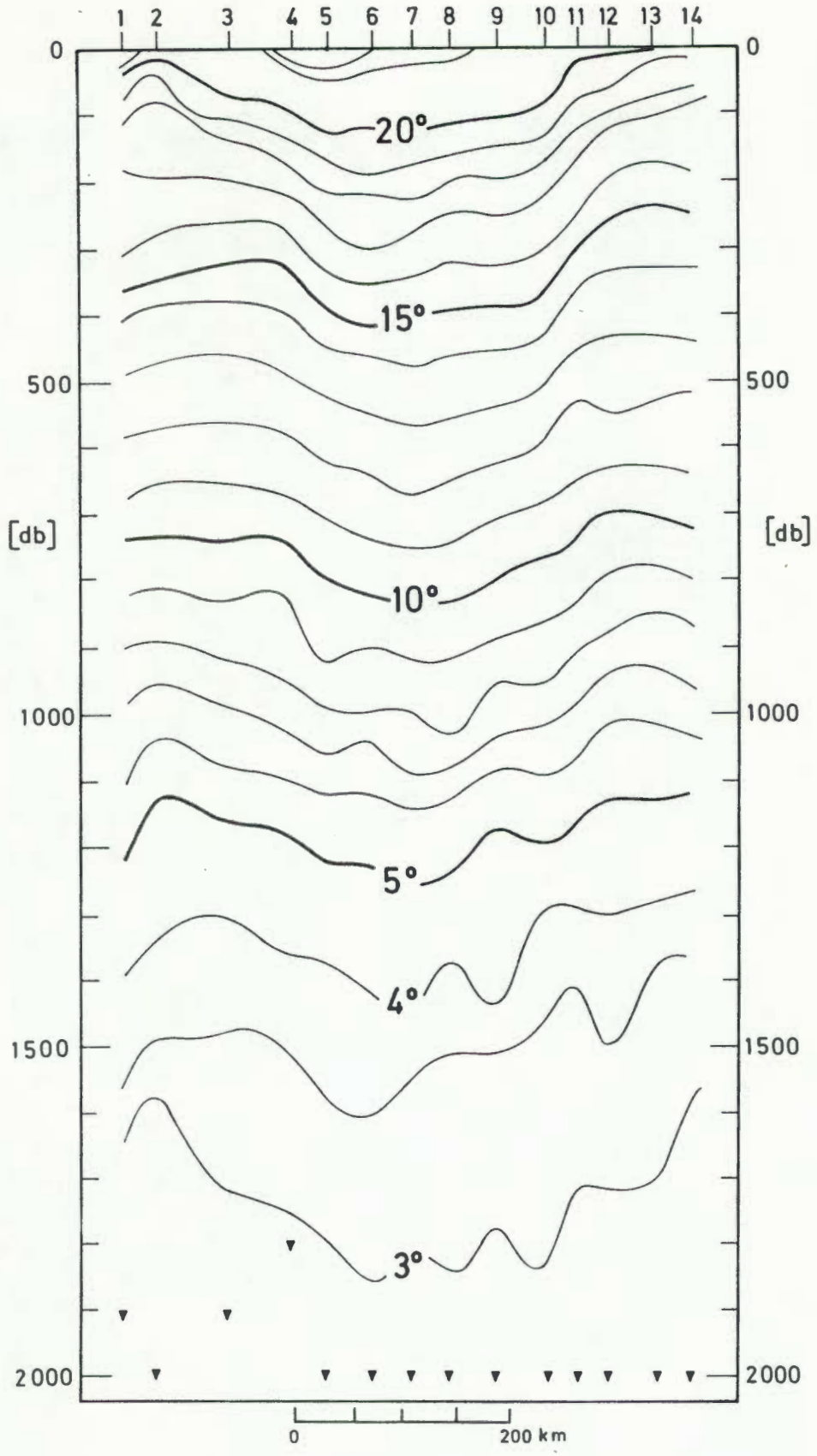

FIG. A5.8 : Vertical section of temperature for stations 1-14 from the *Meiring Naudé* cruise in October, 1981.

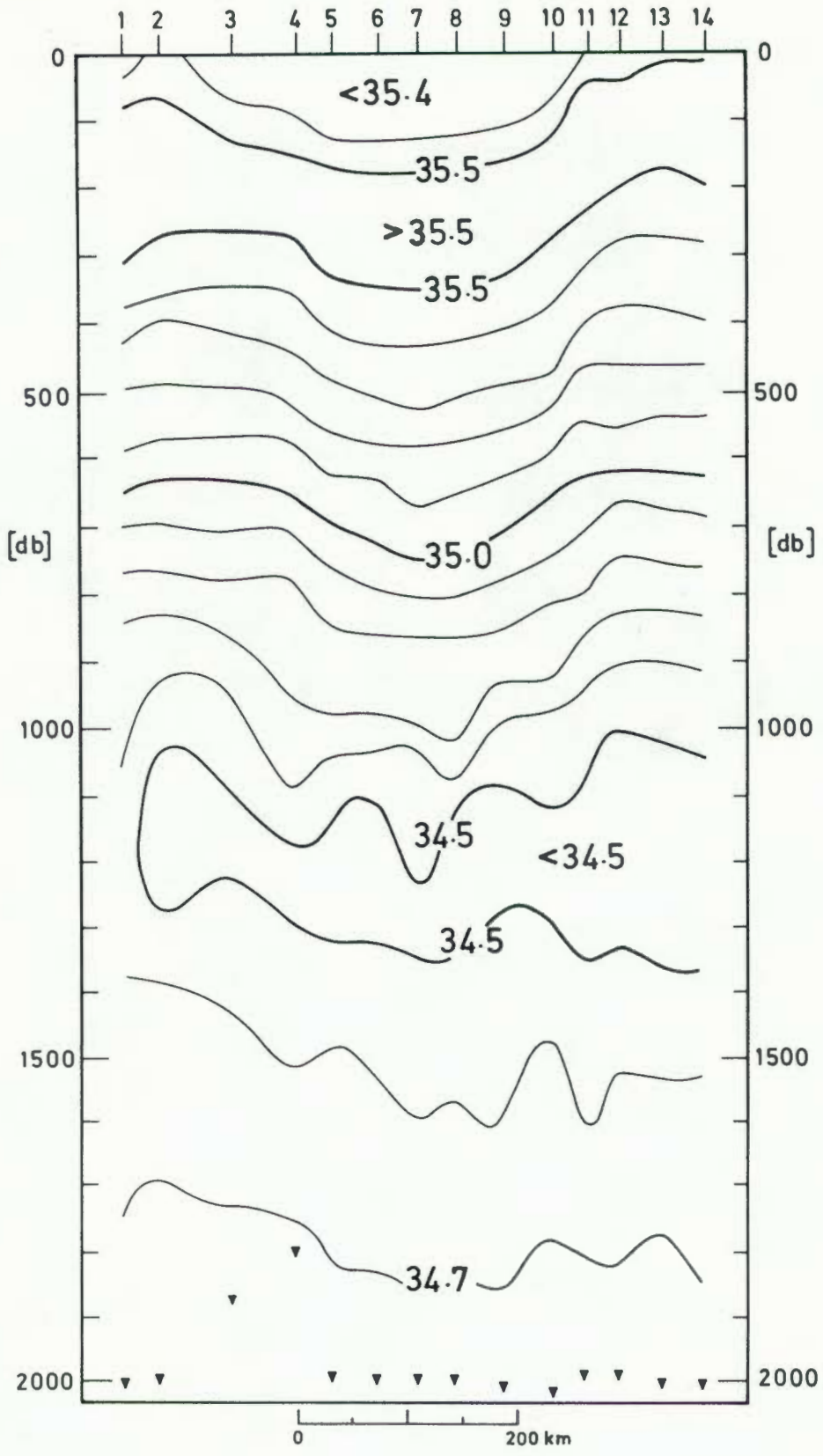

FIG. A5.9 : Vertical section of salinity (in parts per thousand) of stations 1-14 of the *Meiring Naudé* cruise in October, 1981.

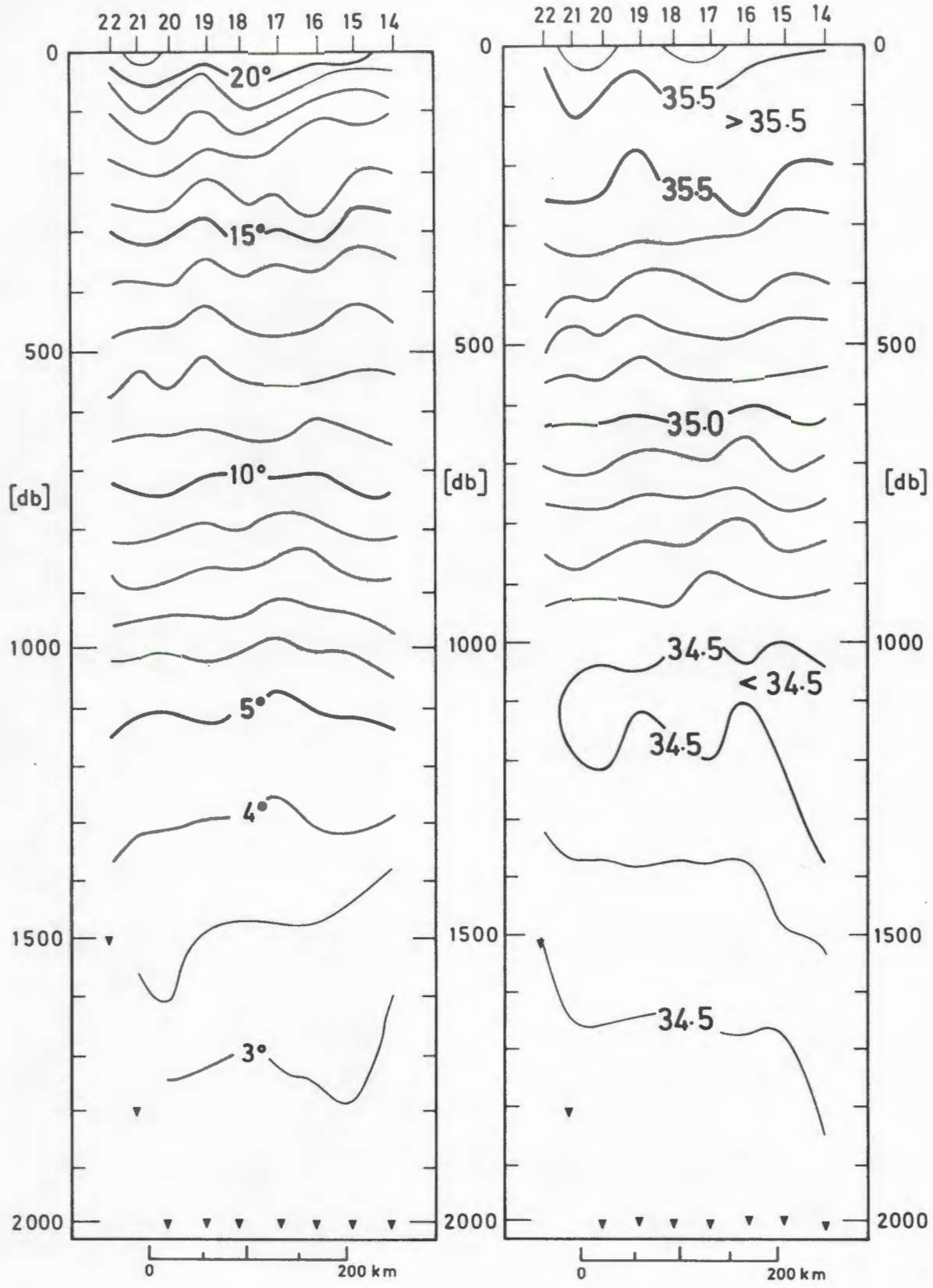

FIG. A5.10 : Vertical section of temperature (left) and salinity (right, in parts per thousand) of stations 14-22 of the *Meiring Naudé* cruise in October, 1981.

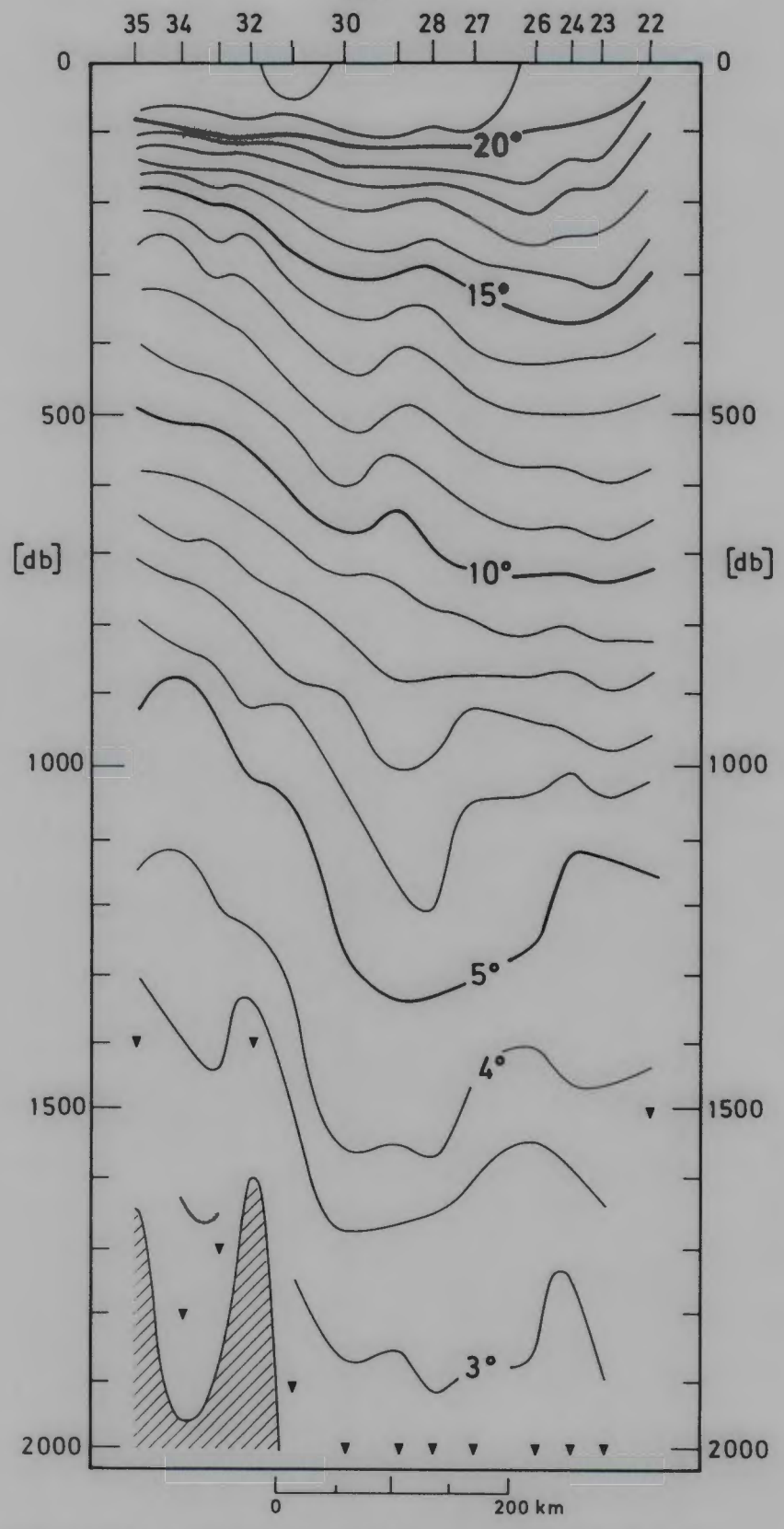

FIG. A5.11 : Vertical section of temperature of stations 22-35 of the *Meiring Naudé* cruise in October, 1981.

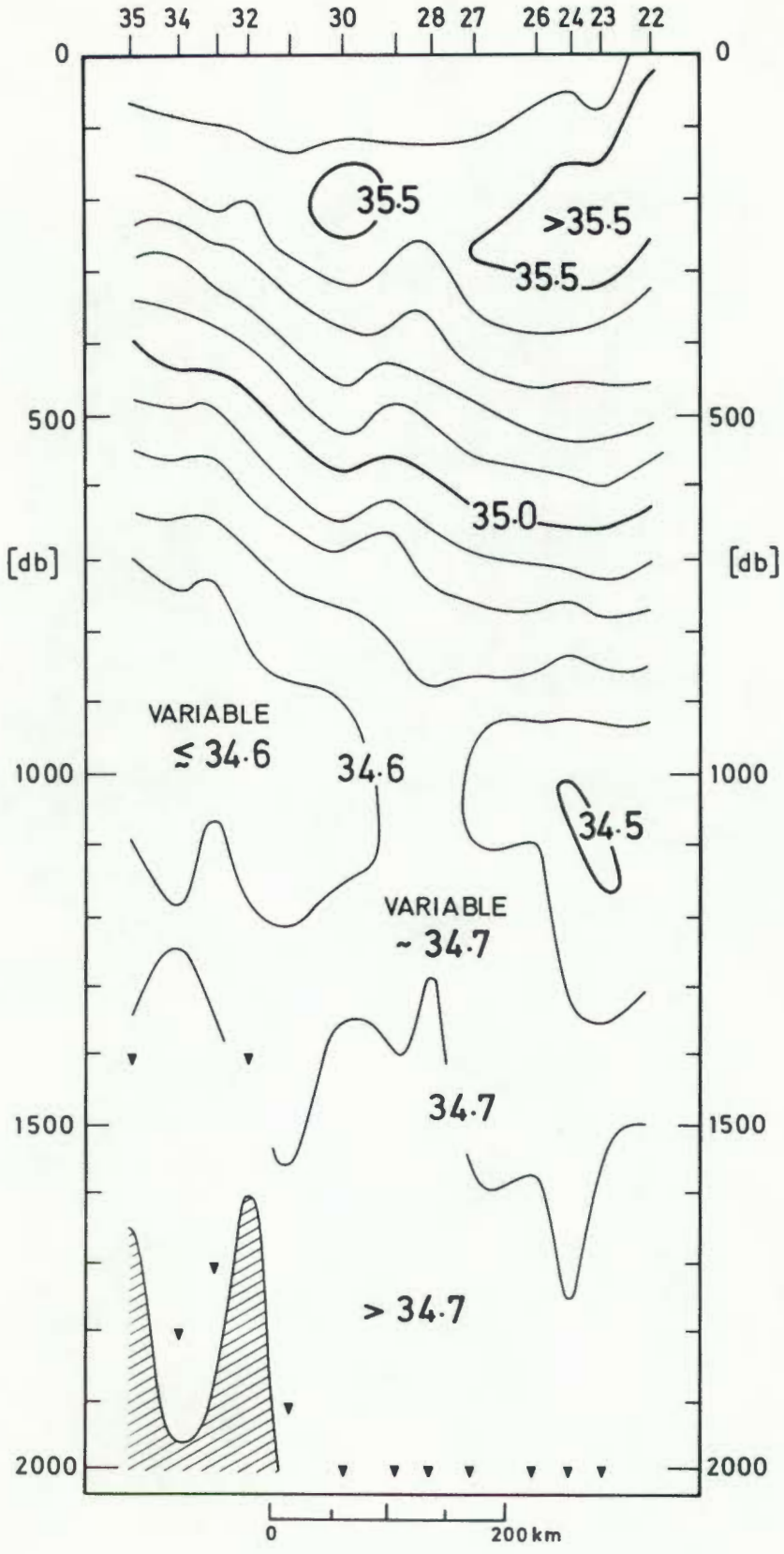

FIG. A5.12 : Vertical section of salinity (in parts per thousand) of stations 22-35 of the *Meiring Naudé* cruise in October, 1981.

APPENDIX 6

VERTICAL SECTIONS ON THE NORTHERN MOZAMBIQUE RIDGE

Soon after the *Meiring Naudé* was commisioned in 1968, a series of stations were executed in the area between Maputo and Durban. The hydrographic sections extended from the coast across the Mozambique Ridge and into the Mozambique Basin (see Fig. A6.1). For several reasons, the data remained "dormant" for more than a decade. In this period changes in the data collecting system and movement of personnel resulted in uncertainty about the quality of the data. Considerable effort was needed to check and process the data, but it is regarded that this data is of much lower quality than the rest of the data presented in this thesis. It is nevertheless included, first because of the paucity of data collected in this region, and second because it throws some light upon the circulation in the area.

The cruise lasted from 13 to 21 August 1968.

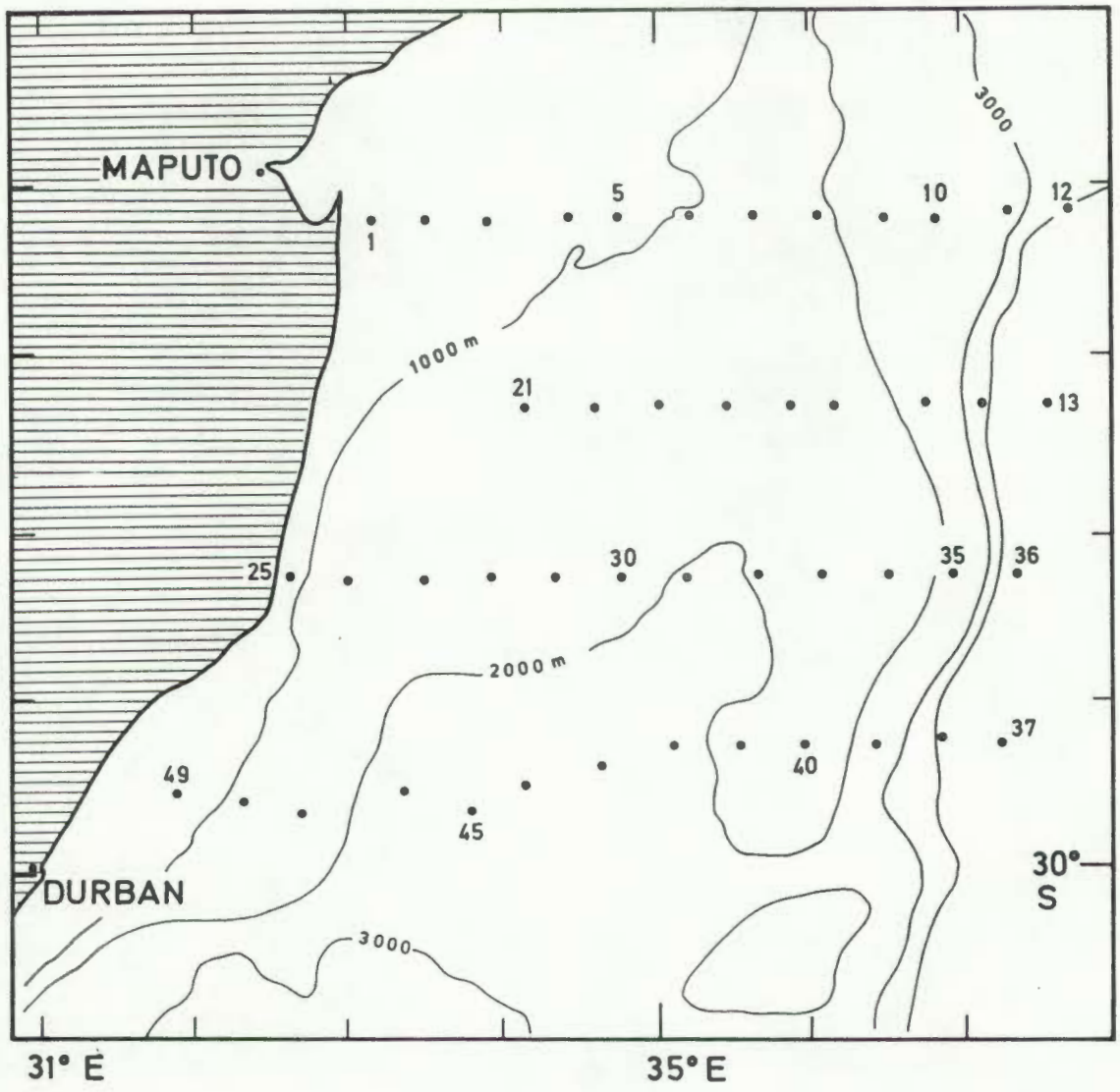

FIG. A6.1 : Station chart of the *Meiring Naudé* cruise in August, 1968.

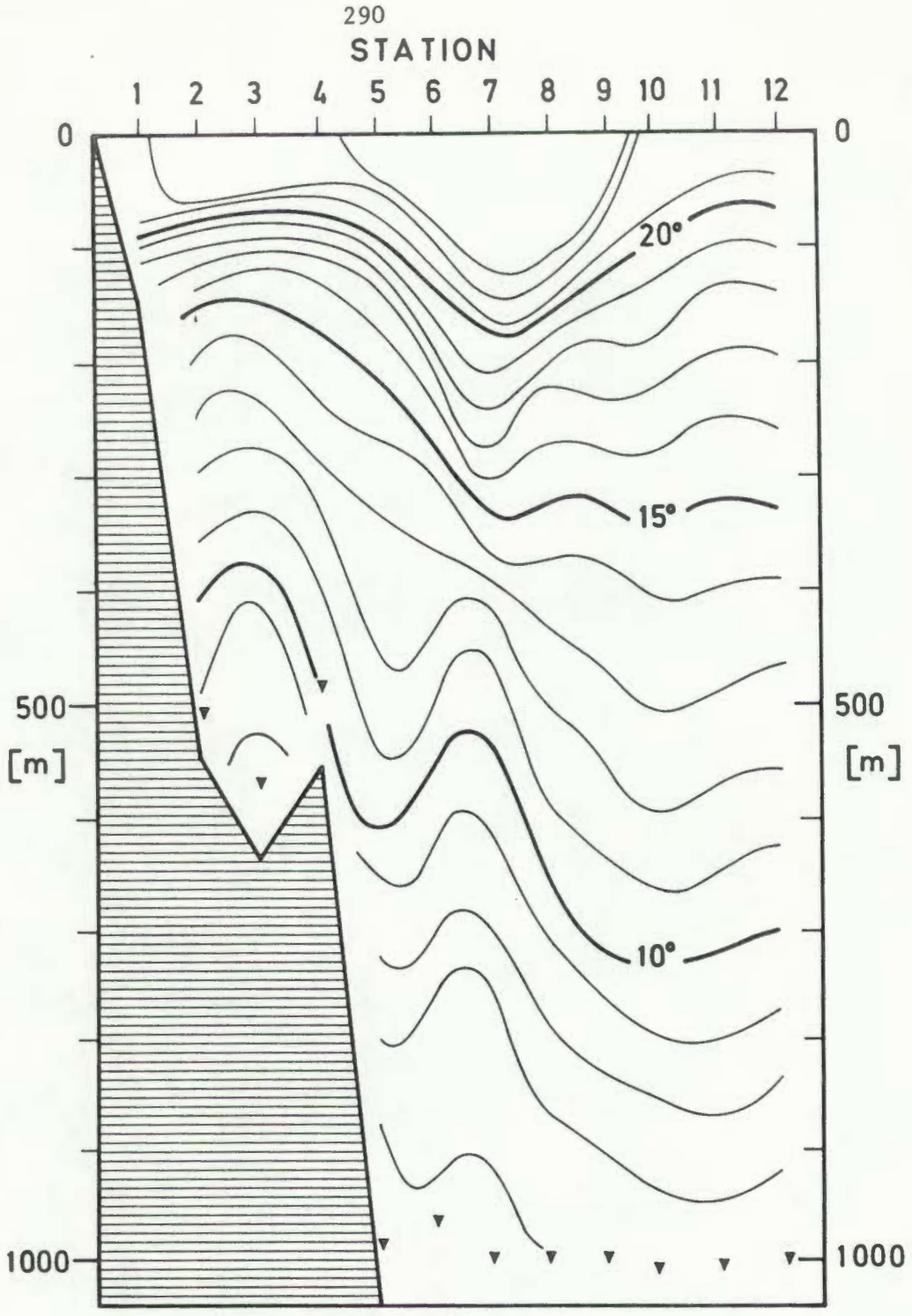

FIG. A6.2 : Vertical section of temperature of stations 1-12 of the *Meiring Naudé* cruise in August, 1968.

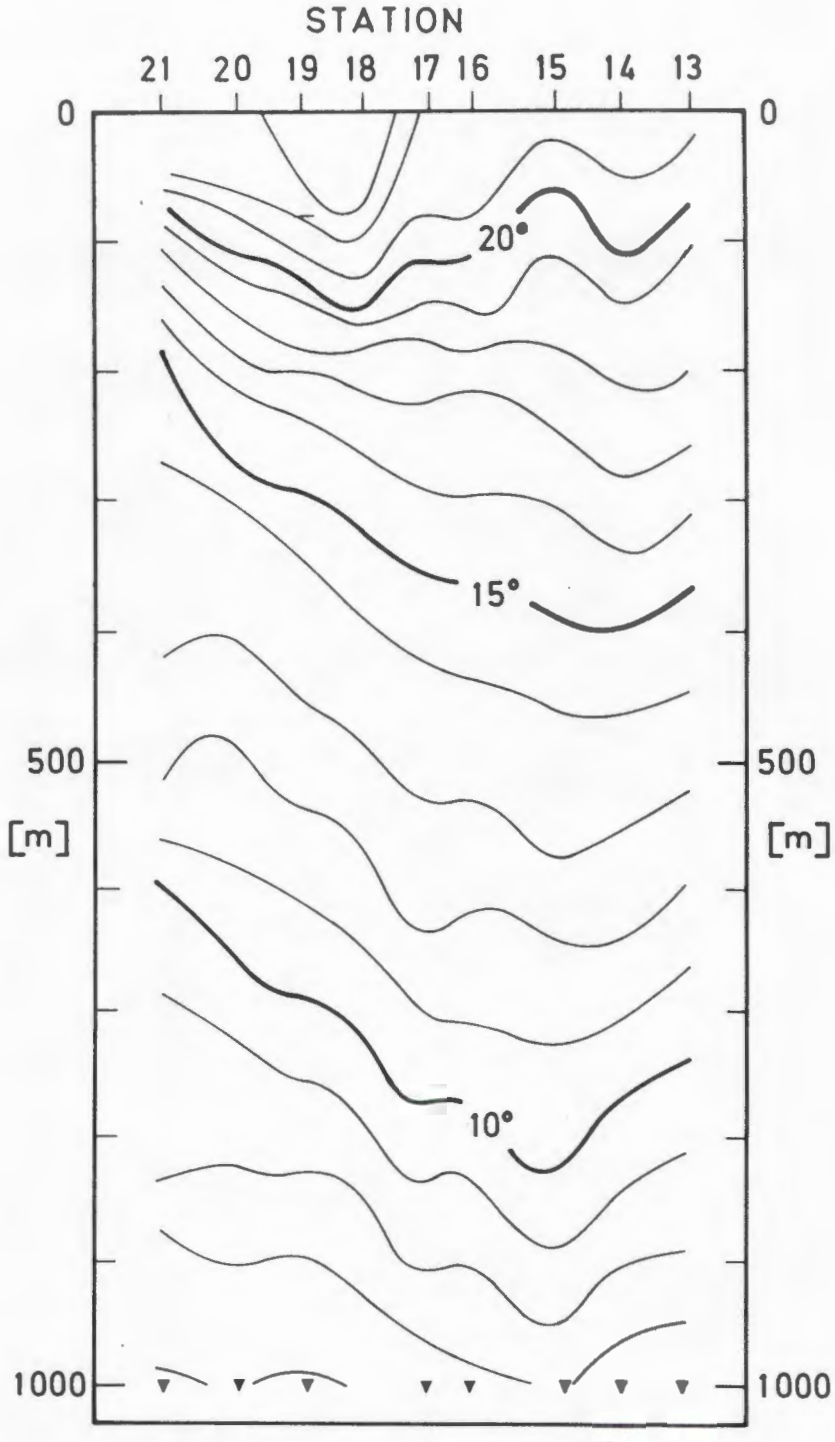

FIG. A6.3 : Vertical section of temperature of stations 13-21 of the *Meiring Naudé* cruise in August, 1968.

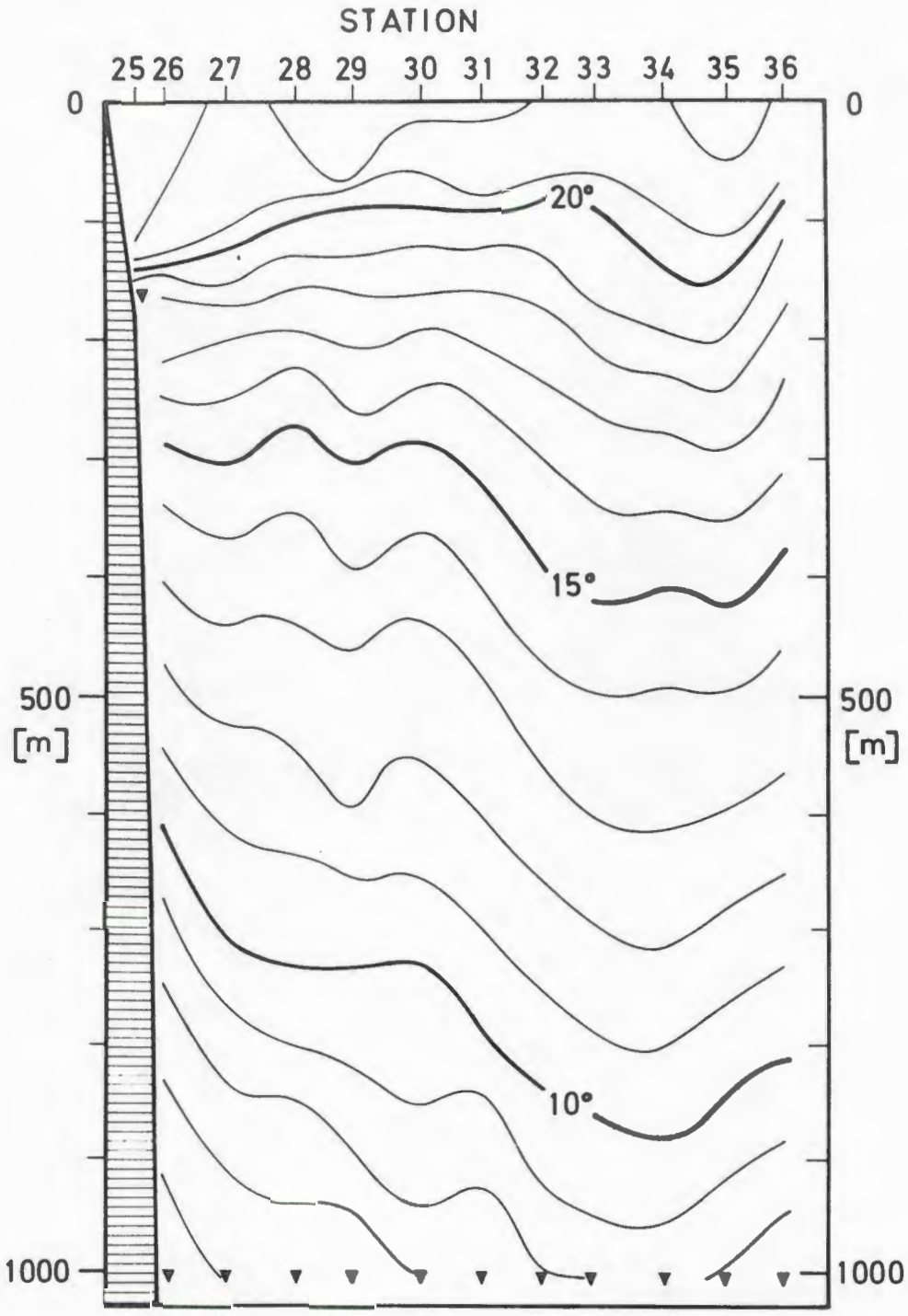

FIG. A6.4 : Vertical section of temperature of stations 25-36 of the *Meiring Naudé* cruise in August, 1968.

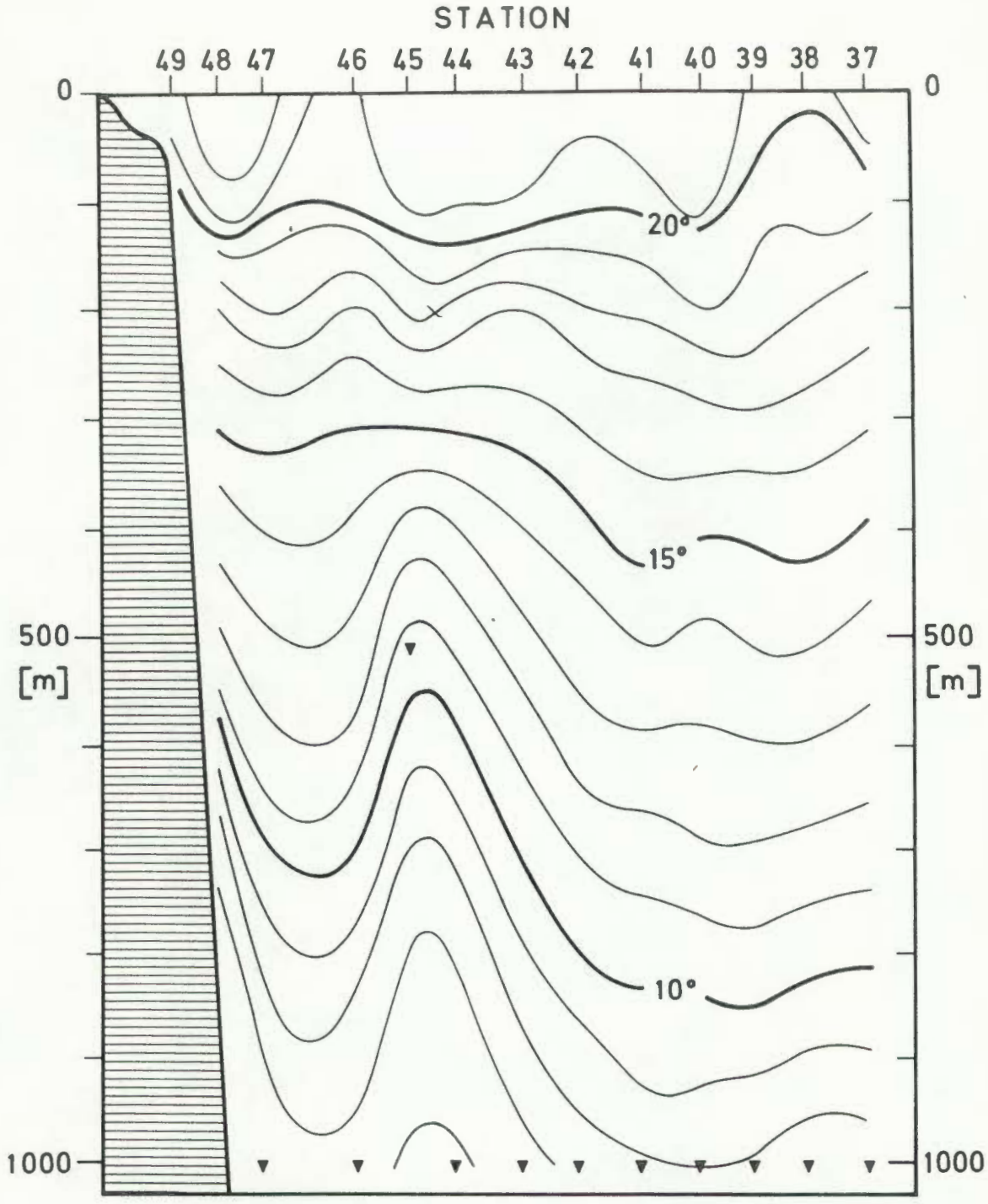

FIG. A6.5 : Vertical section of temperature of stations 37-49 of the *Meiring Naudé* cruise in August, 1968.

APPENDIX 7

FREE-DRIFTING CURRENT METER ARRAY

A7.1 Introduction

Information collected on vortices up to 1979 suffered from the absence of detailed current measurements. The NRIO hydrosonde is incapable of remaining submerged for a long period because its batteries need regular recharging, and this made the hydrosonde unsuitable for continuously-repeated profiling. An array of current meters was therefore designed and deployed in eddy Fred located in December 1979. Because of the time and expense required to moor an array in the anticipated water depth (5000 m), the array was designed to float. By continuously tracking the array with the ship, and using SATNAV for navigation, the velocities recorded by the current meters could be corrected for horizontal drift through the water. The object of this Appendix is to briefly evaluate the performance of the current meters in the light of influences originating from surface swell action, even though the information gleaned from the deployment was only marginally relevant. Also included in this Appendix is an estimate of the drift of eddy Fred based on the current meter results.

A7.2 Design of the array

The design of the floating array is illustrated in Fig. A7.1. The surface float consisted of three heavy-duty oil drums welded together and filled with polyurethane foam. At various depths below the flat were strung five Aanderaa RCM-4 current meters. These meters recorded temperature, current speed and direction every 10 minutes. Had the interconnection between the buoy and the meters been non-elastic as would be the case with steel wire or even with polyprop rope, the current meters would have oscillated vertically in phase with and with the same amplitude as the surface buoy. Since swells of 1½ m were expected in the deployment area, the vertical motion of the current meters would have completely invalidated the measurements.

To decrease or possibly eliminate the effect of the surface float on the current meters, first a 15 m-length of 35 mm rubber cord (the type

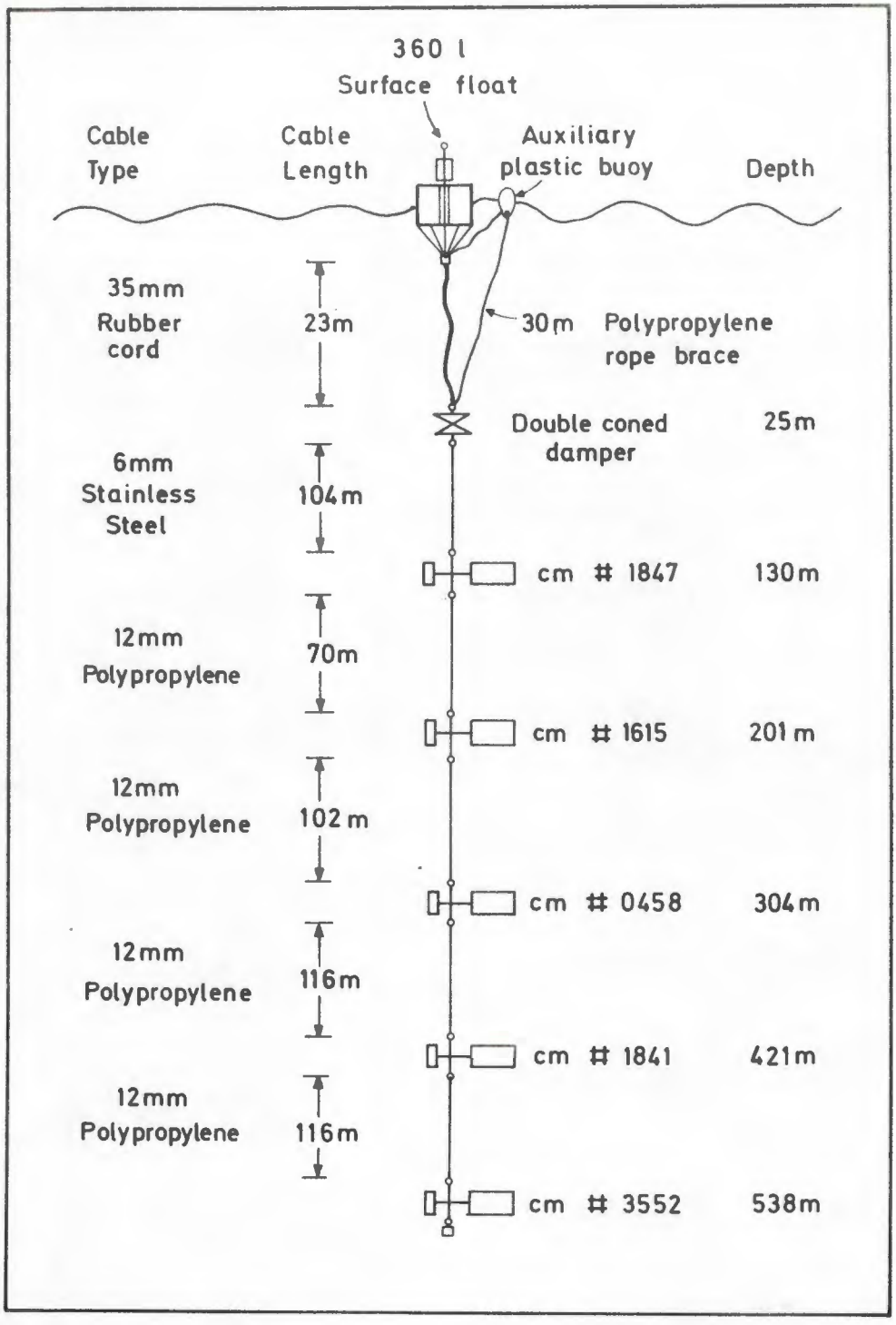

FIG. A7.1 : Configuration of the free-drifting current meter array deployed during the *Meiring Naudé* cruise in December, 1979.

and length commonly used in wave-recorder moorings) was inserted between the surface float and the topmost current meter. Under the weight of the five current meters and other components of the array, the rubber cord elongated to 23 m.

Second, the response of the array to vertical motion was further decreased by installing a stainless steel/glass fibre, double-coned damper immediately below the rubber cord (Fig. A7.2).

To assist in the eventual recovery, a brace in the form of a 30 m polyprop rope was attached between the buoy and the damper. Unfortunately the rope became entangled with the lower end of the surface float and eventually chafed through about 14 hours after deployment. From this time onwards, the surface float was seen to ride the waves much more freely (previously the buoy would become partially submerged in some of the wave crests). The separating of this rope is reflected by a sharp decrease in the current speed, especially visible in the records of the deepest three meters (see Figs. A7.3-A7.7).

Although the movement of the current meters can be assumed to have been much less and the recordings more reliable after the brace had parted, recovery of the array was almost jeopardised because of the difficulty (and danger) in raising the damper with the rubber cord.

A7.3 Deployment period

The deployment of the array was commenced at 09h00 on 3 December, and all the meters were installed by 10h00. Recovery was started at 05h00 on 5 December and concluded by 06h40.

A7.4 Swell-induced motion of the array

In an array such as the one under discussion, the surface swell (the height and period of which varied between 2 m 12 seconds and 5 m 8 seconds) induced two types of motion on the array. First, there was the forced oscillation transmitted via the rubber cord onto the current meters by the buoy movement. Second, there was also the movement of the damper itself due to its being located at a relatively shallow depth where the water

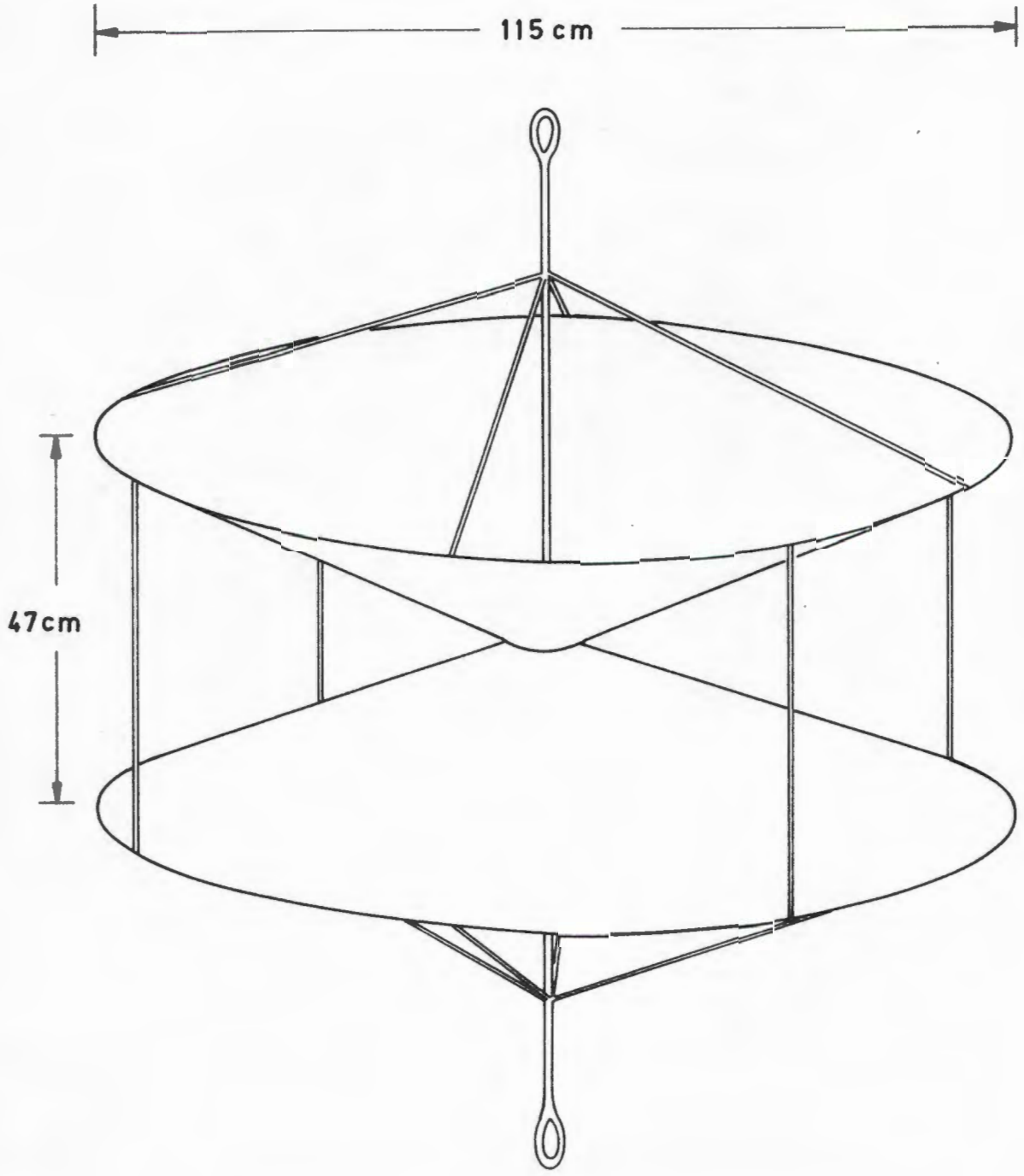

FIG. A7.2 : Double-coned damper used in the free-drifting current meter array. The framework of the damper was made from 6 and 12 mm stainless steel, while the body was fibreglass.

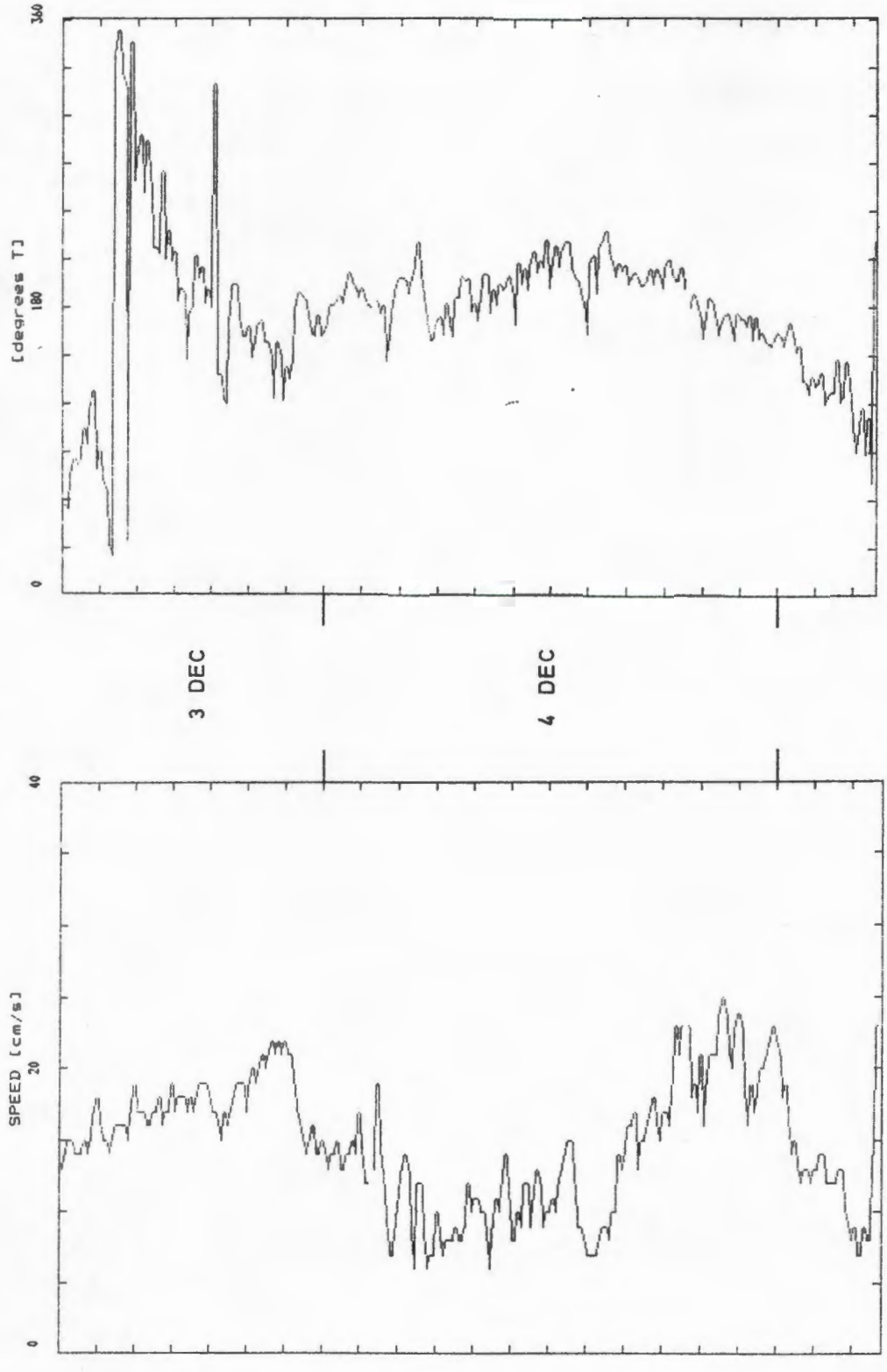

FIG. A7.3 : Current speed and direction of meter 1847, 130 m, in December, 1979.

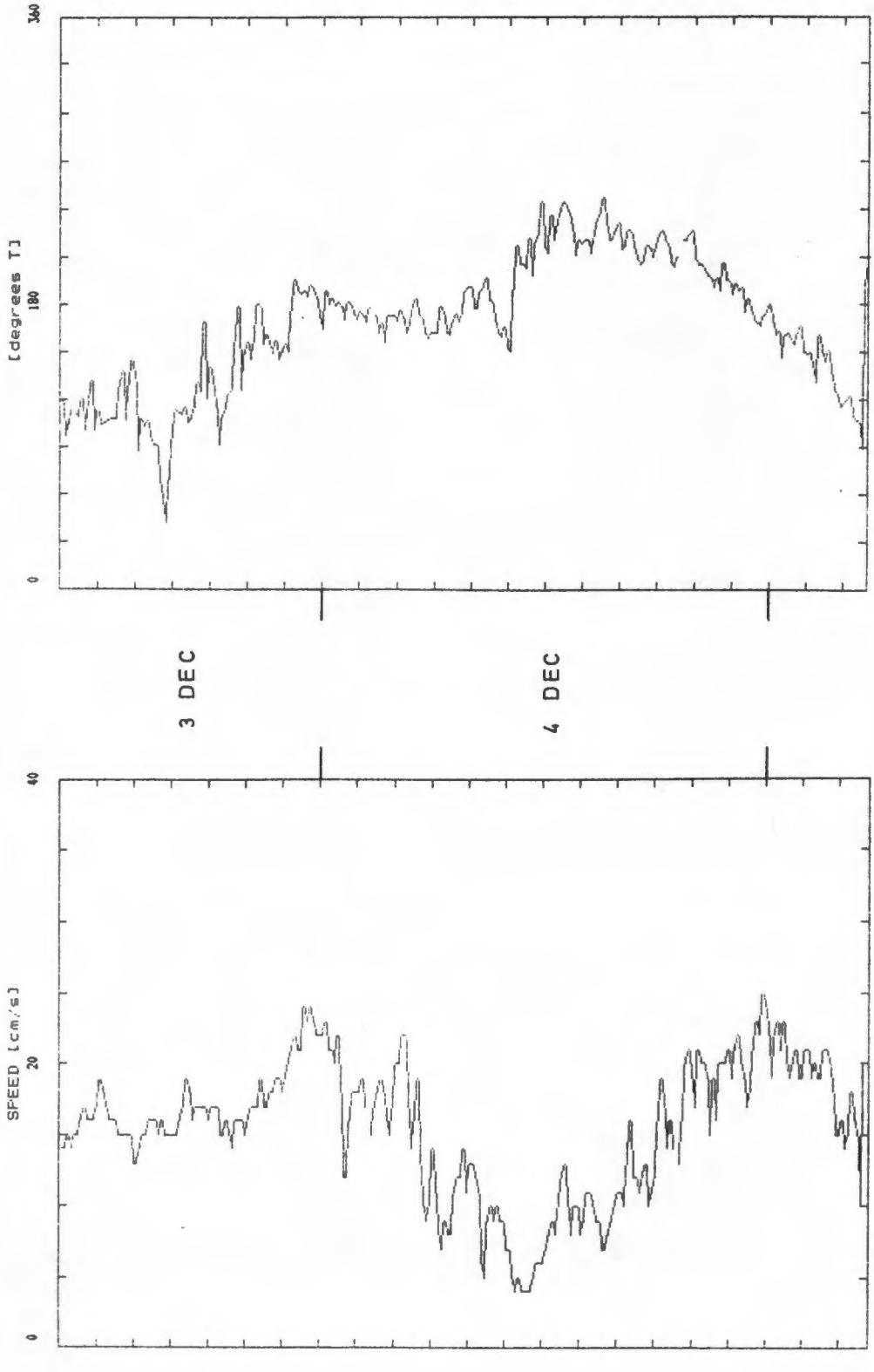

FIG. A7.4 : Current speed and direction of meter 1615, 201 m, in December, 1979.

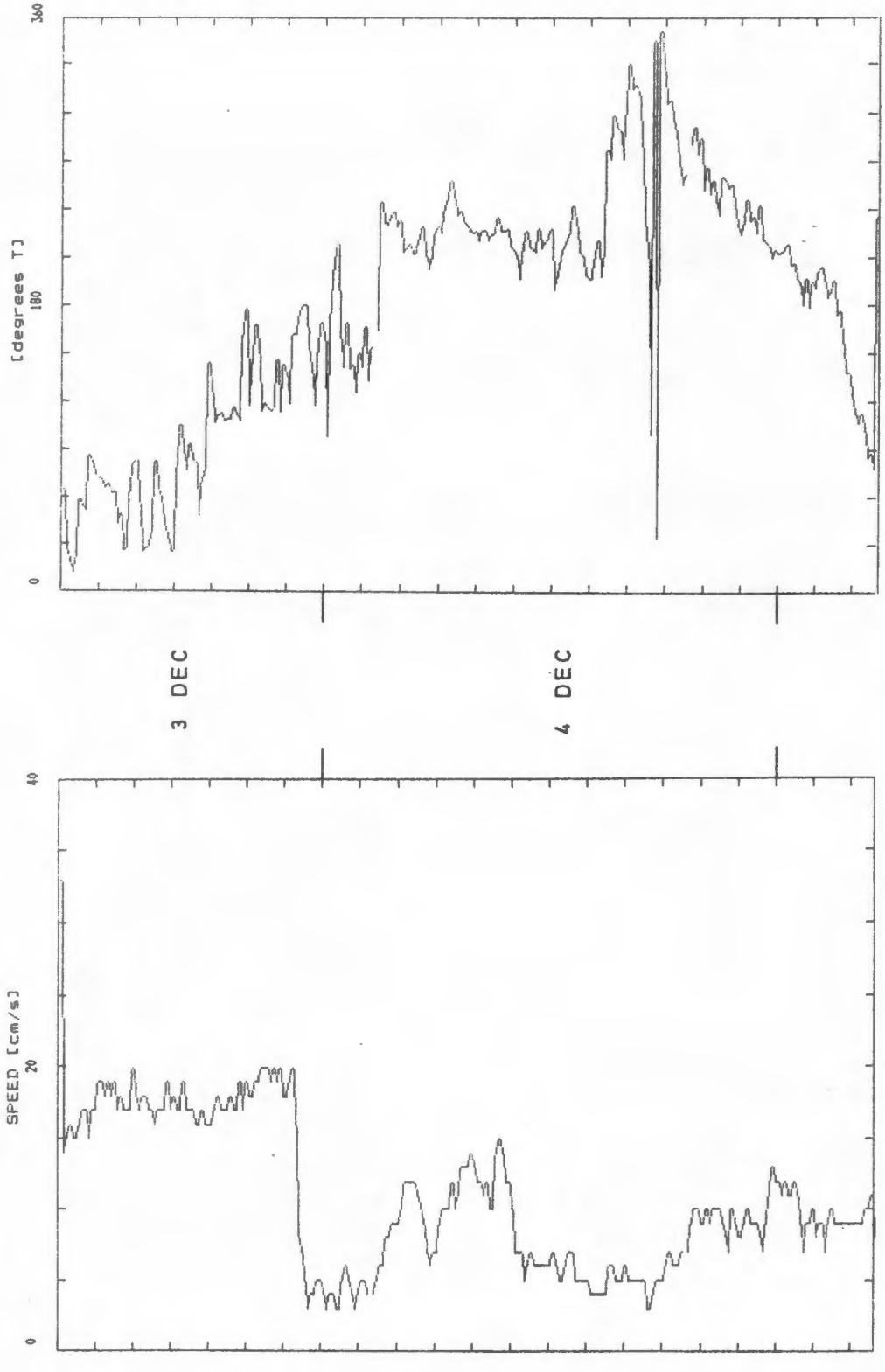

FIG. A7.5 : Current speed and direction, meter 458, 304 m, in December 1979.

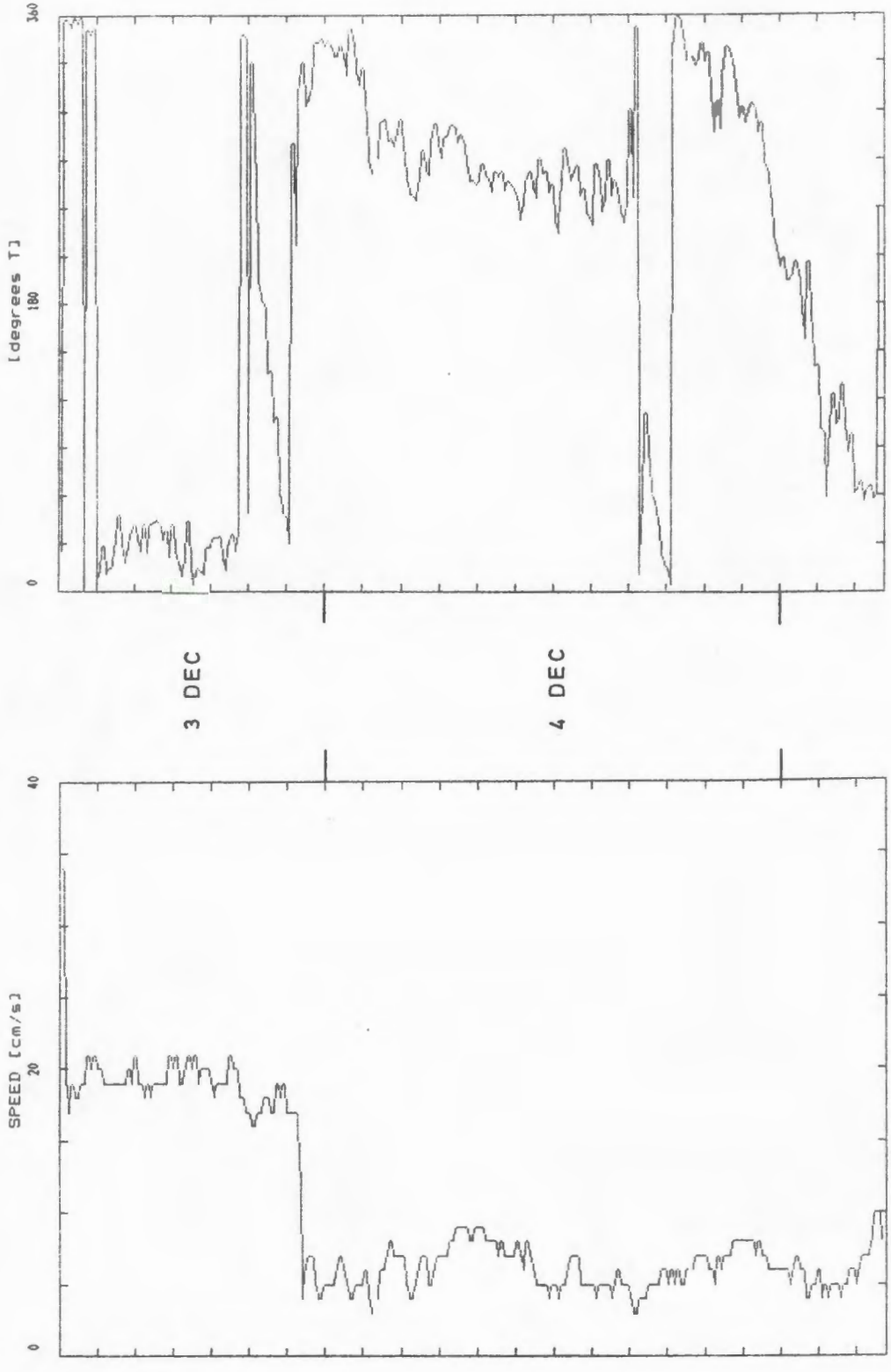

FIG. A7.6 : Current speed and direction of meter 1841, 421 m, for December 1979.

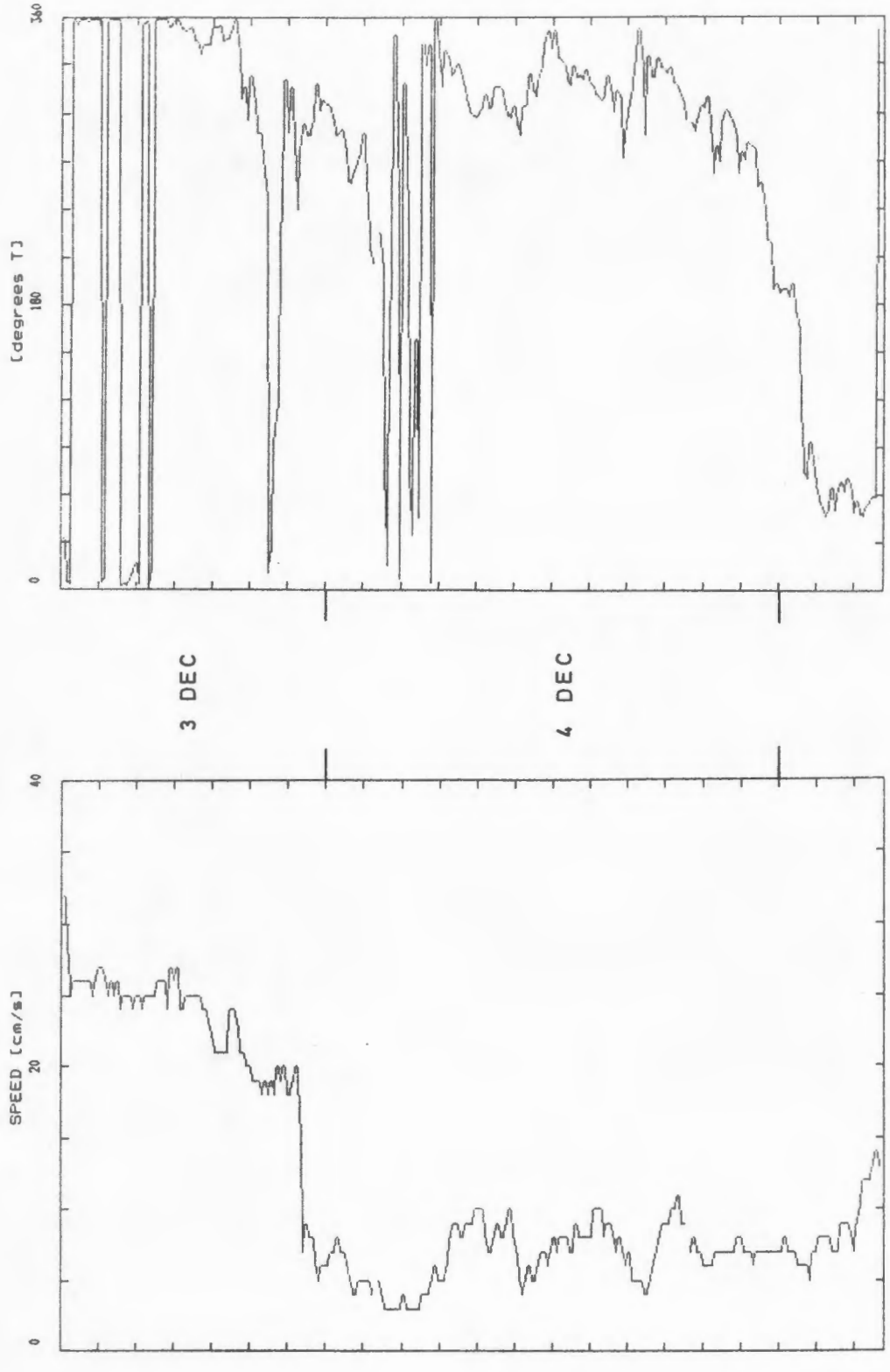

FIG. A7.7 : Current speed and direction of meter 3552, 538 m, in December 1979.

particles exhibit an orbital motion. The resulting motion of the damper because of these two effects can be derived from the superposition of two vectors with a mutual phase difference. It was assumed that at the distance of the meters below the surface (>100 m), the vertical components only of these vectors would play a role in the motion of the meters.

(a) Movement of the damper directly caused by wave action.

At a depth z below deep-water waves the water particles move in approximately circular orbits with radius r where

$$r = \frac{H}{2} e^{\frac{-2\pi z}{156 T^2}} \qquad (1)$$

where H is the swell height and T the period. Because of the assymmetry of the damper it does not necessarily follow that it too was moving in a circular motion. It is, however, assumed that, due to the large drag in the vertical direction (both upward and downward), the vertical component of the *in situ* water motion was transferred almost completely onto the damper.

Using the height and period of the swells observed during the deployment of the array, the radius of the orbital motion at 25 m was calculated. The results (see Fig. A7.8) show that the radius varied between 0.1 and 0.6 m.

(b) Forced movement of the damper caused by the motion of the buoy.

It is assumed that the current meter array can be simplified to a system with the following three components: (i) A surface float that provides a periodic forcing function, (ii) a single representative mass m the motion of which is damped, (iii) an elastic connection between the float and the mass. The differential equation that describes the forced oscillations of this damped, mass-elastic system is

$$m \frac{d^2z}{dt^2} + h \frac{dz}{dt} + kz = F_0 \cos \omega t \qquad (2)$$

where $h\, dz/dt$ is the damping factor provided to a large extent by the damper, kz is the restoring force exerted by the rubber cord, F_0 is the

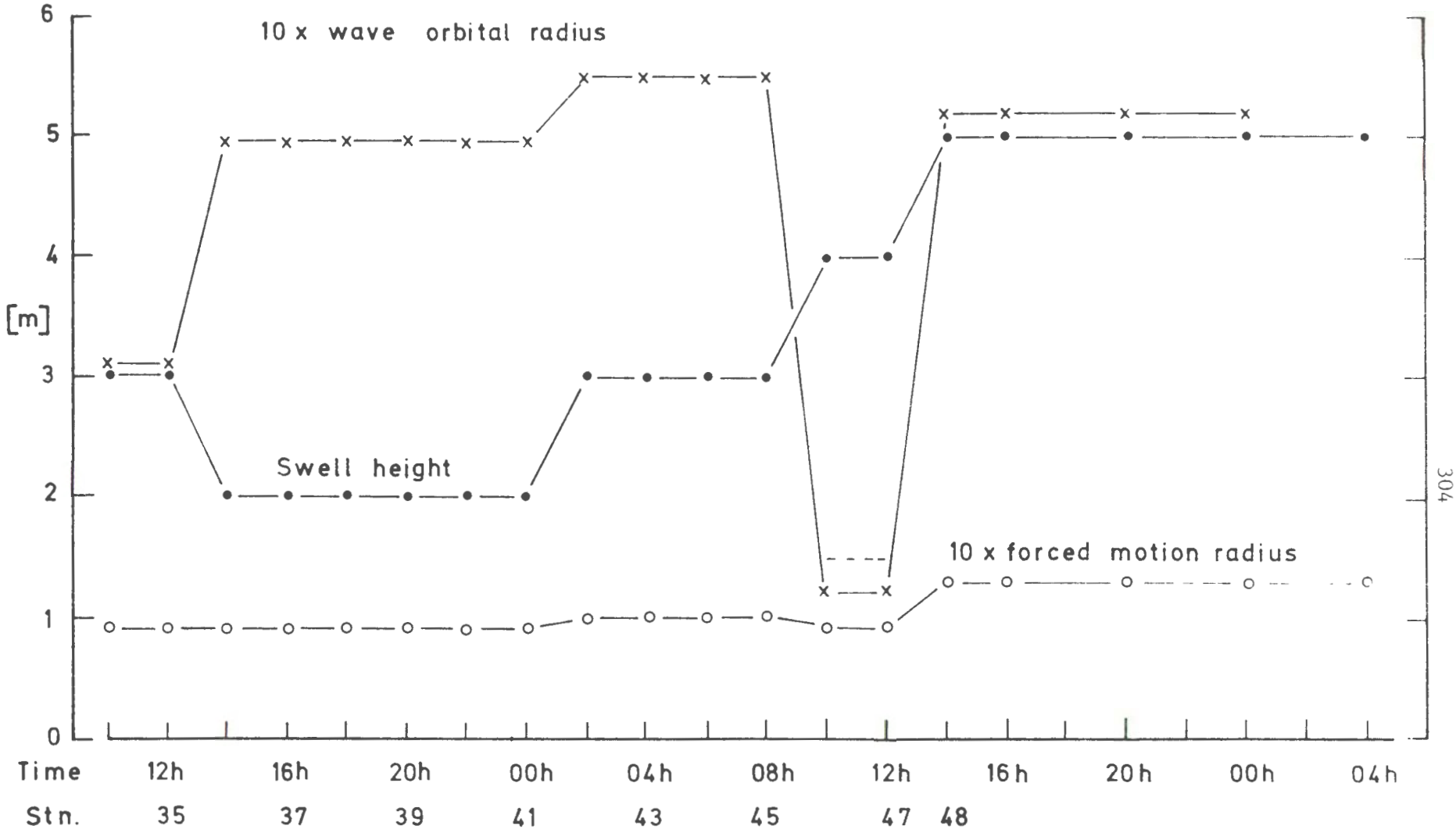

FIG. A7.8 : Variation of swell height, the wave induced orbital radius of water particles at 25 m depth and the radius of the damper forced by the motion of the surface buoy. The orbital radii have been interfaced 10 times for the representation.

forcing function with frequency ω ($= 2\pi/T$, T the period).

In a viscous medium, the damping force or drag is normally taken proportional to the *square* of the velocity rather than the first power as in the equation above. The linear approach is retained here since a solution of the differential equation is readily available. The damping coefficient, h, is however, suitably enlarged.

The real part of the solution of the equation is given by

$$z = e^{-at}\left[A e^{bt} + B e^{-bt}\right] + \frac{F_0 \cos(\omega t - p)}{\left[m^2(\omega_0^2 - \omega^2)^2 + h^2\omega^2\right]^{1/2}} \qquad (3)$$

where $a = h/2m$, $b = \left[(h/2m)^2 - \omega_0^2\right]^{1/2}$

$\omega_0^2 = k/m$ (the free oscillation frequency), and

$\tan p = \omega h / m(\omega_0^2 - \omega^2)$ (the phase difference between the external force and the response of the system).

A and B are constants to be determined from boundary conditions.

The first term describes a transient response to the force, the shape of this response depends on whether $h >$, $=$, or $< 2m\omega_0$ To determine an approximate value of the damping factor h, the following was considered. When a body moves at a velocity v through a medium with density ρ, the drag force on the body is equal to $\frac{1}{2}\rho C_D A v^2$. Here, C_D is the drag coefficient and A the crosssectional area of the moving body exposed to the flow. Taking $C_D = 1.33$, the damper had a drag of about $700\, v^2$ N . Since the expected maximum vertical speed was about 0-1 m/s the drag force would be about 7 N. Using this value, h, which in fact becomes velocity-dependant, was estimated at about 70 kg s^{-1}. This damping would cause the transient motion to disappear rapidly and become negligible within less than 1 second.

For the remaining periodic motion, we assumed that the external force acted only along the rubber cord, so that the amplitude of this force

can be expressed in terms of the coefficient of the restoration force of the rubber, namely $A_0 k$, where A_0 = swell height and $k = 32\ N\ m^{-1}$ (the latter was determined experimentally). The damping coefficient h was replaced by 700 x dz/dt in equation (2) which was then solved numerically for z. The amplitude of the resulting displacement of the damper is plotted in Fig. A7.8, and varied between .09 and .13 m for the swells experienced during the deployment.

Because of the heavy damping, the forcing motion of the buoy and the response of the array remained about $\pi/2$ out of phase. Taking this into consideration, the total displacement-amplitude of the damper was calculated, resulting in values ranging from 0.15 to .92 m. For most of the deployment, wave orbital motion at the depth of the damper contributed more than 95% of the total displacement (see Fig. A7.8).

Corroborating evidence of the validity of the calculations was gathered fortuitously during the recovery of the array. The top end of the rubber was lifted steadily by the crane to about 7 m above deck level before the rubber was secured at deck height. The time taken for this process was roughly ½ minute. The 7 m expanded length of rubber contracted to only 1.75 m after release. If we assume that the array had been raised by a similar height (which is probably an overestimation), this response of the array is the same as its response during deployment to a 7 m-amplitude swell of 50 second period. This period agrees well with the "period" simulated by the movement of the crane (2 x 30 seconds).

A7.5 True relative currents

When the vertical shaft of an Aanderaa current meter is moved up and down, two effects are visible. First, there is a see-saw motion of the current meter and the vane, because of their different drags. As the vertical shaft moves downward, the vane is raised and the current meter faces partially downward. This means that the meter records some of the vertical motion, thus displaying a larger velocity than just the horizontal motion alone. If the current meter was turned through 90° to face vertically, it would record most of the up/down velocity. The current meter is constructed in such a way,

however, that it can at most be deflected 27° from the horizontal, i.e. have at least 63° between its "recording plane" and the vertical. GAUL (1963) found that under these circumstances, the meter records less than 10% of the vertical motion. Added to this, the savonius rotor has a very poor response to oscillatory motion, so that it can safely be assumed that in a vertical motion, say, 0.5 m amplitude and a period of 10 seconds, the meter would register less than 1 cm/s.

Second, if the current meter did not tilt but remained in the same horizontal plane during its vertical motion, the recorded velocity of *horizontal* currents would be *reduced* by 7-11% (GAUL,1963). In our case this reduction has a magnitude of 1-2 cm/s.

We are therefore dealing with two small, almost compensating effects that have a magnitude that falls within the sensitivity and tolerance limits of the current meter. For this reason, the velocities recorded by the meters (see Figs. A7.3-7) were accepted without change.

A7.6 Horizontal drift of the array

This ship closely followed the array, remaining within about 1 km from it for most of the deployment period. From the regular SATNAV fixes that were obtained in this period, five, lying about 6 hours or more apart, were selected and drifts calculated over the intervening periods (see Table A7.1).

TABLE A7.1
DRIFT OF THE ARRAY

PERIOD	DRIFT	
	Speed (m/s)	Direction (°T)
I. 09h04, 3 Dec - 16h44, 3 Dec	0.50	152
II. 16h44, 3 Dec - 00h48, 4 Dec	0.32	149
III. 00h48, 4 Dec - 12h00, 4 Dec	0.35	158
IV. 12h00, 4 Dec - 04h30, 5 Dec	0.29	176

The higher drift speed during the first period cannot be explained in terms of inaccuracy of the SATNAV (see Appendix 2), neither can it be ascribed to a variation of the distance between the ship and the array. It is therefore concluded that the drift speed of the array varied during the deployment period.

On the 4th December, the wind direction was mostly from the southwest, and reached a maximum speed of about 15 m/s in the afternoon. The array was nevertheless drifting toward the south, indicating that it was moving with the water mass.

It would probably not be meaningful to calculate the true currents (i.e. the relative currents and ship's drift vector) for periods shorter than those over which the drift of the ship was obtained. For this reason the 10-minute current vectors recorded by the current meters were averaged to produce relative currents which were vectorially added to the ship's drift to obtain the true currents, (Table A7.2). These vectors are also portrayed in Fig. A7.9.

A7.7 Propagation of eddy Fred

If the eddy had been completely circular and stationary, the magnitude of the current velocity would only be a function of distance from the eddy centre, i.e. the magnitude of the tangential velocity would remain constant at a particular radius. If the eddy itself was, however, advecting, the tangential velocity would be constant only in a frame of reference relative to the eddy. In an absolute frame of reference, the velocity of a particular particle would be the vectorial sum of the tangential velocity V_o and the advection speed V_e of the eddy, and the magnitude of the combined velocity would therefore oscillate as the particle itself described a cycloidal motion (Fig. A7.10).

Inspection of the variation of the tangential velocity of the current meters (depth integrated), shows an irregular fluctuation (Fig. A7.10). However, if the first period (I) is ignored because of possible influence of the swell motion, the variation seems to reveal a slight maximum during the third period. If it is assumed that this (slight) peak occurred as a result of the array (at that moment) being positioned at right angles from the eddy centre relative to the direction of advection (see Fig. A7.10) the following tentative conclusions are reached:

First, judging by the small amplitude of the observed current velocity variation and comparing this with the amplitude of the "model" velocity variation in Fig. A7.10 , it is estimated that the velocity V_e, i.e. the propagation velocity of the eddy, was approximately 5-10 cm/s.

Second, if the velocity V_o and V_e were colinear at 04h00 on 4 December (i.e. this time coincided with t=o, 2π, 4π, etc in Fig. A7.10), the direction in which the eddy propagated was 160°T.

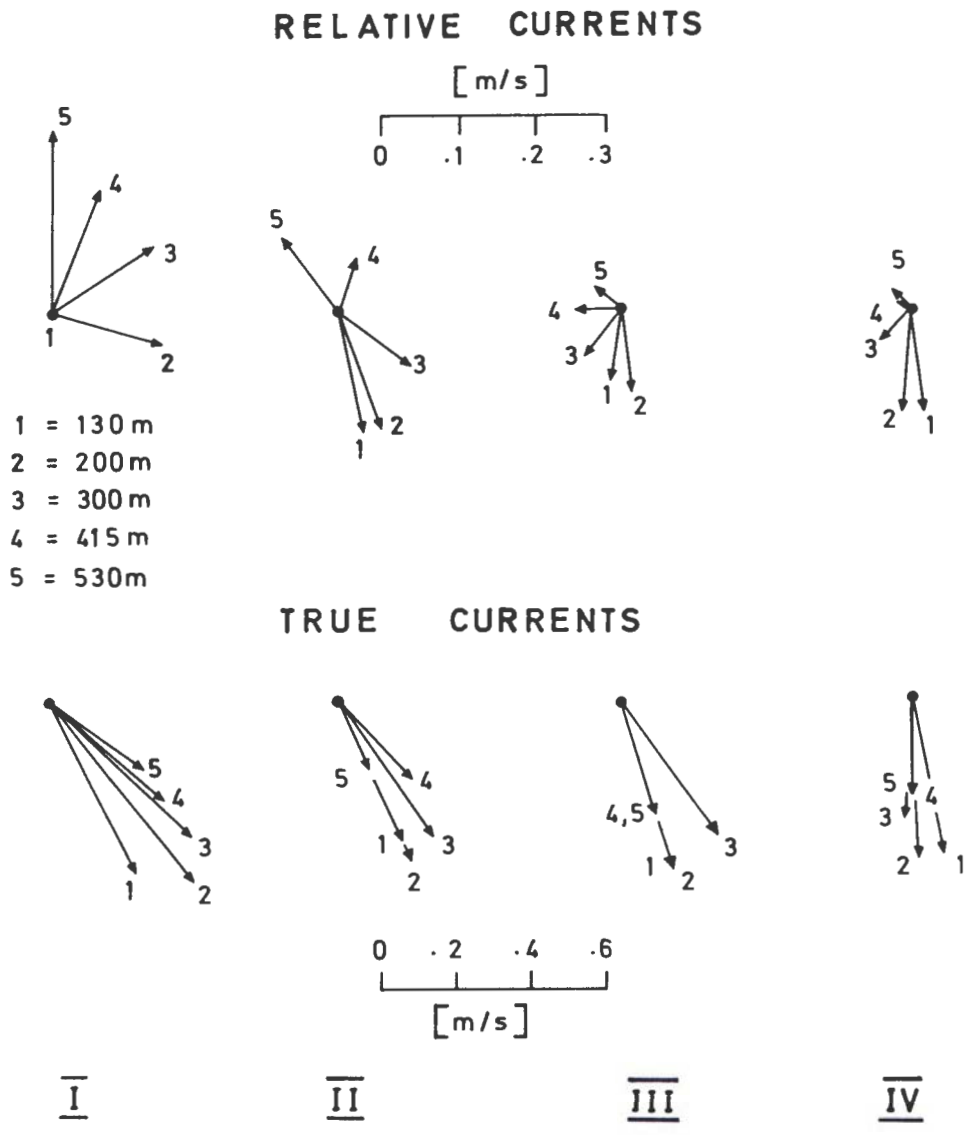

FIG. A7.9 : Current velocities recorded by the 5 current meters during the four periods of deployment (see Table A4.2).
Top : Currrent velocities relative to the drift of the array.
Bottom : Velocities corrected for the drift of the array.

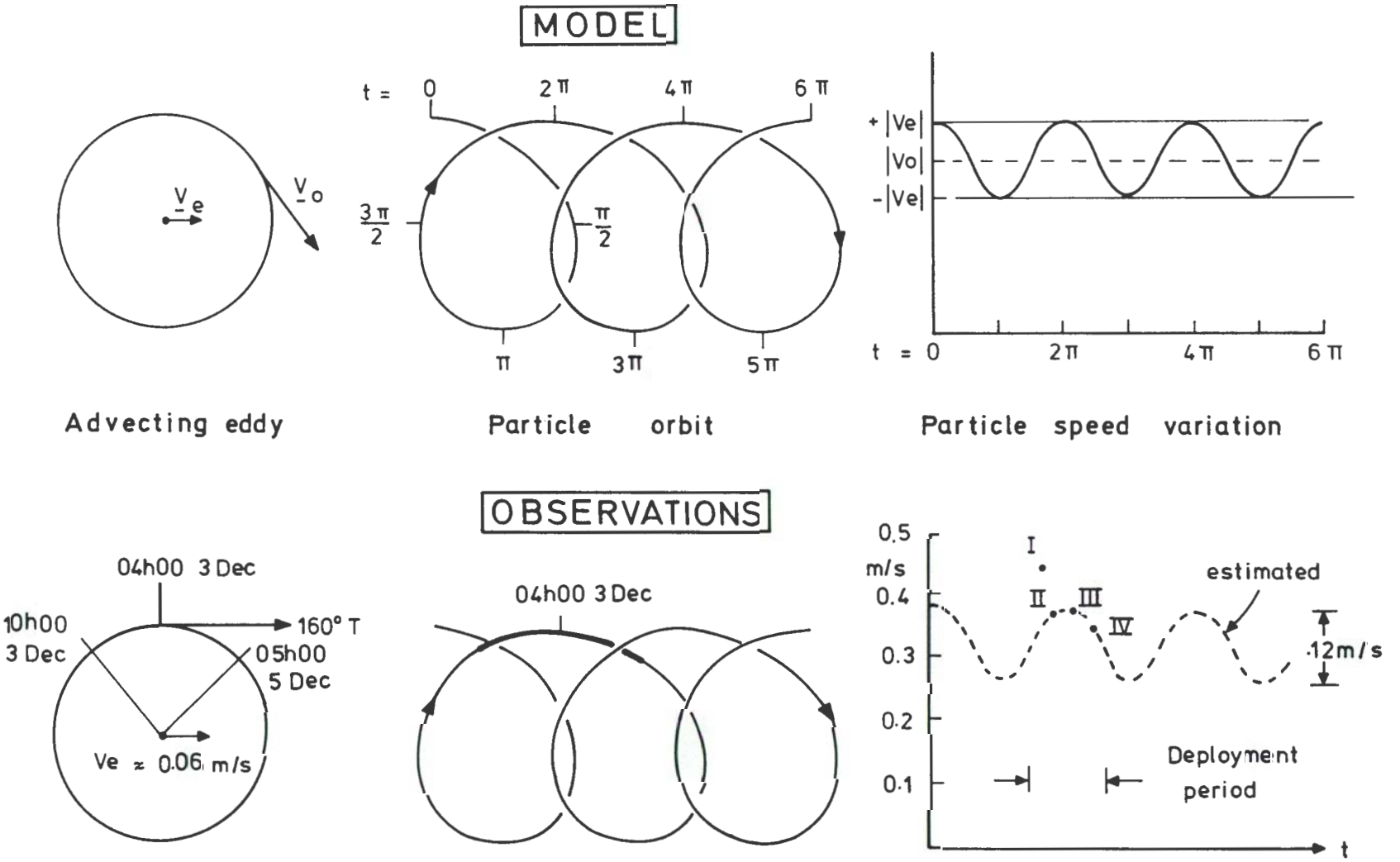

FIG. A7.10 : Comparison between a model representation of the current meter results (top) and the observations (bottom). An eddy (left), advecting at a speed V_e will produce the particle orbit (centre) and the particle speeds will vary as indicated on the right. From the estimated amplitude (12 cm/s) the advection speed of the eddy was estimated at 6 cm/s.

TABLE A7.2

CURRENT VELOCITY RECORDED BY DRIFTING ARRAY

Current Meter ID	Depth (m)	Period (see Table)	Relative		True	
			Speed m/s	Direction	Speed m/s	Direction
1847	130	I	0.01	174	.51	153
		II	0.16	166	.47	154
		III	0.10	189	.44	164
		IV	0.13	174	.42	175
1615	200	I	0.15	107	.61	142
		II	0.17	160	.48	153
		III	0.11	176	.46	162
		IV	0.13	185	.42	179
458	300	I	0.16	057	0.51	134
		II	0.12	127	0.43	143
		III	0.08	221	0.39	169
		IV	0.05	224	0.32	182
1841	415	I	0.18	021	0.40	131
		II	0.08	020	0.28	136
		III	0.06	270	0.33	168
		IV	0.01	300	0.28	179
3552	530	I	0.25	001	0.31	128
		II	0.12	323	0.20	153
		III	0.05	315	0.31	162
		IV	0.04	328	0.26	180

REFERENCES

BACKUS R.H. and J.E. CRADDOCK (1982). Mesopelagic fishes in Gulf Stream cold-core rings. *Journal of Marine Research* 40, 1-20.

BANG N.D. (1970). Major eddies and frontal structures in the Agulhas Current retroflexion area in March 1969. Symposium Oceanography in South Africa, 16pp.

BARRETT J.R. (1971). Available potential energy of Gulf Stream rings. *Deep-Sea Research* 18, 1221-1231.

BECKERLE J.C. *et al* (1980). Sound channel propagation through eddies southeast of the Gulf Stream. *Journal of the Acoustic Society of America* 68, 1750-1767.

BERNSTEIN R.L. and W.B. WHITE (1974). Time and length scales of baroclinic eddies in the central North Pacific Ocean. *Journal of Physical Oceanography* 5, 613-624.

BERTEAUX H.O. *et al* (1979). A study of CTD cables and lowering systems. Woods Hole Oceanographic Institution. Technical Report 7981, 98 pp.

BOYD S.H., P.H. WIEBE and J.L. COX (1978). Limits of Nematoscelis megalops in the northwestern Atlantic in relation to Gulf Stream rings. *Journal of Marine Research* 36, 143-159.

BRETHERTON F.P. (1975). Recent developments in dynamical oceanography. Quarterly *Journal of the Royal Meteorological Society* 101, 705-721.

BRETHERTON F.P. and M.J. KARWEIT (1975). Mid-ocean mesoscale modelling. In: Numerical models of ocean circulation. Ocean Affairs Board; Nat Res Council Washington, 237-249.

BROENKOW W.W. (1982). A comparison between geostrophic and current meter observations in a California eddy. *Deep-Sea Research* 29, 1303-1311.

BRUCE J.G. (1979). Eddies off the Somali coast during the southwest monsoon. *Journal of Geophysical Research* 84, 7742-7748.

BRUCE J.G., D.R. QUADFASEL and J.C. SWALLOW (1980). Somali eddy formation during the commencement of the southwest monsoon 1978. *Journal of Geophysical Research* 85, 6654-6660.

CHANDLER W.S. *et al* (1978). A CTD system: Description; operation; data acquisition and processing. Georgia Marine Science Center Tech. Report 78-7, 75pp.

CHENEY R.E. (1976). A census of rings in the Gulf Stream system. NAVOCEANO Technical Note 3700-44-76, 28 pp.

CHENEY R.E. (1982). Comparison data for SEASAT altimetry in the western North Atlantic. *Journal of Geophysical Research* 87, 3247-3253.

CHENEY R.E. and P.L. RICHARDSON (1976). Observed decay of a cyclonic Gulf Stream ring. *Deep-Sea Research* 23, 143-155.

CHENEY R.E. *et al* (1976). Tracking a Gulf Stream ring with SOFAR floats. *Journal of Physical Oceanography* 6, 741-749.

CHENEY R.E., P.L. RICHARDSON and K. NAGASAKA (1980). Tracking a Kuroshio cold ring with a free-drifting buoy. *Deep-Sea Research* 27A 641-654.

CHENEY R.E. and J.G. MARSH (1981). SEASAT altimeter observations of dynamic topography in the Gulf Stream region. *Journal of Geophysical Research* 86, 473-483.

CHENEY R.E., J.G. MARSH and B.D. BECKLEY (1983). Global mesoscale variability from collinear tracks of SEASAT altimeter data. *Journal of Geophysical Research* 88, 4343-4354.

CLOWES A.J. (1950). An introduction to the hydrology of South African waters. S.A. Fisheries and Marine Biological Investigational Report 12, 66 pp.

COLTON M.T. and R.P.R. CHASE (1983). Interaction of the Antarctic Circumpolar Current with bottom topography: An investigation using satellite altimetry. *Journal of Geophysical Research* 88, 1825-1843.

COX M.D. (1979). A numerical study of Somali Current eddies. *Journal of Physical Oceanography* 9, 311-326.

CRESSWELL G.R. (1982). The Coalescence of two East Australian Current warm-core eddies. *Science* 215, 161-164.

DARBYSHIRE M. (1966). The surface waters near the coasts of southern Africa. *Deep-Sea Research* 13, 57-81.

DARBYSHIRE J. (1972). The effect of bottom topography on the Agulhas Current. *Pure and applied geophysics* 101, 208-220.

DIETRICH G. (1935). Aufbau und Dynamik des sudlichen Agulhasstromgebietes. Veroffentlichungen des Instituts für Meereskunde Berlin A(27), 79pp.

DOBLAR R.A. and R.E. CHENEY (1977). Observed formation of a Gulf Stream cold core ring. *Journal of Physical Oceanography* 7, 944-946.

DUNCAN C.P. (1968). An eddy in the subtropical convergence southwest of South Africa. *Journal of Geophysical Research* 73(2), 531-535.

DUNCAN C.P. (1970). The Agulhas Current. Ph.D. thesis University of Hawaii, 76pp.

DUNCAN C.P. (1976). Comment on "High waves in the Agulhas Current" by E.H. Schumann. *Mariner's Weather Log* 20(1), 3-5.

E E R M (1979). Project marisonde; second dossier. Establissement d'etudes et de Reserches Meteorologiques, Boulogne, 53 pp.

EMERY W.J. (1975). Dynamic height from temperature profiles. *Journal of Physical Oceanography* 5, 369-375.

FEDEROV K.N., A.E. GINZBURG and A.G. ZATSEPIN (1981). Thermohaline structure and traces of mixing in synoptic eddies and Gulf Stream rings. *Oceanology* 21, 15-17.

FIRING E. and R.C. BEARDSLEY (1976). The behaviour of a barotropic eddy on a beta plane. *Journal of Physical Oceanography* 6, 57-65.

FLIERL G.R. (1977). The application of linear quasigeostrophic dynamics to Gulf Stream rings. *Journal of Physical Oceanography* 7, 365-379.

FLIERL G.R. (1979). A simple model for the structure of warm and cold core rings. *Journal of Geophysical Research* 84, 781-785.

FOFONOFF N.P., S.P. HAYES and R.C. MILLARD (1974). WHOI/Brown CTD microprofiler: Methods of calibration and data handling. WHOI technical report 74-89, 64pp.

FU L. and B. HOLT (1983). Some examples of detection of oceanic mesoscale eddies by SEASAT synthetic-aperture radar. *Journal of Geophysical Research* 88, 1844-1852.

FUGLISTER F.C. (1972). Cyclonic rings formed by the Gulf Stream 1965-66. Studies in physical oceanography (Ed. A.L. Gordon), 137-168.

FUGLISTER F.C. (1977). A cyclonic ring formed by the Gulf Stream 1967. In: A voyage of discovery (Ed. M. Angel), Pergamon Press. 177-198.

FUGLISTER F.C. and L.F. WORTHINGTON (1951). Some results of a multiple ship survey of the Gulf Stream. *Tellus* 3, 1-14.

GAUL R.D. (1963). Influence of vertical motion on the Savonius rotor current meter. A & M College of Texas, Ref. 63-AT, 8pp.

GILBERT W.E., A. HUYER and R. SCHRAMM (1981). Hydrographic data First Coastal Ocean Dynamics Experiment. School of Oceanography Oregon State University Rept. 81-12, 34 pp.

GILL A.E. and E.H. SCHUMANN (1979). Topographically induced changes in the structure of an inertial coastal jet: Application to the Agulhas Current. *Journal of Physical Oceanography* 9, 975-991.

GOTTHARDT G.A. (1973). Gulf Stream eddies in the western North Atlantic. U.S. Naval Oceanographic Office Report TN 6150-16-73, 46 pp.

GREGG M.C. *et al* (1982). Dynamic response calibration of the Neil Brown conductivity cell. *Journal of Physical Oceanography* 12, 720-742.

GRüNDLINGH M.L. (1974). A description of inshore current reversals off Richards Bay based on airborne radiation thermometry. *Deep-Sea Research* 21, 47-55.

GRüNDLINGH M.L. (1977a). Drift observations from NIMBUS VI satellite-tracked buoys in the southwestern Indian Ocean. *Deep-Sea Research* 24, 903-913.

GRüNDLINGH M.L. (1977b). A NIMBUS VI satellite-tracked buoy moored on the Mozambique Ridge. *South African Journal of Science* 73, 384-385.

GRüNDLINGH M.L. (1978). Drift of a satellite-tracked buoy in the southern Agulhas Current and Agulhas Return Current. *Deep-Sea Research* 25, 1209-1224.

GRüNDLINGH M.L. (1979). Observation of a large meander in the Agulhas Current. *Journal of Geophysical Research* 84, 3776-3778.

GRüNDLINGH M.L. (1980). On the volume transport of the Agulhas Current. *Deep-Sea Research* 27, 557-563.

GRüNDLINGH M.L. (1983a). On the course of the Agulhas Current. *South African Journal of Science* 65, 49-57.

GRüNDLINGH M.L. (1983b). Eddies in the southern Indian Ocean and Agulhas Current. In: Eddies in Marine Science: Ed. A.R. Robinson. Springer Verlag, 245-264.

GRüNDLINGH M.L. and C.G. SNYMAN (1972). Use of a radiation thermometer in oceanography. C.S.I.R. Symposium on Remote Sensing, May 1972.

GRüNDLINGH M.L. and J.R.E. LUTJEHARMS (1979). Large-scale flow patterns of the Agulhas Current. *South African Journal of Science* 75, 269-270.

GRüNDLINGH M.L., G.A. BROWN and D.W. SMITH (1981). Calibration of the CTD on the R.V. *Meiring Naudé*. CSIR/NRIO Memorandum 8127, 12pp.

HAMON B.V. (1970). Western boundary currents in the South Pacific. National Academy of Science Washington D.C., 50-59.

HANSEN B. and J. MEINCKE (1979). Eddies and meanders in the Iceland-Faroe Ridge area. *Deep-Sea Research* 26A, 1067-1082.

HARRIS T.F.W. (1970). Features of the surface currents in the southwest Indian Ocean. Symposium Oceanography in South Africa. 13 pp.

HARRIS T.F.W. (1972). Sources of the Agulhas Current in the spring of 1964. *Deep-Sea Research* 19, 633-650.

HARRIS T.F.W. (1978). Review of coastal currents in Southern African waters. South African national scientific programme, Report 30; C.S.I.R., Pretoria, 103 pp.

HARRIS T.F.W. and D. van FOREEST (1977). The Agulhas Current System. Department of Oceanography, University Cape Town, 38 pp.

HARRIS T.F.W. and C.C. STAVROPOULOS (1978). Satellite-tracked drifters between Africa and Antarctica. *Bulletin American meteorological Society* 59, 51-59.

HARRIS T.F.W. and D. van FOREEST (1978). The Agulhas Current in March 1969. *Deep-Sea Research* 25, 549-561.

HARRIS T.F.W., W.R. LEGECKIS, D van FOREEST (1978). Satellite infrared images of the Agulhas Current system. *Deep-Sea Research* 25, 543-548.

HOLLAND W.R. (1978). The role of mesoscale eddies in the general circulation of the ocean: numerical experiments using a wind-driven quasi-geostrophic model. *Journal of Physical Oceanography* 8, 363-392.

HOLLAND W.R. and L.B. LIN (1975a). On the generation of mesoscale eddies and their contribution to the oceanic general circulation: I Preliminary numerical experiment. *Journal of Physical Oceanography* 5, 642-657.

HOLLAND W.R. and L.B. LIN (1975b). On the generation of mesoscale eddies and their contribution to the oceanic general circulation: II A parameter study. *Journal of Physical Oceanography* 5, 658-669.

HOLLAND W.R., D.E. HARRISON and A.J. SEMTNER (1983). Eddy-resolving numerical models of large-scale ocean circulation. In: Eddies in Marine Science (Ed. A. Robinson), Springer Verlag, 379-403.

HORNE E.P.W. and J.M. TOOLE (1980). Sensor response mismatches and lag correction techniques for temperature-salinity profilers. *Journal of Physical Oceanography* 10, 1122-1130.

HOWE M.R. and R.I. TAIT (1967). A subsurface cold-core cyclonic eddy. *Deep-Sea Research* 14, 373-378.

IKEDA M. (1981). Eddies detached from a jet crossing over a submarine ridge using a simple numerical model. NOAA Technical Memorandum ERL PMEL-33, 38 pp.

IKEDA M. and J.R. APEL (1981). Mesoscale eddies detached from spatially-growing meanders in an eastward-flowing oceanic jet using a two-layer quasi-geostrophic model. *Journal of Physical Oceanography* 11, 1638-1661

ISELIN C.O'D. (1936). A study of the circulation in the western North Atlantic. *Papers in Oceanography and Meteorology* 4, 101 pp.

ISELIN C.O'D. and F.C. FUGLISTER (1948). Some recent developments in the study of the Gulf Stream. *Journal of Marine Research* 7, 317-329.

JAMES R.W. and R.E. CHENEY (1977). Physical characteristics of ocean fronts and eddies in the North Atlantic. U.S. Naval Oceanographic Office TN 3700-59-77, 52 pp.

JACOBS S.S. and D.T. GEORGI (1977). Observations on the southwest Indian/ Antarctic Ocean. *Deep-Sea Research* 24 (Suppl), 43-84.

JOYCE T.M. and S.L. PATTERSON (1977). Cyclonic ring formation at the polar front in the Drake Passage. *Nature* 265, 131-133.

JOYCE T.M., S.L. PATTERSON and R.C. MILLARD (1981). Anatomy of a cyclonic ring in the Drake Passage. *Deep-Sea Research* 28A, 1265-1287.

KHEDOURI E. and W. GEMMIL (1974). Physical properties and energy distribution of Gulf Stream eddies. NAVOCEANO Tech. note TN-6150-22-74, 27 pp.

KNOWLES C.E. (1974). Salinity determination from use of CTD sensors. *Journal of Physical Oceanography* 4, 275-277.

KRAUSE G. (1968). Struktur und Verteilung des Wassers aus dem Roten Meer im Nordwesten des Indischen Ozeans. *METEOR Forschungsergebnisse* A4, 77-100.

LaFOND E.C. (1951). Processing oceanographic data. U.S. Navy Hydrographic Office Publ. No. 614. 114 pp.

LAI D.Y. and P.L. RICHARDSON (1977). Distribution and movement of Gulf Stream rings. *Journal of Phsyical Oceanography* 7, 670-683.

LAMBERT R.B. (1974). Small-scale dissolved oxygen variations and the dynamics of Gulf Stream eddies. *Deep-Sea Research* 21, 529-546.

LUTJEHARMS J.R.E. (1971). A descriptive physical analysis of water movement in the southwest Indian Ocean during the northeast monsoon season. M.Sc. thesis, University Cape Town. 267 pp.

LUTJEHARMS J.R.E. (1972). A guide to research done concerning ocean currents and water masses in the southwest Indian Ocean. University Cape Town, 577 pp.

LUTJEHARMS J.R.E. (1976). The Agulhas Current system during the northeast monsoon season. *Journal of Physical Oceanography* 6, 655-670.

LUTJEHARMS J.R.E. (1978). Studying the ocean by satellite. *South African shipping news and fisheries industry review* 33, 28-31.

LUTJEHARMS J.R.E. (1979). Interactions between the Agulhas Current and the subtropical convergence. Fourth national oceanographic symposium, Cape Town, July 1979.

LUTJEHARMS J.R.E. (1981a). Physical oceanology of the southwest Indian Ocean. C.S.I.R. Report T/Sea 8016, 82 pp.

LUTJEHARMS J.R.E. (1981b). Features of the southern Agulhas Current circulation from satellite remote sensing. *South African Journal of Science* 77, 231-236.

LUTJEHARMS J.R.E., N.D. BANG and C.P. DUNCAN (1981). Characteristics of the currents east and south of Madagascar. *Deep-Sea Research* 28A, 879-899.

MADELAIN F. and E.G. KERUT (1978). Evidence of mesoscale eddies in the northeast Atlantic from a drifting buoy experiment. *Oceanologica Acta* 1, 159-168.

MALAN O.G. and E.H. SCHUMANN (1979). Natal shelf circulation features revealed by LANDSAT imagery. *South African Journal of Science* 75, 136-137.

MARTIN J. *et al* (1965). Circulation superficielle dans l'ocean indien. *Cahiers oceanographique* 17, 221-240.

McCARTNEY M.S., L.V. WORTHINGTON and W.J. SCHMITZ (1978). Large cyclonic rings from the northeast Sargasso Sea. *Journal of Geophysical Research* 83, 901-914.

MENACHE M. (1963). Premiere campagne oceanographique du Commandant *ROBERT GIRAUD*; Octobre-Novembre 1957. *Cahiers oceanographique* 15, 224-235.

MERCER J.A. and J.R. BOOKER (1983). Long-range propagation of sound through oceanic mesoscale structures. *Journal of Geophysical Research* 88, 689-699.

MIED R.P. and G.J. LINDEMANN (1979). The propagation and evolution of cyclonic Gulf Stream rings. *Journal of Physical Oceanography* 9, 1183-1206.

MIED R.P., G.J. LINDEMANN and J.M. BERGIN (1983). Azimuthal structure of a cyclonic Gulf Stream ring. *Journal of Geophysical Research* 88, 2530-2546.

MODE GROUP (1978). The Mid-Ocean Dynamics Experiment. *Deep-Sea Research* 25, 859-910.

NEUMANN G. and W.J. PIERSON (1966). Principles of physical oceanography. Prentice-Hall Inc., 545 pp.

NIILER P.P. and A.R. ROBINSON (1967). The theory of free inertial jets: A numerical experiment for the path of the Gulf Stream. *Tellus* 19, 601-619.

NILSSON C.S. (1977). Measurement of surface currents around an eddy. R.A.N. Research Laboratory Note 5/77, 21 pp.

NILSSON C.S., J.C. ANDREWS and P. SCULLY-POWER (1977). Observations of eddy formation off East Australia. *Journal of Physical Oceanography* 7, 659-669.

NOF D. (1981). On the beta-induced movement of isolated baroclinic eddies. *Journal of Physical Oceanography* 11, 1662-1672.

OLSON D.B. (1980). The physical oceanography of two rings observed in the Cyclonic Ring Experiment II: Dynamics. *Journal of Physical Oceanography* 10, 514-528.

PAIGE M.A. (1980). Response characteristics of the NBIS Mk III CTD to step changes in temperature and conductivity. U.S. Naval Oceanographic Office; Bay St. Louis Tech. Rep. TR-259, 12 pp.

PARKER C.E. (1971). Gulf Stream rings in the Sargasso Sea. *Deep-Sea Research* 18, 981-994.

PEARCE A.F. (1976). The Agulhas Current off Richards Bay. C.S.I.R. Research Report 348, 21 pp.

PEARCE A.F. (1977a). The shelf circulation off the east coast of South Africa. M.Sc. thesis, University of Natal, 220 pp.

PEARCE A.F. (1977b). Some features of the upper 500 m of the Agulhas Current. *Journal of Marine Research* 35, 731-753.

PEARCE A.F. (1980). Early observations and historical notes on the Agulhas Current circulation. *Transactions Royal Society of South Africa* 44, 205-212.

PEARCE A.F., E.H. SCHUMANN and G.S.H. LUNDIE (1978). Features of the shelf circulation off the Natal Coast. *South African Journal of Science* 74, 328-331.

PERKIN R.G. and E.L. LEWIS (1982). Design of CTD observational programmes i.r.t. sensor time constants and sampling frequencies. *Canadian Technical Report Hydroraphy and ocean science* 7, 47 pp.

PETERSON R.G., W.D. NOWLIN and T. WHITWORTH (1982). Generation and evolution of a cyclonic ring at Drake Passage in early 1979. *Journal of Physical Oceanography* 12, 712.

PETROV A.G. (1980). On motion of Gulf Stream rings. *Oceanology* 20, 635-640.

QUADFASEL D.R. (1983). Structure and variability of the South Equatorial Current in the western Indian Ocean. IUGG/IAPSO Symposium; Hamburg, (abstract only).

QUADFASEL D.R. and F. SCHOTT (1983). Southward subsurface flow below the Somali Current. *Journal of Geophysical Research* 88, 5973-5979.

RABSHACK (1980). Bathymetry of the oceans around southern Africa: Chart 526A. Rabinowitz and Brenner (LAMONT), Shackleton (UCT).

REID J.L., R.A. SCHWARTZLOSE and D.M. BROWN (1963). Direct measurements of a small surface eddy off northern Baja California. *Journal of Marine Research* 21, 205-218.

RENNEL J. (1832). An investigation of the currents of the Atlantic Ocean and those which prevail between the Indian Ocean and the Atlantic. London.

RICHARDSON P.L. (1980). Gulf Stream ring trajectories. *Journal of Physical Oceanography* 10, 90-104.

RICHARDSON P.L., A.E. STRONG and J.A. KNAUSS (1973). Gulf Stream eddies: Recent observations in the western Sargasso Sea. *Journal of Physical Oceanography* 3, 297-301.

RICHARDSON P.L., R.E. CHENEY and L.A. MANTINI (1977). Tracking a Gulf Stream ring with a free-drifting buoy. *Journal of Physical Oceanography* 7, 580-590.

RICHARDSON P.J., R.E. CHENEY and L.V. WORTHINGTON (1978). A census of Gulf Stream rings; Spring 1975. *Journal of Geophysical Research* 83, 6136-6144.

RICHARDSON P.L., C. MAILLARD and T.B. STANFORD (1979). The physical structure and life history of cyclonic Gulf Stream ring Allen. *Journal of Geophysical Research* 84, 7727-7741.

ROCHFORD D.J.(1964). Salinity maxima in the upper 1000 m of the north Indian Ocean. *Australian Journal of Marine and Freshwater research* 15, 1-24.

RODEN G.I. and J.R. IRISH (1975). Electronic digitisation and sensor response effects on salinity computation from CTD field measurements. *Journal of Physical Oceanography* 5, 195-199.

ROSSBY T. and D. WEBB (1970). Observing abyssal motions by tracking swallow floats in the SOFAR channel. *Deep-Sea Research* 17, 359-365.

SAVCHENKO V.G., W.J. EMERY and O.A. VLADIMIROV (1978). A cyclonic eddy in the Antartic Circumpolar Current south of Australia. *Journal of Physical Oceanography* 8, 825-837.

SCHMITZ J.E. and A.C. VASTANO (1975). Entrainment and diffusion in a Gulf Stream cyclonic ring. *Journal of Physical Oceanography* 5, 93-97.

SCHUMANN E.H. (1979). Agulhas Current structure and subtidal fluctuations off Natal. Ph.D. thesis, University of Natal, 162 pp.

SEMTNER A.J. and Y. MINTZ (1977). Numerical simulation of the Gulf Stream and mid-ocean eddies. *Journal of Physical Oceanography* 7, 208-230.

SHACKLETON L. (1982). Southeast Atlantic and southwest Indian Oceans; Chart 126A Bathymetry. Institute of Oceanography, University of Cape Town.

SHIPLEY A.M. and P. ZOUTENDYK (1964). Hydrographic and plankton data collected in the southwest Indian Ocean during the SCOR IIOE 1962-1963. University Cape Town. 210 pp.

SIMPSON E.S.W. (1974). Southeast Atlantic and southwest Indian Oceans: Chart 125A Bathymetry. C.S.I.R. Stellenbosch.

SNYMAN C.G. (1980). An oceanographic data acquisition system using a digital computer. M.Sc. thesis, University Natal, 153 pp.

SPENCE T.W. and R. LEGECKIS (1981). Satellite and hydrographic observations of low-frequency wave motions associated with a cold-core Gulf Stream ring. *Journal of Geophysical Research* 86, 1945-1953.

SPINDEL R.C. and Y. J-F DESAUBIES (1983). Eddies and acoustics. In: Eddies in marine science (Ed. A. Robinson). Springer Verlag. 525-541.

STAVROPOULOS C.C. (1971). Data acquisition on the R.V. *MEIRING NAUDé*. *Electronics and Instrumentation*. 11-15

STAVROPOULOS C.C. and C.P. DUNCAN (1974). A satellite-tracked buoy in the Agulhas Current. *Journal of Geophysical Research* 79, 2744-2746.

STUMPF H.G. and R.V. LEGECKIS (1977). Satellite observations of mesoscale eddy dynamics in the eastern tropical Pacific Ocean. *Journal of Physical Oceanography* 7, 648-658.

SWALLOW J.C. (1976). Variable currents in mid-ocean. *Oceanus* 19, 19-25.

SZEKIELDA K.H. (1983). Satellite investigations on the fluctuations of the Subtropical and Antarctic Convergence zones. *Deutsche Hydrographische Zeitschrift* 36, 25-43.

U S N (1976). Marine climatic atlas of the world: Vol. III. U S Naval Weather Service Publication NAVAIR 50-1C-530, 348 pp.

VASTANO A.C. and D.E. HAGAN (1977). Observational evidence for transformation of tropospheric waters within cyclonic rings. *Journal of Physical Oceanography* 7 938-943.

VASTANO A.C. and G.E. OWENS (1973). On the acoustic characteristics of a Gulf Stream cyclonic ring. *Journal of Physical Oceanography* 3, 470-478.

VASTANO A.C., J.E. SCHMITZ and D.E. HAGAN (1980). The physical oceanography of two rings observed by the Cyclonic Ring Experiment II: Physical structures. *Journal of Physical Oceanography* 10, 493-513.

VISSER G.A. and M.M. VAN NIEKERK (1965). Ocean currents and water masses at 1000, 1500 and 3000 m in the southwest Indian Ocean. South African Division of Sea Fisheries Investigational Report 52. 46 pp.

VUKOVITCH F.M. and B.W. CRISSMAN (1978). Further studies of a cold eddy on the eastern side of the Gulf Stream. *Journal of Physical Oceanography* 8, 838-845.

WARREN B.A. (1963). Topographic influences on the path of the Gulf Stream. *Tellus* 15, 167-183.

WARREN B.A. (1967). Notes on the translatory movement of rings of current with applications to Gulf Stream eddies. *Deep-Sea Research* 14, 505-524.

WATTS D.R. and D.B. OLSON (1978). Gulf Stream ring coalescence with the Gulf Stream off Cape Hatteras. *Science* 202, 971-972.

WIEBE P.H. (1982). Rings of the Gulf Stream *Scientific American* 246, 50-60.

WIEBE P.H. *et al* (1976). Gulf Stream cold core rings: large scale interaction sites for open-ocean plankton communities. *Journal of Marine Research* 23, 695-710.

WYRTKI K. (1971). Oceanographic atlas of the International Indian Ocean Expedition. National Science Foundation Washington. 531 pp.